

# BEACH NOURISHMENT

*An evaluation of equilibration design methods*



Cancún Beach Rehabilitation Project

---

MSc thesis  
April 2004

M.J. Bodegom



# BEACH NOURISHMENT

*An evaluation of equilibration design methods*

Cancún Beach Rehabilitation Project

---



Evaluating Committee:

prof.dr.ir. M.J.F. Stive	(TU Delft)
dr.ir. J. van de Graaff	(TU Delft)
dr.ir. A.J.H.M. Reniers	(TU Delft)
ir. K.G. Nipius	(Hydronamic)

---

MSc thesis  
April 2004

M.J. Bodegom

 <p>TU Delft Delft University of Technology</p>	<p>Delft University of Technology Faculty of Civil Engineering Section of Hydraulic Engineering</p>
 <p>hydRONAMIC</p>	<p>Hydronamic BV Papendrecht</p>





# PREFACE

This report is the result of my MSc thesis study Hydraulic Engineering at Delft University of Technology. This thesis has been performed at Hydronamic BV in Papendrecht, the Netherlands.

This investigation has been carried out within the framework of the Cancún Beach Rehabilitation Project, aiming at restoring Cancún Beach to boost tourist competitiveness. The objective of this thesis is to obtain insight in the cross-shore behaviour of the proposed beach fill by comparing the results of equilibrium models and process-based numerical modelling.

I would like to thank my colleagues at Hydronamic who created a pleasant working environment. I also appreciated the various conversations full of humour with my colleague MSc students at Hydronamic. Furthermore I want to thank ir. K.G. Nipius of Hydronamic and dr.ir. J. van de Graaff, dr.ir. A.J.H.M Reniers and prof.dr.ir. M.J.F. Stive of Delft University of Technology for their valuable advice.

Reaching the end of my studies I can conclude that although it has been a complex job, it was well worth the effort. I would like to express my appreciation for the ongoing support I received from Marijke, my family and my friends during my studies in Delft and abroad.

Martjan Bodegom

Papendrecht, April 2004.



# SUMMARY

## Introduction

Most of the ongoing growth of the world's population takes place in coastal zones, leading to increasing use of these areas. Coasts are dynamic systems characterized by variability in shoreline position and profile shape, induced by natural and human forces at various time scales. Sometimes shore variability conflicts with human interests, which is the case at Cancún Beach in Mexico, used as a case study in this thesis.

In addition to hard coastal structures, beach nourishment or beach fill has become more common to protect human interests as it often has less adverse effects on the surroundings. Beach nourishment consists of the placement of a large volume of (granular) sediment in the active profile, aimed at building additional recreational area and / or offer storm protection.

After placement the fill sediments mix with the native sediments and are distributed across and along the shore by the action of waves and currents. This distribution is split in the following sediment transport processes (see Figure 1):

- The cross-shore equilibration from the construction profile to the equilibrium profile.
- Spread out losses: a transfer of sand out of the nourished area.
- Ongoing background erosion.

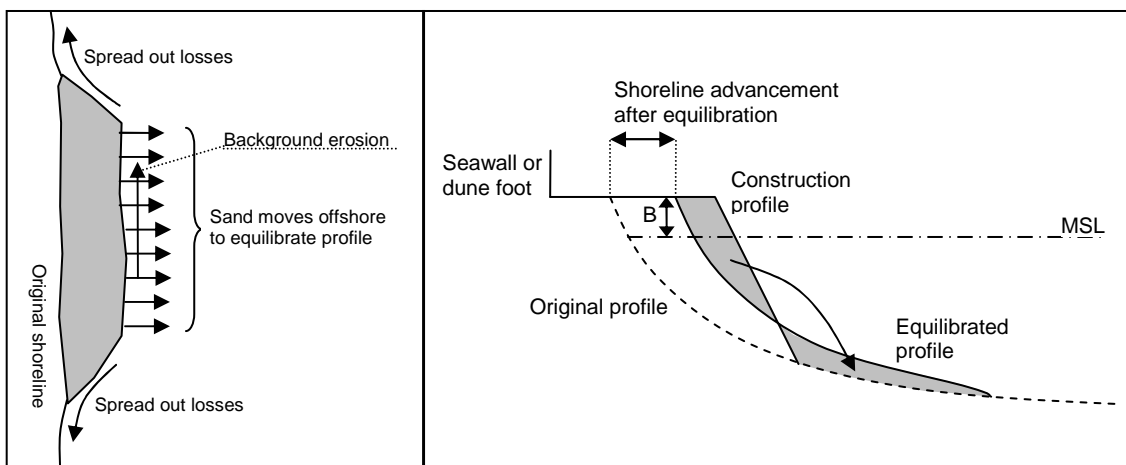


Figure 1: Plan view (left) and cross-section view (right) of the three erosion processes associated with beach nourishment: equilibration, spread-out losses and background erosion.

However, it is difficult to predict the morphological behaviour of a beach fill, especially when fill sediments are used which differ from the native sediments. This complicates the economical, social and environmental assessment of beach nourishment, inducing the need to develop better modelling and design methods.

## Objectives and approach

In this thesis only the cross-shore modelling of beach fill behaviour is considered.

*The scientific objective of this thesis is to compare current design methods for the beach fill equilibration based on equilibrium models (Dean [1974], James [1975], USACE [1994] and Dean [2002]) with process-based numerical modelling (with the software package Unibest-TC of WL | Delft Hydraulics [1999]) and to determine their suitability.*

Furthermore, application of the equilibration design methods leads to practical recommendations regarding the proposed fill at Cancún Beach, such as the shoreline advancement per unit fill volume and the time scale of the beach fill equilibration, for the three considered fill sediments from:

- Borrow area I – Puerto Juárez with an average  $d_{50}$  of 0.27 mm.
- Borrow area II – Punta Sam with an average  $d_{50}$  of 0.42 mm.
- A fictitious borrow area – sediments equal to native with a  $d_{50}$  of 0.33 mm.

Fill volumes  $V$  between 150 and 400 m<sup>3</sup>/m and berm heights  $B$  of 2.0, 2.5 and 3.0 m will be considered.

Furthermore, the stability of the fill sediments during storm conditions will be determined, using the dune erosion prediction model of Vellinga [1986] and the Unibest-TC model.

### **Coastal behaviour of Cancún Beach**

Cancún Beach is used as a case study in this thesis because it is part of a complex coast. An analysis of the coast is made in order to apply the different equilibration design methods. The outer ends of the project area show complex hydrodynamic behaviour, making it difficult to determine their role in the sediment balance of the area. Human intervention in this system has made the system very vulnerable to storms.

### **Equilibration design methods**

The equilibration design methods are characterized by their implementation of relevant model issues: equilibrium profile, granulometry, closure depth, underlying physical and time-varying processes.

The equilibrium models of Dean [1974], James [1975], USACE [1994] and Dean [2002] are characterized by the assumption of an equilibrium profile, while the Unibest-TC model only uses this assumption for calibration purposes. Secondly, the granulometry is modelled differently by each design method. Furthermore, the Unibest-TC model accounts for the underlying time-varying physical processes which cause changes in the morphology.

In order to apply the Unibest-TC model in a sound way, a sensitivity analysis and calibration is carried out. The subsequent model calculations of the beach fill equilibration result in a profile shape and a typical equilibration time scale of approximately 80 days, depending on grain size, berm height and fill volume. The model results should be interpreted with care since the calibration of the model is based on rather uncertain boundary conditions and few bathymetric surveys.

The equilibrium models have been applied using a (rather uncertain) closure depth of 7.5 m. Only the centre of the project area is considered, since the longshore transport gradient is presumed to be small here.

Application of the different equilibration design methods leads to strongly varying results for the shoreline advancement and profile shape. The influence of the grain size on these results varies significantly between the design methods.

The main cause of these differences is the simplified modelling of:

- The grain size variation across the profile.
- The spread of the grain size distribution.
- The dependency of the profile shape on the grain size.

The design method of Dean [2002] and the Unibest-TC model are preferred above the other methods. Both methods aren't perfect and should be used complementary to each other.

### **Storm behaviour of the equilibrated nourished profile**

The profile shape and shoreline retreat after a design storm (return period of 5 years with a deep water significant wave height of 10 m) has been determined with the dune erosion prediction model of Vellinga [1986] and the Unibest-TC model. Three equilibrated nourished ( $V = 250$  m<sup>3</sup>/m and  $B = 2.5$  m) pre-storm profiles with a  $d_{50}$  of 0.27, 0.33 and 0.42 mm are considered.

Uncertainties in the results are caused by uncertain storm parameters and the Unibest-TC parameter setting.

It is expected that:

- The coarse sediments ( $d_{50} = 0.42$  mm) are more stable than the finer sediments.
- A small shoreline retreat or even a seaward shift of the shoreline occurs for the considered fill sediments.
- Erosion volumes of more than  $100 \text{ m}^3/\text{m}$  for  $d_{50} = 0.27$  mm) can occur, while the erosion for  $d_{50} = 0.42$  mm will be in the order of  $50 \text{ m}^3/\text{m}$ .
- The eroded sediment will be deposited between the 4.5 and 9 m depth contours and at the shoreline (at MSL).

The shoreline retreat is relatively small because of the small expected storm surge of approximately MSL +2 m during the design storm.

**Recommendations regarding the Cancún beach fill**

Taking into account the uncertainties in the equilibration design methods and boundary conditions, the following is expected after equilibration of the fill sediments from the two existing borrow areas:

	$d_f = 0.27$ mm	$d_f = 0.42$ mm
Necessary fill volume for a shoreline advancement of 25 m after equilibration	300-375 $\text{m}^3/\text{m}$	200 - 250 $\text{m}^3/\text{m}$
Profile shape after equilibration	Somewhat flatter than the actual profile	Somewhat steeper than the actual profile
Extension of the fill sediments after equilibration	Up to MSL -7.5 m	Up to MSL -7.5 m

Furthermore, it is recommended to:

- Place the fill under a relatively flat construction slope (e.g. 1 to 15) to avoid the occurrence of a scarp.
- Spread the fill across the active profile up to a depth of approximately 4 m, reducing the shoreline retreat after construction and improving public perception.
- Use a berm height of at least MSL +2.5 m, which increases the storm protection.
- Use the coarse fill sediments for better storm protection and more shoreline advancement if this is economically and environmentally feasible.

**Recommendations regarding equilibration modelling methods**

To improve the modelling of beach fill equilibration, it is recommended to:

- Obtain more data on the boundary conditions in the project area for more reliable application of the design methods.
- Improve the equilibrium model of Dean [2002], by:
  - Exclude the very fine particles from the fill volume.
  - Assume a certain mixing with the native sediments, creating a composite sediment volume.
  - Split the composite volume in finer and coarser portions according to James [1975].
  - Split the composite volume in  $N$  (e.g. 5) portions instead of 2.
- Further develop the Unibest-TC model by:
  - Implementing a cross-shore varying grain size.
  - Implementing a dynamic grain size across the profile which is altered by the sediment transport patterns.
  - Implementing an entire grain size distribution (including a spread) instead of a median grain size. This would result in a probability distribution rather than a single estimate of erosion or accretion.



# LIST OF SYMBOLS

LATIN SYMBOLS		
Symbol	Definition	Unit
A	1. profile scale parameter	$m^{1/3}$
	2. wave orbital excursion parameter	m
B	1. berm height	m
	2. general symbol for Unibest-TC boundary conditions	depends
B'	dimensionless berm height = $B/h_*$	[-]
C	1. wave celerity	m/s
	2. Chézy friction factor	$m^{1/2}/s$
$C_r$	correlation coefficient bound long waves (Unibest-TC: C_R)	-
$d_x$	grain diameter where x% of the grain mass has a smaller diameter	m
$d_{50}$	median grain diameter (Unibest-TC: D50)	m
$d_{90}$	$d_{90}$ grain diameter (Unibest-TC: D90)	m
$d_F$	grain diameter of the fill sediments, normally the $d_{50}$	m
$d_N$	grain diameter of the native sediments, normally the $d_{50}$	m
$d_s$	$d_{50}$ of the suspended sediment (Unibest-TC: DSS)	m
D	(storm) duration	hours
$D_f$	wave energy dissipation due to bottom friction	$W/m^2$
Diss	dissipation of roller energy	$W/m^2$
$D_w$	dissipation of wave energy due to breaking	$W/m^2$
$E_r$	roller energy	$J/m^2$
f	1. (probability density) function	[-]
	2. friction factor	[-]
$f_w$	friction factor for bottom friction (Unibest-TC: FWEE)	[-]
g	acceleration of gravity	$m/s^2$
h	water depth	m
$h_c$	closure depth	m
$h_{min}$	minimum water depth where Unibest-TC performs sediment transport calculations	m
$h_*$	closure depth as used in beach nourishment design	m
$h(t)$	water level at offshore boundary (Unibest-TC: H0)	m
$H_e$	effective significant wave height, exceeded only 12 hrs a year	m
$H_{max}$	maximum possible wave height	m
$H_{rms}$	root mean square wave height (Unibest-TC: HRMS)	m
$H_s$	significant wave height	m
i	slope of the water surface	[-]
K	overflow factor according to Dean [1974]	[-]
k	1. local wave number = $2\pi/L$	[rad/m]
	2. roughness height	[m]
$k_s$	friction factor for mean current (Unibest-TC: RKVAL)	m
$k_{s,c}$	current related roughness (Unibest-TC: RC)	m
$k_{s,w}$	wave related roughness (Unibest-TC: RW)	m
L	wavelength	m
$L_p$	peak wavelength	m
$M_\phi$	mean grain diameter in phi units	[-]
p	probability density	[-]
P	1. general symbol for Unibest-TC input parameters	depends
	2. power in weighing function (Unibest-TC: POW)	-
q	sediment transport per unit width	$m^3/s/m$
Q	total sediment transport	$m^3/s$
$Q_b$	fraction of breaking waves	[-]
$q_{tot,x}(x_{end})$	transport at the onshore boundary of the Unibest-TC model (Unibest-TC: USTRA)	$m^3/hr$
$R_A$	overflow factor according to James [1975]	[-]
$R_J$	renourishment factor according to James [1975]	[-]
s	wave steepness	[-]
S	storm surge level	m
t	time	s
$\Delta t$	computational time step	s
$\Delta t_{ubc}$	boundary condition definition time step	S

LATIN SYMBOLS		
Symbol	Definition	Unit
$\tan\phi$	tangent of angle of repose (Unibest-TC: TANPHI)	-
T	simulation time	s
$T^*$	maximum relative wave period (Unibest-TC: TDRY)	-
$T_0$	starting time of the simulation	s
$T_e$	effective mean wave period, corresponding with $H_s$	s
$T_{EQ}$	equilibration time scale	days
$T_p$	peak period (Unibest-TC: T)	s
$T_r$	return period of extreme conditions	year
$T_s$	significant wave period (average period of 33% highest waves)	s
$T_z$	zero crossing wave period	s
$\Delta T$	simulation period	s
u	wave orbital velocity	m/s
v	current velocity	m/s
V	fill volume per unit width	m <sup>3</sup> /m
V(t)	shore parallel current (Unibest-TC: V_TIDE)	m/s
V'	dimensionless fill volume = V/BW*	[-]
$V_{c1}$	critical volume to distinguish between intersecting and non-intersecting profiles	m <sup>3</sup> /m
$V_{c2}$	critical volume to distinguish between emerging and submerged profiles	m <sup>3</sup> /m
$V_E$	eroded volume	m <sup>3</sup> /m
$V_w$	one hour average wind speed at 10 m height (Unibest-TC: V_WIND)	m/s
$W_*$	width of the breaker zone, corresponding with the closure depth $h_*$	m
x	1. shore parallel coordinate 2. coordinate perpendicular to the shore in Unibest-TC, positive in landward direction, with the origin at the seawall	m m
$\Delta x$	computational space step	m
$X_E$	average cross-shore distance over which the eroded volume is moved	m
y	1. coordinate perpendicular to the shore, positive in seaward direction, with the origin at the shoreline 2. shore parallel coordinate in Unibest-TC	m m
$\Delta y_0'$	dimensionless additional dry beach width after equilibration = $\Delta y_{0,EQ} / W_*$	[-]
$\Delta y_0(t)$	additional dry beach width in time	m
$\Delta y_{0,EQ}$	additional dry beach width after equilibration	m
z	bottom height	m

GREEK SYMBOLS		
Symbol	Definition	Unit
$\alpha$	wave breaking parameter (Unibest-TC: ALFAC)	-
$\alpha_w$	viscosity coefficient (Unibest-TC: FCVISC)	-
$\beta$	slope of wave front (Unibest-TC: BETD)	-
$\beta_s$	Bagnold parameter	[-]
$\gamma$	wave breaking parameter (Unibest-TC: GAMMA)	-
$\phi$	phi scale, an alternative measure of sediment size; higher values of $\phi$ indicate smaller sediments $\phi = -^2 \log d$	[-]
$\theta$	angle of wave incidence relative to shore normal (Unibest-TC: A_WAVE)	°
$\theta_w$	wind direction (Unibest-TC: A_WIND)	°
$\lambda$	number of wavelengths for depth integration (Unibest-TC: F_LAM)	-
$\mu_x$	mean of a parameter x	depends
$\nu$	viscosity	m <sup>2</sup> /s
$\rho$	water density	kg/m <sup>3</sup>
$\sigma_x$	standard deviation of a parameter x	depends
$\tau$	shear stress	N/m <sup>2</sup>
$\phi$	phase shift between long and short wave envelope	rad
$\phi_x$	$x^{\text{th}}$ percentile in phi units, x% of the mass of the grains has a smaller phi value, i.e. x% of the grain mass is larger. Note: $\phi_x = -^2 \log(d_{100-x})$	[-]
$\phi_*$	critical phi value	[-]
$\omega$	angular frequency in waves	rad/s



<b>SUBSCRIPTS</b>	
<b>Subscript</b>	<b>Definition</b>
O	subscript referring to deep water wave parameter
c	subscript referring to coarse (portion of) sediments
E	subscript referring to Equilibrated sediments or profile
F	subscript referring to Fill sediments
f	subscript referring to fine (portion of) sediments
m	index
n	index
N	subscript referring to Native sediments

<b>ABBREVIATIONS</b>		
<b>Abbreviation</b>	<b>Explanation</b>	
FONATUR	National Fund for Promotion of Tourism	Fondo Nacional de Fomento al Turismo
HHW	High High Water	
MSL	Mean Sea Level	
SCT	Ministry of Transport and Communications	Secretaría de Transporte y Comunicaciones
SEMARNAT	Ministry of Environmental Issues and Natural Resources	Secretaría de Medio Ambiente y Recursos Naturales
UNAM	National Independent University of Mexico	Universidad Nacional Autónoma de México



# TABLE OF CONTENTS

<b>PREFACE</b> .....	<b>V</b>
<b>SUMMARY</b> .....	<b>VII</b>
<b>LIST OF SYMBOLS</b> .....	<b>XI</b>
<b>1 INTRODUCTION</b> .....	<b>1</b>
<b>2 PROBLEM ANALYSIS</b> .....	<b>3</b>
2.1 INTRODUCTION .....	3
2.2 DESCRIPTION OF THE SITUATION .....	3
2.2.1 <i>Geographical situation</i> .....	3
2.2.2 <i>Geological situation</i> .....	5
2.2.3 <i>Economical and social situation</i> .....	5
2.2.4 <i>Governmental situation</i> .....	5
2.2.5 <i>Future developments</i> .....	6
2.3 DESCRIPTION OF THE ‘CANCÚN BEACH REHABILITATION PROJECT’ .....	6
2.3.1 <i>Historic developments of Cancún Beach</i> .....	6
2.3.2 <i>Cancún Beach Rehabilitation Project</i> .....	6
2.4 OBJECTIVE OF THE THESIS STUDY.....	7
2.4.1 <i>Introduction</i> .....	7
2.4.2 <i>Definition</i> .....	8
2.4.3 <i>Objective</i> .....	8
2.4.4 <i>Available tools</i> .....	9
2.4.5 <i>Approach</i> .....	10
<b>3 ANALYSIS OF THE COASTAL BEHAVIOUR</b> .....	<b>13</b>
3.1 INTRODUCTION .....	13
3.2 BOUNDARY CONDITIONS.....	13
3.2.1 <i>Introduction</i> .....	13
3.2.2 <i>Bathymetry</i> .....	13
3.2.3 <i>Sediment characteristics</i> .....	14
3.2.4 <i>Winds</i> .....	14
3.2.5 <i>Ordinary wave conditions</i> .....	14
3.2.6 <i>Hurricane wave conditions</i> .....	15
3.2.7 <i>Water level variations</i> .....	16
3.2.8 <i>Currents</i> .....	16
3.2.9 <i>Conclusions</i> .....	17
3.3 DIAGNOSIS OF THE ACTUAL SITUATION .....	18
3.3.1 <i>Closure depth</i> .....	18
3.3.2 <i>Shore and shoreline variability</i> .....	19
3.3.3 <i>Cross-shore equilibrium analysis</i> .....	20
3.3.4 <i>Longshore transport gradient</i> .....	21
3.4 HYPOTHESIS OF THE SYSTEM BEHAVIOUR .....	21
3.4.1 <i>Original behaviour of the system</i> .....	21
3.4.2 <i>Human intervention in the coastal system</i> .....	22
3.4.3 <i>Hypothesis system behaviour</i> .....	22
3.5 CONCLUSIONS.....	23

<b>4</b>	<b>THEORY OF BEACH NOURISHMENT BEHAVIOUR AND DESIGN .....</b>	<b>25</b>
4.1	INTRODUCTION .....	25
4.2	BEACH NOURISHMENTS: GOALS AND BEHAVIOUR .....	25
4.2.1	<i>Introduction</i> .....	25
4.2.2	<i>Goals</i> .....	25
4.2.3	<i>Placement</i> .....	25
4.2.4	<i>Behaviour</i> .....	26
4.3	DESIGN OF BEACH NOURISHMENTS .....	28
4.4	COASTAL MODELLING CONCEPTS.....	30
4.4.1	<i>Model subdivision</i> .....	30
4.4.2	<i>Model dimension subdivision</i> .....	31
4.4.3	<i>Application of coastal modelling concepts in beach nourishment design</i> .....	31
4.4.4	<i>Conclusion</i> .....	32
4.5	PROCESS ANALYSIS OF BEACH FILL EQUILIBRATION .....	32
4.6	EQUILIBRATION DESIGN METHODS .....	33
4.6.1	<i>Introduction</i> .....	33
4.6.2	<i>Dean [1974]</i> .....	34
4.6.3	<i>James [1975]</i> .....	36
4.6.4	<i>USACE [1994]</i> .....	39
4.6.5	<i>Dean [2002]</i> .....	41
4.7	CONCLUSIONS .....	46
<b>5</b>	<b>APPLICATION OF EQUILIBRATION DESIGN METHODS.....</b>	<b>47</b>
5.1	INTRODUCTION .....	47
5.2	GRAIN SIZE DISTRIBUTIONS OF THE FILL MATERIAL.....	47
5.3	CALCULATIONS WITH THE EQUILIBRATION DESIGN METHODS .....	48
5.3.1	<i>Dean [1974]</i> .....	48
5.3.2	<i>James [1975]</i> .....	49
5.3.3	<i>USACE [1994]</i> .....	50
5.3.4	<i>Dean [2002]</i> .....	51
5.4	RESULTS OF THE EQUILIBRATION DESIGN METHODS .....	52
5.4.1	<i>Introduction</i> .....	52
5.4.2	<i>Shoreline advancement</i> .....	52
5.4.3	<i>Bottom profiles after equilibration</i> .....	53
5.5	VALIDATION OF THE RESULTS .....	54
5.5.1	<i>Introduction</i> .....	54
5.5.2	<i>Sensitivity to the closure depth</i> .....	54
5.5.3	<i>Sensitivity to variations in grain size distribution</i> .....	55
5.5.4	<i>Conclusions</i> .....	56
<b>6</b>	<b>MODEL SETUP IN UNIBEST-TC.....</b>	<b>57</b>
6.1	INTRODUCTION .....	57
6.2	OBJECTIVES OF THE MODELLING .....	57
6.2.1	<i>Introduction</i> .....	57
6.2.2	<i>Beach fill equilibration</i> .....	57
6.2.3	<i>Storm behaviour</i> .....	58
6.2.4	<i>Required input data</i> .....	58
6.3	MODEL SETUP.....	58
6.3.1	<i>Introduction</i> .....	58
6.3.2	<i>Construction of the model</i> .....	59
6.3.3	<i>Approach sensitivity analysis</i> .....	60
6.3.4	<i>Approach calibration and verification</i> .....	60
<b>7</b>	<b>SENSITIVITY ANALYSIS OF THE UNIBEST-TC MODEL.....</b>	<b>63</b>
7.1	INTRODUCTION .....	63
7.2	REFERENCE MODEL.....	63

7.3	SENSITIVITY FOR THE INPUT PARAMETERS .....	64
7.3.1	<i>TDRY</i> .....	64
7.3.2	<i>USTRA</i> .....	66
7.3.3	<i>ALFAC and GAMMA</i> .....	66
7.3.4	<i>BETD</i> .....	67
7.3.5	<i>FWEE</i> .....	68
7.3.6	<i>F_LAM and POW</i> .....	68
7.3.7	<i>C_R</i> .....	69
7.3.8	<i>D50, D90 and DSS</i> .....	69
7.3.9	<i>FCVISC</i> .....	70
7.3.10	<i>RKVAL</i> .....	71
7.3.11	<i>TANPHI1 and TANPHI2</i> .....	72
7.3.12	<i>RW</i> .....	73
7.3.13	<i>RC</i> .....	73
7.4	SENSITIVITY FOR THE BOUNDARY CONDITIONS .....	74
7.4.1	<i>Water level (h)</i> .....	74
7.4.2	<i>Wave height (<math>H_{rms}</math>)</i> .....	74
7.4.3	<i>Wave angle (<math>\theta</math>)</i> .....	75
7.4.4	<i>Peak period (<math>T_p</math>)</i> .....	75
7.4.5	<i>Wind speed (<math>V_w</math>)</i> .....	75
7.4.6	<i>Longshore velocity <math>V</math></i> .....	75
7.5	CONCLUSIONS.....	76
7.5.1	<i>Input parameters</i> .....	76
7.5.2	<i>Boundary Conditions</i> .....	76
<b>8</b>	<b>CALIBRATION AND VERIFICATION OF THE UNIBEST-TC MODEL.....</b>	<b>77</b>
8.1	INTRODUCTION .....	77
8.2	APPROACH OF THE CALIBRATION AND VERIFICATION .....	77
8.3	BOUNDARY CONDITIONS FOR THE CALIBRATION .....	78
8.3.1	<i>Introduction</i> .....	78
8.3.2	<i>Bottom profiles</i> .....	78
8.3.3	<i>Grain size</i> .....	79
8.3.4	<i>Waves</i> .....	79
8.3.5	<i>Longshore current</i> .....	81
8.3.6	<i>Water levels</i> .....	81
8.3.7	<i>Wind</i> .....	81
8.3.8	<i>Resulting input file</i> .....	81
8.4	RESULTS OF THE CALIBRATION .....	81
8.4.1	<i>General shape of the profile</i> .....	82
8.4.2	<i>Development of individual profiles</i> .....	83
8.4.3	<i>Verification of the equilibration</i> .....	84
8.4.4	<i>Verification of the storm behaviour</i> .....	85
8.4.5	<i>Verification for changed boundary conditions</i> .....	86
8.5	FINAL PARAMETER SETTING.....	88
8.6	CONCLUSIONS.....	88
<b>9</b>	<b>MODELLING OF THE EQUILIBRATION IN THE UNIBEST-TC MODEL.....</b>	<b>91</b>
9.1	INTRODUCTION .....	91
9.2	APPROACH OF THE MODELLING OF THE EQUILIBRATION .....	91
9.3	BOUNDARY CONDITIONS FOR THE MODELLING OF THE EQUILIBRATION .....	92
9.3.1	<i>Introduction</i> .....	92
9.3.2	<i>Bottom profiles</i> .....	92
9.3.3	<i>Grain size</i> .....	93
9.3.4	<i>Wave conditions</i> .....	95
9.3.5	<i>Longshore current</i> .....	95
9.3.6	<i>Water levels</i> .....	95
9.3.7	<i>Wind</i> .....	95
9.3.8	<i>Construction period</i> .....	95
9.3.9	<i>Conclusions</i> .....	95

9.4	RESULTS OF THE MODELLING OF THE EQUILIBRATION .....	96
9.4.1	<i>Introduction</i> .....	96
9.4.2	<i>Bottom profiles and cross-shore transports</i> .....	96
9.4.3	<i>Development of the shoreline position in time</i> .....	99
9.4.4	<i>Comparison with an exponential expression</i> .....	100
9.4.5	<i>Shoreline advancement</i> .....	105
9.4.6	<i>Conclusions</i> .....	105
9.5	VALIDATION OF THE MODELLING RESULTS .....	106
9.5.1	<i>Introduction</i> .....	106
9.5.2	<i>Wave climate</i> .....	106
9.5.3	<i>Difference initial profile and equilibration profile</i> .....	108
9.5.4	<i>Persistency wave conditions</i> .....	111
9.5.5	<i>Seasonal influence</i> .....	112
9.5.6	<i>Computational step size dx</i> .....	114
9.5.7	<i>Conclusions</i> .....	116
9.6	INTERACTION BETWEEN LONGSHORE AND CROSS-SHORE TRANSPORT .....	116
9.6.1	<i>Introduction</i> .....	116
9.6.2	<i>Influence of a longshore transport gradients on the cross-shore transport</i> .....	117
9.6.3	<i>Cross-shore distribution of longshore transport</i> .....	118
9.6.4	<i>Cross-shore gradients in the sediment transport</i> .....	122
9.6.5	<i>Longshore gradients in the sediment transport</i> .....	122
9.6.6	<i>Conclusions</i> .....	122
9.7	CONCLUSIONS AND RECOMMENDATIONS .....	123
<b>10</b>	<b>EVALUATION OF EQUILIBRATION DESIGN METHODS.....</b>	<b>125</b>
10.1	INTRODUCTION .....	125
10.2	COMPARISON OF THE RESULTS .....	125
10.3	EVALUATION OF THE DIFFERENCES IN RESULTS.....	129
10.3.1	<i>Introduction</i> .....	129
10.3.2	<i>Differences in approach of the design methods</i> .....	129
10.3.3	<i>Equilibrium profile</i> .....	129
10.3.4	<i>Granulometry</i> .....	131
10.3.5	<i>Closure depth</i> .....	132
10.3.6	<i>Errors in the model input</i> .....	132
10.3.7	<i>Conclusions</i> .....	132
10.4	CONCLUSIONS AND RECOMMENDATIONS .....	133
10.4.1	<i>Differences in results</i> .....	133
10.4.2	<i>Recommendations for the modelling of the equilibration</i> .....	133
10.4.3	<i>Recommendations for the Cancún Beach Rehabilitation Project</i> .....	134
<b>11</b>	<b>MODELLING OF THE STORM BEHAVIOUR .....</b>	<b>137</b>
11.1	INTRODUCTION .....	137
11.2	APPROACH OF THE MODELLING OF THE STORM BEHAVIOUR .....	137
11.3	BOUNDARY CONDITIONS .....	137
11.3.1	<i>Bottom profile</i> .....	137
11.3.2	<i>Grain size and fall velocity</i> .....	138
11.3.3	<i>Longshore current</i> .....	138
11.3.4	<i>Design storm: waves, winds, water levels and duration</i> .....	138
11.4	RESULTS OF THE UNIBEST-TC MODEL .....	139
11.5	DUNE EROSION PREDICTION MODEL OF VELLINGA [1986].....	139
11.6	DISCUSSION OF RESULTS .....	140
11.7	CONCLUSIONS AND RECOMMENDATIONS .....	141
<b>12</b>	<b>CONCLUSIONS AND RECOMMENDATIONS .....</b>	<b>143</b>
12.1	INTRODUCTION .....	143
12.2	CONCLUSIONS .....	143
12.2.1	<i>Beach fill equilibration</i> .....	143
12.2.2	<i>Storm behaviour</i> .....	147
12.3	RECOMMENDATIONS.....	148
12.3.1	<i>Improving the modelling of the equilibration</i> .....	148
12.3.2	<i>Improving the modelling of the storm behaviour</i> .....	149
12.3.3	<i>Recommendations for the planned fill at Cancún Beach</i> .....	149
	<b>REFERENCES.....</b>	<b>151</b>

# 1 INTRODUCTION

## Background of beach nourishment

With the major part of the ongoing growth of the world's population taking place in coastal zones, economical and social developments make that coasts are more and more intensively used. However, coasts - especially sandy coasts, covering 10 to 15 % of the world's coastline [Van Rijn, 1998] - are dynamic systems characterized by variability in shoreline position and profile shape, induced by natural and human forces at various time scales. Sometimes shore variability conflicts with human interests, which is the case at Cancún Beach in Mexico.

Various techniques are available to influence the coastal behaviour and protect human interests. As an alternative to hard coastal structures, beach nourishment or beach fill has become more common as it often has less adverse effects on the surroundings. For example, in the Netherlands beach nourishments reach 6 million m<sup>3</sup> per annum [d'Angremond and Pluim - Van der Velden, 2001].

Beach nourishment consists of the placement of a large volume of (granular) sediment in the active profile, after which these sediments are distributed across and along the shore by the action of waves and currents. This morphological development consists of longshore spread-out of the fill sediments and of cross-shore equilibration, i.e. the transformation of the construction profile to the dynamic equilibrium profile.

However, it is difficult to predict morphological behaviour of a beach fill. This complicates the economical, social and environmental assessment of beach nourishment, inducing the need to develop better modelling and design methods.

## Objective of this thesis

Various modelling and design methods for beach nourishments are available, covering different aspects of the morphological behaviour. In this thesis cross-shore modelling of the beach fill equilibration and the storm behaviour of the profile will be considered.

*The scientific objective of this thesis is to compare current design methods for the equilibration based on equilibrium models (Dean [1974], James [1975], USACE [1994] and Dean [2002]) with process-based numerical modelling (with the software package Unibest-TC of WL | Delft Hydraulics [1999]) and to determine their suitability.*

Secondly, this thesis will lead to practical conclusions regarding the Cancún Beach Rehabilitation Project such as the shoreline advancement per unit fill volume and the time scale of the beach fill equilibration for the three considered fill sediments:

- Borrow area I – Puerto Juárez with an average  $d_{50}$  of 0.27 mm.
- Borrow area II – Punta Sam with an average  $d_{50}$  of 0.42 mm.
- A fictitious borrow area – sediments equal to native with a  $d_{50}$  of 0.33 mm.

Furthermore, the stability of the fill sediments during storm conditions will be determined. After analyzing the coastal behaviour, various equilibrium models are described and applied. Subsequently the beach fill equilibration is modelled in Unibest-TC. The results of the equilibrium models and the Unibest-TC model are compared, leading to conclusions about the suitability of these design methods. Finally, the behaviour of the nourished beach during a design storm is modelled using the dune erosion prediction model of Vellinga [1986] and the Unibest-TC model.

In this thesis only the centre of Cancún Beach is considered, since the longshore transport gradient is presumed to be small here. Also at this location the model results remain questionable due to uncertainty in the boundary conditions.

### **Structure of this report**

First of all an analysis of the boundary conditions and coastal behaviour of the project area is made in order to apply the various models in a sound way (Chapter 3). Then the theoretical background of the equilibration design methods is discussed. These methods are characterized by their implementation of relevant model issues (Chapter 4). The equilibrium models are applied for the three considered types of fill sediments (Chapter 5). Subsequently, the equilibration is modelled using Unibest-TC. After discussing the model set-up (Chapter 6), a sensitivity analysis is carried out to determine the sensitivity of the model results to the parameter setting and the boundary conditions (Chapter 7). The results of this sensitivity analysis are used to calibrate the model using few available bathymetric surveys and time series of the waves derived from the wave climate (Chapter 8). The calibrated model is used to model the beach fill equilibration for the three considered borrow areas (Chapter 9).

Thereafter the results of the equilibration design according to the equilibrium models and Unibest-TC are compared and explained (Chapter 10).

The calibrated Unibest-TC model is used to determine the profile behaviour during a design storm of the equilibrated nourished profile for the three types of fill sediments. These results are compared with the results of the dune erosion prediction model of Vellinga [1986] (Chapter 11).

Finally, conclusions are drawn regarding the suitability of the considered equilibration design methods and the expected cross-shore behaviour of the proposed beach fill at Cancún Beach. Recommendations are made regarding the modelling of beach fill equilibration and storm behaviour and regarding the Cancún Beach Rehabilitation Project (Chapter 12).

### **Target group**

On the one hand the target group of this report consists of scientists and engineers active in Coastal Engineering or research with interest in cross-shore morphological modelling of sandy coasts. On the other hand this report has been written for coastal engineers active in beach nourishment design in general and the Cancún beach fill in specific.

Readers interested in the scientific background and results of this thesis should focus on Chapter 2, 4, 10 and 12, while readers with special interest in process-based morphological modelling are referred to Chapter 6 to 9 and 11. For information about the Cancún Beach Rehabilitation Project and the behaviour of the coastal system is referred to Chapter 2 and 3.

### **Miscellaneous**

The present text has been written in English by a Dutch author. The English therefore carries a Dutch flavour. British spelling has been used except where reference is made to American literature.

This report is written such that the chapters can be read separately from each other, since it is generally not expected that a reader will read the entire report.

Since data from existing literature and varying sources is used, the use of symbols throughout this report is not unambiguous. The list of symbols should therefore be used with care. In cases where confusion may arise, the symbols are defined and explained as and when they are used.



## 2 PROBLEM ANALYSIS

### 2.1 Introduction

The project considered in this report is located in the municipality of Cancún, Quintana Roo, Mexico. In 1970 the construction of the so-called Zona Hotelera (Hotel Zone) was started on an uninhabited island in front of the coast of the quiet fishing town of Cancún. Now this Hotel Zone is of great importance for the booming tourist industry of Mexico in general and the state of Quintana Roo in special.

However, a decline in the number of visitors in Cancún is partly attributed to a lack of beach, whether or not caused by structural erosion. Therefore one started to investigate the possibilities to increase the beach width in the Zona Hotelera.

In this chapter a description of the geographical, geological, social, economical and governmental situation in Cancún is given (Paragraph 2.2). Subsequently, the Cancún Beach Rehabilitation Project is briefly described (Paragraph 2.3). At the end of this chapter the objective and approach of this thesis study are presented (Paragraph 2.4).

### 2.2 Description of the situation

#### 2.2.1 Geographical situation

Cancún is located on the most eastern tip of the Yucatán Peninsula in the state of Quintana Roo, as can be seen on the map in Figure 2-1 (red arrow).

The Yucatán Peninsula has a tropical climate and is covered by jungle, marsh, mangroves and coastal scrub. The eastern part of the Peninsula consists of the state of Quintana Roo and is also called the Mexican Caribbean, with white sands, clear blue waters and impressive offshore barrier reefs.

The only major surface river in the state of Quintana Roo is the Hondo River (see A in Figure 2-1), forming the border with Belize, more than 250 km south of Cancún. Going up north, one passes a number of lagoons and extensive salt marshes and mangrove forests. Reaching Tulum (B), the coast becomes more closed, with rocky cliffs and small sandy bays. Only 30% of the coast from Tulum to Cancún has a significant beach [\* , personal communication, 2003]. The beaches of the 'Costa Maya' are narrow, but sheltered by reefs. Also Cozumel (C), the nation's largest inhabited island, offers some sheltering to the coast.

Going up further north one reaches the Zona Hotelera (Hotel Zone) of Cancún built on a protuberance on the otherwise more or less straight coast. See the map in Appendix B.2. To the west Laguna Nichupté (see D in Appendix B.2) is a shallow lagoon with two small inlets and filled with mangrove forests. To the north Bahía Mujeres (E), a shallow bay between Isla Mujeres (F) and the main land, borders the Zona Hotelera. Southwards one finds an offshore reef (G), creating sheltered conditions in which mangrove forests (H) flourish.



Figure 2-1: Map of the Yucatán Peninsula [Wereldatlas 2000].

North of the Zona Hotelera one finds Isla Blanca (I), Isla Contoy (J), and Isla Holbox (K), after which the coast bends to the west to the Gulf of Mexico. Sand is abundant in this area as can be seen in Figure 2-2.



Figure 2-2: Left picture: Bahía de Mujeres with Isla Mujeres to the left (east). Right picture: Isla Holbox.

## 2.2.2 Geological situation

### Yucatán Peninsula

The Yucatán Peninsula is geologically young as it emerged from the sea during the Pliocene and Pleistocene periods in the past 10 million years. The enormous shelf of limestone is flat and has an in general infertile soil. In spite of approximately 900 mm of rain per year, the Peninsula lacks significant surface rivers [Editorial Verás, 2002]. The water leaks into the bottom, forming a complex system of 'cenotes' (sinkholes) and underground rivers in the porous limestone rock.

The Yucatán Peninsula is relatively flat, but the east side has only a small continental shelf (approximately 50 km wide), followed by a steep slope, leading to the Caribbean Basin with depths over 4000 m. The flat island Cozumel is in reality a steep mountain emerging from the ocean floor.

Isla Blanca and Isla Holbox are large sand spits, while Isla Mujeres and Isla Contoy consist of limestone rock, old coral reefs and sand. These islands are part of the Meso American Reef, extending from Honduras to the north of Yucatán.

### Zona Hotelera

The Zona Hotelera has an old limestone base with coral rock and young limestone (formed by cementing of the calcareous sand) above it. It has been formed during periods of repeated sea level rise and fall, creating the opportunity for the coral to grow (during high sea water levels) and the young limestone to form (during low sea water levels) [\* , personal communication, 2003].

Erosion of the extensive barrier reefs in the south created calcareous sand, which was carried northwards by the strong oceanic current. Part of this sand was deposited on the rocky base, forming dunes with dense vegetation. The other part was and is deposited further northwards.

## 2.2.3 Economical and social situation

To stimulate the economical and social development of Yucatán in general and Quintana Roo in special, the Mexican government decided to build a large tourist resort on the deserted island before the coast of the quiet fishing village of Cancún.

This location was chosen because of its climate, beaches, reefs, nearby archaeological sites, plentiful labour force and the proximity of the largest tourist market in the world, the USA.

Construction of the Hotel Zone started in 1970 and soon the area attracted large numbers of tourists. Employment in the area boosted and revenues were high.

Now the Hotel Zone has 25.000 rooms and offers a wide spectrum of services to the 2.8 million tourists visiting the area each year, creating employment for thousands of people [\* , 2000e]. This caused the tiny fishing village of Cancún to grow to a major city with over 400,000 inhabitants [Editorial Verás, 2002].

It can be said that Cancún is of great importance for the economy of Quintana Roo and even entire Mexico and offers employment to a large part of the population of Quintana Roo.

## 2.2.4 Governmental situation

Mexico is a federal state, consisting of 31 states and a Federal District. These states are relatively autonomous. The municipality of Cancún is located in the state of Quintana Roo. Also de Zona Hotelera is part of this municipality. However, a zone of 20 m landward from the HHW water line is federal property by law.

The development of the Hotel Zone is in the hands of the following parties:

- The municipality of Cancún
- The government of the state of Quintana Roo
- The federal government in the form of the following institutions:

SCT	Secretaría de Transporte y Comunicaciones	Ministry of Transport and Communication
SEMARNAT	Secretaría de Medio Ambiente y Recursos Naturales	Ministry of Environmental Issues and Natural Resources
FONATUR	Fondo Nacional de Fomento al Turismo	National Fund for Promotion of Tourism

- The hoteliers in the form of the Asociación de los Hoteleros de Quintana Roo (Association of Hoteliers in the state of Quintana Roo).

### 2.2.5 Future developments

The growth of Cancún is not yet over. Hotels are still being constructed. An ambitious plan is 'Puerto Cancún', which implies construction of a marina and luxurious hotels and apartments close to Puerto Juárez (see the map in Appendix B.2). To enable this growth it is considered necessary to increase the beach width between Punta Nizuc and Punta Cancún, which suffered structural erosion over the past 15 years. This project is discussed in the following paragraph.

## 2.3 Description of the 'Cancún Beach Rehabilitation Project'

### 2.3.1 Historic developments of Cancún Beach

While Cancún was going through a period of stable growth, hurricane Gilberto struck the northern part of the Yucatán Peninsula on September 14, 1988, causing heavy damage on the entire peninsula and in the Zona Hotelera of Cancún. Part of this damage was the severe erosion of the 12 km beach between Punta Nizuc and Punta Cancún in the Zona Hotelera, which led to a decrease of beach width of 8 m between 1985 and 1989.

Worried about the influence this could have on the tourism revenues, FONATUR asked UNAM (Universidad Nacional Autónoma de México) to conduct a study of the expected behaviour of the beach in the area. In 1990 UNAM concluded that autonomous recovery would occur in about 16 years [\* , 2000a]. It was decided to take no further action.

However, structural erosion took place in the decade after Gilberto. This was combined with a growing need for beach because of increasing tourist numbers. Some hoteliers decided to construct structures to protect their beaches against storms and to stimulate accretion of sand. They used geotubes or geocontainers. However, these structures weren't successful [\* , 2000a] and an integral investigation was considered necessary, because occupation rates of the hotels were on the down-grade.

### 2.3.2 Cancún Beach Rehabilitation Project

In 2000 the possibilities were investigated to regenerate and protect the beach on the 12 km long coastal stretch between Punta Nizuc in the south and Punta Cancún in the north. This area is further referred to as the project area. The reasons for the Cancún Beach Rehabilitation Project are the decrease in tourism revenues and the large risk induced by hurricanes.

#### Goal of the study

The goal of the study is summarized as follows:

To present the best technical, economical and environmental solution for the beach restoration with the aim to:

- Raise tourist competitiveness.
- Offer protection against extreme conditions at the hotels and infrastructure located in the marine frontage.



### Activities during the study

Between February 2000 and August 2001 the following activities were carried out:

- Bathymetric surveys.
- Measurements of currents, waves and water levels.
- Geotechnical exploration of the project area and surroundings.
- Diagnosis of the actual situation.
- Creating and evaluating different engineering solutions.
- Economical evaluation of the engineering solutions.
- Creating a detailed design and specifications of the proposed solution.

### Proposed solution

The proposed solution for the beach rehabilitation is a beach fill of approximately two million m<sup>3</sup> and the construction of closure structures at the ends of the project area. The nourishment probably has to be carried out on a periodic basis. Two possible borrow areas are considered, indicated on the maps in Appendix B.2:

- Borrow area I – Puerto Juárez with an average  $d_{50}$  of 0.27 mm.
- Borrow area II – Punta Sam with an average  $d_{50}$  of 0.42 mm.

### Planned investigations

Because of the large environmental impact of the proposed borrow locations, a new exploration will be conducted to find other borrow areas. Also more detailed modelling will be used to determine the behaviour and lifetime of the proposed beach fill. The investigation carried out in this thesis will be part of this study. The objective of this thesis is discussed in the following paragraph.

## 2.4 Objective of the thesis study

### 2.4.1 Introduction

As indicated in the preceding paragraph more knowledge has to be obtained about the behaviour of the proposed beach fill. This behaviour can be split in three processes as indicated in Figure 2-3. For further explanation of these terms is referred to Paragraph 4.2.4.

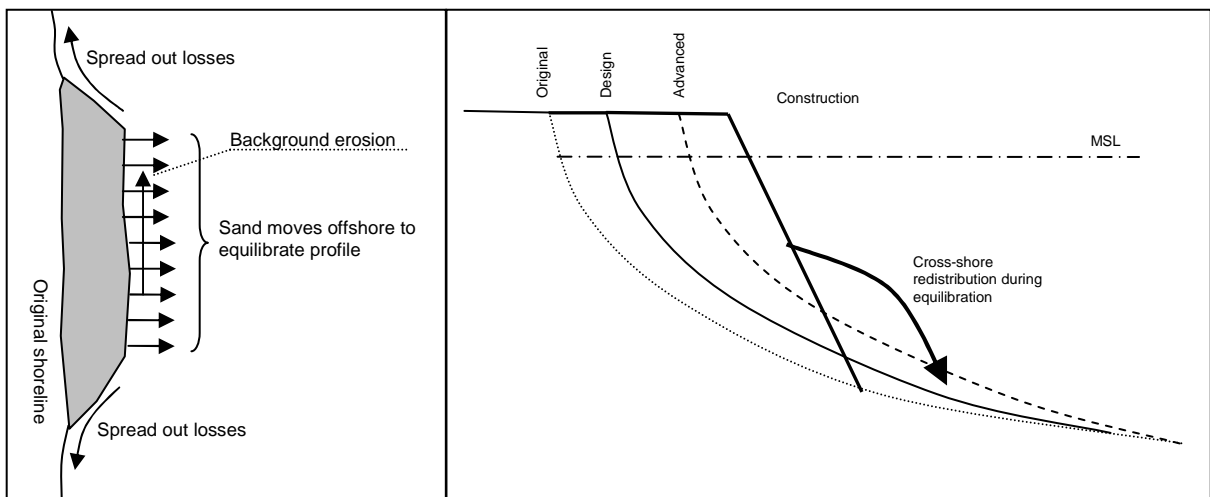


Figure 2-3: Plan view (left) and cross-section view (right) of the three erosion processes associated with beach nourishment: equilibration, spread-out losses and background erosion. In the right figure the four relevant profiles are indicated: construction, advanced, design and original profile.

## 2.4.2 Definition

This thesis will only consider the cross-shore processes associated with beach nourishment design, being the equilibration and storm behaviour.

### Equilibration

Part of this cross-shore behaviour is the transformation process between the construction profile and the equilibrium profile. This process is called equilibration and takes place in the first months to years after construction [NRC, 1995]. Normally spoken, the construction profile is steeper than the equilibrium profile and the shoreline will move towards land during the equilibration. The magnitude of this movement depends amongst others on the grain size used in the fill. The shift of the shoreline is of the utmost importance to determine the project revenues and the remaining protection against hurricanes. Therefore there is a need to determine the shift of the shoreline due to the equilibration process and the time scale in which this occurs. This has to be done for different grain size distributions, as different borrow areas are considered in the project. Various design methods have been defined to determine the necessary fill volume for a certain required beach width after equilibration (Dean [1974], James [1975], USACE [1994] and Dean [2002]). These design methods are equilibrium models and are described in Paragraph 4.6. However, these methods aren't always satisfactory. A more sophisticated approach by means of cross-shore, process-based numerical modelling is therefore desired. The software package Unibest-TC of WL | Delft Hydraulics [1999] is chosen for this purpose (see Paragraph 2.4.4).

### Storm behaviour

Another important aspect in beach nourishment design is the storm response of the profile. A wide beach with a high berm acts like a stockpile of sand, which satisfies the "sand demand" during storm events and can reduce damage to adjacent infrastructure significantly. The (cross-shore) storm behaviour of the equilibrated profile will be determined by process-based numerical modelling with Unibest-TC and according to the method of Vellinga [1986]. Other modelling concepts haven't been considered due to limited time.

This leads to the objective described in the following paragraph.

## 2.4.3 Objective

The objective consists of a scientific part and a practical part. To fulfil the objective a number of sub questions has to be answered.

### Main scientific objective

Compare the results (i.e. shoreline advancement, profile shape) of the equilibrium design methods for the equilibration of Dean [1974], James [1975], USACE [1994] and Dean [2002] with the results of cross-shore process-based numerical modelling of the equilibration in Unibest-TC.

- How do these approaches relate to each other?
- How can the differences in results be explained?
- Which method is preferred?

### Main practical objectives

- What is the shoreline advancement as a function of the fill volume (considering three fill grain size distributions) for the Cancún Beach Rehabilitation Project?
- What is the expected time scale of the equilibration?
- What is the remaining beach width and profile shape after a the occurrence of a design storm on the equilibrated nourished profile?

### Sub questions

1. What is the magnitude of the coastal erosion in the project area in the current situation and which coastal processes have caused this state of erosion? What is the cross-shore equilibrium condition of the beach?

2. What are the theoretical backgrounds of the equilibration design methods (Dean [1974], James [1975], USACE [1994] and Dean [2002])? What are their results regarding the shoreline advancement and profile shape after equilibration?
3. What is the profile shape and shoreline advancement after the equilibration according to process-based cross-shore modelling with Unibest-TC? What is the time scale of the equilibration?
4. What is the profile shape and shoreline retreat after a design storm occurred on an equilibrated nourished profile according to process-based cross-shore modelling with Unibest-TC and according to Vellinga [1986]? What is the influence of the grain size on the post-storm profile shape and shoreline position?

#### **Considered fill sediments**

Three fill sediment distributions will be considered in this thesis, based on two real borrow areas and a fictitious borrow area:

- Borrow area I – Puerto Juárez with an average  $d_{50}$  of 0.27 mm.
- Borrow area II – Punta Sam with an average  $d_{50}$  of 0.42 mm.
- Fictitious borrow area – sediments equal to native with a  $d_{50}$  of 0.33 mm.

In the next paragraph the available tools to fulfil the objective are discussed after which the approach of the thesis study is presented in Paragraph 2.4.5.

#### **2.4.4 Available tools**

Various tools are necessary to fulfil the objective described in Paragraph 2.4.3. In addition, data of the coastal system is required.

##### **Data of the coastal system**

Data of the coastal system is necessary for two reasons:

1. An analysis of the current situation and coastal processes has to be made.
2. The behaviour (equilibration and storm response) of the beach fill has to be modelled.

For both activities information is needed regarding the following:

- The boundary conditions in the project area (waves, wind, currents, bathymetry, grain size).
- History of human interventions in the coastal system.
- Grain size distributions of the fill sediments of the possible borrow areas.

These boundary conditions and human interventions in the project area will be discussed in Chapter 3. Summarizing it can be said that the behaviour of the considered coastal stretch is very complex and that the available data is characterized by lack of temporal resolution, accuracy and reliability.

##### **Available design methods for the equilibration**

Various design methods are available to account for the equilibration of the beach fill:

- Using equilibrium models.
- Using process-based numerical modelling.
- Using physical models.
- Using intuitive methods; the fill behaviour isn't predicted in detail, it is assumed that placement of sediment in the active profile is beneficiary to the coast.

Only the equilibrium models and the process-based modelling will be considered in this thesis, because:

- Time is limited; besides the practical difficulties, physical modelling is very time-consuming.
- Design results should be reproducible, transferable and accurate, which is certainly not the case for intuitive methods.

### **Selection of equilibrium models**

The equilibrium models of Dean [1974], James [1975], USACE [1994] and Dean [2002] have been chosen because:

- Their use is wide spread; James [1975] and the USACE [1994] are recommended in the Shore Protection Manual [USACE, 1984] and the Coastal Engineering Manual [2002] of the USACE.
- The varying implementation of relevant model issues; the USACE [1994] is based on equilibrium profile shapes, while the methods of Dean [1974] and James [1975] consider equilibrium grain size distributions.
- They are interrelated; Dean [2002] is a combination of Dean [1974] and USACE [1994]

These methods will be described in Chapter 4.

### **Selection of the software package for the numerical modelling**

There are various software packages available which model the cross-shore behaviour of sandy coasts based on the physical processes originating the morphology, such as:

- LITCROSS (Danish Hydraulic Institute)
- SEDITEL (Laboratoire National d'Hydraulique)
- Delft3D (WL | Delft Hydraulics)
- Unibest-TC (WL | Delft Hydraulics)

The Unibest-TC software package has been used in this thesis, based on availability and on suitability for the questions addressed in Paragraph 2.4.3. Unibest-TC is suitable to model medium-term cross-shore morphodynamics as they occur after beach nourishment. Furthermore, Unibest-TC uses state-of-the-art model formulations and is still further improved.

### **Modelling of the storm behaviour**

The storm response of the nourished beach will be determined using Unibest-TC because of convenience; a calibrated model is yet available from the modelling of the equilibration. Considering other models such as DUROSTA [Steetzel, 1990] could certainly be useful, but was precluded by limited time.

The method of Vellinga [1986] has been used to determine the storm response, since this method is well-known and based on extensive physical model tests.

## **2.4.5 Approach**

The approach of this study is summarized in the flow chart in Figure 2-4.



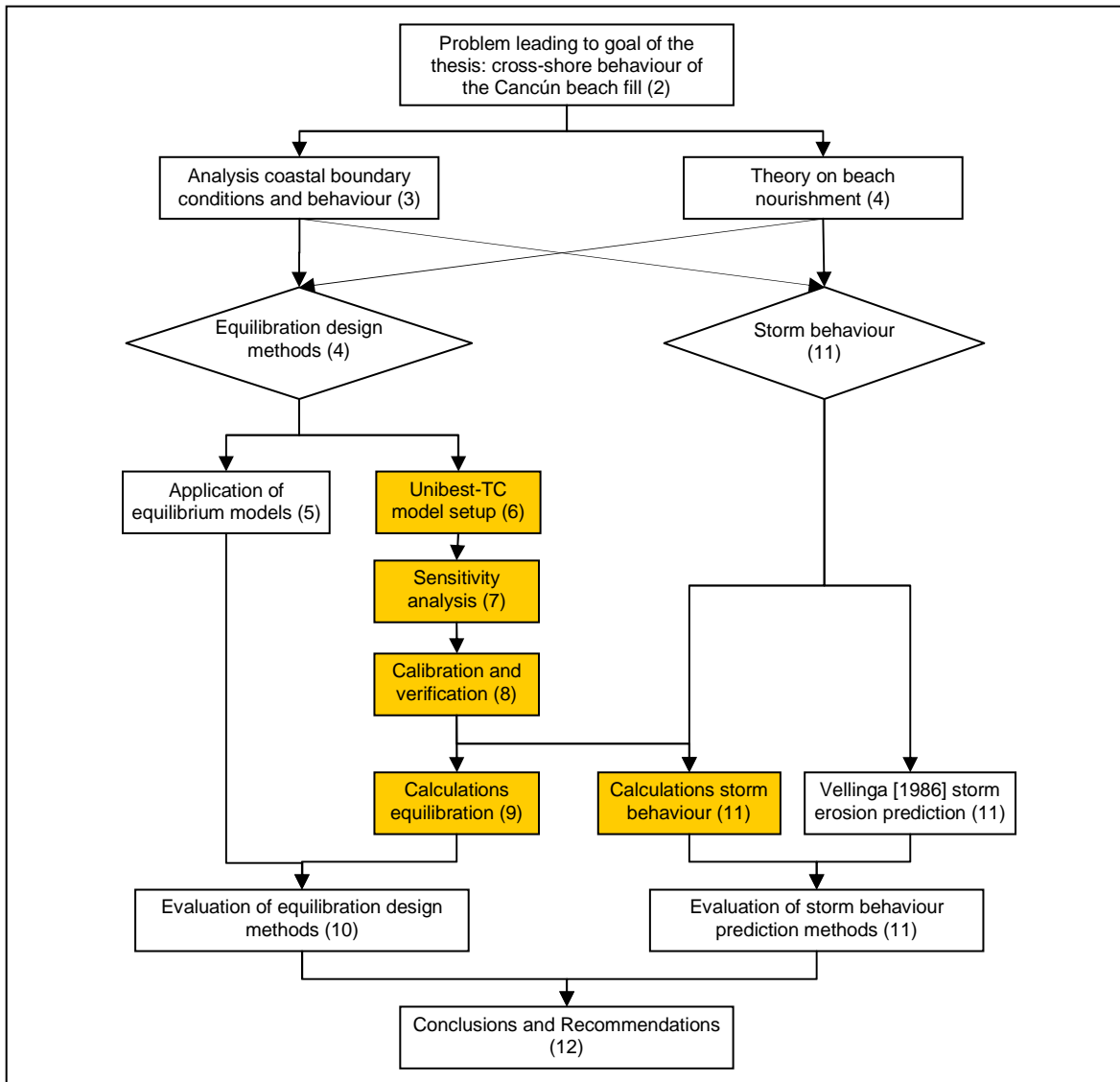


Figure 2-4: Flow chart of the approach of the thesis study. The numbers between parentheses represent the chapters in which the activities are described. The orange coloured boxes represent modelling in Unibest-TC.

First an analysis of the coastal behaviour (Chapter 3) has to be carried out, because an (at least qualitative) understanding of the coastal system is necessary to be able to model its behaviour. Furthermore, insight is necessary in the equilibrium state and boundary conditions of the beach.

In Chapter 4 the theoretical background of beach nourishments is discussed, with emphasis on cross-shore modelling concepts regarding the equilibration. Subsequently, these equilibrium models for the equilibration are applied in Chapter 5.

The Unibest-TC model is discussed in Chapter 6, after which a sensitivity analysis is carried out for the most important input parameters and boundary conditions of the Unibest-TC model (Chapter 7). The model is calibrated and verified in Chapter 8 and is used to model the equilibration in Chapter 9.

In Chapter 10 the modelling results of the equilibration according to the equilibrium models of Dean [1974], James [1975], USACE [1994] and Dean [2002] and the Unibest-TC model are compared and evaluated.

In Chapter 11 the storm behaviour is modelled with the dune erosion prediction model of Vellinga [1986] and with the calibrated Unibest-TC model after which the results are evaluated.

Finally, conclusions are drawn and recommendations are made in Chapter 12, answering the questions posed in Paragraph 2.4.3.



## 3 ANALYSIS OF THE COASTAL BEHAVIOUR

### 3.1 Introduction

The goal of this chapter is to describe the boundary conditions, the current situation in the project area and the behaviour of the coastal system. The results will be used to define the model input in the following chapters.

In Paragraph 3.2 the boundary conditions in the project area will be described, after which the state of the actual beach will be discussed in Paragraph 3.3. Subsequently, in Paragraph 3.4 a hypothesis of the system behaviour will be defined. Finally, conclusions are drawn in Paragraph 3.5.

### 3.2 Boundary conditions

#### 3.2.1 Introduction

In this paragraph the boundary conditions in the project area between Punta Cancún and Punta Nizuc (see maps in Appendix B.2) will be discussed. These consist of bathymetry, sediment characteristics, wind speed and direction, waves, water level variations and currents.

#### 3.2.2 Bathymetry

##### **Bathymetry east of the Yucatán Peninsula**

The Yucatán Peninsula is a flat piece of land, separating the deep basins of the Gulf of Mexico and the Caribbean Sea (see Figure 2-1). While the peninsula is relatively flat, the offshore bathymetry to the East is characterised by a narrow continental shelf and steep slopes to 4500 m water depth. To the north, the continental shelf extends some 200 km into the sea, before dropping into the Gulf Basin. The narrow strait between the main land and Cozumel reaches depths up to 500 m. The entire east coast of the peninsula is characterized by shore parallel coral reefs.

##### **Bathymetry in the project area**

Rocky Punta Cancún and Punta Nizuc protrude further into the sea than the 12 km stretch of sandy beach between them. The beach is characterised by more or less shore parallel depth contours and an average slope of about 1:40 to the 16 m depth contour. Seasonal sandbars occur occasionally. The width of the beach varies between 0 and 30 m, depending on the season and the location. The bathymetry at Punta Cancún and Punta Nizuc is more complex, due to their rocky character. See Appendix B.2.

The bathymetry between Punta Cancún and Punta Nizuc has been measured various times [\*], 2000a, 2000c and 2002]:

- 1985
- 1989
- February 2000
- June 2000
- March 2001

Only the results from the 2000 and 2001 surveys are accurate and to sufficient depth (-15 m). Typical cross-shore profiles can be found in Appendix B.3.

### Chainage system

A chainage system was introduced along the project area. Punta Cancún is at chainage 0+000 m, while Punta Nizuc is at chainage 12+600 m.

### 3.2.3 Sediment characteristics

The white-coloured sediments have a median grain size  $d_{50}$  between 0.2 and 0.5 mm and can be classified as sand of a mainly biological origin, created by the erosion of coral reefs. Another sediment source is the erosion of the limestone base of the Yucatán Peninsula. Both mechanisms are slow-acting [Editorial Verás, 2002].

The sediment characteristics in the project area have been measured various times:

- July 1989
- September 1989
- February 2000
- March 2001

The results determined in March 2001 are most extensive and reliable and are given in Appendix B.4 [\* , 2002], which includes the sediment characteristics of the proposed borrow areas (see Paragraph 2.3.2 and Appendix B.2).

### Thickness of the sediment layers

In May 2001 a diver with a jet tube determined the thickness of the sediment layers in the project area, which is visualized in Appendix B.4.3. It can be seen that the thickness decreases with the water depth.

### 3.2.4 Winds

Wind is an important phenomenon, because it can cause currents, water level differences and aeolian sand transport on the dry beach. During hurricanes, the wind speeds can reach values up to 60 m/s.

The dominant wind direction is from east to south east. However, in the second half of the year so-called 'nortes' occur. These are relatively strong winds from the north and north east, which can last for several days.

In Appendix B.5 detailed information about the wind speed and direction is given, based on satellite measurements acquired from [www.waveclimate.com](http://www.waveclimate.com).

### 3.2.5 Ordinary wave conditions

The ordinary wave climate consists of normal sea and swell. Possible sources are measurements with buoys and wave atlases (composed of visual observations and satellite measurements). Unfortunately, the results of buoy measurements of UNAM (1989-1990) were lost in the course of time, while the results of the buoys placed by \* (2000-2001) have significant imperfections. Therefore, a wave climate based on satellite measurements from [www.waveclimate.com](http://www.waveclimate.com) is used throughout this thesis. Appendix E.3.3 describes this wave climate, which is summarized in Table 3-1.

Table 3-1:

Monthly wave parameters based on 10 years of satellite measurements in the area near Cancún. Direction convention: coming from north = 0°, counting positive clockwise.

Month	$H_s$ [m]	$T_p$ [s]	$\theta$ [°]
January	1.5	6.8	93
February	1.5	6.8	94
March	1.6	6.5	101
April	1.3	6.5	103
May	1.2	6.5	101
June	1.2	6.8	107
July	1.2	6.8	108
August	1.1	6.6	108
September	1.2	6.7	95
October	1.4	6.7	94
November	1.5	6.7	94
December	1.7	6.8	94
<b>Average</b>	<b>1.4</b>	<b>6.7</b>	<b>100</b>

### 3.2.6 Hurricane wave conditions

#### Introduction

The region of Cancún is subject to hurricanes in the entire period between May and December, when the water in the Atlantic Ocean and Caribbean is warm enough to generate these weather systems.

Hurricanes consist of large wind fields, rotating around the low-pressure centre, anticlockwise on the Northern Hemisphere. These winds sometimes exceed 200 km/hr, causing extremely high waves with significant wave heights up to 15 m and high storm surges. In hurricanes, fetch areas in which wind speed and direction remain reasonably constant are usually small. Therefore a typical wave spectrum in front or to either side of a hurricane has multiple peaks. However, close to the centre of the hurricane very large single peaked spectra can occur as well [USACE, 1984].

The influence of a hurricane on the waves at the project area depends largely on the path of these highly dynamic weather systems, as this path determines the direction, fetch and duration of the wind field for a certain location.

#### Hurricanes striking the project area

Hurricanes or tropical storms have struck the Atlantic and Caribbean area 8.8 times per year on average over the period between 1886 and 2002 [\* , internal communication, 2003]. Table 3-2 summarises the tropical storms and hurricanes that affected the project area between 1886 and 2002.

Table 3-2: Summary of hurricanes and tropical storms that affected the project area with wind speeds corresponding to their class [\* , internal communication, 2003].

Monthly resume of tropical cyclones, which affected Punta Cancún in the period 1886-2002.							
Cyclone type	May	Jun	Jul	Aug	Sep	Oct	Nov
Depression	0	0	0	0	3	0	0
Storm	1	7	1	6	4	3	1
Hurricane	0	4	4	14	17	12	1
<b>Total</b>	<b>1</b>	<b>11</b>	<b>5</b>	<b>20</b>	<b>24</b>	<b>15</b>	<b>2</b>

It can be concluded that the project area has a probability of 0.44 per year to be struck by hurricane wind speeds (> 133 km/h).

#### Hurricane wave climate

The probability distribution of the extreme wave heights and the duration of these wave conditions are of large interest for the behaviour of the beach and has been investigated by \* [2000]. The wind fields of 8 hurricanes were used for a hindcast of the wave conditions. The results for hurricane Gilberto (the heaviest recorded hurricane in the project area, 1988) are an  $H_s$  of 13.2 m and a  $T_s$  13.4 s with a direction from the north east on deep water [\* , 2000b]. This wave height is exceeded once in 31 years according to Figure 3-1.

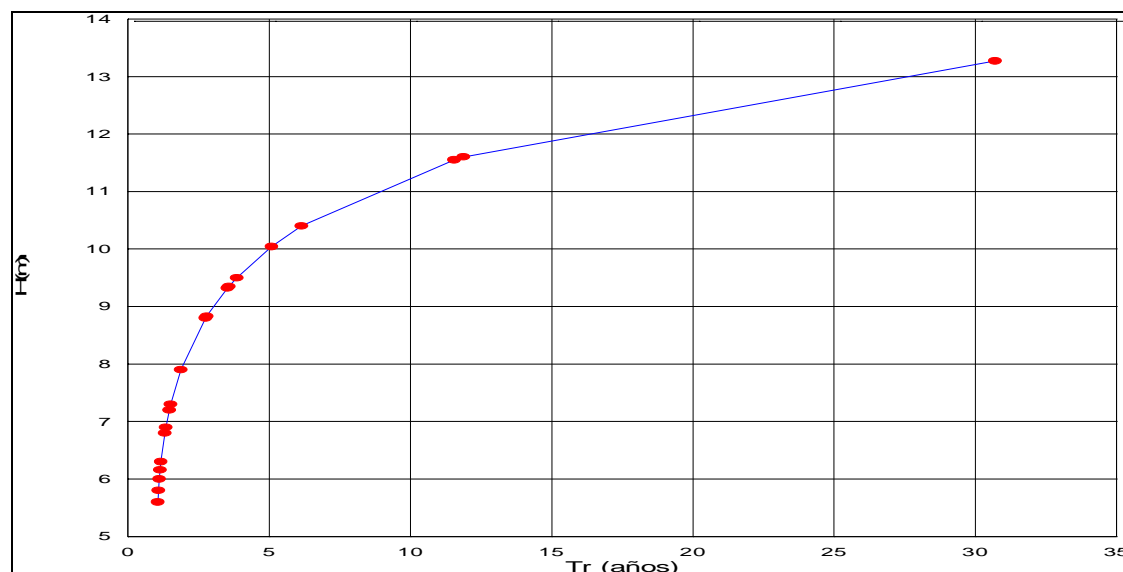


Figure 3-1: Return period ( $T_r$ , in years) of extreme wave heights ( $H_s$ ) caused by hurricanes in the project area [<sup>\*</sup>, 2000a].

The question arises if the number of hurricanes isn't too small for a good analysis.

### 3.2.7 Water level variations

The short-term water level variations in the project area are determined by five phenomena: the astronomical tide, barometric tide, wind stress tide, Coriolis tide and wave set-up.

During normal conditions the water level variations around MSL in the project area are small. The astronomical tide is of the mixed, predominant semi-diurnal type and has a mean tidal range of about 0.20 m [Secretaría de Marina, 2002]. The Coriolis tide does not induce significant water level variations, since the shore parallel oceanic current is practically stationary. Variation in wind, wave and pressure conditions can cause some water level fluctuations during normal conditions.

However, water level variations can be significant during hurricanes. Wind, wave and air pressure reach extreme values and cause large wind and wave set-up and an extraordinary barometric tide.

For example, eyewitnesses stated that the water level during hurricane Gilberto (1988, central pressure 880 mb,  $H_s$  of 13 m) was in the order of MSL +5 m [<sup>\*</sup>, 2003, personal communication]. Hydrodynamic modelling [Bautista et al., 2003] suggests a storm surge (wave set-up not included) of MSL +3 m. The wave set-up at the water line was approximately 2 to 3 m.

### 3.2.8 Currents

The (longshore) currents in the project area consist of different components: the oceanic current, tidal currents, wave-induced currents and currents caused by pressure differences and wind.

Tidal currents are very small, since the astronomical tide has negligible amplitude. The oceanic current reaches values of approximately 2 knots at deep water [Secretaría de Marina, 1999]. Neither the distribution of the current velocity over the depth, nor the magnitude of this current in shallow water is known.

Wave-induced longshore currents are caused by oblique incident waves and by difference in wave set-up along the coastline, caused by varying wave characteristics and bathymetry. These currents occur in or near the breaker zone with velocities in the order of 2 knots. Wind shear stress and longshore differences in wind set-up and barometric tide cause currents too.

**Measurements of currents**

\* [2000] performed measurements of the current pattern in the breaker zone between February 2000 and March 2001 at the locations indicated in Figure 3-2. The results of these measurements are summarized in Table 3-3.

Figure 3-2:

Location of the measurements of the current, wave and water level conditions in the project area [\* , 2002].

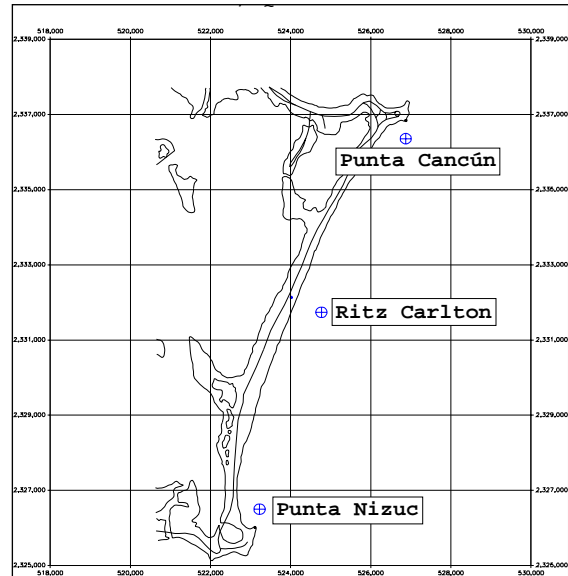


Table 3-3: Summary of the results of the measurements performed \*. Comment: the measurements weren't performed continuously, due to failure and maintenance of the equipment. This is especially the case for the Ritz Carlton location [\* , 2002].

Location	Date measurement	Water depth	Depth measurement	Current velocity	Current direction [degrees]
Punta Cancún	08/02/00 – 06/05/01	5 m	MSL -3.3 m	Mean value 27 cm/s, values up to 81 cm/s occurred	73% of the time the current is directed to the ENE
Ritz Carlton	23/03/00 – 04/04/01	10 m	MSL -8.3 m	Mean value of 15 cm/s, values up to 63 cm/s occurred	Almost always shore parallel (NE / SE), equally distributed between these directions
Punta Nizuc	19/06/00 – 03/05/01	5 m	MSL -3.7 m	Mean value of 8 cm/s, values up to 53 cm/s occurred	Almost always (75%) directed to southeastern directions

From this data it can be concluded that the oceanic current isn't significant in the breaker zone. On the other hand, measurements at Xcaret 60 km south of the project area [\* , 1983] show that the offshore current has a significant influence on the current pattern in the breaker zone.

**3.2.9 Conclusions**

There is a considerable amount of qualitative information available on the boundary conditions. However, there is a lack of quantitative information during a longer period of time, especially of the bathymetry, wave conditions and granulometry. This poses serious limitations on the application of the design methods and process-based modelling with Unibest-TC, which will be discussed in the following chapters.

### 3.3 Diagnosis of the actual situation

#### 3.3.1 Closure depth

The concept of closure depth is discussed in Appendix A.5.1 and is defined as follows: 'The depth of closure ( $h_c$ ) for a given or characteristic time interval is the most landward depth seaward of which there is no significant change in bottom elevation and no significant net sediment transport between the nearshore and the offshore' [Kraus et al., 1998].

The closure depth ( $h_c$ ) in the project area can be determined based on:

1. A visual estimation of the closure depth out of measured bottom profiles.
2. Relations derived by Hallermeier and Birkemeijer (Appendix A.5.1).
3. Numerical modelling with Unibest-TC.

##### Ad 1

Observing the measured profiles of February and June 2000 and March 2001 for the centre of the project area (chainage 5100 to 7000), one can conclude that no significant change in bottom elevation occurs below the following depths:

Period	Closure depth
February to June 2000	-4 m
June 2000 to March 2001	-6 m

These values should be interpreted with care; they are based only on 3 bathymetric surveys. Furthermore it isn't clear whether the bottom changes are predominantly caused by longshore or by cross-shore transport gradients.

##### Ad 2

The relation derived by Hallermeier [1981] reads:

$$h_c = 2.28H_e - 68.5 \left( \frac{H_e^2}{gT_e^2} \right) \quad \text{with} \quad H_e = \bar{H} + 5.6\sigma_H \quad (3.1)$$

Where:	$h_c$	closure depth	[m]
	$H_e$	effective significant wave height, exceeded only 12 hrs per year	[m]
	$T_e$	effective mean wave period, corresponding with $H_e$	[s]
	$\bar{H}$	annual mean significant wave height	[m]
	$\sigma_H$	standard deviation of significant wave height	[m]

Which was approximated later by Birkemeier [1985] as:

$$h_c = 1.57H_e \quad (3.2)$$

These relations demand knowledge of  $H_e$  and  $T_e$ . These have been determined using wave data from [www.waveclimate.com](http://www.waveclimate.com). In Figure 3-3 the results of an extreme value analysis of  $H_s$  is shown for an area with its centre at 20° 00'N, 85° 00'W and a size of 400 x 400 km.



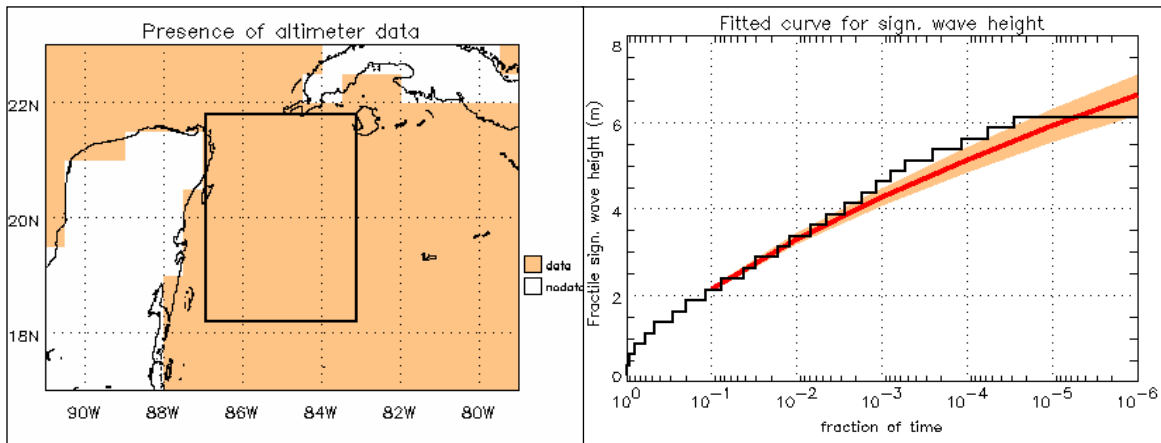


Figure 3-3: Extreme value analysis for the significant wave height  $H_s$  (right panel) and the area where it has been performed (left area) [www.waveclimate.com].

The  $H_e$  used by Hallermeier is exceeded 12 hrs a year (0.137% of time). According to Figure 3-3  $H_e$  is 4.1 m. One finds:  $T_{z,e} = 8.4$  s using the following fitted relation between  $H_s$  and  $T_z$  (see Appendix E.3.3):

$$T_z = 0.73H_s + 5.37 \quad (3.3)$$

This leads to the following values of  $h_c$ :

Method	$h_c$ [m]
Hallermeier	7.68
Birkemeier	6.44

### Ad 3

Cross-shore process-based numerical modelling of the beach fill equilibration with Unibest-TC (see Chapter 9) indicates a closure depth of 7.5 m.

### Conclusion

The closure depth has a value of 6 - 7.7 m. The uncertainty in this value is quite high. For the remainder of this report a value of 7.5 m has been assumed, in accordance with the modelling with Unibest-TC.

## 3.3.2 Shore and shoreline variability

### Introduction

Almost every beach is subject to periodical erosion and accretion. This variability consists of a summation of responses of the morphological system on different time scales as the natural and human forcing occurs at varying time scales too [Stive et. al., 2002]. Within this variability general trends can occur for a certain time span, but extrapolating trend lines is precarious.

### Data on shore variability

Because of the rocky base of the project area and the presence of some Mayan ruins (1200 A.D.) 20 m from the actual shoreline, it can be concluded that the shoreline was located seaward ever since.

The development of the shoreline position between 1985 and 2001 is visualized in Appendix B.6 and can be summarized as follows:

- The average beach width decreased from 30 to 25 m between 1985 and 1989. This shoreline retreat is attributed to hurricane Gilberto in 1988.
- After hurricane Gilberto serious retreat of the shoreline occurred, but close to Punta Nizuc and Punta Cancún accretion took place due to longshore transport

gradients. This statement is confirmed by a hindcast of the current pattern during hurricane Gilberto by Bautista et al. [2003].

- Between 1989 and February 2000 the shoreline retreated even further with 14 m.
- Between February 2000 and March 2001 accretion occurred, resulting in an increase of beach width of 14 m. This can be explained by the extreme quiet wave conditions in this period.
- Between February and June 2000 the shoreline shifted 10 m seaward, caused by seasonal variations in wave conditions. The bar present in the February profiles has moved shoreward and is more pronounced

### Conclusions

It can be concluded that the general trend between 1985 and 2000 has been one of serious shoreline retreat with the major part of this retreat occurring between 1989 and 2000. Between 2000 and 2001 accretion occurred, probably due to extremely quiet wave conditions. Hurricane Gilberto (1988) caused strong erosion in the centre area and strong accretion on the outer ends of the project area. The accreted volumes at the outer ends eroded in the decade after Gilberto. Seasonal variations in shoreline position are significant.

Between 1985 and 1989 the beach eroded above the 6 m depth contour and accreted below this line. Between 1989 and 2000 erosion occurred in the entire profile, with the emphasis on the area between -6 and -12 m. In general, the profile shape hasn't changed significantly between 1985 and 2000.

### 3.3.3 Cross-shore equilibrium analysis

#### Introduction

In this paragraph the measured cross-shore beach profiles on Cancún Beach are compared with a theoretical beach equilibrium profile. The results will be used to apply the equilibration design methods discussed in Paragraph 4.6.

The concept of cross-shore equilibrium profile is the result of a balance of constructive and destructive forces acting on the beach profile. In nature, the equilibrium profile is considered to be dynamic, since the boundary conditions are continually changing in time. In Appendix A.5 different kinds of equilibrium profiles are discussed. Here, the equilibrium profile of Dean [1974] is used, expressed in Equation (3.4). This equation is based on a uniform dissipation of wave energy per unit water volume.

$$h(y) = A(d)y^{2/3} \quad (3.4)$$

Where:	h	depth below MSL	[m]
	y	coordinate perpendicular to the shore, positive in seaward direction, with the origin at the shoreline	[m]
	A(d)	profile scale parameter, a function of the grain size	[m <sup>1/3</sup> ]

Equation (3.4) has been confirmed empirically by (among others) Bruun [1954] and Dean [1977].

#### Comparison with actual beach profiles

A least-square fit of Equation (3.4) to the beach profiles in Cancún has been made. This is done for the centre of the project area (chainage 6+100 to 6+900), since this is the area which will be used in this thesis to assess the equilibration design methods. Profiles measured in June 2000 are used, because this is the planned construction month of the beach fill. The fit is made from MSL to MSL -7.5 m, since this is the closure depth according to the Unibest-TC model.

Averaging the least-square fits of the profile scale parameter  $A$  leads to an average  $A$  of 0.175 m<sup>1/3</sup> for chainage 6+100 to 6+900. The recommended  $A$  for the native grain size of 0.33 mm is 0.131 m<sup>1/3</sup> [Dean, 1977]. So Cancún Beach is significantly steeper than 'recommended'.

A plot of Equation (3.4) with the fitted profile scale parameter can be found in Appendix B.3.

### 3.3.4 Longshore transport gradient

A longshore transport gradient can cause significant shore variability. The average longshore transport gradient can be calculated using a sand balance as derived in Appendix A.3. To do so, accurate measurements of cross-shore profiles at various points in time are necessary. Unfortunately, accurate bathymetry measurements were performed only three times in a 1.5-year period, which is not enough for a sensible determination of the longshore transport gradient.

A qualitative hypothesis of the longshore transport gradient is discussed in Paragraph 3.4.1.

## 3.4 Hypothesis of the system behaviour

### 3.4.1 Original behaviour of the system

#### Longshore transport

Longshore transport plays a significant role in the behaviour of the system, as well in the breaker zone as on deeper water.

The extension of the oceanic current into shallower water is very uncertain. When a parabolic velocity profile is assumed, it can be concluded that this longshore current combined with wave stirring ( $H_{rms} = 1$  m) can move the present sediments at depths smaller than 12 m. The presence of strong gradients in this transport is likely close to rocky outcrops, which modify the current pattern. This hypothesis is supported by the presence of rough sediments at depths of approximately 10 m close to Punta Cancún and Punta Nizuc. Support is also given by a smaller thickness or absence of the sediment at deeper water.

In shallow water the current depends strongly on the wave and wind direction. The waves and wind are mostly from the south east to east. This suggests an average longshore transport from north to south in the breaker zone. Currents because of variable wave set up also occur, especially close to Punta Nizuc and Punta Cancún as is confirmed by current measurements.

In the sketches in Appendix B.7 a qualitative overview of the current and transport patterns in the breaker zone during southeastern and eastern wave and wind directions is given. It can be concluded that during the governing eastern and south eastern wave directions, erosion occurs at the outer ends of the project area.

The occurrence of a large-scale rip current at Punta Nizuc is likely. This can prevent the direct import from sand from the south, which makes that sand import has to occur via deeper water.

#### Cross-shore transport

Cross-shore transport is important, since it causes:

1. Shore or shoreline variability due to seasonal variations in wave climate and variability due to extreme events.
2. Exchange between the breaker zone longshore current regime and the deeper water longshore current regime.

The latter can cause incomplete recovery after storms, because the sediment deposited on deeper water is transported northwards by the offshore current.

#### Presence of dunes

No quantitative data is present regarding the situation between Punta Nizuc and Punta Cancún before the construction of hotels started in 1970. However, locals state that the entire stretch consisted of sand dunes (up to 20 m in height), with rock beneath them. These dunes were very strongly vegetated. A sandy beach was present, with varying width.

The dunes acted like a buffer: accumulating sand during normal conditions by the dense vegetation and releasing this sand during extreme conditions and thus 'satisfying' the sand demand from the sea. Furthermore, the rocky sub layer acted as a fixed limit during periods of severe cross-shore or longshore erosion.

### Wind transport

Wind transport plays an important role. The presence of fine sediments in Laguna Nichupté and the sheltered south west corner of Bahía de Mujeres indicate a significant wind transport.

### 3.4.2 Human intervention in the coastal system

The natural situation, supposed to be in a dynamic equilibrium was significantly disturbed with the construction of the first hotels in 1970. Mankind has made some significant changes in the natural environment:

- Removing sand from the dunes for land reclamation in Laguna Nichupté.
- Removing dune vegetation and replacing it with hotels and greens.
- Building sea walls and hotels and thus creating a fixed boundary instead of a flexible one.
- Systematically removing sargaso (sea grass) washed on the shoreline, because this 'spoils' the white colour of the beach.

A sand buffer, formed by nature in centuries, has been significantly decreased in a few decades by human intervention, which has led to a larger vulnerability to natural forces. This could have caused the following changes in system behaviour:

- Increased wind transport due to removal of the dense dune vegetation.
- Increased erosion of the beach during storms, due to a smaller sand buffer.
- Less accretion at the shoreline, because of the removal of sargaso.
- Less accretion on the dry beach and dunes, because of the removal of vegetation.

These alterations in the natural behaviour of the system lead to a trend of structural erosion, imposed on the normal variability of the beach.

### 3.4.3 Hypothesis system behaviour

It can be assumed that the project area was in a dynamic equilibrium in the past, but the last 18 years are characterised by erosion.

There are three possible explanations for this trend:

1. Caused by structural erosion caused by human intervention (Figure 3-4).
2. Entirely caused by natural middle term (decades) variability (Figure 3-5).
3. A combination of natural variability and structural erosion caused by human intervention (Figure 3-5).

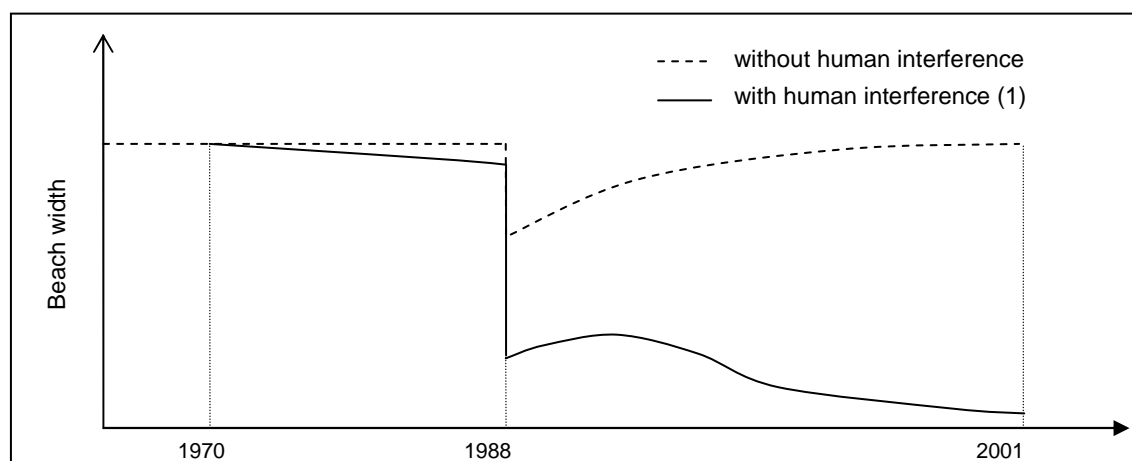


Figure 3-4: Qualitative impression of the shoreline variability according to explanation 1.

A structural erosion trend superimposed on the natural variation of the shoreline results in the continuous line in Figure 3-4. Because of the structural erosion, no full recovery occurred after the extreme erosion caused by Gilberto. Without this structural erosion the

beach probably would have recovered (dashed line). Because of the construction of sea walls the shoreline recession during Gilberto was increased.

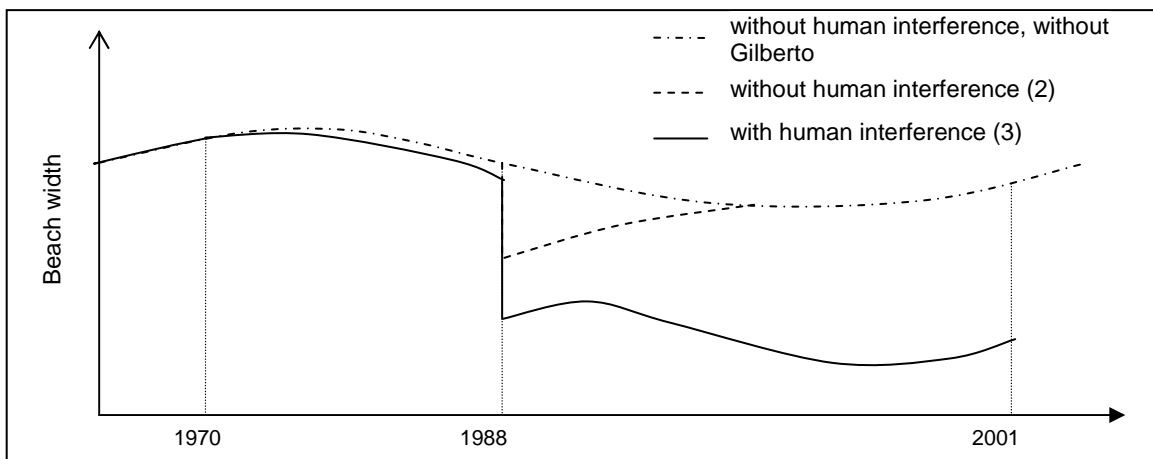


Figure 3-5: Qualitative impression of the shoreline variability according to explanation 2 and 3.

Some middle-term time scale (decades) variability is present with erosion during the past two decades (dashed line). This could explain a shoreline regression (explanation 2), but probably not as strong as occurred in reality. The continuous line in Figure 3-5 is more likely: a combination of structural erosion caused by human intervention and normal natural variability (explanation 3).

### Conclusion

The erosion of the past two decades is probably caused by structural erosion because of human intervention (Paragraph 3.4.2) and a natural middle-term (decades) time scale variability of which the cause remains unknown (explanation 3).

## 3.5 Conclusions

There is a considerable amount of qualitative information available regarding the boundary conditions in the project area. There is however a lack of quantitative information during a longer period of time, especially of the bathymetry, wave conditions and granulometry. The coastal system is characterized by two longshore transport regimes: one in the breaker zone and one in deeper water. Exchange between these two regimes especially occurs during storm events. The outer ends of the project area show complex hydrodynamic behaviour, making it difficult to determine their role in the sediment balance of the area. Human intervention in this system has made the system very vulnerable to storms and has caused a trend of structural erosion.

This (qualitative) picture of the boundary conditions and the behaviour of the coastal system will be used as input for the application of the equilibration design methods in Chapter 5 and for the modelling of the beach fill equilibration with Unibest-TC in Chapter 6 to 9 and Chapter 11.



## 4 THEORY OF BEACH NOURISHMENT BEHAVIOUR AND DESIGN

### 4.1 Introduction

The goal of this chapter is to give the theoretical background of beach nourishment behaviour and to discuss coastal modelling concepts useful for beach nourishment design. Specific attention is paid to the equilibration design methods of Dean [1974], James [1975], the USACE [1994] and Dean [2002].

The mathematical process-based modelling of the equilibration and storm behaviour with Unibest-TC will be discussed in Chapter 6 to 9 and 11.

First the goals and behaviour of a beach nourishment project in general are given (Paragraph 4.2). Then the design process of beach nourishment is described (Paragraph 4.3), after which the available coastal modelling concepts are discussed (Paragraph 4.4). This is followed by a process analysis of beach fill equilibration (Paragraph 4.5). Subsequently, the relevant cross-shore modelling concepts for the equilibration are described (Paragraph 4.6). Finally, this leads to conclusions (Paragraph 0).

The design methods for the equilibration described in Paragraph 4.6 will be applied in Chapter 5 and compared with the results of the Unibest-TC model in Chapter 10.

### 4.2 Beach nourishments: goals and behaviour

#### 4.2.1 Introduction

The placement of sand on a beach, dune or foreshore to restore or build a beach is called beach nourishment or beach fill. Since no hard structures are applied, beach nourishment is called a soft engineering technique and generally has little adverse impact on the surroundings. Beach nourishment projects can be economically very valuable.

#### 4.2.2 Goals

Beach nourishment and the consequently widening of the beach is applied to accomplish several goals [Dean and Dalrymple, 2002]:

- To build additional recreational area.
- To offer storm protection, by reducing wave energy near shore and creating a sacrificial beach.
- To provide environmental habitat for endangered species such as sea turtles.

The first two goals are the most common and are of relevance within the Cancún Beach Rehabilitation Project.

#### 4.2.3 Placement

Sand from onshore or offshore sources can be placed on the beach, dune or foreshore. Placement on the beach is the most common method, since the sand is directly placed where it is needed in most cases. Dune nourishment serves to reinforce the existing dunes to create extra storm protection. Foreshore nourishments are applied as storm protection since they will induce wave breaking further offshore. Secondly, they are used as a

substitute for 'normal' beach nourishment, since it is assumed that all or part of the placed sand will be brought ashore by wave action.

#### 4.2.4 Behaviour

Usually, the beach before the nourishment is subject to structural erosion, and it is likely the structural erosion processes aren't seriously altered by the nourishment. Hence, the nourished beach will eventually erode back to its original state. Therefore, beach nourishments usually are repeated periodically e.g. every few years.

After beach nourishment, the shape of the beach is usually out of equilibrium, both in planform as in cross-shore direction. The subsequent shoreline change can be separated in three processes [Dean and Dalrymple, 2002]:

- The profile equilibration from the construction profile to the (cross-shore) equilibrium profile. This component usually consists of offshore directed transport and thus a shoreline recession, but not of a transfer of sand out of the active profile.
- Spread out losses: a transfer of sand out of the nourished area, due to the planform anomaly created by the placed sand.
- Background erosion, due to ongoing coastal processes before the project was emplaced.

These processes are shown in Figure 4-1 and occur simultaneously, but on different timescales, which is indicated in Figure 4-2.

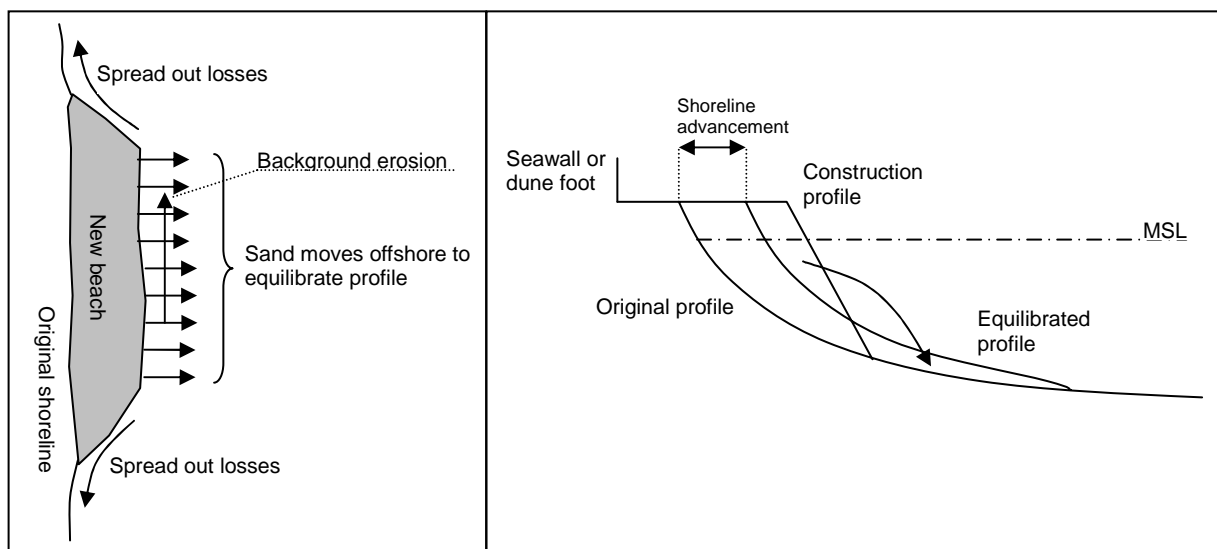


Figure 4-1: Plan view (left) and cross-section view (right) of the three erosion processes associated with beach nourishment: equilibration, spread-out losses and background erosion [NRC, 1995].



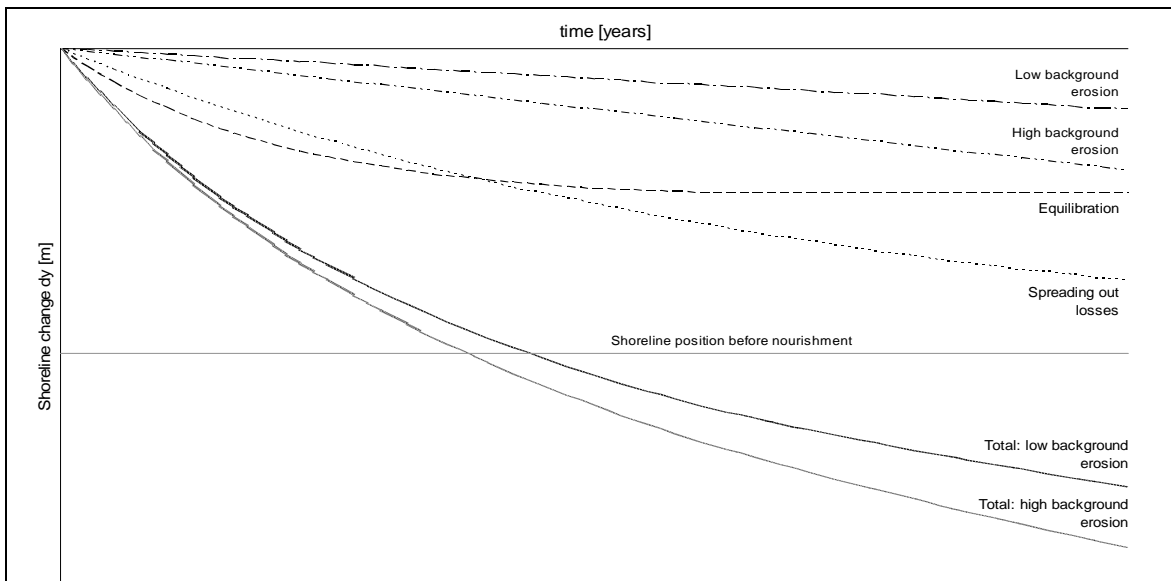
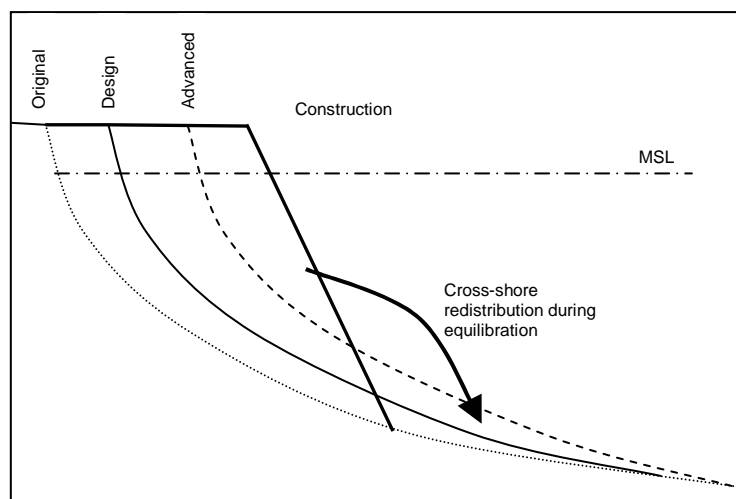


Figure 4-2: Qualitative overview of the erosion processes associated with beach nourishment: background erosion (low and high), equilibration and spread-out losses, leading to a shoreline retreat in time [Dean and Dalrymple, 2002].

- In Figure 4-3 four cross-shore profiles associated with beach nourishment are presented:
- The original profile or pre-nourishment profile is considered to have less sand than required, creating the need for the nourishment.
  - The construction profile is the profile immediately after construction and is usually steeper than the original profile.
  - The advanced profile is the profile that remains after cross-shore equilibration of the construction profile and has theoretically the same shape as the original profile (if the same grain size as native is used in the fill).
  - The design profile is the minimal profile required for the project in the sense that it offers enough beach width for recreation and / or storm protection. What is 'enough' depends on economical considerations.

Figure 4-3: Four cross-shore profiles associated with beach nourishment [NRC, 1995].



The difference between the advanced profile and the design profile is to account for spread-out losses and background erosion and depends on:

- The magnitude of the expected spread-out losses and background erosion.
- The required renourishment frequency, based on economical considerations.

It is emphasized that the advanced profile can be different along the project area to account for longshore differences in background erosion and spread-out losses.

### 4.3 Design of beach nourishments

In a nutshell, the design process of a beach nourishment project can be summarized as follows:

#### Design profile

The design profile is based on the required beach width based on e.g. recreational aspects and on the minimum required storm protection. Increasing beach width will increase costs, but the benefits in the form of increased recreational revenues and decreased damage risk increase too.

The fill volume in the design profile is chosen such that the net annual costs are minimized or the net annual revenues maximized [NRC, 1995]. This is visualized in Figure 4-4.

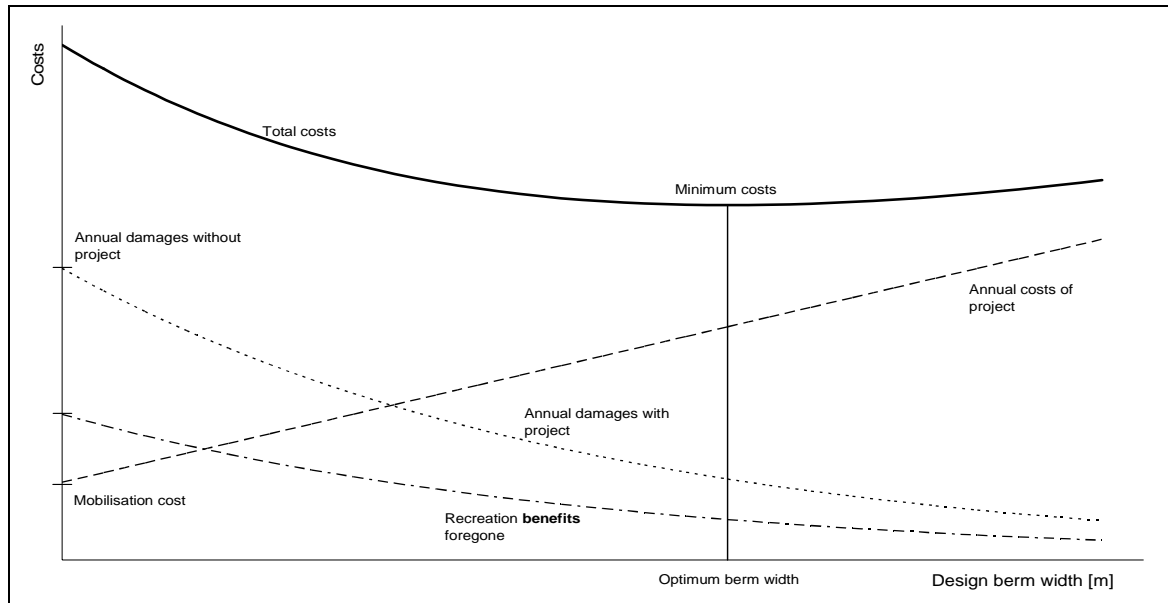


Figure 4-4: Benefits (recreational, storm damage reduction) and cost (annual cost, total cost) of a beach nourishment project versus the design berm width of the fill. The optimum design berm width is where total costs are minimal [NRC, 1995].

To determine the project revenues, information about storm conditions (water levels, wave heights and periods, duration) is needed to calculate the shoreline retreat (and damage to human interest) using short term morphological models.

#### Advanced profile

Above analysis is complicated, since the berm width, and hence the level of protection and recreational area, is a function of time. More specific: the evolution from the advanced to the design profile takes a number of years, during which storm protection and recreational area are higher than for the design profile.

Application of this information requires that the berm width is known (statistically) as a function of time. Therefore quantitative information of the expected background erosion and spread-out losses must be obtained.

#### Construction profile

Also during the equilibration (transformation from the construction profile to the advanced profile) benefits are a function of time. Knowledge must be obtained about the shoreline retreat in time and the 'final' situation after equilibration (shape of the advanced profile). This implies application of modelling concepts that predict the shape of the advanced profile and eventually the time scale of the equilibration.

#### Costs

The costs of the nourishment depend on the distance from the borrow site to the project area and of the volume of the fill and thus on the grain size of the fill material. Another

important parameter is the depth of the borrow site, as this limits the equipment to be used. Also mobilization costs play a role, especially for small projects. This influences the optimum renourishment frequency.

### Additional aspects

Beach nourishment design is more complicated as sketched above. Hybrid solutions are possible: e.g. beach fill combined with groins, underwater sill, detached breakwaters, crenulate bays, etc. Longshore adaptations in the design are also very important. Specific construction and environmental specifications are of relevance too.

Aspects such as financing and organization of the project can be of major influence on the design too. However, these aspects are beyond the scope of this thesis.

The approach discussed above is visualized in Figure 4-5.

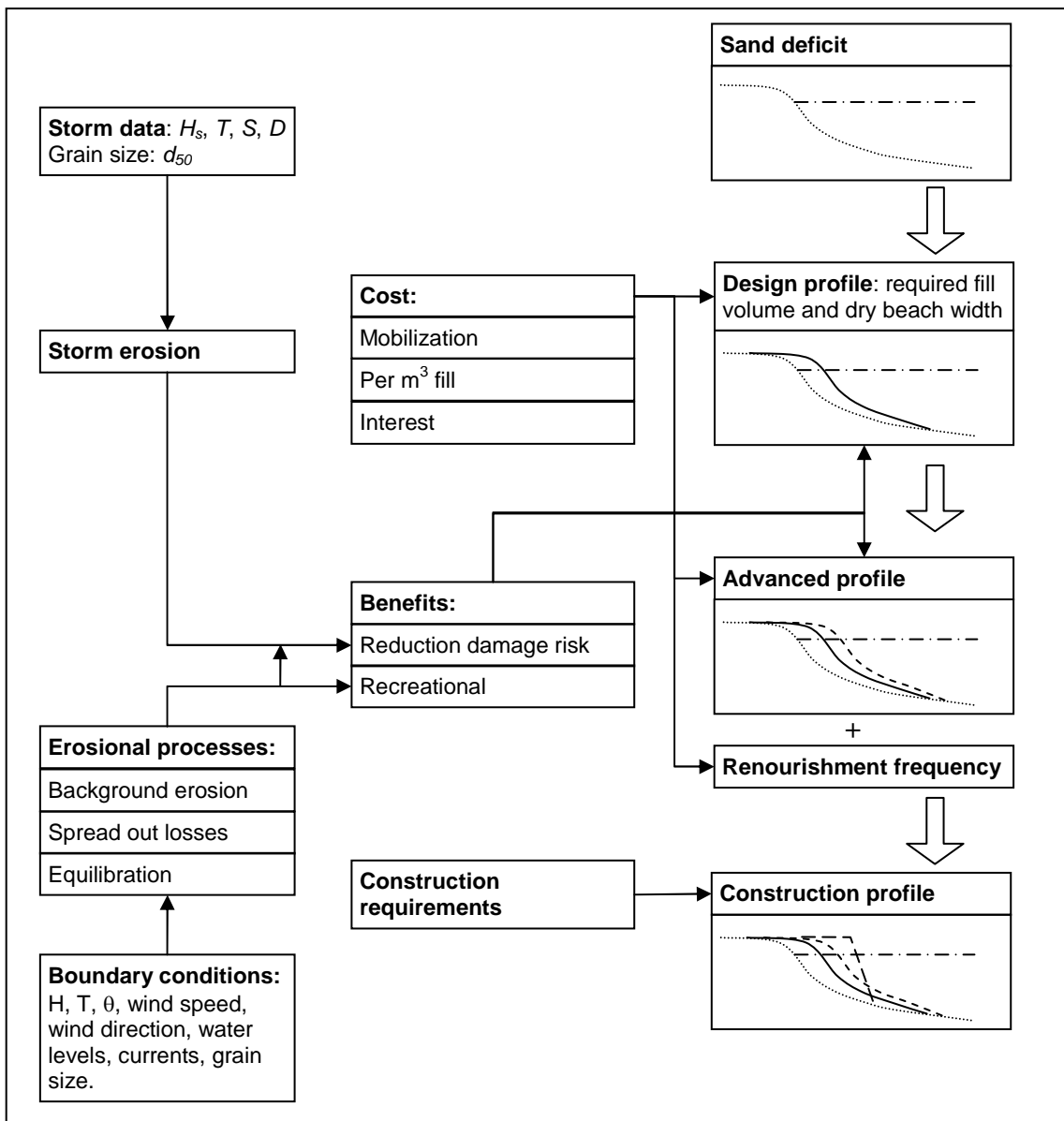


Figure 4-5: Schematic overview of the design of a beach nourishment project with the needed input (boundary conditions), the relevant processes (background erosion, spread out losses, equilibration), cost, benefits and construction aspects influencing the shape of the design profile, the advanced profile & the renourishment frequency and the construction profile. The block arrows indicate the design sequence.

Following this design approach, the following difficulties occur:

- The boundary conditions that will occur during the life time of the project are only known by their statistical distribution; only a probability of occurrence of a certain condition can be given, not when or whether it will occur. This statistical distribution itself is in most cases very unreliable, due to lack of data.
- The modelling concepts used to calculate the storm effects, background erosion, spread-out losses and equilibration are approximate only, since our knowledge of the occurring processes isn't fully developed yet.
- The benefits of the project (recreational, storm protection) vary in time, depending on the remaining beach width. The development of the benefits in time depends on the boundary conditions that will occur after construction and are (in the best case) only known by their statistical distribution and fairly unreliable due to the use of approximate calculation methods.

These difficulties can be partly overcome by using a stochastic approach to determine the costs and benefits and by reducing the uncertainty in boundary conditions by continuous monitoring.

The uncertainty introduced by insufficient modelling methods for the storm effects, background erosion, lateral losses and equilibration is less easy overcome. In the following paragraph, available modelling concepts for these processes are discussed.

## 4.4 Coastal modelling concepts

### 4.4.1 Model subdivision

Coastal models can be subdivided in physical models, which are real models physically smaller than prototype, and equation-based models involving the solutions of the equations governing the relevant physical processes. These equation-based models can be split in analytical models and numerical models.

Another possible subdivision is given by Roelvink and Brøker Hedegaard [1993]. They distinguish four types of *cross-shore* profile models:

#### **Descriptive models**

These models show a qualitative picture of the typical characteristics (e.g. typical beach slope, presence of bars) of a coast as determined by identified parameters and mechanisms (e.g. grain size, tidal range) encountered in the coastal region. Their value for quantitative studies is small, because of the small accuracy and their incapability of predicting effects of man-made interventions in the beach profile.

#### **Equilibrium models**

Equilibrium models are *'based on the a priori identification of an equilibrium state without describing the way such equilibrium is achieved'* [Capobianco et al., 2002]. An example is the beach equilibrium profile found by Bruun [1954] as discussed in Appendix A.5.2.

#### **Empirical profile evolution models**

These models are *'based on an empirical description of the tendency towards the equilibrium'* [Capobianco et al., 2002] and calculate the profile development as a function of time by considering the differences between the local instantaneous bottom profile and the equilibrium profile. An empirical coefficient is needed for every specific situation and is determined by calibration. An example is the numerical model EDUNE [Kriebel and Dean, 1985].

#### **Process-based models**

Also called dynamic or deterministic profile models, these models are *'based on the detailed description of the different processes which originate the morphology'* [Capobianco et al., 2002]. Considering a certain bathymetry, the wave and current fields are calculated. Subsequently, the sediment transports are determined, leading to changes

in the bathymetry, which on their turn cause changes in the wave and current field via the time-stepping mechanism.

#### 4.4.2 Model dimension subdivision

A model subdivision can also be based on the number of horizontal dimensions included in the model. Within these categories, distinction is possible, based on the degree of implementation of vertical information in the model; see TAW [1995] and Sorgedraeger [2002]. This leads to Table 4-1 below.

Table 4-1: Subdivision of models based on the number of implemented horizontal dimensions and the vertical information in the model.

Horizontal subdivision	Vertical subdivision	Description
0-D	0-D	Standard point-model
	q1-DV	Point-model with vertical information
	1-DV	Point-model with complete vertical (z-direction)
1-D	1-D	Standard 1 dimensional line-model
	q2-DV	Ray-model with vertical information
	2-DV	Ray-model with complete vertical (x- and z-direction)
2-D	2-DH	Standard 2 dimensional horizontal field-model
	q3-DV	Field-model with vertical information
	3-D	Complete field-model (x-, y- and z-direction)

#### 4.4.3 Application of coastal modelling concepts in beach nourishment design

The modelling concepts described in Paragraph 4.4.1 can be used to calculate the processes relevant to beach nourishment (storm response, background erosion, spread-out losses, equilibration). For every process the relevant modelling concepts are discussed below.

It is emphasized that the magnitude of the morphological changes can also be determined with frequent bathymetric surveys. This is especially useful for adaptations in the design of subsequent nourishments. This will not be considered here, however.

##### Background erosion and spread-out losses

The background erosion and spread-out losses are both longshore processes and can be modelled in the following ways:

- Using analytical or numerical longshore 1-D modelling of the sediment transports and sediment balance. These models are (partly) process-based in the sense that they recognize one or more dominant processes (e.g. wave induced longshore transport). It is assumed that the profile is in cross-shore equilibrium. An example is the one-line planform model of Pelnard-Consideré [1956].
- Using analytical or numerical 2-D modelling of the sediment transports and sediment balance. These models are (partly) process-based. The cross-shore profile can be considered out of equilibrium. An example is the two-line model of Bakker [1968], in which the cross-shore transport is calculated using an empirical profile evolution model.
- Using 3-D numerical, process-based modelling of the sediment transports and sediment balance, with software packages such as Delft-3D.

##### Equilibration

The equilibration of the construction profile is a pre-dominantly cross-shore process and can be modelled in the following ways:

- Using cross-shore equilibrium models. This method has been widely recognized and has led to the following major design methods: Dean [1974], James [1975], USACE [1994] and Dean [2002].
- Using empirical profile evolution models, both analytical and numerical.

- Using process-based 1-D numerical modelling of the cross-shore transports and sediment balance (e.g. the Unibest-TC software package).
- Using process-based 2-D or 3-D numerical modelling.

### Storm response

The storm response is pre-dominantly cross-shore, although significant longshore erosion can occur too. Here only cross-shore processes are considered. These can be modelled in the following ways:

- Using cross-shore equilibrium models (e.g. Vellinga [1986]).
- Using empirical profile evolution models, both analytical and numerical (e.g. Durosta [Steetzel, 1990] and EDUNE).
- Using process-based 1-D numerical modelling of the cross-shore transports and sediment balance (e.g. Unibest-TC).
- Using process-based 2-D or 3-D numerical modelling.

### 4.4.4 Conclusion

Considering only the cross-shore equilibration, one can conclude that the model concepts suitable for beach nourishment design are on the one hand the equilibrium models (Dean [1974], James [1975], USACE [1994] and Dean [2002]) and on the other hand 1-D process-based numerical modelling (with Unibest-TC). These design methods will be compared, both theoretically and practically, according to the goal of this thesis.

Considering the storm response, only 1-D process-based numerical modelling with Unibest-TC will be considered. These results will be compared with the method of Vellinga [1986]. In the overview below is indicated where the relevant design methods for this thesis are treated:

Process	Model type	Approach	Chapter	Appendix
Equilibration	equilibrium models	<ul style="list-style-type: none"> <li>• Dean [1974]</li> <li>• James [1975]</li> <li>• USACE [1994]</li> <li>• Dean [2002]</li> </ul>	4.6.2 4.6.3 4.6.4 4.6.5	A.5.4
	1-D process-based modelling	<ul style="list-style-type: none"> <li>• Unibest-TC</li> </ul>	6 to 9	C
Storm behaviour	empirical profile evolution models	<ul style="list-style-type: none"> <li>• Vellinga [1986]</li> </ul>	11	
	1-D process-based modelling	<ul style="list-style-type: none"> <li>• Unibest-TC</li> </ul>	11	C

The equilibration design methods will be brought into practice in the Cancún Beach Rehabilitation Project in Chapter 5 after which the results are compared in Chapter 10. The storm behaviour is described in Chapter 11.

## 4.5 Process analysis of beach fill equilibration

### Process analysis

A beach fill causes a severe out-of-equilibrium state of the coast in a cross-shore sense. Not only the profile shape is far different (normally steeper) from the equilibrium state, but also the grain size distribution. The latter is altered in two ways:

1. The composite (i.e. the average of the whole profile) grain size distribution of the fill can differ from the native: the mean and standard deviation of the grain size distribution is different.
2. The cross-shore distribution of the grain size is different; the fill sediments are primarily placed in the upper part of the profile.

Directly after placement the equilibration will start: the out-of-equilibrium profile is transformed to an equilibrium state. The resulting sediment transport is induced by hydrodynamic forcing such as waves and currents and consists of suspended and bed transport. These sediment transports will induce change of the profile shape and change of the grain size distribution across the profile.



assume the actual grain size distribution to be in equilibrium as the USACE method assumes the actual profile shape and median grain size  $d_{50}$  to be in equilibrium. The method of Dean [2002] is a combination of Dean [1974] and USACE [1994].

All methods calculate the shoreline advancement after equilibration for a certain fill volume and fill grain size (distribution).

The design methods can be characterized in the way they implement the relevant modelling issues defined in Paragraph 4.5: equilibrium profile, granulometry, closure depth and modelling of the underlying physical processes.

#### 4.6.2 Dean [1974]

Dean [1974] assumes that the mean grain size of the native sediments is in equilibrium and results in the actual equilibrium profile. It is stated that beach fill equilibration consists of the transformation of the fill sediment grain size distribution to an equilibrated sediment size distribution. This transformation consists of the complete loss of the finer fill sediments until the mean of the transformed (i.e. equilibrated) grain size distribution equals the mean of the native grain size distribution. When the mean fill grain size exceeds the mean native grain size, no losses occur. The design procedure is explained below.

An overfill factor  $K$  is defined, which specifies the number of cubic meters of material to be placed on the beach to retain one cubic meter of sediment. Dean examined the size distributions of the native and fill material, with the latter assumed to be normal distributed using  $\phi$  units [Krumbein, 1936] as defined below:

$$\phi = -2 \log d \quad \text{or} \quad 2^{-\phi} = d \quad (4.2)$$

Where:  $\phi$  phi scale, an alternative measure of size: higher values of phi indicate smaller sediments [-]  
 $d$  sediment sieve diameter [mm]

$$f(\phi) = \frac{1}{\sigma_{\phi} \sqrt{2\pi}} e^{-\frac{(\phi - \mu_{\phi})^2}{2\sigma_{\phi}^2}} \quad (4.3)$$

Where:  $\mu_{\phi}$  mean grain size in phi units [-]  
 $\sigma_{\phi}$  standard deviation in size in phi units [-]

Dean assumed that all sediments finer than sediments with a critical phi value  $\phi_*$  (i.e. larger than  $\phi_*$ ) will be lost, due to longshore or cross-shore transport. The altered size distribution for the fill material that remains is:

$$\begin{aligned} f_E &= K f_F(\phi) & \phi &\leq \phi_* \\ f_E &= 0 & \phi &> \phi_* \end{aligned} \quad (4.4)$$

Where:  $f_E$  sediment size distribution of the equilibrated material in phi units [-]  
 $f_F$  sediment size distribution of the fill material in phi units [-]  
 $\phi_*$  critical phi value, all sediments finer than sediments with a  $\phi_*$  will be lost [-]  
 $K$  overfill factor [-]

With  $K$  chosen so that:

$$1 = K \int_{-\infty}^{\phi_*} f_F(\phi) d\phi = \frac{K}{\sqrt{2\pi}\sigma_F} \int_{-\infty}^{\phi_*} e^{-\frac{(\phi - \mu_F)^2}{2\sigma_F^2}} d\phi \quad (4.5)$$

Where:  $\sigma_F$  standard deviation in size of the fill material [-]

As it is assumed that the size of the material on the beach is in equilibrium with the natural processes, the mean diameter of the fill is to be the same as the native material:



$$\frac{K}{\sqrt{2\pi}\sigma_F} \int_{-\infty}^{\phi} \phi \cdot e^{-\frac{(\phi-\mu_F)^2}{2\sigma_F^2}} d\phi = \mu_N \quad (4.6)$$

Where:  $\mu_N$  mean diameter of the native material in phi units [-]

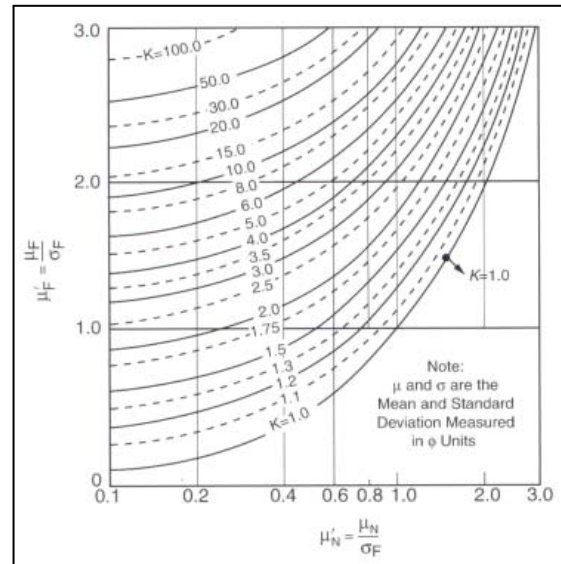
Substituting Equation (4.5) for K in Equation (4.6) leads to:

$$\frac{\int_{-\infty}^{\phi} \phi \cdot e^{-\frac{(\phi-\mu_F)^2}{2\sigma_F^2}} d\phi}{\int_{-\infty}^{\phi} e^{-\frac{(\phi-\mu_F)^2}{2\sigma_F^2}} d\phi} = \mu_N \quad (4.7)$$

The results can be visualized in a design graph as in Figure 4-6:

Figure 4-6:

Design graph for the overfill factor K as a function of mean sediment size of fill and native material and the standard deviation of the size of the fill material [Dean and Dalrymple, 2002].



When the overfill factor  $K$  is known, the effective fill volume can be calculated. By assuming that the profile shape remains the same as the actual profile and by assuming a closure depth, the shoreline advancement  $\Delta y_{0,EQ}$  can be calculated.

#### Implementation of model issues

Table 4-3 summarizes the implementation of relevant model issues in the method of Dean [1974].

Table 4-3: Use of the relevant model issues in the method of Dean [1974].

Model issues		Dean [1974]	
		Used?	Explanation
Equilibrium profile	current profile is in equilibrium	yes	Necessary assumption to calculate the shoreline advancement out of the effective fill volume.
	current sediment is in equilibrium	yes	The fill sediment distribution is modified, since the native <b>mean</b> diameter is assumed to be stable in the actual profile.
	grain size dependent profile shape	no	Only the grain size distribution is altered, not the profile shape.
Granulometry	grain size distribution	$\mu_F + \sigma_F$ $\mu_N$	The fill grain size distribution is assumed to be normally distributed in phi-units. Only the mean of the native distribution is considered.
	grain size distribution across the profile	no	The grain size distribution is assumed to be constant across the profile.
	time-varying grain size distribution across the profile	no	The grain size distribution is assumed to be constant in time.
Depth of closure		yes	Necessary assumption to calculate the shoreline advancement out of the effective fill volume.
Underlying physical processes which cause morphology are considered		no	No processes originating the morphology are described.
Time-varying processes and boundary conditions		no	No dynamic processes and bottom changes are described.

#### 4.6.3 James [1975]

The method developed by James [1975] was adopted for the 1984 edition of the Shore Protection Manual of the U.S. Army Corps of Engineers [USACE, 1984]. The difference compared with the method of Dean [1974] is that only the portion of fines in excess of the native distribution is lost instead of all the fines with a  $\phi$  larger than  $\phi_*$ ; it also takes the spread of the native distribution  $\sigma_N$  into account. This implies that losses may also occur for well-graded fill sediments with a mean grain size larger than the native mean grain size.

James defines an overfill factor  $R_A$  and a renourishment factor  $R_r$ , which depend on the size and sorting of both the native and fill material. Both native and borrow (fill) material are assumed to be log normally distributed. The overfill factor has to be determined using Figure 4-7 [USACE, 1984].

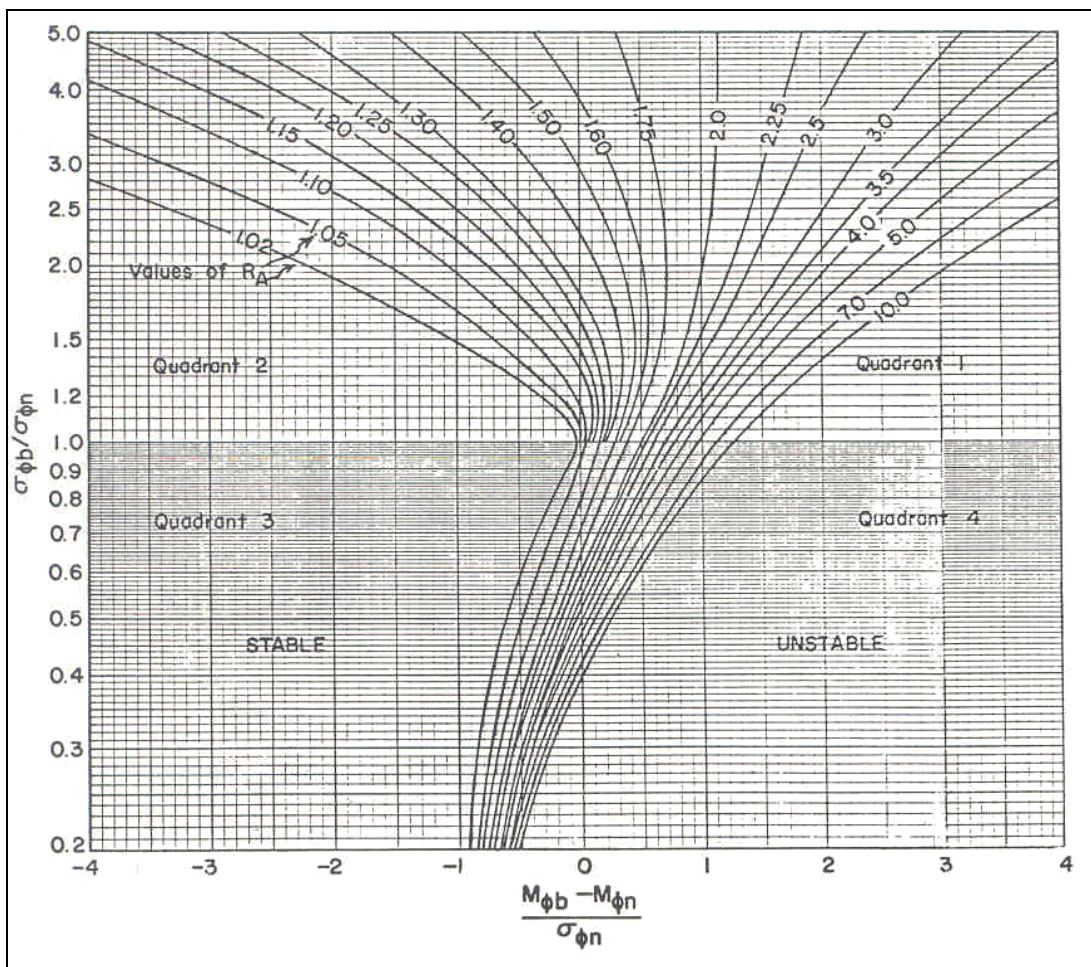


Figure 4-7: Isolines of the adjusted overfill factor  $R_A$  for values of phi mean difference and phi sorting ratio [USACE, 1984]. The subscript 'b' refers to the borrow material and the subscript 'n' refers to the native sand on the beach.

The variables are defined as follows:

$$\sigma_{\phi} = \frac{(\phi_{84} - \phi_{16})}{2} \quad (4.8)$$

Where:

- $\sigma_{\phi}$  the standard deviation of the grain size. High values of  $\sigma$  mean poorly sorted material or well-graded material. [-]
- $\phi_{84}$  the 84<sup>th</sup> percentile in phi units; 84% of the grains has a smaller phi value, i.e. 84% of the grains is larger. [-]
- $\phi_{16}$  the 16<sup>th</sup> percentile in phi units; 16% of the grains has a smaller phi value, i.e. 16% of the grains is larger. [-]

$$M_{\phi} = \frac{(\phi_{84} + \phi_{16})}{2} \quad (4.9)$$

Where:  $M_{\phi}$  the phi mean diameter of the grain size distribution [-]

The meaning of the four quadrants indicated in Figure 4-7 is explained in Table 4-4.

Table 4-4: Relationships of phi means and phi standard deviations of native material and borrow material [USACE, 1984].

Quadrant in Figure 4-7	Relationship of phi means	Relationship of phi standard deviations
1	$M_{\phi b} > M_{\phi n}$ Borrow material is finer than native material	$\sigma_{\phi b} > \sigma_{\phi n}$ Borrow material is more poorly sorted than native material
2	$M_{\phi b} < M_{\phi n}$ Borrow material is coarser than native material	
3	$M_{\phi b} < M_{\phi n}$ Borrow material is coarser than native material	$\sigma_{\phi b} < \sigma_{\phi n}$ Borrow material is better sorted than native material
4	$M_{\phi b} > M_{\phi n}$ Borrow material is finer than native material	

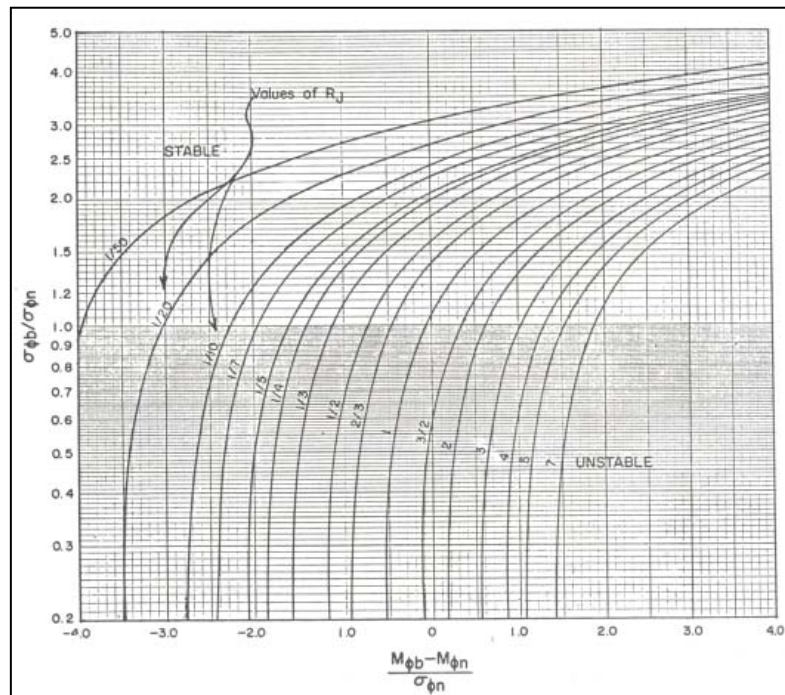
The renourishment factor  $R_j$  is the ratio of the rate at which the borrow material will erode to the rate at which the native beach material is eroding and is given as [USACE, 1984]:

$$R_j = e^{-\left[ \Delta \left( \frac{M_{\phi b} - M_{\phi n}}{\sigma_{\phi n}} \right) - \frac{\Delta^2}{2} \left( \frac{\sigma_{\phi b}^2}{\sigma_{\phi n}^2} - 1 \right) \right]} \quad (4.10)$$

Where:  $R_j$  the renourishment factor. [-]  
 $\Delta$  winnowing function, represents the scaled difference between the phi means of non-eroding and actively eroding native beach sediments [-]

$\Delta = 1$  is recommended for the common situation where the textural properties of non-eroding native sediments are unknown. Equation (4.10) is plotted for  $\Delta = 1$  in Figure 4-8.

Figure 4-8: Isolines of the renourishment factor,  $R_j$ , for values of phi mean difference and phi sorting ratio,  $\Delta=1$  [USACE, 1984].



It is recommended to take  $R_j \geq 1$  for the first nourishment.  $R_j$  accounts for larger / smaller longshore background erosion and spread-out losses due to different grain size

distributions of the fill and native sediments. Therefore it is relevant for the development of the advanced profile to the design profile (see Figure 4-3).  $R_f$  isn't considered further in this thesis.

When the overfill factor  $R_A$  is known, the effective fill volume can be calculated. By assuming that the profile shape remains the same as the actual profile and by assuming a closure depth, the shoreline advancement  $\Delta y_{0,EO}$  can be calculated.

### Implementation of model issues

Table 4-5 summarizes the implementation of relevant model issues in the method of James [1975].

Table 4-5: Use of the relevant model issues in the method of James [1975].

Model issues		James [1975]	
		Used?	Explanation
Equilibrium profile	current profile is in equilibrium	yes	Necessary assumption to calculate the shoreline advancement out of the effective fill volume.
	current sediment is in equilibrium	yes	The fill sediment distribution is modified, since the native <b>grain size distribution</b> is assumed to be stable in the actual profile.
	grain size dependent profile shape	no	Only the grain size distribution is altered, not the profile shape.
Granulometry	grain size distribution	$\mu_N + \sigma_N$ $\mu_F + \sigma_F$	The grain size distributions are assumed to be normally distributed in phi-units.
	grain size distribution across the profile	no	The grain size distribution is assumed to be constant across the profile.
	time-varying grain size distribution across the profile	no	The grain size distribution is assumed to be constant in time.
Depth of closure		yes	Necessary assumption to calculate the shoreline advancement out of the effective fill volume.
Underlying physical processes which cause morphology are considered		no	No processes originating the morphology are described.
Time-varying processes and boundary conditions		no	No dynamic processes and bottom changes are described.

#### 4.6.4 USACE [1994]

This method was presented by Dean [1991] and later adopted by the USACE [1994] and has been incorporated in the 2002 edition of the Coastal Engineering Manual [USACE, 2002]. It can be used to calculate the additional dry beach width after equilibration  $\Delta y_{0,EO}$  as a function of the fill volume  $V$ , the berm height  $B$ , the closure depth  $h_*$  and the size of the native and fill sediments.

It is based on the equilibrium profile concept based on the assumption of uniform dissipation of wave energy per unit volume of water as described in Appendix A.5.2. The resulting equilibrium profile is described as [Dean, 1977]:

$$h(y) = A(d)y^{2/3} \quad (4.11)$$

Where:

$A(d)$	profile scale factor, function of the energy dissipation and indirectly of the grain size of the beach	$[m^{1/3}]$
$h$	depth below MSL	$[m]$
$y$	distance from the shoreline, positive seawards	$[m]$

This relation offers a useful tool to determine the compatibility of fill sediments. A difference compared with the previous methods is that the equilibrium shape of the native and fill sediments is considered, but no attention is paid to the grain size distribution: only



a mean grain size is used. Three beach profiles after equilibration can be distinguished, depending on the fill and native scale parameters ( $A_F$  and  $A_N$ ), the volume  $V$ , the berm height  $B$  and the closure depth  $h_*$ . The nourished profile can be intersecting, non-intersecting or submerged as visualized in Figure 4-9.

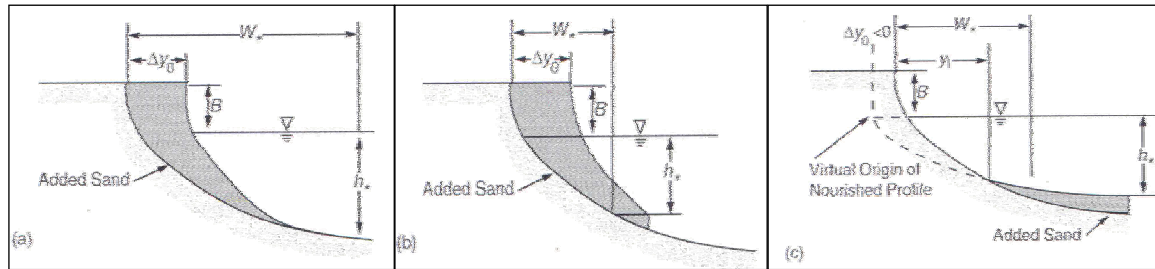


Figure 4-9: Profile types associated with beach nourishment: intersecting (a), non-intersecting & emergent (b) and non-intersecting & submerged profiles. Comment:  $\Delta y_0$  equals  $\Delta y_{0,EQ}$ . [Dean and Dalrymple, 2002]

In Appendix A.5.4, a number of design formulas is derived to calculate the additional dry beach width after equilibration  $\Delta y_{0,EQ}$ . Below the results are summarized using the dimensionless parameters  $V' = V/BW_*$ ,  $\Delta y_0' = \Delta y_{0,EQ}/W_*$  and  $B' = B/h_*$ , where  $W_*$  is the offshore distance associated with the closure depth of the native profile (see Appendix A.5.4).

To distinguish between intersecting and non-intersecting profiles (see Figure 4-9):

$$\Delta y_0' + \left(\frac{A_N}{A_F}\right)^{3/2} - 1 < 0 \quad \text{Intersecting profiles} \quad (4.12)$$

$$\Delta y_0' + \left(\frac{A_N}{A_F}\right)^{3/2} - 1 > 0 \quad \text{Non-intersecting profiles}$$

$$(V')_{c1} = \left(1 + \frac{3}{5B'}\right) \left[1 - \left(\frac{A_N}{A_F}\right)^{3/2}\right] \quad \text{for } (A_F/A_N) > 1 \quad (4.13)$$

Where:  $(V')_{c1}$  critical volume to distinguish between intersecting and non-intersecting profiles [-]

To distinguish between submerged and non-intersecting, but emergent profiles:

$$(V')_{c2} = \frac{3}{5B'} \left(\frac{A_N}{A_F}\right)^{3/2} \left[\frac{A_N}{A_F} - 1\right] \quad \text{for } (A_F/A_N) < 1 \quad (4.14)$$

Where:  $(V')_{c2}$  critical volume to distinguish between emergent and submerged profiles [-]

The relations between berm height  $B$ , added volume  $V$ , native over fill sediment parameter,  $A_N / A_F$  and shoreline advancement  $\Delta y_{0,EQ}$  can be written as follows (using dimensionless parameters):

For intersecting profiles (see Equation (4.12) and Equation (4.13)):

$$V_1' = \Delta y_0' + \frac{3(\Delta y_0')^{5/3}}{5B' \left[ 1 - \left( \frac{A_N}{A_F} \right)^{3/2} \right]^{2/3}} \quad (4.15)$$

For non-intersecting, but emerging profiles (see Equation (4.14)):

$$V_2' = \Delta y_0' + \frac{3}{5B'} \left\{ \left[ \Delta y_0' + \left( \frac{A_N}{A_F} \right)^{3/2} \right]^{5/3} - \left( \frac{A_N}{A_F} \right)^{3/2} \right\} \quad (4.16)$$

These formulas are presented graphically in Figure A-6 in Appendix A.5.4 to ease the design process by avoiding iterative calculations.

#### Implementation of model issues

Table 4-6 summarizes the implementation of relevant model issues in the method of the USACE [1994].

Table 4-6: Use of the relevant model issues in the method of the USACE [1994].

Model issues		USACE [1994]	
		Used?	Explanation
Equilibrium profile	current profile is in equilibrium	yes	The current profile depends on the current grain size via the scale parameter $A$ according to Equation (4.11).
	current sediment is in equilibrium	yes	The current sediment is assumed to be in equilibrium.
	grain size dependent profile shape	yes	The profile shape is fully determined by the grain size.
Granulometry	grain size distribution	$\mu$	Only the mean ( $\mu$ ) or median ( $d_{50}$ ) grain size is considered.
	grain size distribution across the profile	no	The grain size is assumed to be constant across the profile.
	time-varying grain size distribution across the profile	no	The grain size is assumed to be constant in time.
Depth of closure		yes	Necessary assumption to calculate the shoreline advancement and to distinguish between intersecting, non-intersecting and submerged profiles.
Underlying physical processes which cause morphology are considered		minimal	Equilibrium profile shape is based on uniform wave energy dissipation per unit water volume.
Time-varying processes and boundary conditions		no	No dynamic processes and bottom changes are described.

#### 4.6.5 Dean [2002]

Dean [2002] defined a method based on the Dean [1974] and USACE [1994] methods, which takes into account:

- A lognormal grain size distribution of the fill sediments.
- A cross-shore varying grain size.
- A grain size dependent profile shape.

This method eliminates some simplifying assumptions of the methods of Dean [1974] and the USACE [1994].

The method assumes both the native and fill grain size distribution to be normally distributed in  $\phi$ -units according to Equation (4.3). When detailed sediment sieve curves are available, arbitrary sediment size distributions can be used too.

### Coarse and fine portion of the fill volume V

The fill volume  $V$  is split in a coarse (inshore) and fine (seaward) portion. The mean grain size of each portion depends on the grain size distribution of the native and fill sediments. Two cases are distinguished:  $d_F < d_N$  and  $d_F > d_N$ .

#### $d_F < d_N$

A critical grain size  $\phi_*$  separates the finer and coarser fraction of the grain size distribution.  $\phi_*$  is chosen such that the coarser fraction has the same mean grain size as the native sediments:

$$\mu_{Fc} = \mu_N = \frac{\int_{\phi_*}^{\phi_c} \phi_F f(\phi_F) d\phi_F}{\int_{-\infty}^{\phi_*} f(\phi_F) d\phi_F} \quad (4.17)$$

Where:

$\mu_{Fc}$	mean grain size of the coarse portion of the fill volume in phi units	[-]
$\mu_N$	mean grain size of the native sediments in phi units	[-]
$\phi_F$	phi grain size of the fill distribution	[-]
$f(\phi_F)$	sediment size distribution of the fill sediments according to Equation (4.3)	[-]

The mean grain size of the finer fraction is finer than the native mean grain size:

$$\mu_{Ff} = \frac{\int_{\phi_*}^{+\infty} \phi_F f(\phi_F) d\phi_F}{\int_{\phi_*}^{+\infty} f(\phi_F) d\phi_F} \quad (4.18)$$

Where:

$\mu_{Ff}$	mean grain size of the fine portion of the fill volume in phi units	[m <sup>3</sup> /m]
------------	---	---------------------

The volume of the fine seaward portion is calculated as follows:

$$V_{fine} = V \cdot \int_{\phi_*}^{+\infty} f(\phi_F) d\phi_F \quad (4.19)$$

Where:

$V_{fine}$	the fine portion of the fill volume	[m <sup>3</sup> /m]
$V$	the fill volume	[m <sup>3</sup> /m]

The volume of the coarse landward portion is calculated as follows:

$$V_{coarse} = V \cdot \int_{-\infty}^{\phi_*} f(\phi_F) d\phi_F \quad (4.20)$$

Where:

$V_{coarse}$	the coarse portion of the fill volume	[m <sup>3</sup> /m]
$V$	the fill volume	[m <sup>3</sup> /m]



$d_F > d_N$

In the case that the mean fill grain size is larger than native the critical grain size  $\phi_*$  is chosen such that the finer fraction has the same mean grain size as native:

$$\mu_{Ff} = \mu_N = \frac{\int_{\phi_*}^{+\infty} \phi_F f(\phi_F) d\phi_F}{\int_{\phi_*}^{+\infty} f(\phi_F) d\phi_F} \quad (4.21)$$

The mean grain size of the coarser fraction is larger than native mean grain size:

$$\mu_{Fc} = \frac{\int_{-\infty}^{\phi_*} \phi_F f(\phi_F) d\phi_F}{\int_{-\infty}^{\phi_*} f(\phi_F) d\phi_F} \quad (4.22)$$

The volume of the fine (seaward) and coarse (landward) portion is calculated according to Equation (4.19) and (4.20) respectively.

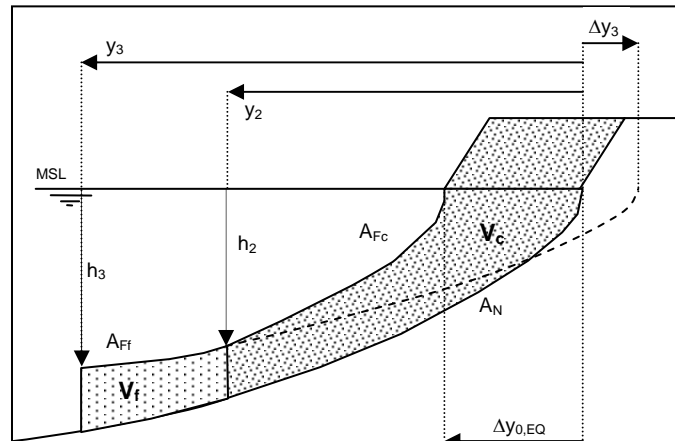
With the mean grain size of the fine and coarse portion known, the corresponding A-parameters according to Equation (4.11) can be determined from Table A-2 in Appendix A.5.2.

### General profile shape

Dean [2002] states that the coarse portion of the fill volume will be located in the upper part, while the fine portion finds its equilibrium position in the lower part of the profile, which is indicated in Figure 4-10. The equilibrated profile is always of the non-intersecting type (see Figure 4-9).

Figure 4-10:

General profile shape of the equilibrated post-nourishment profile according to Dean [2002]. The upper part consists of coarse sediments and has a larger A parameter than the lower part, composed of the fine sediments.



The parameters  $V_c$ ,  $V_f$ ,  $\Delta y_{3r}$ ,  $h_2$  and  $h_3$  are defined in Equation (4.23) to (4.27).

$$V_c = B\Delta y_{0,EQ} + \frac{3}{5} A_N y_2^{5/3} - \frac{3}{5} A_{Fc} (y_2 - \Delta y_{0,EQ})^{5/3} \quad (4.23)$$

Where:	$V_c$	the coarse portion of the fill volume	$[m^3/m]$
	$B$	the berm height	$[m]$
	$\Delta y_{0,EQ}$	the shoreline advancement after equilibration	$[m]$
	$A_N$	the native scale parameter according to Equation (4.11)	$[m^{1/3}]$
	$y_2$	the y-coordinate of the seaward limit of the coarse segment	$[m]$
	$A_{Fc}$	the scale parameter of the coarse part of the fill sediments	$[m^{1/3}]$

$$V_f = \frac{3}{5} A_N (y_3^{5/3} - y_2^{5/3}) - \frac{3}{5} A_{Ff} [(y_3 - \Delta y_{0,EQ})^{5/3} - (y_2 - \Delta y_3)^{5/3}] \quad (4.24)$$

Where:  $V_f$  the fine portion of the fill volume [m<sup>3</sup>/m]  
 $y_3$  the coordinate of the seaward limit of the fine segment [m]  
 $A_{Ff}$  the scale parameter of the fine part of the fill sediments [m<sup>1/3</sup>]  
 $\Delta y_3$  the y-coordinate of the fictitious origin of the lower segment [m]

$$\Delta y_3 = y_2 \left[ 1 - \left( \frac{A_{Fc}}{A_{Ff}} \right)^{3/2} \right] + \Delta y_{0,EQ} \left( \frac{A_{Fc}}{A_{Ff}} \right)^{3/2} \quad (4.25)$$

$$h_2 = A_{Fc} (y_2 - \Delta y_0)^{2/3} \quad (4.26)$$

Where:  $h_2$  the depth of the seaward limit of the coarse segment [m]

$$h_3 = A_{Ff} (y_3 - \Delta y_3)^{2/3} = h_* \quad (4.27)$$

Where:  $h_3$  the depth of the seaward limit of the fine segment [m]  
 $h_*$  the closure depth [m]

**Calculation procedure**

The 6 unknown variables ( $\Delta y_{0,EQ}$ ,  $\Delta y_3$ ,  $y_2$ ,  $y_3$ ,  $h_2$  and  $h_3$ ) are described by 5 equations in Equation (4.23) to (4.27) and must be solved by iteration. This iteration procedure is defined in the flow chart in Figure 4-11 and leads to a value for the shoreline advancement  $\Delta y_{0,EQ}$ .

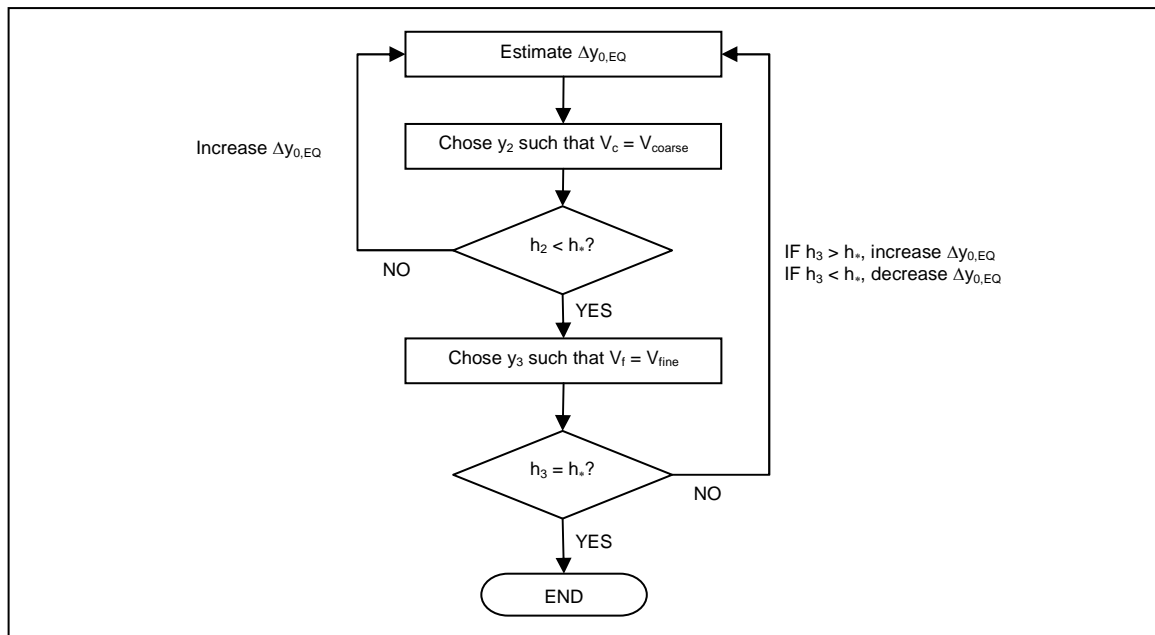


Figure 4-11: Iteration procedure to solve the system of equations from Equation (4.23) to (4.27).

**Comment**

When the coarse portion of the fill volume isn't sufficient to fill the dry beach, the underwater profile is entirely based on the profile scale parameter of the finer fraction.

### Implementation of model issues

Table 4-7 summarizes the implementation of the relevant model issues in the method of Dean[2002].

Table 4-7: Use of the relevant model issues in the method of the Dean [2002].

Model issues		Dean [2002]	
		Used?	Explanation
Equilibrium profile	current profile is in equilibrium	yes	The current profile depends on the current grain size via the scale parameter A according to Equation (4.11).
	current sediment is in equilibrium	yes	The current sediment is assumed to be in equilibrium.
	grain size dependent profile shape	yes	The profile shape is fully determined by the grain size.
Granulometry	grain size distribution	$\mu_F + \sigma_F$ $\mu_N$	The fill grain size distribution is assumed to be normally distributed in phi-units. Only the mean of the native distribution is considered.
	grain size distribution across the profile	$\mu_F(y)$	The equilibrated grain size varies across the profile: a coarse segment in the upper part and a fine segment in the lower part of the profile. The native grain size is assumed to be constant across the profile.
	time-varying grain size distribution across the profile	no	The grain size is assumed to be constant in time.
Depth of closure		yes	Necessary assumption to calculate the shoreline advancement.
Underlying physical processes which cause morphology are considered		minimal	Equilibrium profile shape is based on uniform wave energy dissipation per unit water volume.
Time-varying processes and boundary conditions		no	No dynamic processes and bottom changes are described.

## 4.7 Conclusions

The equilibration design methods presented in this chapter are useful tools, but only implement a few of the relevant model issues, which are summarized in Table 4-8.

Table 4-8: Overview of the use of the relevant model issues in the design methods for equilibration.

Model issues		Design method			
		Dean [1974]	James [1975]	USACE [1994]	Dean [2002]
Equilibrium profile	current profile is in equilibrium	yes	yes	yes	yes
	current sediment is in equilibrium	yes	yes	yes	yes
	grain size dependent profile shape	no	no	yes	yes
Granulometry	grain size distribution:	$\mu_F + \sigma_F$ $\mu_N$	$\mu_F + \sigma_F$ $\mu_N + \sigma_N$	$\mu_N$ $\mu_F$	$\mu_F + \sigma_F$ $\mu_N$
	grain size distribution across the profile	no	no	no	$\mu_F(y)$
	time-varying grain size distribution across the profile	no	no	no	no
Depth of closure		yes	yes	yes	yes
Underlying physical processes which cause morphology are considered		no	no	minimal	minimal
Time-varying processes and boundary conditions		no	no	no	no

### Limitations

The design methods in this chapter have the following limitations caused by the insufficient implementation of relevant model issues:

1. An (uncertain) assumption for the closure depth is needed.
2. None of the four design methods can describe the equilibration in time.
3. None of the four design methods can predict the results for varying boundary conditions, such as a long period of calm waves.
4. All four methods use the uncertain assumption that the prenourishment profile is in dynamic equilibrium.
5. The effect of the grain size on the profile shape is not modelled (Dean [1974] and James) or in a very poor way by the USACE and Dean [2002] methods.
6. A varying grain size across the profile is only implemented in the Dean [2002] method and in a poor way, by considering only two mean grain sizes across the profile.
7. A time-varying grain size distribution across the profile cannot be accounted for in the models; so time-dependent mixing and sorting of the grains is ignored.
8. The USACE method doesn't account for a spread in the grain size distribution.

Limitations 1 to 6 can be eliminated by using process-based modelling with Unibest-TC as will be explained in Chapter 6. Limitations 6,7 and 8 are difficult to eliminate, even in the Unibest-TC model.

In Chapter 5 the design methods described in this chapter will be applied on the Cancún Beach Rehabilitation Project and their results will be discussed.

## 5 APPLICATION OF EQUILIBRATION DESIGN METHODS

### 5.1 Introduction

In this chapter the equilibrium design methods discussed in paragraph 4.6 will be applied to determine the shoreline advancement  $\Delta y_{0,EO}$  of the planned beach fill at Cancún Beach. Only the center area of Cancún Beach (between chainage 6+100 and 6+900) will be considered. The fill grain size distributions of the two considered borrow areas near Puerto Juárez and Punta Sam (see Appendix B.2) will be considered, together with a fictitious borrow site with the a grain size distribution equal to native.

In Chapter 10 the results of this chapter will be compared with the results of the process-based modelling of the equilibration with Unibest-TC (Chapter 6 to 9).

The sediments of the borrow areas are described in Paragraph 5.2. With these sediment parameters calculations are performed in Paragraph 5.3 using the equations of Paragraph 4.6. In Paragraph 5.4 the shoreline advancement  $\Delta y_{0,EO}$  will be determined for various values of the fill volume  $V$  and the berm height  $B$ . The results will be validated in Paragraph 5.5.

### 5.2 Grain size distributions of the fill material

The design methods of Dean [1974] and James [1975] (Paragraph 4.6.2 and 4.6.3) require the mean and standard deviation in  $\phi$ -units of the native and fill sediments, which are assumed to have a normal distribution. The USACE-method requires the  $A$  parameters according to Equation (4.11), based on the median grain size  $d_{50}$  of the native and fill sediments. This required input is given in this paragraph.

In Appendix B.4.1 the grain sizes  $d_{16}$ ,  $d_{50}$  and  $d_{84}$  of the available samples on the actual beach and in the two considered borrow sites are presented. Applying Equation (4.2) results in the corresponding  $\phi$ -values from which the  $\phi$ -mean diameter ( $M_{\phi}$ , see Equation (4.9)) and the  $\phi$ -standard deviation ( $\sigma_{\phi}$ , see Equation (4.8)) of each sample can be calculated. Thereafter the composite mean  $\mu_T$  and composite standard deviation  $\sigma_T$  are determined (both in  $\phi$ -units), which can be found in Table 5-1. Also the recommended  $A$  parameters according to Dean and Dalrymple [2002] are given. The fitted  $A$  parameter for the native sediments is obtained by a least square fit of Equation (4.11) to the original profile up to MSL -7.5 m (see Paragraph 3.3.3). The other "fitted"  $A$  parameters are proportional to this value.

Table 5-1: Composite sediment parameters of the native sediments and the two considered borrow areas.

	$d_{50}$ [mm]	$\mu_{\phi}$ [-]	$\sigma_{\phi}$ [-]	$A$ recommended [ $m^{1/3}$ ]	$A$ fitted [ $m^{1/3}$ ]
native sediments	0.33	1.58	0.63	0.131	0.175
Borrow area I – Puerto Juárez	0.27	1.85	1.04	0.119	0.159
Borrow area II – Punta Sam	0.42	1.27	1.10	0.148	0.198

In Figure 5-1 to Figure 5-3 the sediment size distributions are presented graphically, assuming that they are normally distributed in  $\phi$ -units.

### 5.3 Calculations with the equilibration design methods

Knowing the grain parameters described in Paragraph 5.2, the design methods of Paragraph 4.6.2 and 4.6.3 can be applied, leading to the shoreline advancement and profile shapes presented in Paragraph 5.4.

#### 5.3.1 Dean [1974]

In Table 5-2 the parameters necessary to use the design graph in Figure 4-6 are presented together with the resulting overfill factor  $K$ .

Table 5-2: Sediment parameters necessary to use the design graph of Figure 4-6 in Paragraph 4.6.2 and the resulting overfill factor  $K$ .

	$d_{50}$ [mm]	$\mu_N/\sigma_F$ [-]	$\mu_F/\sigma_F$ [-]	Dean $K$ [-]
native sediments	0.33	1.00	1.00	1.00
Borrow area I – Puerto Juárez	0.27	1.52	1.78	1.16
Borrow area II – Punta Sam	0.42	1.44	1.15	1.00

The sediment size distribution of the equilibrated material is visualized in Figure 5-1, together with the native sediments and fill sediments of borrow area I.

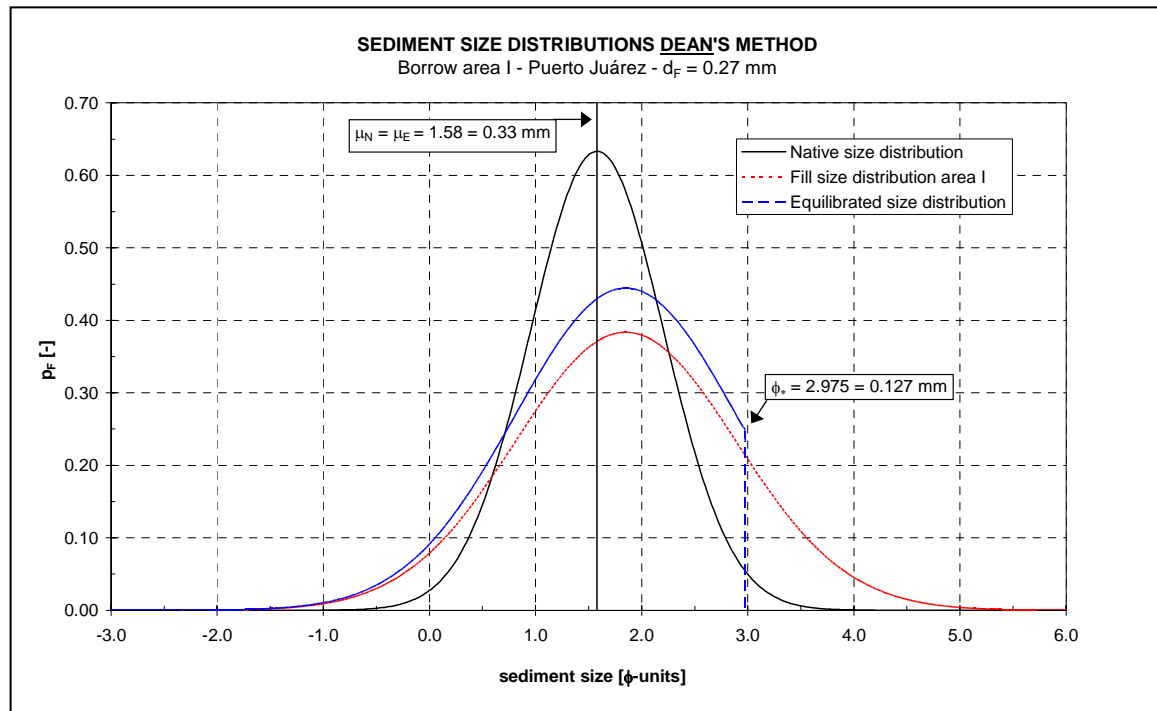


Figure 5-1 Idealized grain size distributions of the native sediments and fill sediments of **borrow area I** and the equilibrated sediment size distribution according to Dean [1974].  $\mu_E$  is the mean grain size of the equilibrated material.

Knowing the overfill factors  $K$ , the shoreline advancement  $\Delta y_{0,EQ}$  can be calculated, assuming that the profile shape doesn't change:

$$\Delta y_{0,EQ} = \frac{V}{K(B + h_*)} \quad (5.1)$$

Where:	$\Delta y_{0,EQ}$	additional dry beach width after equilibration	[m]
	$V$	fill volume	[m <sup>3</sup> /m]
	$K$	overfill factor ( $R_A$ for James' method)	[-]
	$B$	berm height	[m]
	$h_*$	closure depth	[m]

The results are presented in Appendix H.

### 5.3.2 James [1975]

In Table 5-3, the parameters necessary to use the design graph in Figure 4-7 on page 37 are given, together with the resulting overfill factor  $R_A$ .

Table 5-3 Sediment parameters necessary to use the design graph of Figure 4-7 in Paragraph 4.6.3 and the resulting overfill factor  $R_A$ . The subscript "n" refers to "native", "b" to "borrow".

	$d_{50}$ [mm]	$(M_{\phi b} - M_{\phi n}) / \sigma_{\phi n}$ [-]	$\sigma_{\phi b} / \sigma_{\phi n}$ [-]	James $R_A$ [-]
native sediments	0.33	1.00	1.00	1.05
Borrow area I – Puerto Juárez	0.27	0.43	1.65	1.50
Borrow area II – Punta Sam	0.42	-0.49	1.75	1.09

The value of  $R_A$  of 1.05 for fill sediments the same as native is to account for a loss of fines during construction. The sediment size distributions of the equilibrated material of borrow area I and II are visualized in Figure 5-2 and Figure 5-3, together with the native and fill sediments.

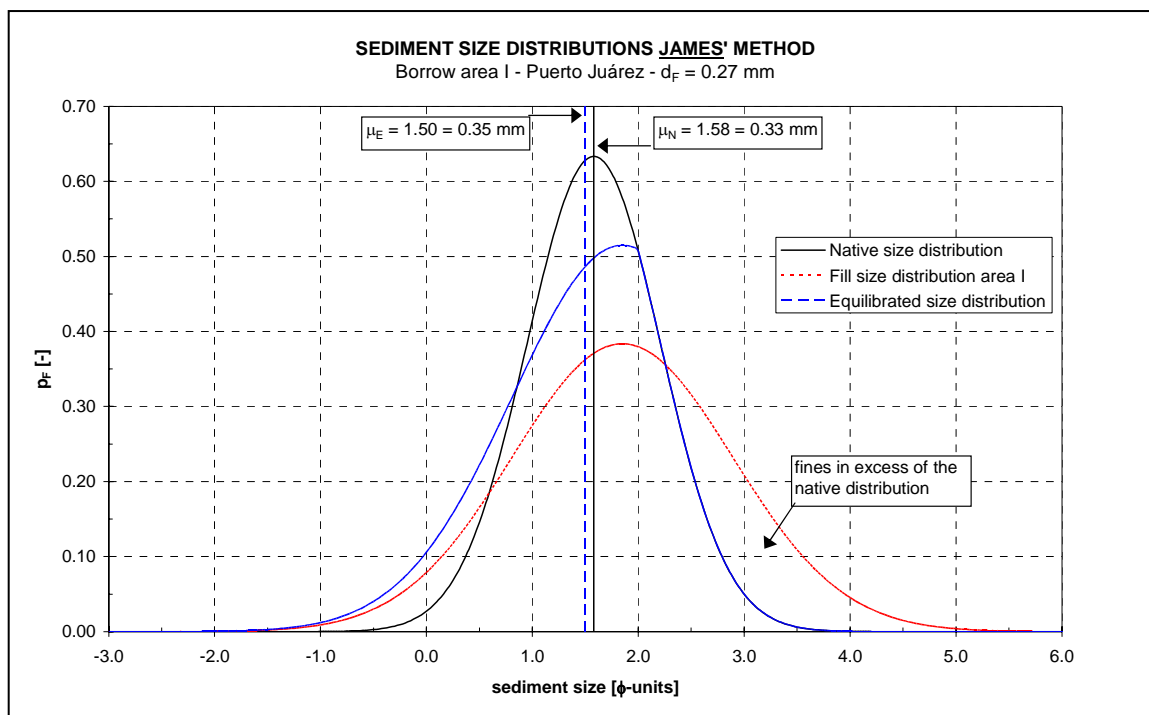


Figure 5-2 Idealized grain size distributions of the native sediments and fill sediments of **borrow area I** and the equilibrated sediment size distribution according to James [1975].

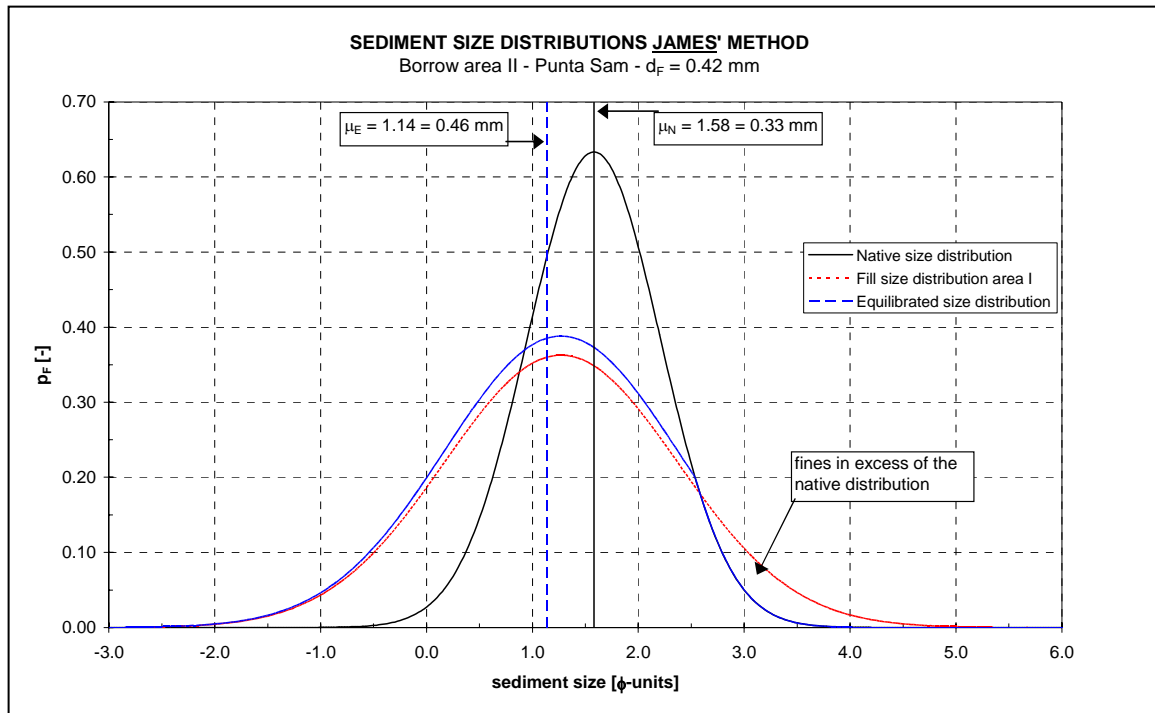


Figure 5-3 Idealized grain size distributions of the native sediments and fill sediments of borrow area II and the equilibrated sediment size distribution according to James [1975].

Knowing the overfill factors  $R_{A_v}$ , the shoreline advancement  $\Delta y_{0,EQ}$  can be calculated using Equation (5.1), assuming that the profile shape doesn't change. The results are presented in Appendix H.

### 5.3.3 USACE [1994]

The critical (dimensionless) volumes necessary to distinguish between intersecting, non-intersecting and submerged profiles (see Figure 4-9) are presented in Table 5-4 and Table 5-5 for three different values of the berm height  $B$  and the closure depth  $h_*$ . These values were calculated using Equation (4.13) and Equation (4.14). For the fill sediments equal to native, the associated profile is of the non-intersecting type.

Table 5-4: Critical (dimensionless) volumes to distinguish between emerging and submerged profiles for borrow area I – Puerto Juárez ( $d_{50} = 0.27$  mm).

	Closure depth $h_*$ [m]					
	6.0		7.5		9.0	
B [m]	$V'_{c2}$ [-]	$V_{c2}$ [m <sup>3</sup> /m]	$V'_{c2}$ [-]	$V_{c2}$ [m <sup>3</sup> /m]	$V'_{c2}$ [-]	$V_{c2}$ [m <sup>3</sup> /m]
2.0	0.209	83.97	0.261	146.70	0.314	231.41
2.5	0.167	83.97	0.209	146.70	0.251	231.41
3.0	0.139	83.97	0.174	146.70	0.209	231.41

Table 5-5: Critical (dimensionless) volumes to distinguish between intersecting and non-intersecting profiles for borrow area II – Punta Sam ( $d_{50} = 0.42$  mm).

	Closure depth $h_*$ [m]					
	6.0		7.5		9.0	
B [m]	$V'_{c1}$ [-]	$V_{c1}$ [m <sup>3</sup> /m]	$V'_{c1}$ [-]	$V_{c1}$ [m <sup>3</sup> /m]	$V'_{c1}$ [-]	$V_{c1}$ [m <sup>3</sup> /m]
2.0	0.473	190.08	0.550	308.35	0.626	461.46
2.5	0.413	207.06	0.473	332.07	0.534	492.64
3.0	0.372	224.03	0.423	355.79	0.473	523.81



Applying Equation (4.15) and Equation (4.16) leads to the additional dry beach width  $\Delta y_{0,EQ}$  according to the USACE-method. The results are presented in Appendix H.

### 5.3.4 Dean [2002]

The method of Dean [2002] is described in Paragraph 4.6.5 and uses the grain size distribution to split the fill volume  $V$  in a coarse and fine portion. The mean grain size of each portion determines its sediment scale parameter  $A$ . These data are used to calculate the shoreline advancement  $\Delta y_{0,EQ}$  according to the flow chart in Figure 4-11.

In Figure 5-4 and Figure 5-5 the fill sediment size distributions are split in a fine and coarse portion according to Equation (4.17) to (4.22). The critical grain size  $\phi_*$  is indicated, together with the mean sediment sizes of the coarse and fine portions.

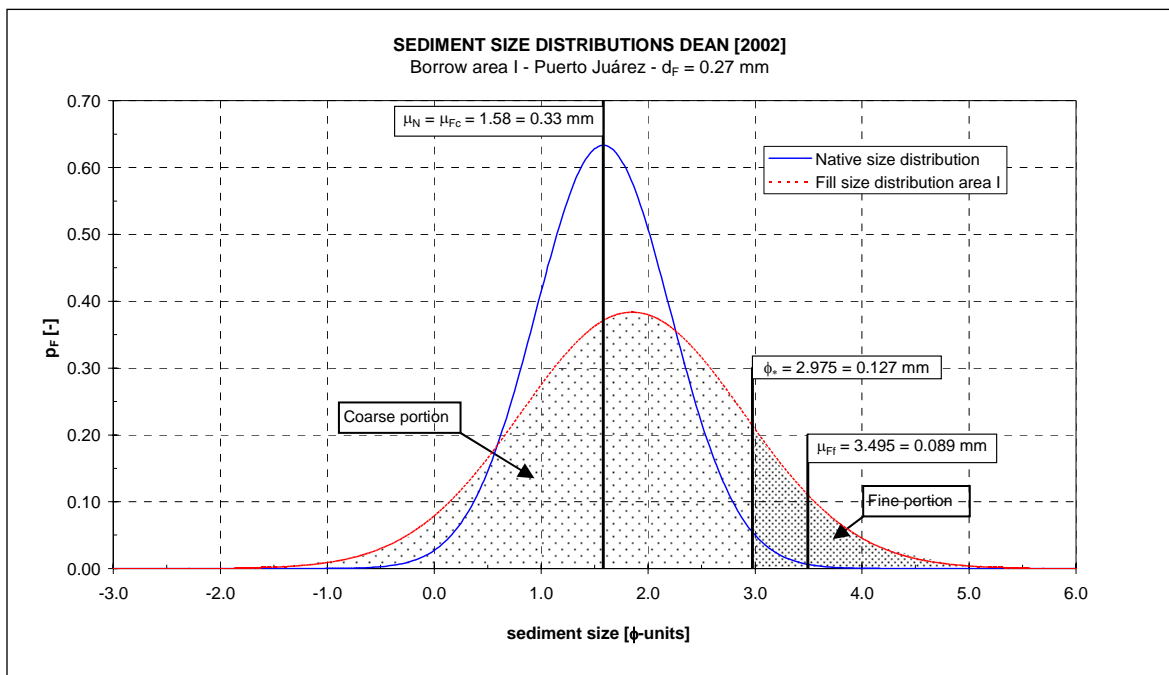


Figure 5-4 Idealized grain size distributions of the native sediments and fill sediments of **borrow area I**. The coarse portion ( $V_{coarse}$ ) to the left of  $\phi_*$  has a mean  $\mu_{Fc}$  equal to the mean of the native size distribution. The fine portion ( $V_{fine}$ ) to the right of  $\phi_*$  has a mean of 0.089 mm.

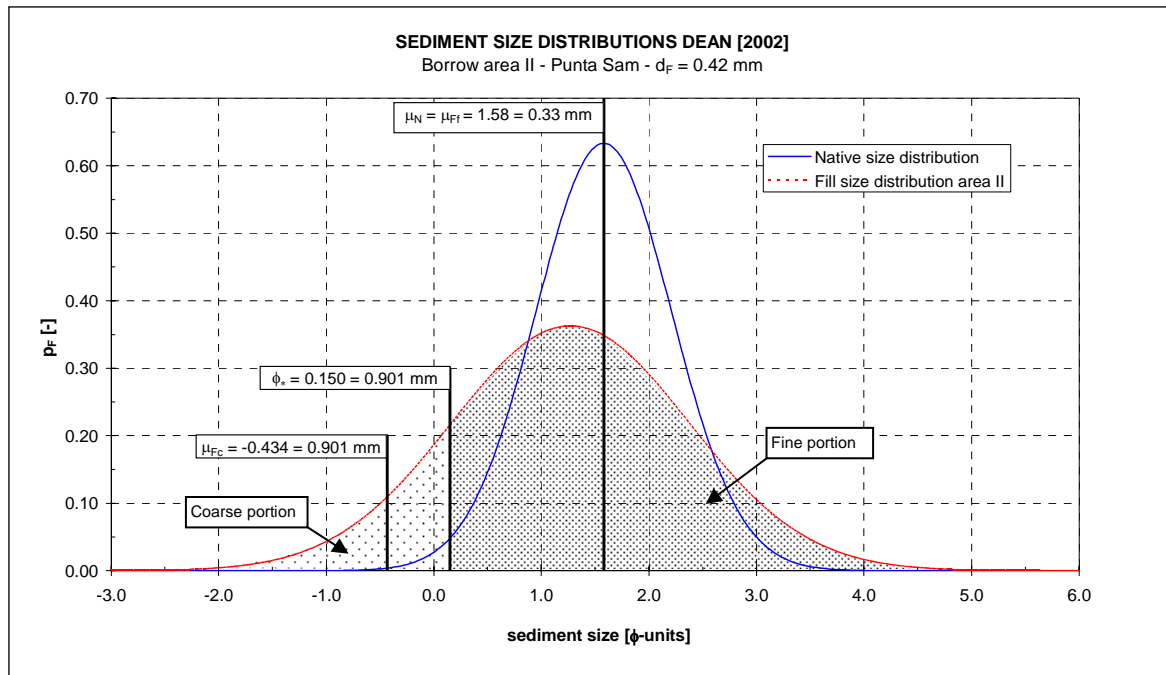


Figure 5-5 Idealized grain size distributions of the native sediments and fill sediments of **borrow area II**. The coarse portion ( $V_{coarse}$ ) to the left of  $\phi_*$  has a mean  $\mu_{Fc}$  of 0.901 mm. The fine portion ( $V_{fine}$ ) to the right of  $\phi_*$  has a mean equal to the native size distribution.

The key parameters of both borrow areas are indicated in Table 5-6 and are used to calculate the shoreline advancement in Paragraph 5.4.2 according to the flow chart in Figure 4-11.

Table 5-6: Key parameters of the two borrow areas for the method of Dean [2002].

Borrow area	$d_F$ [mm]	$V_{coarse}$ [m <sup>3</sup> /m]	$V_{fine}$ [m <sup>3</sup> /m]	$\mu_{Fc}$ [mm]	$\mu_{Ff}$ [mm]	$A_{Fc}^{1/3}$ [m <sup>1/3</sup> ]	$A_{Ff}^{1/3}$ [m <sup>1/3</sup> ]
I – Puerto Juárez	0.27	0.862 V	0.149 V	0.330	0.089	0.175	0.076
II- Punta Sam	0.42	0.138 V	0.851 V	0.901	0.330	0.406	0.175

## 5.4 Results of the equilibration design methods

### 5.4.1 Introduction

With the calculation results of Paragraph 5.3, the shoreline advancement after equilibration are given. Thereafter the bottom profiles after equilibration according to the methods of Dean, James and the USACE can be drawn. A closure depth  $h_*$  of 7.5 m has been used since this is the closure depth according to the Unibest-TC model (see Paragraph 3.3.1).

The following ranges of variables are considered:

- The fill volume  $V$ : 150 – 200 – 250 – 300 – 350 – 400 m<sup>3</sup>/m.
- The berm height  $B$ : 2.0 – 2.5 – 3.0 m.
- The fill grain size  $d_F$ : 0.27 – 0.33 – 0.42 mm.

### 5.4.2 Shoreline advancement

The calculated values of  $\Delta y_{0,EQ}$  are presented in Appendix H and Figure 5-6 for a berm height  $B$  of 2.5 m.

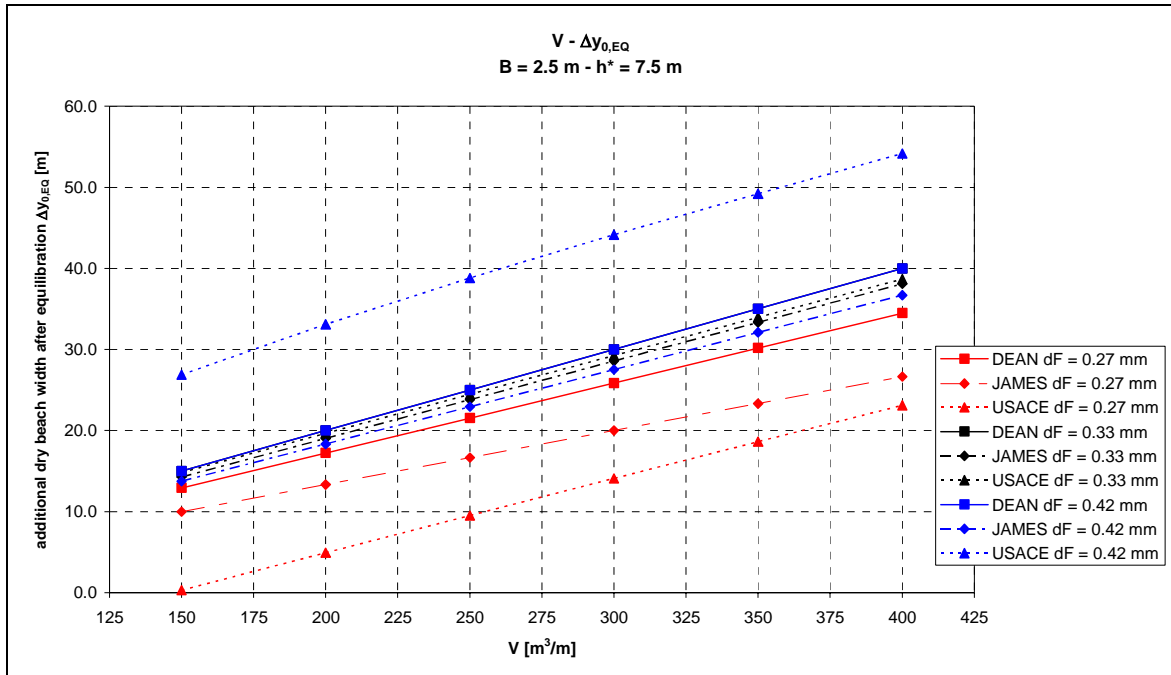


Figure 5-6: Additional dry beach widths for three fill sediment size distributions according to the methods of Dean, James and USACE for fill volumes  $V$  between 150 and 400  $\text{m}^3/\text{m}$  and, with  $B = 2.5 \text{ m}$  and  $h^* = 7.5 \text{ m}$ . The results for the Dean [2002] method are not plotted since they are practically equal to the Dean [1974] (for  $d_F = 0.27$  and  $0.42 \text{ mm}$ ) method and the USACE-method (for  $d_F = 0.33 \text{ mm}$ ).

The following can be concluded:

- All methods predict a larger  $\Delta y_{0,EQ}$  for increasing fill volume  $V$ .
- The  $\Delta y_{0,EQ}$  for  $d_F = d_N = 0.33 \text{ mm}$  is slightly different for the USACE-method, due to the manner in which the toe of the profile is accounted for.
- The USACE-method accounts for grain size dependent profile shapes which leads to:
  - Distinction between intersecting and non-intersecting profiles.
  - A non-linear relation between the fill volume  $V$  and the shoreline advancement  $\Delta y_{0,EQ}$  for the coarse fill sediments ( $d_F = 0.42 \text{ mm}$ ).
  - A threshold volume for incipient shoreline advancement for the fine fill sediments ( $d_F = 0.27 \text{ mm}$ ).
  - A larger sensitivity of  $\Delta y_{0,EQ}$  to the grain size of the fill.
- The  $\Delta y_{0,EQ}$  according to the methods Dean [1974] and [2002] is independent of the grain size for  $d_F > d_N$ .
- The differences in  $\Delta y_{0,EQ}$  between the design methods for the fill sediments other than native are in the same order of magnitude as the values of  $\Delta y_{0,EQ}$  itself.
- Significant differences in assumed profile shape occur between the USACE and Dean [2002] method on the one hand and the methods of James and Dean [1974] on the other hand.

### 5.4.3 Bottom profiles after equilibration

Knowing the additional dry beach width after equilibration, the resulting bottom profiles can be drawn. The USACE-method and the method of Dean [2002] prescribe a certain bottom profile shape according to Equation (4.11), while the methods of James and Dean [1974] only give an effective fill volume. To be able to draw the bottom profiles for the latter two methods the same bottom profile shape as native and a closure depth are assumed. This leads to the bottom profiles indicated on page H-2 to H-4 in Appendix H.

It can be observed that:

- The fit of  $h=Ay^{2/3}$  to the measured profile is very poor.
- The toe of the profile is vertical for the USACE and Dean [2002] methods and is not accounted for by the methods of James and Dean [1974].

## 5.5 Validation of the results

### 5.5.1 Introduction

The results of Paragraph 5.4 are influenced by deviations of the assumed values for the closure depth  $h_*$ , the median fill grain size  $d_F$  and the shape of the grain size distribution. In this paragraph the influence of these parameters on (a) the calculated *values* of the additional dry beach widths  $\Delta y_{0,EQ}$  and (b) the *differences* between the three design methods is determined.

### 5.5.2 Sensitivity to the closure depth

The resulting additional dry beach width  $\Delta y_{0,EQ}$  for different values of the assumed closure depth  $h_*$  is presented in Table 5-7 and visualized in Figure 5-7. Values of  $h_*$  smaller than 6 m and larger than 9 m are unlikely to occur.

Table 5-7: Additional dry beach width  $\Delta y_{0,EQ}$  for values of the closure depth  $h_*$  between 6 and 9 m for  $B = 2.5$  m and  $V = 250$  m<sup>3</sup>/m.

Description fill source			Dean			James			USACE			Dean [2002]		
			$h_*$ [m]			$h_*$ [m]			$h_*$ [m]			$h_*$ [m]		
Fill source	$d_{50}$ [mm]	A [m <sup>1/3</sup> ]	6.0	7.5	9.0	6.0	7.5	9.0	6.0	7.5	9.0	6.0	7.5	9.0
Native	0.33	0.175	29.4	25.0	21.7	28.0	23.8	20.7	28.5	24.5	21.4	28.5	24.5	21.4
Area I	0.27	0.159	25.4	21.6	18.7	19.6	16.7	14.5	17.9	9.5	1.5	25.4	21.7	18.9
Area II	0.42	0.198	29.4	25.0	21.7	27.0	22.9	19.9	39.0	38.8	38.8	39.0	38.8	38.8

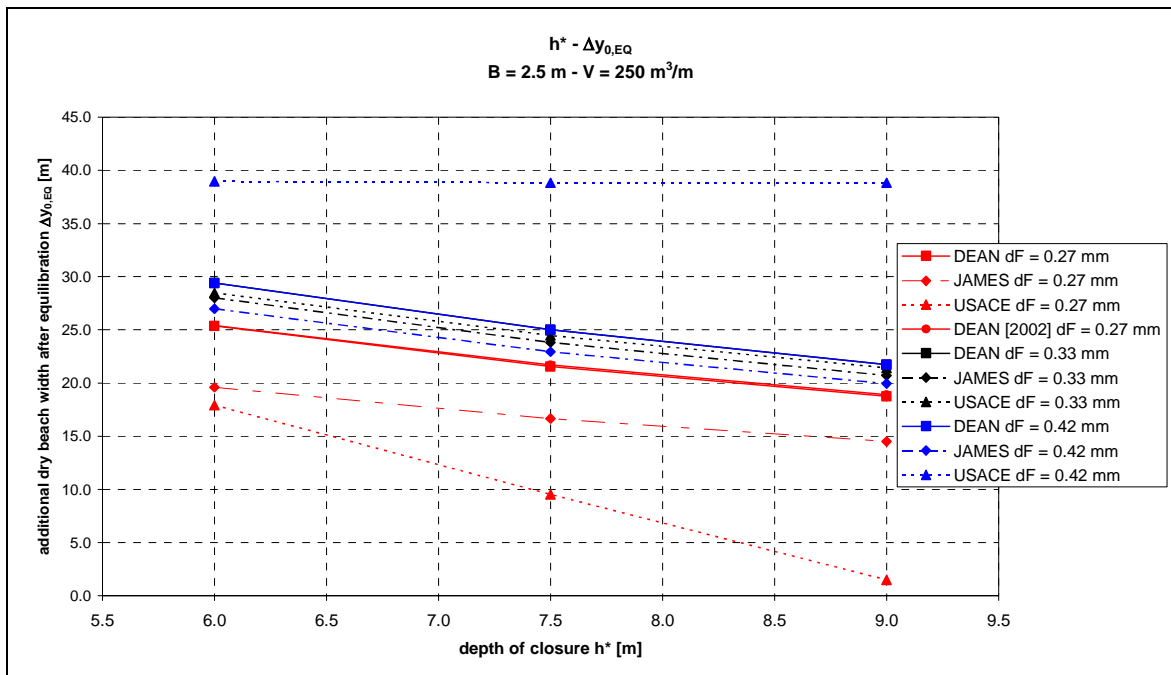


Figure 5-7: Additional dry beach width  $\Delta y_{0,EQ}$  for different values of the closure depth  $h_*$  for  $B = 2.5$  m and  $V = 250$  m<sup>3</sup>/m. Results of the method of Dean [2002] for  $d_F = 0.33$  and  $0.42$  mm equal those of the USACE-method for  $d_F = 0.33$  mm.

The following observations can be made:

- The USACE-method for  $d_F = 0.42$  mm is almost insensitive to changes in the  $h_*$  due to the occurrence of an intersecting profile.
- The USACE-method for  $d_F = 0.27$  mm is very sensitive to changes in the  $h_*$  due to relatively flat slope of the equilibrated profile.
- The Dean [2002] method is far less sensitive to the closure depth, because only non-intersecting profiles occur.
- For the other fill grain sizes and methods, the sensitivity to  $h_*$  is relatively low: deviations up to 17% relative to the results for  $h_* = 7.5$  m occur. This is significantly smaller than the mutual differences between the design methods (see Figure 5-6 in Paragraph 5.4.2).

### 5.5.3 Sensitivity to variations in grain size distribution

#### Median grain size $d_{50}$ of the fill material

In Figure 5-8 the additional dry beach width  $\Delta y_{0,EQ}$  for  $V = 200$  m<sup>3</sup>/m and  $B = 2.5$  m is plotted versus the median grain diameter  $d_{50}$ .

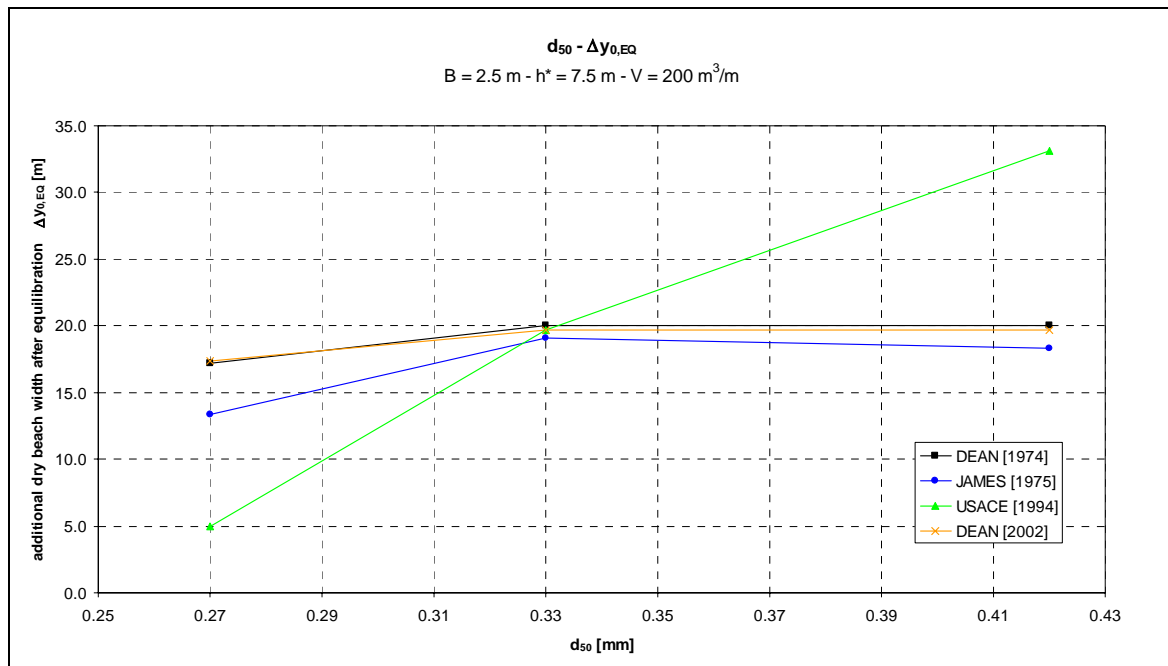


Figure 5-8: Additional dry beach width  $\Delta y_{0,EQ}$ , versus median sediment size  $d_{50}$  of the fill material for  $V = 200 \text{ m}^3/\text{m}$ ,  $B = 2.5 \text{ m}$  and  $h_* = 7.5 \text{ m}$ .

The following observations can be made:

- The calculated additional dry beach width  $\Delta y_{0,EQ}$  for a certain grain size other than native differs a lot for each method.
- The sensitivity of  $\Delta y_{0,EQ}$  to small errors in the  $d_{50}$  is relatively low compared with the mutual differences between the design methods.
- The  $\Delta y_{0,EQ}$  according to the USACE-method is very sensitive to the median grain size due to the strong grain size dependent slope of the profile.

#### Standard deviation of the grain size $\sigma$

This parameter only influences the results of the methods of James and Dean [1974] and Dean [2002]. Small errors in the input for this parameter cause small errors in the calculated  $\Delta y_{0,EQ}$ .

#### Shape of the grain size distribution

For the methods of James and Dean, the grain size in  $\phi$ -units is assumed to have a normal distribution. This is a reasonable assumption for almost all individual sediment samples found in nature. The sediment placed on the beach is extracted from a relatively large area during the dredging process and thus consists of a very large number of individual sediment samples. All these samples together (which are assumed to have a normal distribution) form a new composite distribution which again is normal distributed, because:

- Mixing is present in the hopper dredge, during pumping and during the placement.
- The composite sand consists of a large number of normal distributed samples, which leads to a uni-modal normal distributed composite sand.

The small deviations that might occur are of negligible influence on the calculated  $\Delta y_{0,EQ}$ .

### 5.5.4 Conclusions

Concluding it can be stated that the calculated shoreline advancement  $\Delta y_{0,EQ}$  is sensitive to deviations in the closure depth and the median grain size. However the influence of deviations of these variables on the *mutual differences* between the design methods is low.

The shape and standard deviation  $\sigma_\phi$  of the grain size distribution are only of relevance for the James and Dean methods. Sensitivity of the additional dry beach width  $\Delta y_{0,EQ}$  is low for the small expected variations in these parameters.

## 6 MODEL SETUP IN UNIBEST-TC

### 6.1 Introduction

Goal of this chapter is to describe the setup of the model for the beach fill equilibration in the software package Unibest-TC. The model setup in Unibest-TC consists of the objectives of the modelling, the construction of the model and the approach followed with the sensitivity analysis, calibration and verification of the model. This chapter serves as a framework for Chapters 7 to 9.

First, the objectives of the modelling are described (Paragraph 6.2). Then the model set-up is discussed, which consists of the construction of the model (Paragraph 6.3.2), the approach of the sensitivity analysis (Paragraph 6.3.3) and the calibration and verification (Paragraph 6.3.4).

### 6.2 Objectives of the modelling

#### 6.2.1 Introduction

Part of the goal of this thesis is to compare the results of the equilibrium methods described in Paragraph 4.6 with process-based numerical modelling. In Paragraph 2.4.4 it has been decided to use the Unibest-TC program of WL | Delft Hydraulics. Unibest-TC can be classified as a numerical process-based q2-DV model (see Paragraph 4.4.2).

The Unibest-TC model consists of 5 sub-models:

- Wave propagation model.
- Mean current profile model.
- Wave orbital velocity model.
- Bed load and suspended load transport model.
- Bed level change model.

The Unibest-TC model is further described in Appendix C.

The objective is to model the equilibration of the construction profile to the equilibrium profile and the behaviour during storm conditions, thereby answering the questions described in the following subparagraphs.

#### 6.2.2 Beach fill equilibration

The following questions regarding the equilibration must be answered by the Unibest-TC model:

- What is the development of the equilibration in time, i.e. what is the characteristic time scale and end state for the equilibration of a construction profile to the equilibrium profile?
- What is the influence of the fill grain size on the equilibrium shape of the profile and the time scale of the equilibration?

By using Unibest-TC some limitations of the design methods described in Paragraph 4.7 are eliminated:

1. No uncertain assumption of the closure depth is needed.
2. The equilibration in time can be described.

3. Varying boundary conditions can be applied (milder wave climate, etc.).
4. The assumption that the actual profile is in (dynamic) equilibrium isn't used.
5. The effect of the grain size on the profile shape is modelled, based on the occurring physical processes.
6. A varying grain size across the profile can be used in the model.

Limitations of the Unibest-TC model are:

1. No grain size distribution can be used, the  $d_{50}$  is considered representative for the grain size distribution.
2. The grain size distribution across the profile  $d_{50}(x)$  cannot be varied in time.
3. A lot of detailed boundary conditions are necessary, which aren't always available.
4. A detailed calibration is necessary to adjust the model to the local conditions. This is a complex procedure for which a lot of data of the boundary conditions is required.

### 6.2.3 Storm behaviour

The following questions regarding the storm response must answered by the Unibest-TC model:

- What is the profile shape and shoreline retreat after the occurrence of a design storm on an equilibrated nourished profile?
- What is the influence of the fill grain size on the post-storm profile shape and shoreline retreat?

### 6.2.4 Required input data

The Unibest-TC model needs input data to answer the questions posed in Paragraph 6.2.2 and 6.2.3. This required input can be split in boundary conditions and input parameters.

The program requires the following boundary conditions:

- An initial cross-shore bottom profile.
- A (linear varying) grain size in the profile ( $d_{50}$  and  $d_{90}$ ).
- A longshore current velocity at a certain depth, if desired varying in time.
- Water level variations at the offshore boundary, if desired varying in time.
- Wave height, angle to shore normal and peak period at the offshore boundary, if desired varying in time.
- Wind velocity and direction, if desired varying in time.

The used boundary conditions differ for the consecutive phases of the modelling process as discussed in Paragraph 6.3 and are defined in the corresponding chapters.

For an overview of the various input parameters (roughness heights, time step etc.) is referred to Appendix D.

## 6.3 Model setup

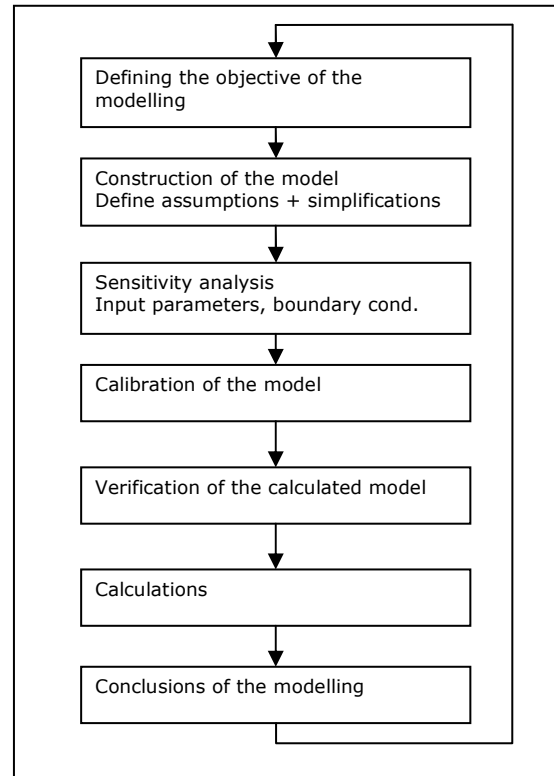
### 6.3.1 Introduction

A proper mathematical modelling process consists of the phases as described in Figure 6-1.



Figure 6-1:

Phases in (mathematical) modelling, including a feedback loop.



The objective of the modelling has been discussed in Paragraph 6.2. The other phases and their set-up will be discussed in the following paragraphs.

### 6.3.2 Construction of the model

The Unibest-TC software package is a very useful tool to investigate the morphodynamic behaviour of cross-shore profiles. However, it must be kept in mind that even this state-of-the-art model has its restraints.

A model represents by definition only a part of the real world. Certain processes are omitted or simplified in the model. The construction of a model consists of the following phases:

1. Schematization
2. Representation
3. Discretization

In each phase assumptions and simplifications are made, which are discussed below.

#### Ad 1: Schematization

The developers of Unibest-TC have omitted some (cross-shore) physical processes from the mathematical model formulations, like wind set-up, local wave generation, wind transport over the dry profile, swash zone dynamics etc.

Since Unibest-TC can be characterised as a q2-DV model (see Paragraph 4.4.2), it assumes uniform longshore conditions. Longshore effects such as rip currents, edge waves, shear waves and beach cusps are not accounted for. These originally longshore processes do influence the cross-shore development of the profile. To improve results, a longshore gradient can be imposed on the calculated longshore transport.

Furthermore, the processes which are accounted for are described by mathematical formulations. These formulations have their restraints, e.g. transport formulae as discussed by Camenen and Larroudé [2003].

#### Ad 2: Representation

The occurring boundary and initial conditions are represented in the model. Differences between the model and reality occur because of:

- Measurement errors (biased or random).

- Omission of persistancy when using random generated wave and wind conditions.
- Omission of relations between boundary conditions when using uncorrelated probability distributions of boundary conditions.
- Lack of knowledge of conditions that have occurred (during calibration phase).
- Lack of knowledge of conditions that will occur (during calculation phase).

### Ad 3: Discretization

Unibest-TC uses a numerical approach with a space step  $\Delta x$  and a fixed time step  $\Delta t$ . This can lead to inaccuracies and instabilities. Furthermore, the boundary conditions are known only on discrete times with a mutual time step  $\Delta t_{ubc}$ . Furthermore, the boundary conditions are divided into classes with a certain class size, reducing the precision, e.g. wave height classes of 20 cm.

### 6.3.3 Approach sensitivity analysis

The sensitivity analysis (see Chapter 7) is necessary for two reasons.

- First, the influence of the input parameters (see Appendix D) on the different output parameters has to be defined. These results will be used to calibrate the model.
- Secondly, the sensitivity to changing boundary conditions of the output must be known to be able to draw conclusions about the reliability of the modelling results in relation with the uncertainties in the boundary conditions.

The general approach of the sensitivity analysis is as in Figure 6-2:

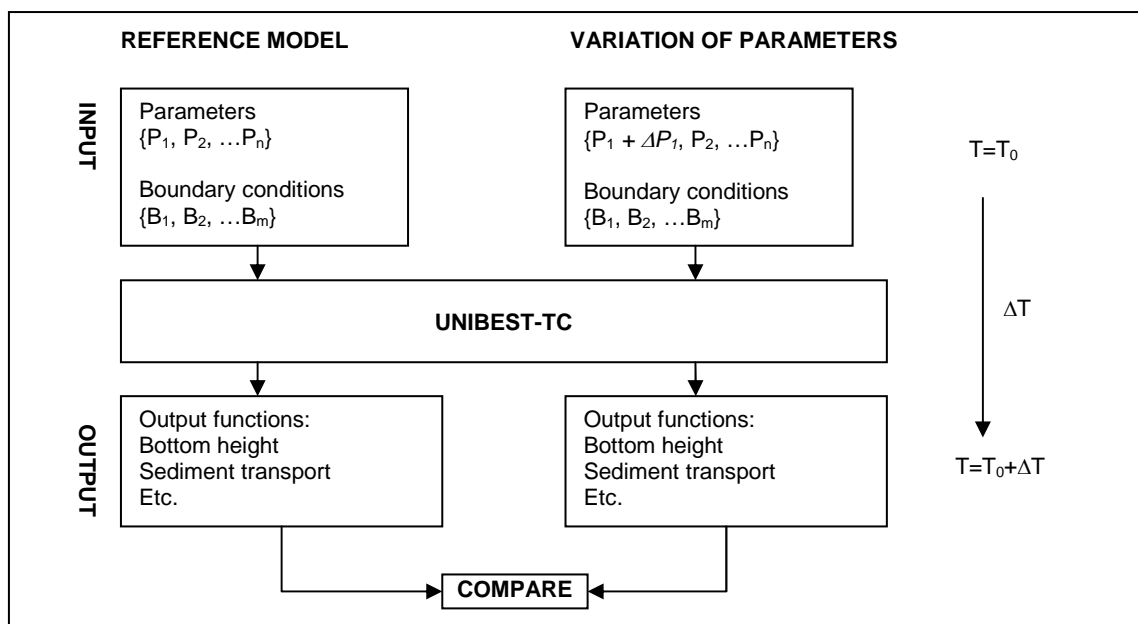


Figure 6-2: Schematic representation of the sensitivity analysis.

A reference model is made after which each of the input parameters or boundary conditions is varied with a value  $\Delta P_i$  or  $\Delta B_j$ . The consequences of this changes on the output functions are determined. Distinction is made of direct influence of a parameter on a function (at  $t = t_1$ ) or indirect influence via the time stepping mechanism (at  $t > t_1$ ).

### 6.3.4 Approach calibration and verification

#### Calibration

Calibration (see Chapter 8) is necessary to make the model a sufficient representation of reality. What can be called 'sufficient' depends on the objective of the modelling. Ideally, the development of a given initial state (at  $T_0$ ) with given boundary conditions is modelled during a time  $\Delta T$ . The results are compared with the known real state at  $T_0 + \Delta T$ . The goal

is achieving the best resemblance between the model results and the physical reality, by changing the input parameters. Iteration is needed until the resemblance is satisfactory or maximal. This is shown in Figure 6-3.

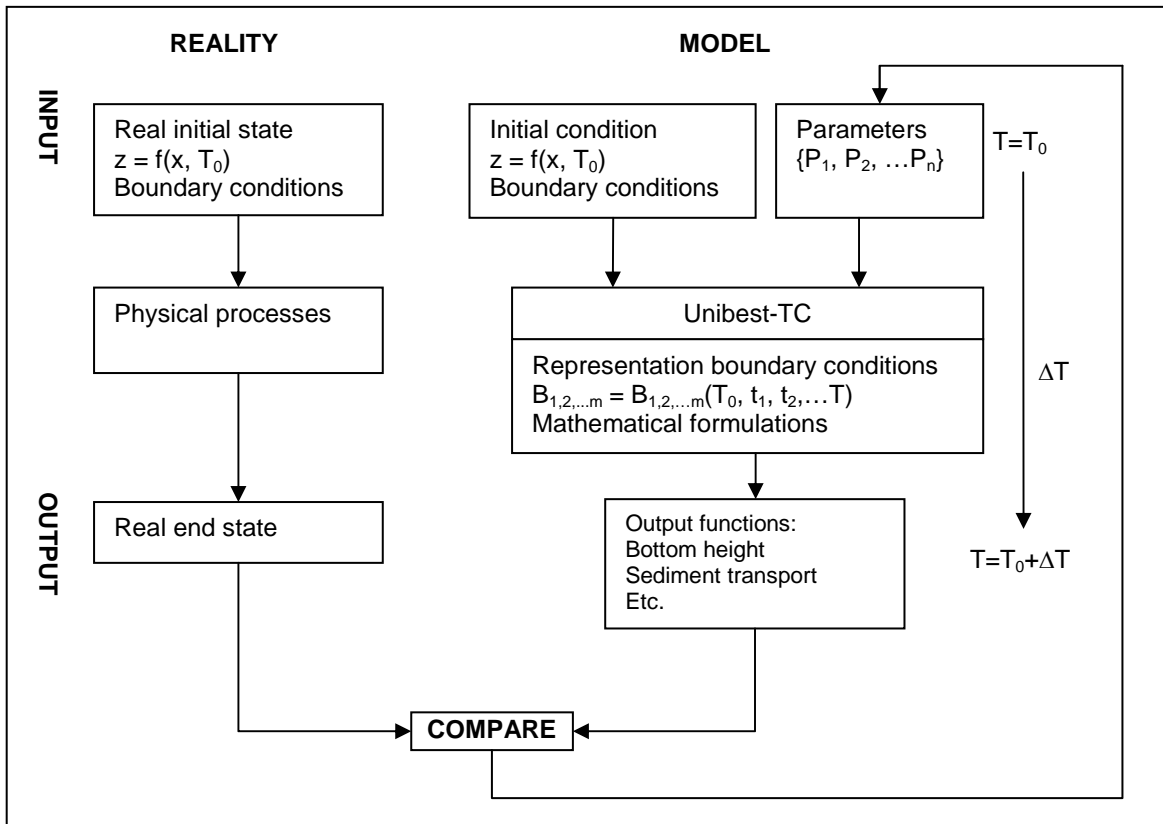


Figure 6-3: Idealized schematic representation of the calibration process.

An exact representation of reality probably won't occur. Focus will not be on calibration of the model on a detailed scale, e.g. it is impossible to model every small bottom irregularity. Furthermore, bathymetry has been measured only three times in only 14 months and the available wave, wind and current data is of a poor quality.

Therefore first a less detailed approach is used, which focuses on the correct representation of the general profile shape in the considered coastal stretch. For a detailed description of the calibration approach is referred to Paragraph 8.2.

### Verification

Verification (see Chapter 8) of the calibrated model is necessary to check whether the model represents reality in a sufficient manner. Ideally, a *new* initial state or a new profile is taken and the development of the profile is calculated with known boundary conditions (waves, wind, etc.) and the parameter setting of the calibration phase. After  $T = T_0 + \Delta T$  the model results are compared with the real situation. The resemblance should be sufficient; if not another parameter setting should be considered.

Verification of the results will also be carried out for the storm behaviour of the profile and the equilibration. Common sense arguments will be used to determine if the modelling results are reasonable in a qualitative sense.



## 7 SENSITIVITY ANALYSIS OF THE UNIBEST-TC MODEL

### 7.1 Introduction

In this chapter the sensitivity of the Unibest-TC output functions (such as transports, bottom changes) to changes in the input parameter setting (bottom roughness, wave breaking parameters, etc.) and the boundary conditions (e.g. wave height and period) is determined. The approach of the sensitivity analysis was already discussed in Paragraph 6.3.3.

This sensitivity analysis is necessary for the calibration process described in Chapter 8, since the default parameter setting doesn't give satisfactory results. Furthermore, insight in the model behaviour is necessary for the calibration.

For the model formulations reference is made to Bosboom et al. [2000] and to Appendix C. For more information on model behaviour and sensitivity to input parameters is referred to Sorgedragger [2002] and Van Thienen [2003].

The structure of this chapter is as follows. First the reference model is described (Paragraph 7.2). Then the sensitivity for the input parameters is discussed (Paragraph 7.3). After that the sensitivity for the boundary conditions is analyzed (Paragraph 7.4). Finally conclusions regarding the sensitivity of the model behaviour are drawn (Paragraph 7.5).

Graphs of the sensitivity analysis can be found in Appendix F.

### 7.2 Reference model

#### Reference values of the input parameters and boundary conditions

The input parameters and boundary conditions to be varied in the reference model are indicated in Table 7-1, together with their reference value. The boundary conditions are average values of the real conditions occurring in the project area. For the complete set of input parameters is referred to Appendix D.

#### Bottom profile

The used bottom profile is a measured profile at chainage 6+300 m (in the middle of Punta Cancún and Punta Nizuc) to a depth of 16 m, extended to -30 m with soundings from nautical chart SM922 [Secretaría de Marina, 1999]. A constant median grain size  $d_{50}$  of 0.33 mm is used across the profile.

Table 7-1: Description of input parameters and boundary conditions to be varied during the sensitivity analysis, including their reference values.

Parameter type	Input parameter	Symbol	Description	Reference value	Unit	Appendix	Par.
General	TDRY	$T^*$	Maximum relative wave period	20	-	F.2.1	7.3.1
	USTRA	$q_{tot,x}(x_{end})$	Transport at the onshore boundary	0	m <sup>3</sup> /hr	F.2.2	7.3.2
Wave	GAMMA	$\gamma$	Wave breaking parameter	0	-	F.2.3	7.3.3
	ALFAC	$\alpha$	Wave breaking parameter	1	-	F.2.4	7.3.3
	BETD	$\beta$	Slope of wave front	0.1	-	F.2.5	7.3.4
	FWEE	$f_w$	Friction factor for bottom friction	0.01	-	F.2.6	7.3.5
	F_LAM	$\lambda$	Number of wavelengths for depth integration	2	-	F.2.7	7.3.6
	POW	P	Power in weighing function	1	-	F.2.8	7.3.6
	C_R	$C_r$	Correlation coefficient bound long waves	0.25	-	F.2.9	7.3.7
Sediment	D50	$d_{50}$	$d_{50}$ grain diameter	0.00033	m	F.2.10	7.3.8
	D90	$d_{90}$	$d_{90}$ grain diameter	0.00040	m	-	7.3.8
	DSS	$D_s$	$d_{50}$ of suspended sediment	0.000264	m	F.2.11	7.3.8
Current	FCVISC	$\alpha_w$	Viscosity coefficient	0.1	-	F.2.12	7.3.9
	RKVAL	$k_s$	Friction factor for mean current	0.01	m	F.2.13	7.3.10
Transport	TANPHI1	$\tan\phi_1$	Tangent of angle of repose	0.15	-	F.2.14	7.3.11
	TANPHI2	$\tan\phi_2$	Tangent of angle of repose	0.5	-	F.2.15	7.3.11
	RW	$k_{s,w}$	Wave related roughness	0.002	m	F.2.16	7.3.12
	RC	$k_{s,c}$	Current related roughness	0.01	m	F.2.17	7.3.13
Boundary condition		Symbol	Description	Reference value	Unit	Appendix	Par.
H0		$h(t)$	Water level at offshore boundary	0	m	F.2.18	7.4.1
HRMS		$H_{rms}$	Root mean square wave height at offshore boundary	1.1	m	F.2.19	7.4.2
A_WAVE		$\theta$	Angle of wave incidence relative to shore normal at offshore boundary	10	°	F.2.20	7.4.3
T		$T_p$	Peak period of wave field	6	s	F.2.21	7.4.4
V_WIND		$V_w$	Wind speed	4	m/s	F.2.22	7.4.5
V_TIDE		$V(t)$	Shore parallel current	1	m/s	F.2.22	7.4.6
A_WIND		$\theta_w$	Wind direction	10	°	-	-

In the following paragraphs the input parameters and boundary conditions are varied to determine the influence on the model output.

### Monitored output functions

The monitored output functions are the average suspended transport, average bed load transport and average total transport during the computed time span of 1 year and the resulting bottom profile. For plots of these output functions is referred to Appendix F.2.

## 7.3 Sensitivity for the input parameters

### 7.3.1 TDRY

TDRY [-] is a user-defined maximum value for  $T^*$ , the relative wave period, a dimensionless parameter indicating the non-linearity of the wave field:

$$T^* = T_p \sqrt{g/h} \quad (7.1)$$

Where:	$T_p$	peak wave period	[s]
	$T^*$	relative wave period	[-]
	$g$	gravity acceleration	[m/s <sup>2</sup> ]
	$h$	local water depth	[m]

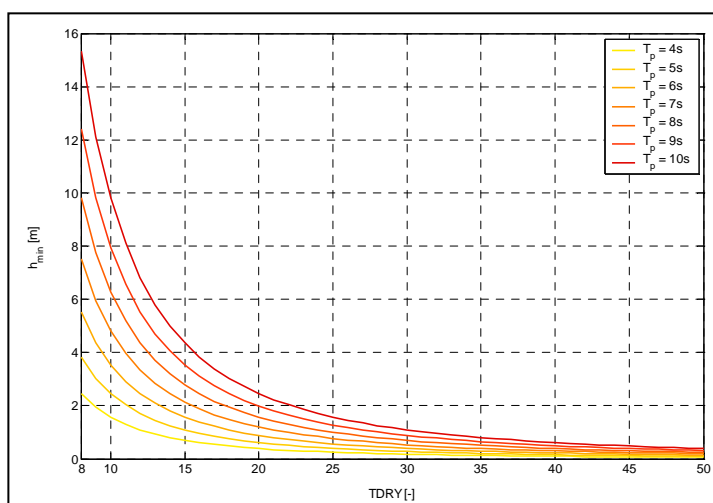
The larger  $T^*$ , the more non-linear the wave field is. TDRY is used to define the most shoreward calculation point of the model. Once  $T^*$  exceeds TDRY, the sediment transport calculations are stopped at the corresponding minimum water depth ( $h_{min}$ ) at the up wave boundary:

$$h_{min} = \frac{T_p^2 g}{TDRY^2} \quad (7.2)$$

In the figure below  $h_{min}$  is plotted as a function of TDRY for different  $T_p$ .

Figure 7-1:

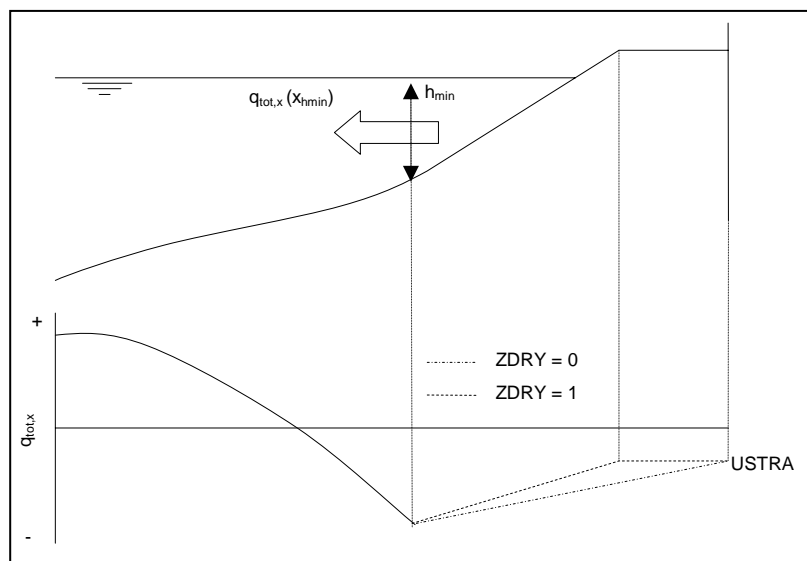
The depth of the last shoreward calculation point ( $h_{min}$ ) plotted for the relative wave period parameter (TDRY) for different values of the peak period ( $T_p$ ).



Between  $h_{min}$  and the most landward grid point, the sediment transport is calculated via linear interpolation with the height of the profile (parameter ZDRY = 1) or with the distance (parameter ZDRY = 0). The parameter USTRA defines the transport at the most shoreward grid point (see Paragraph 7.3.2). This is visualized in Figure 7-2.

Figure 7-2:

Extrapolation of the total cross-shore transport  $q_{tot,x}$  from the last calculation point with depth  $h_{min}$  to the most landward grid point with a user defined cross-shore transport USTRA (see Paragraph 7.3.2). The parameter ZDRY indicates the extrapolation method: ZDRY = 1 indicates linear extrapolation over the height of the profile, ZDRY = 0 indicates linear extrapolation with the distance.



### Observations

Plots of the output functions (average suspended transport, average bed load transport and average total transport during the computed time span of 1 year and the resulting bottom profile) can be found in Appendix F.2. From these graphs it can be observed that:

- TDRY influences the transport ( $q_{tot,x}$ ) above  $h_{min}$  directly. Via the time stepping mechanism the other processes are also influenced.
- The development of the dry profile depends to a large extent on the value of TDRY. The erosion or accretion introduced to the dry profile influences the development of the wet profile above the 6 m depth contour.
- The variation of the total transport is relatively low for values of TDRY between 20 and 30. Larger values result in unacceptable use of linear wave theory in very shallow water, which leads to unrealistic transport rates. Smaller values lead to a very large  $h_{min}$ , which causes the extrapolation area to expand seaward severely.

### 7.3.2 USTRA

USTRA [ $m^3/hr/m$ ] defines the value of the total cross-shore transport at the most shoreward grid point and is of direct influence on the cross-shore transport shoreward of  $h_{min}$ . Therefore, it can be used to calibrate the model to represent the development of the dry profile in a satisfactory manner. Indirectly, USTRA influences the bar development in the wet profile too.

Physically USTRA is determined by the wind transport at the shoreward boundary or by beach mining.

### Observations

- USTRA determines the sediment import or export at the shoreward boundary of the computational domain.
- USTRA influences the bottom height and total transport up to the 7 m depth contour during the sensitivity calculation runs with a duration of 1 year.
- USTRA can be used to calibrate the development of the dry profile, but this isn't realistic.

### 7.3.3 ALFAC and GAMMA

ALFAC [-] and GAMMA [-] are discussed simultaneously because both influence the dissipation of organized wave energy ( $D_w$ ) due to wave breaking, according to the bore model of Battjes and Janssen [1978]:

$$D_w = \frac{\rho g \cdot ALFAC \cdot H_{max}^2 Q_b}{4T_p} \quad (7.3)$$

Where:

$D_w$	dissipation of organised wave energy due to breaking	[ $W/m^2$ ]
$\rho$	density of the water	[ $kg/m^3$ ]
$H_{max}$	maximum possible wave height	[m]
$Q_b$	fraction of breaking waves	[-]

$$H_{max} = \frac{0.88}{k} \tanh\left(\frac{GAMMA \cdot kh}{0.88}\right) \quad (7.4)$$

Where:  $k$  local wave number [rad/m]

Battjes and Stive [1985] found an empirical relationship for GAMMA, for ALFAC assumed 1:

$$GAMMA = 0.5 + 0.4 \tanh(33s_0) \quad (7.5)$$



$$s_0 = \frac{H_{rms,0}}{L_0} \quad (7.6)$$

Where:	$s_0$	offshore wave steepness	[-]
	$H_{rms,0}$	offshore root-mean-square wave height	[m]
	$L_0$	offshore wavelength	[m]

This relationship is used as the default setting in Unibest-TC.

According to Equation (7.6)  $s_0$  is a function of the offshore wave height and wavelength. Since a strong relation between these two exists (depending on the wave field),  $s_0$  and thus GAMMA can be expressed as a function of  $H_{rms,0}$  for a certain wave data set.

It's also possible for the user to vary ALFAC and GAMMA according to his own view and calibrate the model in this way. Equation (7.3) reveals that  $D_w$  varies linearly with ALFAC. The variation of  $D_w$  with GAMMA isn't straightforward, because the fraction of breaking waves,  $Q_{br}$ , also depends on  $H_{max}$  (see Appendix C.3).

### Observations

Equation (7.5) is probably the best representation of physical reality and therefore recommended. When the modelling results aren't satisfactory, ALFAC and GAMMA can be varied at own insight. This leads to the following observations:

- Lower values of GAMMA result in lower values for the dissipation of wave energy due to bottom friction ( $D_r$ ) and higher values for the dissipation of wave energy due to breaking ( $D_w$ ).
- Lower values of GAMMA result in lower wave heights at a given depth.
- The magnitude of both suspended and bottom transport decreases for lower values of GAMMA.
- The magnitude of the bottom changes decreases for lower values of GAMMA.
- Increasing ALFAC leads to increasing dissipation due to wave breaking ( $D_w$ ) and to decreasing dissipation due to bottom friction ( $D_r$ ).
- With decreasing ALFAC, the magnitudes of cross-shore bottom and suspended transport increase [Van Thienen, 2003].
- Total cross-shore transport is more offshore directed with decreasing ALFAC.

### 7.3.4 BETD

BETD [-] is the slope of the face of the wave (normally between 0.05 and 0.10) and influences the dissipation of roller energy linearly.

$$\frac{\partial}{\partial x}(2E_r C \cos \theta) = D_w - Diss \quad (7.7)$$

Where:	$E_r$	roller energy	[J/m <sup>2</sup> ]
	$C$	wave celerity	[m/s]
	$\theta$	wave angle	[°]
	$Diss$	dissipation of roller energy	[W/m <sup>2</sup> ]

$$Diss = BETD \cdot 2g \frac{E_r}{C} \quad (7.8)$$

$Diss$  influences the shear stress in the direction of wave propagation on the middle layer (see Appendix C.3).

$$\tau_{s,wave} = \frac{Diss}{c} \quad (7.9)$$

Where:	$\tau_{s,wave}$	surface shear stress due to waves	[N/m <sup>2</sup> ]
--------	-----------------	-----------------------------------	---------------------

Together with the depth-independent forcing (see Appendix C.3) this shear stress induces the undertow. It also influences the streaming velocity near the bed, because the

dissipation term is used for the determination of the depth-averaged viscosity due to breaking waves. Influence outside the breaker zone is negligible, because no rollers are present.

#### Observations

- Increasing BETD leads to larger dissipation of roller energy.
- Increasing BETD leads to a smaller cross-shore velocity at 10 cm from the bottom.
- The magnitude of the total transport increases for larger values of BETD. The influence on the bottom and suspended transport depends on the value of non-dimensional parameter  $kh$  as stated by Sorgedraeger [2002].
- The influence on the bottom height is very small.

### 7.3.5 FWEE

FWEE [-] influences the dissipation of wave energy due to bottom friction ( $D_f$ ) in the organized wave energy balance (see Appendix C.3). It is of no direct influence in other physical processes in the model. In normal circumstances the dissipation due to bottom friction ( $D_f$ ) is approximately 10 times smaller than dissipation due to wave breaking ( $D_w$ ). Only outside the breaker zone, in relatively shallow water,  $D_f$  is important.

$$D_f = \frac{FWEE \cdot \rho}{\sqrt{\pi}} u_{orb}^3 \quad (7.10)$$

Where:  $D_f$  wave energy dissipation due to bottom friction [W/m<sup>2</sup>]  
 $u_{orb}$  amplitude of the wave orbital velocity based on linear wave theory and the  $H_{rms}$  [m/s]

#### Observations

- Bottom friction increases for increasing values of FWEE.
- The total transport is more onshore directed for higher values of FWEE.

### 7.3.6 F\_LAM and POW

F\_LAM [-] and POW [-] are treated simultaneously because both influence the breaker delay concept in Unibest-TC. This concept was introduced because wave breaking not only depends on the local water depth, but on the water depths to some distance seaward of the considered point. This is because a wave needs a distance in the order of one wavelength to start or stop breaking [Bosboom et al., 2000].

Therefore, a reference depth  $h_r$  is introduced, which replaces the depth  $h$  in Equation (7.4).  $h_r$  is determined by taking a weighed water depth seawards of the computational point, over a length  $X$ .

$$X = F\_LAM \cdot L_p \quad (7.11)$$

Where:  $X$  integration distance (seaward from computational point) [m]  
 $L_p$  local peak wavelength [m]  
 F\_LAM number of wavelengths for depth integration

The parameter POW determines the shape of the weighing function. For POW = 1, the weighing function is linear, for POW = 2 parabolic (more influence of water depths close to the computational point) etc. Hence a larger value of POW decreases the influence of the breaker delay function.

The influence of breaker delay is especially relevant in parts with large gradients in the bottom height, such as bars.

#### Observations

- Smaller values of F\_LAM result in less difference between the actual depth and the reference depth.
- Higher values of F\_LAM causes the dissipation due to wave breaking to concentrate more onshore, thereby increasing suspended sediment transport and thus increasing total transport in offshore direction.

- The higher total transport in offshore direction for higher values of F\_LAM causes a slightly higher bar.
- Higher values of POW result in less difference between the actual depth and the weighed depth.
- Smaller values of POW causes the dissipation due to wave breaking to concentrate more onshore, thereby increasing suspended sediment transport and thus increasing total transport in offshore direction.
- The higher total transport in offshore direction for smaller values of POW causes a slightly higher bar.

### 7.3.7 C\_R

C\_R influences the instantaneous current velocity, which is used to calculate bed load transport. It doesn't influence the average velocity and concentration profile, so the suspended transport is not altered. It determines the phase shift  $\varphi$  (see Equation (7.13)) between the long wave envelope and the short wave envelope.  $\varphi = -\pi$  for bound long waves, where high waves correspond with lowering of the water level and thus an offshore directed long wave velocity.

$$U(t) = \hat{u} \cos\left(\frac{\omega t}{m} + \varphi\right) \quad (7.12)$$

Where:	$\hat{u}$	amplitude of long wave orbital velocity	[m/s]
	$\omega/m$	frequency of long wave	[rad/s]
	t	time	[s]
	$\varphi$	phase shift between long and short wave envelope	[rad]
	m	number of waves in a wave group (=7)	[-]

$$\cos(\varphi) = C_R \cdot \left[ 1 - 2 \left( \frac{H_{rms}}{H_{rms,0}} \right)^2 \right] \quad (7.13)$$

Since the sediment concentration below high waves is larger than below low waves (due to a larger bottom shear stress), the bed load transport caused by bound long waves ( $\varphi = -\pi$ ) is directed offshore. The default value of C\_R is 0.25 according to an empirical relation by Roelvink and Stive [1989]. This leads to a low value of  $\varphi$ . When C\_R is increased, the situation approaches the bound long wave and the bed load transport is directed less onshore [Sorgedraeger, 2002].

The suspended transport isn't influenced directly by C\_R, but indirectly (via the bottom changes) the influence is quite large.

#### Observations

- The bottom transport is more on shore directed for lower values of C\_R.
- The suspended transport is only indirectly influenced, and the yearly average value increases.
- The total transport is more onshore directed for lower values of C\_R.
- Empirically C\_R should be 0.25, but this parameter can be altered to calibrate the model.

### 7.3.8 D50, D90 and DSS

D50, D90 and DSS are treated in the same paragraph because all three are sediment parameters. A strong correlation exists between these three variables. According to Van Rijn [1993], the diameter of suspended sediment ( $d_s$ ) is 60 to 100% of  $d_{50}$ . The relation between  $d_{90}$  and  $d_{50}$  depends on the grading of the material. For marine sands,  $d_{90}$  is between 120-140% of  $d_{50}$  [Van Rijn, 1998].

The incorporation of the grain size parameters in Unibest-TC is discussed below.

- Bed load transport.  $d_{50}$  is included in the dimensionless effective and critical shear stress. The transport diminishes with increasing  $d_{50}$ .
- Reference concentration near the bed. This is the concentration near the bottom, which is used as a boundary condition to solve the sediment concentration profile in the middle layer. On the one hand a larger  $d_{50}$  increases the reference concentration directly. On the other hand, a larger  $d_{50}$  increases the time averaged critical bed shear stress, thereby diminishing the reference concentration. It depends on the magnitude of  $d_{50}$  which effect is stronger.
- Suspended transport.  $d_s$  is included in the fall velocity and the mixing coefficient near the bed. A larger  $d_s$  therefore results in a smaller concentration and a smaller suspended transport. Therefore, the total transport becomes more onshore directed, since the suspended transport is directed offshore for the whole profile. This is confirmed by Veuger [2001].
- Effective bed shear stress. The effective bed shear stress is that part of the total bed shear stress which acts directly on the grains. It is calculated by multiplying the total bed shear stress with a factor  $\mu$ , defined in Equation (7.14). A larger  $d_{90}$  results in a larger effective bed shear stress and thus a larger suspended and bed load transport (while keeping RC constant).

$$\mu = \frac{f'_c}{f_c} = \frac{\left[ \log \frac{12h}{3d_{90}} \right]^{-2}}{\left[ \log \frac{12h}{RC} \right]^{-2}} \quad (7.14)$$

Where:  $d_{90}$  diameter which is exceeded by only 10% of the grains by weight [m]  
 RC current related roughness (see 7.3.12) [m]

In this sensitivity analysis the grain parameters  $d_{50}$  and  $d_{90}$  should have the same proportion to each other. Therefore, when the  $d_{50}$  is varied,  $d_{90}$  and  $d_s$  are varied with the same factor. However, since no measurements were done of  $d_s$  and no fixed ratio of  $d_{50}/d_s$  exists, also a variation of  $d_s$  (while keeping  $d_{50}$  and  $d_{90}$  constant) is performed.

The sets of grain sizes indicated in Table 7-2 are used as input in Unibest-TC. Run 1 and 2 have respectively smaller and larger grain sizes, while keeping the mutual proportions equal to the reference model; that is  $d_{90} = 1.2d_{50}$  and  $d_s = 0.8d_{50}$ . With run 3 and 4 the influence of varying  $d_s$  is investigated.

Table 7-2: Sets of grain sizes used in the sensitivity analysis.

	reference	run 1	run 2	run 3	run 4
D50 ( $d_{50}$ ) [mm]	0.33	0.25	0.40	0.33	0.33
D90 ( $d_{90}$ ) [mm]	0.40	0.30	0.48	0.40	0.40
DSS ( $d_s$ ) [mm]	0.264	0.20	0.32	0.20	0.33

### Observations

- With increasing D50, the suspended and bottom transport rates decrease. The total transport decreases too, except for some local maxima (due to the summation of positive and negative suspended and bottom transports).
- A larger D50 leads to more sediment import from deeper water.
- The suspended sediment transport increases for decreasing DSS (direct influence).
- The bottom transport is influenced only indirectly by DSS.
- The total transport is more offshore directed for smaller values of DSS.

### 7.3.9 FCVISC

In order to solve the equation in which the depth-mean velocity is related to the surface stress, the depth independent forcing and the streaming term, the depth averaged

viscosity  $\bar{\nu}_t$  must be known. This depth-averaged viscosity consists of the depth-averaged viscosity for a purely slope driven current, for a wind-driven current and of depth-averaged viscosity generated by wave breaking. This last term is modelled according to Battjes [1975]:

$$\bar{\nu}_{t,3} = FCVISC \cdot \left( \frac{Diss}{\rho} \right)^{1/3} L \quad (7.15)$$

Where:	$\bar{\nu}_{t,3}$	depth-averaged turbulent viscosity due to wave breaking	[m <sup>2</sup> /s]
	Diss	Dissipation of roller energy	[W/m <sup>2</sup> ]
	$\rho$	density of the water	[kg/m <sup>3</sup> ]
	L	typical length scale, set to $H_{rms}$ in Unibest-TC	[m]

Model experiments indicate that FCVISC [-] should be in the range of 0.05-0.10 when L is set to  $H_{rms}$ . A higher FCVISC gives a higher total turbulent viscosity, leading to a smaller velocity gradient over the depth.

Sorgedraeger [2002] states that increasing FCVISC leads to an increase of bed load sediment transport for breaking waves. The bed load transport for non breaking waves is decreased.

### Observations

- Cross-shore suspended transport decreases for increasing FCVISC.
- Cross-shore bottom transport becomes less onshore directed for non-breaking waves when FCVISC is increased.
- For breaking waves, cross-shore bottom transport becomes more onshore directed when FCVISC is increased.
- As a result, the total transport decreases for increasing values of FCVISC at  $T = 0$ . Van Thienen [2003] confirms that this behaviour occurs over a longer period too.

### 7.3.10 RKVAL

RKVAL [m] is the user-defined Nikuradse roughness height, directly influencing two parameters in the cross-shore mean current module:

#### The non-dimensional thickness of the wave boundary layer $\delta$

$$\delta = 0.09\alpha h A^{0.82} RKVAL^{0.18} \quad (7.16)$$

Where:	$\alpha$	coefficient to represent the influence of the irregularity of the wave field. $\alpha=1$ for regular waves, $\alpha = 20$ for irregular waves (fixed value in Unibest-TC)	[-]
	h	local waterdepth	[m]
	A	wave orbital excursion parameter	[m]

An increase of RKVAL results in a larger thickness of the wave boundary layer, thereby decreasing the velocity in the wave boundary layer and thus also in the middle layer. The influence of RKVAL via  $\delta$  on the on the cross-shore velocities is small due to the small power (0.18) in Equation (7.16).

#### The friction factor for dissipation due to bottom friction $f_w$

$$f_w = 1.39 \left( \frac{33A}{RKVAL} \right)^{-0.52} \quad (7.17)$$

An increase of RKVAL results in a larger  $f_w$  and thus a larger dissipation due to bottom friction ( $D_f$ ). This will increase the streaming function.  $f_w$  also has a positive quadratic influence on the turbulence in the wave boundary layer, which on its turn has a positive influence on both the undertow as the streaming velocity [Sorgedraeger, 2002].

Concluding we can state that an increase in RKVAL [Sorgedraeger, 2002]:

- Increases the on shore directed streaming induced suspended transport.
- Increases the offshore directed undertow induced suspended transport.
- Increases the on shore directed streaming induced bottom transport.
- The magnitude and net effect of a change in RKVAL depends on the local depth and wave parameters.

### The longshore water surface slope $i$

RKVAL also influences the longshore mean current. The longshore slope in the water surface is calculated with a user-defined longshore velocity at a certain depth and the equation of Chézy:

$$U = C\sqrt{hi} \quad C = 18 \log \left( \frac{12h}{RKVAL} \right) \quad (7.18)$$

Increasing RKVAL will lead to smaller longshore velocities and transports [Van Thienen, 2003]. Also the cross shore transport will decrease, since the longshore velocity influences the instantaneous velocity near the bed and thus the instantaneous bed shear stress.

### Observations

- Increasing RKVAL leads to a shift of energy dissipation in shoreward direction. This causes higher waves to reach the same depth [Van Thienen, 2003].
- Higher values of RKVAL cause higher suspended sediment transports (offshore directed) [Van Thienen, 2003] and higher bottom transports (onshore directed).
- The total transport becomes more onshore directed for higher values of RKVAL.

### 7.3.11 TANPHI1 and TANPHI2

The bed load transport is influenced by the bottom slope in two ways. First, the critical shear stress for a down slope movement is smaller than for an upslope movement. Secondly, the transport directly induced by gravity once the grains have been set in motion is taken into account. For this purpose the Bagnold parameter  $\beta_s$  (see for example Nipius [1998]) is introduced in the bed load transport formulation.  $\beta_s$  influences the bed load transport in a linear manner.

$$\beta_s = \left( 1 + \frac{\frac{u_{bx}}{|u_b|} \frac{dz_b}{dx}}{\tan \varphi} \right)^{-1} \quad (7.19)$$

Where:	$u_{bx}$	cross-shore component of near bottom velocity	[m/s]
	$u_b$	near bottom velocity	[m/s]
	$dz_b/dx$	bottom slope	[-]
	$\tan \varphi$	tangent of angle of repose	[-]

$\beta_s$  depends on  $\tan \varphi$ , a user-defined angle of repose, which may vary from the natural angle of repose.  $\tan \varphi$  can be defined at two cross-shore locations (XF1, XF2) with the corresponding parameters TANPHI1 (most offshore location) and TANPHI2 (most shoreward location). Unibest-TC uses linear interpolation to calculate  $\tan \varphi$  across the profile.

When the term between the brackets in Equation (7.19) approaches zero,  $\beta_s$  approaches infinity, leading to very large, unrealistic transports. This can only occur when  $u_{bx}$  is negative (seaward) or when  $dz_b/dx$  is negative (downward directed slope in onshore direction). Negative values for  $u_{bx}$  are not likely to occur. However, negative values for  $dz_b/dx$  are possible (bars). To avoid very large values of  $\beta_s$  and numerical instabilities, the proportion  $(dz_b/dx)/\tan \varphi$  should be smaller than ca 0.6. In Table 7-3 the values of TANPHI1 and TANPHI2 are indicated.

Table 7-3: Sets of values for TANPHI1 and TANPHI2 used in the sensitivity analysis.

		reference	run 1	run 2	run 3	run 4
XF1 = -500 m (seaward)	TANPHI1 [-]	0.15	0.05	0.30	0.15	0.15
XF2 = -10 m (landward)	TANPHI2 [-]	0.50	0.50	0.50	0.25	0.80

### Observations

- Small values of TANPHI in combination with downward slopes can cause unrealistic high transports.
- Higher values of TANPHI1 lead to higher bottom and total transports for upward slopes. This makes it a powerful tool to modify the sediment import from deep water.
- Higher values of TANPHI2 lead to higher bottom and total transports for upward slopes. For downward slopes, the transport decreases.
- Higher values of TANPHI2 cause a more pronounced bar.

### 7.3.12 RW

RW [m] represents the wave related bed roughness ( $k_{s,w}$ ) used to calculate the bed shear stress due to waves in the suspended load model. This bed shear stress determines the reference concentration near the bed and thus to a large extent the sediment concentration in the entire water column. In the bed load model RW is not used, since in this model  $k_s$  is a function of  $d_{90}$  and the critical shear stress parameter  $\theta'$ .

$$\langle |\tau_{b,w}| \rangle = \frac{1}{4} \rho f_w \hat{U}_\delta^2 \quad f_w = \exp \left[ -6 + 5.2 \left( \frac{\hat{A}_\delta}{k_{s,w}} \right)^{-0.19} \right] \quad (7.20)$$

Where:	$f_w$	wave friction factor according to Swart	[-]
	$\hat{A}_\delta$	peak value of near-bed orbital excursion parameter, based on $H_s$ and linear wave theory	[m]
	$k_{s,w}$	wave related roughness height. Equals RW in case of suspended load, function of $d_{90}$ in case of bed load	[m]
	$\tau_{b,w}$	bed shear stress, due to waves	[N/m <sup>2</sup> ]
	$\hat{U}_\delta$	peak value of near bed orbital velocity, based on linear wave theory and $H_s$	[m/s]

An increase in RW will lead to a higher value for  $f_w$  and a higher bed shear stress and reference concentration near the bed. This will cause larger suspended sediment transports.

### Observations

- Increasing values of RW lead to increasing suspended sediment transport, which causes more offshore directed sediment transport.
- The development of the dry and upper wet profile is influenced by RW, because RW indirectly determines the reference transport for the landward extrapolation procedure from  $h_{min}$  to the landward boundary.

### 7.3.13 RC

RC [m] represents the current related friction factor ( $k_s$ ) used to calculate the bed shear stress due to currents (with or without the presence of waves) in the suspended and bed load model.



$$\tau_{b,c} = \frac{1}{8} \alpha_r \rho f_c \bar{v}^2 \quad f_c = 0.24 \left[ \log \frac{12h}{k_s} \right]^{-2} \quad (7.21)$$

Where:	$f_c$	current friction factor	[-]
	$\alpha_r$	coefficient representing presence of waves	[-]
	$k_s$	current related roughness height (=RC)	[m]
	$\tau_{b,c}$	bed shear stress, due to currents (in presence of waves)	[N/m <sup>2</sup> ]
	$\bar{v}$	depth-averaged velocity	[m/s]

RC influences the efficiency factor for currents (see Equation (7.14)) too. It also influences  $\alpha_r$ . Furthermore, RC influences the current related mixing coefficient via the Chézy coefficient. So, the effect of a variation of RC isn't straightforward.

### Observations

- RC has no direct influence on the bottom transport.
- The suspended transport increases severely for decreasing values of RC.
- The total transport is directed more shoreward for increasing values of RC.
- For values of RC larger than 0.01m, the sediment concentrations in the water decrease severely [Van Thienen, 2003].

## 7.4 Sensitivity for the boundary conditions

The sensitivity of the model output to a variation of the boundary conditions is needed to make a founded statement about the reliability and accuracy of the model. The reference values of the boundary conditions (see Table 7-1) are varied to determine the influence on the model output. For plots of these output functions is referred to Appendix F.2.

### 7.4.1 Water level ( $h$ )

The water level variations in the project area during normal conditions are small: a tidal range of maximal 0.30 m and minor wind set-up (in the order of decimetres). The influence of these variations on the morphological behaviour is determined by implementing tidal water level variations in the reference model.

#### Conclusions

- Introducing the astronomical tide (with an amplitude of approximately 0.20 m) has a negligible influence on the bottom height.
- It is emphasized that very high water level variations (storm surges) will have severe influence on the profile development.

### 7.4.2 Wave height ( $H_{rms}$ )

The wave height has been varied to compare the results with the reference model ( $H_{rms} = 1.1$  m, see Table 7-1). The peak period ( $T_p$ ) has been held constant at its reference value of 6 s. Since the energy dissipation is proportional to the second or third power of the wave height, the influence of  $H_{rms}$  on the transports is very large. Higher  $H_{rms}$  will lead to higher transport rates because there is more energy present.

#### Conclusions

- Both the bottom and suspended transport increase for increasing  $H_{rms}$ .
- The total transport is directed onshore over the entire profile for lower values of  $H_{rms}$  and directed more offshore for high values of  $H_{rms}$ .
- It can be concluded that a correct input of  $H_{rms}$  is very important to achieve correct model results.



### 7.4.3 Wave angle ( $\theta$ )

The wave angle  $\theta$  has been varied to compare the results with the reference model ( $\theta = 10^\circ$ ). The influence of the wave angle on the transport rates and the bottom development depends to a large extent on the longshore (oceanic) current. As can be seen in Appendix F.2.20 the influence of  $\theta$  is small when the longshore current is absent. When a current of 1 m/s on a depth of 30 m is used, the influence of  $\theta$  is considerable. This can be explained by the fact that for  $\theta > 0$  the orbital velocity is partly longshore directed. This causes the instantaneous velocity (vector sum of longshore current and wave orbital motion) in longshore direction to increase severely, causing more sediment to be set in motion and thus increasing the bottom transport and suspended transport (via the reference concentration near the bed) in longshore and cross-shore direction.

#### Conclusions

- The influence of the wave angle depends on the presence of a longshore current.
- The influence can be significant, so attention has to be paid to a correct representation of  $\theta$  in the model.

### 7.4.4 Peak period ( $T_p$ )

The peak period has been varied to compare the results with the reference model ( $T_p = 6$  s).

#### Conclusions

- An increase of  $T_p$  causes an increase in both suspended and bottom transport.
- The total transport is directed more onshore for higher values of  $T_p$ .
- An accurate input of  $T_p$  is required for correct model output.

### 7.4.5 Wind speed ( $V_w$ )

The wind speed influences the cross-shore velocity distribution in the Unibest-TC model and is therefore important for the occurring transports. The wind speed has been varied to determine the consequences of this variation.

#### Conclusions

- Increasing wind speed causes a slightly lower onshore directed bottom transport, due to the slightly lower onshore current velocity near the bed. This is caused by the offshore directed return current in the lower part of the middle layer.
- The suspended sediment transport is slightly more offshore directed.
- The total transport is slightly more offshore directed.
- Since the influences are small it is assumed that an average wind speed can be used in the calibration procedure, because no exact measurements are available.

### 7.4.6 Longshore velocity $V$

The longshore velocity at a certain depth influences the longshore transport, but also the cross-shore transport. This because the instantaneous bed shear stress is calculated from the instantaneous current velocity, which is the vector sum of the longshore and cross-shore velocities. A higher value of  $V$  is expected to lead to higher bed load cross-shore transports. Also the suspended transport is expected to increase, since the reference concentration at the bed increases too.

#### Conclusions

- For moderate values of  $V$  (<1.0 m/s) no large influence is present on the occurring transports.
- For larger values of  $V$ , the offshore directed suspended sediment transport increases dramatically, due to a very large reference concentration.
- As discussed in Paragraph 7.4.3, the longshore velocity has a large influence on the transports in combination with the wave angle  $\theta$ .

## 7.5 Conclusions

### 7.5.1 Input parameters

It can be concluded that the input parameters determine model outcome to a large extent. The parameters have a direct (at  $t = t_i$ ) and indirect influence (via the time-stepping mechanism) on the output functions; the magnitude of this influence on the output functions differs per parameter.

The influence of each parameter on the output is summarized in Table 7-4, partly obtained from Van Thienen [2003]. Attention is paid to the suspended, bed and total transport, separately above and below the 5 m depth contour and to the development of the dry profile. Table 7-4 will be used for the calibration of the model in Chapter 8.

Table 7-4: Overview of the influence of input parameters on the important output functions, separately for below and above the 5m depth contour. The grading is as follows:

White	0	Practically no influence
Yellow	1	Little influence
Orange	2	Moderate influence
Red	3	Big influence

Comment: the influence of TANPHI depends on the location where it is imposed. Partly obtained from Van Thienen [2003].

Parameter type	Input parameter	Symbol	Suspended transport below MSL -5m	Bottom transport below MSL -5m	Total transport below -MSL -5m	Suspended transport from MSL -5m to 0m	Bottom transport from MSL -5m to 0m	Total transport from MSL -5m to 0m	Development of dry profile
General	TDRY	$T^*$	0	0	0	1	1	1	3
	USTR	$q_{tot,x}(x_{end})$	1	1	1	2	2	3	3
Wave	ALFAC	$\alpha$	0	0	0	1	1	1	0
	GAMMA	$\gamma$	1	1	1	3	3	3	2
	BETD	$\beta$	0	0	0	0	0	0	0
	FWEE	$f_w$	0	0	0	1	1	1	0
	F_LAM	$\lambda$	0	0	0	2	2	2	1
	POW	$P$	0	0	0	1	1	1	0
	C_R	$C_r$	0	2	2	3	3	3	2
Sediment	D50	$d_{50}$	0	3	3	3	3	3	2
	DSS	$D_s$	3	0	3	2	2	2	1
Current	FCVISC	$\alpha_w$	0	0	0	2	2	2	1
	RKVAL	$k_s$	1	3	3	3	3	3	1
Transport	TANPHI1	$\tan\phi_1$	0	2	2	0	0	0	0
	TANPHI2	$\tan\phi_2$	0	0	0	0	2	2	1
	RW	$k_{s,c}$	2	2	3	3	2	3	2
	RC	$k_{s,w}$	1	0	1	3	0	3	2

### 7.5.2 Boundary Conditions

Although a good representation of the boundary conditions is necessary for good modelling results, some boundary conditions are of minor importance.

The wave height ( $H_{rms}$ ) and the wave period ( $T_p$ ) are very important for the model results. The wave direction ( $\theta$ ) is less important. The normal water level variations  $h(t)$  can be neglected. The wind speed  $V_w$  cannot be neglected, but the use of monthly average values is permitted within reasonable limits. The longshore current  $V$  has almost no influence on the cross-shore transports for values up to 1 m/s (as occurring in reality). However, different combinations of  $V$  and  $\theta$  can cause differences in transport rates. So attention has to be paid to a correct representation of these two boundary conditions.

## 8 CALIBRATION AND VERIFICATION OF THE UNIBEST-TC MODEL

### 8.1 Introduction

The goal of this chapter is to adjust the default parameter setting of Unibest-TC in such a way that the model represents the real coastal behaviour in a sufficient way. Furthermore, the limitations of the calibrated model will be defined.

The sensitivity analysis of Chapter 7 serves as a reference for the calibration and verification described in this chapter. The final parameter setting will be used for the calculations in Chapter 9.

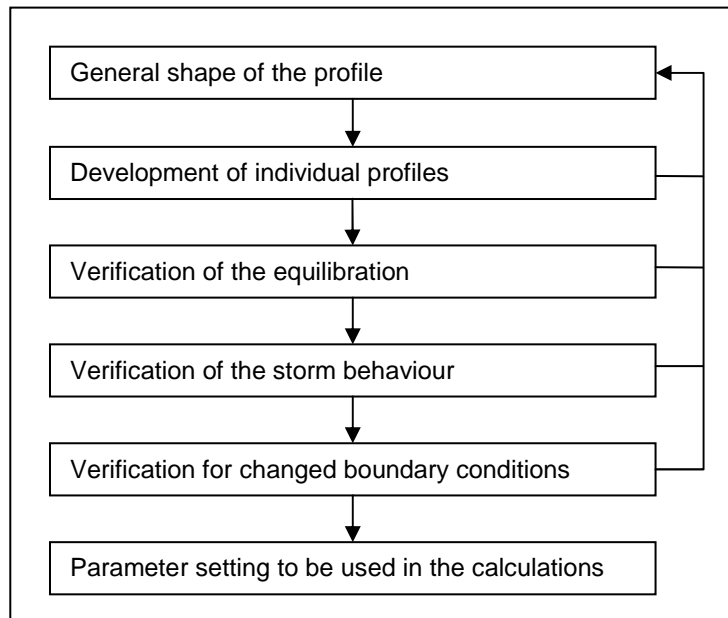
First, the approach of the calibration and verification is discussed (Paragraph 8.2). Then the boundary conditions are treated (Paragraph 8.3). The results for the final parameter setting are given in Paragraph 8.4. Subsequently, the changed input parameters will be discussed (Paragraph 8.5). Finally, the conclusions are presented in Paragraph 8.6.

### 8.2 Approach of the calibration and verification

The calibration and verification process can be characterized as a trail-and-error process. The input parameters are repeatedly changed to achieve the best correspondence between the model output and reality (see figure Figure 6-3 in Paragraph 6.3.4), following the approach illustrated in Figure 8-1.

Figure 8-1:

*Approach of the calibration.*



#### General shape of the profile

First the general shape of the profile has to be reproduced. To achieve this, the input parameters are changed until the calculated profile resembles the initial profile. Average

boundary conditions (varying per month) are used. The initial profile consists of longshore averaged profiles measured in February and June 2000.

#### **Development of individual profiles**

The development of a cross-section from a known initial state to a known end state should be modelled sufficiently accurate. Profiles measured at chainage 5+100, 6+100 and 8+300 in February 2000, June 2000 and March 2001 are used.

#### **Verification of the equilibration**

The development from a typical construction profile to an equilibrium profile is calculated. Common sense arguments are used to determine if the results are satisfactory.

#### **Verification of the storm behaviour**

The development of an equilibrium profile during a moderate storm is modelled. Common sense arguments are used to determine if the results are satisfactory.

#### **Verification for changed boundary conditions**

The influence of changes in the offshore longshore current and the grain size on the model results is determined, since both boundary conditions are uncertain.

## **8.3 Boundary conditions for the calibration**

### **8.3.1 Introduction**

Since the boundary conditions are uncertain, choices have to be made how these boundary conditions should be represented during the calibration. In this paragraph, the possibilities for each boundary condition are discussed, where after is decided which options are used in the various calibration stages.

### **8.3.2 Bottom profiles**

Ideally, the calibration consists of the calculation of the development of a given initial state (at  $T_0$ ) with given boundary conditions during a time  $\Delta T$ . The results are compared with the known real state at  $T_0 + \Delta T$  (see Figure 6-3). Therefore it is desired to have various measured bottom profiles at different times, e.g. every 3 months for 10 years. However, suitable measurements of bottom profiles were only performed in February and June 2000 and March 2001.

The following questions arise:

- Which cross-sections in the project area should be considered?
- Should individual or longshore averaged cross-sections be considered?

Cross-sections in the center of the project area (chainage 5+100m to 8+300m) will be used, since the longshore transport gradient is presumed to be small in this area (see Appendix B.7).

For the reproduction of the general shape of the profile (Paragraph 8.4.1) averaged profiles will be used to filter out noise in the bottom height like measurement errors, rip currents, beach cusps etc. This approach is recommended for profile models by Van Rijn et al. [2003, p. 299]:

*'Analysis of field data shows that the assumptions of longshore uniformity for Profile models often are severely violated because of the presence of rhythmic and non-rhythmic features. Thus, a basic question is whether a Profile model can be applied to an individual transect, because longshore variability may be so large that bed level changes of individual transects over short periods are not significantly different in statistical sense. A better approach is to apply the Profile models to longshore-averaged profiles.'*

For simulation of the development of individual profiles (Paragraph 8.4.2), single cross-sections will be used. This because averaged profiles have the disadvantage that bar -

trough features can disappear due to the averaging of the profile. It must be stated that no firm conclusions can be drawn based on the results for just one individual profile, since rip currents or longshore irregularities could be present.

### 8.3.3 Grain size

The grain size has a large influence on the sediment transports and bottom profiles in the area. Therefore it is desired to have detailed and precise information of the grain size across the profile. In the Unibest-TC model a cross-shore constant or varying grain size can be used. The latter means that the grain size  $d_{50}$  is a function of the water depth. Measurements of the grain size in the area are scarce (see Paragraph 3.2.3) so that only very little is known about the variation of the grain size in cross-shore sense. A first choice is to use a constant median grain size  $d_{50} = 0.32$  mm for the entire calibration process. The sensitivity of the calibration results for this assumption will be tested (see Paragraph 8.4.5).

### 8.3.4 Waves

Unibest-TC requires a definition file with the wave conditions ( $H_{rms}$ ,  $T_p$  and  $\theta$ ) defined in time. It is desired to use realistic wave input which resembles the wave conditions as occurred prior to the measurements of the bottom profiles in February and June 2000 and March 2001.

#### Possible sources of wave input

There are five options to create the time series of the waves ( $H_{rms}$ ,  $T_p$ ,  $\theta$ ):

1. From an average wave climate obtained from satellite data.
2. From the wave conditions measured by buoys (see Paragraph 3.2.5) in the considered period.
3. From the wave conditions measured by satellites in the considered period.
4. From a combination of source 1 and 2.
5. From a combination of source 1 and 3: scaled time series.

#### Ad 1

A monthly 3-dimensional scatter diagram of  $H_{rms}$ ,  $T_p$  and  $\theta$  is available based on satellite observations from [www.waveclimate.com](http://www.waveclimate.com) (see Appendix E.3.3).

The disadvantage is that these wave conditions differ from the wave conditions which occurred in reality. Secondly, this wave climate is based on satellite observations in a large area (400,000 km<sup>2</sup>), which is not necessarily representative for the project area. Finally the persistency of the real wave conditions isn't reproduced.

#### Ad 2

The second method does not have these restrictions. However, two buoys were on sheltered positions and the third buoy did not measure the wave height on an accurate manner. In addition, the measurements of the buoys were interrupted a number of times.

#### Ad 3

The third option gives reliable observations of the wave height, but observations of  $T_p$  and  $\theta$  aren't available. Furthermore, the temporal resolution of the measurements is very low (every 2 or 3 days).

#### Ad 4

The fourth option combines the advantages of the first two options. The directions and periods measured by the buoy are used (and transformed to the seaward border of the model). The wave heights measured by the buoy are corrected with a factor obtained from a comparison with the satellite observations in the same period. In the periods that the buoy didn't function, random drawings from the three-dimensional ( $H_{rms}$ ,  $T_p$ ,  $\theta$ ) scatter diagram obtained from satellite observations are used.

Although this method seems satisfactory, the wave heights measured by satellite and measured by the buoy are only moderately correlated (correlation factor of 0.70) and a

clear relation between the  $H_s$  measured by the buoy and the  $H_s$  measured by the satellite is not present. See Figure 8-2.

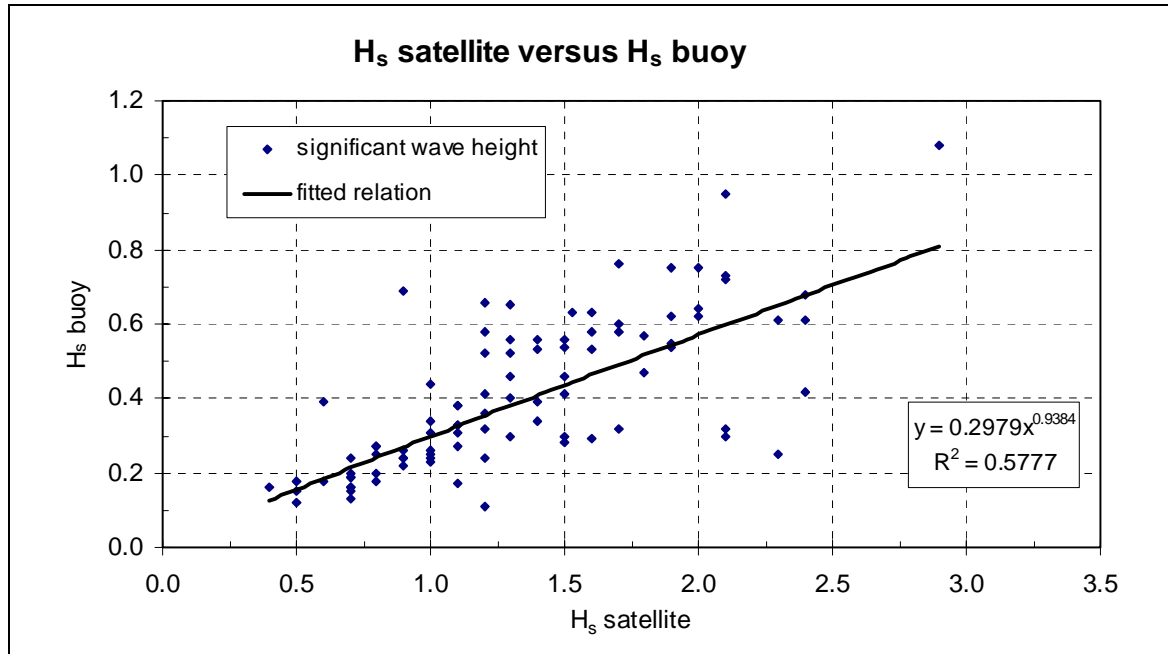


Figure 8-2: Satellite measurements [www.waveclimate.com] of the significant wave height ( $H_s$  satellite) versus the significant wave height measured by a (malfunctioning) buoy ( $H_s$  buoy) at the same time [\*, 2002]. The R-squared value of 0.577 indicates that no clear relation can be distinguished from the cloud of points. The fitted relation is therefore indicative only.

The absence of a proper relation between the wave heights measured by satellite and those measured by the buoy prevents the application of a correction factor for the wave height measured by the buoy. Furthermore, the buoy functioned only 50% of the time. Therefore this wave input isn't satisfactory.

#### Ad 5

This method uses both the monthly wave climate based on 10 years of satellite measurements and the satellite measurements of  $H_s$  during the considered period of the calibration (February 2000 to March 2001). The procedure is as follows:

- The following variables are defined:
  - $\bar{H}_{s,wc}$  monthly average significant wave height of the wave climate based on 10 years of satellite measurements.
  - $\bar{H}_{s,m}$  monthly average significant wave height based on satellite measurements between February 2000 and March 2001.
- Secondly, the generated wave height from the average wave climate is scaled with the proportion between  $\bar{H}_{s,wc}$  and  $\bar{H}_{s,m}$  according to Equation (8.1).

$$H_{s,wc,scaled}(t_i) = \frac{\bar{H}_{s,m}}{\bar{H}_{s,wc}} \cdot H_{s,wc}(t_i) \quad (8.1)$$

Where:  $H_{s,wc,scaled}(t_i)$  scaled significant wave height at time  $t = t_i$  in the considered month [m]  
 $H_{s,wc}(t_i)$  significant wave height at  $t = t_i$  generated from the average wave climate [m]

Finally, the wave period is corrected using a  $H_s$ - $T_p$  relation (see Appendix E.3.4). The result is a scaled time series of wave data for the calibration period.

## Conclusion

Every source of wave input has its specific disadvantages. Options 2 and 3 cannot be used since they lack sufficient temporal resolution (option 3) or give incorrect information (option 2). Option 1 might not represent the real conditions as they occurred in reality during the considered period and the persistency of the wave conditions is omitted. Option 4 cannot be used since the buoy measurements cannot be corrected in a statistically sound manner. Since the buoy only recorded during 50% of time, the difference between option 1 and 4 is small anyway.

Therefore a straightforward choice has been made: option 1, random generated time series of the waves out of a monthly 3-dimensional probability distribution of  $H_{rms}$ ,  $T_p$  and  $\theta$  based on 10 years of satellite measurements will be used to model the general shape of the profile. To improve the similarity of the model input with the real world, the scaled method (option 5) will be used in the modelling of the individual profiles.

In Appendix E.3.3 the generation of the time series of the waves is described, together with the other boundary conditions.

### 8.3.5 Longshore current

A constant longshore current on deep water with velocities up to 1 m/s from south to north occurs (see Appendix B.7). Ideally, this current should be measured accurately across the active profile to determine the velocity distribution close to shore. However, this measurements aren't available. The most likely value is a depth-mean velocity of 0.5 m/s to the north at a depth of 30 m. This value is used in the entire calibration and verification procedure. The influence of this boundary condition on the results will be checked (see Paragraph 8.4.5).

### 8.3.6 Water levels

The variation in water level during normal conditions is small (see Paragraph 3.2.7) and the influence on the profile development is very low (see Paragraph 7.4.1). Therefore, water level variations during normal conditions are omitted. For storm simulations a storm surge will be included.

### 8.3.7 Wind

Ideally, measurements of the wind speed and direction in the period prior to the measurements of the bottom profiles should be used as a model input. However, no measurements of the winds were performed during this period. The influence of the wind on the model results is quite small (see Paragraph 7.4.5). Therefore average wind speeds and directions for each month are used, based on satellite measurements from [www.waveclimate.com](http://www.waveclimate.com) (see Appendix B.5).

### 8.3.8 Resulting input file

The input files for the boundary conditions are presented in Appendix E.6.1.

## 8.4 Results of the calibration

In this paragraph the final results of the calibration phase are discussed. The approach described in Figure 8-1 has been used. In each subparagraph one step of the flow chart of Figure 8-1 is treated. The goal, approach, boundary conditions, results, discussion and conclusions of each step are briefly discussed. As indicated in Figure 8-1 the calibration is an iterative process: the parameter setting is changed repeatedly until all steps in Figure 8-1 are completed successfully. Only the results with the final parameter setting (see Appendix D) are discussed.

Reference is made to Appendix G for graphs of the results.



### 8.4.1 General shape of the profile

Stage:	<b>General shape of the profile</b> (see graphs in Appendix G.1)		
Goal:	Sufficient similarity between the averaged calculated profiles and the averaged measured profiles.		
Approach:	The parameter setting is changed until the calculated bottom profile after 1, 2 and 3 years resembles the initial measured bottom profile.		
Boundary conditions:	Waves	E.3.3	Generated time series of $H_{rms}$ , $T_p$ and $\theta$ out of the monthly averaged wave climate based on 10 years of satellite measurements.
	Wind	E.4	Constant monthly averaged wind speed and direction.
	Current	E.4	Constant depth-mean velocity of -0.5 m/s at 30 m water depth
	Water level	E.4	Constant water level at MSL.
	Bottom profile	E.5.2	Averaged bottom profiles over chainage 6+100, 6+300, 6+500, 6+700 and 6+900 measured in February 2000 and June 2000.
	Grain size	B.4.1	Constant across the profile: $d_{50} = 0.32$ mm
Results:	<p><b>Profiles</b> In Figure G-1 it can be seen that the calculated profiles in February each year resemble the averaged measured profile in February 2000, as is the case for the June profiles (Figure G-4). The area between <math>x = -40</math> m and <math>x = -100</math> m draws the attention: here the calculated profiles are significantly higher than the measured ones.</p> <p><b>Transport rates</b> From the average cross-shore transport rates in Figure G-2, it can be concluded that the bottom and suspended transport almost cancel each other out. The resulting average total transport is plotted in Figure G-3. The total transport is offshore directed in the upper part of the profile above the 2 m depth contour. More seaward, to MSL -8 m, the total transport is onshore directed, reaching a maximum of <math>7 \text{ m}^3/\text{year}/\text{m}</math> at the MSL -5 m line. Even further offshore, the total transport is directed seaward again.</p>		
Discussion:	<p>The upper part of the wet profile (above MSL-2 m) isn't modelled correctly. This is due to the extrapolation procedure from <math>h_{min}</math> (see Paragraph 7.3.1) to the seawall. This extrapolation is linear with the height and is a poor representation of the physical processes occurring in this area.</p> <p>The offshore directed bottom transport at deeper water is probably due to secondary wind-driven currents and stirring action of the longshore current and the wave orbital motion.</p>		
Conclusions:	<p>The Unibest-TC model can represent the averaged measured profiles reasonably well. The transport rates seaward of the 8 m line might be too much offshore directed, but this doesn't influence the upper part of the profile significantly in the considered calculation period. The model represents the average equilibrium conditions quite well, assuming that the averaged measured profiles are a good representation of the equilibrium conditions.</p>		



## 8.4.2 Development of individual profiles

Stage:	<b>Development of individual profiles</b> (see graphs in Appendix G.2)		
Goal:	Sufficient similarity between the measured individual profiles (in February 2000, June 2000 and March 2001) and the calculated profiles on the same dates.		
Approach:	The parameter setting is changed until the calculated bottom profile resembles the measured reference bottom profile. Profiles measured in February 2000 are used as initial profiles, profiles measured in June 2000 and March 2001 as reference profiles.		
Boundary conditions:	Waves	E.3.4	Scaled time series of $H_{rms}$ , $T_p$ and $\theta$ out of the monthly averaged wave climate based on 10 years of satellite measurements.
	Wind	E.4	Constant monthly averaged wind speed and direction.
	Current	E.4	Constant depth-mean velocity of -0.5 m/s at 30 m water depth.
	Water level	E.4	Constant water level at MSL.
	Bottom profile	E.5.1	Individual profiles at chainage 5100, 6100 and 8300, measured in February 2000.
	Grain size	B.4.1	Constant across the profile: $d_{50} = 0.32$ mm
Results:	<p><b>February to June 2000</b> (see Figure G-5)                  With the measured profiles of February 2000 as input, the calculated profiles of June 2000 correspond reasonably well with the measured ones. In general the erosion of the dry profile is slightly overestimated and the calculated bottom height between MSL -1 m and -3 m is slightly too high.</p> <p><b>February 2000 to March 2001</b> (see Figure G-6)                  The similarity between the measured and calculated profiles is quite low. The erosion of the dry profile is severely overestimated (chainage 5100 and 8300), as is the bottom height around the 4 m depth contour (all profiles).</p>		
Discussion:	<p>The discrepancy between the calculated and measured profiles can have three causes:</p> <ol style="list-style-type: none"> <li>1. Incorrect representation of the boundary conditions.</li> <li>2. Incorrect representation of (magnitude of) the physical processes.</li> <li>3. Errors in the measured profiles.</li> </ol> <p>As was concluded in Paragraph 3.5, quantitative information regarding the boundary conditions is lacking. Secondly, since individual profiles are considered, longshore effects might cast a cloud upon the results. Due to a lack of reliable data the question whether or not the (magnitude of the) physical processes is represented correctly remains unanswered.</p>		
Conclusions:	<p>The results for individual profiles are doubtful. The question arises whether or not the model can represent changes in profiles in an accurate manner. The weak foundation of the boundary condition input is probably a huge error source. It remains uncertain whether or not the model reacts correctly on time-varying boundary conditions.</p>		

### 8.4.3 Verification of the equilibration

Stage:	<b>Verification of the equilibration</b> (see graphs in Appendix G.3)		
Goal:	Reasonable results for the equilibration of a construction profile in the sense that the calculations are stable and the equilibrated profile shape is similar to the pre-nourishment profile shape.		
Approach:	The development of a construction profile to an equilibrium profile is modelled. The parameter setting is adapted until results are reasonable.		
Boundary conditions:	Waves	E.3.3	Generated time series of $H_{rms}$ , $T_p$ and $\theta$ out of the monthly averaged wave climate based on 10 years of satellite measurements.
	Wind	E.4	Constant monthly averaged wind speed and direction.
	Current	E.4	Constant depth-mean velocity of -0.5 m/s at 30 m water depth.
	Water level	E.4	Constant water level at MSL.
	Bottom profile	G-4	Calculated (equilibrium) profile by Unibest-TC in June, with a superimposed construction profile: slope 1:10, berm height of 2.5 m, added volume of 150 m <sup>3</sup> /m (see Figure G-7).
	Grain size	B.4.1	Constant across the profile: $d_{50} = 0.32$ mm
Results:	<p><b>Bottom height</b> (see Figure G-7) The construction profile evolves rapidly towards a new equilibrium state. Between MSL +0 m and MSL -5 m the pre-nourishment profile is shifted approximately 15 m seaward. Below MSL -5 m the bottom profile becomes steeper and meets the original profile at approximately MSL -7.5 m.</p> <p><b>Shoreline position</b> (see Figure G-8) First, the shoreline position decreases rapidly in time. The magnitude of this change (<math>dx/dt</math>) decreases with time, leading to a more or less exponential decay of beach width. This qualitative picture of exponential decay is confirmed by Dean [2002]. The low seasonal variation in shoreline position (approximately 4 m) draws the attention, because it is lower than observed in reality (approximately 10 m).</p> <p><b>Transport rates</b> (see Figure G-9) The yearly-averaged transport rate during the first year after construction reaches its maximum value of 126 m<sup>3</sup>/year/m at 90 m from the seawall.</p>		
Discussion:	The results discussed above seem to be qualitatively correct. Since no earlier nourishments were performed in the project area, no quantitative comparison with measurements could be performed. When the average transport rate during the first year of equilibration is compared with the average transport calculated in Paragraph 8.4.1, it can be concluded that the offshore directed transports during equilibration are 40 times as high.		
Conclusions:	The modelling results of the equilibration are qualitatively correct. No firm conclusions can be drawn whether the model represents reality correctly in a quantitative sense.		

#### 8.4.4 Verification of the storm behaviour

Stage:	<b>Verification of the storm behaviour</b> (see graphs in Appendix G.4)	
Goal:	Reasonable results for the storm behaviour of a profile in the sense that the calculations are stable and the equilibrated profile shape is similar to the pre-nourishment profile shape.	
Approach:	The development of an initial profile during a 2-day storm and the subsequent year is modelled. The parameter setting is changed until the results are reasonable. The assumed storm conditions represent a storm with a return period of approximately 5 year.	
Boundary conditions:	Waves	$H_{rms}(t) = 1 + 4.5\sin(\pi t)$ and $T_p = 7 + 11\sin(\pi t)$ during a 2-day storm. Average conditions during recovery phase.
	Wind	$V_w(t) = 8 + 30\sin(\pi t)$ during a 2-day storm. Average conditions during recovery phase.
	Current	Constant depth-mean velocity of -0.5 m/s at 30 m water depth.
	Water level	$h(t) = 0 + 1.6\sin(\pi t)$ during a 2-day storm. Average conditions during recovery phase.
	Bottom profile	G.5 A calculated equilibrium profile by Unibest-TC is used as the pre-storm profile(see Figure G-10).
	Grain size	B.4.1 Constant across the profile: $d_{50} = 0.32$ mm
Results:	<p><b>Bottom height</b> (see Figure G-10) It can be seen that the 2-day storm causes a severe shoreline retreat of about 17 m. This sediment is deposited between MSL -4 m and -8 m. After the storm the major part of this material is transported upwards again, but no full recovery to the original beach width occurs.</p> <p><b>Transport rates</b> (see Figure G-11) The 2-day storm causes severe transport rates. On average the maximum offshore directed transport rate is 32 m<sup>3</sup>/day/m. Even higher peaks occur.</p>	
Discussion:	Qualitatively the results seem correct. Since no measurements after storm conditions were performed in the project area, no quantitative comparison with measurements could be performed. When the average transport rate during the storm is compared with the normal conditions (see Paragraph 8.4.1), it can be concluded that the transports during the storm are in the order of 1000 times as high than during normal conditions.	
Conclusions:	The modelling results of the storm behaviour are qualitatively correct. No conclusions can be drawn whether the model represents reality correctly in a quantitative sense.	

### 8.4.5 Verification for changed boundary conditions

Stage:	<b>Variation of the longshore current</b> (see graphs in Appendix G.5)		
Goal:	Determine the influence of the longshore current on the calibration results.		
Approach:	The development of a measured profile is modelled during a period of one year for various values of the longshore current. The results are compared and the sensitivity of the calibration to this boundary condition is determined. This is done with the final parameter setting.		
Boundary conditions:	Waves	E.3.3	Generated time series of $H_{rms}$ , $T_p$ and $\theta$ out of the monthly averaged wave climate based on 10 years of satellite measurements.
	Wind	E.4	Constant monthly-averaged wind speed and direction.
	Current		Constant depth-mean velocity of -0.25, -0.50 and -0.75 m/s at 30 m depth.
	Water level	E.4	Constant water level at MSL.
	Bottom profile	E.5.2	Averaged bottom profiles over chainage 6+100, 6+300, 6+500, 6+700 and 6+900 measured in February 2000
	Grain size	B.4.1	Constant: $d_{50} = 0.32$ mm
Results:	<p><b>Transport rates</b> (see Figure G-12) The influence on the cross-shore total transports is high. For a lower longshore current (-0.25 m/s) the transport is more onshore directed. For a higher longshore current (-0.75 m/s) the transport is more offshore directed. The relatively high differences in total transports are caused by relatively small differences in suspended and bed transport.</p> <p><b>Bottom height</b> (see Figure G-13) In spite of the large changes in total cross-shore transports the influence on the calculated bottom heights after three years is low. This is because the gradients in the transport hardly change.</p>		
Discussion:	For time scales up to 3 years, the influence of the longshore current on the bottom elevation can be neglected. For longer time scales the cross-shore sediment balance can be altered significantly when using different longshore currents. Of course the longshore transport (especially just outside the surf zone) is very sensitive for the magnitude of the longshore current. Since the longshore transport gradient is assumed to be zero, this has no influence on the results.		
Conclusions:	The longshore current of -0.5 m/s is a safe assumption for the calculation of the beach fill equilibration in Chapter 9.		

<b>Stage:</b>	<b>Cross-shore variation of the grain size</b> (see graphs in Appendix G.5)		
Goal:	Determine the influence of a cross-shore varying grain size on the calibration results.		
Approach:	The development of a measured profile is modelled during a period of one year for a constant and a varying grain size distribution across the profile. The results are compared and the sensitivity of the calibration to this boundary condition is determined. This is done with the final parameter setting.		
Boundary conditions:	Waves	E.3.3	Generated time series of $H_{rms}$ , $T_p$ and $\theta$ out of the monthly averaged wave climate based on 10 years of satellite measurements.
	Wind	E.4	Constant monthly-averaged wind speed and direction.
	Current	E.4	Constant depth-mean velocity of -0.5 m/s at 30 m water depth.
	Water level	E.4	Constant water level at MSL +0 m
	Bottom profile	E.5	Averaged bottom profiles over chainage 6+100, 6+300, 6+500, 6+700 and 6+900 for February 2000
	Grain size	G.6	Constant: $d_{50} = 0.32$ mm. Varying along the profile: $d_{50} = f(z)$ , see Figure G-14.
Results:	<p><b>Transport rates</b> (see Figure G-15) The total cross-shore transport rate hardly changes: it is slightly more offshore directed on deeper water and slightly more onshore directed on shallow water.</p> <p><b>Bottom height</b> (see Figure G-16) The bottom heights after three years of calculations hardly differ.</p>		
Discussion:	The transport is different for the two considered grain size distributions. The differences are especially significant on deeper water and on the dry profile, where the transport is calculated by extrapolation.		
Conclusions:	The use of a constant grain size across the profile is permitted during the calibration.		

## 8.5 Final parameter setting

In this paragraph the final parameter setting which will be used for the calculations is discussed. In general the intention was to use the default parameter setting as much as possible. Only a few parameters have been changed. These are discussed below. For a complete list of the parameter setting, reference is made to Appendix D.

### **TDRY**

TDRY is the maximum value for the relative wave period  $T^*$ . A value for TDRY larger than 20 is preferred; smaller values limit the calculation area too much. For TDRY = 24 the best fit with the dry profile was created. Therefore this value has been chosen.

### **F\_LAM**

F\_LAM is the number of wavelengths for the depth integration in the breaker delay function. The default value for F\_LAM is 2, but the developers of Unibest-TC suggest that its value can be chosen smaller than 1 for steep beach profiles. The profile used here can be considered steep (approximately 1:40), so a value of 0.5 has been chosen. This gives best results for the bottom elevation around the 4 m depth contour.

### **TANPHI 1 & TANPHI 2**

The user-defined angle of repose ( $\tan\phi$ ) influences the bottom transport.  $\tan\phi$  can be defined at two cross-shore locations (XF1, XF2) as the corresponding parameters TANPHI1 (most offshore location) and TANPHI2 (most shoreward location). These parameters have been used to tune the cross-shore transport and to optimize the resemblance between the measured and the calculated bottom elevations.

### **RKVAL**

RKVAL [m] is the user-defined Nikuradse roughness height. This parameter has been increased to raise the offshore directed suspended sediment transport. In combination with an increase of RC, this leads to a better distribution of the suspended transport across the profile.

### **RC**

RC is the current related friction factor. RC has been increased to decrease the suspended sediment transport. Together with an increase of RKVAL, this leads to a better resemblance between measured and calculated bottom elevations.

### **ZDRY**

ZDRY can be either 0 or 1. The default value is 0, indicating that the extrapolation over the dry profile takes place linearly with the distance. When changed to 1, the extrapolation occurs linearly with the height. This is a better representation of reality during erosion conditions as occurring during beach fill equilibration. Therefore, ZDRY has been set to 1.

## 8.6 Conclusions

### **Limitations**

In general, the calibration phase was characterized by lack of good, reliable data of the boundary conditions and the bottom elevations. This has been a serious restraint for the calibration phase.

### **Calibration results**

The results of the Unibest-TC model with the final (calibrated) parameter setting can be characterized as follows:

- The representation of the average equilibrium conditions is good.
- The representation of changes in individual profiles remains questionable.
- The representation of the equilibration and storm behaviour is qualitatively OK.

Furthermore it can be concluded that:

- The model outcome is relatively insensitive to changes in the longshore current.
- The use of constant grain size along the profile is permitted in the calibration.

The final parameter setting resulting from the calibration process is presented in Appendix D and will be used in the modelling of the beach fill equilibration (Chapter 9) and storm behaviour (Chapter 11).

**Implementation of model issues**

Table 8-1 summarizes the way in which the relevant model issues (defined in Paragraph 4.5) are implemented in the calibrated Unibest-TC model for the equilibration of the beach fill.

Table 8-1: Use of the relevant model issues in the Unibest-TC model

Model issues		Unibest-TC model	
		Used?	Explanation
Equilibrium profile	current profile is in equilibrium	implicitly	Assumption used in the calibration of the model.
	current sediment is in equilibrium	implicitly	Assumption used in the calibration of the model.
	grain size dependent profile shape	implicitly	The profile shape is based on the underlying physical processes.
Granulometry	grain size distribution:	$d_{50F}$ $d_{50N}$	The grain size distributions are represented by the median grain size.
	grain size distribution across the profile	$d_{50}$ (h) not used	Median grain size can vary across the profile.
	time-varying grain size distribution across the profile	no	The grain size distribution is assumed to be constant in time.
Depth of closure		no	The assumption is not used
Underlying physical processes which cause morphology are considered		yes	Underlying physics are (partly) modelled
Time-varying processes and boundary conditions		yes	Boundary conditions and physical processes vary in time.

**Implications for the modelling of the equilibration and storm behaviour**

The following implications for the modelling of the equilibration and storm behaviour are defined:

- Since the final parameter setting is predominantly based on the correct representation of the –assumed- equilibrium profile, the calibrated model is based on the a priori identification of such an equilibrium profile. This implies that the Unibest-TC model fulfils part of the definition for equilibrium models (see Paragraph 4.4.1). The difference with real equilibrium models is that the model does describe the physical processes which cause the morphology.
- It remains questionable whether the final parameter setting gives quantitatively good results of severe out-of-equilibrium processes as the equilibration and storm behaviour in Chapter 9 and 11.
- This uncertainty can only be taken away with the use of measurements of both boundary conditions and bottom elevations. Since these aren't available, further validation of the model remains impossible.
- The results presented in the next chapters should therefore be interpreted with care.





## 9 MODELLING OF THE EQUILIBRATION IN THE UNIBEST-TC MODEL

### 9.1 Introduction

The goal of this chapter is to present the results of the modelling of the beach fill equilibration with Unibest-TC. The calibrated parameter setting created in Chapter 8 and presented in Appendix D is used for the calculations. In Chapter 10 part of the results presented in this chapter will be compared with the results of the equilibration design methods described in Paragraph 4.6 and Chapter 5.

First the approach of the modelling of the equilibration in Unibest-TC is discussed (Paragraph 9.2), after which the boundary conditions used in the model are defined (Paragraph 9.3). Subsequently, the results of the modelling are presented (Paragraph 9.4) and validated (Paragraph 9.5). Part of this validation is the interaction between the longshore and cross-shore transports (Paragraph 9.6). The chapter is completed with the conclusions (Paragraph 9.7).

### 9.2 Approach of the modelling of the equilibration

#### Goal of the modelling

The goal of the Unibest-TC model is to model the profile equilibration of the construction profile to a (dynamic) equilibrium profile. The following questions have to be answered by the model:

1. What is the dynamic equilibrium profile after equilibration?
2. What is the development of the equilibration in time and what is the characteristic time scale of the equilibration?

#### Parameter ranges

The influence of the following parameters on both the dynamic equilibrium profile after equilibration and the development of the equilibration in time has to be determined:

- The fill volume  $V$ : 150 – 200 – 250 – 300 – 350 – 400 m<sup>3</sup>/m.
- The berm height  $B$ : 2.0 – 2.5 – 3.0 m.
- The fill grain size  $d_f$ : 0.27 – 0.33 – 0.42 mm.
- The random generated time series of the waves [ $H_{rms}$ ,  $T_{pr}$ ,  $\theta$ ], all with the same statistical properties, but with a varying sequence (5 series in total).

Calculation runs have been made for all combinations of above parameters. A selection of the results is discussed in Paragraph 9.4.

#### Validation of the model results

The model results will be validated by investigating the influence of the following (uncertain) model input and assumptions (Paragraph 9.5):

- Wave climate; all  $H_{rms}$  in the normal time series of the waves will be made smaller by 10% (calm year) and larger by 10% (heavy year).
- Shape of the construction profile.
- Omission of persistency of wave conditions.
- Starting time of the calculations.
- Computational step size  $dx$ .
- Presumed absence of a longshore transport gradient.

## 9.3 Boundary conditions for the modelling of the equilibration

### 9.3.1 Introduction

The boundary conditions in the project area are uncertain. In this paragraph the various options to represent these boundary conditions are discussed, where after is decided which options are used in the modelling of the equilibration. In general the same boundary conditions as in the calibration and verification phase are used (see Paragraph 8.3).

### 9.3.2 Bottom profiles

The following questions arise:

1. Which cross-sections in the project area should be considered?
2. Should individual or longshore averaged cross-sections be considered?
3. Which profile(s) should be used as a base for the fill: profiles calculated by Unibest-TC or measured profiles?
4. Which slope(s) of the construction profiles should be considered?

#### Ad 1

The cross-sections in the center of the project area (chainage 6+100 to 6+900 m) will be used, since the longshore transport gradient is assumed to be low at this location (see Appendix B.7).

#### Ad 2

Longshore averaged profiles will be considered as this filters out longshore rhythmic and non-rhythmic features (see Paragraph 8.3.2). Profiles between chainage 6+100 to 6+900 will be averaged, since the longshore transport gradient is probably low in this area (see Appendix B.7).

#### Ad 3

As has been concluded in the previous chapter (see Paragraph 8.4 and 8.6), differences between the measured and calculated profiles are present. To avoid interference of these differences with the interpretation of the calculation results, an equilibrium profile calculated by Unibest-TC is used as a base for the fill. The equilibrium profile is calculated in June, since this is the planned construction month [\*, 2002], see Paragraph 9.3.8. The equilibrium profile is visualized in Figure 9-1, together with the construction profiles.

#### Ad 4

In reality the construction slope depends on the grain size, wave conditions, tide, currents and construction methods. Values between 1 to 5 and 1 to 15 are reasonable for medium size sands. Therefore a slope of 1 to 10 has been used in the calculations, both above and below the water line. The sensitivity of the final profile shape, the equilibration time scale and the shoreline advancement to this assumption is low (see Paragraph 9.5.3).

Using above assumptions, various construction profiles have been created with different berm heights and fill volumes, which can be seen in Figure 9-1.

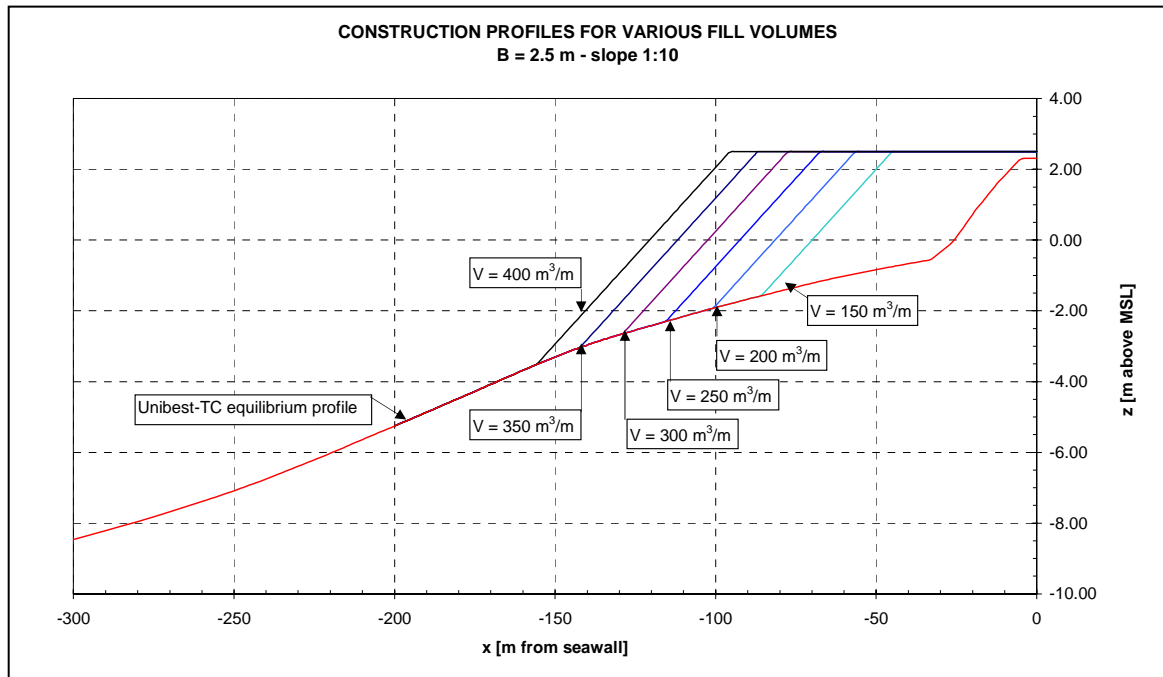


Figure 9-1: Construction profiles for various fill volumes. The equilibrium profile of Unibest-TC in June is used as a base for the fills. This equilibrium profile has been created in Chapter 8.

### 9.3.3 Grain size

In reality the grain size varies across the profile. In Unibest-TC the grain size can be varied over the height or can be held constant. The latter option was used in the calibration phase; sensitivity of the model results to this assumption was low (see Paragraph 8.4.5).

The placement of the fill introduces new grain sizes in the profile. In Paragraph 4.5 it was concluded that the distribution of the grain size over the height will vary in time because of the following processes:

1. Sorting due to construction processes.
2. Displacement of the fill sediments during equilibration.
3. Sorting of the fill sediments across the profile.
4. Mixing of the fill and native sediments.

The magnitude and time scale of these processes depend on the size distribution of the fill and native sediments and on the occurring wave and current conditions after and during construction, but in general the following characteristic time scales can be recognised: the first process has a time scale of hours to days, the second of weeks to months (see Paragraph 9.4.3) and the third and fourth of weeks to years.

With the current state of knowledge regarding this subject, the distribution of sediment size over the height and its variation in time cannot be determined. However, there are a few simplifying ways to incorporate a grain size variation over the bottom height in the Unibest-TC modelling of the profile equilibration, which are visualized in Figure 9-2:

1. **Block:** the grain size equals the fill grain size ( $d_f$ ) above the intersection point (here set at -2.5 m, see Figure 9-1) with the original profile; below this point the grain size changes to the native  $d_N$ . Process 2 to 4 are assumed to have minor influence on the profile equilibration and are disregarded.
2. **Linear:** the grain size equals the  $d_f$  in the upper part of the profile after which it increases/decreases gradually in the  $d_N$ . Process 1, 2 and 4 are incorporated and are assumed to occur instantaneously.
3. **Mixed:** The grain size has a constant value across the profile, between the sizes of the native and fill sediments, depending on the proportion between the sediment

volumes involved. Below the intersection point (MSL -7.5 m) the grain size is the same as native. With this approach, process 2 and 4 are assumed to be dominant and to occur instantaneously.

4. **Covered:** the fill grains cover the native grains up to the intersection point. Process 2 is assumed to be dominant during the profile equilibration
5. **Time varying:** a distribution as in the linear type is used, but the point of intersection and the degree of mixing vary in time. Calculations with Unibest-TC are stopped after e.g. 50 days after which the grain size distribution across the profile is changed and calculations are continued again, etc. Process 1, 2 and 4 are incorporated and differences in time scales can be applied.

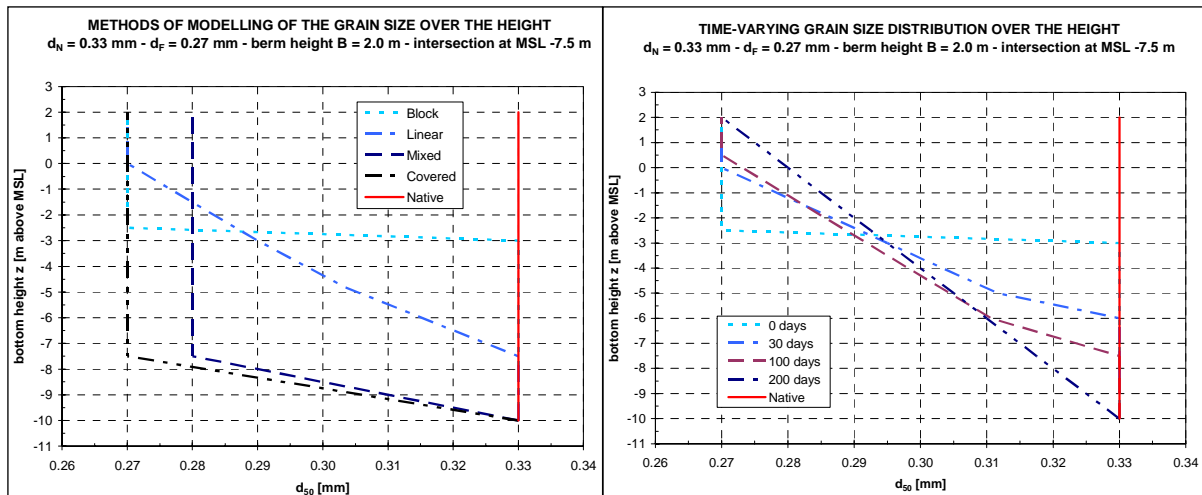


Figure 9-2: Methods to model the variation of the grain size over the height in the cross-shore profile during the equilibration. The native grain size is assumed to be constant over the height. The values of the distributions have been chosen arbitrarily; the objective is to visualize the differences in approach, not to give real values for the grain size distributions over the height. Left frame: block, linear, mixed and covered method. Right frame: time-varying linear method.

Comparison of the profile equilibration with the five cross-shore grain size distributions above shows that the differences in bottom heights are low in the considered one year period. This can be seen in Figure 9-3.

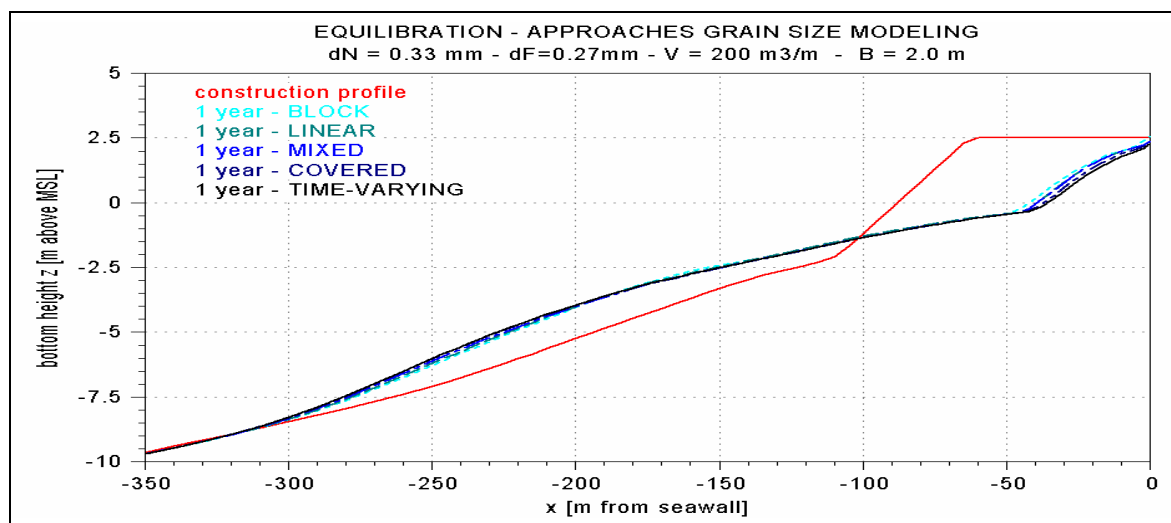


Figure 9-3: Equilibrated profiles according to Unibest-TC after one year for 5 types of grain size distribution over the height.

Since very little is known about the variation of sediment size over the height and its variation in time, a simple approach is chosen. Method 4 (the fill grains cover the native grains instantaneously) will be used to model the equilibration in Unibest-TC. It is emphasized that this is an incorrect representation of reality, since it ignores dynamic sorting and mixing of the grains.

### 9.3.4 Wave conditions

Unibest-TC requires a definition file with the wave conditions ( $H_{rms}$ ,  $T_p$  and  $\theta$ ) defined in time. The possibilities to generate the wave input for the model have already been discussed in Paragraph 8.3.4. The wave input used in the modelling of the equilibration will consist of random generated time series out of a monthly 3-dimensional probability distribution of  $H_{rms}$ ,  $T_p$  and  $\theta$  based on 10 years of satellite measurements (see Appendix E.3.3). Various time series will be used to determine the influence of variations due to the random character of the time series.

Furthermore, the sensitivity of the modelling results to variations in the wave climate will be investigated in Paragraph 9.5.2. A heavier year and a calmer year will be considered by increasing and decreasing the random generated root-mean-square wave height with 10%.

### 9.3.5 Longshore current

A mean velocity of 0.5 m/s from south to north at a depth of 30 m will be used, just as during the calibration phase, see Paragraph 8.3.5. Sensitivity of the model results to this uncertain boundary condition is low, see Paragraph 8.4.5.

### 9.3.6 Water levels

The variation in water level during normal conditions is small (see Paragraph 3.2.7) and the influence on the profile development is very low (see Paragraph 7.4.1). For simplicity's sake, water level variations during normal conditions are omitted.

### 9.3.7 Wind

Monthly averages of wind speed and a yearly average wind direction are used, as more detailed information isn't available, just as during the calibration phase, see Paragraph 9.3.7.

### 9.3.8 Construction period

According to \* [2002], the fill is placed during the summer months. It is expected that the considered chainage 6100 – 6900 m in the centre of the project area will be constructed at the end of June or beginning of July. Therefore the calculation starting time  $T_0$  is at day 180 in the year (end of June). The influence of the starting time on the results will be determined in Paragraph 9.5.5. Unless stated otherwise,  $T_0$  will represent day 180 of the year and day 0 of the simulation time.

### 9.3.9 Conclusions

Above boundary conditions are assumed to be a fair representation of reality, relevant for the modelling of the profile equilibration. The results of the modelling with these boundary conditions are presented and discussed in Paragraph 9.4. The results are validated in Paragraph 9.5 to determine the sensitivity of the results for assumptions made in this paragraph.

## 9.4 Results of the modelling of the equilibration

### 9.4.1 Introduction

With the boundary conditions defined in Paragraph 9.3, a large number of runs with the Unibest-TC model are made for all combinations of variables ( $d_F$ ,  $V$ ,  $B$ , wave time series) discussed in Paragraph 9.2. A selection of the model results is discussed in this paragraph.

### 9.4.2 Bottom profiles and cross-shore transports

#### The first year after construction

In Figure 9-4 the development of a construction profile ( $V = 250 \text{ m}^3/\text{m}$ ,  $B = 2.5 \text{ m}$ ,  $d_F = 0.33 \text{ mm}$ ) during the first year after construction is visualized. Also the occurring total cross-shore transport for standard wave conditions is plotted.

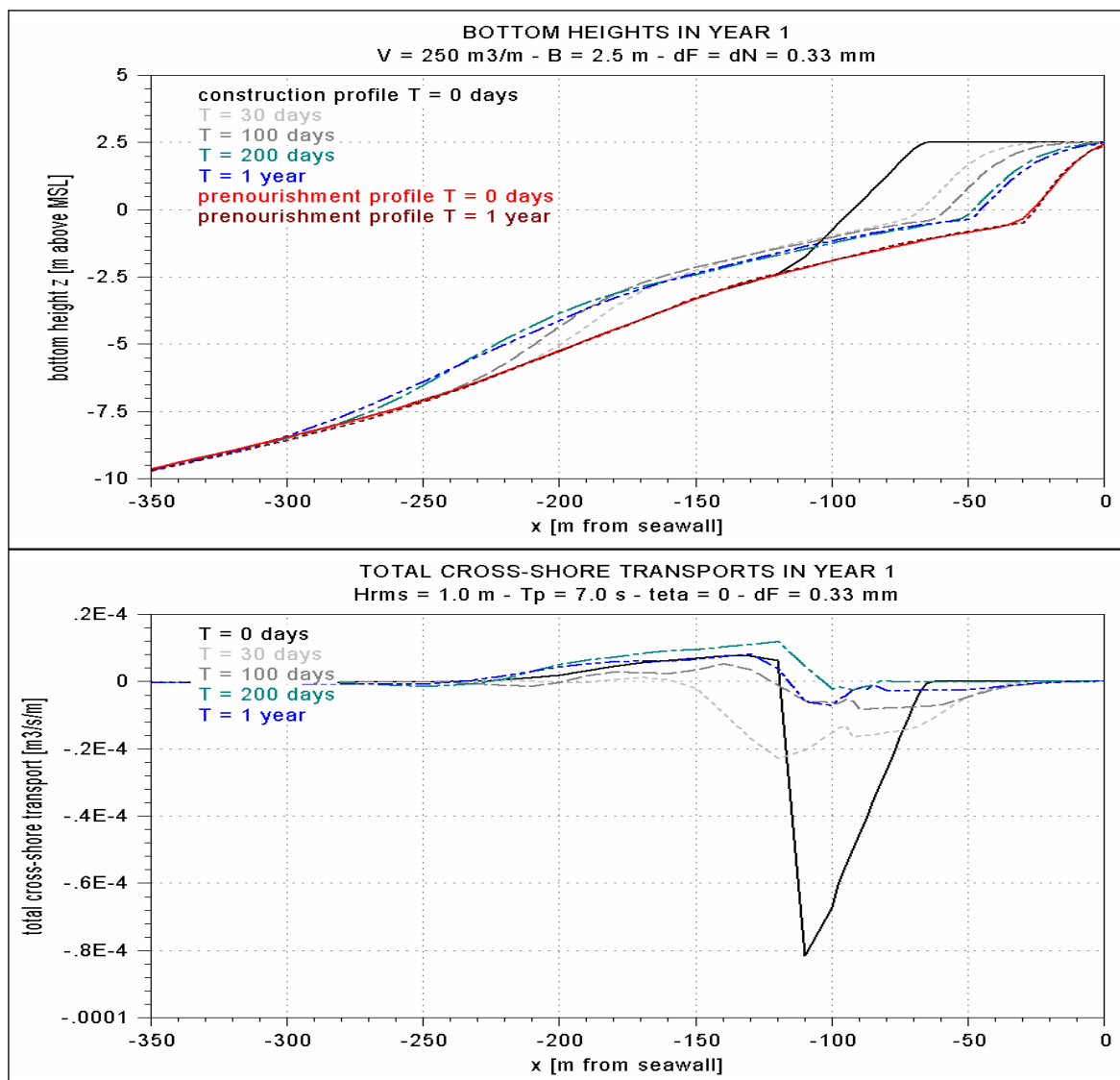


Figure 9-4: Upper panel: Development of a construction profile at  $T = 0$  days to an equilibrated profile at  $T = 1$  year compared with the autonomous development of the dry profile according to Unibest-TC for a normal wave climate  
 Lower panel: Total (bed + suspended load) instantaneous cross-shore transports during the equilibration for standard wave conditions.

The following observations can be made:

- Rapid erosion of the upper part and accretion of the lower part of the profile occur.
- This profile change slows down as the equilibration continues.
- The deposition in the lower profile extends to MSL -8.5 m, but significant changes occur to MSL -7.5 m.
- The profile shape after one year is almost parallel to the prenourishment profile.
- The offshore directed total cross-shore transport (for standard wave conditions) is very high for the initial profile and becomes smaller as the equilibration continues.

### The second year after construction

The behaviour of the prenourishment and nourished profiles in the second year after construction is shown in Figure 9-5. The average total cross-shore transports during this year are plotted too.

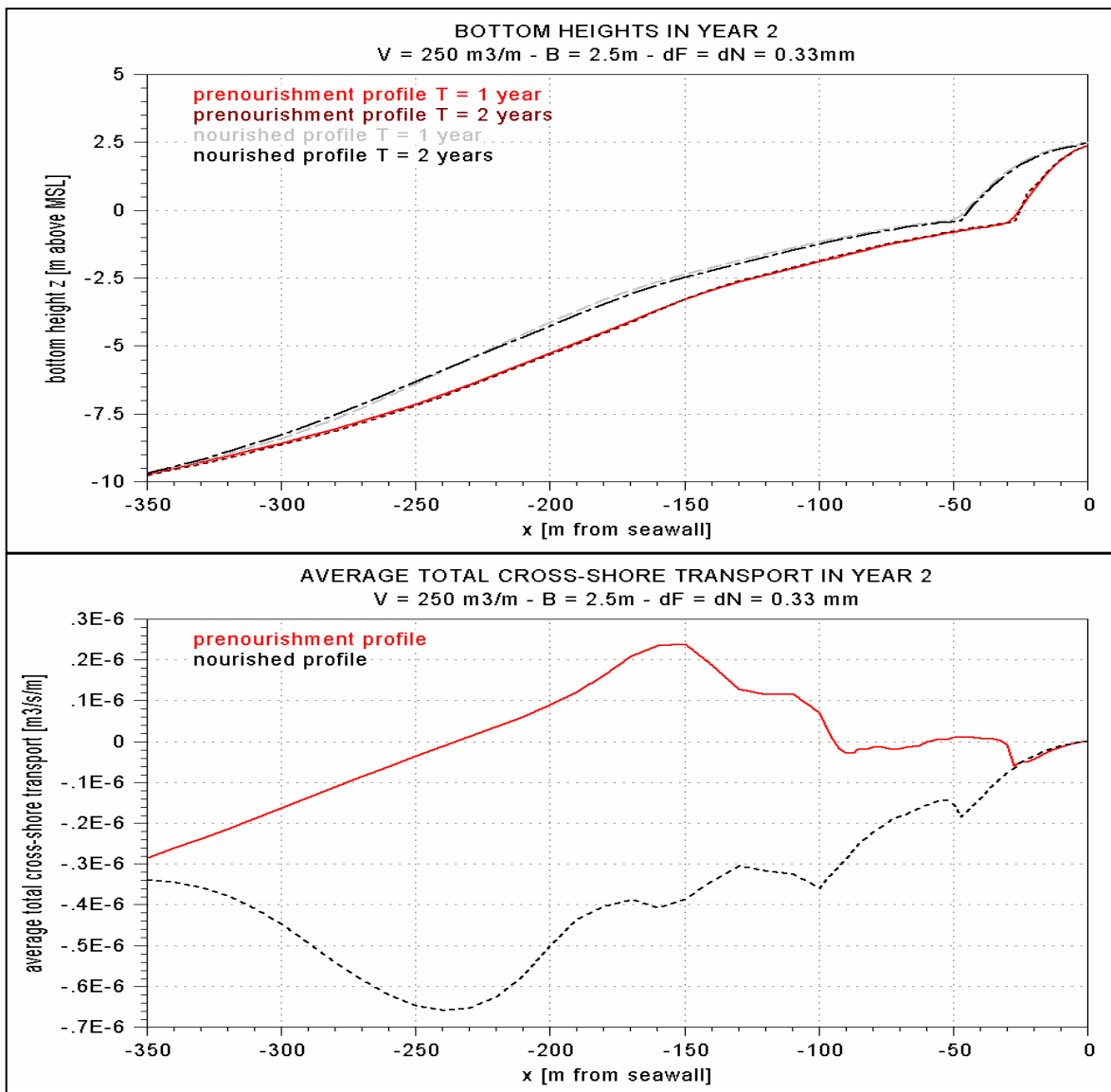


Figure 9-5: Upper panel: profile development during the second year after construction of the nourished (black and grey lines) and the prenourishment profile (red lines)  
 Lower panel: average total (bed + suspended load) cross-shore transport in the second year after construction for both the nourished and prenourishment profile.

The following observations can be made:

- In the second year, the shape of the nourished profile hardly changes. Some sediment is eroded from the upper part and deposited near the toe of the profile.
- The not-nourished profile is slightly accreting in the upper part of the profile.
- The average total cross-shore transports of the original and nourished profile differ a lot.
- The average total cross-shore transport is low: a maximum of approximately 20 m<sup>3</sup>/m/year for the nourished profile.

### Results for fill sediments other than native

In Figure 9-6 the calculated profiles after one year for three fill grain sizes are plotted.

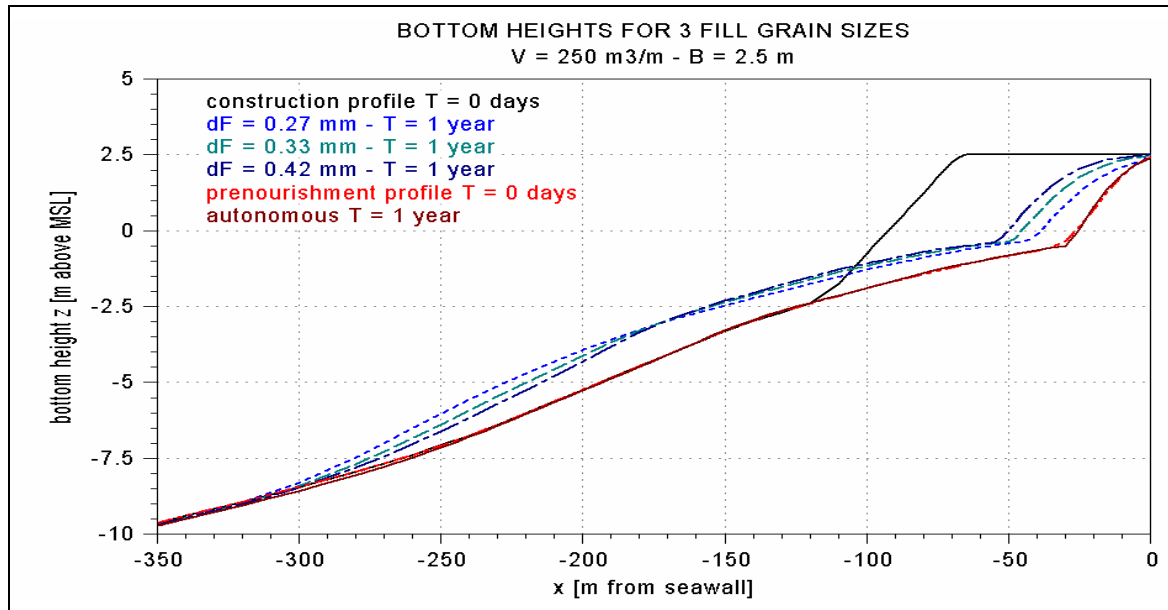


Figure 9-6: Calculated bottom profiles after one year for different fill grain sizes  $d_f$ .

The following observations can be made:

- The larger the fill sediments, the steeper the deeper part of the profile.
- Finer fill grains result in smaller shoreline advancement.

### Discussion

The large cross-shore transports and rapid erosion can be explained by the severe out-of-equilibrium state of the profile. Wave energy is dissipated in a small water volume compared with the prenourishment profile, leading to high turbulence and high transports. When the equilibration continues, wave energy dissipation is more spread out and the cross-shore transports decrease.

The eroded volume for the larger grains is smaller compared with the fine grains. This is caused by the fact that the large grains can resist larger forces and thus erosion is smaller, i.e. the wave energy dissipation is spread out over a smaller water volume for larger grains, resulting in a steeper and higher bottom profile.

The profile changes in the second year after construction are low. The results in this period are less reliable than in the first year. The profile is almost in dynamic equilibrium and sediment transports are low, making that small errors in the Unibest-TC model (see Paragraph 8.6) can cast a cloud upon the results.

### Conclusions

The following conclusions can be drawn:

- The equilibration is almost complete one year after placement of the fill.
- The model results after more than one year become less reliable due to inaccuracies in the calibrated model.
- Larger fill grains result in steeper deep water profiles and more shoreline advancement.



### 9.4.3 Development of the shoreline position in time

#### Introduction

In Paragraph 9.4.2 was determined that rapid profile change occurs, because the construction profile is in a severe out-of-equilibrium state. This profile change consists of erosion in the upper part of the profile and deposition in the lower part, leading to a shoreline retreat in time.

The symbol for the shoreline position used in this paragraph is  $y_0$ , since this is in correspondence with the coordinate system used in this thesis (see Appendix A.2). The origin of this  $y$ -axis is at the seawall. The additional dry beach width  $\Delta y_0$  is defined as the difference in shoreline position between the prenourishment profile and the nourished profile and is a function of time. The shoreline is defined as the intersection between MSL and the bottom profile.

#### Shoreline position in time

The retreat of the shoreline is visualized in Figure 9-7 for a fill volume  $V$  of  $250 \text{ m}^3/\text{m}$  with a median fill grain size  $d_F$  of  $0.33 \text{ mm}$  and a berm height  $B$  of  $2.5 \text{ m}$  placed under a 1 to 10 slope. The shoreline position has been calculated for five time series of the waves with the same statistical properties, but a different sequence of wave conditions.

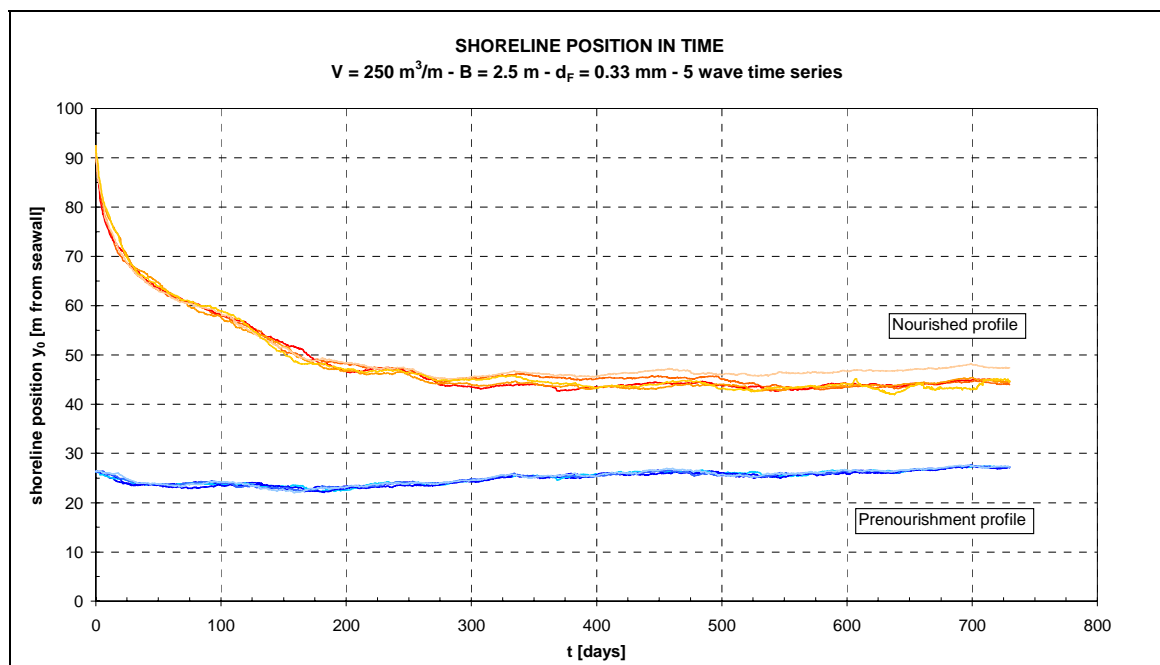


Figure 9-7: Development of the shoreline position  $y_0$  in time according to Unibest-TC for a construction profile and the prenourishment profile. Five time series of the waves with the same statistical properties have been used (see Paragraph 9.3.4).

The following observations can be made from this graph:

- The rate of shoreline change decreases in time.
- After approximately 300 days no significant change of shoreline position occurs.
- The shoreline position varies a little depending on the time series of the waves used. These variations are especially present after the equilibration is (almost) complete and are in the order of meters.
- The autonomous development (without the fill) of the prenourishment shoreline is slightly seaward.
- Sensitivity of the autonomous development of the shoreline to the time series of the waves used is negligible.

In Figure 9-8 the additional dry beach width  $\Delta y_0$  is plotted for three median fill grain sizes  $d_F$ . It shows the same behaviour as the shoreline position  $y_0$  in Figure 9-7.

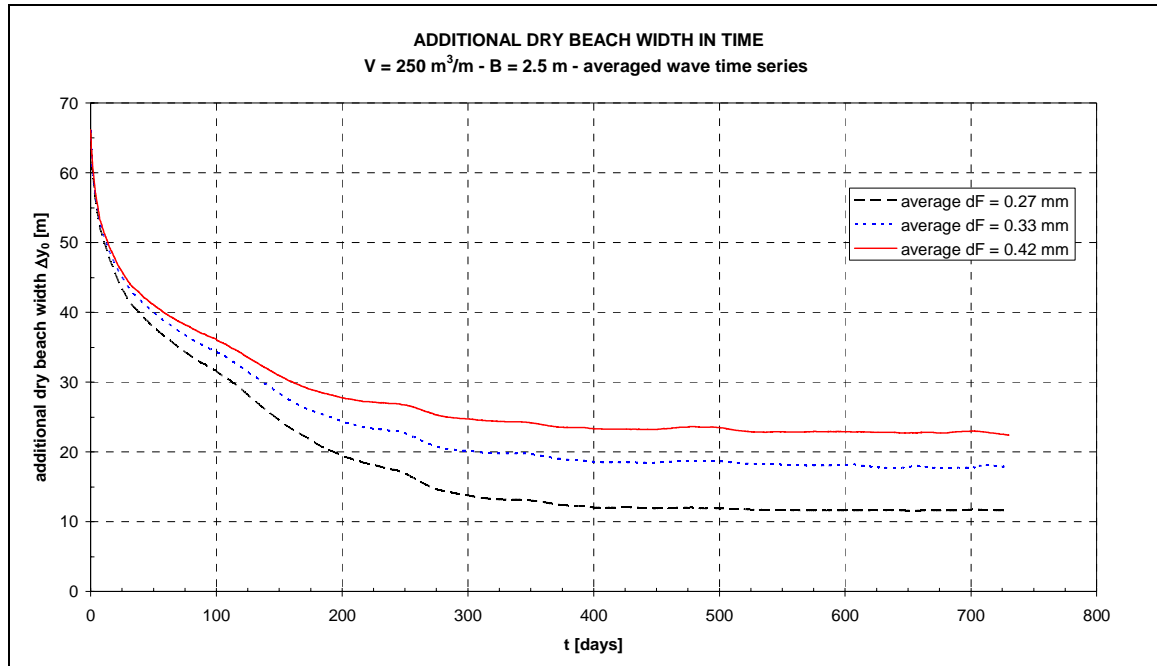


Figure 9-8: Development of the additional dry beach width  $\Delta y_0$  in time for three fill grain sizes  $d_F$ . Each line is an average of five different time series of the waves (see Figure 9-7).

The following observations can be made from this graph:

- The additional dry beach width  $\Delta y_0$  increases significantly with the median fill grain size  $d_F$ .
- The equilibration time scale is approximately the same for the grain sizes considered.

#### 9.4.4 Comparison with an exponential expression

##### Introduction

Dean [2002] suggested an expression with an exponential decay of the additional dry beach width  $\Delta y_0$  in time as in Equation (9.1).

$$\Delta y_0(t) = \Delta y_{0,EQ} + [\Delta y_0(0) - \Delta y_{0,EQ}] \cdot e^{-t/T_{EQ}} \quad (9.1)$$

Where:	$\Delta y_0(t)$	additional dry beach width in time	[m]
	$\Delta y_{0,EQ}$	additional dry beach width after equilibration	[m]
	$\Delta y_0(0)$	additional dry beach width of the construction profile	[m]
	$T_{EQ}$	equilibration time scale	[days]

Equation (9.1) is fitted to and compared with the results from the Unibest-TC model according to the following definitions:

- The values of  $\Delta y_{0,EQ}$  are averages of  $\Delta y_0(t)$  between  $t = 400$  days and  $t = 450$  days after construction to filter out short term variations.
- The fit is made for values of  $\Delta y_0(t)$  in the range given by Equation (9.2). This to avoid influence of the very small values of  $\Delta y_0(t)$  in the results of the fit of  $T_{EQ}$ .

$$1 \geq \frac{|\Delta y_0(t) - \Delta y_{0,EQ}|}{|\Delta y_0(0) - \Delta y_{0,EQ}|} \geq 0.025 \quad (9.2)$$

The influence of the following variables on the equilibration time scale  $T_{EQ}$  is investigated:

- The fill grain size  $d_F$ .
- The berm height  $B$ .
- The fill volume  $V$ .

To explain these influences, the eroded (and deposited) volume  $V_e$  is determined together with the distance  $X_e$  over which this eroded volume is moved to the location where it is deposited. These two parameters are defined in Figure 9-9.

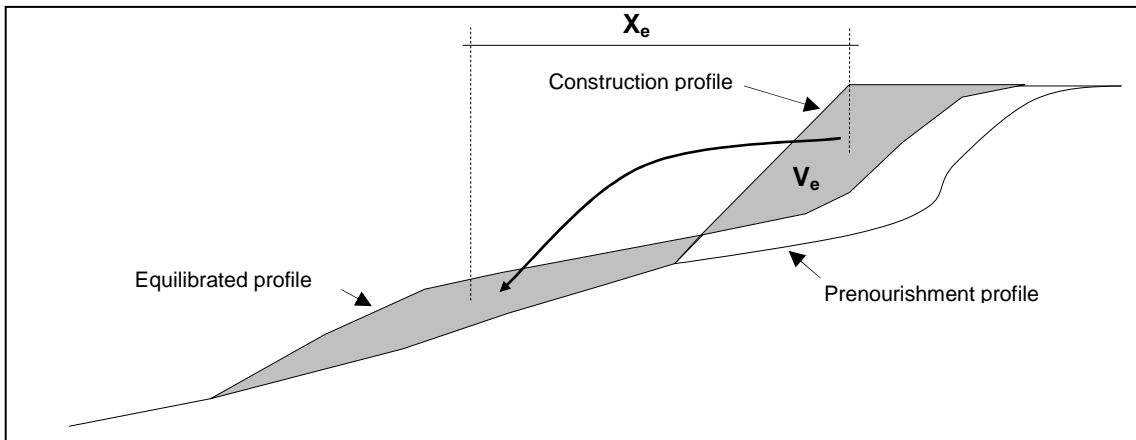


Figure 9-9: Definitions of the eroded volume  $V_e$  (which equals the deposited volume) and the cross-shore distance  $X_e$  over which this volume is moved.  $X_e$  is defined as the horizontal distance between the centres of gravity of the eroded and deposited areas (shaded grey).

**Fill grain size  $d_f$**

In Figure 9-10 the results from Unibest-TC are plotted according to Equation (9.1). It can be seen that the equilibration time scale is approximately the same for the grain sizes considered. In the same graph a least-square fit of Equation (9.1) for  $T_{EO}$  is drawn for  $d_f = 0.33$  mm. The fits for the other grain sizes are nearly the same and therefore not plotted. A visual inspection reveals that Equation (9.1) is a reasonable expression for the development of the additional dry beach width in time, especially for  $t > 100$  days. In Table 9-1 the least-square fits for  $T_{EO}$  and the  $R$ -squared values are shown.

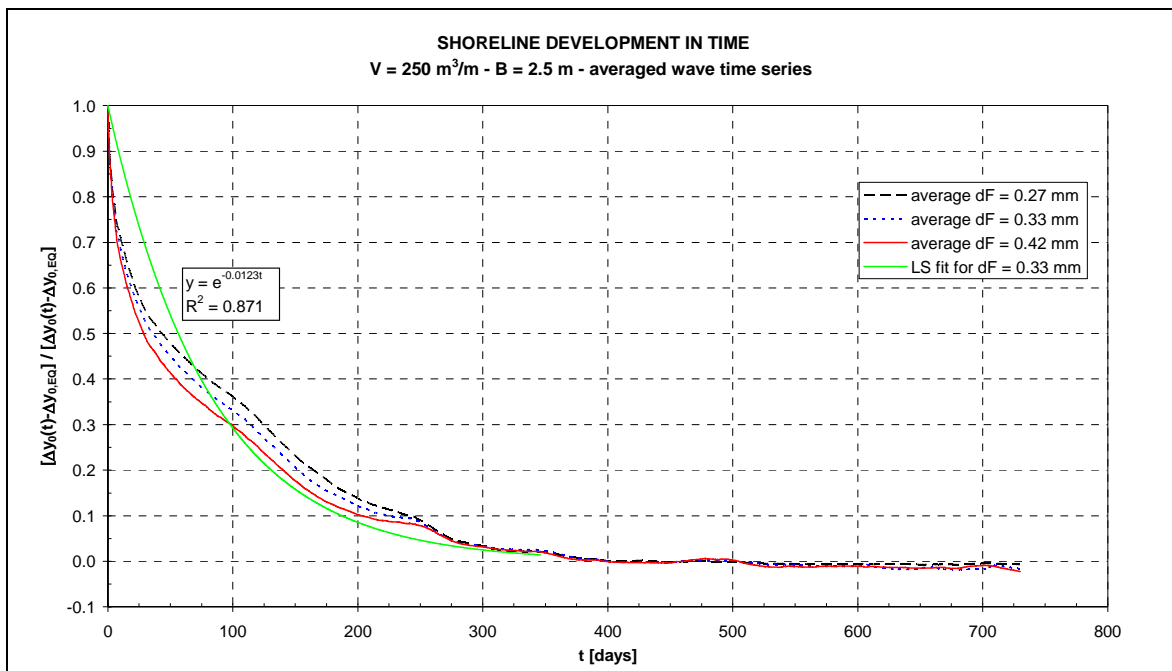


Figure 9-10: The development of the additional dry beach width according to Equation (9.1) for three fill grain sizes  $d_f$ . A least-square fit according to Equation (9.1) for  $d_f = 0.33$  mm has been made.

Table 9-1: Key figures of the equilibration for three fill grain sizes, a fill volume  $V$  of  $250 \text{ m}^3/\text{m}$  and a berm height  $B$  of  $2.5 \text{ m}$ .  $T_{EQ}$  was determined according to Equation (9.1) using the least-square method. The  $R^2$  values close to one indicate a good fit.

fill grain size $d_F$ [mm]	$V_e$ [ $\text{m}^3/\text{m}$ ]	$X_e$ [m]	$T_{EQ}$ [days]	$R^2$ [-]
0.27	185.5	145.3	89.0	0.878
0.33	159.1	130.4	81.3	0.871
0.42	141.7	119.1	71.7	0.835

Discussion:

It can be concluded that the grain size has a small influence on the equilibration time scale, which can be explained as follows. On the one hand the larger the grain, the less transport occurs. This implies that profile changes take place more slowly for a larger grain size. On the other hand the difference between the construction profile and the equilibrium profile is smaller for larger grains, i.e. less sand needs to be transported to achieve equilibrium conditions. Furthermore, small sized sediments need to be transported further offshore. These three processes don't level each other out, resulting in a decreasing  $T_{EQ}$  for larger grains for the grain size range considered here.

**The berm height  $B$**

In Figure 9-11 the shoreline development in time according to Equation (9.1) is plotted for the three considered berm heights  $B$ : 2.0, 2.5 and 3.0 m. It can be seen that the fitted relations for the three berm heights give different results for  $T_{EQ}$ , which are summarized in Table 9-2.

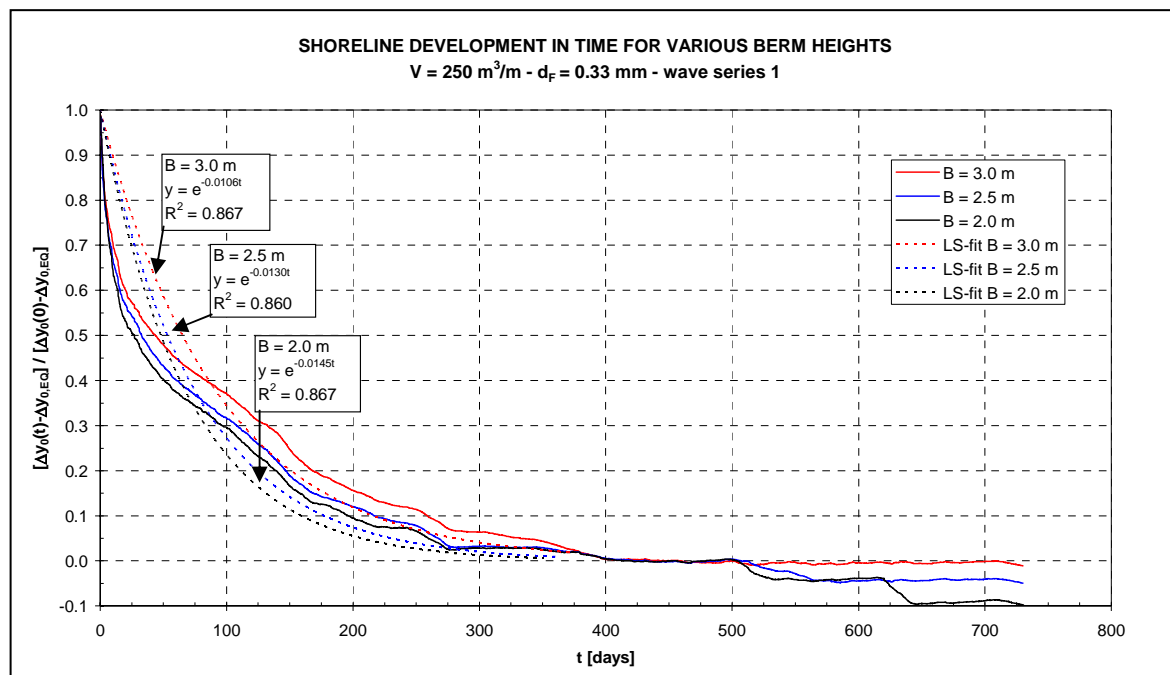


Figure 9-11: Shoreline development in time according to Unibest-TC for various berm heights  $B$ . Three least-square fits according to Equation (9.1) are plotted.

Table 9-2: Key figures of the equilibration for three berm heights  $B$ , a fill volume  $V$  of  $250 \text{ m}^3/\text{m}$  and a fill grain size  $d_F$  of  $0.33 \text{ mm}$ .  $T_{EQ}$  was determined according to Equation (9.1) using the least-square method. The  $R^2$  values close to one indicate a good fit.

berm height $B$ [m]	$V_e$ [ $\text{m}^3/\text{m}$ ]	$X_e$ [m]	$T_{EQ}$ [days]	$R^2$ [-]
2.0	157.7	128.1	69.2	0.839
2.5	159.1	130.4	77.0	0.860
3.0	160.0	133.5	93.9	0.867

**Discussion:**

It can be concluded that the berm height  $B$  has a small influence on the equilibration time scale. This can be explained by the following mechanisms:

- A higher  $B$  means that a little more sand has to be moved to the lower part of the profile to achieve equilibrium conditions. This slightly increases the equilibration time scale.
- A higher  $B$  means that on average the eroded sand is moved over a larger cross-shore distance to the deposition area, increasing  $T_{EQ}$ .
- A lower  $B$  means more shoreline retreat during extreme conditions. Post-storm recovery in the model is weak, leading to a larger permanent shoreline retreat after a storm for a lower  $B$ . This leads to a smaller equilibration time scale.

These three mechanisms lead to a smaller  $T_{EQ}$  for lower berm heights  $B$ .

**The fill volume  $V$** 

In Figure 9-12 the shoreline development in time according to Equation (9.1) is plotted for three considered fill volumes:  $V = 200, 300$  and  $400 \text{ m}^3/\text{m}$ . It can be seen that the fitted relations for the three fill volumes give different results for  $T_{EQ}$ , which are summarized in Table 9-3.

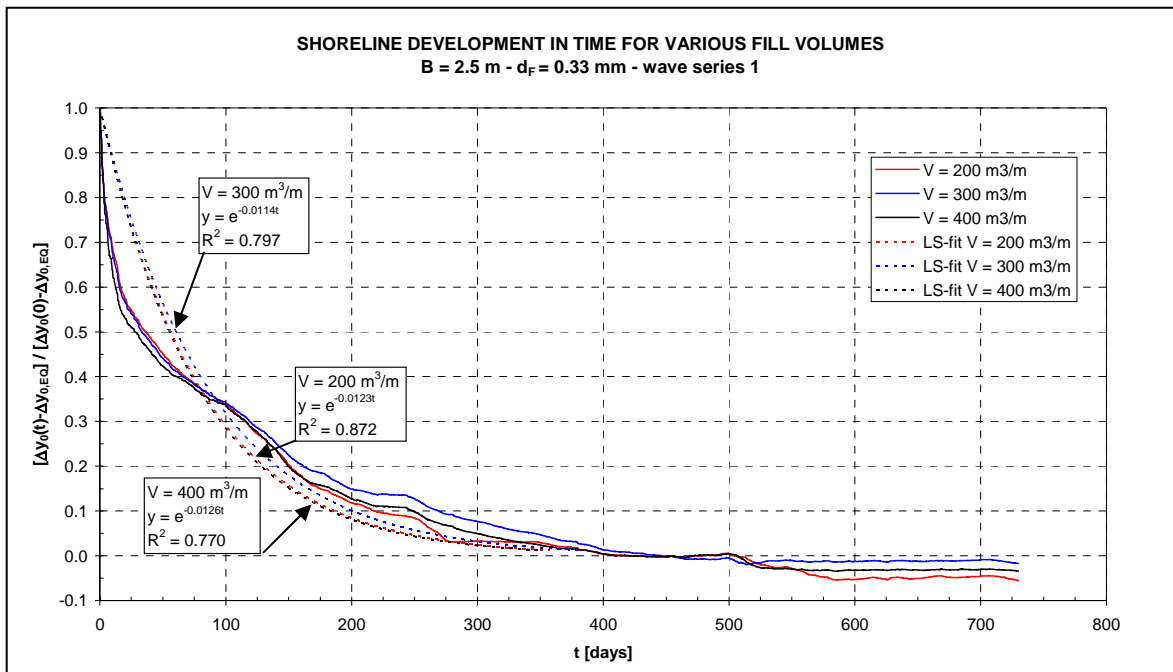


Figure 9-12: Shoreline development in time according to Unibest-TC for various fill volumes  $V$ . Three least-square fits according to Equation (9.1) are plotted.

Table 9-3: Key figures of the equilibration for three fill volumes  $V$ , a berm height  $B$  of 2.5 m and a fill grain size  $d_f$  of 0.33 mm.  $T_{EQ}$  was determined according to Equation (9.1) using the least-square method. The  $R^2$  values close to one indicate a good fit.

fill volume $V$ [ $\text{m}^3/\text{m}$ ]	$V_e$ [ $\text{m}^3/\text{m}$ ]	$X_e$ [m]	$T_{EQ}$ [days]	$R^2$ [-]
200	134.1	129.0	81.0	0.872
300	182.5	131.6	87.4	0.797
400	213.7	131.4	79.6	0.770

The following observations can be made:

- During the first 100 days, the shoreline retreat of the fill with  $V = 400 \text{ m}^3/\text{m}$  is a little higher than those of the other fills.
- Thereafter, the small fill ( $V = 200 \text{ m}^3/\text{m}$ ) shows the fastest retreat.

## Explanation:

One would expect a larger equilibration time scale for larger fill volumes, because a larger volume has to be eroded. However, the modelling results show a fast shoreline retreat for the large fill volume during the first 100 days after construction. This is caused by the fact that the construction profile extends to relatively deep water (see upper panel in Figure 9-13), causing the waves to break over a relatively small distance (see lower panel in Figure 9-13), speeding up the equilibration. After a while, the profile approaches equilibrium conditions, spread wave breaking over a larger area, which leads to a decrease in the shoreline retreat rate.

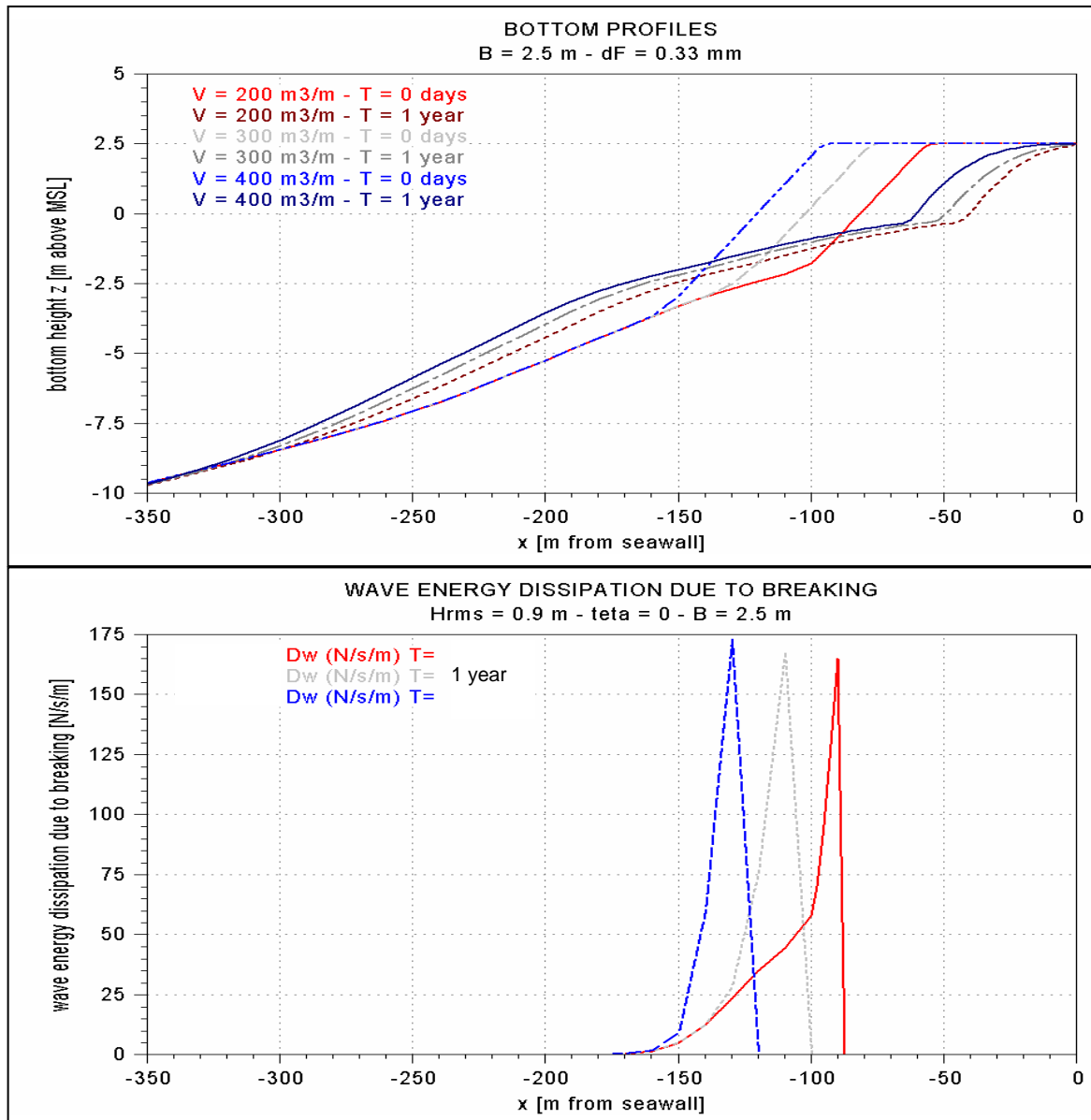


Figure 9-13: Upper panel: Construction profiles and calculated profiles after one year for various fill volume  $V$  according to Unibest-TC.  
Lower panel: Wave energy dissipation due to breaking according to Unibest-TC for the three construction profiles in the upper panel.

## Conclusion

It can be concluded that the equilibration time scale  $T_{EO}$  lies in the order of 80 days. This time scale is (slightly) influenced by the fill grain size  $d_F$ , the berm height  $B$  and the fill volume  $V$ . This influence can be explained by:

- The magnitude of the eroded volume  $V_{e_i}$ ; larger eroded volumes result in larger time scales.

- The distance  $X_e$  over which the eroded volume is moved; larger eroded volumes lead to larger time scales.
- The berm height; higher berm heights act as a stockpile of sand.
- The extension of the construction profile into the breaker zone; more focused wave breaking causes higher transports.
- The grain size; a smaller grain size results in higher transports.

Summarized it can be stated that (for the ranges of variables considered):

- A larger fill grain size  $d_F$  results in a smaller equilibration time scale  $T_{EQ}$ .
- A higher berm height  $B$  results in a larger equilibration time scale  $T_{EQ}$ .
- No clear relation is present between the fill volume  $V$  and the equilibration time scale  $T_{EQ}$ .

### 9.4.5 Shoreline advancement

In this paragraph the calculated shoreline advancement (or additional dry beach width) after equilibration  $\Delta y_{0,EQ}$  are presented. The values of  $\Delta y_{0,EQ}$  are averages of  $\Delta y_0$  between  $t = 400$  days and  $t = 450$  days after construction to filter out short term variations, like in Paragraph 9.4.3.

The calculated values of the additional dry beach width  $\Delta y_{0,EQ}$  for a range of fill volumes  $V$  and the three considered fill sediments are summarized in Appendix H.

The results are visualized in Figure 9-14.

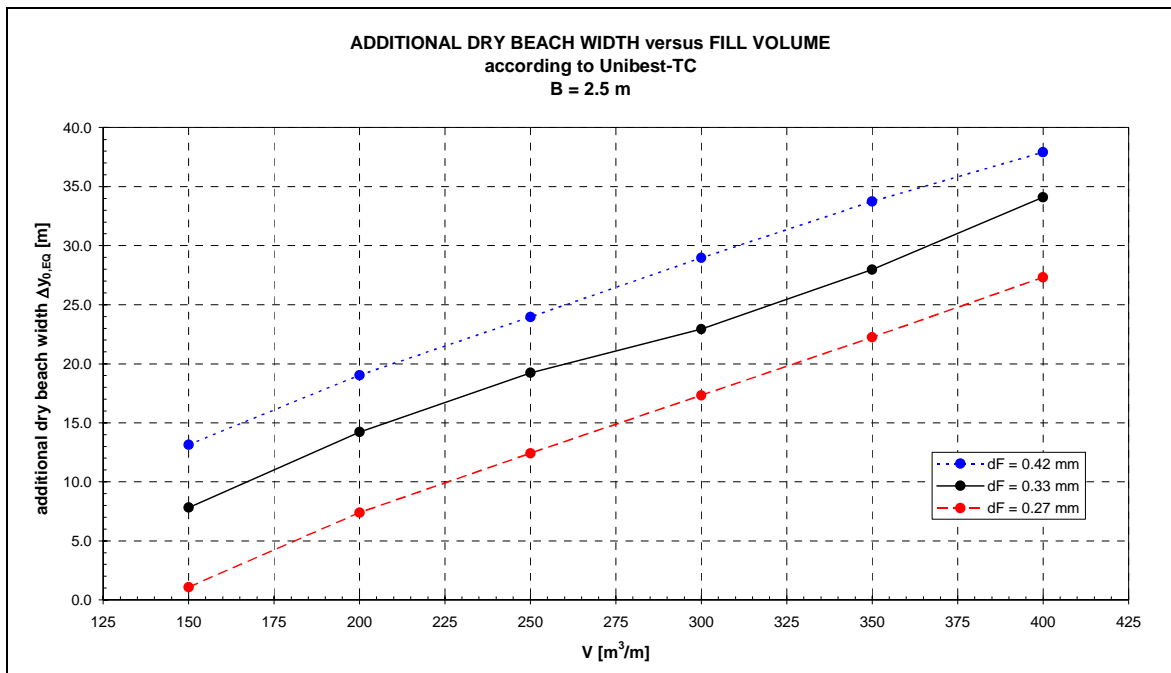


Figure 9-14: Additional dry beach width  $\Delta y_{0,EQ}$  versus the fill volume  $V$  for a berm height  $B$  of 2.5 m according to the Unibest-TC model.

It can be concluded that:

- Larger fill volumes result in a larger  $\Delta y_{0,EQ}$ .
- Larger fill sediments results in a larger  $\Delta y_{0,EQ}$ .
- The fills with the fine sediments ( $d_F = 0.27$  mm) and small volumes ( $V < 150$   $m^3/m$ ) result in practically zero additional dry beach widths.

### 9.4.6 Conclusions

The most important conclusions of this paragraph are:

- Larger fill sediments result in a steeper bottom profile.
- Larger fill sediments and larger fill volumes result in larger additional dry beach width  $\Delta y_{0,EQ}$ .

- The equilibration is practically complete after approximately 1 year. The Unibest-TC model becomes less reliable for larger time spans.
- The shoreline retreat rate decreases in time.
- The exponential expression of Equation (9.1) shows reasonable resemblance with the Unibest-TC model results.
- Differences in the equilibration time scale  $T_{EQ}$  can be explained by the eroded volume  $V_e$ , the distance  $X_e$  over which the sediment is moved, the grain size  $d_f$ , the berm height  $B$  and the extension of the construction profile into the breaker zone.
- The larger the grain size  $d_f$ , the smaller equilibration time scale  $T_{EQ}$ .
- The higher the berm height  $B$ , the higher equilibration time scale  $T_{EQ}$ .
- No clear relation between the fill volume  $V$  and the equilibration time scale  $T_{EQ}$  is present.

## 9.5 Validation of the modelling results

### 9.5.1 Introduction

In this paragraph the sensitivity of the model results discussed in Paragraph 9.4 to the assumptions made in Paragraph 9.3 is investigated.

### 9.5.2 Wave climate

In Figure 9-15 a construction profile with  $V = 250 \text{ m}^3/\text{m}$ ,  $B = 2.5 \text{ m}$  and  $d_f = 0.33 \text{ mm}$  is plotted. In the same figure the equilibrated profiles after one year are shown for three wave climates to investigate the sensitivity of the equilibration to deviations in the occurring wave climate:

1. A normal wave climate, represented by time series of the waves1 as used in Paragraph 9.4 and defined by random drawings out of a monthly 3-dimensional ( $H_{rms}$ ,  $T_{pr}$ ,  $\theta$ ) probability distribution based on 10 years of satellite measurements (see Paragraph 9.3.4).
2. A calm wave climate with the wave heights of series 1 multiplied by 0.9.
3. A heavy wave climate with the wave heights of series 1 multiplied by 1.1.

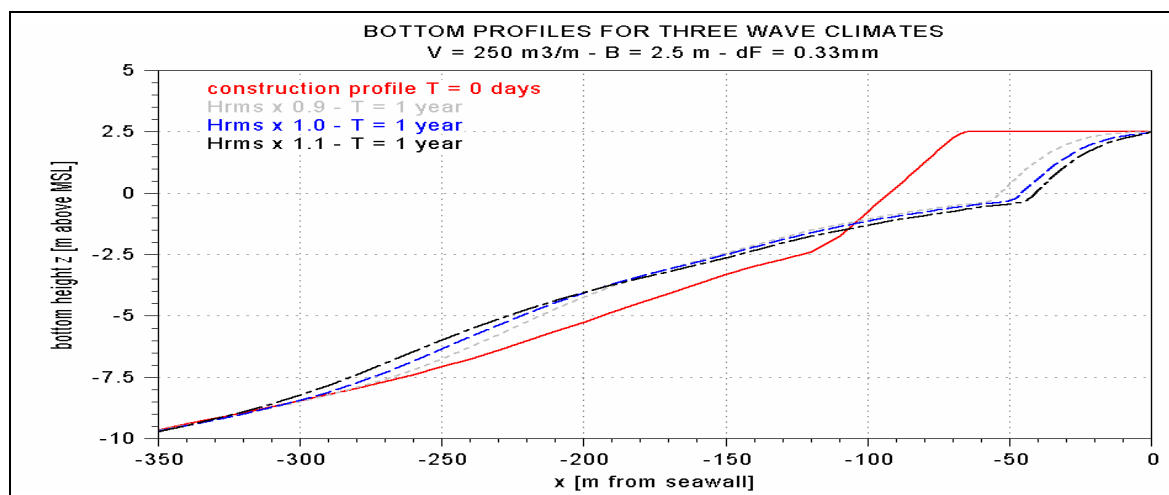


Figure 9-15: Calculated bottom profiles with Unibest-TC after one year for three wave climates.

The additional dry beach width  $\Delta y_0$  in time is plotted in Figure 9-16, which is transformed to Figure 9-17 according to Equation (9.1).



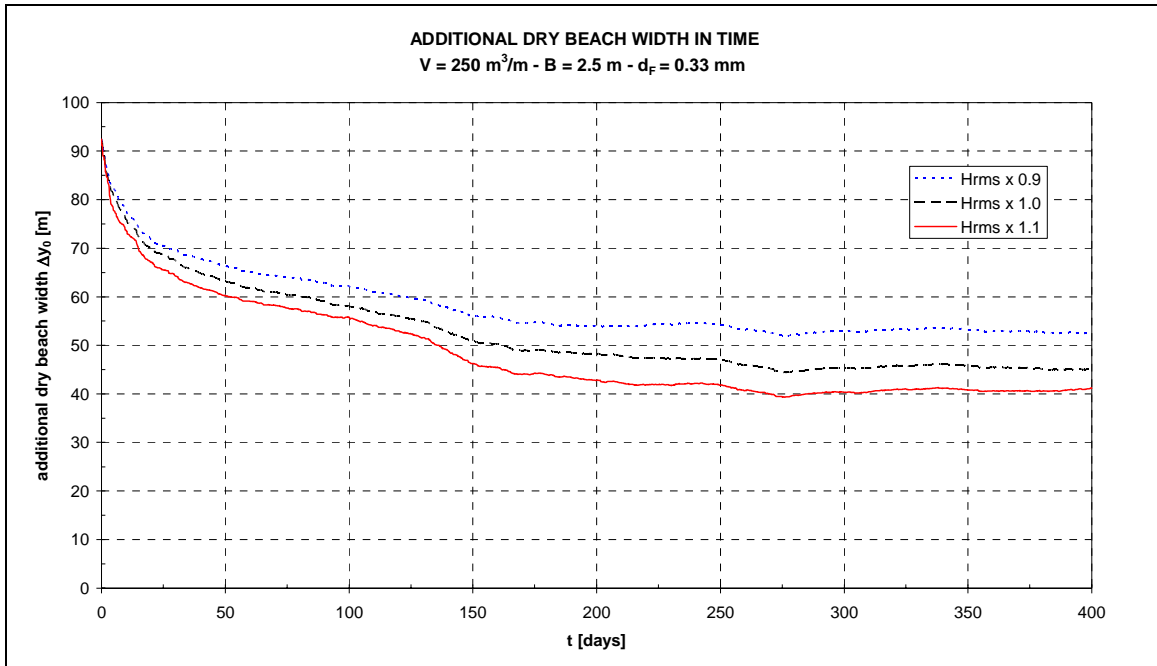


Figure 9-16: The development of the additional dry beach width in time according to Unibest-TC for three wave climates.

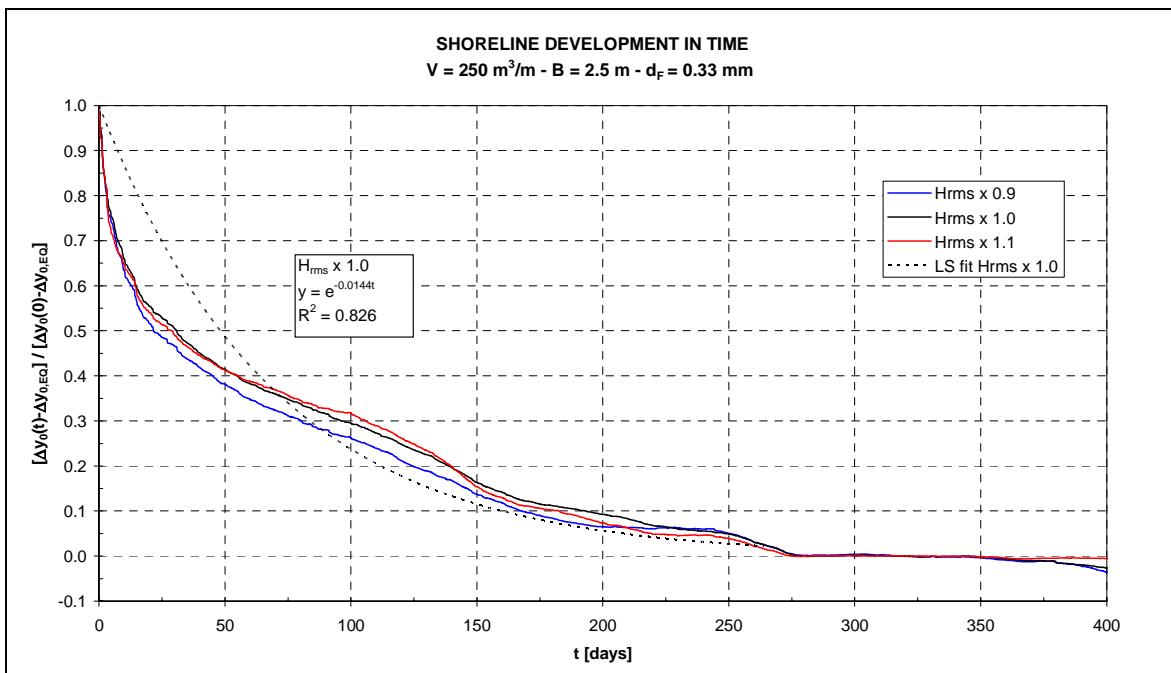


Figure 9-17: Shoreline development in time according to Unibest-TC for three wave climates. A least-square fit according to Equation (9.1) is plotted for  $H_{rms} \times 1.0$ .

In Table 9-4 the key figures of the equilibration for the three wave climates are given.

Table 9-4: Key figures of the equilibration for a fill volume  $V$  of  $250 \text{ m}^3/\text{m}$ , a fill grain size of  $d_f = 0.33 \text{ mm}$  and a berm height  $B$  of  $2.5 \text{ m}$ . Three wave climates have been considered: a normal wave climate, a calm wave climate (all wave heights 10% lower) and a heavy wave climate (all wave heights 10% higher).

wave height $\overline{H}_{rms}$ [m]	$\Delta y_0$ [m]	$V_e$ [ $\text{m}^3/\text{m}$ ]	$X_e$ [m]	$h_c$ [m]	$T_{EQ}$ [days]	$R^2$ [-]
$0.9 \overline{H}_{rms}$	28.19	131.2	114.1	7.0	60.5	0.804
$1.0 \overline{H}_{rms}$	20.68	158.5	132.4	7.5	69.5	0.826
$1.1 \overline{H}_{rms}$	15.74	179.3	148.2	8.0	69.3	0.802

The following observations can be made:

- The more energetic (higher waves) the wave conditions, the smaller the additional dry beach width  $\Delta y_0$ .
- For higher waves the equilibrium bottom height is lower in the upper part of the profile.
- The more energetic (higher waves) the wave conditions, the larger the eroded  $V_e$  volume and the distance  $X_e$  over which the sediment is transported.
- The more energetic (higher waves) the wave conditions, the larger the closure depth  $h_c$ .
- No significant influence of the average wave height on the equilibration time scale  $T_{EQ}$  is present.

#### Explanation

Higher waves carry more wave energy into the breaker zone, leading to more turbulence, higher longshore and cross-shore currents and higher wave-orbital velocities, causing higher sediment transports.

The wave conditions influence the equilibrium shape to which the construction profile evolves. Higher waves cause a larger closure depth  $h_{cr}$ , a wider breaker zone and a lower bottom height in the shallow part of the breaker zone. Therefore for higher waves more sediment has to be moved over a larger distance to achieve equilibrium conditions. Regarding the equilibration time scale  $T_{EQ}$  these two contributions level each other out to a great extent.

#### Conclusion

One can conclude that the equilibrium shape and the shoreline retreat are highly sensitive to the wave climate in the project area. The time scale on which the equilibration takes place is rather insensitive to small deviations in the wave climate. It is emphasized that the occurrence of hurricanes can have significant influence on the equilibration time scale. Also the sequence in which wave conditions occur can have significant influence on the equilibration time scale (see Paragraph 9.5.4).

### 9.5.3 Difference initial profile and equilibration profile

In Figure 9-18 three construction profiles of  $V = 250 \text{ m}^3/\text{m}$  and  $d_f = 0.33 \text{ mm}$  with construction slopes 1 to 5, 1 to 10 and 1 to 15 have been plotted. In the same figure the equilibrated profiles after 450 days are shown. The additional beach width  $\Delta y_0$  in time is plotted in Figure 9-19, which is transformed to Figure 9-20 according to Equation (9.1).

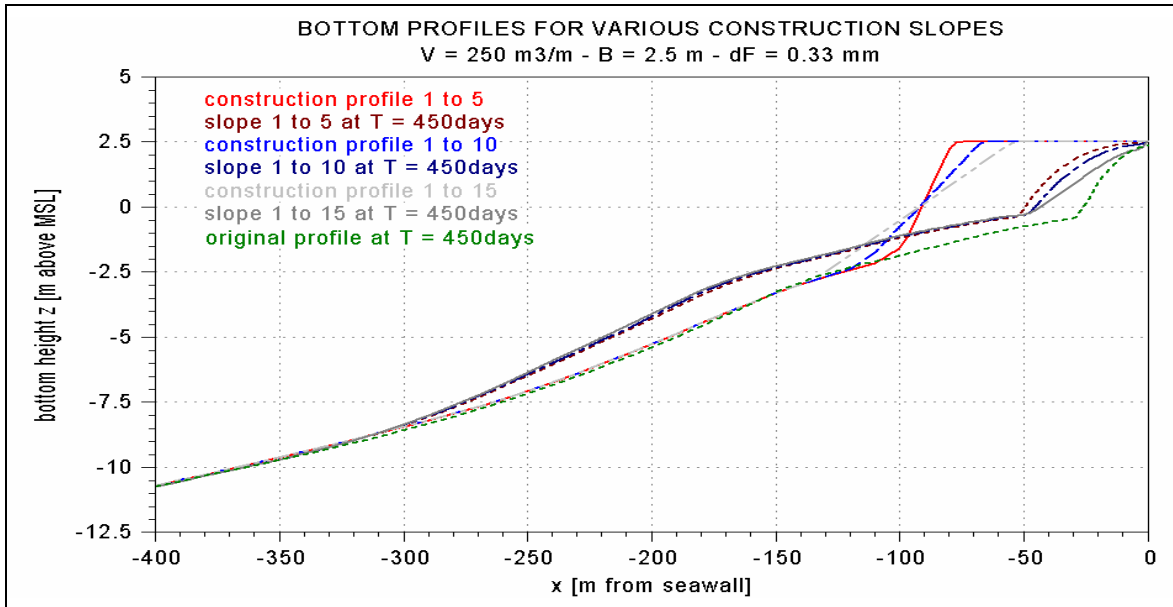


Figure 9-18: Construction profiles for three construction slopes and the corresponding calculated bottom profiles after 450 days. The calculated development of the prenourishment profile is also plotted.

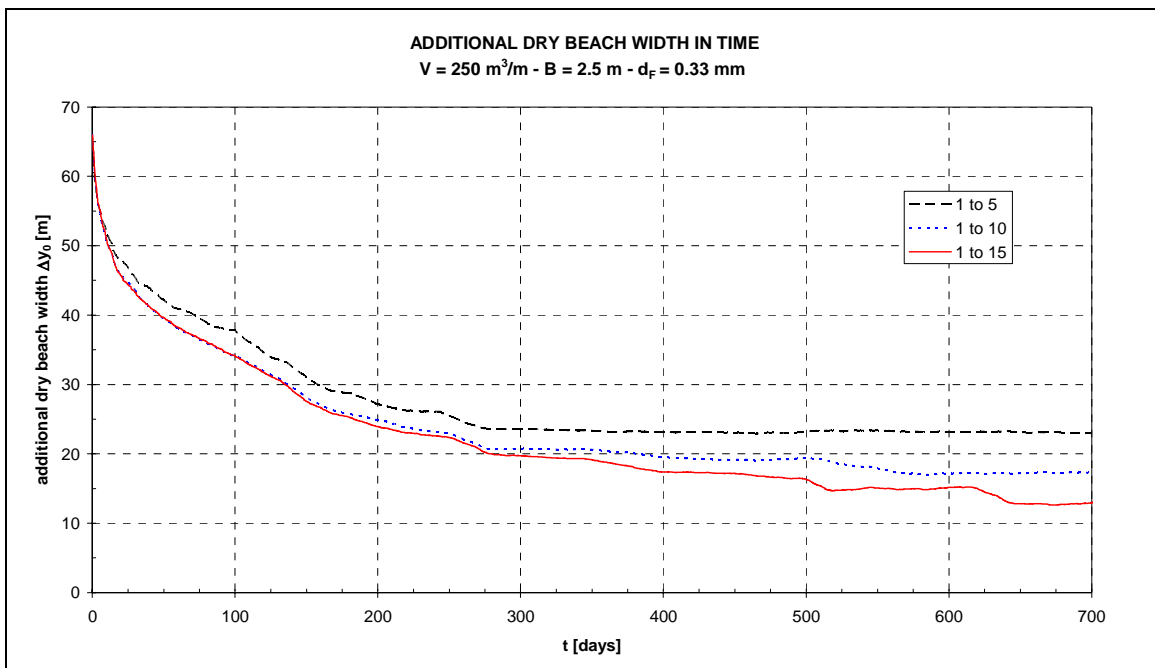


Figure 9-19: Development of the additional dry beach width in time according to Unibest-TC for three construction slopes.

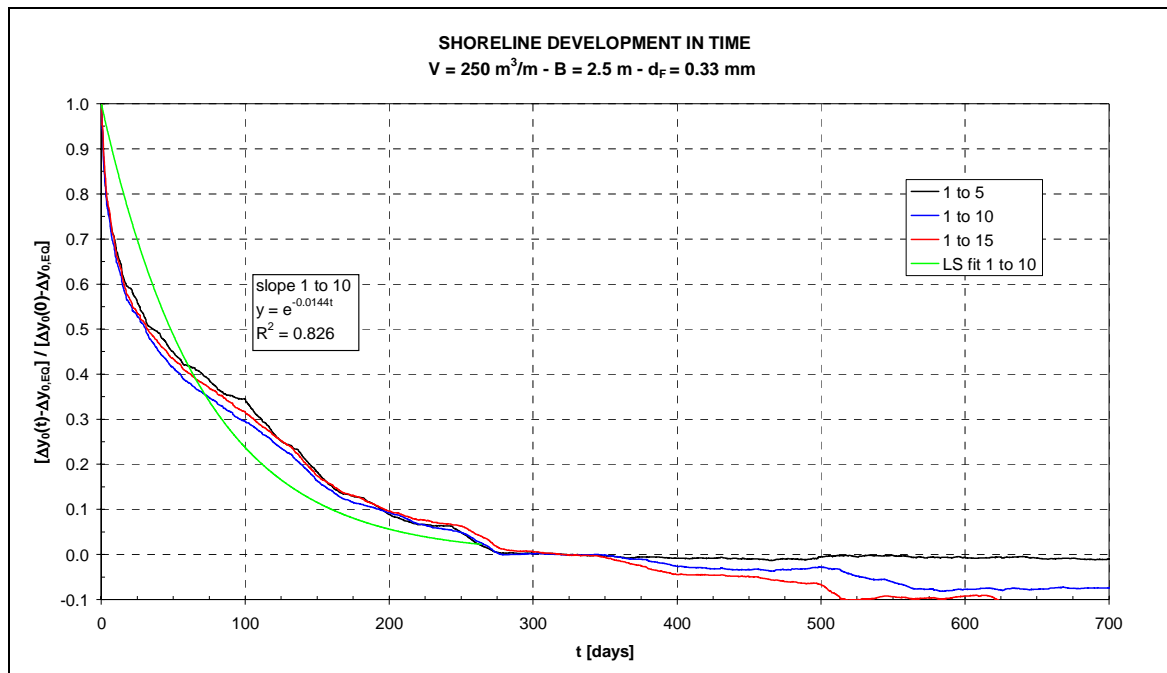


Figure 9-20: Shoreline development in time according to Unibest-TC for three construction slopes. A least-square fit according to Equation (9.1) is plotted for a construction slope of 1 to 10.

In Table 9-5 the key figures for the 1 to 5, 1 to 10 and 1 to 20 slopes are given. The least-square fits of  $T_{EQ}$  have been obtained from Figure 9-20 by fitting between  $t = 0$  and  $t = 325$  days. This deviant period has been chosen because the long term behaviour of the 1 to 15 profile shows a trend of shoreline retreat, caused by different storm response due to differences in the shape of the berm. This effect isn't part of the equilibration in the narrow sense of the word.

Table 9-5: Key figures of the equilibration for three construction slopes, a fill volume  $V$  of  $250 \text{ m}^3/\text{m}$ , a fill grain size of  $d_f = 0.33 \text{ mm}$  and a berm height  $B$  of  $2.5 \text{ m}$ .  $T_{EQ}$  was determined according to Equation (9.1) using the least-square method. The  $R^2$  values close to one indicate a good fit.

slope [-]	$\Delta y_0$ [m]	$V_e$ [ $\text{m}^3/\text{m}$ ]	$X_e$ [m]	$T_{EQ}$ [days]	$R^2$ [-]
1 to 5	23.47	153.6	122.7	76.7	0.857
1 to 10	20.68	159.1	130.3	69.5	0.826
1 to 15	19.44	161.3	141.1	74.3	0.841

The following observations can be made:

- The steeper slope of the profile remains partly intact after equilibration.
- Smoothing of the sharp edge between the berm and the slope occurs; this has a numerical cause (see Paragraph 9.5.6).
- The additional dry beach width  $\Delta y_0$  is higher for the steeper slopes.
- The eroded volume  $V_e$  is slightly higher for flatter slopes.
- The distance  $X_e$  over which the eroded volume has to be moved is larger for flatter profiles.
- The flatter slopes show ongoing shoreline recession, caused by the lower average berm height (lower storm reserve).
- The fitted equilibration time scales  $T_{EQ}$  are almost equal.

**Explanation**

One would expect the flatter profile to equilibrate in a shorter time span, because it's closer to the equilibrium state. However, the latter isn't true for this specific case because:

- The total eroded volume is somewhat larger for the flatter profiles.

- The average distance over which the eroded volume has to be moved before it is deposited is somewhat larger for the flatter profiles.

This is caused by the fact that the dry profiles of the three construction slopes keep their distinct shapes. In reality the dry profile shapes should evolve to the same shape. This doesn't happen in the model, because the mechanisms responsible for the dry profile shape (wind transport, swash zone dynamics) aren't incorporated in the Unibest model. So in reality we would expect the eroded volume to be somewhat larger for the steep slopes and somewhat smaller for the flat slopes, leading to larger  $T_{EQ}$  for the steep slopes and smaller  $T_{EQ}$  for the flatter slopes, contradictory to the results found by the Unibest-TC model.

### Conclusion

The construction slope influences the results of the Unibest-TC model: the additional beach width  $\Delta y_{0,EO}$  is smaller for flatter slopes. This is caused by an incorrect modelling of the development of the dry profile. No significant changes are expected to occur in reality for different construction slopes. The equilibration time scale  $T_{EQ}$  is hardly influenced by the construction slope.

The assumption of a construction slope of 1 to 10 has practically no influence on the results.

### 9.5.4 Persistency wave conditions

In the calculations so far random generated wave series have been used. These wave series don't represent the persistency of wave conditions. The question arises if this influences the equilibration time scale and the final shape of the equilibrated profile. Therefore two situations are compared: one run with a random generated wave series as used in Paragraph 9.4 and the same wave series, but then sorted per month. The  $H_{rms}$  in time of these two wave series is plotted in Figure 9-21. The statistical properties of the random and sorted wave series are identical; only the sequence in which the wave conditions occur differs. The calculated shoreline positions in time are plotted in Figure 9-22.

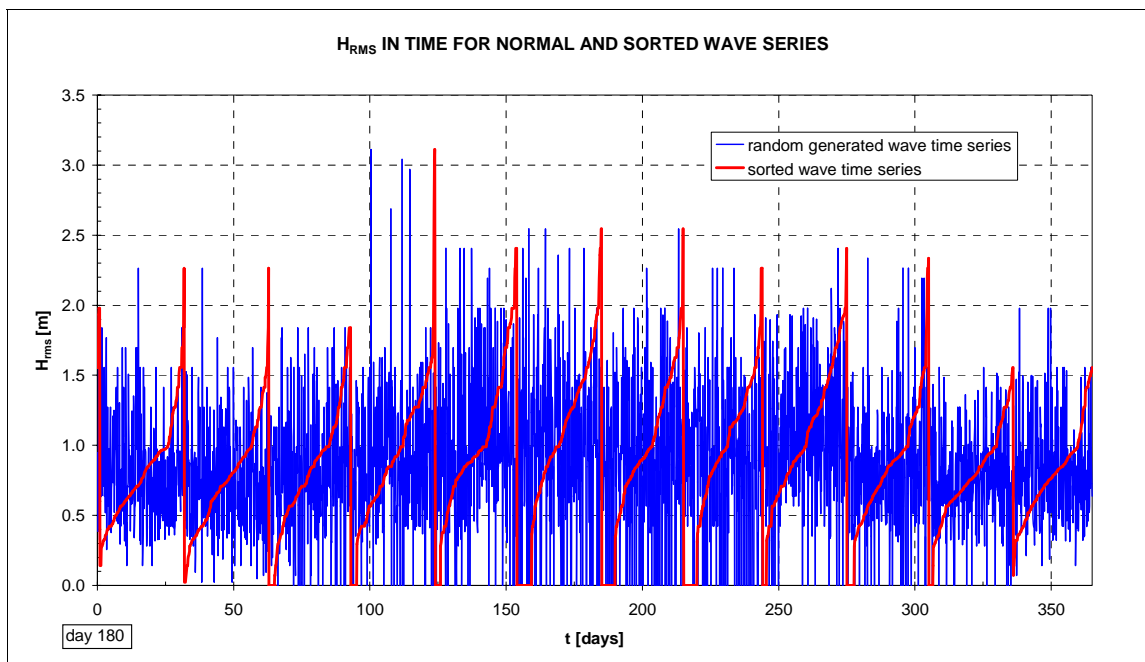


Figure 9-21:  $H_{rms}$  in time for normal and sorted wave time series.  $T = 0$  days is day 180 of the year, since the calculations start at this day.

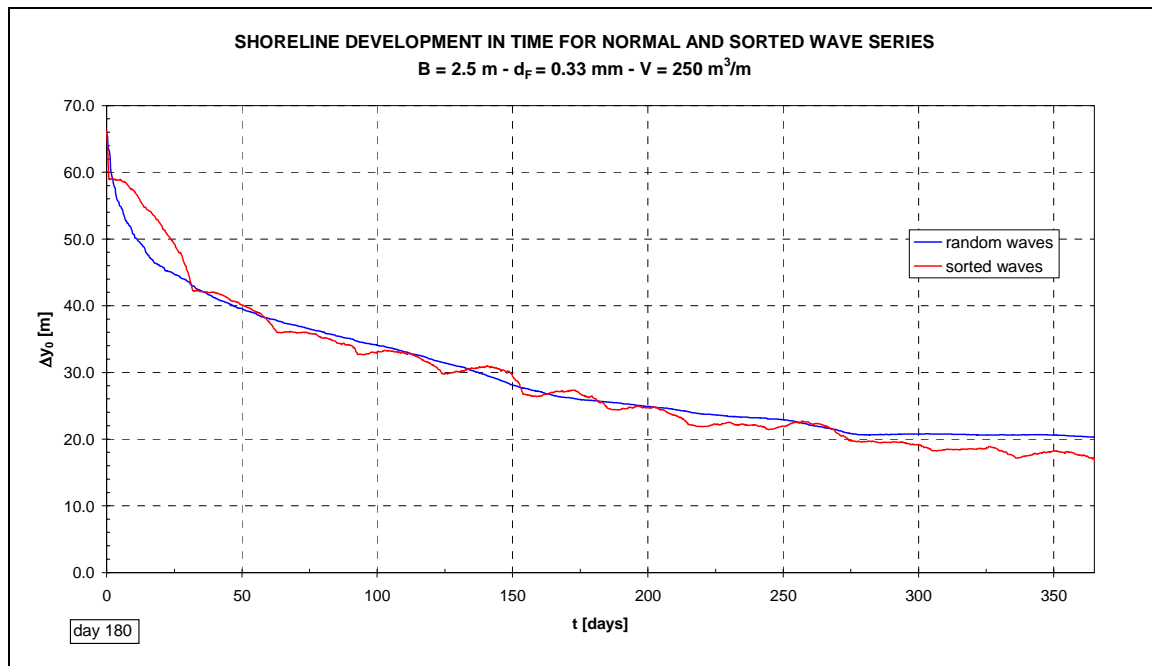


Figure 9-22: Shoreline development in time for normal and sorted time series of the waves (see Figure 9-21) according to Unibest-TC.

The following observations can be made:

- The final shape of the profile is almost identical for both runs (not shown here).
- The profile with the sorted wave series is more dynamic; the shoreline position and profile shape show more variation in time.
- The equilibration time scale  $T_{EQ}$  is approximately equal.
- The  $\Delta y_0$  after equilibration is smaller for the sorted wave series.

### Explanation

It is clear that the sorted wave series results in a more dynamic profile: erosion and accretion are more persistent and can cause larger profile fluctuations. The difference in  $\Delta y_0$  is probably due to the absence of post-erosion recovery in the Unibest-TC model: recovery after a long period of high waves does not fully occur.

### Conclusion

Since we are interested in the average conditions after equilibration, in other words in the dynamic equilibrium condition, the absence of the persistency of wave conditions in the model doesn't influence the conclusions of the modelling in a significant way.

## 9.5.5 Seasonal influence

When observing the graphs of the shoreline development in time, one notices that the shoreline retreat rate doesn't decrease monotonically. This is caused by the seasonal variation in wave conditions (see Paragraph 3.2.5). As stated in Paragraph 9.3.8, the starting time  $T_0$  for the calculations is the end of June ( $T_0 = 180$  days).

This starting time has been varied to determine the influence on the results (shoreline retreat, end state). Five runs with random generated wave series (wave series 1 to 5) have been made for all three starting times. The additional dry beach width  $\Delta y_0$  in time has been determined for all runs after which these shoreline positions have been averaged over 5 wave series for one starting time. The results are plotted in Figure 9-23.

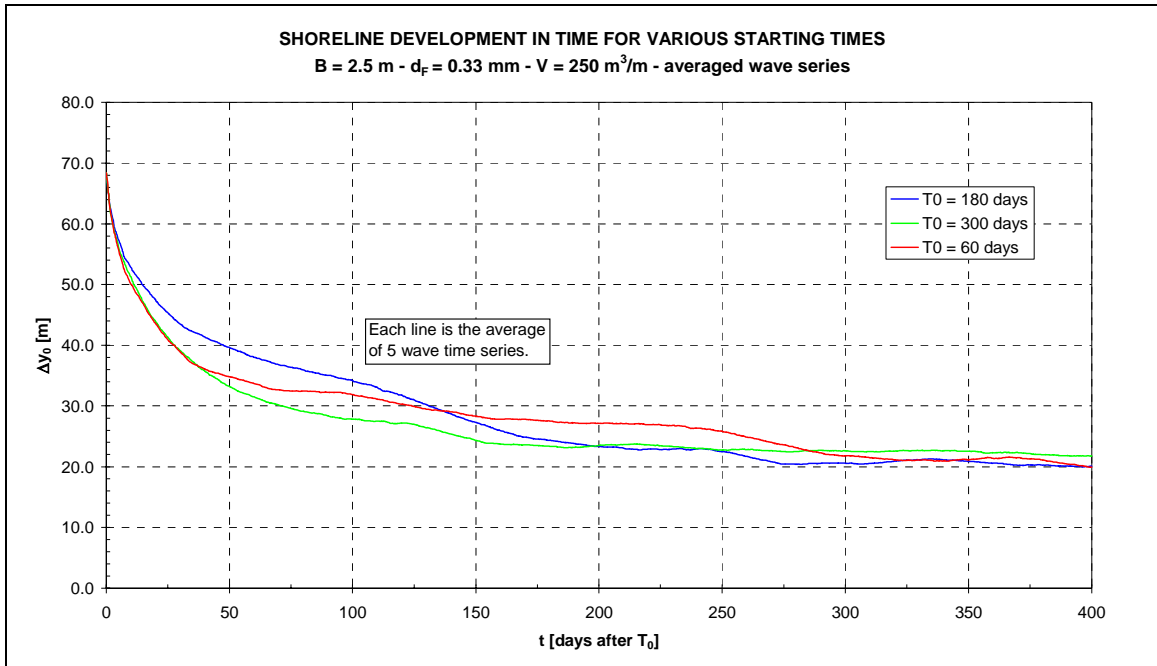


Figure 9-23: Shoreline development in time according to Unibest-TC for three starting times. Each line is an average of five wave time series.

The next step comprises the averaging of the shoreline position in time for all three starting times. The results can be found in Figure 9-24. A least-square fit for this average has been plotted too. The results are summarized in Table 9-6.

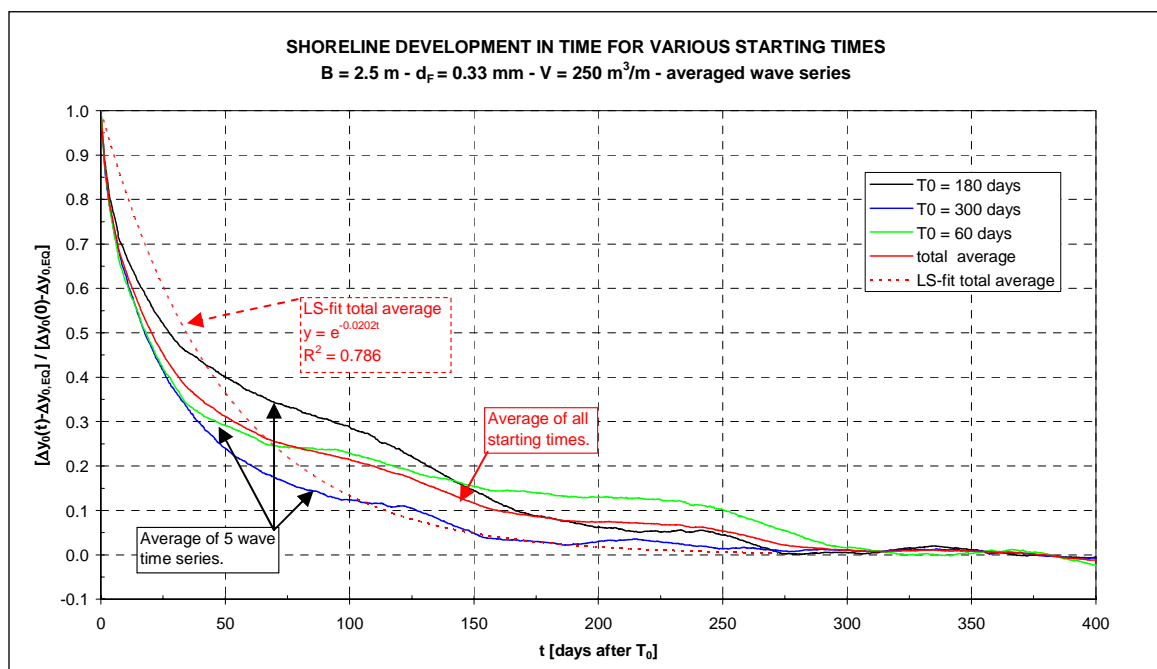


Figure 9-24: Shoreline development in time according to Unibest-TC for three starting times. The red line is the average of the black, blue and green line. The dashed red line is a least-square fit according to Equation (9.1).

Table 9-6: Key figures of the equilibration for three starting times  $T_0$  for a fill volume  $V$  of 250  $m^3/m$  and a berm height  $B$  of 2.5 m and a fill grain size of 0.33 mm. No significant differences in eroded volume are present.  $T_{EQ}$  was determined according to Equation (9.1) using the least-square method.  $R^2$  values close to one indicate a good fit.

starting time $T_0$ [days]	$\Delta y_0$ [m]	$T_{EQ}$ [days]	$R^2$ [-]
60	21.0	51.0	0.494
180	20.3	65.2	0.859
300	22.1	34.8	0.911
average	21.1	49.6	0.786

The following observations can be made:

- The final (dynamic) equilibrium shape of the profile is insensitive to the starting time of the calculations  $T_0$ .
- The additional dry beach width after equilibration is almost insensitive to  $T_0$ .
- The equilibration time scale  $T_{EQ}$  is severely influenced by  $T_0$ .

### Explanation

The influence of  $T_0$  on  $T_{EQ}$  can be explained by the seasonal variation of the wave height (see Paragraph 3.2.5): a starting time  $T_0$  of 300 days at the beginning of winter (higher waves) gives a small  $T_{EQ}$ .

### Conclusion

The sequence in which the wave conditions occur has a significant influence on the equilibration time scale. The dynamic equilibrium state however isn't significantly influenced by the starting time / sequence of wave conditions, provided that the statistical properties of the time series of the waves are equal.

## 9.5.6 Computational step size $dx$

The computational step size  $dx$  indicates the grid points where Unibest-TC performs its calculations, and has to be chosen such that:

- The spatial resolution is sufficiently accurate.
- Numerical stability is guaranteed.
- The maximum number of grid points of Unibest-TC (i.e. 399) is not exceeded.

The first criterion implies an upper limit for  $dx$ , the second and third a lower limit. For the offshore part of the profile ( $z < \text{MSL} - 15 \text{ m}$ ) a spatial step of 100 m is chosen, since the required spatial resolution is low. In the shallower ( $\text{MSL} - 15 \text{ m} < z < \text{MSL} - 2.0 \text{ m}$ ) part a spatial step of 10 m is taken, to increase spatial resolution. Values of  $dx$  smaller than 10 m give numerical instability in the wave module of Unibest-TC (see Appendix C.3.2).

For the upper part of the profile ( $z > \text{approximately MSL} - 2.0 \text{ m}$ ) the spatial step size is of particular relevance. The transport rates in this part of the profile are calculated by linear extrapolation with the height from the last calculation point with depth  $h_{min}$  which is approximately 0.85 m in this model (see Appendix C.3.6). The spatial discretization leads to numerical smoothing of the sharp edges, which is indicated in Figure 9-25.

In Figure 9-26 the original and calculated cross-shore profiles are plotted together with the initial cross-shore transports for a step size  $dx = 5, 2.5$  and  $1.25 \text{ m}$  on the dry profile.



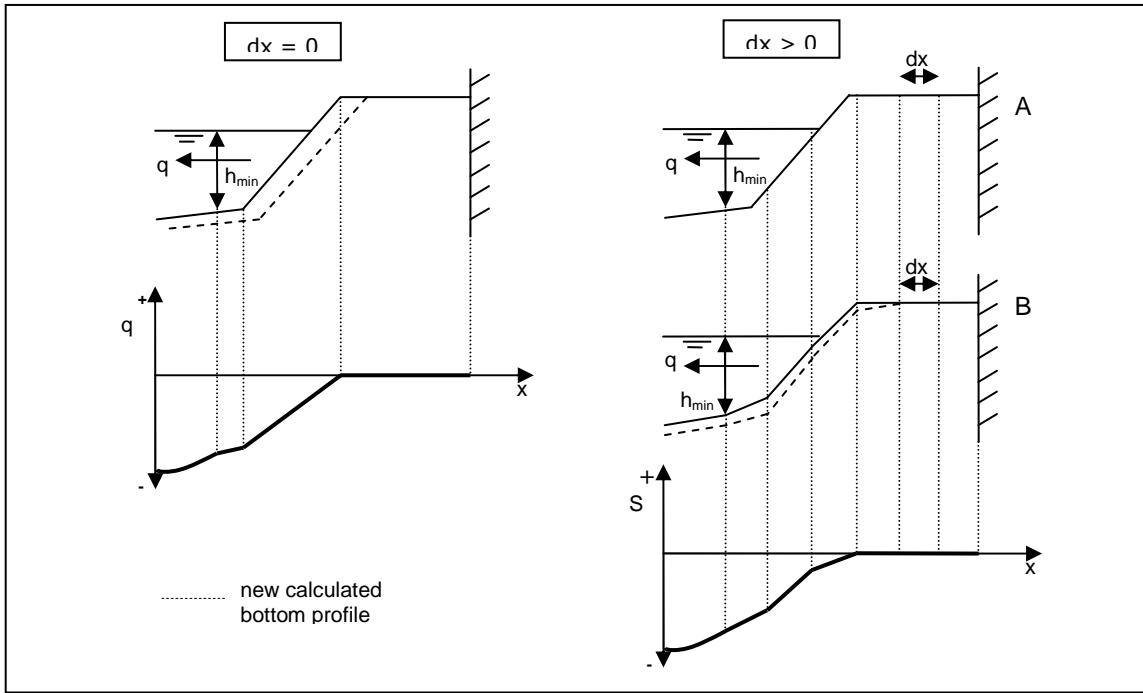


Figure 9-25: Calculation of the cross-shore transport over the dry profile. On the left-hand side the theoretical transport rates for an infinitely small computational step size  $dx$ . On the right hand side the original profile (A) with the profile as it is seen by Unibest for a finite  $dx$  (B), resulting in a different transport rate over the dry profile, causing smoothing of the sharp edges (dashed line in B).

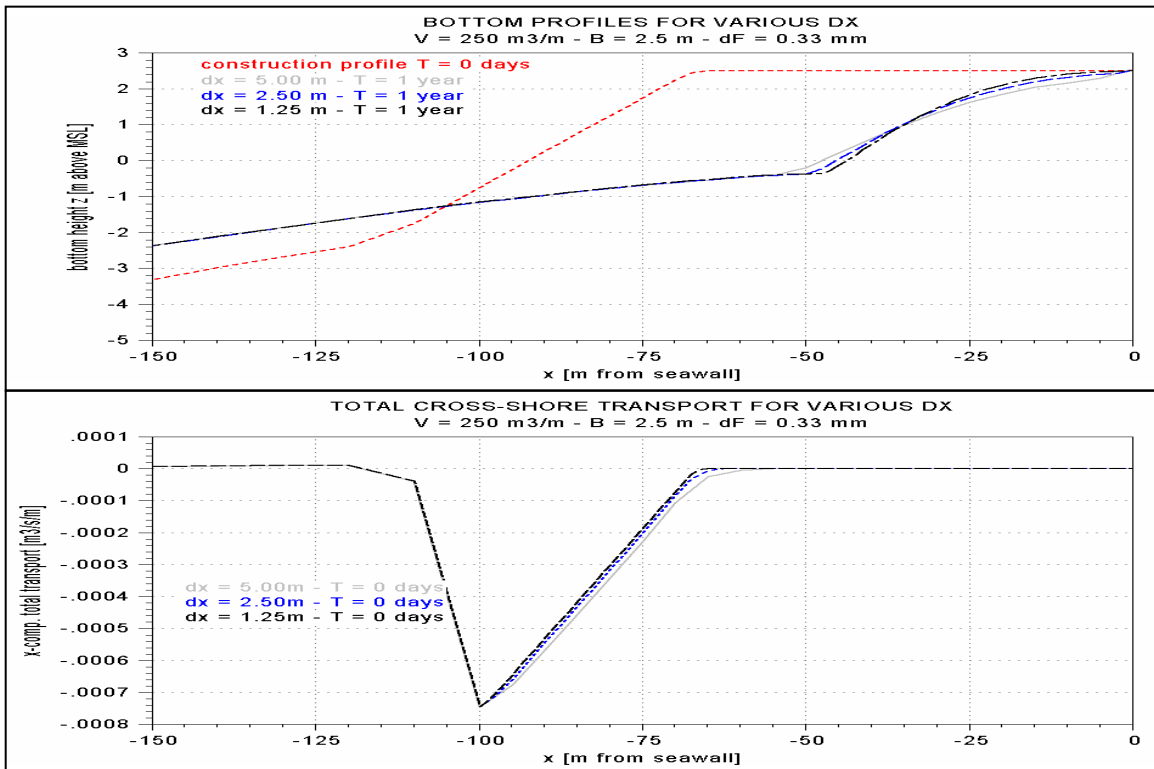


Figure 9-26: Upper panel: Construction profile and calculated profiles after one year by Unibest-TC for various computational step sizes  $dx$ . Lower panel: Total cross shore transports (bed + suspended load) on the construction profile at  $T = 0$  days for three values  $dx$ .

The following observations can be made:

- The cross-shore transport on the dry profile is influenced by the step size  $dx$  at locations where strong differences in bottom height gradients occur (i.e. at the edge of the fill).
- The smaller the step size  $dx$  the better the original dry profile shape is preserved.
- The shoreline recession is a little smaller for larger  $dx$ .
- The bottom profile below MSL -1.0 m is the same for all  $dx$  considered.

### Conclusion

The step size  $dx$  influences the development of the dry profile. This influence has a numerical cause and is not process-based. In reality we would also expect smoothing of the sharp edges of the dry profile, caused by wind transport, walking people, wave run-up and construction practice. So it can be stated that a little smoothing of the edges in the model represents reality to some extent, although the underlying physics aren't incorporated. It can also be concluded that the influence of the step size on the dry profile on the final results is relatively low. Therefore the step size of 2.5 m used for the calculations in this chapter is a safe choice.

## 9.5.7 Conclusions

The sensitivity of the model results to the boundary conditions and assumptions can be summarized as follows:

- The wave climate has a significant influence on the bottom profile shape and shoreline position (Paragraph 9.5.2).
- The construction slope has some influence on the additional dry beach width  $\Delta y_{0,EO}$  while this influence in reality isn't expected to occur. A slope of 1 to 10 as considered here is expected to give good modelling results (Paragraph 9.5.3).
- The omission of persistency in the time series of the waves is of minor influence when dynamic profile equilibrium conditions are considered (Paragraph 9.5.4).
- The starting time of the calculations has significant influence on the equilibration time scale, due to the varying wave conditions during the year. The dynamic equilibrium state is hardly influenced by the starting time (Paragraph 9.5.5).
- The computational step size  $dx$  has a minor influence on the development of the dry profile. A finite  $dx$  causes some smoothing of sharp edges of the dry profile (Paragraph 9.5.6).

## 9.6 Interaction between longshore and cross-shore transport

### 9.6.1 Introduction

It has been assumed that an eventually present longshore transport gradient in the center area of Cancún Beach can be neglected (see Paragraph 9.3.2). The goal of this paragraph is to check if a longshore transport gradient could influence the results of the cross-shore modelling of the beach fill equilibration.

The longshore transport  $q_y$  consists of bed load and suspended transport and is caused by turbulence, a longshore current and wave orbital motion. The longshore transport increases for (amongst others):

- Decreasing grain size.
- Increasing wave height (more turbulence and higher current).
- Increasing angle of wave incidence (up to 45°) (higher current).
- Increasing wind speed component parallel to the shore (higher current).
- Increasing tidal or oceanic current.

Gradients in the longshore transport  $q_y/\partial y$  are caused by differences in the above parameters along the coast.

The total longshore transport across the profile  $Q_y$  is the integral of the longshore transport across the profile ( $x$ -axis) and thus depends (amongst others) on the width over which the transport  $q_y$  is present, i.e. the width of the breaker zone.

### Questions

The following questions must be answered:

1. Does the beach nourishment (with material the same as native) influence the longshore erosion / accretion, compared with the original profile?
2. Does a longshore transport gradient (if present) influence the results of the cross-shore equilibration?

The following sub-questions have to be answered:

- a. When (in general) will longshore transport gradients influence the cross-shore transport? (Paragraph 9.6.2)
- b. What is the distribution of the longshore transport across the profile for the pre-nourishment profile and the nourished profile? (Paragraph 9.6.3)
- c. How do the cross-shore gradients of the cross-shore transport  $q_x/\partial x$  and the longshore transport  $q_y/\partial x$  compare? (Paragraph 9.6.4)
- d. Are there differences in the longshore transport gradient  $q_y/\partial y$  across the profile for the pre-nourishment and the nourished profile? (Paragraph 9.6.5)

## 9.6.2 Influence of a longshore transport gradients on the cross-shore transport

During the modelling of the equilibration in this chapter, the gradient in longshore transport has been assumed zero. In the case that this assumption is not true, longshore erosion or accretion will influence the cross-shore sediment balance. Where in the (cross-shore) profile this erosion or accretion will take place depends on the distribution across the profile of (a) the longshore transport  $q_y(x)$  and (b) the gradients of this transport  $q_y/\partial y(x)$ .

Assuming that longshore erosion or accretion occurs, two cases can be distinguished:

### Case 1

The cross-shore differences in bottom changes caused by longshore erosion or accretion are reworked by the cross-shore transport such that no significant changes in the shape of the cross-shore profile due to longshore transport occur. The loss or gain of sediments due to longshore erosion is thus equally distributed across the active cross-shore profile. This is the case if the longshore transport gradient is small compared with the cross-shore transport gradient:

$$\frac{\partial q_y}{\partial y} \ll \frac{\partial q_x}{\partial x} \quad (9.3)$$

Where:	$q_x$	total cross-shore transport per unit width	$[\text{m}^3/\text{s}/\text{m}]$
	$q_y$	total longshore transport per unit width	$[\text{m}^3/\text{s}/\text{m}]$
	$y$	longshore coordinate	$[\text{m}]$

**Or** when the differences in longshore transport across the profile are small (the whole active profile will have almost the same bottom change due to the longshore transport gradient) compared with the cross-shore transport gradient:

$$\frac{\partial q_y}{\partial x} \ll \frac{\partial q_x}{\partial x} \quad (9.4)$$

Where:	$x$	cross-shore coordinate	$[\text{m}]$
--------	-----	------------------------	--------------

So if Equation (9.3) or (9.4) is true, two conclusions can be drawn:

- The cross-shore profile shape and transport in the active profile isn't significantly changed by the longshore erosion or accretion.
- The longshore sediment loss or gain can be superimposed on the cross-shore bottom changes, equally distributed over the entire active profile.

### Case 2

When **both** Equation (9.3) and Equation (9.4) aren't fulfilled, changes in profile shape will occur.

For this case the following conclusions can be drawn:

- The cross-shore profile shape and transport is changed by the longshore erosion or accretion.
- The longshore sediment loss or gain cannot be superimposed on the cross-shore bottom changes after e.g. one year.

### 9.6.3 Cross-shore distribution of longshore transport

#### Construction profile versus pre-nourishment profile

The question arises what the differences in longshore transport are for a construction profile and the pre-nourishment profile. Therefore three runs (two construction profiles and the pre-nourishment profile) have been made with Unibest-TC with the following parameters:

Parameter	symbol	value
root-mean-square wave height	$H_{rms}$	1.1 m
peak wave period	$T_p$	7.0 s
wave direction	$\theta$	-45°
ocean current	$V$	-0.5 m/s at 30 m depth
wind speed and direction	$V_w$ and $\theta_w$	8 m/s and 0°
bottom profiles	$z_b(x)$	original profile $V = 250 \text{ m}^3/\text{m}$ $V = 400 \text{ m}^3/\text{m}$

The bottom profiles with the transport rates have been plotted in Figure 9-27 and Figure 9-28. No bottom changes were calculated; only the initial transports are considered here.

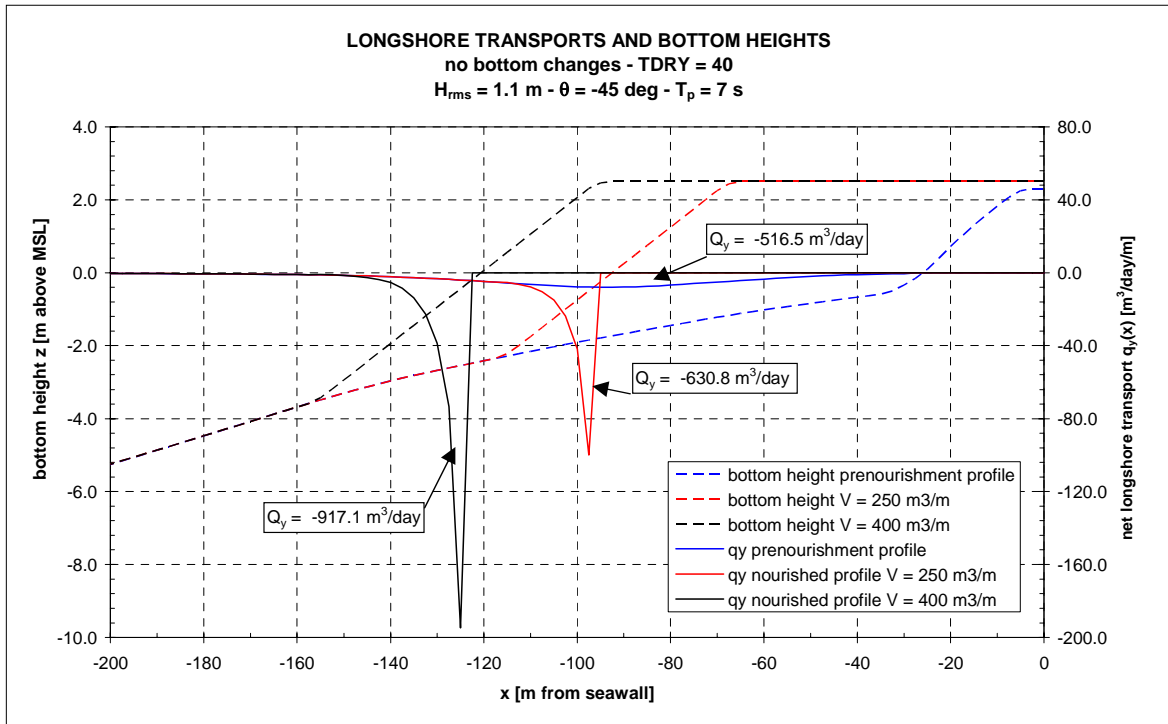


Figure 9-27: **Initial** longshore transports for the pre-nourishment profile and two construction profiles for standard wave conditions. The total longshore transports  $Q_y$  were determined from  $x = -180$  m until the  $x$ -coordinate where  $h = h_{min}$  (approximately at  $h = 0.31$  m).

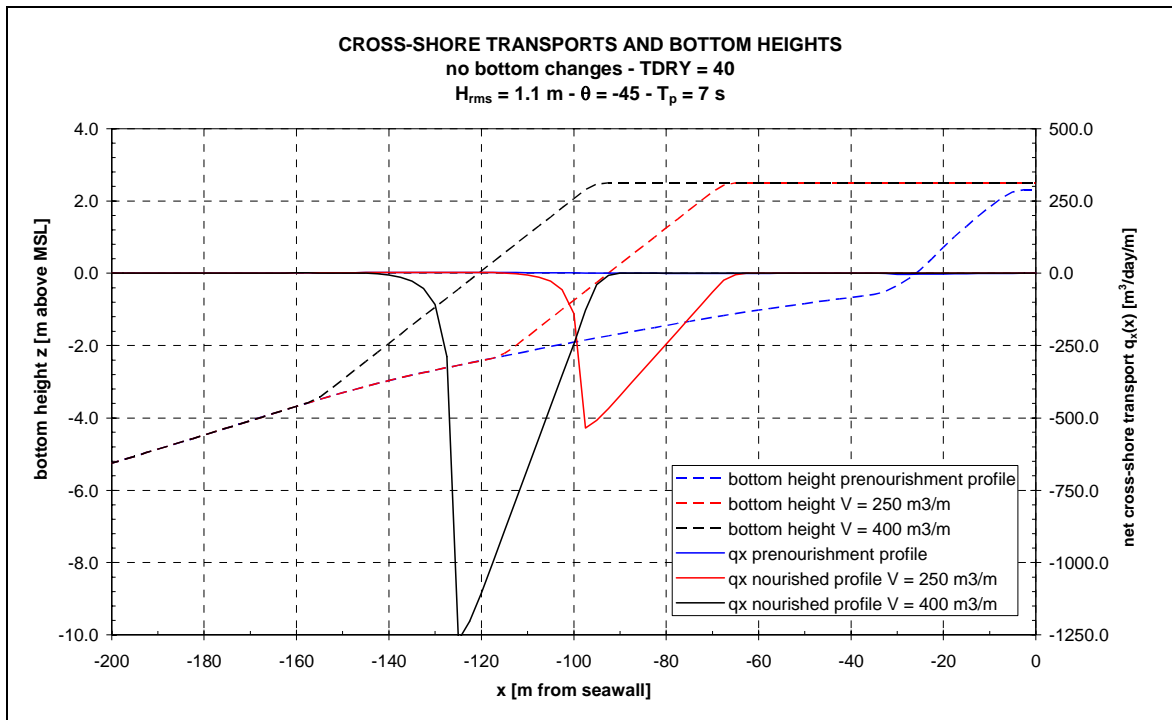


Figure 9-28: **Initial** cross-shore transports for the pre-nourishment profile and two construction profiles for standard wave conditions.

The following observations can be made:

- The peak values of the cross-shore transport  $q_x(x)$  are far higher for the construction profiles.
- The peak values of the longshore transport  $q_y(x)$  are far higher for the construction profiles.

- The longshore transports are calculated to the last grid point where  $h > h_{min}$  (= 0.31 m in this case with TDRY = 40, see Appendix C.3.6); for the next grid point they are set zero.
- The cross-shore transports are calculated to the last grid point where  $h > h_{min}$ ; for the next grid points the transport is extrapolated with the height (see Appendix C.3.6).
- The net total longshore transport  $Q_y$  from  $x = -150$  m to the shoreline has the highest value for the nourished profile with  $V = 400$  m<sup>3</sup>/m (917.1 m<sup>3</sup>/day).
- Due to the fact that Unibest-TC sets the longshore transport to zero for depths smaller than  $h_{min}$  (= 0.31 m for TDRY = 40 and  $T_p = 7$  s, see Paragraph 7.3.1), the total longshore transport  $Q_y$  is slightly underestimated for the steep construction profiles, because a small part of the breaker zone is ignored.

#### Conclusion:

Significant differences in the total longshore transport  $Q_y$  and the cross-shore distribution of the longshore transports  $q_y(x)$  occur between the construction profiles and the pre-nourishment profiles. These differences aren't fully accounted for by the Unibest-TC model due to the fact that the calculations are stopped at  $h_{min}$ . Total longshore transports are higher for the steep construction profiles.

#### First 60 days after construction with a normal wave climate

The distribution of the longshore transport on the pre-nourishment profile and the equilibrating nourished profile ( $V = 250$  m<sup>3</sup>/m) during the first 60 days after construction (when nourished and not-nourished profiles are still significantly different in shape) is plotted in Figure 9-29. The transports in this graph are *net* transports of the first 60 days after construction.

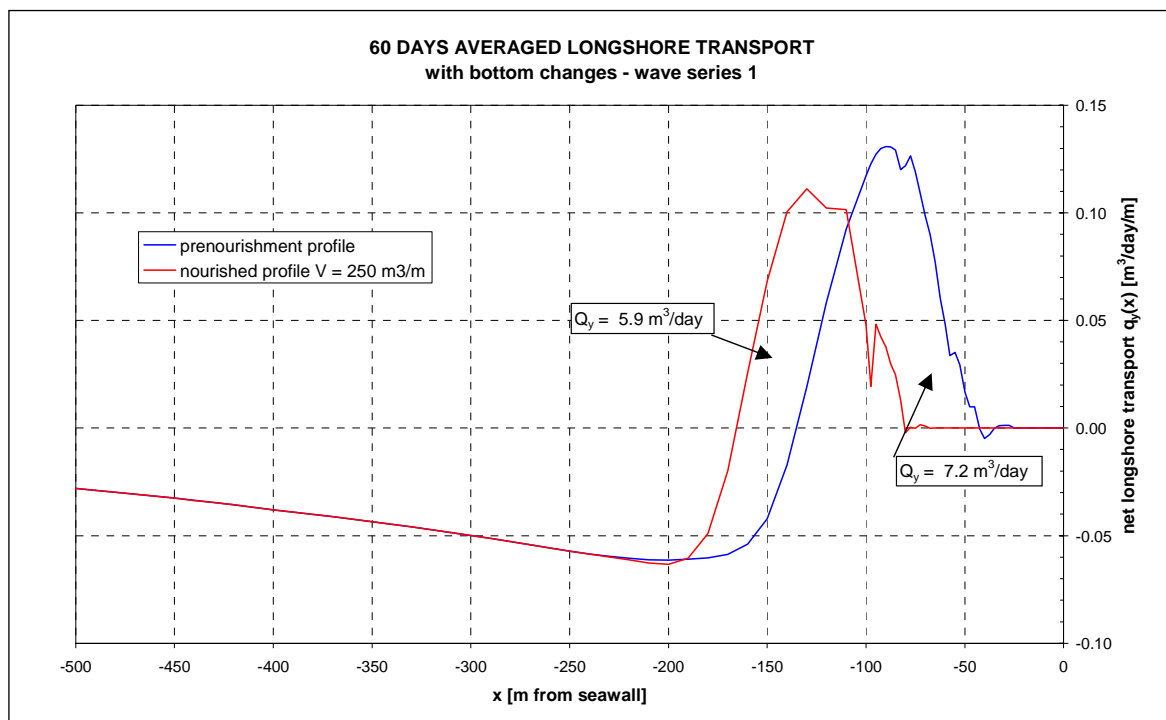


Figure 9-29: Net longshore transport across the profile during the first 60 days after construction for a **normal wave climate**.

The following observations can be made:

- The deep water longshore transport (caused by the oceanic current and wave stirring) is the same for both cases.
- The longshore transport in the breaker zone  $q_y(x)$  has a lower peak for the nourished profile.
- The net total transport  $Q_y$  in the breaker zone (positive, southwards) is  $7.2 \text{ m}^3/\text{day}$  for the original profile and  $5.9 \text{ m}^3/\text{day}$  for the nourished profile. These small values are caused by the small incident wave angles during this period and the fact that the average incident wave angle is almost shore normal.

Conclusions:

- Both the cross-shore distribution of the longshore transport  $q_y(x)$  as the net total longshore transport  $Q_y$  are different for the construction and the original profile in the first 60 days after construction.
- The magnitude of the net longshore transport for the considered period is very low, because of the small average angle of wave incidence  $\theta$ . Bottom changes caused by longshore transport gradients will therefore be small.

### First year after construction

The distribution of the longshore transport across the profile for the original and the equilibrating profile is shown in Figure 9-30. The transports in this graph are net transports of the first year after construction.

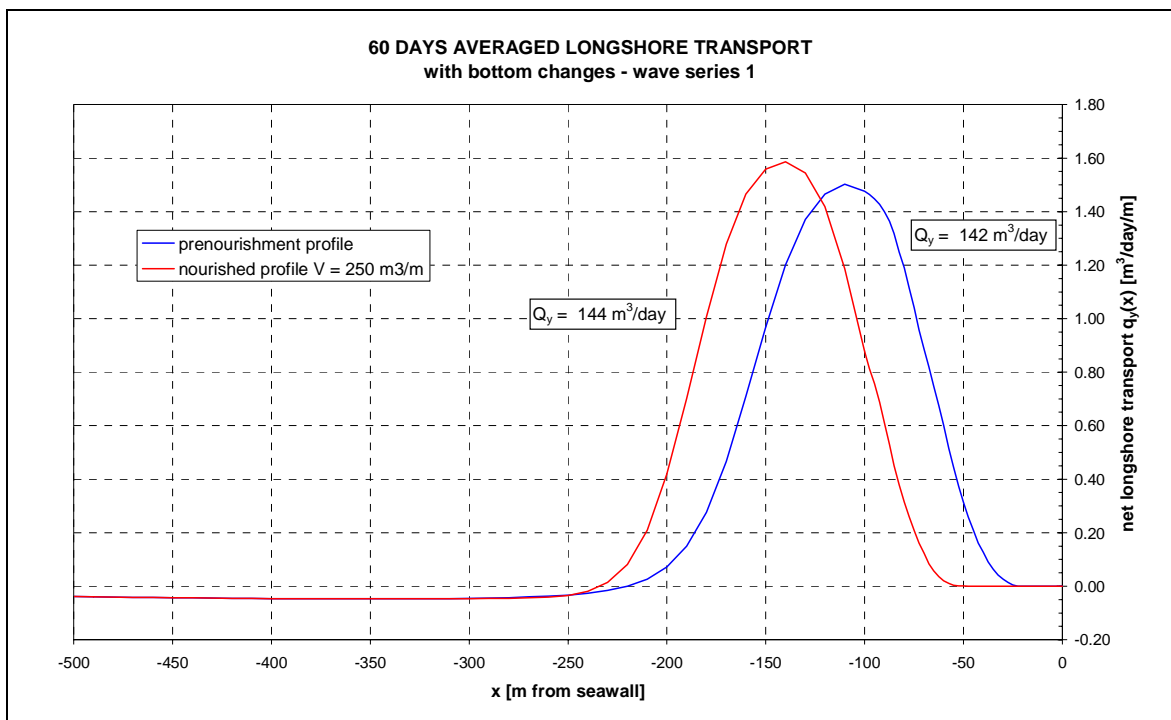


Figure 9-30 Net longshore transport across the profile during the first year after construction for a normal wave climate.

The following observations can be made:

- The deep water longshore transport (caused by the oceanic current) is the same for both cases.
- The transport in the breaker zone has a slightly higher peak for the nourished profile.
- The net total transport in the breaker zone (positive, southwards) is  $142 \text{ m}^3/\text{day}$  for the original profile and  $144 \text{ m}^3/\text{day}$  for the nourished profile.
- The distribution across the profile is nearly the same.

**Conclusion:**

The net cross-shore distribution of the longshore transport  $q_y(x)$  and the net total longshore transport  $Q_y$  are almost the same for the construction and original profile in the first year after construction. This can be explained by small average angle of wave incidence during the first months after construction.

**9.6.4 Cross-shore gradients in the sediment transport**

In Table 9-7 the maximum transports and gradients in the breaker zone are summarized for an initial construction profile with a fill volume  $V = 400 \text{ m}^3/\text{m}$ ,  $B = 2.5 \text{ m}$ , slope = 1 to 10,  $d_F = 0.33 \text{ mm}$ ,  $H_{rms} = 1.1 \text{ m}$ ,  $T_p = 7 \text{ s}$ ,  $\theta = -45^\circ$ .

Table 9-7: Maximum values of the cross-shore and longshore transports and their gradients for a construction profile with  $V = 400 \text{ m}^3/\text{m}$ ,  $B = 2.5 \text{ m}$  and  $d_F = 0.33 \text{ mm}$  at  $T=0$  days. Used wave input:  $H_{rms} = 1.1 \text{ m}$ ,  $T_p = 7 \text{ s}$  and  $\theta = -45^\circ$ . The results are obtained from Figure 9-27 and Figure 9-28.

Variable		maximum	unit
longshore transport	$q_y(x)$	192	$[\text{m}^3/\text{day}/\text{m}]$
cross-shore transport	$q_x(x)$	108	$[\text{m}^3/\text{day}/\text{m}]$
longshore transport gradient across the profile	$\frac{\partial q_y}{\partial x}$	7	$[(\text{m}^3/\text{day}/\text{m})/\text{m}]$
cross-shore transport gradient across the profile	$\frac{\partial q_x}{\partial x}$	23	$[(\text{m}^3/\text{day}/\text{m})/\text{m}]$

From this table can be concluded that the condition of Equation (9.4) is fulfilled.

**9.6.5 Longshore gradients in the sediment transport**

The gradient in the longshore transport can be different for the deep water longshore transport and the transport in the breaker zone, since both are caused by different phenomena. The latter is predominantly caused by the oceanic current and wave stirring. Differences along the coast of these two processes can cause gradients in the longshore transport on deep water. This transport is of negligible importance for the equilibration process, since this occurs on relatively deep water and will not be treated further.

The gradient in longshore transport in the breaker zone is predominantly caused by differences along the coast of wave height and wave angle. This can occur due to varying refraction, diffraction and shoaling along the coast and thus depends on the direction of the incoming waves. So the longshore transport gradient can be different depending on the direction of the longshore transport.

The gradient can also vary across the breaker zone, but this effect is estimated to be negligible. This implies that the beach fill has a negligible influence on the gradients too.

**9.6.6 Conclusions**

The answers to the questions in the introduction (Paragraph 9.6.1) are as follows:

1. The beach fill influences the (net) cross-shore distribution of the longshore transport  $q_y(x)$  in the breaker zone, as it does the total net longshore transport  $Q_y$  in the breaker zone. Since the gradient in the longshore transport can be assumed to be independent on the shape of the cross-shore profile, the longshore erosion or accretion volume during the equilibration process is different from that of the original profile.
2. The results of the cross-shore equilibration aren't significantly disturbed by a longshore transport gradient because the cross-shore gradient of the cross-shore transport is much bigger than the cross-shore gradient of the longshore transport:  $\partial q_x / \partial x \gg \partial q_y / \partial x$ .



It can be concluded that for the modelling of the equilibration the omission of possible occurring longshore transport gradients is justified and of no significant influence on the results.

It must be stated however, that if longshore transport gradients occur, the profile will be shifted. This development can be superimposed on the results of the cross-shore modelling within reasonable limits of accuracy.

## 9.7 Conclusions and recommendations

In this paragraph the conclusions of this chapter are presented. This answers the questions posed in Paragraph 9.2, which are repeated here for convenience:

- What is the dynamic equilibrium profile after equilibration?
- What is the development of the equilibration in time, i.e. what is the characteristic time scale of the equilibration?

### Dynamic equilibrium profile

In general, the equilibrated profile has approximately the same shape as the pre-nourishment profile. The toe of the profile is located between MSL -7.5 and -8.5 m, depending on the fill volume. The dry profile shape remains approximately the same as the construction profile, because physical processes such as swash zone dynamics and wind transport are not incorporated in the model.

The following parameters influence the shape of the dynamic equilibrium profile:

- A larger fill volume  $V$  results in a larger seaward shift of the profile.
- A higher berm height  $B$  causes a slightly smaller seaward shift of the profile since more sediment is stocked on the dry beach.
- A larger fill grain size  $d_f$  results in a steeper deep water profile. More sediment is available for the upper part of the profile, resulting in a larger shoreline advancement  $\Delta y_{0,EQ}$ .
- Different time series of the waves have a negligible influence on the profile shape.

### Development of the equilibration in time

The profile equilibration is practically complete after one year: both the profile changes as the cross-shore transports have become very low at that time. The minor profile changes in the following years can partly be contributed to further equilibration and partly to imperfections in the Unibest-TC model, and therefore aren't reliable.

The exponential expression in Equation (9.5) suggested by Dean [2002] for the development of the shoreline position in time is a reasonable approximation for the shoreline development calculated by Unibest-TC.

$$\Delta y_0(t) = \Delta y_{0,EQ} + [\Delta y_0(0) - \Delta y_{0,EQ}] \cdot e^{-t/T_{EQ}} \quad (9.5)$$

Where:	$\Delta y_0(t)$	additional dry beach width in time	[m]
	$\Delta y_{0,EQ}$	additional dry beach width after equilibration	[m]
	$\Delta y_0(0)$	additional dry beach width of the construction profile	[m]
	$T_{EQ}$	equilibration time scale	[days]

Least-square fits for the equilibration time scale  $T_{EQ}$  lie between 70 and 95 days and depend on the following quantities:

- The grain size  $d_f$  as a larger grain size results in smaller transports.
- The berm height  $B$  as higher berm heights act like a stockpile of sand, only moved by high waves.
- The extension of the construction profile in the breaker zone, as more focused wave breaking causes larger transports.
- The eroded volume  $V_{er}$  as higher volumes take more time to erode.
- The cross-shore distance  $X_e$  over which the eroded volume is transported.

In general it can be stated that:

- The larger the grain size  $d_F$ , the smaller the equilibration time scale  $T_{EQ}$ .
- The higher the berm height  $B$ , the larger the equilibration time scale  $T_{EQ}$ .
- No clear relation is present between the fill volume  $V$  and  $T_{EQ}$ .

### Validation of the model results

The validation of the model can be summarized as follows:

- A wave climate with higher waves increases the eroded volume and shoreline retreat during equilibration and changes the dynamic equilibrium profile shape significantly.
- In reality no influence of the construction slope on the dynamic equilibrium profile shape is expected. In the Unibest-TC model a small difference in additional dry beach width  $\Delta y_0$  is present, caused by an incorrect modelling of the dry profile. The equilibration time scale  $T_{EQ}$  is hardly influenced. The construction slope of 1 to 10 used for the modelling probably is a good representation of reality.
- The omission of persistency of wave conditions in the time series of the waves has no significant influence on the dynamic equilibrium profile shape and the equilibration time scale.
- When the modelling starts in a different time of the year, large differences in the equilibration time scale  $T_{EQ}$  result, caused by seasonal variations in wave climate. No significant differences in dynamic equilibrium profile shape occur.
- The computational time step  $dx$  influences the development of the dry profile a little. No significant changes in results occur.
- The assumption that a possibly present gradient in the longshore transport doesn't influence the results of the cross-shore equilibration is justified.

It can be stated that the model results are rather robust for changes in the slope of the construction profile, the omission of persistency of wave conditions and the computational time step  $dx$ . The wave climate and seasonal wave variations are of significant influence on the model results.

### Discussion of model results

Model results remain uncertain, in spite of an extensive validation of the Unibest-TC model. This is caused by:

- The uncertain boundary conditions result in uncertainties in the calibrated parameter setting and the calculation results.
- The shoreline position is just one indicator of the calculated profile and could be calculated wrongly. This might cause errors in the determination of the equilibration time scale  $T_{EQ}$ .
- The omission of mixing and sorting of the grains. This could cause errors in the calculated profile shape and equilibration time scale.

It is concluded that the results discussed in this chapter should be interpreted with care.

### Recommendations for the Cancún Beach fill

The following recommendations regarding the planned fill at Cancún Beach are made:

- A potentially dangerous scarp is likely to occur, because of the very high erosion rates directly after construction.
- It is advised to spread the fill across the active profile up to a depth of approximately 4 m, since this will reduce the shoreline retreat after construction and thus improves public perception of the project.
- It is advised to apply a berm height of at least MSL +2.5 m, since this relatively high berm acts like a stockpile of sand which is only drawn on during extreme conditions.

## 10 EVALUATION OF EQUILIBRATION DESIGN METHODS

### 10.1 Introduction

The objective of this chapter is to describe and explain the differences in calculated shoreline advancement and profile shape after equilibration between the equilibrium models and process-based modelling with Unibest-TC.

These equilibrium models of Dean [1974], James [1975], the USACE [1994] and Dean [2002] have been described in Paragraph 4.6 and applied in Chapter 5. The process-based modelling with Unibest-TC has been discussed in Chapter 6 to 9.

First, the calculated shoreline advancement and profile shape according to above design methods are compared in Paragraph 10.2. Subsequently, the differences are evaluated and explained in Paragraph 10.3. Finally, the conclusions and recommendations are discussed in Paragraph 10.4.

### 10.2 Comparison of the results

#### Shoreline advancement

In Paragraph 5.4.2 and 9.4.5 the shoreline advancement after equilibration  $\Delta y_{0,EQ}$  (or additional dry beach width) according to the methods of Dean [1974], James [1975], USACE [1994], Dean [2002] and the Unibest-TC model has been determined. In Appendix H the values of  $\Delta y_{0,EQ}$  are summarized for a berm height  $B$  of 2.5 m and a closure depth  $h_*$  of 7.5 m. These shoreline advancements are visualized in Figure 10-1 to Figure 10-3.

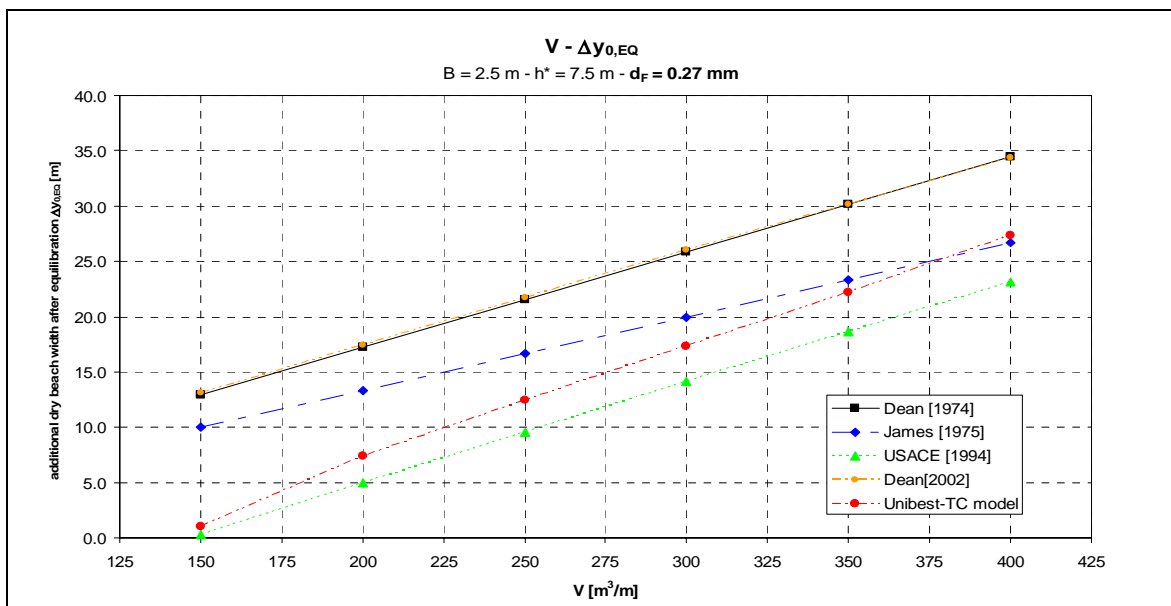


Figure 10-1: The shoreline advancement after equilibration  $\Delta y_{0,EQ}$  versus the fill volume  $V$  for  $B = 2.5$  m,  $h_* = 7.5$  m and  $d_F = 0.27$  mm.

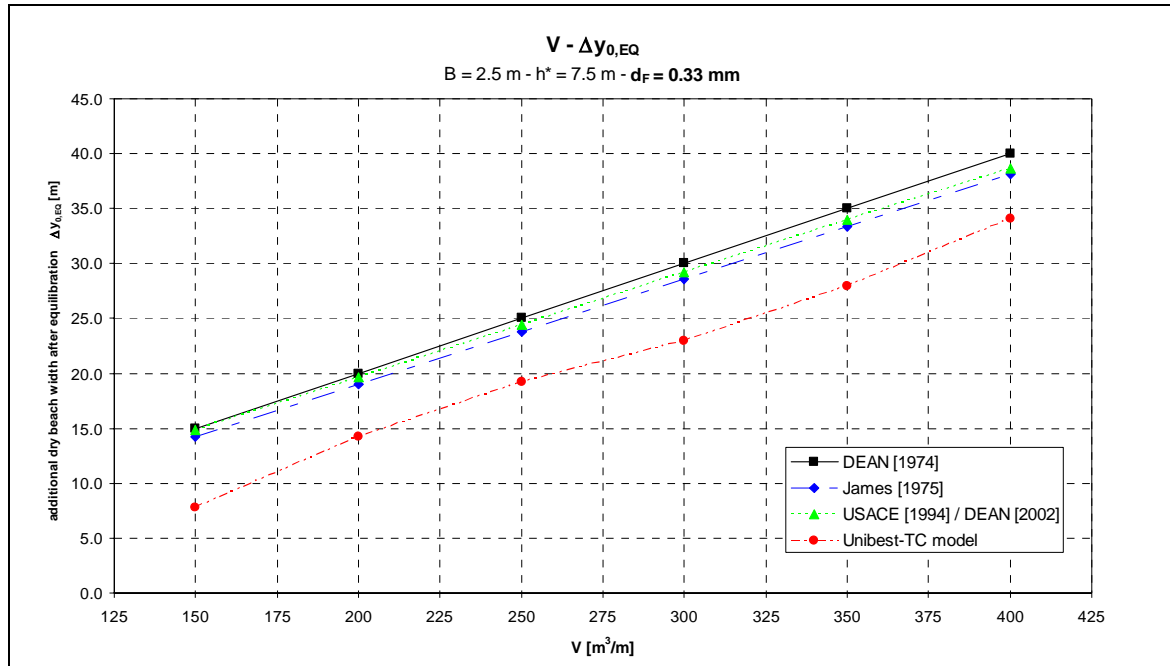


Figure 10-2: The shoreline advancement after equilibration  $\Delta y_{0,EQ}$  versus the fill volume  $V$  for  $B = 2.5$  m,  $h_* = 7.5$  m and  $d_f = 0.33$  mm.

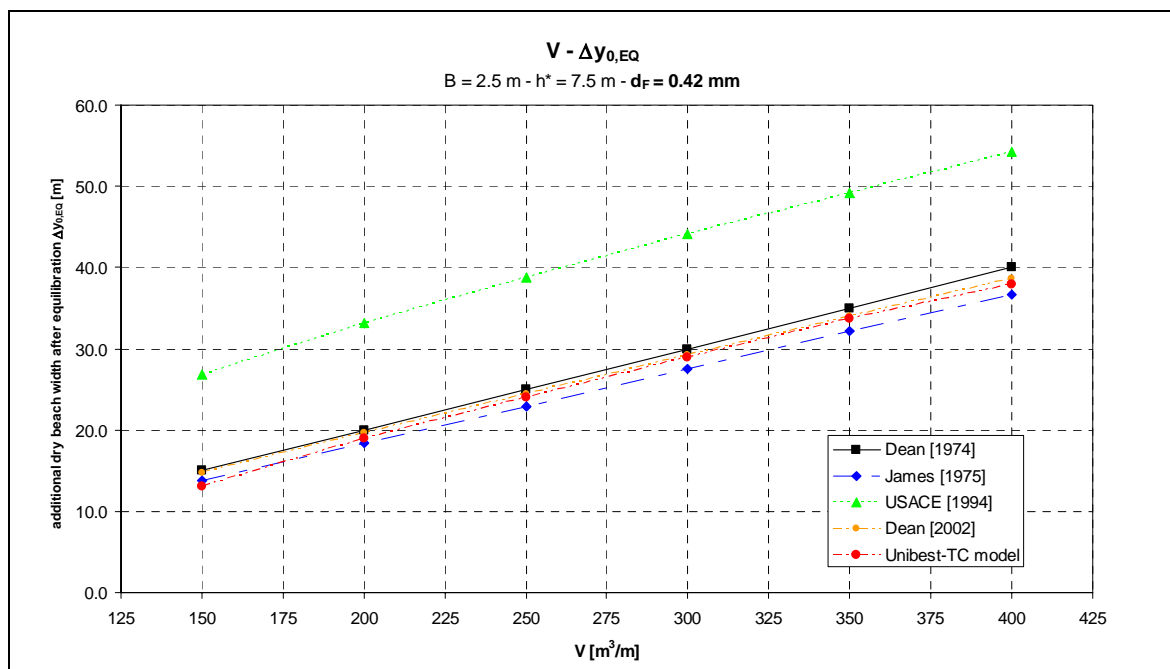


Figure 10-3: The shoreline advancement after equilibration  $\Delta y_{0,EQ}$  versus the fill volume  $V$  for  $B = 2.5$  m,  $h_* = 7.5$  m and  $d_f = 0.42$  mm.

In Figure 10-4 the results are presented in another manner: the median fill grain size  $d_f$  has been plotted on the horizontal axis and the additional dry beach width  $\Delta y_{0,EQ}$  on the vertical axis for a fill volume  $V$  of  $200$   $m^3/m$  and a berm height  $B$  of  $2.5$  m. It is clear that large differences exist between the design methods in the sensitivity of the shoreline advancement and the fill grain size.

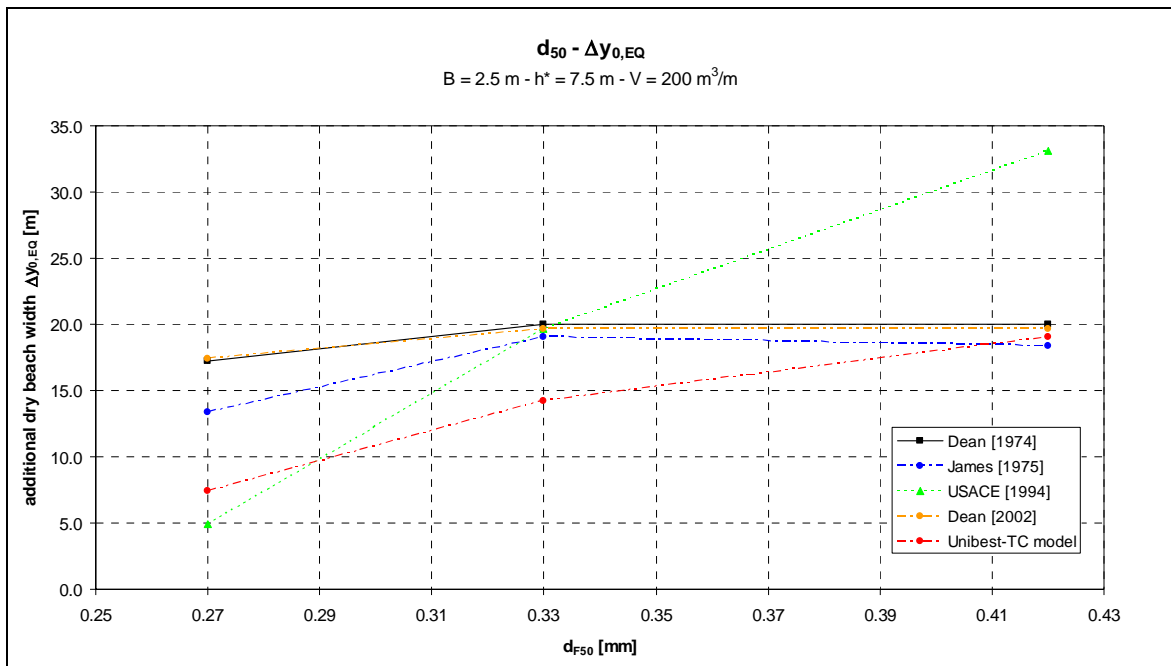


Figure 10-4: The shoreline advancement versus the median fill grain size  $d_{F50}$ .

### Profile shape

On page H-5 to H-7 in Appendix H the following initial and equilibrated bottom profiles are drawn for the three fill grain sizes considered ( $d_F = 0.27 - 0.33 - 0.42$  mm), using a fill volume  $V$  of  $250 \text{ m}^3/\text{m}$  and a berm height  $B$  of 2.5 m:

Initial profiles	Profiles after equilibration
Measured June 2000, averaged chainage 6100 – 6900	According to the USACE method
A least-square fit according to Equation (4.11)	According to the Dean [2002] method
An Unibest-TC equilibrium profile (see Paragraph 8.4.1)	According to the Unibest-TC model

The equilibrated profiles according to Dean [1974] and James have been omitted from these plots to maintain a clear view. For these profiles is referred to page H-2 to H-4 in Appendix H.

The following remarks can be made:

- The fit of  $h = Ay^{2/3}$  to the measured profile is poor.
- The fit of the Unibest-TC equilibrium profile to the measured profile is reasonable (see Paragraph 8.4.1).

### Summary of the results

In Table 10-1 the results of the applied design methods are summarized.

Table 10-1: Comparison of the results of the design methods. N.A. means Not Applicable. Scores (+ +/+ /0/-/-) are relative to each other.  
 \* Milder for finer grains, steeper for coarse grains.  
 # Finer fraction in lower profile with a milder slope, coarse fraction in upper profile with a steeper slope.

Results		Design method				
		Dean [1974]	James [1975]	USACE [1994]	Dean [2002]	Unibest-TC
Shoreline advancement [m] for $V = 250 \text{ m}^3/\text{m}$	$d_F = 0.27$	25.0	23.8	24.5	24.5	19.2
	$d_F = 0.33$	21.6	16.7	9.5	21.7	12.4
	$d_F = 0.42$	25.0	22.9	38.8	24.5	24.0
Threshold volume for shoreline advancement		No	No	Yes	No	Yes
Shoreline advancement per unit fill volume	$d_F = 0.27$	0	-	0	0	+
	$d_F = 0.33$	0	0	0	0	0
	$d_F = 0.42$	0	-	+	0	0
Sensitivity $\Delta y_{0,EQ}$ for $d_F$		-	0	++	-	+
Profile shape		No change	No change	*	#	*
Non-intersecting profiles		Yes	Yes	Yes	Yes	N.A.
Intersecting profiles		No	No	Yes	No	N.A.
Toe of the profile		No toe	No toe	Vertical if non-inters.	Vertical	N.A.
Change in dry beach shape		No	No	No	No	Small

Some unexpected features of Table 10-1 are explained below.

#### Threshold volume

A threshold volume for shoreline advancement occurs in the Unibest-TC model for  $d_F = 0.27 \text{ mm}$ , because the sediment size in the profile is assumed to equal the fill grain size, i.e. no mixing with the native sediments occurs. Therefore the calculated shoreline advancement for  $V < 200 \text{ m}^3/\text{m}$  is probably too low.

#### Shoreline advancement per unit fill volume

The shoreline advancement per unit fill volume ( $d\Delta y_{0,EQ} / dV$ ) according to the methods of James and Dean [1974] is independent of the fill volume and can be written as:

$$\frac{d(\Delta y_{0,EQ})}{dV} = \frac{1}{K(h_* + B)} \quad (10.1)$$

Where:	$\Delta y_{0,EQ}$	additional dry beach width	[m]
	$V$	fill volume	[m <sup>3</sup> /m]
	$K$	overflow factor according to Dean or James	[-]
	$h_*$	closure depth	[m]
	$B$	berm height	[m]

The occurrence of intersecting and non-intersecting profiles with the USACE method causes a high, respectively low shoreline advancement per unit fill volume.

#### Sensitivity of the shoreline advancement $\Delta y_{0,EQ}$ to the fill grain size

Intersecting and non-intersecting profiles and a grain size dependent profile shape cause a large sensitivity of the shoreline advancement to the fill grain size.

#### Toe of the profile and dry beach

The way the toe of the profile and the dry beach are modelled is of negligible influence on the shoreline advancement.

## 10.3 Evaluation of the differences in results

### 10.3.1 Introduction

Significant differences occur between the design methods regarding profile shape, threshold volumes, shoreline advancement per unit fill volume and sensitivity to the fill grain size. This is caused by a varying implementation of relevant model issues and by the input of uncertain boundary conditions in the design methods.

In Paragraph 10.3.2 an overview is presented of the implementation of the relevant model issues, where after the consequences of these model issues on the results are discussed in Paragraph 10.3.3 to 10.3.5. Subsequently, the influence of the uncertain boundary conditions is discussed (Paragraph 10.3.6). Finally conclusions are drawn in Paragraph 10.3.7.

### 10.3.2 Differences in approach of the design methods

The equilibration design methods can be characterized by the implementation of the relevant model issues as defined in Paragraph 4.5 and summarized in Table 10-2.

Table 10-2: Overview of the implementation of model issues.

Model issues		Design method				
		Dean [1974]	James [1975]	USACE [1994]	Dean [2002]	Unibest-TC
Equilibrium profile	current profile is in equilibrium	yes	yes	yes	yes	implicitly
	current sediment is in equilibrium	yes	yes	yes	yes	implicitly
	grain size dependent profile shape	no	no	yes	yes	implicitly
Granulometry	grain size distribution	$\mu_F + \sigma_F$ $\mu_N$	$\mu_F + \sigma_F$ $\mu_N + \sigma_N$	$\mu_N$ $\mu_F$	$\mu_F + \sigma_F$ $\mu_N$	$d_{50F}$ $d_{50N}$
	grain size distribution across the profile	no	no	no	$\mu_F$ (y)	$d_{50}$ (h) not used
	time-varying grain size distribution across the profile	no	no	no	no	no
Depth of closure		yes	yes	yes	yes	no
Underlying physical processes which cause the morphology are considered		no	no	minimal	minimal	yes
Time-varying processes and boundary conditions		no	no	no	no	yes

The design methods of Dean [1974] and [2002], James and the USACE are equilibrium models, i.e. 'based on the a priori identification of an equilibrium state without describing the way such equilibrium is achieved' [Capobianco et al., 2002]. The Unibest-TC model is a process-based profile model, i.e. 'based on the detailed description of the different processes which cause the morphology' [Capobianco et al., 2002], although it is implicitly based on an assumed equilibrium condition for calibration purposes.

The implication of the implementation of the model issues indicated in Table 10-3 on the results of the design methods is discussed in the following paragraphs.

### 10.3.3 Equilibrium profile

#### Current profile and sediment is in equilibrium

This assumption is used –implicitly or explicitly– by all design methods and is highly uncertain due to lack of profile measurements during sufficient time. If the profile and sediment are out-of-equilibrium instead of in-equilibrium, the consequences indicated in Table 10-3 occur.

Table 10-3: Implications of an incorrectly assumed equilibrium profile and sediment.

Method	Used?	Implication when assumption is not true
Dean [1974]	yes	Another equilibrated profile shape and grain size distribution will occur.
James [1975]	yes	Idem to Dean [1974].
USACE [1994]	yes	The fitted profile scale parameter $A_N$ will change, as does the equilibrated profile shape and shoreline advancement.
Dean [2002]	yes	The fitted profile scale parameter $A_N$ will change, as does the equilibrated profile shape and shoreline advancement.
Unibest-TC	implicitly	The calibrated parameter setting needs to be altered, leading to differences in equilibrated profile shape and shoreline advancement.

The consequences are qualitatively similar, but can differ in a quantitative sense. It is estimated that the assumption of an equilibrium state of the current profile is at least more or less correct. This assumption is therefore no large error source; neither causes it large differences between the methods.

**Grain size dependent profile shape**

A grain size dependent profile shape is observed in nature: profile slopes are milder when composed of finer sediments [Dean, 1977]. This model issue should be implemented in a design method for a good representation of reality. In Table 10-4 the implications of the implementation of this model issue are discussed.

Table 10-4: Implications of a grain size dependent profile shape.

Method	Used?	Implication of model issue
Dean [1974]	no	<p>This is an incorrect representation of reality which has the following implications:</p> <div style="border: 1px solid black; padding: 10px; margin: 10px auto; width: fit-content;"> <p style="text-align: center;">Same profile slope for all <math>d_F</math></p> <p style="text-align: center;">↓</p> <ul style="list-style-type: none"> <li>No intersecting profiles</li> <li>No sensitivity of <math>\Delta y_{0,EQ}</math> to <math>d_F</math>, and thus a overestimation of the shoreline advancement for <math>d_F &lt; d_N</math> and an underestimation for <math>d_F &gt; d_N</math></li> </ul> </div>
James [1975]	no	Idem to Dean [1974].
USACE [1994]	yes	<p>The profile shape (<math>h=Ay^{2/3}</math>) is strongly grain size dependent, but not adequate for this situation. The grain size dependent profile shape has the following implications:</p> <div style="display: flex; justify-content: space-around;"> <div style="border: 1px solid black; padding: 5px; margin: 5px;"> <p>Steeper slopes for <math>d_F &gt; d_N</math></p> <p style="text-align: center;">↓</p> <ul style="list-style-type: none"> <li>Intersecting profiles</li> <li>Large (<math>d\Delta y_{0,EQ} / dV</math>)</li> <li>Large sensitivity of <math>\Delta y_{0,EQ}</math> to <math>d_F</math></li> </ul> </div> <div style="border: 1px solid black; padding: 5px; margin: 5px;"> <p>Flatter slopes for <math>d_F &lt; d_N</math></p> <p style="text-align: center;">↓</p> <ul style="list-style-type: none"> <li>submerged profiles and treshold fill volume</li> <li>Small (<math>d\Delta y_{0,EQ} / dV</math>)</li> <li>Large sensitivity of <math>\Delta y_{0,EQ}</math> to <math>d_F</math></li> </ul> </div> </div>
Dean [2002]	yes	Idem to USACE [1994], but only non-intersecting profiles occur, due to the cross-shore variation of the grain size.
Unibest-TC	implicitly	The profile shape is grain size dependent, based on the underlying physical processes.



### 10.3.4 Granulometry

In reality the grain size distribution varies across the profile and in time, due to mixing and sorting. When we assume the grain size in  $\phi$ -units at every location and time to be normally distributed, we can express the grain size distribution as follows:

$$f(x, t, \phi) = \frac{1}{\sigma_\phi \sqrt{2\pi}} e^{-\frac{(\phi - \mu_\phi)^2}{2\sigma_\phi^2}} \quad \text{with} \quad \begin{aligned} \mu_\phi &= f(y, t) \\ \sigma_\phi &= f(y, t) \end{aligned} \quad (10.2)$$

Where:  $\mu_\phi$  mean grain size in phi units [-]  
 $\sigma_\phi$  standard deviation in size in phi units [-]

This idealized real situation is considered in a very simplified way in the design methods.

#### Spread of the grain size distribution ( $\sigma$ )

Accounting for the spread in the grain size distribution has its consequences, which is indicated in Table 10-5.

Table 10-5: Consequences of the implementation of the spread in the grain size distribution in the equilibration design methods

Design method	Implementation	Consequences
Dean [1974] James [1975]	Yes: loss of finer fraction	Recognizes that fines are less stable, but ignores that fine grains can be stable in the lower part of the profile Underestimates $\Delta y_{0,EQ}$ slightly because fines are lost.
Dean [2002]	Yes: finer fraction in lower part of profile	Recognizes that fines are less stable, but could be stable in the lower part of the profile
USACE [1994] Unibest-TC	No: finer fraction remains in profile	Ignores that fines are less stable, but recognizes that fine grains can remain in the profile Overestimates $\Delta y_{0,EQ}$ for $d_F > d_N$ . Underestimates $\Delta y_{0,EQ}$ for $d_F < d_N$

In general, accounting for the spread in the grain size distribution has the following consequences:

- $d_F > d_N$ : a larger spread leads to less compatible sediment and less shoreline advancement.
- $d_F < d_N$ : a larger spread leads to more compatible sediment and more shoreline advancement.

#### Grain size distribution varies across the profile $\mu(y)$

When sufficient data is available, a median grain size varying over the height can be incorporated in the Unibest-TC model. This possibility hasn't been exploited in this thesis, due to a lack of data of the grain size variation across the profile.

The Dean [2002] method does account for a varying grain size across the profile, although in a very simplifying way: the fill sediments are split in a fine and a coarse fraction. The former is placed in the lower part of the profile, whereas the latter is located in the upper part of the profile. Taking a varying grain size across the profile into account leads to less sensitivity of the shoreline advancement to the grain size.

#### Time-varying grain size distribution

Neither the equilibrium-based methods (Dean [1974] and [2002], James [1975] and USACE [1994]) nor the Unibest-TC model accounts for a location- and time-varying grain size distribution. Unibest-TC describes dynamic processes, but no dynamic grain size changes across the profile. None of the models can therefore model the sorting and mixing of the fill and native sediments. This omission of a time-varying grain size distribution can

cause serious deviations (compared with reality) in the dynamic development of the bottom profile.

### 10.3.5 Closure depth

This model issue is of importance the equilibrium models, as it indicates to which depth the fill sediments extend, determining the shoreline advancement to a great extent. This concept isn't used in the process-based modelling in Unibest-TC.

The closure depth is held equal for all design methods, based on the results of the Unibest-TC model. This assumption could be wrong and cause errors in the calculated shoreline advancement compared with reality. The sensitivity of the calculated shoreline advancement and profile shape to variations in the closure depth is however far smaller than the mutual differences between the results of the design methods (see Paragraph 5.5.2).

### 10.3.6 Errors in the model input

The differences in model results are also caused by incorrect input in the models: all methods require different input of boundary conditions as is indicated in Table 10-6.

Table 10-6: Necessary input of boundary conditions for the considered design methods.

Method	Input
Dean [1974]	Grain size distribution of the fill sediment and a mean grain size of the native sediment. Current (equilibrium) profile shape.
James [1975]	Grain size distributions of fill and native sediments. Current (equilibrium) profile shape.
USACE [1994]	Mean grain size of fill and native sediments. Fit of Equation (4.11) to the current (equilibrium) profile.
Dean [2002]	Grain size distribution of the fill sediment and a mean grain size of the native sediment. Fit of Equation (4.11) to the current (equilibrium) profile.
Unibest-TC	<ul style="list-style-type: none"> <li>• Wave height, period and direction in time.</li> <li>• Water level in time.</li> <li>• Wind speed and direction in time.</li> <li>• Longshore current velocity.</li> <li>• Grain size <math>d_{50}</math>.</li> <li>• Bottom profiles.</li> </ul>

The Unibest-TC model needs a lot of input, while the other methods only need information about the grain size and profile shape. This implies that the uncertainty in results caused by the model input is higher for the Unibest-TC model.

### 10.3.7 Conclusions

The differences between the design methods regarding the calculated shoreline advancement and profile shape can have two causes:

- Varying implementation of model issues.
- Varying reliability of the input data (boundary conditions) for each method.

The main cause of the difference in results is the (incorrect) modelling of the granulometry in the form of the following model issues:

1. Spread in the grain size distribution.
2. Grain size variation across the profile.
3. A grain size dependent profile shape.

Not accounting for the first two phenomena causes a too severe sensitivity of the shoreline advancement to the mean grain size of the fill sediments, while the third feature decreases this sensitivity.

Only the method of Dean [2002] accounts for all three model issues, but in a very poor way because:

- The profile shape is poorly represented with the  $h=Ay^{2/3}$  equation.
- The fill sediments are only split in two portions.

The Unibest-TC model is process-based, which results in a more realistic grain size dependent profile shape. However, neither a spread in the grain size distribution nor a varying grain size across the profile is incorporated in the model. Furthermore, the model requires more uncertain boundary conditions.

## 10.4 Conclusions and recommendations

### 10.4.1 Differences in results

Significant differences occur in predicted shoreline advancement and profile shape between the design methods, such as:

- Sensitivity of the shoreline advancement to the fill grain size.
- Shoreline advancement per unit fill volume.
- The occurrence of intersecting profiles.
- A grain size dependent profile shape.

Furthermore, the Unibest-TC model has the advantage that it describes the development of the equilibration in time.

These differences have two causes:

- Varying implementation of model issues.
- Varying reliability of the input data (boundary conditions) for each method.

The implementation of relevant model issues is indicated in Table 10-2.

The main cause of the difference in results is the (simplified) modelling of the granulometry in the form of the following model issues:

1. Spread in the grain size distribution.
2. Grain size variation across the profile.
3. A grain size dependent profile shape.

### 10.4.2 Recommendations for the modelling of the equilibration

First of all, frequent monitoring is recommended to obtain more data on the boundary conditions in the project area to increase the reliability of all design methods.

It should be pointed out that the equilibration occurs very rapidly in this case and that the exact time scale isn't relevant for the design of the beach nourishment in this case.

However, the shape of the equilibrated profile is important for beach nourishment design, since it determines the revenues of the project. Also the grain size distribution across the profile after equilibration is of relevance, because it determines the longshore transport in the area and thus the lifetime of the fill. Recommendations to improve the prediction of the equilibrated profiles and the grain size distribution regarding the equilibrium models and the Unibest-TC model are made:

#### Equilibrium models

Of the equilibrium models, the method of Dean [2002] is preferred, since it accounts for grain size dependent profile shape, spread in the grain size distribution and a cross-shore varying grain size. However, it should be considered to:

1. Exclude the very fine particles (e.g.  $< 50 \mu\text{m}$ ) from the fill volume, as these will be washed out and removed very quickly after placement or during the dredging process with a hopper dredge.
2. Assume a certain mixing with the native sediments, depending on the involved volumes of fill and native sediments. This leads to a composite grain size distribution of the active volume in the profile.

3. Split the composite volume in finer and coarser portions according to James [1975], since it is likely that only the fines in excess of the native distribution move to deep water.
4. Split the composite volume in  $N$  (e.g. 5) portions instead of 2, to increase the cross-shore variability of the grain size. This has already been suggested by Dean [2002].

In spite of these improvements, this method remains a poor representation of reality, since the profile shape is very poorly modelled by  $h=Ay^{2/3}$  equation and the degree of mixing between the native and fill sediments remains unclear. It is recommended to monitor the development of the grain size distribution during the equilibration at various locations to extend the knowledge regarding this subject.

#### Unibest-TC model

Regarding the Unibest-TC model, improvements could be made in the hydrodynamics and sediment transport formulations and the modelling of the development of the dry profile. To improve modelling of the beach fill equilibration special attention should be paid to the implementation of the granulometry in the model:

1. An expected cross-shore varying grain size  $d_{50}(x)$  after equilibration can be incorporated in the model. In this way the expected sorting and mixing is implemented in the model.
2. This cross-shore varying grain size should be dynamic in time  $d_{50}(y,t)$ ; the initial  $d_{50}(y,0)$  can be altered according to the sediment transport patterns, as has been suggested by Capobianco et al. [2002]. This would incorporate time-dependent sorting and mixing in the model.
3. To be even more realistic, the entire grain size distribution instead of mean / median values should be used. This would result in a probability distribution rather than a single estimate of erosion or accretion.

The feasibility of these enhancements remains questionable, but they are essential for good modelling of the beach fill equilibration, since profile shape development is inextricably bound up with the development of the grain size distribution across the profile due to mixing and sorting [Medina et al., 1995].

However, serious efforts lie ahead to be able to predict the (probabilistic) development of a grain size distribution across a profile. For example, stochastic sediment transport patterns will lead to stochastic bottom changes. The question arises whether morphological development, based on non-linear equations with a stochastic character, can be predicted over longer time scales or that model results will have a chaotic nature, leading to an unpredictable end state.

#### 10.4.3 Recommendations for the Cancún Beach Rehabilitation Project

Recommendations in this chapter focus on the predicted equilibrium profile shape and shoreline advancement. The dynamic development of the equilibration is only predicted by the Unibest-TC model and has been treated in Paragraph 9.4.

The results for the fictitious borrow area with  $d_F = d_N = 0.33$  mm aren't discussed here, since no such borrow area exists; these sediments were only used as a reference case.

##### Borrow area I – Puerto Juarez – $d_F = 0.27$ mm

The method of Dean [2002] and the Unibest-TC model are the most realistic design methods. The method of the USACE [1994] is probably too pessimistic regarding the shoreline advancement. It is therefore justified to say that the real shoreline advancement will probably be between the results of the Dean [2002] method and the Unibest-TC method (see Figure 10-3). This leads to the following statements:

- A fill volume of 300 – 375 m<sup>3</sup>/m is needed to achieve a shoreline advancement of 25 m after cross-shore equilibration.
- The equilibrated profile will be somewhat flatter than the actual profile. The profile shape is best represented by the Unibest-TC model results (see page H-5 to H-7 in Appendix H). It is likely that the fill sediments will extend to a depth of 7.5 m.

**Borrow area II – Punta Sam –  $d_F = 0.42$  mm**

The results of the USACE method are probably far too optimistic regarding the shoreline advancement, due to the assumed occurrence of intersecting profiles. The other models give approximately the same results, but might be too pessimistic since they don't (or insufficiently) account for a grain size dependent profile shape. Only the method of James [1974] accounts for the large spread in the fill grain size distribution.

Taking into account all uncertainties in the considered design methods the following statements can be made:

- A fill volume of 200 – 250 m<sup>3</sup>/m is necessary to achieve a shoreline advancement of 25 m after cross-shore equilibration.
- The equilibrated profile will be somewhat steeper than the actual profile. The profile shape is best represented by the Unibest-TC model results. It is likely that the fill sediments will extend to a depth of 7.5 m.



# 11 MODELLING OF THE STORM BEHAVIOUR

## 11.1 Introduction

The objective of this chapter is to determine the shoreline retreat and profile shape after the occurrence of a design storm on an equilibrated nourished profile.

The storm response will be determined using the dune erosion prediction model of Vellinga [1986] and the Unibest-TC model. Vellinga's model is well-known and based on extensive laboratory tests, while the Unibest-TC model is chosen primarily because of the availability of a calibrated model (see Chapter 8).

The structure of this chapter is as follows. In Paragraph 11.2 the approach of the modelling of the storm behaviour is discussed, after which the boundary conditions are defined in Paragraph 11.3. Subsequently, the results of the Unibest-TC model and Vellinga's dune erosion prediction model are discussed in Paragraph 11.4 and 11.5 respectively. In Paragraph 11.6 the results are compared and discussed, leading to conclusions in Paragraph 11.7.

## 11.2 Approach of the modelling of the storm behaviour

### Goal of the modelling

The goal is to determine:

- The profile shape and shoreline retreat after the occurrence of a design storm on an equilibrated nourished profile.
- The influence of the fill grain size on the post-storm profile shape and shoreline retreat.

### Parameter ranges

The profile shape after the storm depends on various parameters. First of all, the berm height, fill volume and fill grain size of the original profile are of importance. Secondly, the storm characteristics have a huge influence.

The following parameter ranges will be considered:

- Fill volume  $V$ : 250 m<sup>3</sup>/m
- Berm height  $B$ : 2.5 m
- Fill grain size  $d_F$ : 0.27 – 0.33 – 0.42 mm
- Design storm: return period of 5 years

## 11.3 Boundary conditions

In this paragraph the boundary conditions needed to calculate the storm behaviour with Unibest-TC and Vellinga [1986] are defined. Especially the wave and surge conditions and the storm duration are very uncertain.

### 11.3.1 Bottom profile

An equilibrated nourished profile with a fill volume  $V$  of 250 m<sup>3</sup>/m and a berm height  $B$  of 2.5 m is considered. This equilibrated profile was generated by the Unibest-TC model with a normal wave climate after 15 months of simulation and represents a typical profile state at the end of September, which is at the start of the hurricane season. Plots of the profiles for  $d_F = 0.27, 0.33$  and  $0.42$  mm can be found in Appendix J.

### 11.3.2 Grain size and fall velocity

Again the sediments from the two borrow areas are used. The native sediments serve as a reference case. The fall velocity  $w_s$  is used in the method of Vellinga [1986], while the  $d_{50}$  is used in the Unibest-TC model. The  $d_{50}$  is assumed to represent the entire grain size distribution in both cases. The sediment fall velocity in fresh water is calculated according to Sisternans [2002], and corrected to the fall velocity in seawater with Van Rijn [1993], see Appendix I.

The values of  $d_{50}$  and  $w_s$  can be found in Table 11-1.

Table 11-1: Median grain size  $d_{50}$  and sediment fall velocity  $w_s$ . The fall velocity is calculated according to Equation (I-6) in Appendix I using  $\rho_s = 2650 \text{ kg/m}^3$ ,  $\rho_w = 1025 \text{ kg/m}^3$ ,  $T = 28 \text{ }^\circ\text{C}$  and  $g = 9.81 \text{ m/s}^2$ .

Sediment source	$d_{50}$ [mm]	$w_s$ [cm/s]
fictitious borrow area with sediments equal to native	0.33	4.73
Borrow area I – Puerto Juárez	0.27	3.90
Borrow area II – Punta Sam	0.42	5.85

### 11.3.3 Longshore current

The offshore longshore current during the storm is assumed to be the same as during normal conditions: a depth-mean velocity of 0.5 m/s to the north at a depth of 30 m.

### 11.3.4 Design storm: waves, winds, water levels and duration

The hurricanes in the project area have a relatively small duration (e.g. 6 hrs) of the storm surge level due to the relatively fast movement of these weather systems. The severe wave conditions can persist for longer periods of time. The storm surge levels are relatively low because the sea is relatively deep. A storm with a return period of 5 years is considered here.

#### Wave conditions

According to Figure 3-3, the deep water significant wave height  $H_{s,0}$  with a return period of 5 years is 10 m. The deep water wave steepness  $s_{p,0}$  is defined according to Equation (11.1) and is seldom higher than 5% to 5.5% [d'Angremond and Van Roode, 2001].

$$s_{p,0} = \frac{H_{s,0}}{1.56T_p^2} \quad (11.1)$$

With  $s_{p,0} = 5.3\%$  this leads to a design peak wave period  $T_p$  of 11 s.

#### Storm surge level and wind speed

No extreme value distribution of the storm surge level  $S$  is available, but Bautista et al. [2003] state that the storm surge during hurricane Gilberto with a return period of 30 years was approximately 2.5 m. A storm surge level of 2 m is therefore assumed, combined with a wind speed of 35 m/s (12 on the Beaufort scale).

#### Storm duration

The variation in time of the storm parameters is modelled according to Equation (11.2) during a duration  $D$  of 1.5 days.

$$X = \hat{X} \sin^2\left(\frac{2\pi t}{D}\right) \quad (11.2)$$

Where:

X	storm parameter: $H_s$ , $T_p$ , wind speed or storm surge	
D	storm duration	[hrs]
t	time	[hrs]
$\hat{X}$	amplitude of the storm parameter	



The design storm is presented in Figure 11-1.

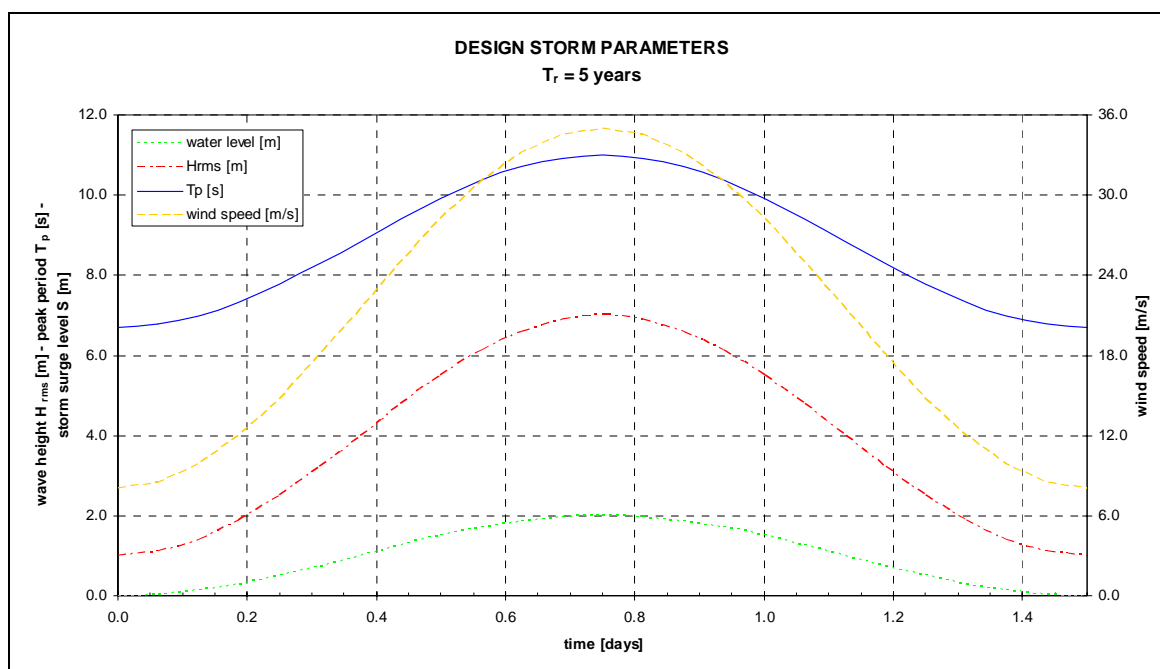


Figure 11-1: Variation of the storm parameters in time for a design storm with a return period of 5 years.

## 11.4 Results of the Unibest-TC model

The Unibest-TC model has been used to calculate the development of the equilibrated profiles during a design storm. The pre- and post-storm profiles can be found in Appendix J. The key parameters of the post-storm profile are given in Table 11-2.

Table 11-2: Key parameters of the post-storm profile according to the Unibest-TC model.

$d_{50}$ [mm]	Shoreline retreat at MSL [m]	Eroded volume [ $\text{m}^3/\text{m}$ ]
0.27	-2.1	42.6
0.33	-3.3	39.9
0.42	-2.8	37.9

It can be observed that:

- The shoreline does not retreat, but shifts seawards for the considered grain sizes.
- The eroded volume decreases slightly for larger grain sizes.
- The seaward extension of the erosion profile decreases for larger grains.

## 11.5 Dune erosion prediction model of Vellinga [1986]

Vellinga [1986] conducted extensive laboratory experiments to find an answer on the following question: "how much dune erosion will occur under extreme storm surge conditions?"

The investigations led to scale relations for the laboratory reproduction of dune erosion during storm surges, a dune erosion prediction model and a better understanding of the process of dune erosion.

The dune erosion prediction model is based on the observation that a typical erosion profile develops during storm surges. This profile can be represented as a function of

storm surge level, wave height and the settling velocity of the beach sand as can be seen in Figure 11-2.

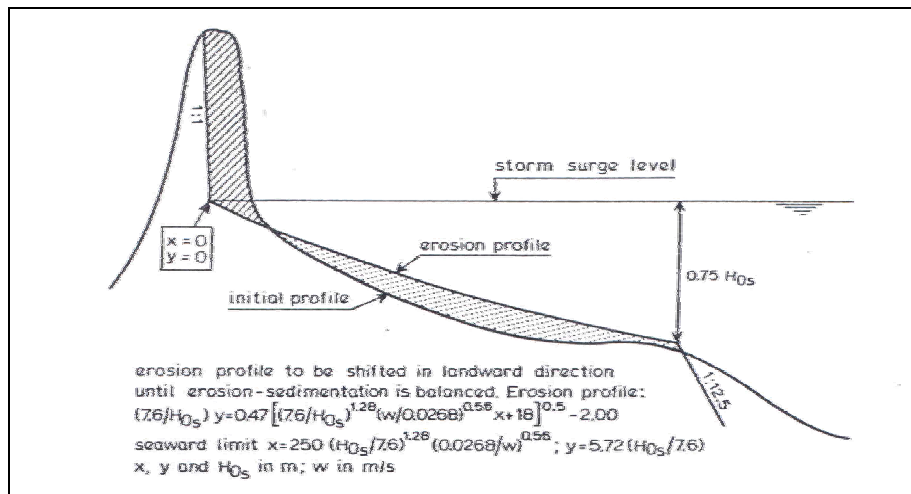


Figure 11-2: Principle of the dune erosion prediction model [Vellinga, 1986].

This erosion profile has been verified with field measurements. It should be noted that the dune erosion prediction model is only applicable in situations where a two-dimensional (cross-shore) idealization of the dune erosion process is possible, i.e. where no large longshore transport gradient exists. Furthermore, the dune erosion prediction model was primarily derived for relatively high storm surges combined with wave action.

In Appendix J the post-storm profiles for the three grain sizes ( $d_{50} = 0.27 - 0.33 - 0.42$  mm) are plotted. In Table 11-3 the key parameters of the post-storm profiles are given.

Table 11-3: Key parameters of the post-storm profile according to the dune erosion prediction model of Vellinga [1986].

$d_{50}$ [mm]	Shoreline retreat at SSL [m]	Shoreline retreat at MSL [m]	Seaward extension of erosion profile [m]	Eroded volume [ $m^3/m$ ]
0.27	27.0	9.2	287.9	144.5
0.33	10.0	-2.9	258.4	92.3
0.42	-6.0	-14.8	229.4	64.8

It can be observed that:

- For  $d_{50} = 0.42$  mm the shoreline during the storm (at SSL = MSL + 2 m) shifts seawards.
- For  $d_{50} = 0.33$  and 0.42 mm the shoreline after the storm (at MSL) shifts seawards.
- The seaward extension of the post-storm profile increases for smaller  $d_{50}$ .
- The eroded volume increases significantly for smaller  $d_{50}$ .
- For  $d_F = 0.27$  mm, the erosion extends behind the positions of the seawall, which can't occur in reality.

## 11.6 Discussion of results

The Unibest-TC model and the dune erosion prediction model of Vellinga [1986] have a very different approach, since the Unibest-TC model is clearly process-based, while the model of Vellinga [1986] is based on empirical model results.

It must be kept in mind that none of the methods accounts for scour near the seawall, underestimating the erosion near that location.

### Comparison of the results

A comparison between the two methods reveals the following similarities and differences:

1. Both methods result in approximately the same cross-shore location of erosion / sedimentation.
2. The eroded volume decreases for larger grains.
3. The seaward extension of the erosion profile decreases for larger grains.
4. Seaward shifts of the shoreline (at MSL) occur.
5. Vellinga's model predicts a larger erosion volume than the Unibest-TC model.
6. Vellinga's model predicts a larger shoreline retreat for  $d_{50} = 0.27$  mm than the Unibest-TC model.
7. Vellinga's model predicts a larger seaward shift of the shoreline for  $d_{50} = 0.33$  and  $0.42$  mm than the Unibest-TC model.

### Explanation of results

Point 2 and 3 are in correspondence with the expectations; the larger grains are more stable and settle less offshore due to their large fall velocity.

The observed seaward shift of the shoreline occurs because the eroded dune sediments are deposited around the shoreline (at MSL). Furthermore, a large part of the profile erosion takes place in the part of the profile that is below MSL and not on the dune and dry beach.

The cause of the differences between Vellinga's model and the Unibest-TC model isn't known exactly. The following causes could apply:

- The Unibest-TC model was primarily developed for longer-term morphological developments.
- The parameter setting of the Unibest-TC model is kept the same as for the modelling of the equilibration (see Chapter 8). No calibration has been carried out for storm behaviour.
- The Unibest-TC model uses time-dependent boundary conditions (see Paragraph 11.3.4), while Vellinga's model uses constant boundary conditions.

### Conclusions

Taking these factors into account the impression arises that Vellinga's model is more reliable than the Unibest-TC model.

It should also be kept in mind that the boundary conditions of the design storm are very uncertain, causing a large uncertainty in the results.

## 11.7 Conclusions and recommendations

### Conclusions

Regarding the use of the dune erosion prediction model of Vellinga and the Unibest-TC model it can be concluded that:

- The Unibest-TC model results in small erosion volumes compared with Vellinga's model.
- The parameter setting of the Unibest-TC model isn't calibrated for storm conditions.
- The use of the maximum storm surge level and maximum deep water significant wave height in Vellinga's model probably leads to an overestimation of the erosion.
- Vellinga's model results in a seaward shift of the profile for  $d_{50} = 0.33$  and  $0.42$  mm.
- None of the models accounts for scour near the seawall, underestimating the erosion at this location.

The following conclusions for a design storm with a return period of 5 years can be drawn:

- The coarse sediments ( $d_{50} = 0.42$  mm) are far more stable than the finer sediments.
- Erosion volumes of more than  $100 \text{ m}^3/\text{m}$  for  $d_{50} = 0.27$  mm) can occur, while the erosion for  $d_{50} = 0.42$  mm will be in the order of  $50 \text{ m}^3/\text{m}$ .

- The eroded sediment will be deposited between the 4.5 and 9 m depth contours and at the shoreline (at MSL).

It should be pointed out that the uncertainty in the used storm conditions is probably as high as the uncertainty in the model results. Furthermore, the used pre-storm profiles are based on Unibest-TC calculations. Therefore, the results of this chapter should be interpreted with care.

### **Recommendations**

To achieve a better prediction of the beach erosion during a design storm, the following recommendations are made:

- Apply frequent monitoring to obtain sound data to determine the extreme value distributions of the storm parameters ( $H_{sr}$ ,  $T_{pr}$ , wind speed, surge level and storm duration).
- Use other storm erosion prediction models, such as DUROSTA [Stetzel, 1990].

To achieve a better storm resistance of Cancún Beach it is recommended to use the fill sediments of borrow area II – Punta Sam ( $d_{50} = 0.42$  mm), since these sediments show far less erosion than the finer sediments.

## 12 CONCLUSIONS AND RECOMMENDATIONS

### 12.1 Introduction

In this chapter the questions posed in Paragraph 2.4.3 will be answered, fulfilling the objective of this thesis. Recommendations will be made regarding the Cancún Beach Rehabilitation Project and the modelling of the equilibration and storm behaviour.

Cancún Beach has been used as a case study in this thesis and shows complex coastal behaviour. The coastal system is characterized by two longshore transport regimes: one in the breaker zone and one in deeper water. Exchange between these two regimes especially occurs during storm events. The outer ends of the project area show complex hydrodynamic behaviour, making it difficult to determine their role in the sediment balance of the area. Human intervention in this system has made the system very vulnerable to storms.

A beach fill has been proposed as a mitigating measure. The centre of the project area has been used to model beach fill behaviour, since this area has a presumed low longshore transport gradient. Three possible fill sediment sources have been used:

- Borrow area I – Puerto Juárez with an average  $d_{50}$  of 0.27 mm.
- Borrow area II – Punta Sam with an average  $d_{50}$  of 0.42 mm.
- Fictitious borrow area – sediments equal to native with a  $d_{50}$  of 0.33 mm.

Fill volumes  $V$  between 150 and 400 m<sup>3</sup>/m and berm heights  $B$  of 2.0; 2.5 and 3.0 m have been considered, while the closure depth has been set to 7.5 m.

### 12.2 Conclusions

#### 12.2.1 Beach fill equilibration

Below the questions posed in Paragraph 2.4.3 regarding the equilibration will be answered.

*How do the approaches of the equilibration design methods relate to each other?*

This question can be answered by comparing the implementation of relevant model issues as in Table 12-1.

Table 12-1: Overview of the implementation of model issues.

Model issues		Design method				
		Dean [1974]	James [1975]	USACE [1994]	Dean [2002]	Unibest-TC
Equilibrium profile	current profile is in equilibrium	yes	yes	yes	yes	implicitly
	current sediment is in equilibrium	yes	yes	yes	yes	implicitly
	grain size dependent profile shape	no	no	yes	yes	implicitly
Granulometry	grain size distribution	$\mu_F + \sigma_F$ $\mu_N$	$\mu_F + \sigma_F$ $\mu_N + \sigma_N$	$\mu_N$ $\mu_F$	$\mu_F + \sigma_F$ $\mu_N$	$d_{50F}$ $d_{50N}$
	grain size distribution across the profile	no	no	no	$\mu_F (y)$	$d_{50} (h)$ not used
	time-varying grain size distribution across the profile	no	no	no	no	no
Depth of closure		yes	yes	yes	yes	no
Underlying physical processes which cause the morphology are considered		no	no	minimal	minimal	yes
Time-varying processes and boundary conditions		no	no	no	no	yes

The distinction between the process-based modelling with Unibest-TC and the equilibrium models is clearly visible. Secondly, large differences are present in the modelling of the granulometry.

What are the differences in results between the equilibration design methods?

The results of the equilibration design methods are summarized in Table 12-2. The cross-shore profiles after equilibration can be found in Appendix H.

Table 12-2: Comparison of the results of the design methods. N.A. means Not Applicable. Scores (+ +/+/-/0/-/-) are relative to each other.

\* Milder for finer grains, steeper for coarse grains.

# Finer fraction in lower profile with a milder slope, coarse fraction in upper profile with a steeper slope.

@ The shoreline advancement per unit fill volume represents the slope of the lines in Figure 12-1 and Figure 12-2 and is a measure of the effectiveness of the fill volume.

Results		Design method				
		Dean [1974]	James [1975]	USACE [1994]	Dean [2002]	Unibest-TC
Shoreline advancement [m] for $V = 250 \text{ m}^3/\text{m}$	$d_F = 0.27$	25.0	23.8	24.5	24.5	19.2
	$d_F = 0.33$	21.6	16.7	9.5	21.7	12.4
	$d_F = 0.42$	25.0	22.9	38.8	24.5	24.0
Threshold volume for shoreline advancement		No	No	Yes	No	Yes
Shoreline advancement per unit fill volume (@)	$d_F = 0.27$	0	-	0	0	+
	$d_F = 0.33$	0	0	0	0	0
	$d_F = 0.42$	0	-	+	0	0
Sensitivity $\Delta y_{0,EQ}$ for $d_F$		-	0	++	-	+
Profile shape		No change	No change	*	#	*
Non-intersecting profiles		Yes	Yes	Yes	Yes	N.A.
Intersecting profiles		No	No	Yes	No	N.A.

Large differences occur in predicted shoreline advancement after equilibration. Furthermore, the sensitivity of the shoreline advancement to the fill grain size varies a lot. Differences in profiles shape occur in the distribution of the fill sediments across the profile and the occurrence of intersecting and non-intersecting profiles. In addition to Table 12-2 the Unibest-TC model has the advantage that it describes the development of the equilibration in time.

*How can the differences in results between the equilibration design methods be explained?*

The main cause of the difference in results is the (simplified) modelling of the granulometry represented by the following model issues:

1. Spread in the grain size distribution.
2. Grain size variation across the profile.
3. A grain size dependent profile shape.

The grain size distribution influences the profile shape severely and should therefore be modelled accurately.

*Which equilibration design method is preferred?*

All design methods disregard the fact that the profile shape development is inextricably bound up with the development of the grain size distribution across the profile due to mixing and sorting.

The design method of Dean [2002] implements the granulometry related model issues, but in a poor way by splitting the fill volume in only two fractions and using a very poor representation of the equilibrium profile shape ( $h = Ay^{2/3}$ ). In spite of these limitations Dean [2002] is preferred above the even more simplifying methods of Dean [1974], James [1975] and the USACE [1994].

In contrary to the Unibest-TC model, Dean [2002] accounts for a spread in the grain size distribution. On the other hand, the Unibest-TC model describes the physical processes originating the morphology. Both methods aren't perfect and should be interpreted with care. No definitive choice for one method should be made at this moment; they complement each other.

*What is the shoreline advancement as a function of the fill volume?*

Only an answer with a certain bandwidth can be given, due to the imperfections in the equilibration design methods as described above. Below the results for the two existing borrow areas are discussed.

**Borrow area I – Puerto Juarez –  $d_F = 0.27$  mm**

The shoreline advancement will probably be between the results of the Dean [2002] method and the Unibest-TC method (see Figure 12-1).

**Borrow area II – Punta Sam –  $d_F = 0.42$  mm**

The results of the USACE method are probably far too optimistic regarding the shoreline advancement, due to the assumed occurrence of intersecting profiles. The other models give approximately the same results (see Figure 12-2), but might be too pessimistic since they don't (or insufficiently) account for a grain size dependent profile shape.

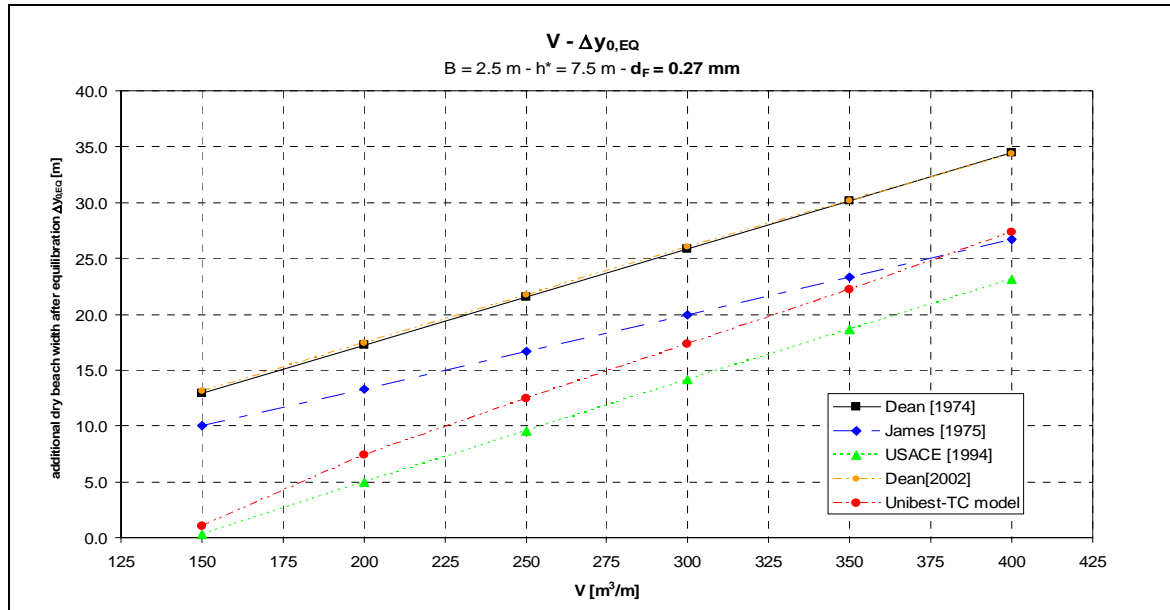


Figure 12-1: The shoreline advancement after equilibration  $\Delta y_{0,EQ}$  versus the fill volume  $V$  for a berm height  $B = 2.5$  m and a closure depth  $h_* = 7.5$  m. Only the results for borrow area I – Puerto Juárez with a  $d_{F50}$  of 0.27 mm are plotted.

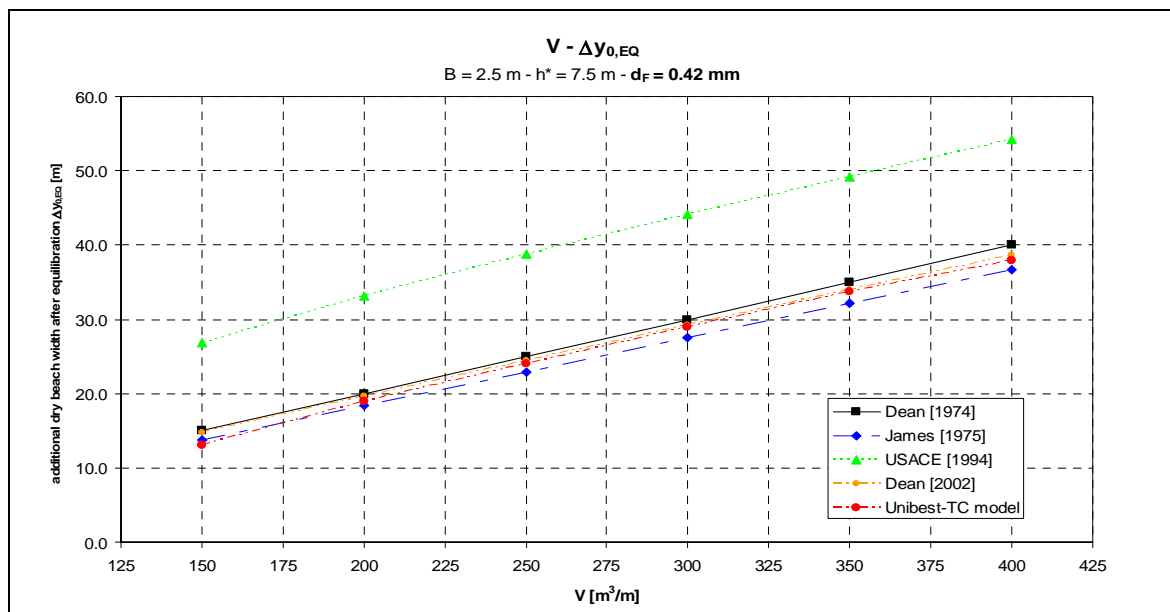


Figure 12-2: The shoreline advancement after equilibration  $\Delta y_{0,EQ}$  versus the fill volume  $V$  for a berm height  $B = 2.5$  m and a closure depth  $h_* = 7.5$  m. Only the results for borrow area II – Punta Sam with a  $d_{F50}$  of 0.42 mm are plotted.

Taking into account the uncertainties in the considered design methods and boundary conditions, the following statements can be made:

	$d_F = 0.27$ mm	$d_F = 0.42$ mm
Necessary fill volume for a shoreline advancement of 25 m after equilibration	300-375 $m^3/m$	200 – 250 $m^3/m$
Profile shape	Somewhat flatter than actual profile	Somewhat steeper than actual profile
Extension of the fill sediments after equilibration	Up to MSL –7.5 m	Up to MSL –7.5 m

The profile shape is best represented by the Unibest-TC results in Appendix H.



### What is the time scale of the equilibration?

According to the Unibest-TC model it can be concluded that the profile equilibration is practically complete after one year.

The exponential expression in Equation (12.1) suggested by Dean [2002] for the development of the shoreline position in time is a reasonable approximation for the shoreline development calculated by Unibest-TC.

$$\Delta y_0(t) = \Delta y_{0,EQ} + [\Delta y_0(0) - \Delta y_{0,EQ}] \cdot e^{-t/T_{EQ}} \quad (12.1)$$

Where:	$\Delta y_0(t)$	additional dry beach width in time	[m]
	$\Delta y_{0,EQ}$	shoreline advancement after equilibration	[m]
	$\Delta y_0(0)$	additional dry beach width of the construction profile	[m]
	$T_{EQ}$	equilibration time scale	[days]

Least-square fits for the equilibration time scale  $T_{EQ}$  lie between 70 and 95 days, which is short, making that the exact time scale isn't relevant for the design of the beach nourishment in this case.

It can be stated that:

- The larger the grain size  $d_f$ , the smaller the equilibration time scale  $T_{EQ}$ .
- The higher the berm height  $B$ , the larger the equilibration time scale  $T_{EQ}$ .
- No clear relation is present between the fill volume  $V$  and the equilibration time scale  $T_{EQ}$ .

The Unibest-TC model results should be interpreted with care, because:

- The uncertain boundary conditions result in uncertainties in the calibrated parameter setting and the calculation results.
- The shoreline position is just one indicator of the calculated profile and could be calculated wrongly. This might cause errors in the determination of the equilibration time scale  $T_{EQ}$ .

## 12.2.2 Storm behaviour

Below, the questions posed in Paragraph 2.4.3 regarding the storm behaviour of the nourished profile are answered.

### What is the shoreline retreat and profile shape after the occurrence of a design storm on an equilibrated nourished profile?

This question has been answered with the dune erosion prediction model of Vellinga [1986] and the Unibest-TC model using a design storm with a return period of 5 years ( $H_{s,0} = 10$  m).

Regarding the use of the dune erosion prediction model of Vellinga and the Unibest-TC model it can be concluded that:

- The parameter setting of the Unibest-TC model isn't calibrated for storm conditions.
- Vellinga's model results in a seaward shift of the profile for  $d_{50} = 0.33$  and  $0.42$  mm.
- None of the models accounts for scour near the seawall, underestimating the erosion at this location.

This leads to the following conclusions for a design storm with a return period of 5 years:

- The coarse sediments ( $d_{50} = 0.42$  mm) are more stable than the finer sediments.
- Erosion volumes of more than  $100 \text{ m}^3/\text{m}$  for  $d_{50} = 0.27$  mm can occur, while the erosion for  $d_{50} = 0.42$  mm will be in the order of  $50 \text{ m}^3/\text{m}$ .
- The eroded sediment will be deposited between the 4.5 and 9 m depth contours and at the shoreline (at MSL).

It should be pointed out that the uncertainty in the used storm conditions is probably as high as the uncertainty in the model results. Furthermore, the used pre-storm profiles are based on Unibest-TC calculations.

## 12.3 Recommendations

### 12.3.1 Improving the modelling of the equilibration

#### Frequent monitoring

First of all, frequent monitoring is recommended to obtain more data on the boundary conditions in the project area to increase the reliability of all design methods.

It should be pointed out that the equilibration occurs very rapidly in this case and that the exact time scale isn't relevant for the design of the beach nourishment in this case. However, the shape of the equilibrated profile is important for beach nourishment design, since it determines the revenues of the project. Also the grain size distribution across the profile after equilibration is of relevance, because it determines the longshore transport in the area and thus the lifetime of the fill. Recommendations to improve the prediction of the equilibrated profiles and the grain size distribution regarding the equilibrium models and the Unibest-TC model are made:

#### Equilibrium models

Of the equilibrium models, the method of Dean [2002] is preferred, since it accounts for grain size dependent profile shape, spread in the grain size distribution and a cross-shore varying grain size. However, it should be considered to:

1. Exclude the very fine particles (e.g.  $< 50 \mu\text{m}$ ) from the fill volume, as these will be washed out and removed very quickly after placement or during the dredging process with a hopper dredge.
2. Assume a certain mixing with the native sediments, depending on the involved volumes of fill and native sediments. This leads to a composite grain size distribution of the active volume in the profile.
3. Split the composite volume in finer and coarser portions according to James [1975], since it is likely that only the fines in excess of the native distribution move to deep water.
4. Split the composite volume in  $N$  (e.g. 5) portions instead of 2, to increase the cross-shore variability of the grain size. This has already been suggested by Dean [2002].

In spite of these improvements, this method remains a simplified representation of reality, since the profile shape is very poorly modelled by  $h=Ay^{2/3}$  equation and the degree of mixing between the native and fill sediments remains unclear. It is recommended to monitor the development of the grain size distribution during the equilibration at various locations to extend the knowledge regarding this subject.

#### Unibest-TC model

Regarding the Unibest-TC model, improvements could be made in the hydrodynamics and sediment transport formulations and the modelling of the development of the dry profile. To improve modelling of the beach fill equilibration special attention should be paid to the implementation of the granulometry in the model:

1. An expected cross-shore varying grain size  $d_{50}(x)$  after equilibration can be incorporated in the model. In this way the expected sorting and mixing is implemented in the model.
2. This cross-shore varying grain size should be dynamic in time  $d_{50}(y, t)$ ; the initial  $d_{50}(y, 0)$  can be altered according to the sediment transport patterns, as has been suggested by Capobianco et al. [2002]. This would incorporate time-dependent sorting and mixing in the model.
3. To be even more realistic, the entire grain size distribution instead of mean / median values should be used. This would result in a probability distribution rather than a single estimate of erosion or accretion.

The feasibility of these enhancements remains questionable, but they are essential for good modelling of the beach fill equilibration, since profile shape development is inextricably bound up with the development of the grain size distribution across the profile due to mixing and sorting [Medina et al., 1995].

### 12.3.2 Improving the modelling of the storm behaviour

To achieve a better prediction of the beach erosion during a storm, the following recommendations are made:

- Apply frequent monitoring to obtain sound extreme value distributions of the storm parameters ( $H_{st}$ ,  $T_{pr}$ , wind speed, surge level and storm duration).
- Use other storm erosion prediction models, such as DUROSTA [Steetzel, 1990], which was precluded in this thesis due to limited time.

### 12.3.3 Recommendations for the planned fill at Cancún Beach

The equilibration and storm behaviour of the planned beach fill on Cancún Beach cannot be predicted exactly, due to large uncertainties in the boundary conditions and modelling methods. In spite of these uncertainties it is clear that the planned beach fill will be beneficiary to Cancún Beach in the sense that it will result in additional beach width and storm protection.

Regarding the planned beach fill at Cancún Beach it can be said that:

- The fill sediments of borrow area II – Punta Sam ( $d_F = 0.42$  mm), result in the largest shoreline advancement and storm protection per unit fill volume.
- A potentially dangerous scarp is likely to occur, because of the very high erosion rates directly after construction.
- It is advised to spread the fill across the active profile up to a depth of approximately 4 m, since this will reduce the shoreline retreat after construction and thus improves public perception of the project.
- It is advised to apply a berm height of at least MSL +2.5 m, since this relatively high berm acts like a stockpile of sand which is only drawn on during extreme conditions.

Furthermore it is recommended to start monitoring of the coast (bathymetry, grain size distributions, waves, wind and currents) as soon as possible. This monitoring should continue after the beach fill has taken place so that future nourishments can be assessed better.



## REFERENCES

- d'Angremond, K. and E.T.J.M. Pluim – Van der Velden, *Introduction Coastal Engineering, lecture notes*. Delft: Delft University of Technology, 2001.
- d'Angremond K. and F.C. van Roode, *Breakwaters and closure dams*. Delft: Delft University Press, 2001.
- Bakker, W.T., 'The dynamics of a coast with a groin system'. *Proc. 11<sup>th</sup> Int. Conf. on Coastal Eng.* London, I-31 (1968), p. 492-517.
- Battjes, J.A., 'Modelling of turbulence in the surf zone'. *Proc. Symp. On Modelling Techniques*, San Francisco, ASCE p. 1050-1061, 1975.
- Battjes, J.A., and J.P.F.M. Janssen, 'Energy loss and set-up due to breaking in random waves'. *Proc. 16<sup>th</sup> Int. Conf. on Coastal Eng.*, ASCE, p. 569-587, 1978.
- Battjes, J.A., and M.J.F. Stive, 'Calibration and verification of a dissipation model for random breaking waves'. *J. of Geophysical Research*, 90 (1985), p. 9159-9167.
- Bautista, E.G., R. Silva, P. Salles, 'Prediction of storm surges generated by tropical storms'. *Ingeniería Hidráulica en México*, 18-2 (2003), p. 5-19 (in Spanish).
- Birkemeier, W.A., 'Field data on seaward limit of profile change'. *Journal of the Waterways, Port, Coastal and Ocean Engineering*, ASCE, 111-3 (1985), p. 598-602.
- Bodge, K.R., 'Representing equilibrium beach profiles with an exponential expression,' *Journal of Coastal Research*, 8 (1992), p. 47-55.
- Bosboom, J., S.G.J. Aarninkhof, A.J.H.M. Reniers, J.A. Roelvink, D.J.R. Walstra, *Unibest-TC 2.0, overview of model formulations*. Delft: WL | Delft Hydraulics, 2000.
- Bowen, A.J., 'Simple models of nearshore sedimentation; beach profiles and longshore bars,' *Coastline of Canada*, Geol. Survey of Canada, Paper 80-11, p. 1-11, 1980.
- Bruun, P., 'Coast erosion and the development of beach profiles'. U.S. Army Corps of Engineers, Beach Erosion Board, Tech. Memo. NO. 44, 1954.
- Camenen, Benoît, Philippe Larroudé, 'Comparison of sediment transport formulae for the coastal environment'. *Coastal Engineering*, 48 (2003), p. 111-132.
- Capobianco, M., H. Hanson, M. Larson, H. Steetzel, M.J.F. Stive, Y. Chatelus, S. Aarninkhof, T. Karambas, 'Nourishment design and evaluation: applicability of model concepts'. *Coastal Engineering* 47 (2002), p. 113-135.
- Dean, R.G., 'Compatibility of borrow material for beach fills'. *Proc. 14<sup>th</sup> Intl. Conf. on Coastal Eng.* ASCE, Copenhagen, p. 1319-1333, 1974.
- Dean, R.G., 'Equilibrium beach profiles: U.S. Atlantic and Gulf Coasts'. Department of Civil Engineering, Ocean Engineering Report No. 12, University of Delaware, January, 1977.
- Dean, R.G., 'Equilibrium beach profiles: characteristics and applications'. *Journal of Coastal Research* 7 (1991), p. 53-83.

Dean, Robert G., Robert A. Dalrymple, *Water wave mechanics for engineers and scientists*. Teaneck, NJ, USA: World Scientific Publishing Cooperation, 1991.

Dean, R.G., *Beach nourishment, theory and practice*. Singapore: World Scientific Publishing Co. Pte. Ltd., 2002

Dean, R.G., and R.A. Dalrymple, *Coastal processes with engineering applications*. Cambridge, United Kingdom: Cambridge University Press, 2002.

Editorial Verás, *Mexican Caribbean, Quintana Roo, map and visitors guide*. Cancún: Grupo Editorial Regiomontano, 2002.

Hallermeier, R.J., 'A profile zonation for seasonal sand beaches from wave climate'. *Coastal Engineering* 4 (1981), p. 253-277.

Holthuijsen, L.H., "Windwaves: observation techniques," Lecture notes Wind Waves, Delft University of Technology, 2002.

James, W.R., 'Technique for evaluating suitability of borrow material for beach nourishment'. U.S. Army Coastal Engineering Research Centre, Tech. Memo No. 60, 1975.

Kraus, N.C., M. Larson, R.A. Wise, 'Depth of closure in beach fill design', *Coastal and Hydraulic Engineering Technical Note II-40*, Vicksburg, USA: USACE, 1998.

Kriebel, D.L. and R.G. Dean, 'Numerical simulation of time-dependent beach and dune erosion'. *Coastal Engineering* 9 (1985), p. 221-245.

Krumbein, W.C., 'Applications of Logarithmic Moments to Size Frequency Distribution of Sediments'. *Journal of Sediment Petrology*, 6 (1936), p. 35-47.

Larson, M., 'Quantification of beach profile change,' Rept. 1008, Dept. Water Resources Eng., Univ. Lund, 1998.

Longuet-Higgins, M.S., 'Mass transport in water waves,' *Philosophical Transactions of the Royal Society of London*, 245A (1953), p. 535-581.

Medina, R., I. Losada, M.A. Losada, C. Vidal, 'Variability of beach profiles: profile shape and granulometric distribution'. *Ingeniería del Agua* 2 Num. Extraordinario (1995) (in Spanish).

Nicholls, R.J., W.A. Birkemeier, and R.J. Hallermeier, 'Application of the closure depth concept,' Proc. 25<sup>th</sup> Intl. Conf. Coastal Eng., ASCE, Orlando, p. 3874-3887, 1996.

Nipius, K.G., *Modelling of cross-shore transport using Bailard, applied on the Outer Delta of the Grevelingen*. MSc thesis, Delft University of Technology, 1998 (in Dutch).

NRC / National Research Council, *Beach nourishment and protection*. Committee on Beach Nourishment and Protection. Washington, DC:National Academic Press, 1995.

Pelnard-Considere, R., 'Theoretical essay on the evolution of coastal shapes consisting of sand or gravel,' 4<sup>th</sup> *Journées de l'Hydraulique, Les Energies de la Mer*, Question III, Rapport No. 1, 1956 (in French).

Rienecker, M.M. and J.D. Fenton, 'A Fourier approximation method for steady water waves'. *Journal of Fluid Mechanics*, 104 (1981), p. 119-137.

Rijn, L.C. van, 1993. *Principles of sediment transport in rivers, estuaries and coastal seas*. Amsterdam: Aqua Publications, 1993.

Rijn, L.C. van et al., *Yearly averaged sand transport at the 20 m and 8 m depth contours of the JARKUS-profiles 14, 40, 76 and 103*. Report H1887, Delft Hydraulics, 1995.

- Rijn, L.C. van, *Principles of coastal morphology*. Amsterdam: Aqua Publications, 1998.
- Rijn, L.C. van, D.J.R. Walstra, B. Grasmeijer, J. Sutherland, S. Pan, J.P. Sierra, 'The predictability of cross-shore bed evolution of sandy beaches at the time scale of storms and seasons using process-based Profile models'. *Coastal Engineering*, 47 (2003), p. 295-327.
- Roelvink, J.A. and M.J.F. Stive, 'Bar generating cross-shore flow mechanisms on a beach'. *J. Geophys. Res.*, 94-C4 (1989), p. 4785-4800.
- Roelvink, J.A. and I. Broker Hedegaard, 'Cross-shore profile models'. *Coastal Engineering* 21 (1993), p. 163-191.
- Sand, S.E., 'Long wave problems in laboratory models'. *J. Waterw. Port Coastal Ocean Div. ASCE*, 108 (1982), p. 492-503
- SCT, *Manual for the design of ports*. Mexico City: Secretaría de Comunicaciones y Transportes, 2001.
- Secretaría de Marina, *Isla Mujeres, Cancún and proximities, Nautical Chart SM 922*. Mexico City: Secretaría de Marina, 1999 (in Spanish).
- Secretaría de Marina, *Tide tables 2003, Gulf of Mexico and Caribbean Sea*. Mexico City: Secretaría de Marina, 2002 (in Spanish).
- Sisternans, P.G.J., *Graded sediment transport by non-breaking waves and a current*, PhD thesis Delft University of Technology; also Communications on Hydraulic and Geotechnical Engineering, Report No. 02-2. Delft: Delft University of Technology, 2002.
- Sorgedragter, J.M., *Cross-shore sediment transport on the shoreface, behaviour analysis of Unibest-TC sediment transport formulas*. MSc thesis, Delft University of Technology, 2002.
- Steezel, H.J., *DUROSTA: time-dependent model for cross-shore transport during extreme conditions: part III*. Delft: WL | Delft Hydraulics Report no. WL H 298, 1990 (in Dutch).
- Stive, M.J.F., S.G.J. Aarninkhof, L. Hamm, H. Hanson, M. Larson, K.M. Wijnberg, R.J. Nicholls, M. Capobianco, 'Variability of shore and shoreline evolution'. *Coastal Engineering*, 47 (2002), p. 211-235.
- TAW, Basic report sandy coast, part of the guide Sandy Coast, Delft: TAW, 1995 (in Dutch).
- Thienen, P.M. van, *Behaviour of a steep reclaimed profile exposed to a North Sea wave climate*. MSc thesis, Delft University of Technology, 2002.
- USACE, *Shore Protection Manual, 4th edition*. Washington, D.C.: USACE, Coastal Engineering Research Centre, 1984.
- USACE, 'Beach-fill volumes required to produce specified dry beach width'. Coastal Eng. Tech. Note II-32, Coastal Engineering Research Centre, 6pp., 1994.
- USACE, *Coastal Engineering Manual Part III (version 30 April 2002)*. Washington D.C.: USACE, Coastal Engineering Research Centre, 2002.
- Vellinga, P., *Beach and dune erosion during storm surges*. PhD thesis Delft University of Technology; also Delft Hydraulics Communications no. 372, Delft: WL | Delft Hydraulics, 1986.

Veuger, A.J., *Gradient in longshore transport of sediment in Unibest-TC*. MSc thesis, Delft University of Technology, 2001.

Wereldatlas 2000. Munchen: Publisher Areopagus, 1995 (in Dutch).

WL | Delft Hydraulics, *Settling velocity of sand in sea water of 5 C*, Report M1263, Part IV-b. Delft: WL | Delft Hydraulics, 1983.

WL | Delft Hydraulics, *'Unibest-TC, a generic tool to investigate the morphodynamic behaviour of cross-shore profiles. User manual'*, Delft: WL | Delft Hydraulics, 1999.

### **Websites:**

[www.waveclimate.com](http://www.waveclimate.com)



# BEACH NOURISHMENT

*An evaluation of equilibration design methods*

## APPENDICES

---



Cancún Beach Rehabilitation Project

---

MSc thesis  
April 2004

M.J. Bodegom



# BEACH NOURISHMENT

*An evaluation of equilibration design methods*

Cancún Beach Rehabilitation Project

## APPENDICES

---

Evaluating Committee:

prof.dr.ir. M.J.F. Stive	(TU Delft)
dr.ir. J. van de Graaff	(TU Delft)
dr.ir. A.J.H.M. Reniers	(TU Delft)
ir. K.G. Nipius	(Hydronamic)

---

MSc thesis  
April 2004

M.J. Bodegom



Delft University of Technology  
Faculty of Civil Engineering  
Section of Hydraulic Engineering



Hydronamic BV  
Papendrecht



# TABLE OF CONTENTS

<b>A</b>	<b>THEORY ON MORPHOLOGICAL PROCESSES IN THE COASTAL ZONE .....</b>	<b>A-1</b>
A.1	INTRODUCTION .....	A-1
A.2	COORDINATE SYSTEM .....	A-1
A.3	SEDIMENT BUDGET .....	A-2
A.4	CROSS-SHORE FORCES ACTING IN THE NEARSHORE .....	A-3
A.5	EQUILIBRIUM BEACH PROFILES .....	A-6
A.5.1	<i>Closure depth</i> .....	A-6
A.5.2	<i>Equilibrium beach profile concepts</i> .....	A-6
A.5.3	<i>Extensions of the equilibrium beach profile concept</i> .....	A-8
A.5.4	<i>Application of the equilibrium profile to beach nourishment design</i> .....	A-9
<b>B</b>	<b>DESCRIPTION OF THE COASTAL SYSTEM.....</b>	<b>B-1</b>
B.1	INTRODUCTION .....	B-1
B.2	MAPS OF THE PROJECT AREA .....	B-1
B.3	TYPICAL CROSS-SHORE PROFILES IN THE PROJECT AREA.....	B-1
B.4	SEDIMENT CHARACTERISTICS .....	B-1
B.4.1	<i>Characteristics of the native and fill sediments</i> .....	B-1
B.4.2	<i>Longshore and cross-shore distribution of sediment size</i> .....	B-3
B.4.3	<i>Thickness of the sediment layers</i> .....	B-3
B.5	WIND DATA .....	B-4
B.6	DEVELOPMENT OF THE SHORELINE POSITION .....	B-5
B.7	CURRENT AND TRANSPORT PATTERNS.....	B-6
<b>C</b>	<b>OVERVIEW OF MODEL FORMULATIONS IN UNIBEST-TC .....</b>	<b>C-1</b>
C.1	INTRODUCTION .....	C-1
C.2	COORDINATE SYSTEM .....	C-1
C.3	SUB-MODELS .....	C-2
C.3.1	<i>Model set-up</i> .....	C-2
C.3.2	<i>Wave propagation model</i> .....	C-2
C.3.3	<i>Mean current profile model</i> .....	C-4
C.3.4	<i>Wave orbital velocity model</i> .....	C-5
C.3.5	<i>Bed load and suspended load transport model</i> .....	C-6
C.3.6	<i>Bed level change model</i> .....	C-8
<b>D</b>	<b>UNIBEST-TC PARAMETER SETTINGS.....</b>	<b>D-1</b>
<b>E</b>	<b>BOUNDARY CONDITIONS IN UNIBEST-TC .....</b>	<b>E-1</b>
E.1	INTRODUCTION .....	E-1
E.2	TIME STEP DEFINITION BOUNDARY CONDITIONS .....	E-1
E.3	GENERATION OF WAVE INPUT .....	E-1
E.3.1	<i>Introduction</i> .....	E-1
E.3.2	<i>Background of satellite wave data</i> .....	E-2
E.3.3	<i>Wave climate based on satellite data</i> .....	E-2
E.3.4	<i>Scaled wave conditions based on satellite data</i> .....	E-5
E.4	WIND, CURRENT AND WATER LEVEL INPUT .....	E-8
E.5	BOTTOM PROFILES .....	E-8
E.5.1	<i>Individual bottom profiles</i> .....	E-8
E.5.2	<i>Averaged bottom profiles</i> .....	E-8
E.5.3	<i>Input files bottom profiles</i> .....	E-9
E.6	INPUT FILES BOUNDARY CONDITIONS .....	E-10
E.6.1	<i>Input file: normal conditions, average waves</i> .....	E-10
E.6.2	<i>Input file: storm1</i> .....	E-12

<b>F</b>	<b>RESULTS SENSITIVITY ANALYSIS.....</b>	<b>F-1</b>
F.1	INTRODUCTION.....	F-1
F.2	GRAPHS.....	F-2
F.2.1	Sensitivity to model parameter TDRY.....	F-1
F.2.2	Sensitivity to model parameter USTRA.....	F-2
F.2.3	Sensitivity to model parameter GAMMA.....	F-3
F.2.4	Sensitivity to model parameter ALFAC.....	F-5
F.2.5	Sensitivity to model parameter BETD.....	F-6
F.2.6	Sensitivity to model parameter FWEE.....	F-7
F.2.7	Sensitivity to model parameter F_LAM.....	F-9
F.2.8	Sensitivity to model parameter POW.....	F-10
F.2.9	Sensitivity to model parameter C_R.....	F-11
F.2.10	Sensitivity to model parameter D50.....	F-12
F.2.11	Sensitivity to model parameter Dss.....	F-13
F.2.12	Sensitivity to model parameter FCVISC.....	F-14
F.2.13	Sensitivity to model parameter RKVAL.....	F-15
F.2.14	Sensitivity to model parameter TANPHI1.....	F-16
F.2.15	Sensitivity to model parameter TANPHI2.....	F-17
F.2.16	Sensitivity to model parameter RW.....	F-18
F.2.17	Sensitivity to model parameter RC.....	F-19
F.2.18	Sensitivity to boundary condition $h(t)$ .....	F-20
F.2.19	Sensitivity to root-mean-square wave height $H_{rms}$ .....	F-21
F.2.20	Sensitivity to wave angle $\theta$ .....	F-22
F.2.21	Sensitivity to peak wave period $T_p$ .....	F-23
F.2.22	Sensitivity to wind speed $V_{wind}$ .....	F-24
F.2.23	Sensitivity to longshore current $V(t)$ .....	F-25
<b>G</b>	<b>RESULTS CALIBRATION PHASE.....</b>	<b>G-1</b>
G.1	INTRODUCTION.....	G-1
G.2	GENERAL SHAPE OF THE PROFILE.....	G-2
G.3	DEVELOPMENT OF INDIVIDUAL PROFILES.....	G-4
G.4	VERIFICATION OF THE EQUILIBRATION.....	G-6
G.5	VERIFICATION OF THE STORM BEHAVIOUR.....	G-7
G.6	VERIFICATION FOR CHANGED BOUNDARY CONDITIONS.....	G-8
<b>H</b>	<b>RESULTS EQUILIBRATION DESIGN METHODS.....</b>	<b>H-1</b>
<b>I</b>	<b>SEDIMENT FALL VELOCITY.....</b>	<b>I-1</b>
I.1	INTRODUCTION.....	I-1
I.2	SEDIMENT FALL VELOCITY.....	I-1
<b>J</b>	<b>POST-STORM PROFILES.....</b>	<b>J-1</b>



### A.3 Sediment budget

The sediment budget is the bookkeeping of all the sediment entering and leaving a reference area. When we examine the reference area in Figure A-2 with length  $dy$  and width  $dx$ , Equation (A-1) can be derived (conservation of volume argument).

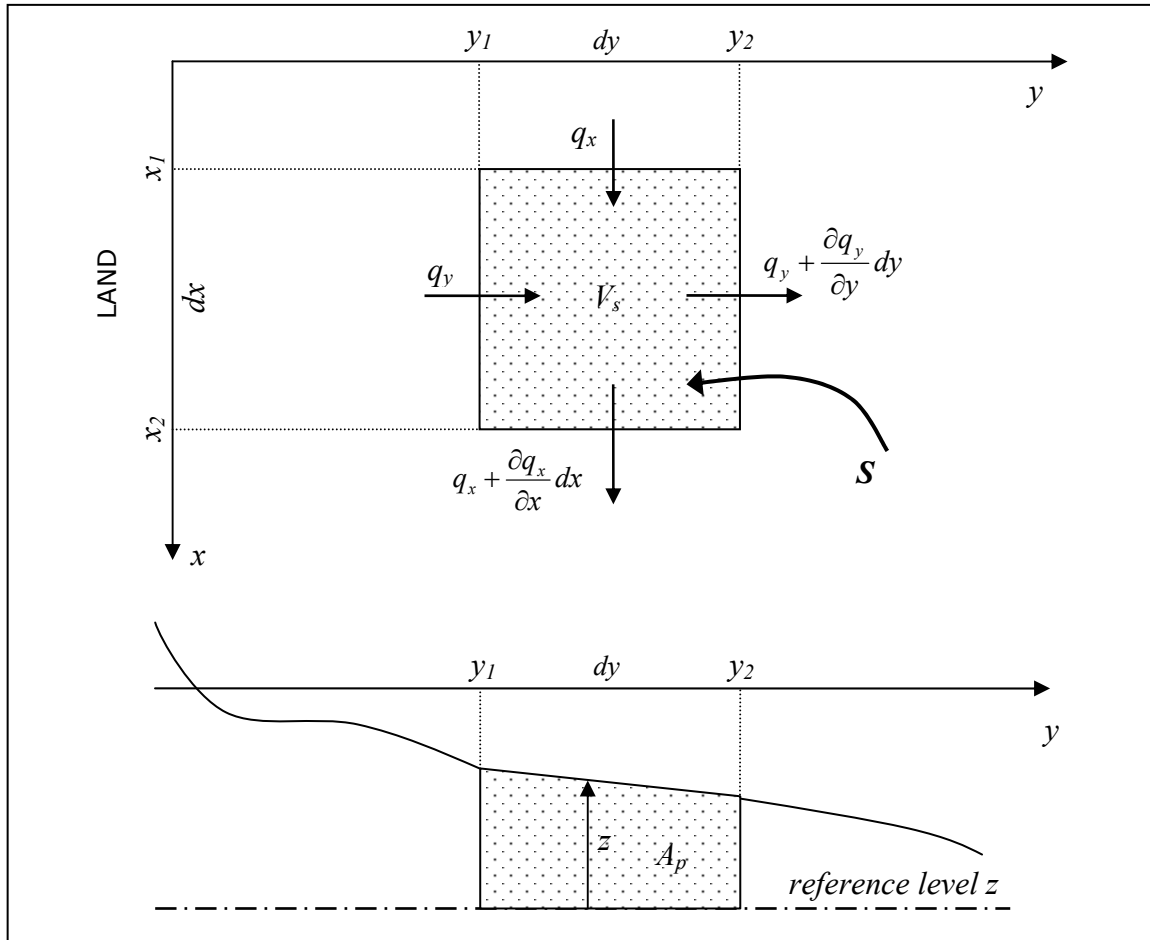


Figure A-2: Plane view (above) and cross section (below) of the reference area for the derivation of the conservation of sediment equation.

$$dV_s = \left[ q_x - \left( q_x + \frac{\partial q_x}{\partial x} dx \right) \right] dy dt + \left[ q_y - \left( q_y + \frac{\partial q_y}{\partial y} dy \right) \right] dx dt + S \quad (A-1)$$

- Where:
- $V_s$  sediment volume in reference area above the reference level  $z$ . [m<sup>3</sup>]
  - $q_x$  sediment transport in  $x$  direction (longshore) per unit width. varies with  $x$ ,  $y$  and time  $t$ . [m<sup>3</sup>/s/m]
  - $q_y$  sediment transport in  $y$  direction (cross-shore) per unit width. varies with  $x$ ,  $y$  and time  $t$ . [m<sup>3</sup>/s/m]
  - $S$  source term for added sediment in the reference area. [m<sup>3</sup>]

Re-arranging and dividing by  $dx dy dt$  leads to the conservation of sediment equation:

$$\frac{\partial z}{\partial t} = -\frac{\partial q_x}{\partial x} - \frac{\partial q_y}{\partial y} + s \quad (A-2)$$

- Where:
- $z$  bottom height above the reference level. [m]
  - $s$  source term for added sediment volume per m<sup>2</sup> and per second. [m<sup>3</sup>/m<sup>2</sup>/s]



Integrating from the onshore ( $y_1$ ) to the offshore boundary ( $y_2$ ) results in:

$$\frac{\partial}{\partial t} \int_{y_1}^{y_2} z dy = -\frac{\partial}{\partial x} \int_{y_1}^{y_2} q_x dy - [q_y(x, y_2, t) - q_y(x, y_1, t)] + \int_{y_1}^{y_2} s dy \quad (\text{A-3})$$

This equals to:

$$\frac{\partial A_p}{\partial t} = -\frac{\partial Q_x}{\partial x} + q_y(x, y_1, t) - q_y(x, y_2, t) + \int_{y_1}^{y_2} s dy \quad (\text{A-4})$$

Where:

$A_p$	the area enclosed by the reference level $z$ , the offshore boundary $y_2$ , the onshore boundary $y_1$ and the bottom profile.	[m <sup>2</sup> ]
$Q_x$	total volumetric sand transport between $y_1$ and $y_2$ in $x$ (longshore) direction.	[m <sup>3</sup> /s]

Integrating along the beach profile from  $x_1$  to  $x_2$  and then integrating over time results in:

$$\Delta V_s = V_{x_1} - V_{x_2} + V_{y_1} - V_{y_2} + S \quad (\text{A-5})$$

Where:

$\Delta V_s$	change in total sediment volume in the reference area.	[m <sup>3</sup> ]
$V_{x_1}$	longshore imported sediment volume at the upward boundary.	[m <sup>3</sup> ]
$V_{x_2}$	longshore exported sediment volume at the downward boundary.	[m <sup>3</sup> ]
$V_{y_1}$	cross-shore imported sediment volume from the onshore direction.	[m <sup>3</sup> ]
$V_{y_2}$	cross-shore exported sediment volume from the offshore direction.	[m <sup>3</sup> ]
$S$	source term for artificially added sediment volume.	[m <sup>3</sup> ]

## A.4 Cross-shore forces acting in the nearshore

There are several forces that occur in the nearshore and cause sediment transport and profile response. The magnitude of these forces varies within the profile. When the profile is in equilibrium, these forces are in balance. Cross-shore transport gradients and profile change occur when the equilibrium of forces is disturbed by changing hydrodynamic boundary conditions. The forces occurring in the nearshore area are summarized in Table A-1 and explained below. Onshore- and offshore-directed forces are referred to as 'constructive' and 'destructive', respectively. Some forces can be constructive or destructive, depending on the hydrodynamic conditions. It is noted that the term 'force' is used in a generic sense. The most important source for this appendix has been the Coastal Engineering Manual [USACE, 2002].

Table A-1: Constructive and destructive cross-shore 'forces' in the nearshore.

Description of 'force'	Constructive / Destructive	Most important in:
Average bottom shear stress due to non-linear waves	constructive	just outside the breaker zone
Streaming velocities	constructive	whole profile, increasing for shallow water
Overtopping	constructive	whole profile, increasing for shallow water
Gravity	destructive	whole profile
Undertow due to mass transport	destructive	whole profile, increasing for shallow water
Return flow due to momentum flux transfer	destructive	breaker zone only
Intermittent suspension	both	shallow water
Turbulence	both	the breaker zone
Wind effects	both	shallow water

### Average bottom shear stress due to non-linear waves

Non linear waves, occurring when ocean waves approach shallow water, have higher wave crests and of shorter duration than the wave troughs. This results in higher onshore (crest) than offshore (trough) directed orbital velocities, even since the time-mean water particle velocity is zero. However, the time-mean bottom shear stress is larger than zero (onshore directed), since it is proportional to the square of the velocity. This feature is most pronounced just outside the breaker zone.

### Streaming function

Another constructive force is the so-called streaming velocity, occurring in the bottom boundary layer. The onshore directed streaming motion has been quantified by Longuet-Higgins [1953] as:

$$v_s = -\frac{3\sigma k H^2}{16 \sinh^2 kh} \quad (\text{A-6})$$

Where:  $v_s$  maximum (over depth) value of the streaming velocity [m/s]  
 $k$  local wave number [rad/m]  
 $h$  water depth [m]  
 $\sigma$  wave angular frequency [rad/s]  
 $H$  wave height [m]

The bottom shear stress, induced by the streaming velocity can be expressed as:

$$\tau_{bs} = -\frac{\rho \varepsilon^{1/2} \sigma^{3/2} H^2 k}{8\sqrt{2} \sinh^2 kh} \quad (\text{A-7})$$

Where:  $\tau_{bs}$  bottom shear stress induced by the streaming velocity [N/m<sup>2</sup>]  
 $\varepsilon$  eddy viscosity [m<sup>2</sup>/s]

### Overtopping

Overtopping (e.g. of a barrier island) can be considered a constructive 'force', since it reduces the magnitude of the seaward directed undertow or even replaces it by a landward directed current.

### Gravity

Gravity acts as a destructive force and 'pulls' the sediment particles in a down slope direction. However, it may also serve as a stabilizing force, since: it hinders particles to be lifted from the bed by turbulence, it creates frictional resistance of the sediment and it causes suspended sediment to settle out of the water column.

### Undertow due to mass transport

The undertow is a seaward directed cross-shore current, counteracting the mass transport

caused by (linear) waves. The time-averaged seaward discharge is [Dean and Dalrymple, 1991]:

$$Q = \frac{E}{\rho C} \quad (A-8)$$

Where: Q time-averaged seaward discharge due to mass transport [m<sup>3</sup>/s]  
 E wave energy density [J/m<sup>2</sup>]  
 C wave celerity [m/s]

This flow carries suspended sediment in a seaward direction and is destructive.

### Return flow due to momentum flux transfer

Wave propagation towards shore implies a shoreward flux of momentum. When the waves break, this momentum is transferred to the water column. The distribution of this momentum is non-uniform over the depth with its centroid in the upper part of the water column. The total force induced by this momentum transfer is balanced by a pressure force due to a slope of the water surface. This pressure force is uniform over the depth, resulting in a landward flow in the upper part of the water column and a seaward flow in the lower part (see Figure A-3). The net effect will be a seaward flux of sediment.

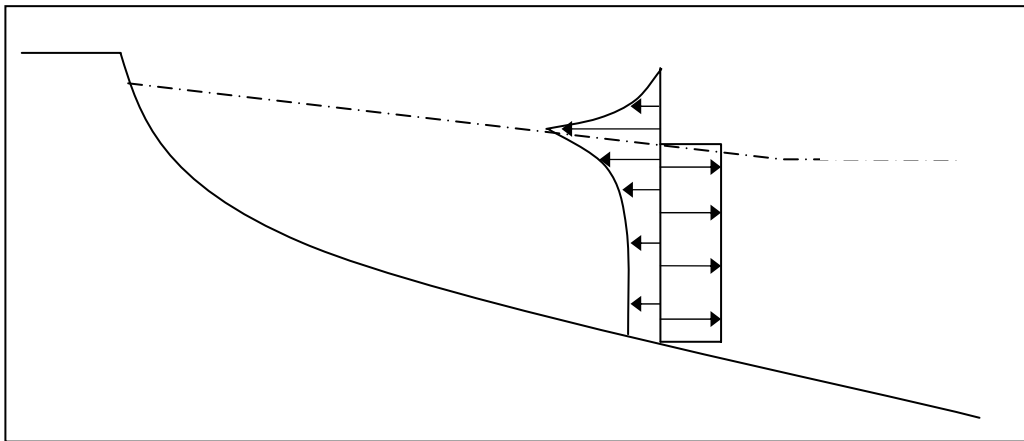


Figure A-3: Onshore wave-induced momentum flux and counterbalancing pressure force (assuming no wind or longshore effects).

### Intermittent suspension

If the suspension is intermittent, occurring each wave period, the direction of suspended transport due to wave orbital motion depends on the average water particle velocity during the period that a sediment particle is suspended. So suspended transport due to wave orbital motion can be destructive or constructive, depending on the time lag between orbital velocity and sediment mobilization and on the sediment fall velocity.

### Turbulence

Turbulence can be effective in mobilizing sediment. Depending on whether the net forces on the moment of mobilization are shoreward or seaward, turbulence has a constructive or destructive effect, respectively.

### Wind effects

Wind blowing over a water surface exerts a shear stress on this surface, inducing a surface flow in the direction of the wind and a water level slope when meeting land. The wind shear stress is the largest at the surface and the smallest at the bottom. The counterbalancing pressure force is depth-uniform. This leads to a secondary flow system: in the direction of the wind at the water level and in opposite direction near the bottom. Thus, landward-directed winds cause seaward directed bottom flows and can be considered destructive. Seaward-directed winds cause landward directed bottom flows and can be considered constructive.

### Forces acting on the dry profile

It is emphasized that also the dry profile is subject to forces and thus transports. One force is the wind stress acting on the soil and capable of moving the grains in seaward or landward direction.

The transition between the sea and land (swash zone) is subject to wave uprush and downrush, depositing or eroding sand in this area. The outflow from the beach face during low tide causes offshore directed sediment transport. During high tide water percolates into the beach face and thus creating a difference in uprush and downrush volume, leading to accretion of sand.

## A.5 Equilibrium beach profiles

### A.5.1 Closure depth

'The closure depth ( $h_c$ ) for a given or characteristic time interval is the most landward depth seaward of which there is no significant change in bottom elevation and no significant net sediment transport between the nearshore and the offshore' [Kraus et al., 1998].

Based on field data and correlations with the Shields parameter, Hallermeier [1981] defined the closure depth as follows:

$$h_c = 2.28H_e - 68.5 \left( \frac{H_e^2}{gT_e^2} \right) \quad \text{with} \quad H_e = \bar{H} + 5.6\sigma_H \quad (\text{A-9})$$

Where:	$h_c$	closure depth	[m]
	$H_e$	effective significant wave height, exceeded only 12hrs per year	[m]
	$T_e$	effective wave period, exceeded only 12hr per year	[s]
	$\bar{H}$	annual mean significant wave height	[m]
	$\sigma_H$	standard deviation of significant wave height	[m]

Which was approximated later by Birkemeier [1985] as:

$$h_c = 1.57H_e \quad (\text{A-10})$$

Nicholls et al. [1996] provided a generalized closure depth for time frames other than one year, resulting in:

$$h_c(t) = 2.28H(t)e - 68.5 \left[ \frac{H(t)^2}{gT(t)^2} \right] \quad (\text{A-11})$$

Where:	t	considered period	[years]
	$H_e(t)$	effective significant wave height, exceeded only 12hr in the time t	[m]

In the following applications,  $h_c$  is assumed to represent the closure depth for profile changes over long (seasonal to years) time scales. For short-term profile changes, e.g. during storms, the breaking depth  $h_b$  is a better delineation of the active profile [USACE, 2002].

### A.5.2 Equilibrium beach profile concepts

#### Dynamic equilibrium

It can be assumed that if all the forces in the cross-shore profile are in balance, there is no net cross-shore sediment transport and the profile is in equilibrium. A change in hydrodynamic conditions will disturb the balance of forces and cause a change in profile shape. In reality, the hydrodynamic conditions are constantly changing and so is the corresponding equilibrium profile. This is called the dynamic equilibrium concept.

### Characteristics of equilibrium beach profiles

Generally observed characteristics of equilibrium profiles are [Dean, 1977]:

- They tend to be concave upward.
- Finer sediments give milder slopes.
- Steeper waves give flatter slopes.
- Sediments tend to be sorted; finer sediments in deeper water, coarser sediments in shallower water.

On many beaches one encounters longshore bars, seasonal or permanent, changing in position and shape.

### Quantitative description of equilibrium beach profiles

Dean and Dalrymple [2002] examined several models to predict the manner in which the depth varies across the surf zone.

1. Uniform wave energy dissipation per unit water volume.
2. Uniform wave energy dissipation per unit area.
3. Uniform bottom shear stress in cross-shore direction.
4. A sediment transport approach.
5. Other models.

#### Ad 1: Uniform wave energy dissipation per unit water volume

It is assumed that turbulence caused by wave breaking is the dominant destructive force. The concept is simply that, if sediment of a given size is considered to be able to withstand a given level of wave energy dissipation per unit water volume, then the energy dissipation per unit volume may be considered to be representative of the magnitude of turbulent fluctuations per unit volume [Dean and Dalrymple, 2002]. This leads to:

$$\frac{1}{h} \frac{dF}{dy} = D_*(d) \quad (\text{A-12})$$

Where:	h	still water depth	[m]
	F	wave energy flux = $EC_g$	[J/ms]
	y	shore normal coordinate directed offshore, originating at the shoreline	[m]
	$D_*(d)$	uniform energy dissipation per unit volume for a certain grain size d.	[J/s/m <sup>3</sup> ]

According to linear wave theory in shallow water we can write:

$$\frac{d \left( \frac{1}{8} \rho g \kappa^2 h^2 \sqrt{gh} \right)}{dy} = h D_*(d) \quad (\text{A-13})$$

Where:	$\kappa$	breaking index (= approximately 0.8)	[-]
--------	----------	--------------------------------------	-----

Differentiating gives:

$$D_*(d) = \frac{5}{16} \rho g^{3/2} \kappa^2 h^{1/2} \frac{dh}{dy} \quad (\text{A-14})$$

Integrating for  $h$  leads to:

$$h(y) = \left( \frac{24 D_*(d)}{5 \rho g \sqrt{g} \kappa^2} \right)^{2/3} y^{2/3} = A(d) y^{2/3} \quad (\text{A-15})$$

Where:	A(d)	profile scale factor, function of the energy dissipation and indirectly of the grain size of the beach	[m <sup>1/3</sup> ]
--------	------	--	---------------------

The dimensional parameter A is the profile scale factor and is a function of the grain size of the beach. The profile described by Equation (A-15) is concave upward, as encountered

in nature. Drawbacks are an infinite beach slope at the shoreline, its inability to describe sand bars and the limitation to the breaker zone.

**Ad 2: Uniform wave energy dissipation per unit area**

If it is assumed that it is the wave energy dissipation per unit surface which gives the equilibrium profile, the previous derivation leads to [Dean and Dalrymple, 2002]:

$$h = A_2^{2/5} \tag{A-16}$$

Where:  $A_2$  a dimensional constant [m<sup>3/5</sup>]

**Ad 3: Uniform bottom shear stress in cross-shore direction**

One could argue that an equilibrium shape exists when the cross-shore bottom shear stress is constant across the surf zone. This leads to a similar relation as Equation (A-16).

**Ad 4: A sediment transport approach**

Bowen's [1980] model is based on a zero net suspended transport at each location in the profile, leading to:

$$h = Ay^{2/3} \quad \text{with} \quad A = \left( \frac{(7.5w)^2}{g} \right)^{1/3} \tag{A-17}$$

Where:  $w$  sediment fall velocity [m/s]

**Ad 5: Other beach equilibrium profile models**

Other models are given by e.g. Larson [1988] and Bodge [1992].

**Recommended beach equilibrium concept**

The USACE [2002] recommends the beach equilibrium concept based on Equation (A-15), since this relation had been found empirically by Bruun [1954] and has been confirmed by various empirical studies. Dean found empirically:

$$A = 0.067w^{0.44} \tag{A-18}$$

Where:  $w$  sediment fall velocity [cm/s]

The recommended A-values for sand are given in Table A-2.

Table A-2: Summary of recommended A-values [m<sup>1/3</sup>] for diameters from 0.10 to 1.09mm [USACE, 2002]. In the left column one finds the first digit of the grain size, in the upper row the second digit of the grain size.

d <sub>50</sub> (mm)	0	0.01	0.02	0.03	0.04	0.05	0.06	0.07	0.08	0.09
0.1	0.0630	0.0672	0.0714	0.0756	0.0798	0.0840	0.0872	0.0904	0.0936	0.0968
0.2	0.1000	0.1030	0.1060	0.1090	0.1120	0.1150	0.1170	0.1190	0.1210	0.1230
0.3	0.1250	0.1270	0.1290	0.1310	0.1330	0.1350	0.1370	0.1390	0.1410	0.1430
0.4	0.1450	0.1466	0.1482	0.1498	0.1514	0.1530	0.1546	0.1562	0.1578	0.1594
0.5	0.1610	0.1622	0.1634	0.1646	0.1658	0.1670	0.1682	0.1694	0.1706	0.1718
0.6	0.1730	0.1742	0.1754	0.1766	0.1778	0.1790	0.1802	0.1814	0.1826	0.1838
0.7	0.1850	0.1859	0.1868	0.1877	0.1886	0.1895	0.1904	0.1913	0.1922	0.1931
0.8	0.1940	0.1948	0.1956	0.1964	0.1972	0.1980	0.1988	0.1996	0.2004	0.2012
0.9	0.2020	0.2028	0.2036	0.2044	0.2052	0.2060	0.2068	0.2076	0.2084	0.2092
1.0	0.2100	0.2108	0.2116	0.2124	0.2132	0.2140	0.2148	0.2156	0.2164	0.2172

**A.5.3 Extensions of the equilibrium beach profile concept**

**Gravity as an extra destructive force**

Introducing this extra force flattens the profile, especially in the steep parts, thereby removing the infinite slope at the shoreline. The following relation applies [USACE, 2002]:

$$y = \frac{h}{m_0} + \left(\frac{h}{A}\right)^{\frac{3}{2}} \quad (\text{A-19})$$

Where:  $m_0$  beach face slope [-]

### Non-uniform sand sizes

The sand size across the beach profile usually varies and so does the profile scale factor  $A(d)$ . This can be accounted for by splitting the beach profile into different sections with constant  $A$  parameters for each section. See for example Dean and Dalrymple [2002].

### A.5.4 Application of the equilibrium profile to beach nourishment design

According to Dean [1991], the concept of beach equilibrium profiles is a useful tool for beach nourishment design. With this concept, the post-nourishment equilibrium profile can be calculated, depending on the fill volume and the grain size of the fill. Three types of nourished profiles are possible: non-intersecting, intersecting and submerged. These profiles are shown in Figure A-4.

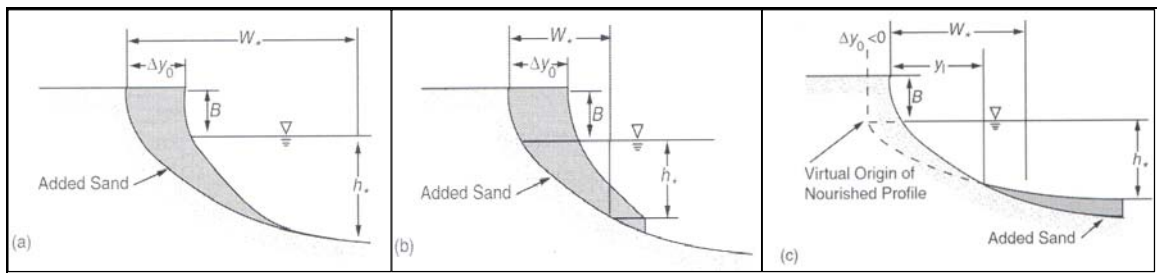


Figure A-4: Profile types associated with beach nourishment: intersecting (a), non-intersecting & emergent (b) and non-intersecting & submerged profiles. [Dean and Dalrymple, 2002]

A necessary but insufficient requirement for intersecting profiles is that fill sediments are coarser than native. A necessary but insufficient requirement for submerged profiles is that the fill sediments are finer than native. The profiles in Figure A-4 can be quantified by using the equilibrium profile concept of Equation (A-15). For intersecting profiles the volume placed per unit shoreline length  $V_1$  can be expressed as a function of shoreline advancement  $\Delta y_0$ :

$$V_1 = B\Delta y_0 + \int_0^{y_i} A_N y^{2/3} dy - \int_0^{(y_i - \Delta y_0)} A_F y^{2/3} dy \quad (\text{A-20})$$

Where:

$V_1$	placed volume per unit shoreline length	[m <sup>3</sup> /m]
$B$	berm height	[m]
$\Delta y_0$	shoreline advancement	[m]
$y_i$	distance from original shoreline to intersection point	[m]
$A$	profile scale parameter according to Equation (A-9). 'F' refers to the fill sediment and 'N' refers to the native sediment	[m <sup>1/3</sup> ]

Integrating leads to:

$$V_1 = B\Delta y_0 + \frac{3}{5} A_N y_i^{5/3} - \frac{3}{5} A_F (y_i - \Delta y_0)^{5/3} \quad \text{with} \quad y_i = \frac{\Delta y_0}{1 - \left(\frac{A_N}{A_F}\right)^{3/2}} \quad (\text{A-21})$$

Substituting yields:

$$V_1 = B\Delta y_0 + \frac{3}{5} A_N \frac{\Delta y_0^{5/3}}{\left[1 - \left(\frac{A_N}{A_F}\right)^{3/2}\right]^{2/3}} \quad (\text{A-22})$$

This can be written in non-dimensional form by introducing the parameters  $V' = V/BW_*$ ,  $\Delta y_0' = \Delta y_0/W_*$  and  $B' = B/h_*$ , where  $W_*$  is the offshore distance associated with the closure depth  $h_*$  of the native profile.

$$V_1' = \Delta y_0' + \frac{3(\Delta y_0')^{5/3}}{5B' \left[1 - \left(\frac{A_N}{A_F}\right)^{3/2}\right]^{2/3}} \quad (\text{A-23})$$

In a similar way one finds for non-intersecting, but emergent profiles:

$$V_2' = \Delta y_0' + \frac{3}{5B'} \left\{ \left[ \Delta y_0' + \left(\frac{A_N}{A_F}\right)^{3/2} \right]^{5/3} - \left(\frac{A_N}{A_F}\right)^{3/2} \right\} \quad (\text{A-24})$$

To distinguish between intersecting and non-intersecting profiles the following relations apply:

$$\begin{aligned} \Delta y_0' + \left(\frac{A_N}{A_F}\right)^{3/2} - 1 < 0 & \quad \text{Intersecting profiles} \\ \Delta y_0' + \left(\frac{A_N}{A_F}\right)^{3/2} - 1 > 0 & \quad \text{Non-intersecting profiles} \end{aligned} \quad (\text{A-25})$$

$$(V')_{c1} = \left(1 + \frac{3}{5B'}\right) \left[1 - \left(\frac{A_N}{A_F}\right)^{3/2}\right] \quad \text{for } (A_F/A_N) > 1 \quad (\text{A-26})$$

Where:  $(V')_{c1}$  critical volume to distinguish between intersecting and non-intersecting profiles [-]

To distinguish between non-intersecting but emergent and submerged profiles the following relation applies:

$$(V')_{c2} = \frac{3}{5B'} \left(\frac{A_N}{A_F}\right)^{3/2} \left[\frac{A_N}{A_F} - 1\right] \quad \text{for } (A_F/A_N) < 1 \quad (\text{A-27})$$

Where:  $(V')_{c2}$  critical volume to distinguish between emergent and submerged profiles [-]

Equation (A-26) and Equation (A-27) can be visualized for different values of  $h_*/B$  as in Figure A-5.



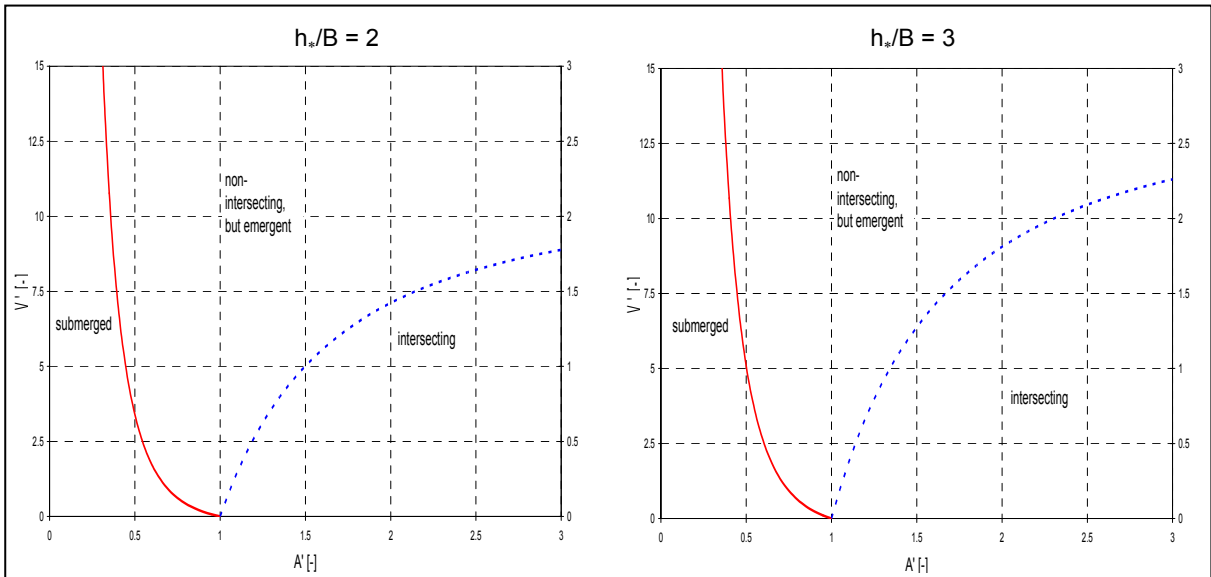


Figure A-5: Distinction between intersecting, non-intersecting & emergent and submerged profiles as a function of dimensionless parameters  $A' = (A_F/A_N)$  and  $V' (=B/BW_*)$ . The lines are plotted for  $h_*/B = 2$  and  $h_*/B = 3$ . The red solid line represents Equation (A-27) and the blue dotted line Equation (A-26).

Equation (A-23) and Equation (A-24) can be used to calculate the dry beach width  $\Delta y_0'$  for a certain applied volume  $V'$ . This means that there are three independent variables:  $B'$ ,  $V'$  and  $A' = A_F/A_N$ . Equation (A-23) and Equation (A-24) can be displayed for different values of  $B'$  as in Figure A-6.

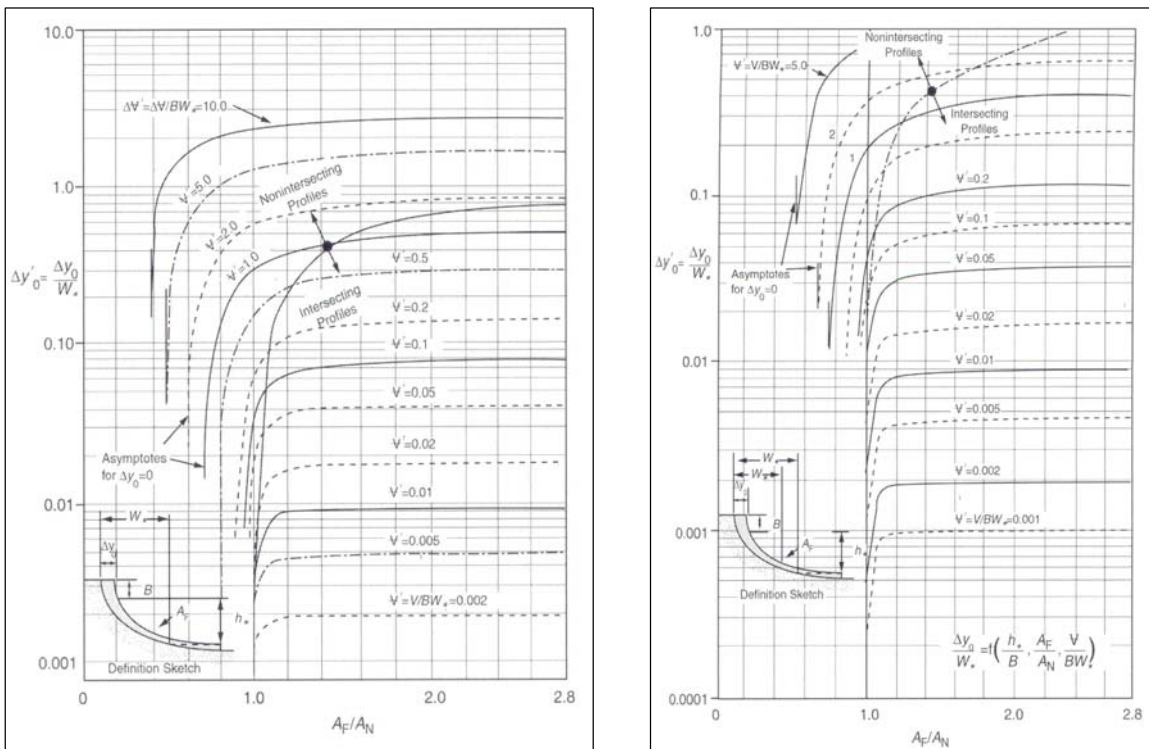


Figure A-6: Design graphs for  $B' = h_*/B = 4$  (left panel) and  $B' = 3$  (right panel) to determine the dimensionless shoreline translation  $\Delta y_0'$  as a function of  $A_F/A_N$  and the dimensionless fill volume  $V'$ . [Dean and Dalrymple, 2002]

The graphs above can be used to design beach nourishment volumes for certain required beach widths after equilibration. It is emphasized however, that longshore losses or are not accounted for.



## B DESCRIPTION OF THE COASTAL SYSTEM

### B.1 Introduction

In this appendix a description of the coastal system is given, which is used as a reference throughout this thesis. In Paragraph B.2 maps of the project area (between Punta Cancún and Punta Nizuc) are presented. Subsequently, some typical cross-shore profiles are presented in Paragraph B.3. In Paragraph B.4 the sediment characteristics of the current beach and the proposed borrow areas are discussed. Then the wind climate is discussed in Paragraph B.5. In Paragraph B.6 the development of the shoreline position is presented. Finally, in Paragraph B.7, the current and transport patterns in the project area are discussed.

### B.2 Maps of the project area

On the next pages four maps are shown:

Yucatán Peninsula	
Isla Mujeres, Cancún and surroundings	soundings in meters, relative to MLLW
Bahía de Mujeres	soundings in meters, relative to MLLW
Project area	soundings in meters, relative to MLLW

The letters below indicate important locations on these maps. The red arrow indicates Cancún.

A	Hondo river	
B	Tulum	
C	Cozumel	
D	Laguna Nichupté	Filled with fine sediments and mangrove
E	Bahía Mujeres	Relatively shallow and sheltered by reef fragments and Isla Mujeres and filled with fine to medium sediments
F	Isla Mujeres	Consists of sand, rock and coral
G	Reef	Creates sheltered conditions
H	Mangrove forests	
J	Isla Contoy	Consists of sand, rock and coral
K	Isla Holbox	Consists of sand
L	Isla Blanca	Consists of sand
I	Borrow area I	Near Puerto Juárez, $d_{50} = 0.27$ mm
II	Borrow area II	Near Punta Sam, $d_{50} = 0.42$ mm

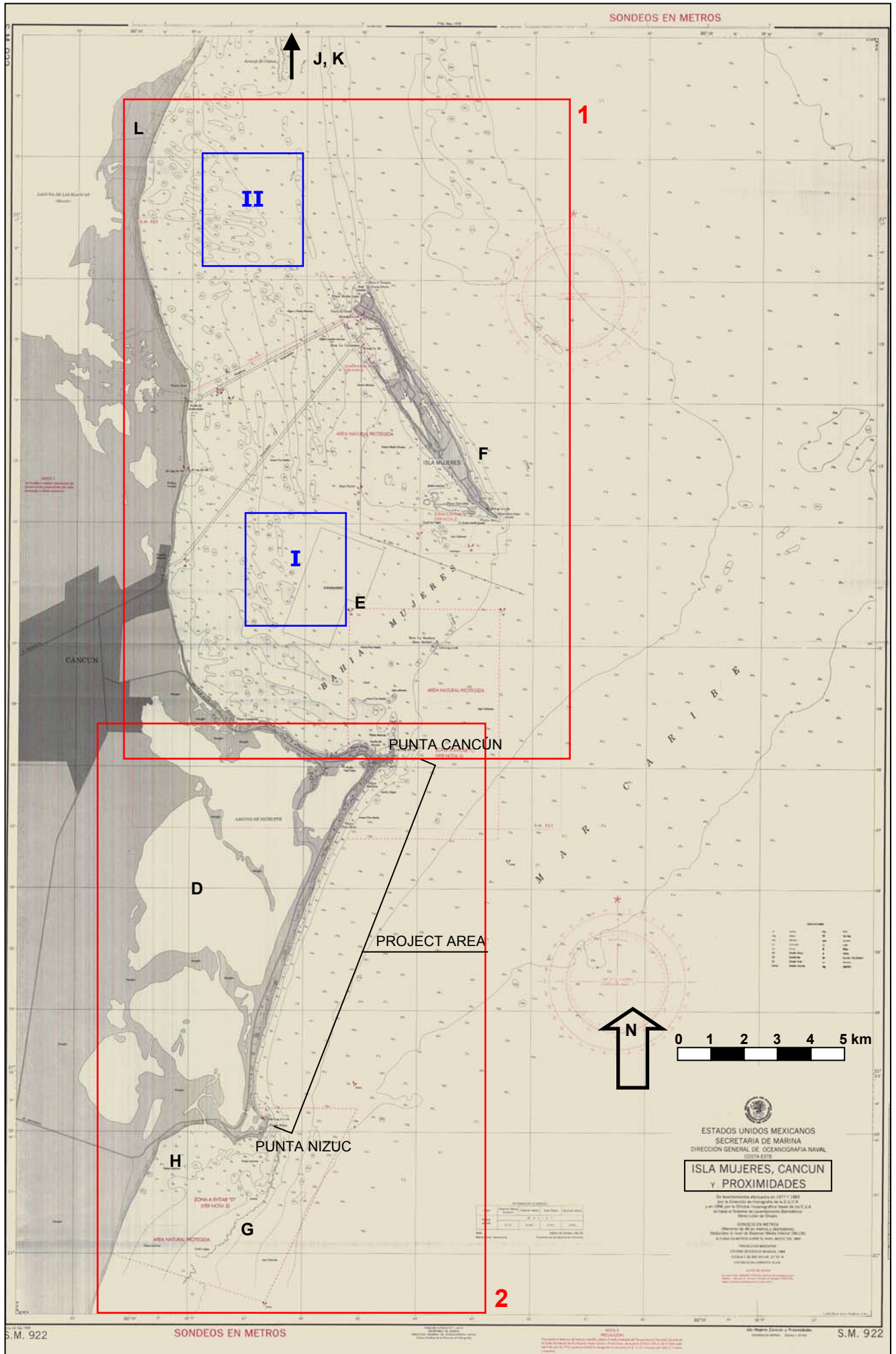


# YUCATÁN PENINSULA



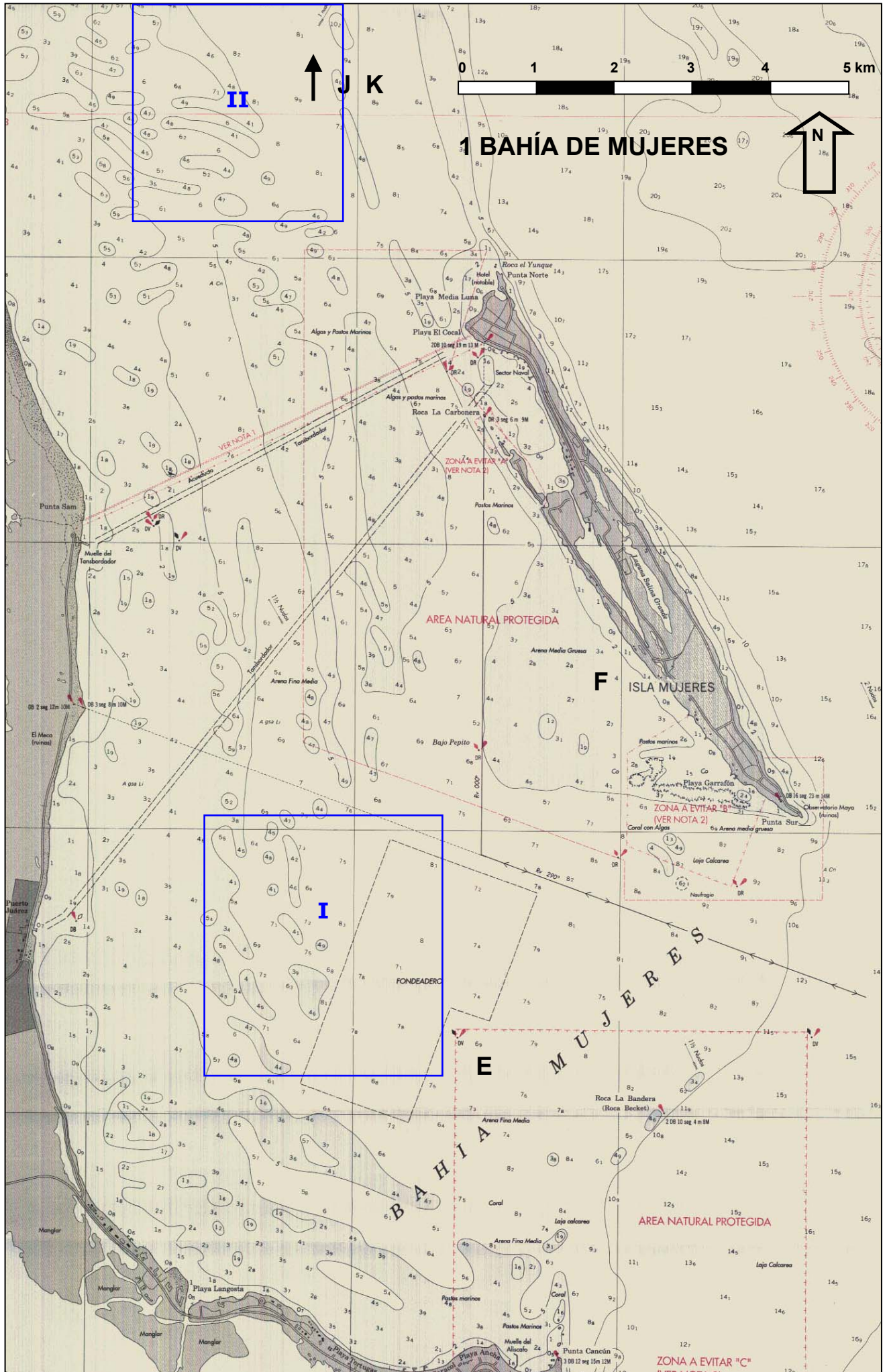






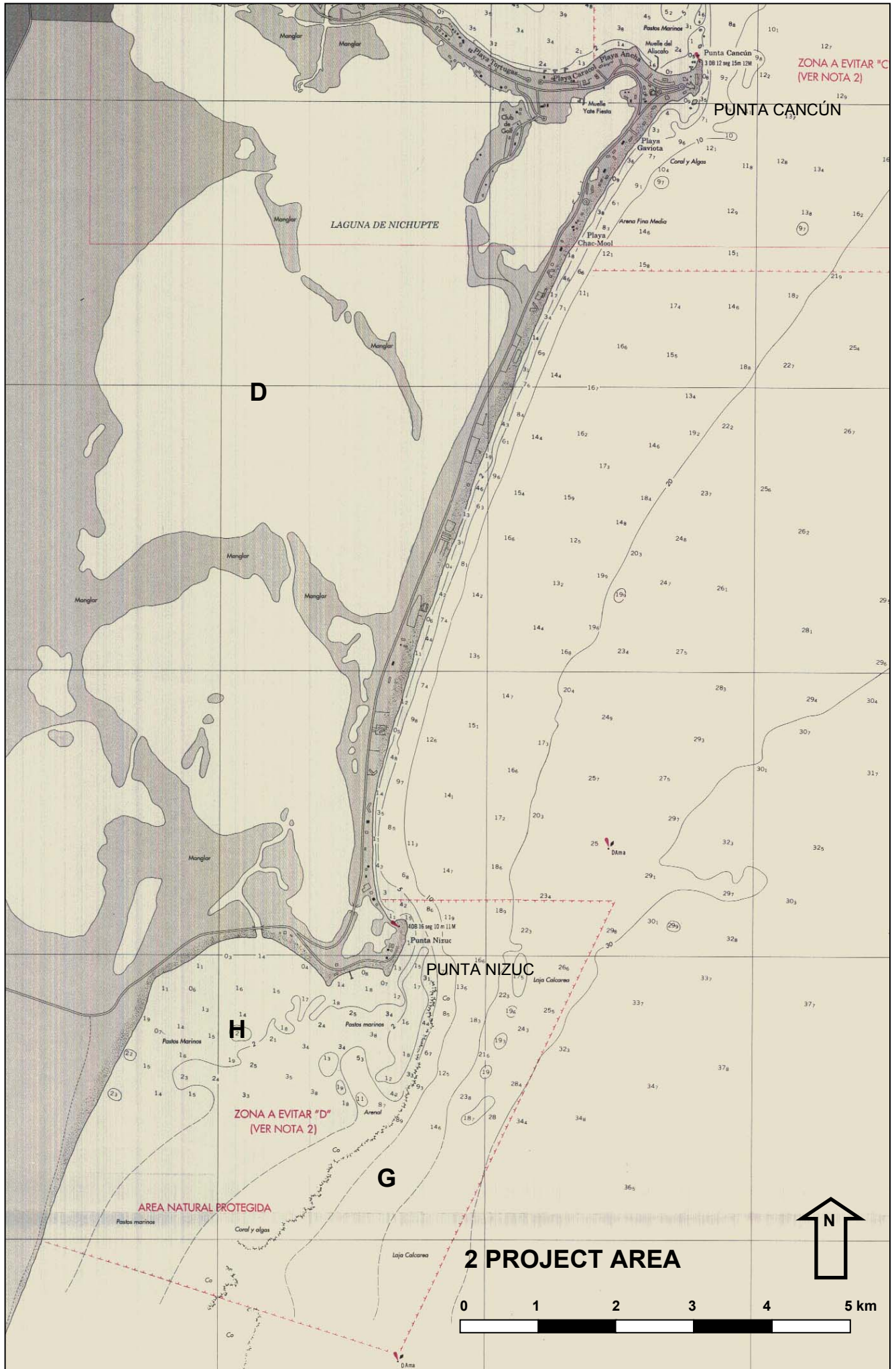














## B.3 Typical cross-shore profiles in the project area

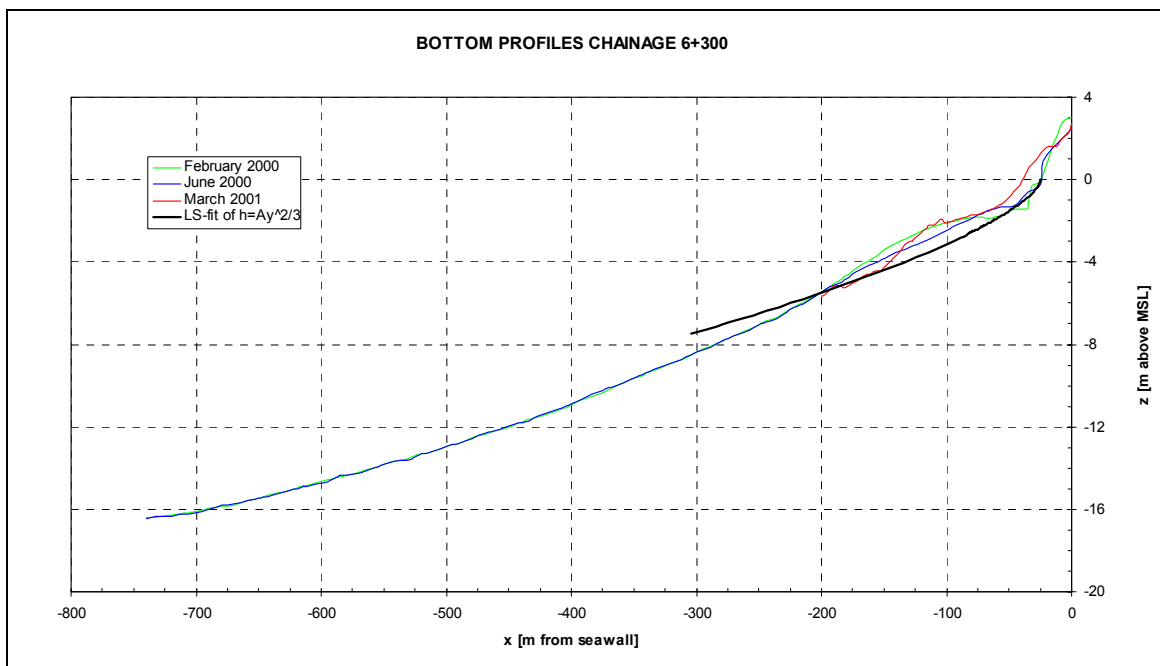


Figure B-1: Bottom profiles at chainage 6+300 measured in February and June 2000 (up to MSL -16m) and in March 2001 (up to MSL -6 m). A least-square fit of  $h=Ay^{2/3}$  to the June 2000 profile up to a depth of 7.5 m is plotted too ( $A = 0.175 \text{ m}^{1/3}$ ).

## B.4 Sediment characteristics

### B.4.1 Characteristics of the native and fill sediments

The characteristics of the native and fill sediments are indicated in the tables below.

Native sediment chainage 6100 - 6900									
sample	depth [m]	$d_{16}$ [mm]	$d_{84}$ [mm]	$d_{50}$ [mm]	$\phi_{16}$	$\phi_{84}$	$\phi_{50}$	$M_\phi$	$\sigma_\phi$
1	-10	0.42	0.19	0.28	1.25	2.40	1.84	0.57	1.82
2	-5	0.42	0.15	0.25	1.25	2.74	2.00	1.99	0.74
3	-3	0.42	0.18	0.28	1.25	2.47	1.84	1.86	0.61
4	-2	0.47	0.22	0.33	1.09	2.18	1.60	1.64	0.55
5	-1	0.60	0.28	0.38	0.74	1.84	1.40	1.29	0.55
6	water line	0.50	0.27	0.38	1.00	1.89	1.40	1.44	0.44
7	dry beach	0.66	0.28	0.40	0.60	1.84	1.32	1.22	0.62
8	dune	0.44	0.24	0.32	1.18	2.06	1.64	1.62	0.44
<b>composite</b>		0.50	0.23	0.33	1.02	2.15	1.60	<b>1.58</b>	<b>0.63</b>

Note: the values of MSL -10 m are not included in the calculation of the mean, because the fill won't extend to this depth.

<b>Borrow area I – Puerto Juárez</b>									
sample	depth [m]	d <sub>16</sub> [mm]	d <sub>84</sub> [mm]	d <sub>50</sub> [mm]	φ <sub>16</sub>	φ <sub>84</sub>	φ <sub>50</sub>	M <sub>φ</sub>	σ <sub>φ</sub>
1	0.30 m below the sea floor	0.76	0.18	0.32	0.40	2.47	1.64	1.43	1.04
2		0.45	0.13	0.22	1.15	2.94	2.18	2.05	0.90
3		0.45	0.10	0.24	1.15	3.32	2.06	2.24	1.08
4		0.40	0.17	0.22	1.32	2.56	2.18	1.94	0.62
5		0.48	0.13	0.23	1.06	2.94	2.12	2.00	0.94
6		0.24	0.09	0.12	2.06	3.47	3.06	2.77	0.71
7		0.90	0.23	0.40	0.15	2.12	1.32	1.14	0.98
8		0.75	0.25	0.42	0.42	2.00	1.25	1.21	0.79
<b>composite</b>		0.55	0.16	0.27	0.96	2.73	1.98	<b>1.85</b>	<b>1.04</b>

<b>Borrow area II – Punta Sam</b>									
sample	depth [m]	d <sub>16</sub> [mm]	d <sub>84</sub> [mm]	d <sub>50</sub> [mm]	φ <sub>16</sub>	φ <sub>84</sub>	φ <sub>50</sub>	M <sub>φ</sub>	σ <sub>φ</sub>
1	0.30 m below the sea floor	0.77	0.20	0.38	0.38	2.32	1.40	1.35	0.97
2		0.48	0.15	0.25	1.06	2.74	2.00	1.90	0.84
3		0.80	0.17	0.34	0.32	2.56	1.56	1.44	1.12
4		0.50	0.11	0.23	1.00	3.18	2.12	2.09	1.09
5		0.75	0.19	0.34	0.42	2.40	1.56	1.41	0.99
6		1.10	0.31	0.43	-0.14	1.69	1.22	0.78	0.91
7		1.30	0.40	0.80	-0.38	1.32	0.32	0.47	0.85
8		1.10	0.33	0.57	-0.14	1.60	0.81	0.73	0.87
<b>composite</b>		0.85	0.23	0.42	0.31	2.23	1.37	<b>1.27</b>	<b>1.10</b>

The composite mean and standard deviation (bold in above tables) are calculated using Equation (B-1) and Equation (B-2).

$$\mu_T = \frac{1}{N} [\mu_1 + \mu_2 + \dots + \mu_N] \quad (B-1)$$

Where: N number of samples [-]  
 $\mu_T$  composite mean [-]  
 $\mu_n$  mean of individual sample [-]

$$\sigma_T^2 = \frac{1}{N} \left[ \sum_1^N \sigma_n^2 + \sum_1^N (\mu_n - \mu_T)^2 \right] \quad (B-2)$$

Where:  $\sigma_T$  composite standard deviation [-]  
 $\sigma_n$  standard deviation of individual sample [-]

So the composite mean is simply the average of the means of the individual samples. The composite standard deviation is the square root of the composite variance. The latter is the average of the variances of the individual samples plus the sum of the squared differences of the mean of the individual samples and the composite mean [Dean, 2002].

### B.4.2 Longshore and cross-shore distribution of sediment size

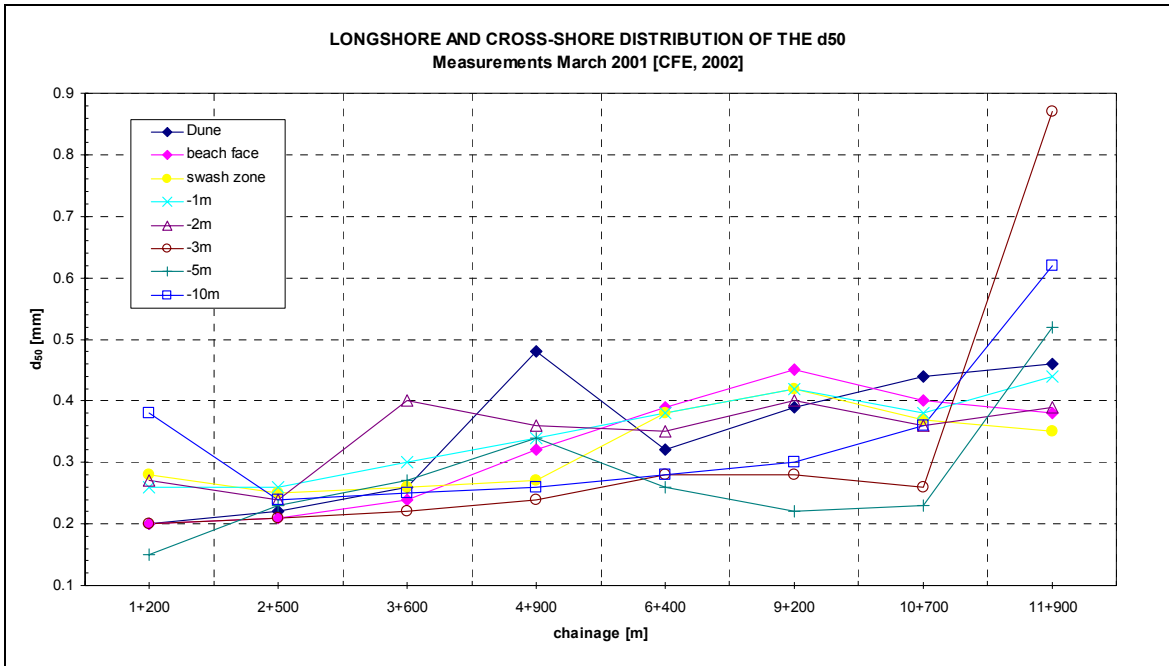


Figure B-2: Longshore and cross-shore distribution of the median grain size  $d_{50}$ .

### B.4.3 Thickness of the sediment layers

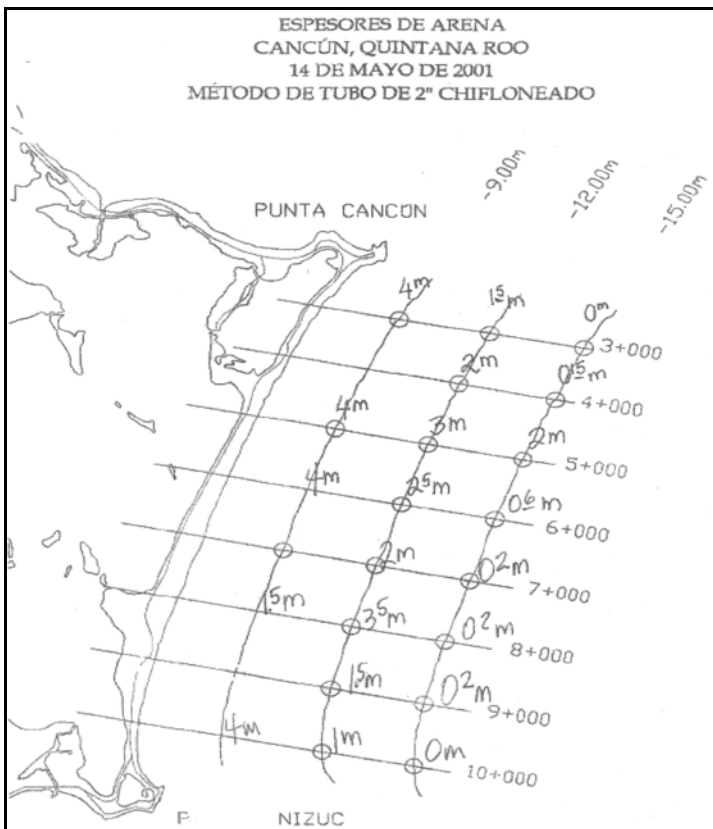


Figure B-3: Thickness of the sediment layers in the project area is indicated. Values and locations are indicative only, since they were determined by a diver with a jet tube.

## B.5 Wind data

The monthly distribution of the offshore wind speed is indicated in Table B-1. Information regarding the wind direction is indicated in Figure B-4.

Table B-1: Monthly distribution of offshore wind speed [www.waveclimate.com].

Monthly percentage of occurrence of wind speed [m/s] in rows												
Wind speed [m/s]	Jan	Feb	Mar	Apr	May	Jun	Jul	Aug	Sep	Oct	Nov	Dec
0 – 2	0.5	0.9	1.3	4.6	5.7	0.9	2.7	5.8	5.9	1.3	1.7	2.0
2 – 4	3.6	8.9	5.8	5.4	10.1	5.3	19.9	21.4	16.0	6.9	6.0	6.4
4 – 6	13.1	25.2	21.9	26.4	30.1	35.6	44.7	39.6	42.8	25.2	21.8	12.6
6 – 8	26.1	31.0	35.2	39.2	35.2	37.9	26.2	26.3	27.1	29.5	27.3	36.3
8 – 10	27.7	19.9	18.9	16.9	14.7	15.6	5.0	5.4	4.4	19.3	18.8	23.0
10 – 12	19.1	9.3	11.6	6.9	3.8	4.5	1.0	1.3	2.8	8.6	10.9	11.5
12 – 14	7.7	3.8	4.9	0.6	0.4	0.2	0.6	0.2	1.0	7.4	8.4	5.9
14 – 16	2.1	1.0	0.4	0	0	0.1	0	0.1	0.0	1.7	5.0	2.3
16 – 18	0.0	0	0	0	0	0	0	0	0	0.3	0	0
> 18	0	0	0	0	0	0	0	0	0	0	0	0
<b>Average [m/s]</b>	<b>8.5</b>	<b>7.2</b>	<b>7.4</b>	<b>6.6</b>	<b>6.1</b>	<b>6.5</b>	<b>5.3</b>	<b>5.2</b>	<b>5.4</b>	<b>7.5</b>	<b>7.9</b>	<b>7.8</b>

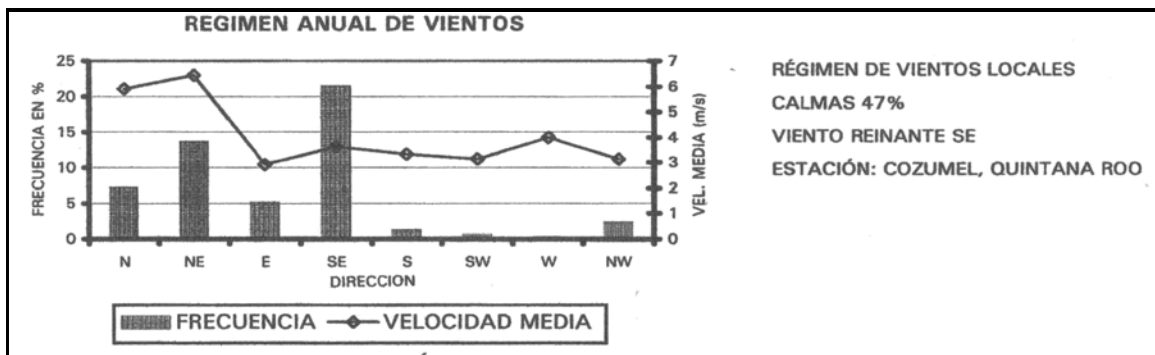


Figure B-4: Annual wind climate for the project area with frequency of occurrence (left axis) and mean velocity (right axis) per direction (horizontal axis) [SCT, 2001].



## B.6 Development of the shoreline position

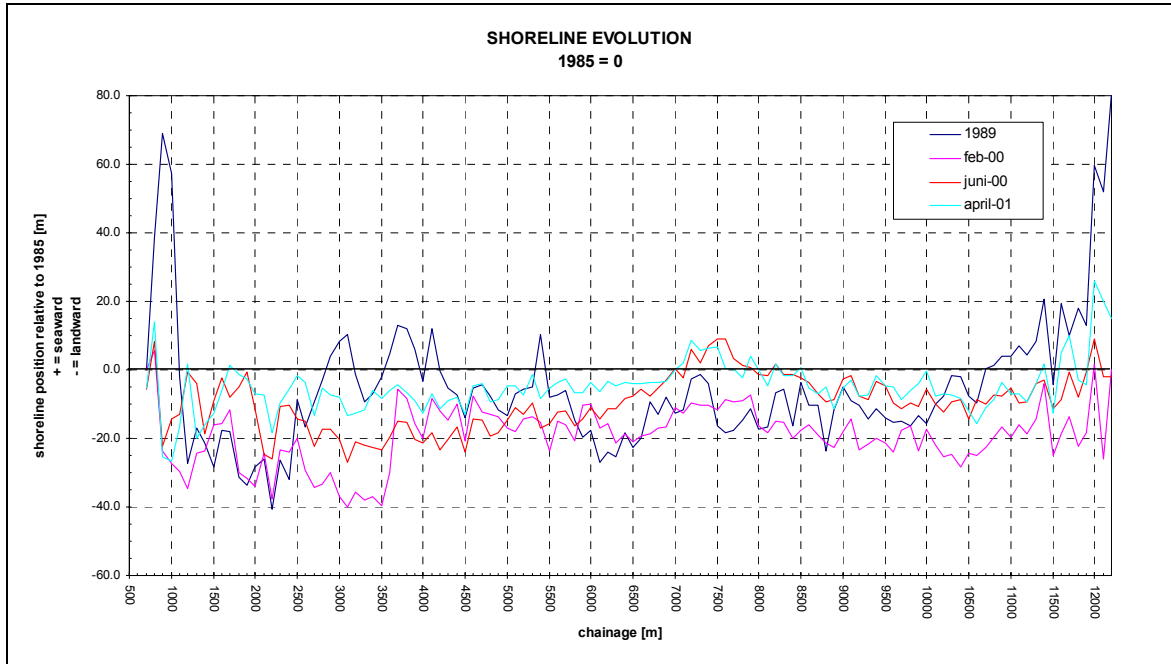


Figure B-5: Shoreline development in time. Punta Cancún is at chainage 0+000 and Punta Nizuc at chainage 12+600. Note that the 1985 and 1989 data aren't accurate.

## B.7 Current and transport patterns

In Figure B-6 the offshore current patterns are indicated.

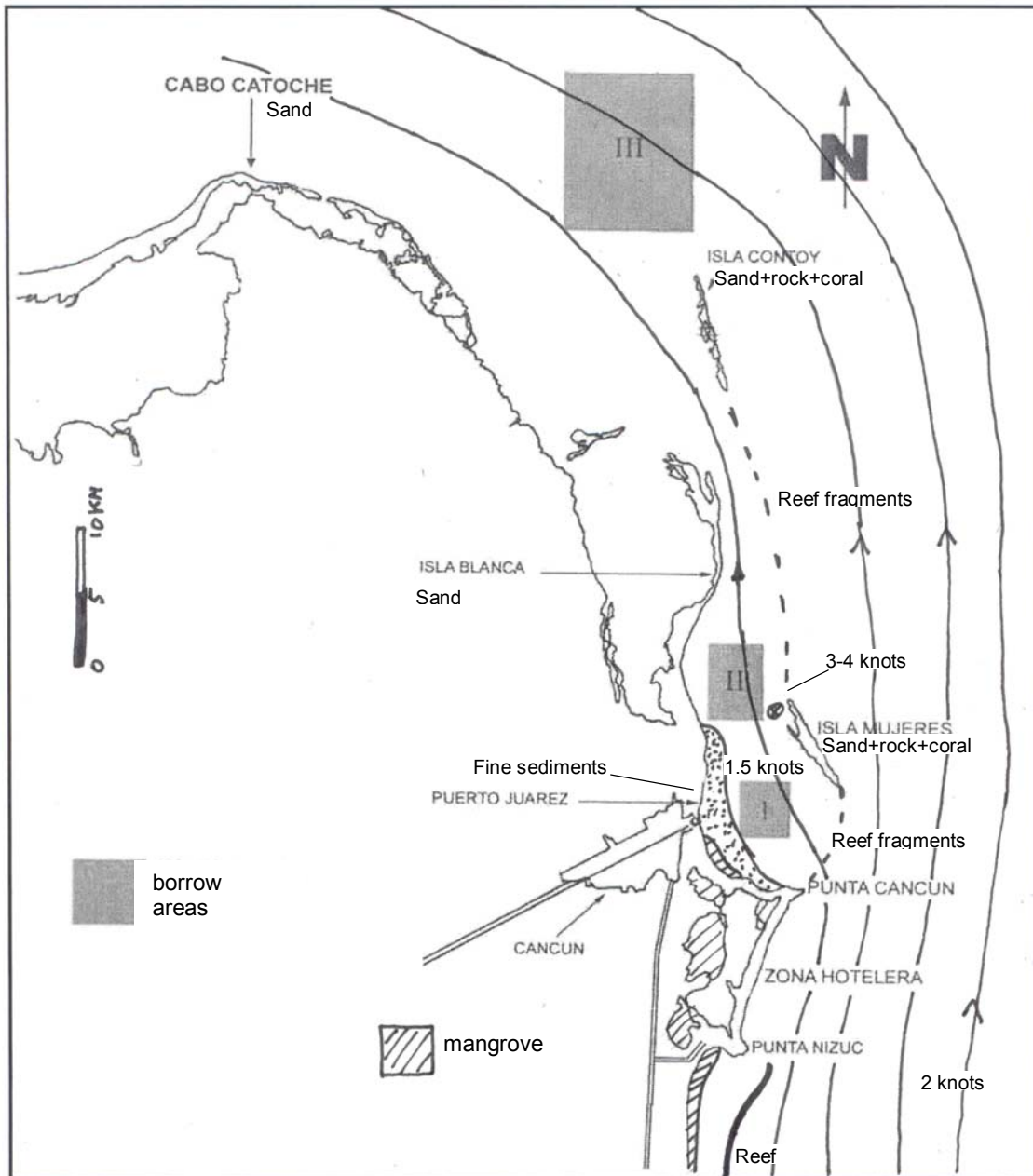


Figure B-6: Offshore current patterns and location of reef fragments and sediment types.

In Figure B-7 and Figure B-9 the nearshore current patterns are indicated for southeastern and eastern wave conditions respectively. In Figure B-8 and Figure B-10 the longshore erosion and accretion patterns are derived for the considered wave directions. It is concluded that longshore erosion at the outer ends of the project area (at Punta Cancún and Punta Nizuc) can occur for all wave directions between southeast and northeast. The centre of the project area has a small expected longshore transport gradient.

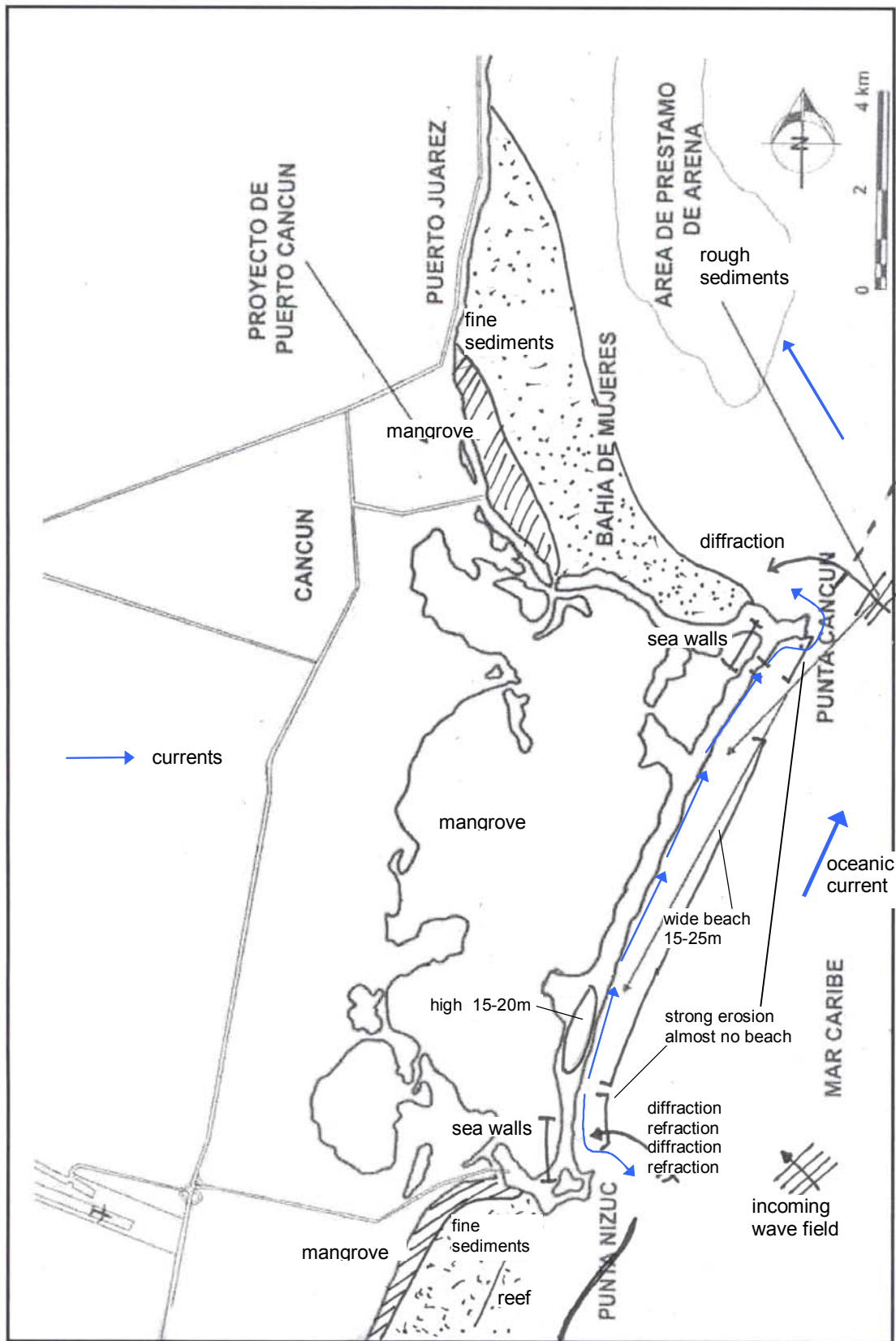


Figure B-7: Nearshore current patterns for southeastern wave conditions.

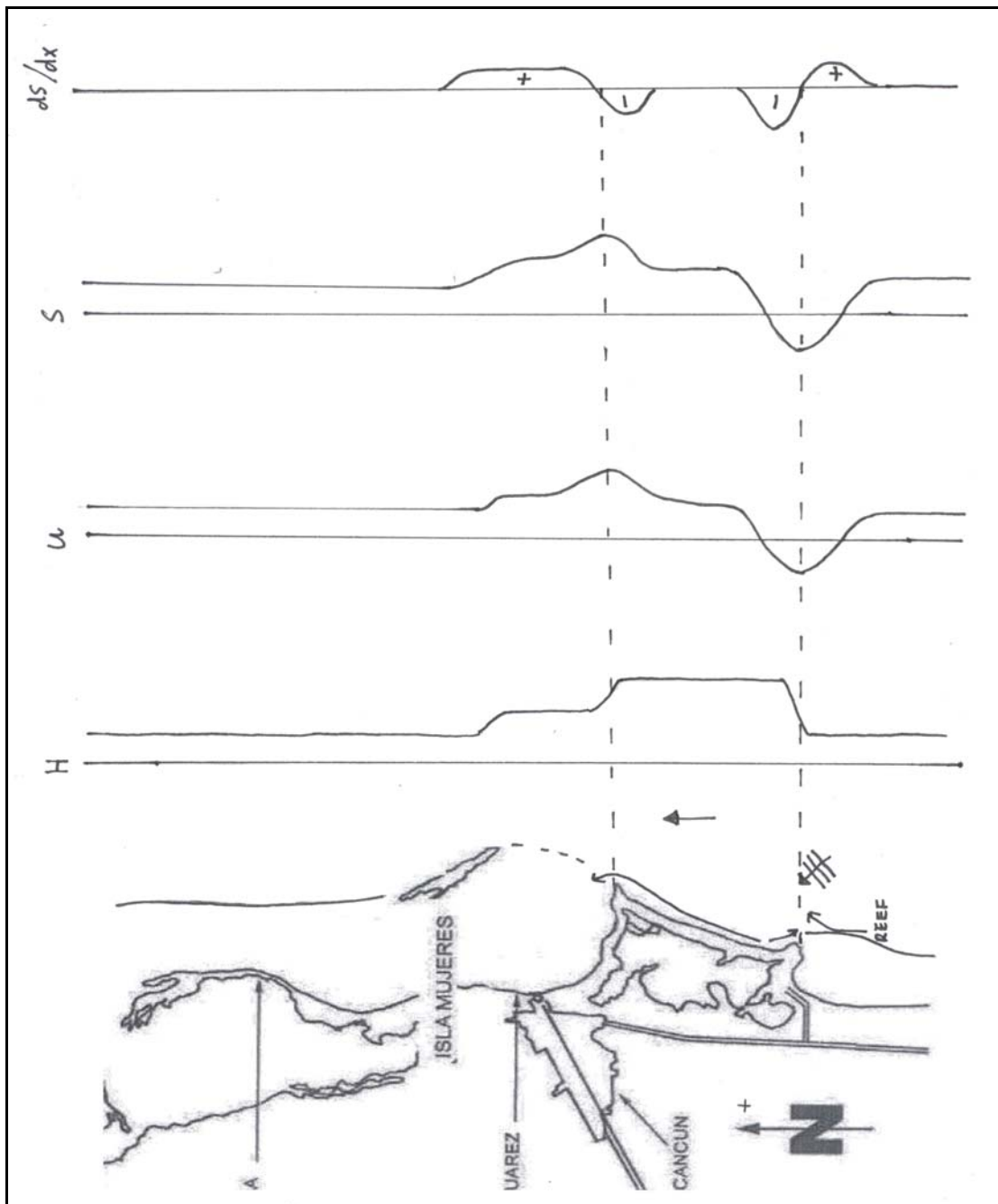


Figure B-8: Nearshore longshore sediment transport patterns for southeastern wave conditions. + means accretion, - erosion.

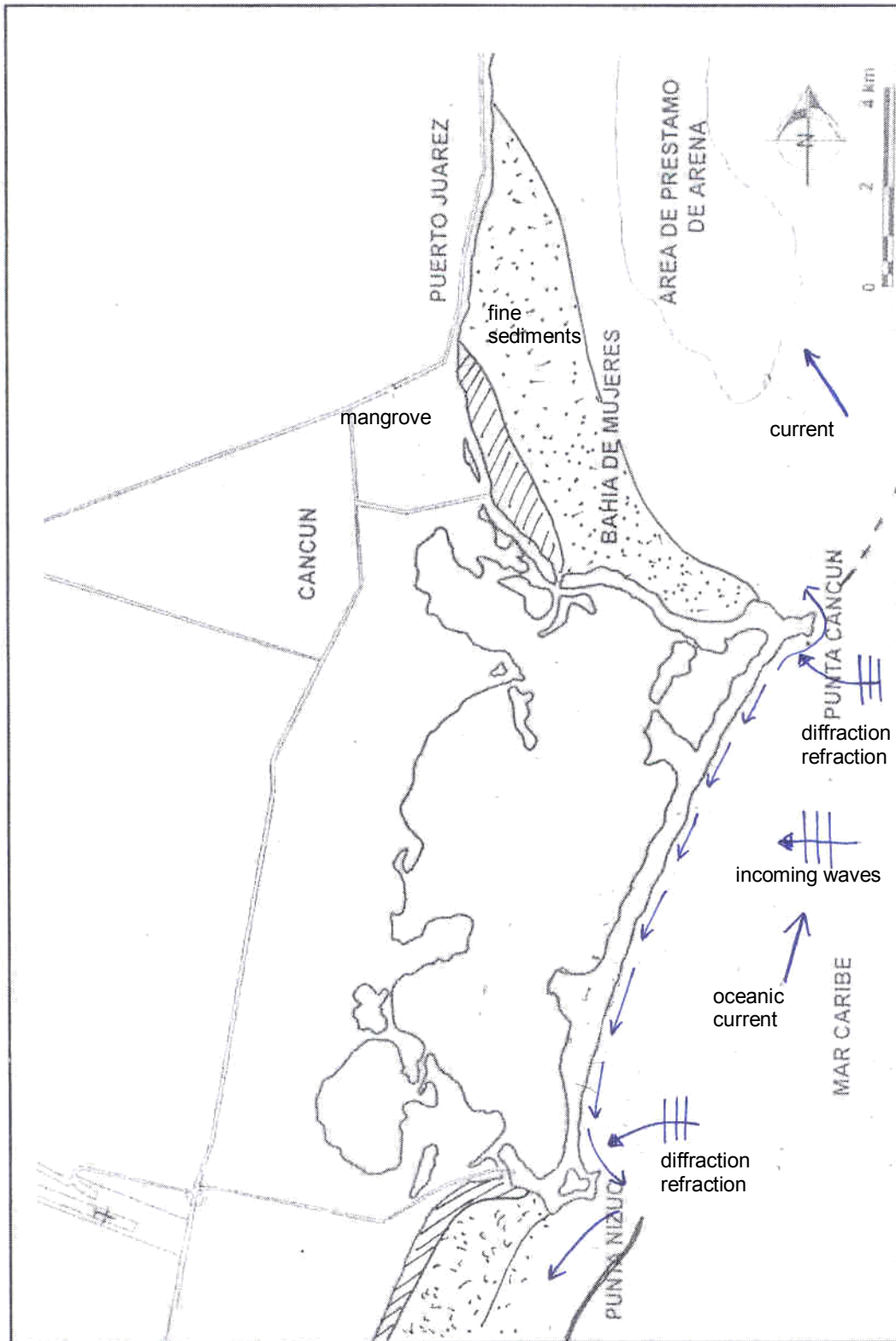


Figure B-9: Nearshore current patterns for eastern wave conditions.

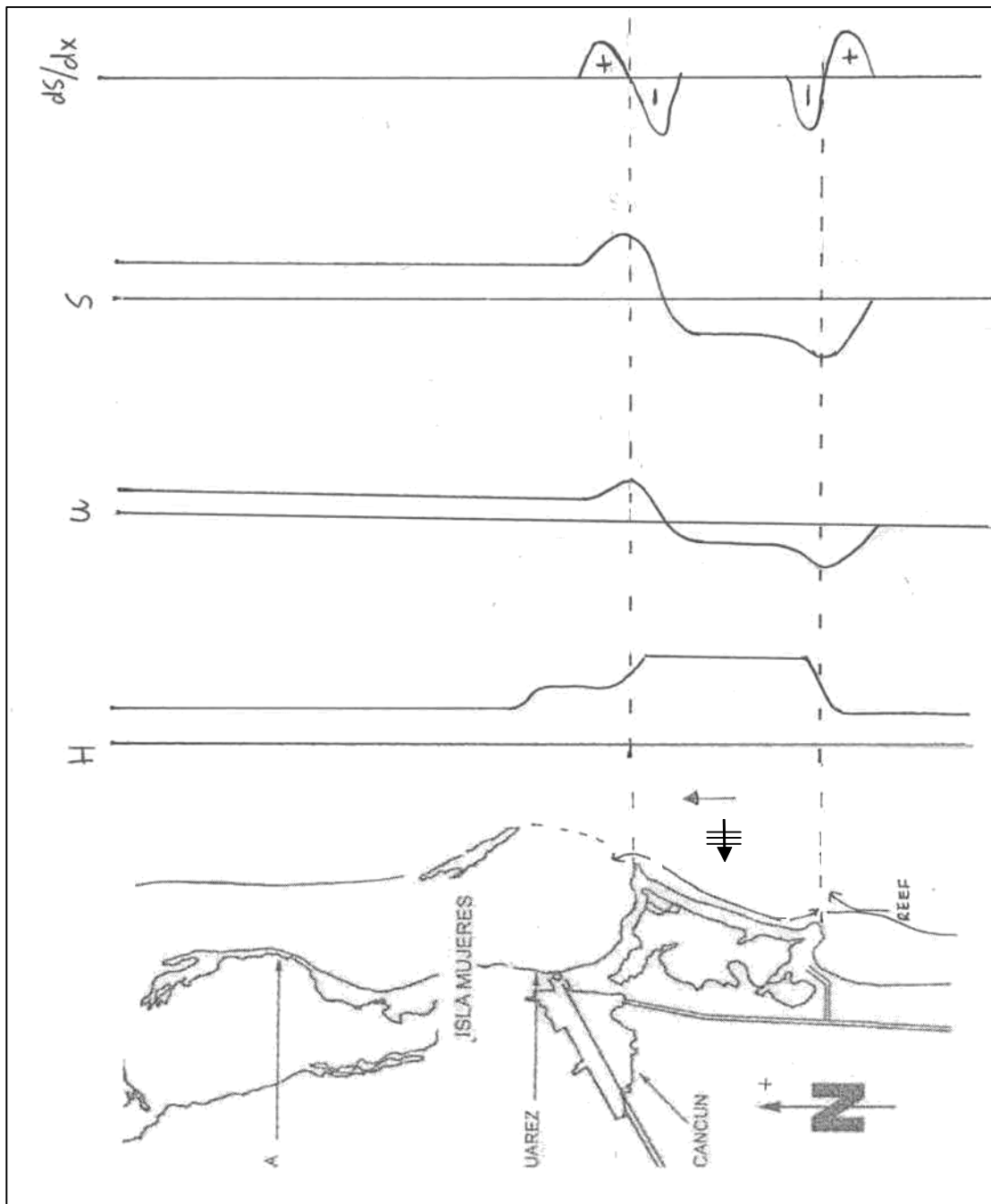


Figure B-10: Nearshore longshore sediment transport patterns for southeastern wave conditions. + means accretion, - erosion.

## C OVERVIEW OF MODEL FORMULATIONS IN UNIBEST-TC

### C.1 Introduction

In this appendix an overview of the model set-up and formulations in Unibest-TC version 2.04beta is given. Goal of this overview is to explain the basic assumptions and working of the program. For more detailed and exhaustive information is referred to Bosboom et al. [2000]. Other useful references include: Sorgedrager [2002] and Van Thienen [2003]. The structure of this appendix is as follows. First the used coordinate system is defined (Paragraph C.2). Then the model set-up is discussed (Paragraph C.3.1 ) after which the various sub-models are described (Paragraph C.3.2 to C.3.6).

### C.2 Coordinate system

The coordinate system used in Unibest-TC is shown in Figure C-1.

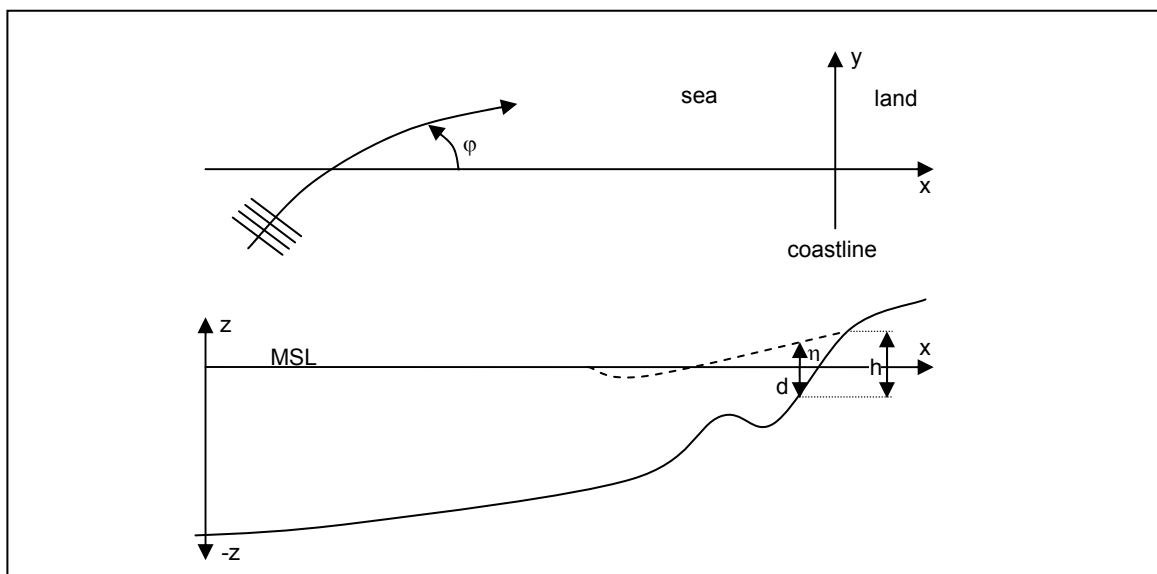


Figure C-1: Definition of coordinate system and water level in Unibest-TC. The origin of the vertical  $z$ -axis is at MSL. The  $x$ -axis is positive landwards, while the  $y$ -axis is rotated  $90^\circ$  counter-clockwise, relative to the  $x$ -axis. Wave angles are defined between the  $x$ -axis and the direction of wave propagation, positive angles counting counter-clockwise. The water level  $\eta$  and the bottom level  $d$  together form the water depth  $h$ .

Because of the used calculation scheme, Unibest-TC can only calculate in positive  $x$ -direction. This implies that the incoming wave direction  $\varphi$  must be between  $-90^\circ$  and  $+90^\circ$ .

## C.3 Sub-models

### C.3.1 Model set-up

The Unibest-TC model consists of five sub-models:

- Wave propagation model.
- Mean current profile model.
- Wave orbital velocity model.
- Bed load and suspended load transport model.
- Bed level change model.

A schematic representation of the various sub-models is given in Figure C-2.

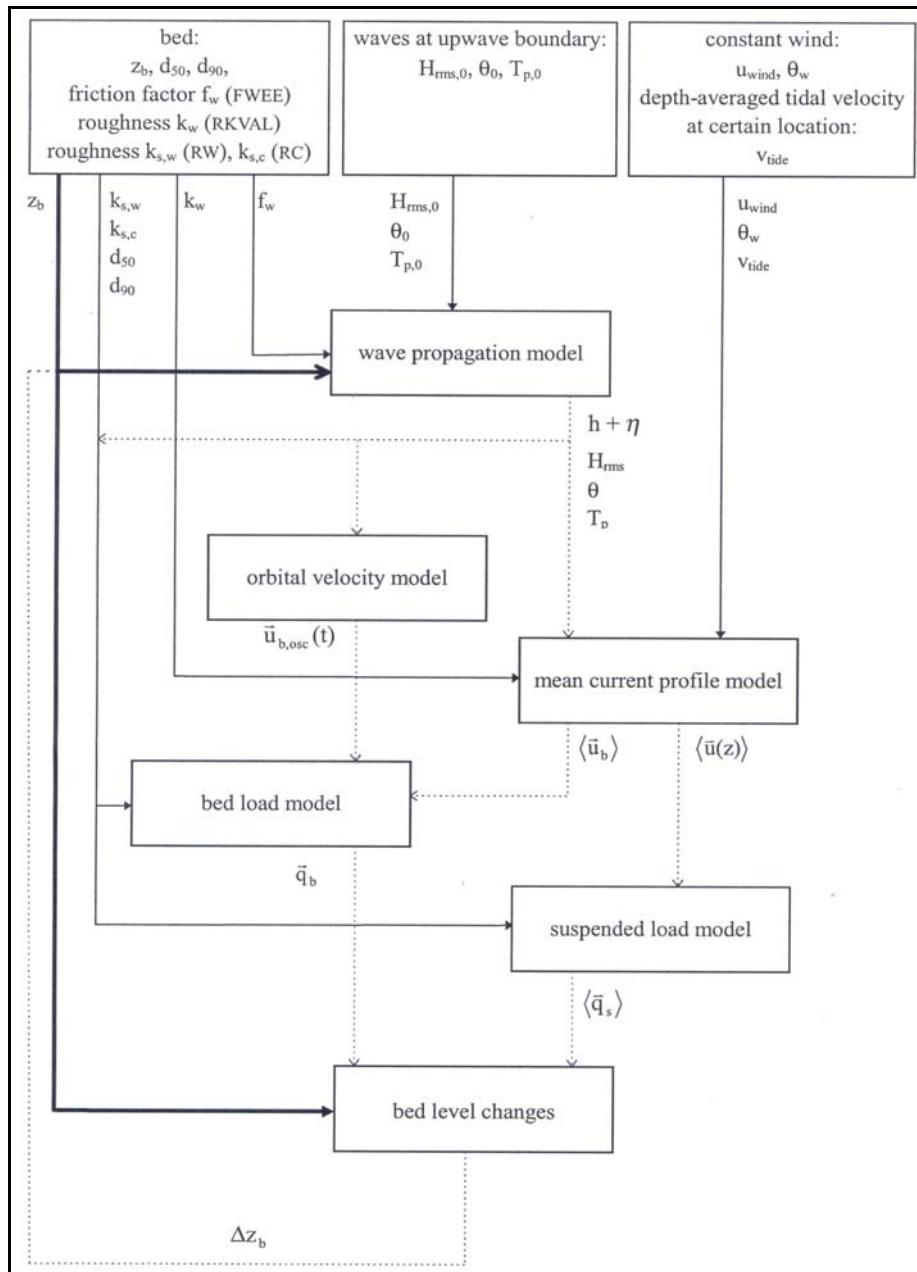


Figure C-2: Overview of Unibest-TC sub-models [Bosboom et al., 2000].

### C.3.2 Wave propagation model

The wave propagation model computes the wave energy decay along a cross-shore ray including effects of shoaling, refraction and energy dissipation. This is done by three



coupled first-order differential equations, viz. the time-averaged wave energy balance, the balance equation for the roller energy and the horizontal momentum balance. The first equation reads:

$$\frac{\partial}{\partial x}(EC_g \cos \theta) = -D_w - D_f \quad (C-1)$$

Where:	$C_g$	wave group velocity	[m/s]
	$\theta$	angle of incidence of the wave field	[°]
	$D_w$	dissipation of wave energy due to breaking	[W/m <sup>2</sup> ]
	$D_f$	dissipation of wave energy due to bottom friction	[W/m <sup>2</sup> ]

The organised wave energy  $E$  is defined according to linear wave theory:

$$E = \frac{1}{8} \rho g H_{rms}^2 \quad (C-2)$$

Where:	$\rho$	density of water	[kg/m <sup>3</sup> ]
	$g$	gravitational acceleration	[m/s <sup>2</sup> ]
	$H_{rms}$	root-mean-square wave height	[m]

For the dissipation of organised wave energy the following expression is used:

$$D_w = \frac{\rho g \alpha H_{max}^2 Q_b}{4T_p} \quad \text{with} \quad H_{max} = \frac{0.88}{k} \tanh\left(\frac{\gamma k h}{0.88}\right) \quad (C-3)$$

Where:	$\alpha$	dissipation coefficient (ALFAC)	[-]
	$T_p$	peak wave period	[s]
	$H_{max}$	maximum possible wave height	[m]
	$Q_b$	fraction of breaking waves	[-]
	$\gamma$	dissipation coefficient (GAMMA)	[-]
	$k$	local wave number	[1/m]
	$h$	water depth	[m]

The fraction of breaking waves  $Q_b$  is calculated from the ratio between  $H_{rms}$  and  $H_{max}$ . A delay for the breaking of the waves is applied, as waves require a certain distance to start breaking. Therefore the used water depth is not the local water depth, but a weighed depth over a certain distance seaward of the computational point.

The dissipation due to bottom friction is modelled as:

$$D_f = \frac{f_w \rho}{\sqrt{\pi}} u_{orb}^3 \quad (C-4)$$

Where:	$f_w$	user-defined friction factor (FWEE)	[-]
	$u_{orb}$	amplitude of the wave orbital velocity based on linear wave theory and $H_{rms}$ .	[m/s]

The second differential equation is the balance equation for the roller energy:

$$\frac{\partial}{\partial x}(2E_r C \cos \theta) = D_w - Diss \quad \text{with} \quad Diss = \beta 2g \frac{E_r}{C} \quad \text{with} \quad E_r = \frac{1}{2} \rho C^2 \frac{A}{L} \quad (C-5)$$

Where:	$E_r$	roller energy	[J/m <sup>2</sup> ]
	$C$	wave celerity	[m/s]
	$\beta$	slope of the face of the wave (BETD)	[-]
	$Diss$	dissipation of roller energy	[W/m <sup>2</sup> ]
	$A$	area of the roller	[m]
	$L$	length of the roller	[m]

The third differential equation is the cross-shore momentum equation, which reads:

$$\frac{\partial \bar{\eta}}{\partial x} = -\frac{1}{\rho g h} \frac{\partial S_{xx}}{\partial x} \quad \text{with} \quad S_{xx} = \left( (n + n \cos^2 \theta - 0.5) E + 2E_r \cos^2 \theta \right) \quad (\text{C-6})$$

Where:

$\eta$	mean wave set-up	[m]
$S_{xx}$	cross-shore radiation stress	[N/m]
$n$	group velocity / wave propagation speed ( $C_g/C$ )	[-]

With given boundary conditions for  $H_{rms}$ ,  $T_p$  and  $\theta$  at the upwave boundary and a given bottom profile  $z_b(x)$ , the equation system can be solved for the three unknowns  $E$ ,  $E_r$  and  $\eta$ .

### C.3.3 Mean current profile model

This model calculates the vertical distribution of the wave-averaged mean current in both longshore and cross-shore direction, accounting for vertical non-uniform driving forces: wind shear stress, wave breaking, bottom dissipation in the wave boundary layer and the slope of the free surface due to a longshore (tidal) current.

In order to calculate this velocity distribution, the horizontal momentum balance needs to be solved. This is done using a quasi 3-D model which consists of three layers as can be seen in Figure C-3.

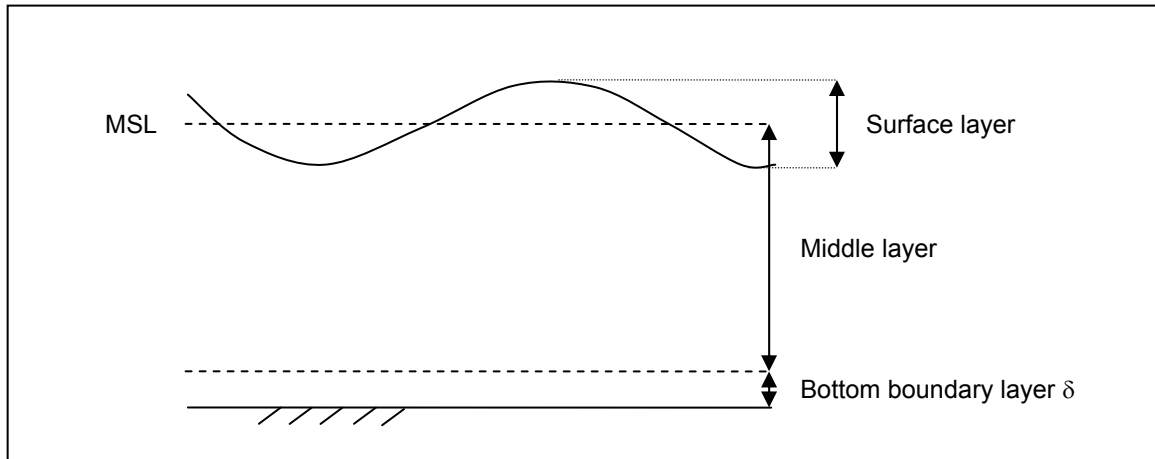


Figure C-3: Three layer model to determine the vertical distribution of the wave-averaged mean current. The surface layer extends from the wave trough to the wave crest. The middle layer extends from MSL to the top of the bottom boundary layer.

The surface layer is replaced by an effective shear stress at wave trough level induced by wind and surface rollers and by a mass flux, compensating for the mass transport in the surface layer.

The total shear stress can be calculated by integrating a momentum balance of the following form:

$$\frac{\partial \tau_i}{\partial \sigma} = R_i \quad (\text{C-7})$$

Where:

$\tau_i$	horizontal shear stress	[N/m <sup>2</sup> ]
$\sigma$	dimensionless depth ( $z/h$ )	[-]
$R_i$	pressure gradient forcing, assumed to be depth-independent	[N/m <sup>2</sup> ]
$i$	$i$ -direction, with $i = x$ or $y$	

Integration of Equation (C-7) from the surface downwards leads to:

$$\tau_i = \tau_{s,i} - R_i (1 - \sigma) \quad (\text{C-8})$$

Where:  $\tau_{s,i}$  known surface stress at MSL due to wind stress and stress of surface rollers [m<sup>2</sup>]

It must be stated that for the bottom boundary layer the streaming term induced shear stress must be included at the right-hand-side of Equation (C-8). For simplicity, this term is not considered here. See for details Bosboom et al. [2000].

The shear stress is related to the velocity gradients by:

$$\tau_i = \frac{\rho \nu_t}{h} \frac{\partial u_i}{\partial \sigma} \quad (C-9)$$

Where:  $\nu_t$  eddy viscosity [m<sup>2</sup>/s]

The vertical structure of the eddy viscosity is calculated separately for the middle and the bottom layer. The eddy viscosity is written as the product of the depth-averaged viscosity and a parabolic shape function. The depth-averaged viscosity is defined as the root-mean-square of the depth-averaged viscosity contributions due to breaking, wind and the slope-driven current. In the boundary layer, the eddy viscosity is increased to account for the increased turbulence due to the wave orbital motion.

Integrating Equation (C-9) gives an expression for the velocity profile as a function of the eddy viscosity. Integrating once more gives an expression for the depth-mean velocity in  $x$ - and  $y$ -direction as a function of the forcing: wind shear stress, the roller shear stress, the streaming function and the depth-independent pressure gradient.

The depth-mean velocity in  $x$ -direction follows from the mass flux in the surface layer:

$$\bar{u}_x = -\frac{q_{drift} \cos \theta}{h} \quad \text{with} \quad q_{drift} = \frac{E + 2E_r}{c} \quad (C-10)$$

Where:  $q_{drift}$  mass flux in the surface layer due to the progressive character of the waves and the surface roller in breaking waves [m<sup>2</sup>/s]

The depth-independent pressure gradient in  $y$ -direction  $R_y$  follows from the Chézy equation:

$$v = C \sqrt{h \frac{\partial h}{\partial y}} \quad \text{with} \quad C = 18 \log \left( \frac{12h}{k_s} \right) \quad (C-11)$$

Where:  $v$  (tidal) velocity at a reference depth [m/s]  
 $k_s$  roughness height (RKVAL) [m]

The remaining unknowns are the depth-mean velocity in  $y$ -direction and the pressure gradient  $R_x$  in  $x$ -direction. These values depend on the depth-averaged velocity, which itself depends on  $R_x$  (via the slope-driven current). Therefore an iterative procedure is followed to solve the equations, leading to a solution for the depth-mean current and the current profile in  $x$ - and  $y$ -direction.

### C.3.4 Wave orbital velocity model

The wave orbital velocity model calculates time series of the near-bed wave orbital velocity, containing contributions due to wave asymmetry; wave group related amplitude modulation and bound long waves. The shortest time-series which can exhibit all of these features has a length of one short wave group, which is  $m$  waves long.

A time series of the near-bed velocity including wave asymmetry in the case of regular waves is based on the Rienecker and Fenton [1981] model:

$$U_1(t) = \sum_{j=1}^n B_j \cos(j\omega t) \quad (C-12)$$

Where:  $B_j$  amplitudes, determined such that the difference between the max and min velocity of the asymmetric waves equals the difference in case of monochromatic waves [m]

The amplitude modulation on the time scale of a wave group is introduced by adding a second velocity time series:

$$U_2(t) = \sum_{j=1}^n \cos(j\omega t) \left[ \frac{1}{2} (1 + \cos(\Delta\omega t)) \right]^j \quad (C-13)$$

Where:  $\Delta\omega$  =  $\omega/m$ ,  $m$  being the number of waves in a wave group [rad/s]  
(set to 7 by default)

The magnitude of  $U_2$  is corrected to  $U_2'$ :

$$U_2'(t) = \left( \frac{\frac{1}{T} \int_0^T U_1^3 dt}{\frac{1}{mT} \int_0^{mT} U_2^3 dt} \right)^{1/3} U_2(t) \quad (C-14)$$

Where:  $T$  the wave period [s]

The long wave velocity  $U_3$  is computed according to Roelvink and Stive [1989] such that the wave-group related features of a random wave field are represented by a bi-chromatic wave train and a bound long wave with amplitude  $\xi_a$ :

$$U_3(t) = \xi_a \frac{\sqrt{gh}}{h} \cos\left(\frac{\omega}{m}t + \varphi\right) \quad \text{with} \quad \xi_a = -G_{nm} \frac{a_n a_m}{h} \quad \text{and} \quad (C-15)$$

$$m_0 = \frac{1}{8} H_{rms}^2 = \frac{1}{2} a_n^2 + \frac{1}{2} a_m^2 + \frac{1}{2} \xi_a^2$$

Where:  $\xi_a$  long wave amplitude [m]  
 $\varphi$  phase shift [rad]  
 $G_{nm}$  transfer function according to Sand [1982] [-]  
 $a_n, a_m$  amplitudes of the bichromatic wave train  $a_n = a_m$  [m]  
 $m_0$  total surface variance [m<sup>2</sup>]

The phase shift  $\varphi$  is calculated according to an empirical expression by Roelvink and Stive [1989]:

$$\cos(\varphi) = C_r \left[ 1 - 2 \left( \frac{H_{rms}}{H_{rms,0}} \right)^2 \right] \quad (C-16)$$

Where:  $C_r$  a correlation coefficient (C\_R) [-]  
 $H_{rms,0}$  the incoming wave height at the seaward boundary [m]

Finally the total orbital velocity  $U_4$  is calculated:

$$U_4(t) = U_2'(t) + U_3(t) \quad (C-17)$$

### C.3.5 Bed load and suspended load transport model

#### Bed load transport

Bed load is defined as being that part of the load which is in more or less continuous contact with the bed. The bed load is computed as a function of the instantaneous bed shear stress, which depends on the near-bed velocity signals. These are composed of the generated time series of near-bed wave orbital velocity according to Equation (C-17) and the time-averaged current velocity near the bed.

The non-dimensional instantaneous bed-load vector  $\Phi_{bd}$  according to Ribberink [Van Rijn et al., 1995] is defined as follows:

$$\Phi_{bd}(t) = \frac{q_b(t)}{\sqrt{\Delta g d_{50}^3}} = 9.1 \frac{\beta_s}{(1-p)} (|\theta'(t)| - \theta_c)^{1.8} \frac{\theta'(t)}{|\theta'(t)|} \quad (C-18)$$

Where:	$q_b(t)$	bed-load transport rate in volume per unit time and width including pores	[m <sup>3</sup> /s/m]
	$d_{50}$	median grain diameter	[m]
	$p$	porosity of the sediment (=0.4)	[-]
	$\theta'$	dimensionless effective shear stress	[-]
	$\theta_c$	dimensionless critical shear stress	[-]
	$\beta_s$	slope factor	[-]

The instantaneous dimensionless effective shear stress  $\theta'$  is due to current and waves and only represents the sediment forcing (drag force on the grains) and not the form drag (induced by bed forms):

$$\theta'(t) = \frac{1/2 f_{cw}' |u_b(t)| u_b(t)}{(\rho_s - \rho) g d_{50}} \quad (C-19)$$

Where:	$f_{cw}'$	weighed friction factor due to currents and waves	[-]
	$u_b$	near-bottom horizontal velocity of the combined wave-current motion	[m/s]

The Bagnold slope correction factor  $\beta_s$  increases the transport rates in the case of downslope transport and decreases the transport rates for upslope transports:

$$\beta_s = \left( 1 + \frac{u_{bx} \frac{dz_b}{dx}}{|u_b| \tan \varphi} \right)^{-1} \quad (C-20)$$

Where:	$u_{bx}$	cross-shore component of near bottom velocity	[m/s]
	$dz_b/dx$	bottom slope	[-]
	$\tan \varphi$	angle of repose (TANPHI)	[-]

The instantaneous cross- and longshore bed load transport rates are obtained from:

$$q_{bx} = \frac{u_{bx}}{|u_b|} |q_b| \quad \text{and} \quad q_{by} = \frac{u_{by}}{|u_b|} |q_b| \quad (C-21)$$

### Suspended load transport

In Unibest-TC the wave-related suspended sediment transport is assumed to be small compared to the current-related suspended transport. Therefore the suspended sediment flux is computed as the product of the wave-averaged current and concentration profiles, which are obtained from the mean current profile model (see Paragraph C.3.3) and a time-averaged advection-diffusion equation:

$$q_{s,c} = \frac{\int_a^h (vc) dz}{(1-p)\rho_s} \quad (C-22)$$

Where:	$v$	time-mean velocity profile	[m/s]
	$c$	time-mean concentration profile	[kg/m <sup>3</sup> ]

The time-mean concentration profile  $c$  is calculated from the following equation:

$$w_{s,m} c + \varphi_d \varepsilon_{s,cw} \frac{dc}{dz} = 0 \quad (C-23)$$

Where:	$w_{s,m}$	fall velocity of suspended sediment	[m/s]
	$\varepsilon_{s,cw}$	sediment mixing coefficient of combined currents and waves	[m <sup>2</sup> /s]
	$\varphi_d$	damping coefficient dependent on the concentration	[-]

The wave-related mixing coefficient  $\varepsilon_{s,w}$  is assumed to be constant in the upper half of the water column and in the layer near the bed with a linear variation in between. Its magnitude depends on (among others): the wave height ( $H_{rms}$ ), period ( $T_p$ ), kinematic viscosity ( $\nu$ ) and grain size ( $d_{50}$ ).

The current-related mixing coefficient  $\varepsilon_{s,c}$  is assumed to be constant in the upper half of the water column and to decrease linearly to zero in the lower half of the column. Its magnitude depends on the bed roughness ( $k_{s,c}$ ) and the kinematic viscosity ( $\nu$ ).

The combined current and wave sediment mixing coefficient ( $\varepsilon_{s,cw}$ ) is defined as follows:

$$\varepsilon_{s,cw} = \sqrt{(\varepsilon_{s,w})^2 + (\varepsilon_{s,c})^2} \quad (C-24)$$

In order to solve Equation (C-23) a boundary condition for the concentration is required. The reference concentration near the bed is given by:

$$c_a = 0.015 \rho_s \frac{d_{50}}{a} \frac{T^{1.5}}{D_*^{0.3}} \quad \text{with } T = \frac{\tau'_{b,cw} - \tau_{b,cr}}{\tau_{b,cr}} \quad \text{and } D_* = d_{50} \left( \frac{g\Delta}{\nu^2} \right)^{1/3} \quad (C-25)$$

Where:	$c_a$	reference concentration near the bed	[kg/m <sup>3</sup> ]
	$a$	reference level	[m]
	$T$	dimensionless bed-shear parameter	[-]
	$D_*$	dimensionless particle parameter	[-]
	$\tau_{b,cw}$	time-averaged effective bed-shear stress due to currents and waves	[N/m <sup>2</sup> ]
	$\tau_{b,cr}$	time-averaged critical bed-shear stress according to Shields	N/m <sup>2</sup> ]
	$\nu$	kinematic viscosity	[m <sup>2</sup> /s]

### C.3.6 Bed level change model

The bed level changes are computed from the depth-averaged mass balance:

$$\frac{\partial z_b}{\partial t} + \frac{\partial q_{bot,sus}}{\partial x} = 0 \quad (C-26)$$

Where:	$z_b$	bottom height	[m]
--------	-------	---------------	-----

It is possible to introduce a longshore gradient in Equation (C-26) leading to:

$$\begin{aligned} \frac{\partial z_b}{\partial t} + \frac{\partial q_{bot,sus}}{\partial x} + FL\_POS \cdot q_y &= 0 \quad \text{for } q_y > 0 \\ \frac{\partial z_b}{\partial t} + \frac{\partial q_{bot,sus}}{\partial x} + FL\_MIN \cdot q_y &= 0 \quad \text{for } q_y < 0 \end{aligned} \quad (C-27)$$

Where:	$q_y$	longshore transport rate	[m <sup>3</sup> /s/m]
	$FL\_POS$	coefficient to introduce longshore transport gradient	[1/m]
	$FL\_MIN$	coefficient to introduce longshore transport gradient	[1/m]

Approaching the water line calculations stop when the water becomes too shallow. This depth is calculated from the user-defined relative wave period:

$$T^* = T_p \sqrt{g/h} \quad (C-28)$$

Where:	$T_p$	peak wave period	[s]
	$T^*$	relative wave period (TDRY)	[-]
	$g$	gravity acceleration	[m/s <sup>2</sup> ]
	$h$	local water depth	[m]

Landward of the depth calculated with Equation (C-28), the sediment transport is interpolated over the 'dry' profile. The cross-shore sediment transport  $q_{tot}$  varies linearly (with the height or the distance) between the last calculation point and the user-defined transport (USTRA) at the most landward grid point.





## D UNIBEST-TC PARAMETER SETTINGS

In the following table three complete sets of relevant input parameters are presented:

- The default parameter setting of Unibest-TC.
- The parameter setting used for the sensitivity analysis.
- The parameter setting after calibration of the model.

Table D-1: Parameter settings for the different model phases (sensitivity analysis, calibration + calculations) and the default values of Unibest-TC. If appropriate, the symbol for a parameter as used in Appendix C is given (second column).

PARAMETER		DESCRIPTION	Unit	PARAMETER SETTING		
Name	Symbol			Default	Sensitivity	Calibration
DT	$\Delta t$	Time step	days	1	0.2	0.125
NT	-	Number of time steps	-	5	1825	8760
USTRA	$q_{tot,x}(X_{end})$	Transport at shoreward boundary	m <sup>3</sup> /hr	0	0	0
JFR	-	Frequency to generate output	days	1	20	20
IBOD	-	Calculate bottom changes switch	-	1	1	1
TDRY	T*	Maximum relative wave period	-	40	20	24
K_IJL	-	Breaker delay switch	-	1	1	1
F_LAM	-	Number of wavelengths for depth integration	-	2	2	0.5
POW	-	Power in weighing function	-	1	1	1
TANPHI1	$\tan\phi_1$	Internal friction angle at X1	-	0.03	0.15	0.15
TANPHI2	$\tan\phi_2$	Internal friction angle at X2	-	0.1	0.5	0.4
XF1	-	Most seaward location	m	500	-500	-400
XF2	-	Most shoreward location	m	1200	-10	-10
DVAR	-	Cross-shore varying grain size switch	-	0	0	0
FCVISC	$\alpha_w$	Viscosity coefficient	-	0.1	0.1	0.1
GAMMA	$\gamma$	Wave breaking parameter ( $H_{max}$ )	-	0	0	0
ALFAC	$\alpha$	Wave breaking parameter	-	1	1	1
FWEE	$f_w$	Friction factor for bottom friction	-	0.01	0.01	0.01
RKVAL	$k_s$	Friction factor for mean current	m	0.01	0.01	0.02
DIEPV	-	Reference depth for tidal velocity	m	5	30	30
REMLG	-	Fixed bottom layer (zero transport)	m	0.1	0.1	0.1
BETD	$\beta$	Slope of wave front	-	0.1	0.1	0.1
D50	$d_{50}$	D50 grain size	m	0.0002	0.00033	0.00033
D90	$d_{90}$	D90 grain size	m	0.0003	0.0004	0.0004
DSS	$d_s$	D50 grain size of suspended material	m	0.00017	0.000264	0.000264
RC	$k_{s,c}$	Current related roughness	m	0.01	0.01	0.02
RW	$k_{s,w}$	Wave related roughness	m	0.002	0.002	0.002
ZDRY	-		-	0	0	1
TEMP	Te	Water temperature	°C	10	28	28
SALIN	Sa	Water salinity	* 0.01	30	30	30
C_R	$C_r$	Correlation coefficient bound long waves	-	0.25	0.25	0.25
FL_POS	-	Gradient in longshore transport	-	0	0	0
FL_NEG	-	Gradient in longshore transport	-	0	0	0

# E BOUNDARY CONDITIONS IN UNIBEST-TC

## E.1 Introduction

In this appendix an overview of the used boundary conditions in Unibest-TC is given. Goal of this overview is to make clear how the boundary conditions for the calibration and calculation of the equilibration and storm behaviour were generated.

In Paragraph E.2 the time step for the definition of the boundary conditions will be chosen. In Paragraph E.3 the generation of the wave input based on satellite data is discussed. Then the wind, current and water level input are treated (Paragraph E.4). The bottom profiles are discussed in Paragraph E.5. In Paragraph E.6 the boundary conditions definition files are listed.

## E.2 Time step definition boundary conditions

Unibest-TC uses an interpolation procedure to determine the boundary conditions on every computational point in time. Therefore it is allowed to use non-equidistant time points in the boundary condition definition file. Furthermore, it is allowed to use a time step in the boundary condition definition file which is different from the computational time step. However, in this particular case of a random generated wave climate without persistency of wave conditions, interpolation can lead to unrealistic wave directions. To avoid this, the boundary condition definition time step ( $\Delta t_{ubc}$ ) and the computational time step ( $\Delta t$ ) should be equal and are set to 0.125 days = 3 hours.

## E.3 Generation of wave input

### E.3.1 Introduction

Unibest-TC requires a definition file with the wave conditions ( $H_{rms}$ ,  $T_p$  and  $\theta$ ) defined in time. It is desired that the input of the wave conditions is as realistic as possible, i.e. shows as much resemblance as possible with the wave conditions as they occurred prior to the measurements of the bottom profiles in February and June 2000 and March 2001.

There are three sources available to generate the wave input for the Unibest-TC model:

- Measurements of buoys in the mentioned period.
- A wave climate based on 10 years of satellite observations of  $H_{rms}$ ,  $T_p$  and  $\theta$ .
- Satellite measurements in the mentioned period.

It was decided not to use the data from the buoys, since these measurements are very unreliable and inaccurate (see Paragraph 8.3.4). Satellite measurements in the mentioned period have a low resolution and only individual measurements of the wave height are made public.

In this paragraph the background of wave data based on satellite observations is described (Paragraph E.3.2). Then the wave climate based on satellite observations and the resulting input file for Unibest-TC is discussed (Paragraph E.3.3). Finally, in an attempt to improve the resemblance with reality, scaled wave conditions are created (Paragraph E.3.4).

### E.3.2 Background of satellite wave data

Satellite observations form an increasingly important source of wave data. Since the 1980's satellites equipped with various remote sensing instruments have been launched to gather wave data all over the world, which form a useful supplement to measurements with buoys and visual estimates. Modern satellites can measure the wave height, period and direction of the wave field. For more detailed information about these measurement techniques, reference is made to Holthuijsen [2002] and [www.waveclimate.com](http://www.waveclimate.com).

A satellite takes samples of the wave conditions while it passes a certain area. One pass results in a distribution of the wave conditions in the area during this pass. This is visualized in Figure A-1.

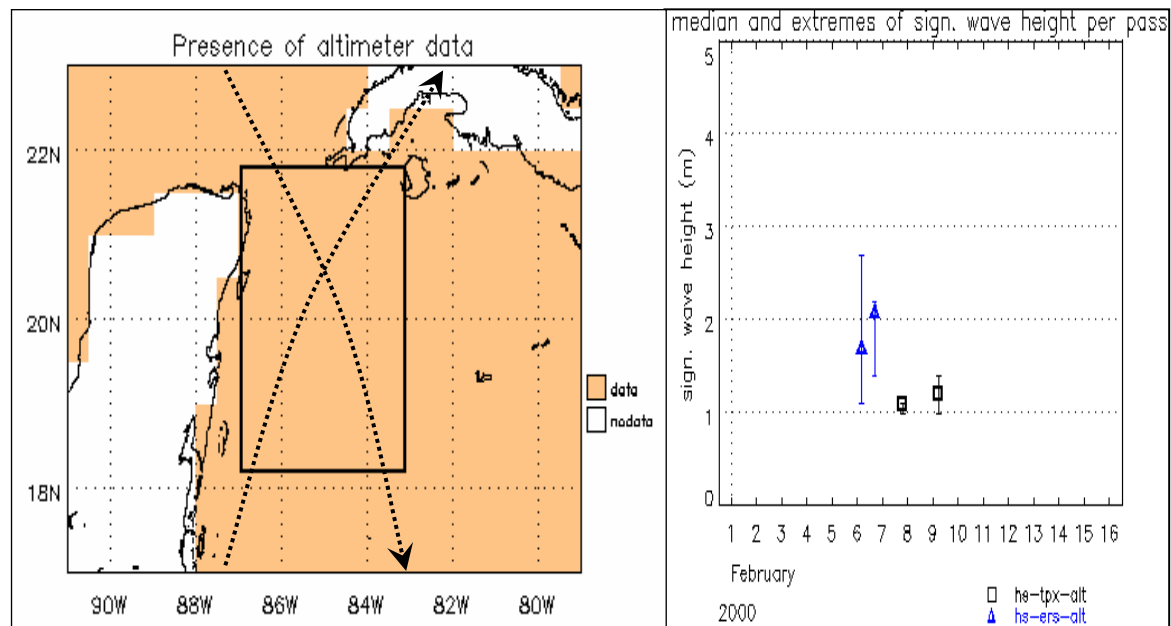


Figure E-1: Left panel: Passes of a satellite across an area of interest (arrows) and samples during such a pass (dots). Right panel: Distribution of significant wave height per pass (the codes in the right bottom corner indicate the names of the satellites). [www.waveclimate.com].

For engineering purposes, one is interested in general in wave data at a certain point or small area. To obtain these, a representative area has to be defined. Increasing the area leads to an increase of the amount of data, but this data could be less representative for the point considered, depending on the variability in geography and bathymetry. When observations are carried out in a certain area during a number of years a wave climate for this area can be defined.

The company ARGOS has gathered wave measurements of satellites and has created a databank with world cover, which is accessible via [www.waveclimate.com](http://www.waveclimate.com). This databank has been used in this thesis to create wave input for the morphological model Unibest-TC (see Appendix C).

### E.3.3 Wave climate based on satellite data

#### Offshore wave climate

An offshore wave climate based on 10 years of satellite measurements between 1991 and 2001 is available. The area from which the measurements were taken has a size of 400 x 400 km with its centre at 20° 00'N, 85° 00'W and is shown in Figure E-2. The size of the area is maximal to obtain as many measurements as possible and has been chosen such that small variability in wave conditions is expected.

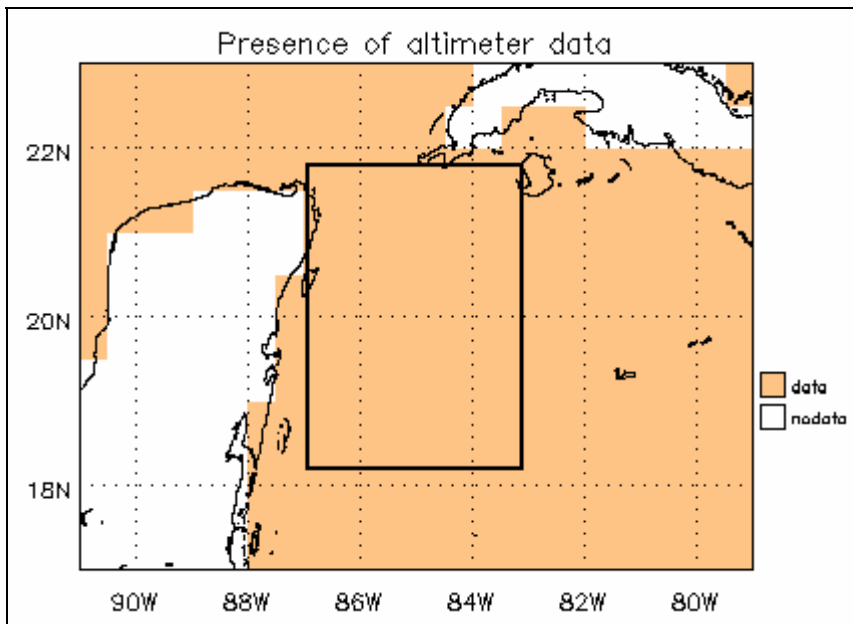


Figure E-2: Area from which the wave climate is obtained (400 x 400 km).

The offshore wave climate obtained from the area in Figure E-2 consists of a monthly 3-dimensional probability distribution of  $H_{rms}$ ,  $T_p$  and  $\theta$  based on 10 years of satellite measurements. Key figures of this wave climate are given in Table E-1.

Table E-1:

Average values of the wave climate based on 10 years of satellite measurements in the area of Figure E-2. Direction convention: coming from north = 0°, counting positive clockwise.

Month	$H_s$ [m]	$T_p$ [s]	$\theta$ [°]
January	1.5	6.8	93
February	1.5	6.8	94
March	1.6	6.5	101
April	1.3	6.5	103
May	1.2	6.5	101
June	1.2	6.8	107
July	1.2	6.8	108
August	1.1	6.6	108
September	1.2	6.7	95
October	1.4	6.7	94
November	1.5	6.7	94
December	1.7	6.8	94
<b>Average</b>	<b>1.4</b>	<b>6.7</b>	<b>100</b>

This monthly 3-D probability distribution can be visualized in a 3-dimensional scatter diagram. Per directional section of 22.5°, combinations of certain classes of wave height and period are listed. The number of times a certain combination ( $H_s$ ,  $T_z$ ,  $\theta$ ) occurs, represents the probability of occurrence of this combination in the considered month. In Table E-2 a part of this list is presented.

Table E-2

Part of the scatter diagram of the monthly averaged offshore wave climate in January. Every value of  $H_s$ ,  $T_p$  or  $\theta$  represents the centre of its class. A smaller class width means that there are many available measurements for that range of values to justify this smaller class width. The number of times a combination is listed indicates the probability of occurrence of this combination.

month	Hs	Tz	direction
1	0.60	5.00	315.0
1	0.80	5.00	315.0
1	0.80	6.00	315.0
1	1.00	5.00	315.0
1	1.00	6.00	315.0
1	1.10	4.50	315.0
1	1.20	5.00	315.0
1	1.20	6.00	315.0
1	1.27	4.33	315.0
1	1.33	4.67	315.0
1	1.40	5.00	315.0
1	1.30	5.50	315.0
1	1.40	6.00	315.0
1	1.40	7.00	315.0
1	1.60	5.00	315.0
1	1.60	6.00	315.0
1	1.80	5.00	315.0
1	1.80	6.00	315.0
1	2.00	5.00	315.0
1	2.20	5.00	315.0
1	2.20	6.00	315.0
1	2.40	5.00	315.0
1	2.60	5.00	315.0
1	2.80	5.00	315.0

### Generation of time series and correction of 'impossible' directions

When random drawings are taken from this scatter diagram (see Table E-2), a wave time series is generated, which represents the average wave climate. This is done for every month of the year, every three hours. In this way a time series is generated, representative for the average wave climate, but without the persistency of wave conditions as occurring in reality. The  $H_s$  is replaced by  $H_{rms}$  by dividing with  $\sqrt{2}$ .  $T_z$  is replaced by  $T_p$  by multiplying with 1.3 [d'Angremond and Van Roode, 2001]. The direction is transformed from the normal coordinate system ( $y$ -axis perpendicular to the shoreline, positive seawards, see Appendix A.2) to the coordinate system of Unibest-TC ( $x$ -axis perpendicular to the shoreline, positive landwards, see Appendix C.2). Part of the resulting time series is presented in Table E-3.

Table E-3

Part of the time series of  $H_{rms}$ ,  $T_p$  and  $\theta$ , generated with random drawings from the average wave climate scatter table as in Table E-2.

time [days]	Hrms [m]	wave angle [deg]	Tp [s]
0.000	0.001	110.00	5.85
0.125	0.849	-25.00	7.80
0.250	0.940	87.50	6.03
0.375	1.980	42.50	9.10
0.500	0.601	65.00	5.53
0.625	1.556	-2.50	7.80
0.750	0.001	110.00	6.21
0.875	2.546	42.50	6.50
1.000	1.930	42.50	6.07
1.125	0.658	-2.50	6.07
1.250	1.237	65.00	6.18
1.375	0.849	20.00	5.20
1.500	1.273	-2.50	7.80
1.625	0.856	-2.50	6.59
1.750	1.344	65.00	5.85
1.875	0.516	-2.50	7.37
2.000	0.792	20.00	7.25
2.125	1.464	42.50	5.63
2.250	0.926	87.50	5.92
2.375	0.424	20.00	9.10
2.500	0.001	110.00	9.10
2.625	0.615	20.00	6.93
2.750	0.976	42.50	6.36
2.875	0.969	-25.00	6.32
3.000	0.849	20.00	9.10

Since the area of the satellite observations is large (400 x 400 km), also waves travelling eastward are observed (although rarely). In reality, these waves cannot occur close to shore, since they would be originating from the beach. Therefore, such a wave condition should be defined as a calm period. This has been done by setting  $H_{rms}$  to 0.001 m when the wave angle is larger than  $90^\circ$  or smaller than  $-90^\circ$ :

If  $\theta > 90^\circ$  or  $\theta < -90^\circ$  then  $H_{rms} = 0.001$  m

The result of this rule can be seen in Table E-3, where the  $H_{rms}$  has been changed to 0.001 m for an impossible wave angle of  $110^\circ$ .

The resulting time series of wave conditions has been used as input at the offshore boundary of the Unibest-TC model at 30 m depth. This is sufficiently deep to use the offshore wave climate without transformation of the direction and wave height to shallow water conditions.

### E.3.4 Scaled wave conditions based on satellite data

For the calibration and verification of the Unibest-TC model (see Chapter 8), the wave conditions between February 2000 and March 2001 should be known as exactly as possible. As discussed in Paragraph 3.2.5, no correct measurements of buoys are available. It was therefore decided to scale the average wave climate of Paragraph E.3.3 with the use of satellite measurements of  $H_s$  in the mentioned period.

#### Satellite measurements of the significant wave height $H_s$

It is possible to obtain satellite measurements of  $H_s$  (unfortunately not of  $T_p$  and  $\theta$ ) on specified dates and areas from [www.waveclimate.com](http://www.waveclimate.com). Every time a satellite passes an area it takes a number of samples of the wave height. These samples give a distribution of the wave height with upper and lower limits and a median. These parameters are indicated in a graph as in Figure E-3. The measurements of  $H_s$  available in a  $200 \times 200$  km area near the project area (see Figure E-3) have been gathered. The size of the area has been chosen smaller as in Paragraph E.3.3 to improve the similarity between the measured wave height and the wave height close to the project area.

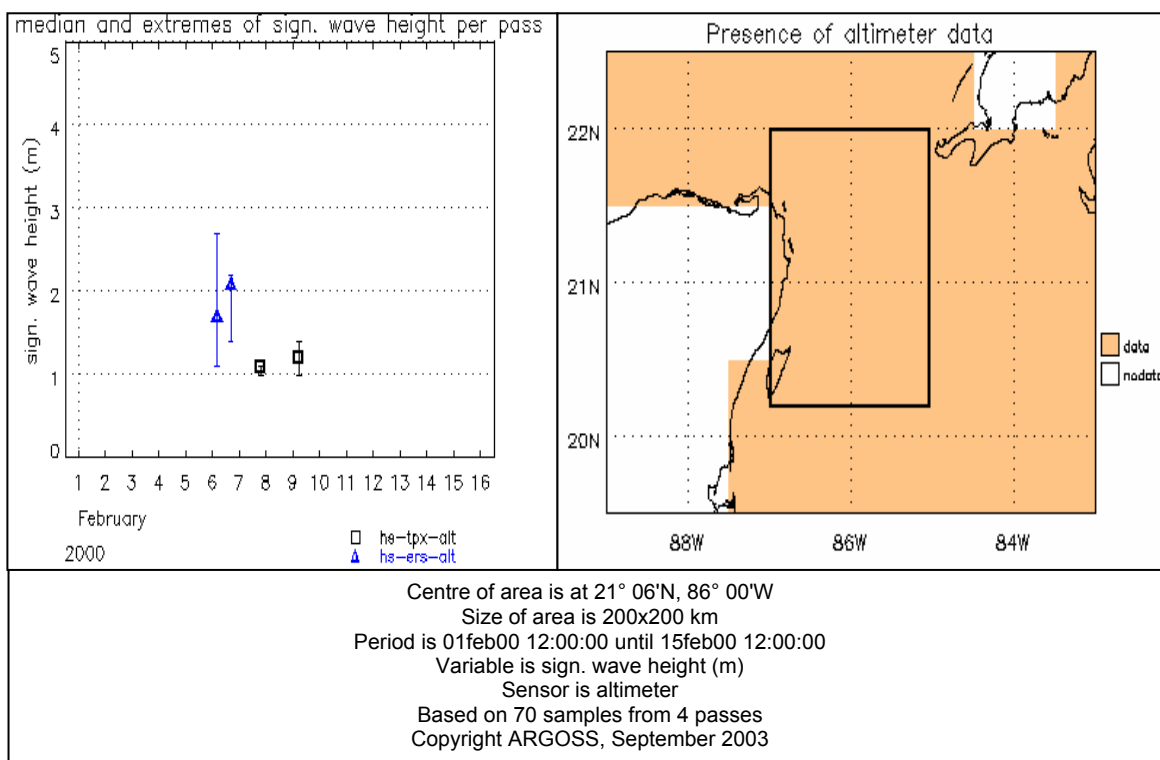


Figure E-3: Satellite measurements of  $H_s$  in the area in the right panel. The measurements have a time resolution of about 2.5 days [[www.waveclimate.com](http://www.waveclimate.com)].

#### Scaling factor for the significant wave height $H_s$

The satellite measurements of  $H_s$  in the area indicated in Figure E-3 for the period between February 2000 and March 2001 have been averaged for each month in the mentioned period. The monthly averaged values of the measured significant wave height  $\overline{H}_{s,measured}$  are compared with the monthly averaged  $H_s$  of the wave climate  $\overline{H}_{s,climate}$  described in E.3.3 (see Table E-4). This leads to a scaling factor according to:

$$F_H(j) = \frac{\bar{H}_{s,measured}(j)}{\bar{H}_{s,c}(j)} \quad (E-1)$$

Where:  $F_H$  scaling factor for wave height [-]  
 $j$  month number [-]  
 $\bar{H}_{s,measured}(j)$  average of the measured wave height by satellites for month j [m]  
 $\bar{H}_{s,c}$  average wave height based on the wave climate for month j [m]

Table E-4:

Monthly averages of satellite measurements of  $H_s$  and monthly averaged  $H_s$  from the wave climate described in E.3.3 [www.waveclimate.com].

Month	number of passes	$\bar{H}_{s,measured}$ [m]	$\bar{H}_{s,c}$ [m]	scaling factor $F_H$ [-]
February-00	12	1.38	1.54	0.89
March-00	12	1.23	1.59	0.78
April-00	10	0.97	1.31	0.74
May-00	13	1.18	1.16	1.01
June-00	13	1.12	1.18	0.95
July-00	11	0.66	1.19	0.56
August-00	11	1.07	1.05	1.02
September-00	13	0.93	1.22	0.76
October-00	11	1.77	1.40	1.26
November-00	10	1.24	1.51	0.82
December-00	13	1.75	1.72	1.01
January-01	11	1.44	1.54	0.93
February-01	10	1.49	1.54	0.97
March-01	11	1.65	1.59	1.04

**Scaling factor for the peak period  $T_p$**

The next step is to define a scaling factor for the peak period  $T_p$ . No measurements of  $T_p$  are available between February 2000 and March 2001. It is therefore decided to calculate the  $T_p$  based on a relation between  $H_s$  and  $T_p$ . Such a relation has been established based on the wave climate described in Paragraph E.3.3. A two-dimensional scatter diagram of  $T_z$  and  $H_s$  is created (see Table E-5).

Table E-5: Scatter diagram of  $H_s$  versus  $T_z$  [www.waveclimate.com]. It can be seen that the average spectrum is slightly double-peaked, due to the presence of some swell with low wave heights and long periods.

Percentage of occurrence of sign. wave height [m] in rows versus mean wave period [s] in columns									
$H_s$ [m]	$T_z$ [s]								total
	0 - 4	4 - 5	5 - 6	6 - 7	7 - 8	8 - 9	9 - 10	> 10	
0.0 – 0.6	0	0	0	0	0	0	0	0	0.0
0.6 – 0.8	0	3.3	4.7	3.3	0.7	0.7	0	0	12.7
0.8 – 1.0	0	5.3	7.3	11.3	4.0	0.7	0.7	0	29.3
1.0 – 1.2	0	1.3	9.3	5.3	0.7	0	0	0	16.6
1.2 – 1.4	0	4.0	6.0	2.7	0	0	0	0	12.7
1.4 – 1.6	0	0	4.0	3.3	0	0	0	0	7.3
1.6 – 1.8	0	0	3.3	2.7	0	0	0	0	6.0
1.8 – 2.0	0	0	0.7	2.7	2.0	0	0	0	5.4
2.0 – 2.2	0	0	0	1.3	0	0	0	0	1.3
2.2 – 2.4	0	0	0	1.3	0	0	0	0	1.3
2.4 – 2.6	0	0	0	2.0	0	0	0	0	2.0
2.8 – 3.0	0	0	0	0.7	0	0	0	0	0.7
3.0 – 3.2	0	0	0	0	0	0	0	0	0.0
3.2 – 3.4	0	0	0	0	3.3	0	0	0	3.3
3.4 – 3.6	0	0	0	0	0	0	0	0	0.0
> 3.6	0	0	0	0	1.3	0	0	0	1.3
<b>total</b>	<b>0.0</b>	<b>13.9</b>	<b>35.3</b>	<b>36.6</b>	<b>12.0</b>	<b>1.4</b>	<b>0.70</b>	<b>0.0</b>	<b>0.0</b>



This scatter diagram has been plotted in Figure E-4, using  $T_p = 1.3T_z$  [d'Angremond and Van Roode, 2001] and  $H_{rms} = H_s / \sqrt{2}$ .

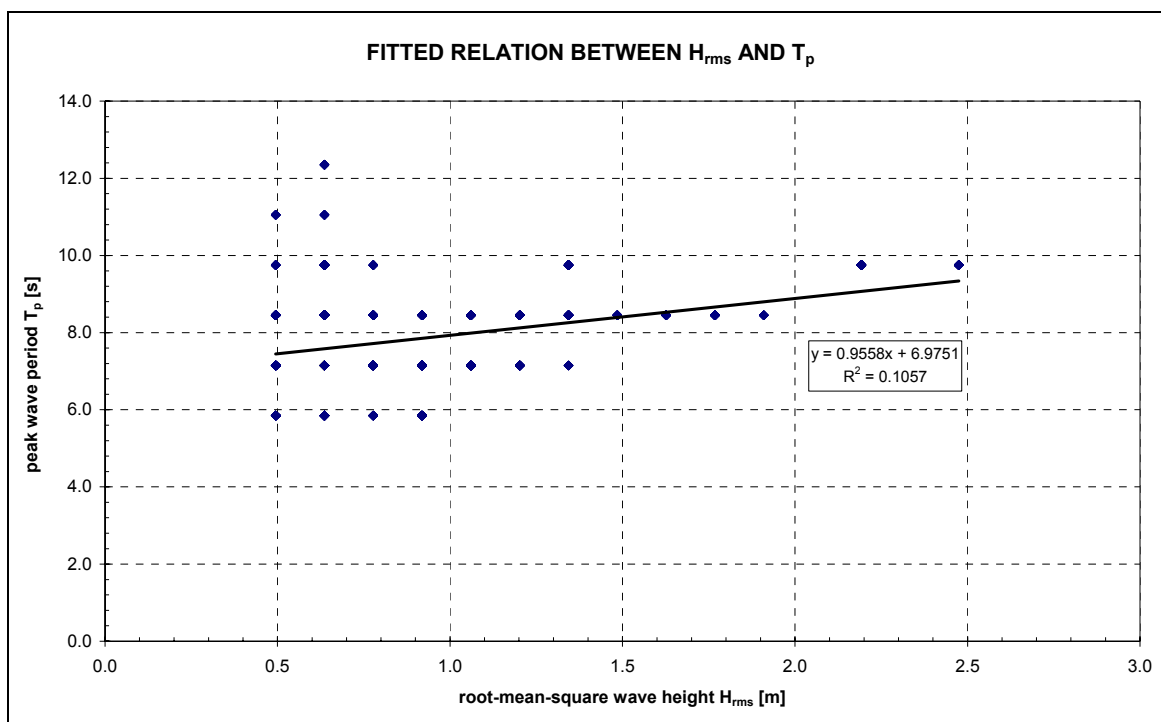


Figure E-4: Root-mean-square wave height ( $H_{rms}$ ) versus peak wave period ( $T_p$ ) with a least-square fit. Each point in the figure represents a number of samples, based on the percentage of occurrence indicated in Table E-5.

Figure E-4 leads to:

$$T_p = 0.9558H_{rms} + 6.975 \quad (\text{E-2})$$

The scaling factor ( $F_{T_p}$ ) for  $T_p$  varies for each drawing out of the average wave climate and is calculated with the following formula:

$$F_{T_p}(t_i) = \frac{a \cdot H_{rms}(t_i) + b}{a \cdot H_{rms}(t_i) \cdot F_H + b} \quad (\text{E-3})$$

Where:

$F_{T_p}$	scaling factor for peak period	[-]
$t_i$	time point in time series	[-]
$H_{rms}$	root-mean-square wave height	[m]
a,b	coefficients from Equation (E-2)	

### Scaled wave time series

The  $H_s$  and  $T_p$  in the time series of Paragraph E.3.3 are multiplied with their corresponding scaling factors, leading to a scaled wave time series. The wave direction isn't changed.

### Comments

The statistical foundations of this method are rather weak, because of the following reasons:

- The number of measurements of  $H_s$  is low.
- The relation between  $H_{rms}$  and  $T_p$  is based on little samples.
- It isn't correct to take the scaling constant for the entire month.

## E.4 Wind, current and water level input

### Wind input

Almost no wind data is available. The input consists of monthly averages based on satellite measurements and indicated below [www.waveclimate.com]. The wind direction is predominantly from the east to south east (see Appendix B.5). The relation between the wave conditions and the wind speeds is not known. The wind direction has been set to 0° (perpendicular to the shoreline), since this is the average wind direction.

Month	Jan	Feb	Mar	Apr	May	Jun	Jul	Aug	Sep	Oct	Nov	Dec
Average wind speed [m/s]	8.5	7.2	7.4	6.6	6.1	6.5	5.3	5.2	5.4	7.5	7.9	7.8

### Longshore current input

The longshore current in northern direction of about 1 m/s in deep water has to be incorporated in the model. However, the current velocities closer to shore remain uncertain. A reasonable estimate is 0.5 m/s on 30 m depth. This value is held constant during the calculations.

### Water level input

The water level during normal conditions is set to MSL 0 m, since the tide is negligible.

## E.5 Bottom profiles

### E.5.1 Individual bottom profiles

Along the entire project area cross-shore profiles have been measured in February and June 2000 and in March 2001. This has been done every 200 m in longshore direction. A few of these profiles have been used for calculations in Unibest-TC. The profiles have been transformed from the coordinate system used by the surveyors ( $x$ -axis pointing seaward, origin at the shoreline at MSL) to the coordinate system used by Unibest-TC ( $x$ -axis pointing landward, origin at the seawall). This results in profiles as in Figure B-1 in Appendix B.

These profiles have been extended to -30 m depth contour (at  $x = -5850$  m) with the use of nautical charts, to be able to impose the boundary conditions at approximately deep water.

### E.5.2 Averaged bottom profiles

Averaged profiles have been used in the calibration phase of the modelling with Unibest-TC to omit 'noise' like longshore effects and measurement errors (see Chapter 8.3.2). Averaging has been carried out around the shoreline (at MSL) between chainage 6+100 and 6+900.

First the average beach width (distance between the sea wall and the shoreline) has been determined. Profiles with a larger beach width are 'cut-off' at the average beach width; profiles with a smaller beach width than average are extended linearly up to the average beach width. In Figure E-5 the individual and averaged profiles for June 2000 are plotted.



Figure E-5: Individual profiles and averaged profile at June 2000 for chainage 6+100 to 6+900.

### E.5.3 Input files bottom profiles

Below an example is given of an input file of a bottom profile (.bot – file) for chainage 6+300, measured in February 2000.

```

1
524027      2332147      290
Site: Cancún, Mexico, 6300_feb2000
x           z
-5850.00   -30.00
-2275.00   -20.00
-739.99    -16.42
-732.70    -16.42
-722.10    -16.29
-711.57    -16.21
-709.35    -16.19
-700.97    -16.12
-690.37    -15.98
-679.84    -15.87
-678.63    -15.86
-669.24    -15.77
-658.71    -15.58
-648.11    -15.44
-647.99    -15.44
-637.58    -15.24
-626.98    -15.12
-617.34    -14.92
-616.39    -14.90
-605.86    -14.72
-595.26    -14.55
-586.69    -14.43
-584.73    -14.41
-574.13    -14.28
-563.59    -14.07
-555.98    -13.97
-553.00    -13.93
-542.40    -13.68
-531.87    -13.56
-525.33    -13.42
-521.27    -13.34
-510.74    -13.17
-500.14    -12.95
-494.69    -12.86
-489.61    -12.78
-479.02    -12.52
-468.42    -12.35
-464.04    -12.25
-457.89    -12.12
-447.29    -11.97
-436.75    -11.68
-433.33    -11.64
-426.16    -11.54
    
```

-415.56	-11.29
-405.03	-11.09
-402.68	-11.02
-394.43	-10.76
-383.90	-10.53
-373.30	-10.27
-372.04	-10.23
-362.77	-9.96
-352.17	-9.70
-341.58	-9.44
-341.39	-9.43
-331.05	-9.17
-320.45	-8.94
-310.68	-8.72
-309.91	-8.70
-299.32	-8.37
-288.78	-8.09
-280.03	-7.85
-278.19	-7.81
-267.59	-7.53
-257.12	-7.26
-249.44	-7.03
-246.53	-6.93
-235.99	-6.70
-225.40	-6.31
-218.80	-6.10
-214.87	-5.99
-204.27	-5.63
-193.67	-5.23
-188.09	-5.01
-183.14	-4.80
-172.54	-4.31
-162.01	-3.93
-157.44	-3.75
-151.41	-3.50
-140.88	-3.10
-130.28	-2.82
-126.79	-2.70
-119.68	-2.48
-109.15	-2.27
-98.56	-2.06
-96.15	-2.04
-88.02	-1.96
-77.43	-1.82
-66.90	-1.85
-65.44	-1.85
-56.30	-1.75
-45.70	-1.43
-35.17	-1.44
-34.79	-1.40
-32.22	-0.30
-24.57	0.00
-7.63	2.77
0.00	2.50

## E.6 Input files boundary conditions

### E.6.1 Input file: normal conditions, average waves

Below the boundary condition definition file (.ubc) defined in Paragraph E.3 and E.4 is given. For convenience only the first 10 days are printed.

6							
0							
time [days]	water level [m]	Hrms [m]	wave angle [deg]	Tp [s]	wind speed [m/s]	wind dir [deg]	
0.000	0.000	0.509	20.000	7.280	8.500	0.000	
0.125	0.000	1.768	65.000	5.850	8.500	0.000	
0.250	0.000	0.905	87.500	6.994	8.500	0.000	
0.375	0.000	1.032	20.000	6.877	8.500	0.000	
0.500	0.000	0.537	-2.500	6.240	8.500	0.000	
0.625	0.000	0.813	87.500	7.475	8.500	0.000	
0.750	0.000	0.891	42.500	6.903	8.500	0.000	
0.875	0.000	1.414	-25.000	7.800	8.500	0.000	
1.000	0.000	0.926	65.000	5.902	8.500	0.000	
1.125	0.000	0.778	65.000	8.450	8.500	0.000	
1.250	0.000	0.884	-2.500	8.125	8.500	0.000	
1.375	0.000	0.658	20.000	6.071	8.500	0.000	

**Beach Nourishment: an evaluation of equilibration design methods**

1.500	0.000	0.001	110.000	6.071	8.500	0.000
1.625	0.000	0.354	-2.500	7.150	8.500	0.000
1.750	0.000	0.926	20.000	8.541	8.500	0.000
1.875	0.000	1.131	87.500	6.500	8.500	0.000
2.000	0.000	1.605	-2.500	6.929	8.500	0.000
2.125	0.000	0.863	65.000	6.643	8.500	0.000
2.250	0.000	0.001	155.000	6.500	8.500	0.000
2.375	0.000	1.209	20.000	7.241	8.500	0.000
2.500	0.000	1.414	65.000	7.800	8.500	0.000
2.625	0.000	0.001	110.000	7.150	8.500	0.000
2.750	0.000	0.001	155.000	6.500	8.500	0.000
2.875	0.000	0.891	-2.500	5.590	8.500	0.000
3.000	0.000	1.131	42.500	6.500	8.500	0.000
3.125	0.000	0.834	20.000	6.344	8.500	0.000
3.250	0.000	1.259	20.000	6.370	8.500	0.000
3.375	0.000	0.001	132.500	5.850	8.500	0.000
3.500	0.000	1.273	65.000	6.500	8.500	0.000
3.625	0.000	0.757	-2.500	5.668	8.500	0.000
3.750	0.000	0.001	110.000	6.500	8.500	0.000
3.875	0.000	0.735	42.500	5.460	8.500	0.000
4.000	0.000	0.905	-2.500	5.720	8.500	0.000
4.125	0.000	0.495	87.500	7.150	8.500	0.000
4.250	0.000	1.803	20.000	7.475	8.500	0.000
4.375	0.000	0.001	155.000	6.500	8.500	0.000
4.500	0.000	0.955	65.000	6.201	8.500	0.000
4.625	0.000	0.976	20.000	6.370	8.500	0.000
4.750	0.000	1.520	42.500	7.475	8.500	0.000
4.875	0.000	1.273	20.000	9.100	8.500	0.000
5.000	0.000	0.707	20.000	9.100	8.500	0.000
5.125	0.000	1.032	20.000	6.877	8.500	0.000
5.250	0.000	0.001	132.500	7.150	8.500	0.000
5.375	0.000	1.697	42.500	7.800	8.500	0.000
5.500	0.000	1.485	87.500	5.850	8.500	0.000
5.625	0.000	1.414	42.500	6.500	8.500	0.000
5.750	0.000	0.990	42.500	6.500	8.500	0.000
5.875	0.000	1.435	-2.500	5.421	8.500	0.000
6.000	0.000	1.450	65.000	5.525	8.500	0.000
6.125	0.000	0.813	-25.000	6.175	8.500	0.000
6.250	0.000	0.672	65.000	6.175	8.500	0.000
6.375	0.000	0.905	20.000	6.994	8.500	0.000
6.500	0.000	0.940	87.500	7.319	8.500	0.000
6.625	0.000	0.001	177.500	6.500	8.500	0.000
6.750	0.000	0.481	20.000	7.020	8.500	0.000
6.875	0.000	0.990	-47.500	6.500	8.500	0.000
7.000	0.000	0.898	-2.500	5.655	8.500	0.000
7.125	0.000	0.955	42.500	8.775	8.500	0.000
7.250	0.000	1.485	-2.500	7.150	8.500	0.000
7.375	0.000	0.940	-2.500	7.332	8.500	0.000
7.500	0.000	1.202	20.000	8.450	8.500	0.000
7.625	0.000	0.976	42.500	6.357	8.500	0.000
7.750	0.000	1.485	42.500	5.850	8.500	0.000
7.875	0.000	1.980	42.500	7.800	8.500	0.000
8.000	0.000	0.849	20.000	7.800	8.500	0.000
8.125	0.000	0.467	20.000	5.577	8.500	0.000
8.250	0.000	0.750	65.000	5.577	8.500	0.000
8.375	0.000	1.626	20.000	7.150	8.500	0.000
8.500	0.000	1.626	20.000	5.850	8.500	0.000
8.625	0.000	0.863	20.000	5.330	8.500	0.000
8.750	0.000	1.697	87.500	6.500	8.500	0.000
8.875	0.000	0.001	155.000	6.500	8.500	0.000
9.000	0.000	0.516	-2.500	7.371	8.500	0.000
9.125	0.000	1.605	-2.500	6.929	8.500	0.000
9.250	0.000	0.969	42.500	7.605	8.500	0.000
9.375	0.000	0.001	110.000	6.500	8.500	0.000
9.500	0.000	0.976	-2.500	6.370	8.500	0.000
9.625	0.000	0.764	20.000	7.046	8.500	0.000

## E Boundary conditions in Unibest-TC

9.750	0.000	0.424	-2.500	6.500	8.500	0.000
9.875	0.000	0.870	-2.500	6.682	8.500	0.000
10.000	0.000	1.556	-2.500	9.100	8.500	0.000

### E.6.2 Input file: storm1

Below the boundary conditions definition file (.ubc) of the design storm used in Chapter 11 is given.

```
6
0
```

time [days]	water level [m]	Hrms [m]	wave angle [deg]	Tp [s]	wind speed [m/s]	wind dir [deg]
0.0000	0.000	1.000	0.000	6.700	8.000	0.000
0.0625	0.034	1.102	0.000	6.773	8.460	0.000
0.1250	0.134	1.402	0.000	6.988	9.809	0.000
0.1875	0.293	1.879	0.000	7.330	11.954	0.000
0.2500	0.500	2.500	0.000	7.775	14.750	0.000
0.3125	0.741	3.224	0.000	8.294	18.006	0.000
0.3750	1.000	4.000	0.000	8.850	21.500	0.000
0.4375	1.259	4.776	0.000	9.406	24.994	0.000
0.5000	1.500	5.500	0.000	9.925	28.250	0.000
0.5625	1.707	6.121	0.000	10.370	31.046	0.000
0.6250	1.866	6.598	0.000	10.712	33.191	0.000
0.6875	1.966	6.898	0.000	10.927	34.540	0.000
0.7500	2.000	7.000	0.000	11.000	35.000	0.000
0.8125	1.966	6.898	0.000	10.927	34.540	0.000
0.8750	1.866	6.598	0.000	10.712	33.191	0.000
0.9375	1.707	6.121	0.000	10.370	31.046	0.000
1.0000	1.500	5.500	0.000	9.925	28.250	0.000
1.0625	1.259	4.776	0.000	9.406	24.994	0.000
1.1250	1.000	4.000	0.000	8.850	21.500	0.000
1.1875	0.741	3.224	0.000	8.294	18.006	0.000
1.2500	0.500	2.500	0.000	7.775	14.750	0.000
1.3125	0.293	1.879	0.000	7.330	11.954	0.000
1.3750	0.134	1.402	0.000	6.988	9.809	0.000
1.4375	0.034	1.102	0.000	6.773	8.460	0.000
1.5000	0.000	1.000	0.000	6.700	8.000	0.000

# F RESULTS SENSITIVITY ANALYSIS

## F.1 Introduction

In this appendix the results of the sensitivity analysis discussed in Chapter 7 are described. Goal of this analysis is to determine the sensitivity of the Unibest-TC output functions (such as transports and bottom changes) for changes in the input parameter setting (e.g. roughness, wave breaking parameters, etc.) and the boundary conditions (e.g.  $H_{rms}$ ,  $T_p$ ). This sensitivity analysis is necessary for the calibration described in Chapter 8 and Appendix G, since the default parameter setting doesn't give satisfactory results. In Table F-1 the parameters and boundary conditions that have been varied are summarized. On the next pages the influence of variations in these parameters on the relevant output functions (such as transports and bottom changes) is visualized in graphs.

Table F-1: Description of input parameters and boundary conditions to be varied during the sensitivity analysis, including their reference values.

Parameter type	Input parameter	Symbol	Description	Reference value	Unit	Appendix	Par.
General	TDRY	$T^*$	Maximum relative wave period	20	-	F.2.1	7.3.1
	USTRA	$q_{tot,x}(X_{end})$	Transport at the onshore boundary	0	m <sup>3</sup> /hr	F.2.2	7.3.2
Wave	GAMMA	$\gamma$	Wave breaking parameter	0	-	F.2.3	7.3.3
	ALFAC	$\alpha$	Wave breaking parameter	1	-	F.2.4	7.3.3
	BETD	$\beta$	Slope of wave front	0.1	-	F.2.5	7.3.4
	FWEE	$f_w$	Friction factor for bottom friction	0.01	-	F.2.6	7.3.5
	F_LAM	$\lambda$	Number of wavelengths for depth integration	2	-	F.2.7	7.3.6
	POW	P	Power in weighing function	1	-	F.2.8	7.3.6
	C_R	$C_r$	Correlation coefficient bound long waves	0.25	-	F.2.9	7.3.7
Sediment	D50	$d_{50}$	$d_{50}$ grain diameter	0.00033	m	F.2.10	7.3.8
	D90	$d_{90}$	$d_{90}$ grain diameter	0.00040	m	-	7.3.8
	DSS	$D_s$	$d_{50}$ of suspended sediment	0.000264	m	F.2.11	7.3.8
Current	FCVISC	$\alpha_w$	Viscosity coefficient	0.1	-	F.2.12	7.3.9
	RKVAL	$k_s$	Friction factor for mean current	0.01	m	F.2.13	7.3.10
Transport	TANPHI1	$\tan\phi_1$	Tangent of angle of repose	0.15	-	F.2.14	7.3.11
	TANPHI2	$\tan\phi_2$	Tangent of angle of repose	0.5	-	F.2.15	7.3.11
	RW	$k_{s,w}$	Wave related roughness	0.002	m	F.2.16	7.3.12
	RC	$k_{s,c}$	Current related roughness	0.01	m	F.2.17	7.3.13
Boundary condition		Symbol	Description	Reference value	Unit	Appendix	Par.
H0		$h(t)$	Water level at offshore boundary	0	m	F.2.18	7.4.1
HRMS		$H_{rms}$	Root mean square wave height at offshore boundary	1.1	m	F.2.19	7.4.2
A_WAVE		$\theta$	Angle of wave incidence relative to shore normal at offshore boundary	10	°	F.2.20	7.4.3
T		$T_p$	Peak period of wave field	6	s	F.2.21	7.4.4
V_WIND		$V_w$	Wind speed	4	m/s	F.2.22	7.4.5
V_TIDE		$V(t)$	Shore parallel current	1	m/s	F.2.22	7.4.6
A_WIND		$\theta_w$	Wind direction	10	°	-	-

For the complete parameter setting during the sensitivity analysis reference is made to Appendix D.

## **F.2 Graphs**

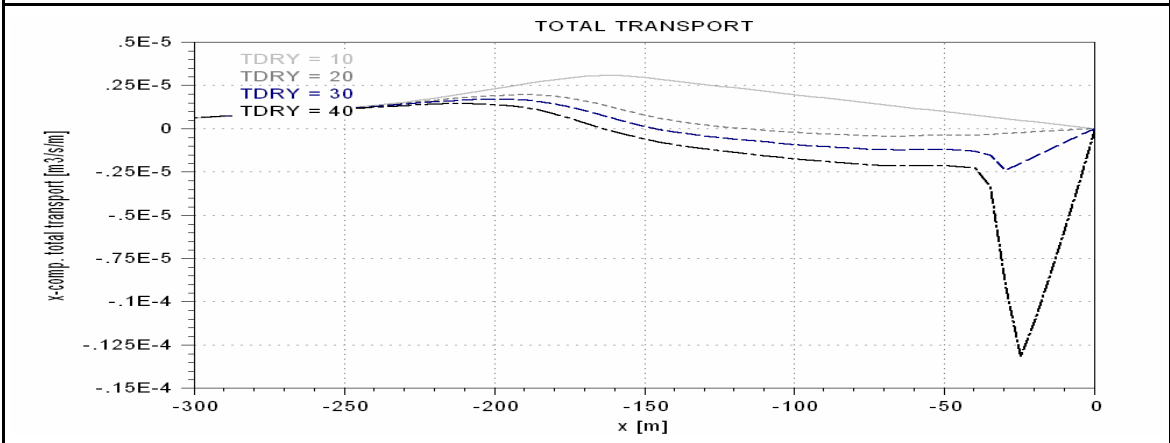
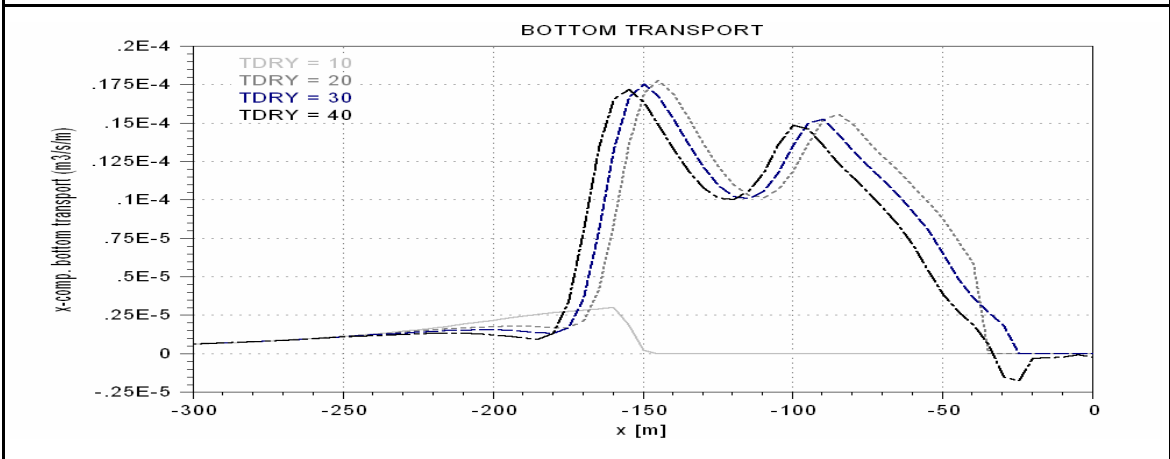
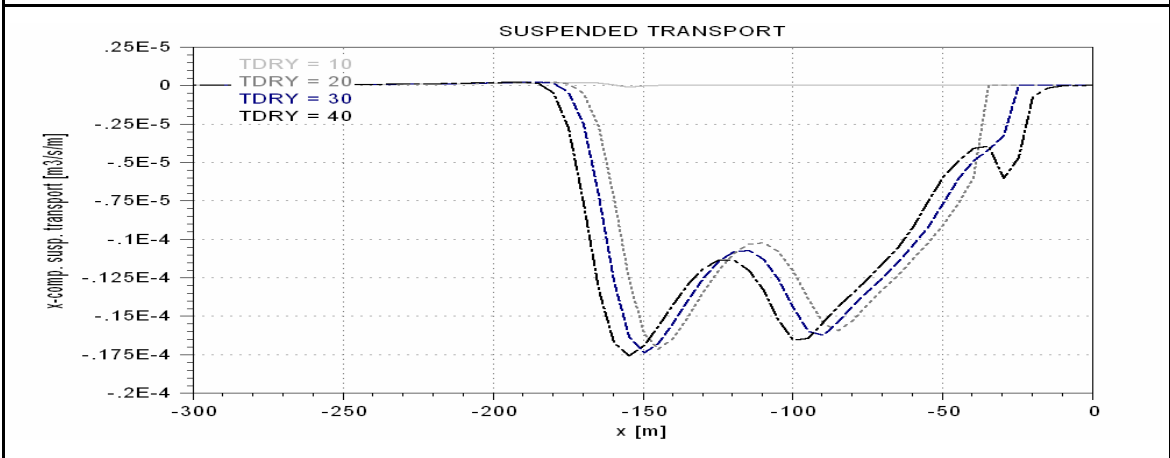
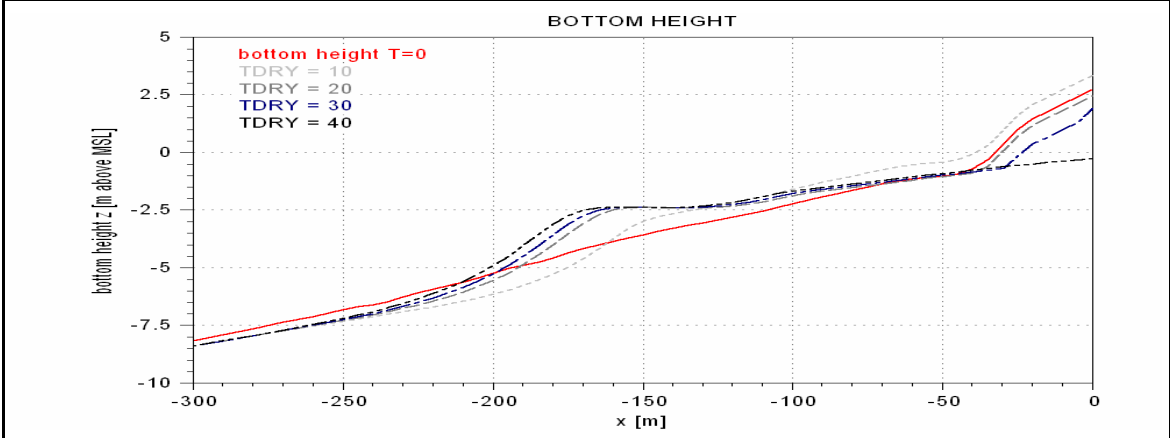
On the next pages the results of the sensitivity analysis are presented in graphical form. Reference is made to the corresponding paragraph in the main text and to the relevant Equations in Appendix C.



### F.2.1 Sensitivity to model parameter TDRY

Paragraph 7.3.1

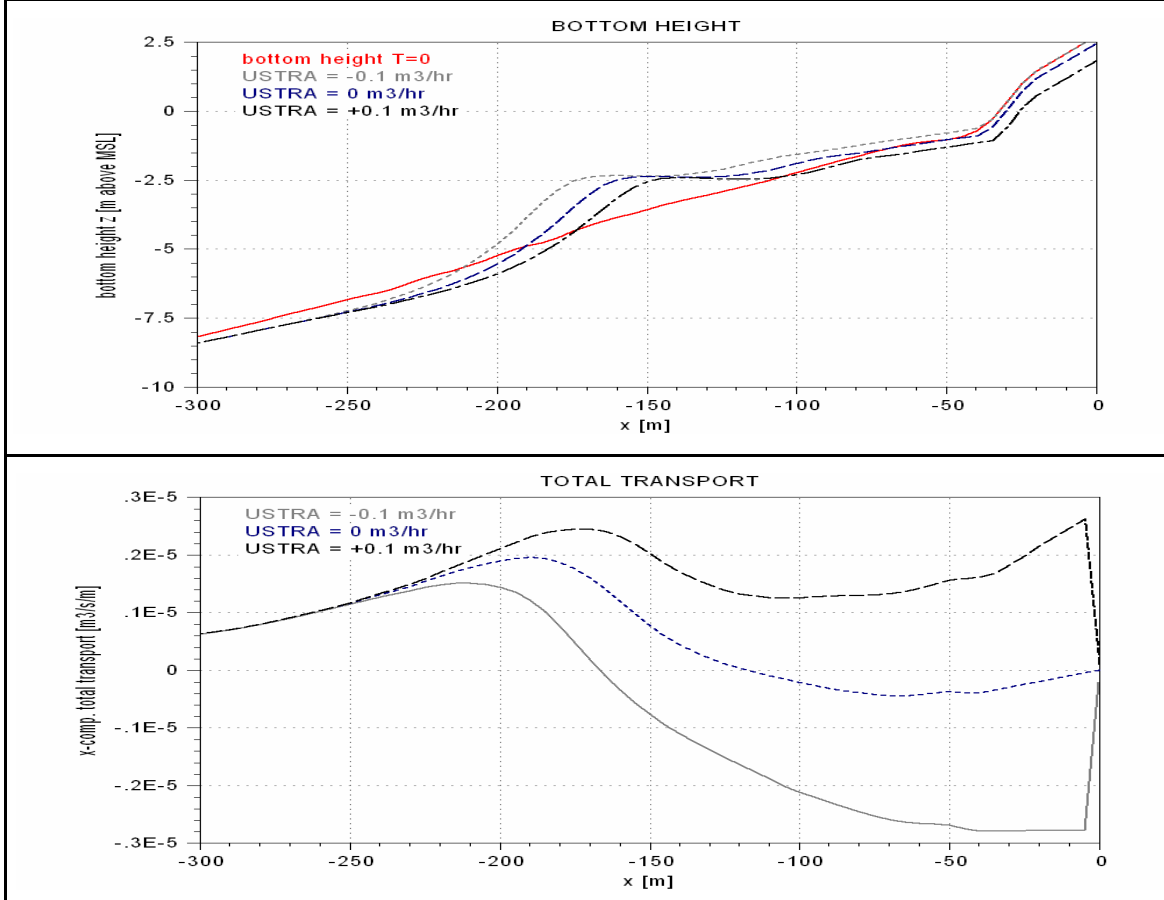
Equation (C-28), page C-9



### F.2.2 Sensitivity to model parameter USTRA

Paragraph 7.3.2

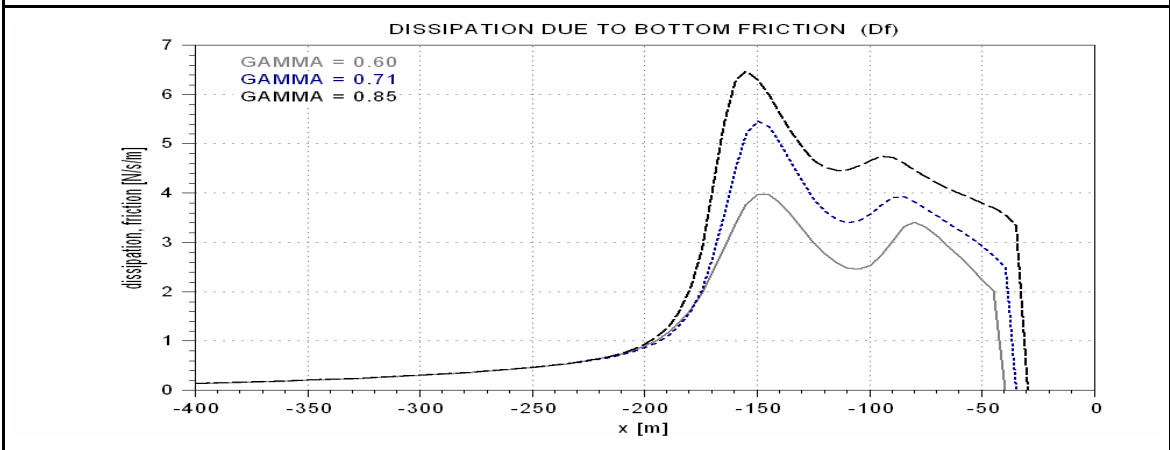
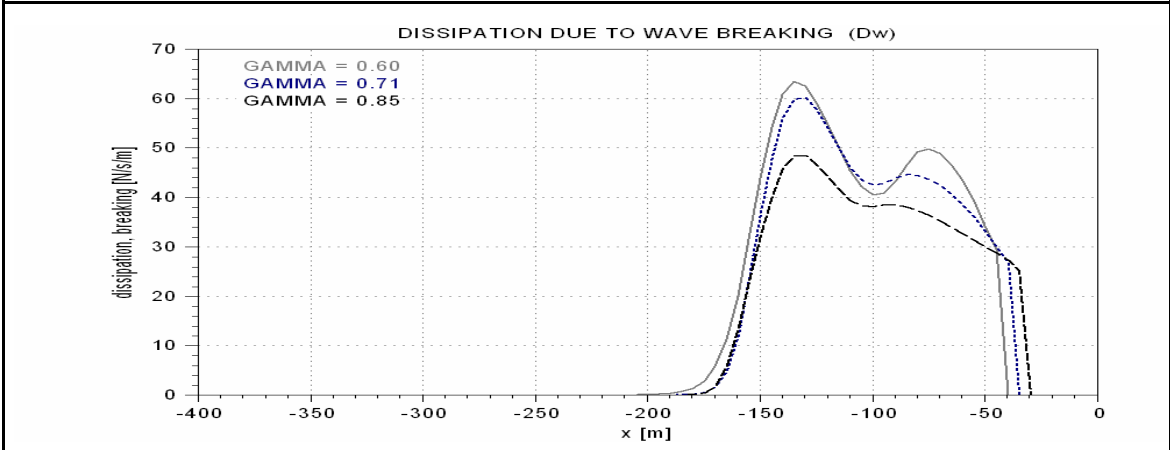
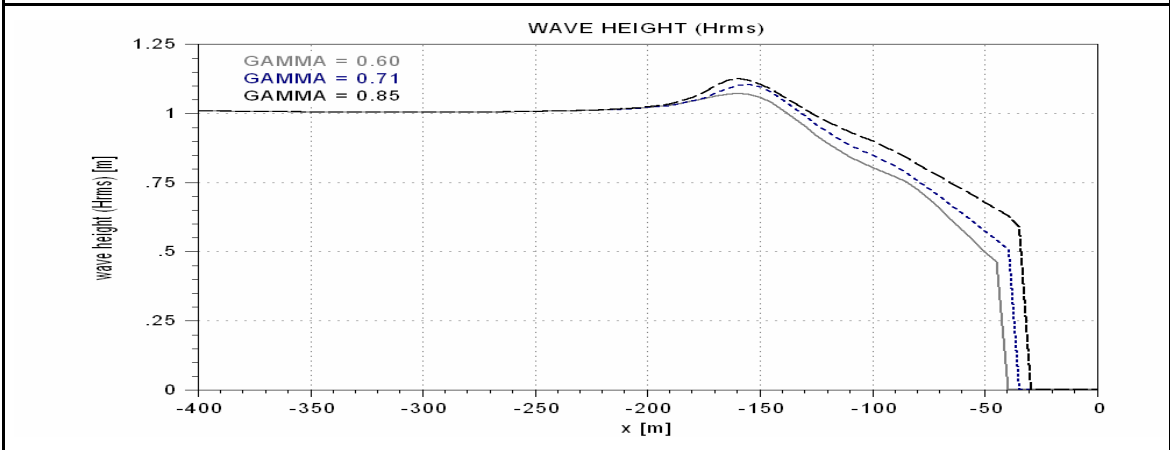
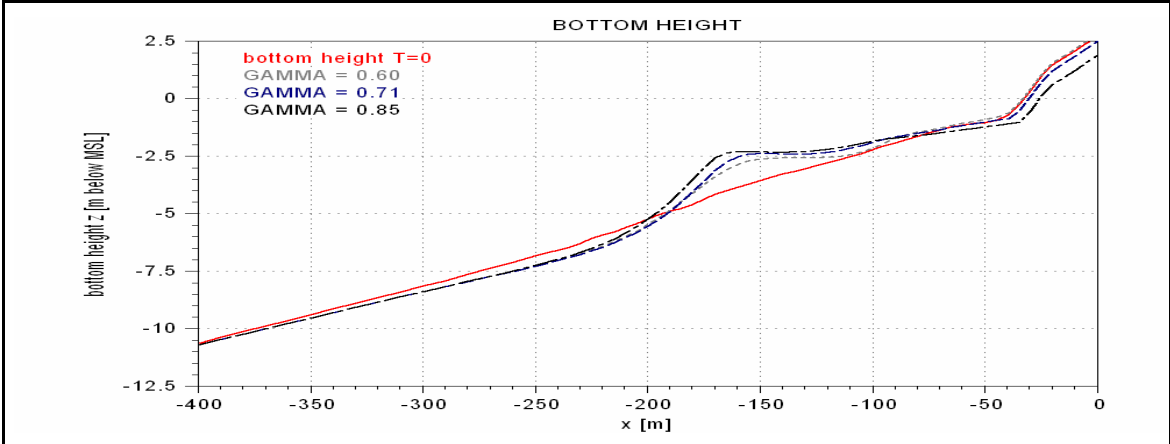
page C-8



### F.2.3 Sensitivity to model parameter GAMMA

Paragraph 7.3.3

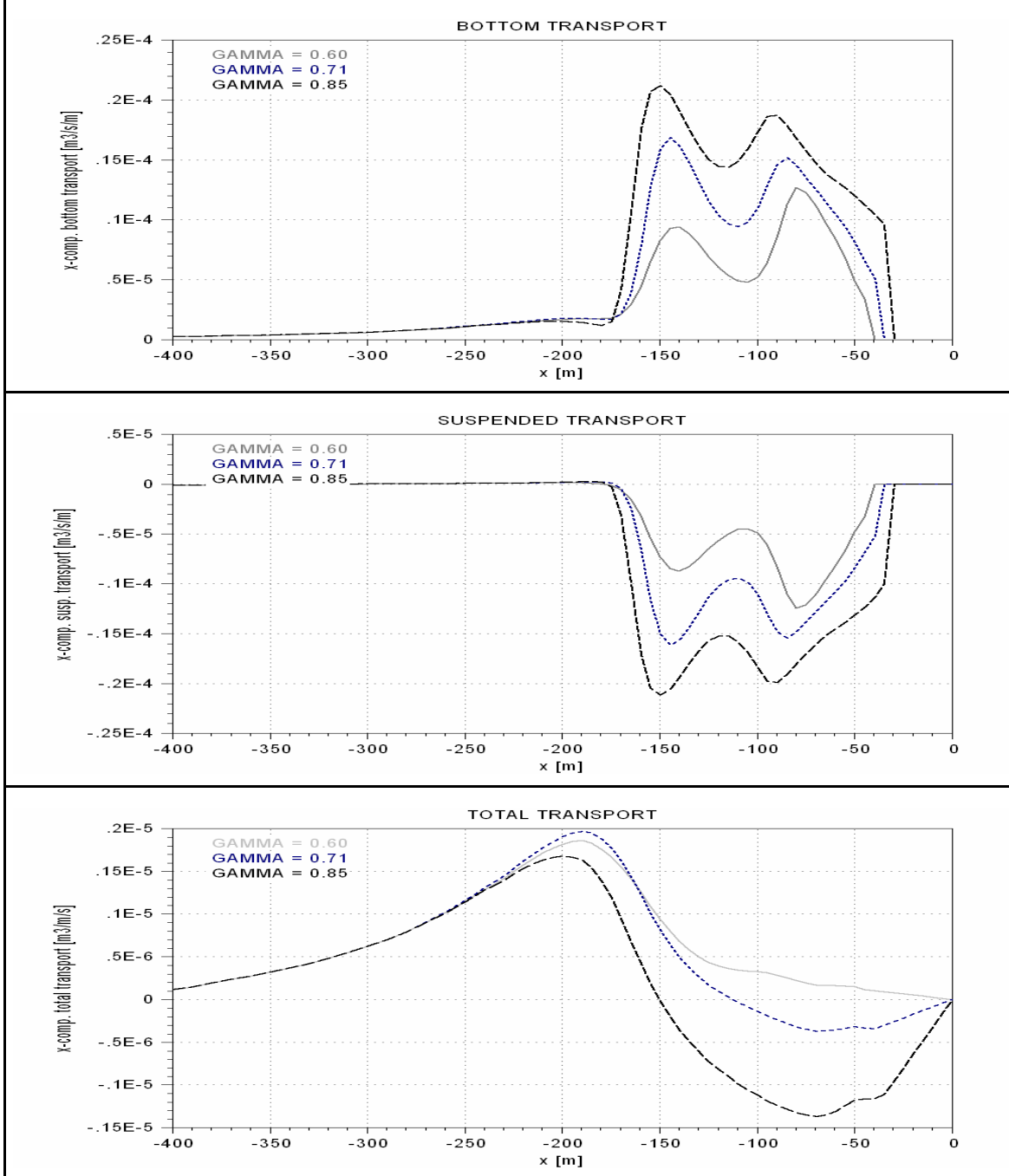
Equation (C-3), page C-3



### Sensitivity to model parameter GAMMA (2)

Paragraph 7.3.3

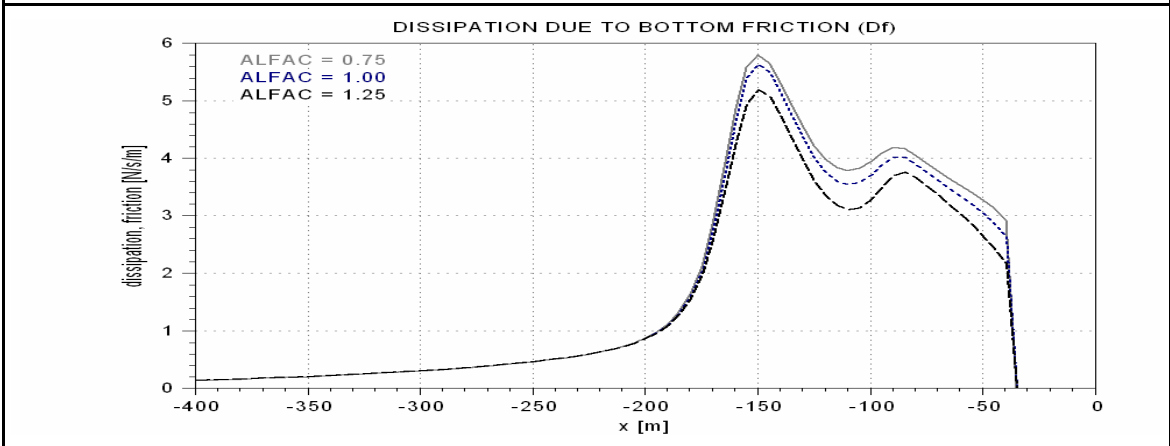
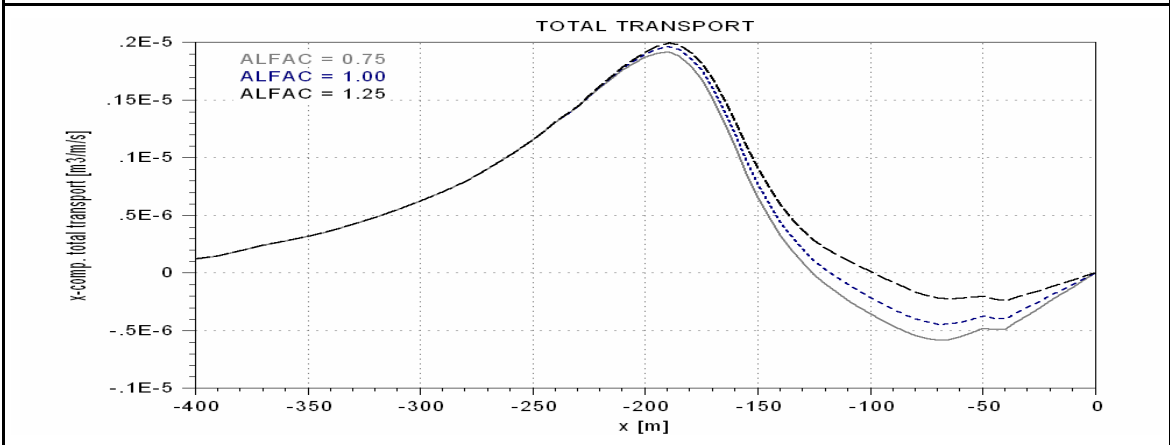
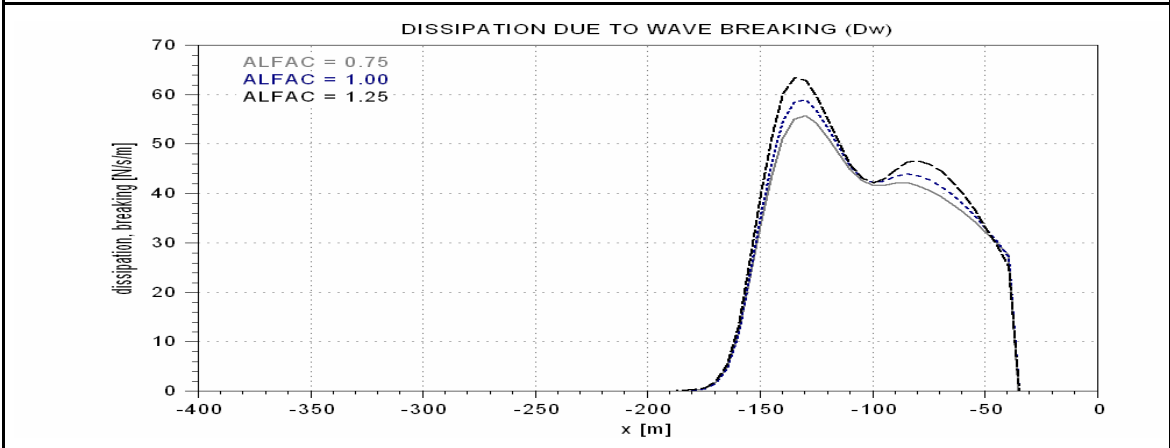
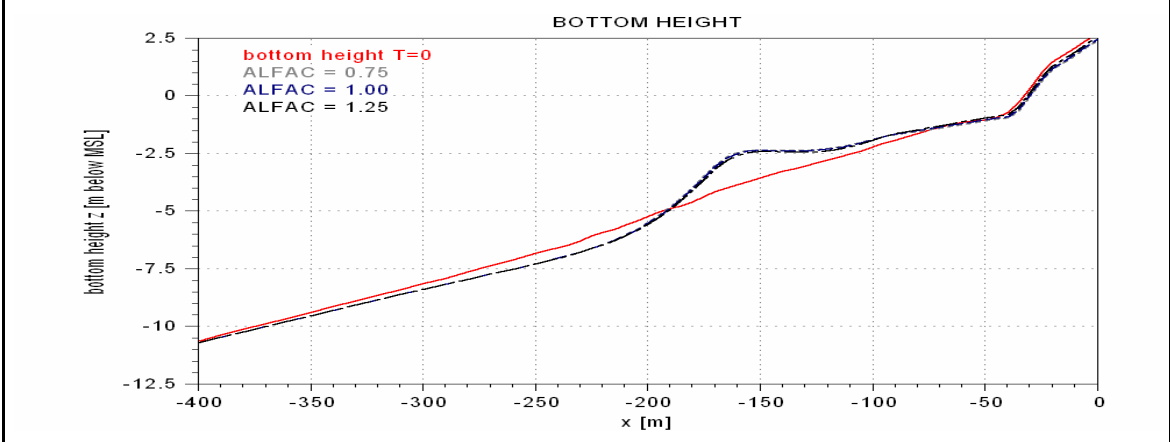
Equation (C-3), page C-3



### F.2.4 Sensitivity to model parameter ALFAC

Paragraph 7.3.3

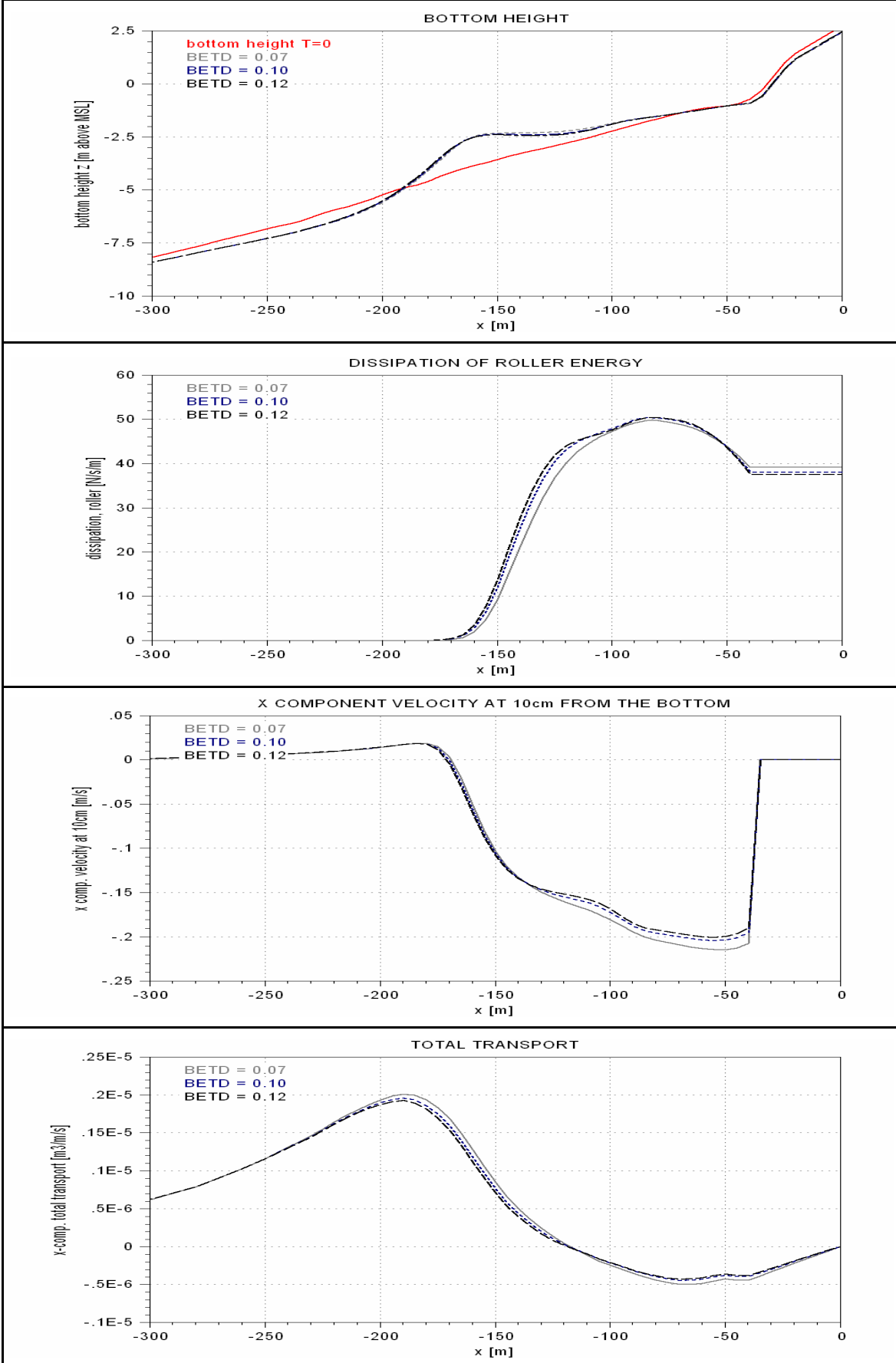
Equation (C-3), page C-3



### F.2.5 Sensitivity to model parameter BETD

Paragraph 7.3.4

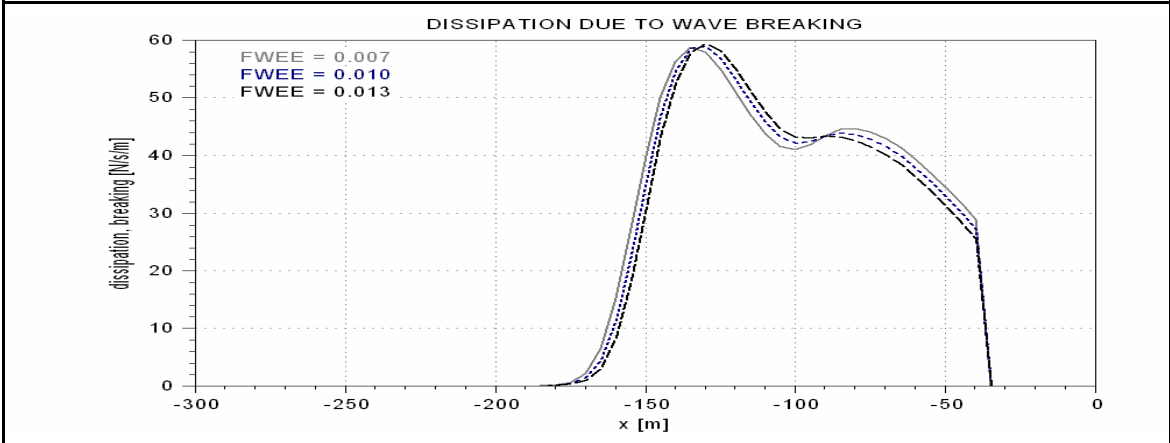
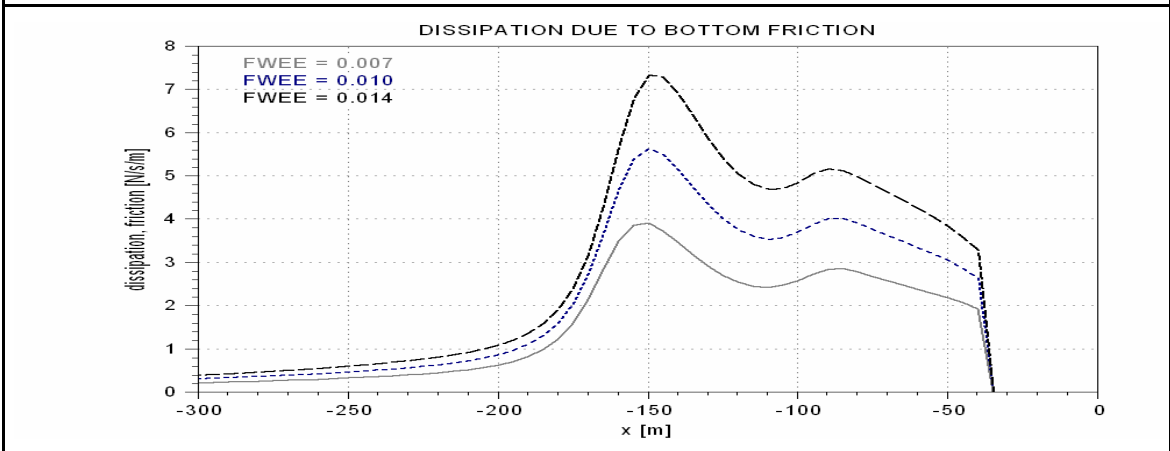
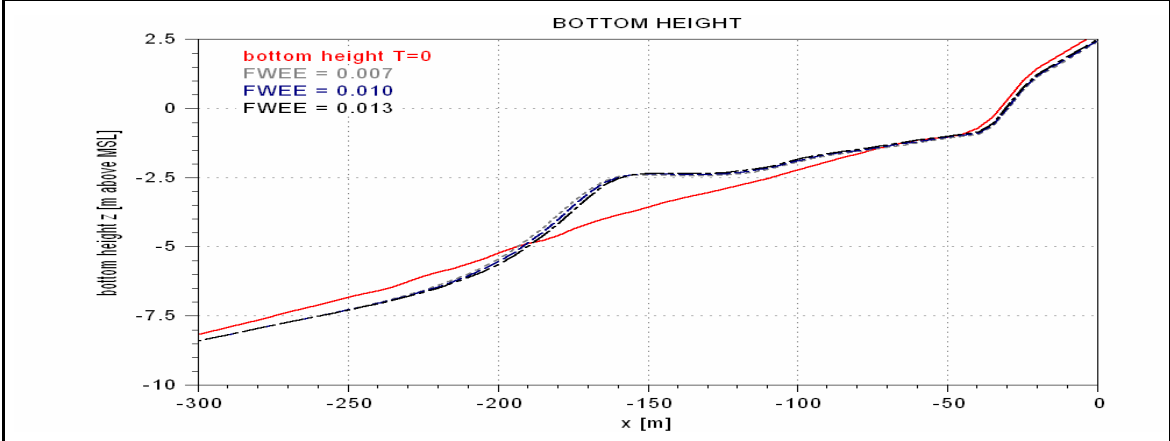
Equation (C-5), page C-3



### F.2.6 Sensitivity to model parameter FWEE

Paragraph 7.3.5

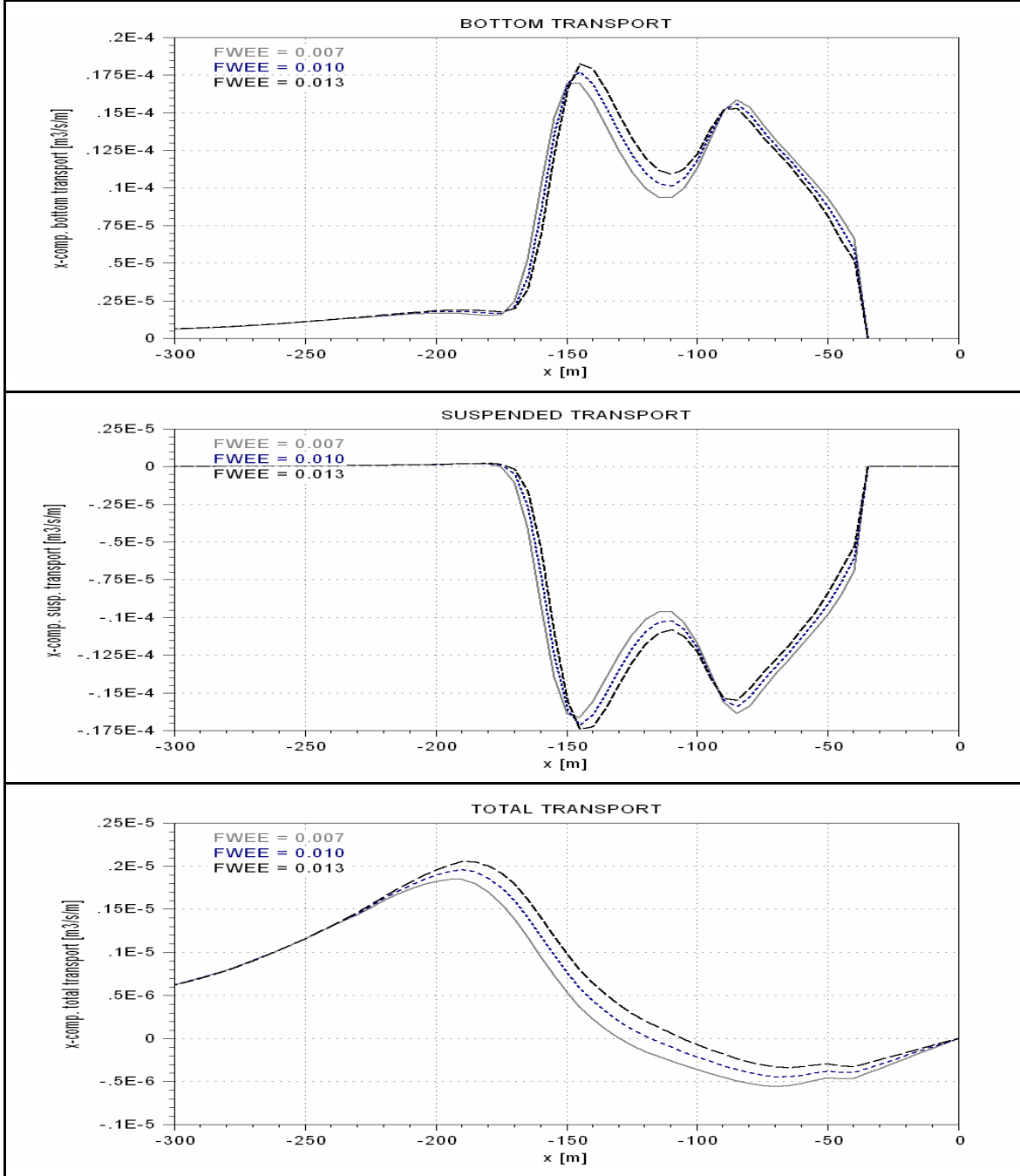
Equation (C-4), page C-3



**Sensitivity to model parameter FWEE (2)**

Paragraph 7.3.5

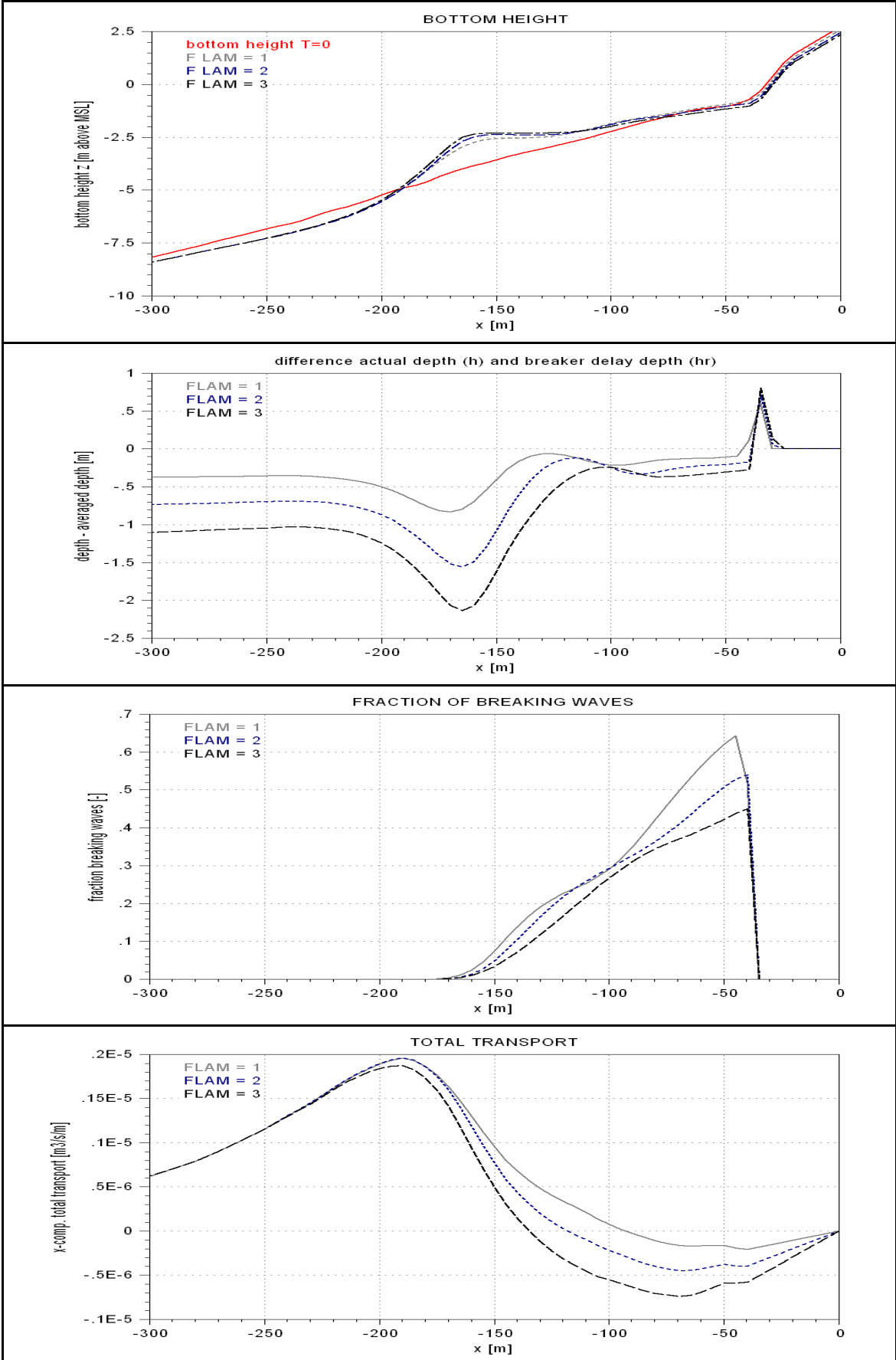
Equation (C-4), page C-3





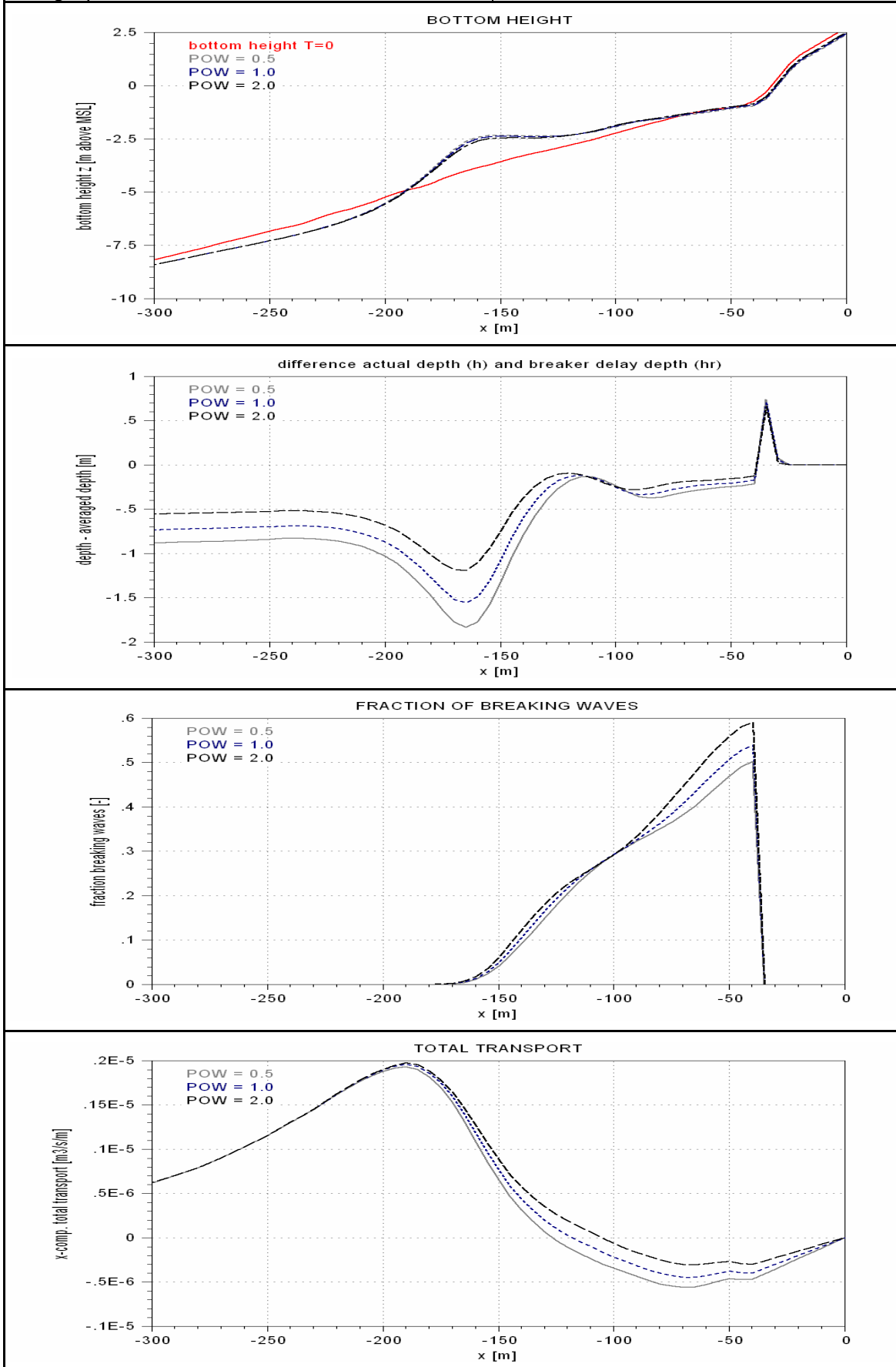
### F.2.7 Sensitivity to model parameter F\_LAM

Paragraph 7.3.6



### F.2.8 Sensitivity to model parameter POW

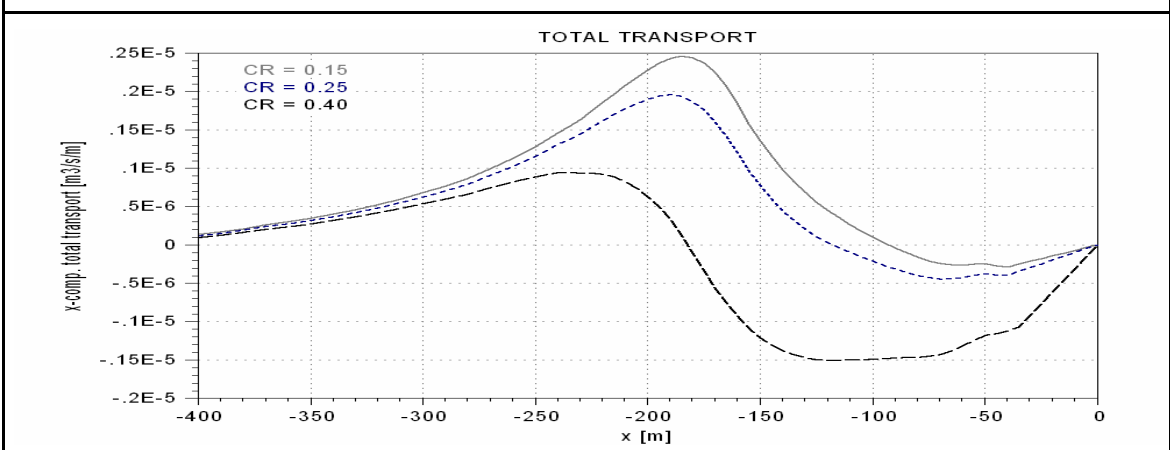
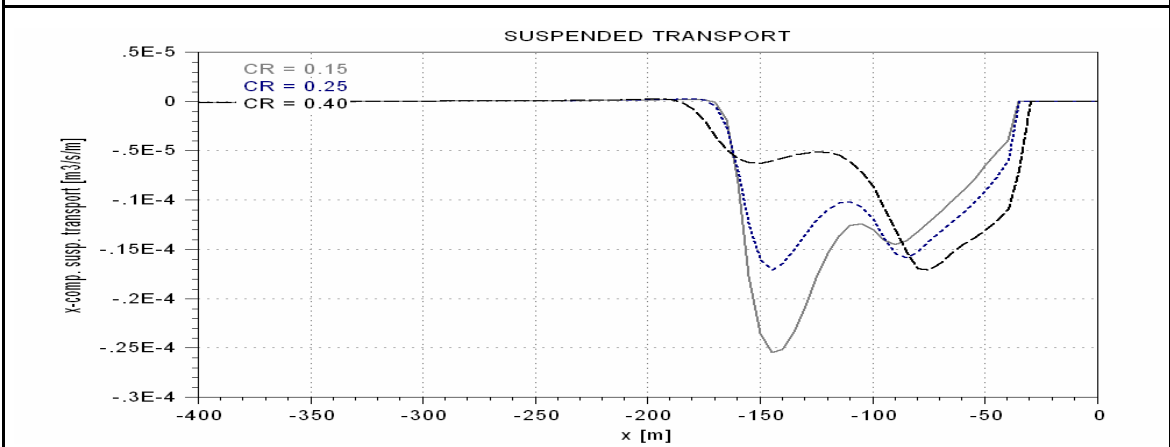
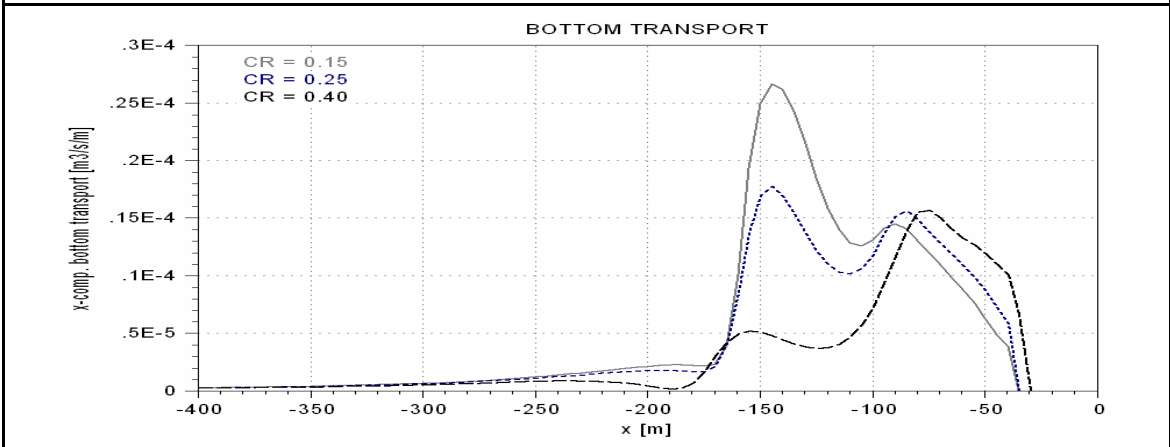
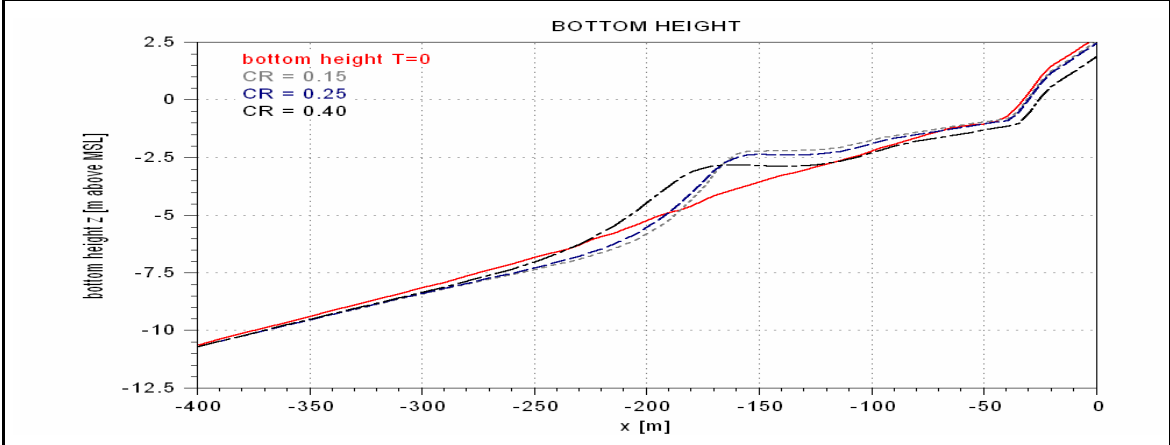
Paragraph 7.3.6



### F.2.9 Sensitivity to model parameter C\_R

Paragraph 7.3.7

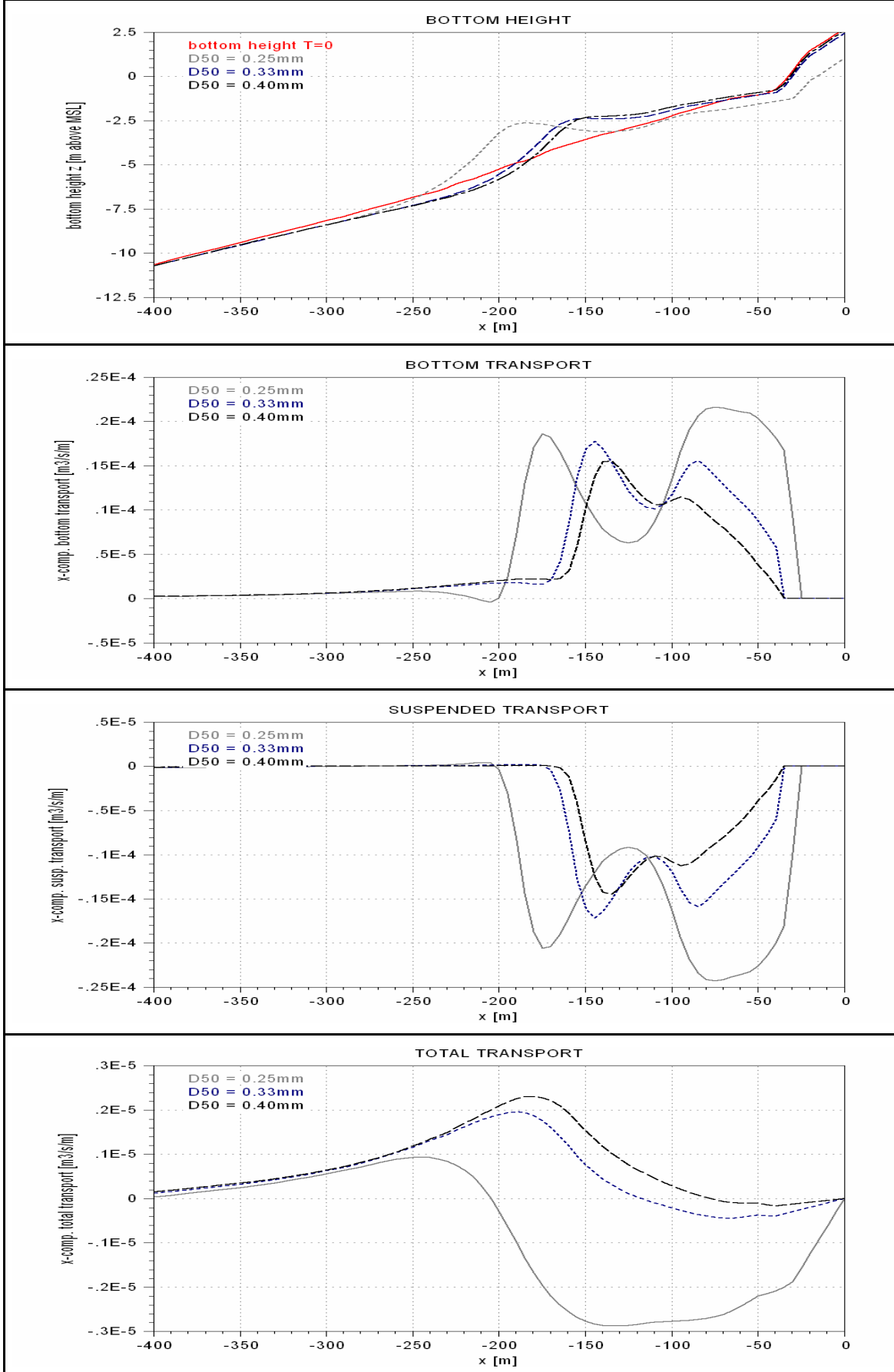
Equation (C-16), page C-6



### F.2.10 Sensitivity to model parameter D50

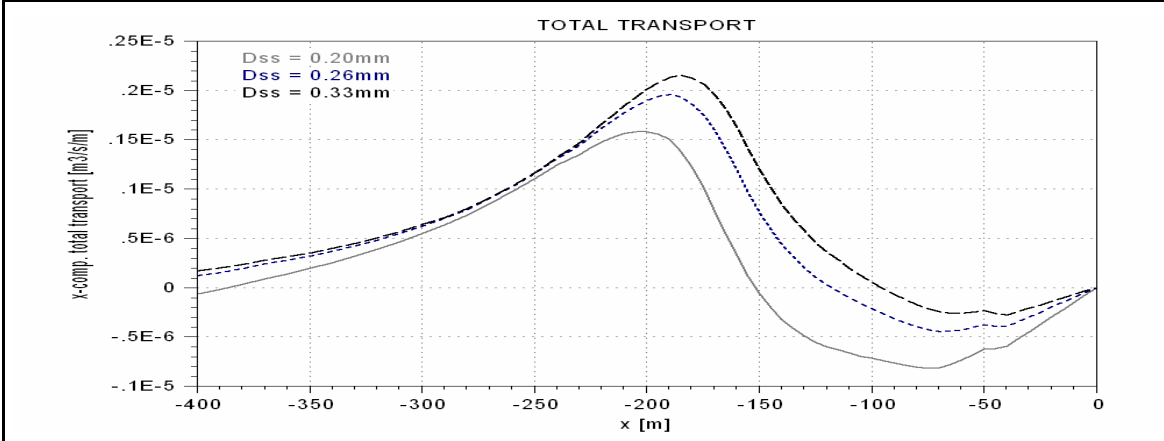
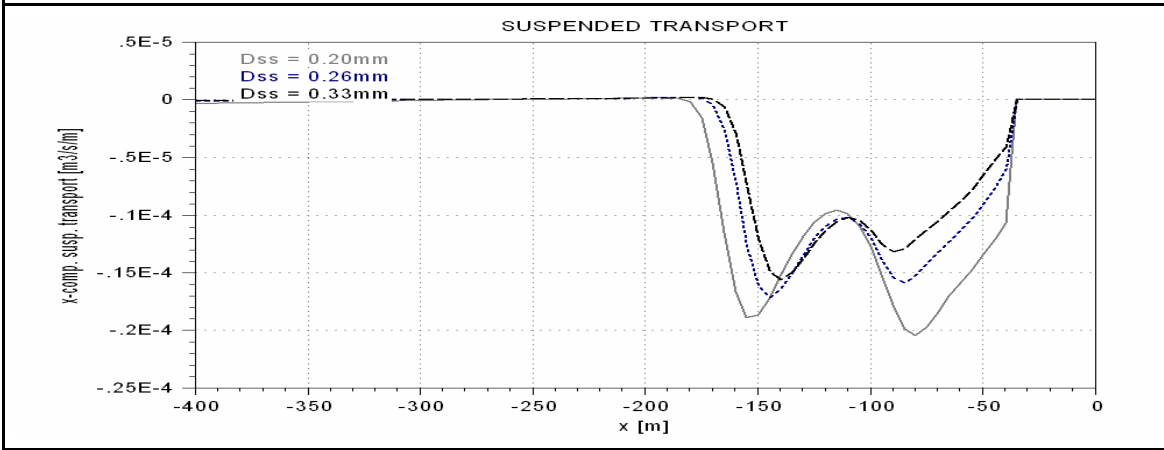
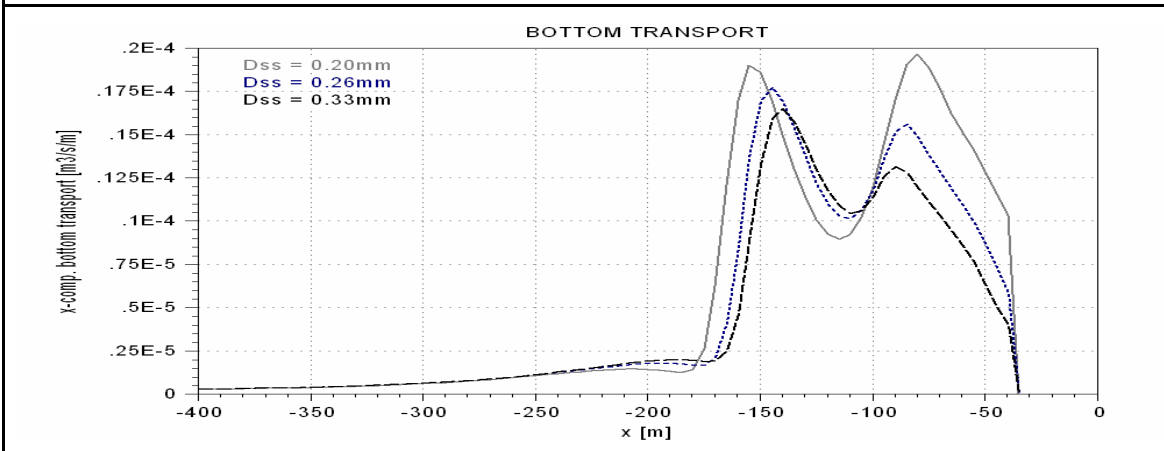
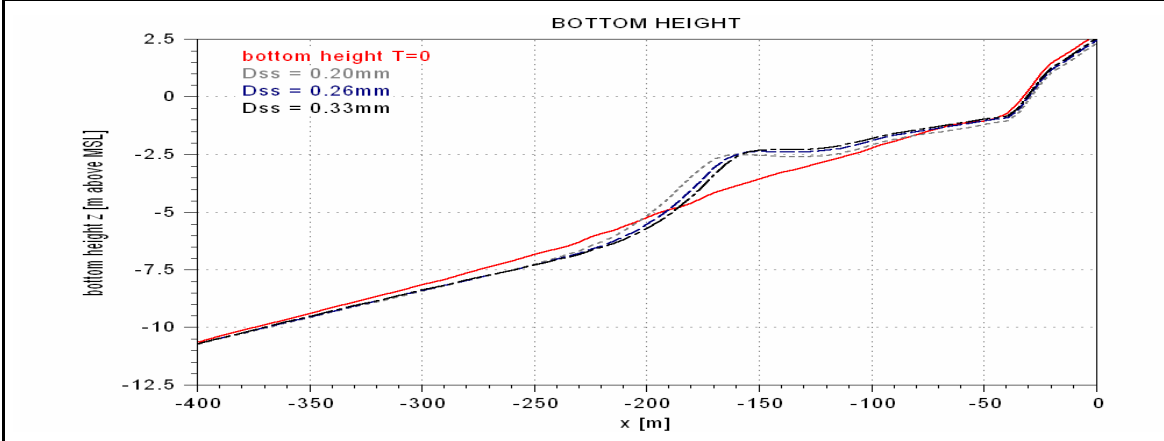
Paragraph 7.3.8

Equation (C-18), page C-7



### F.2.11 Sensitivity to model parameter Dss

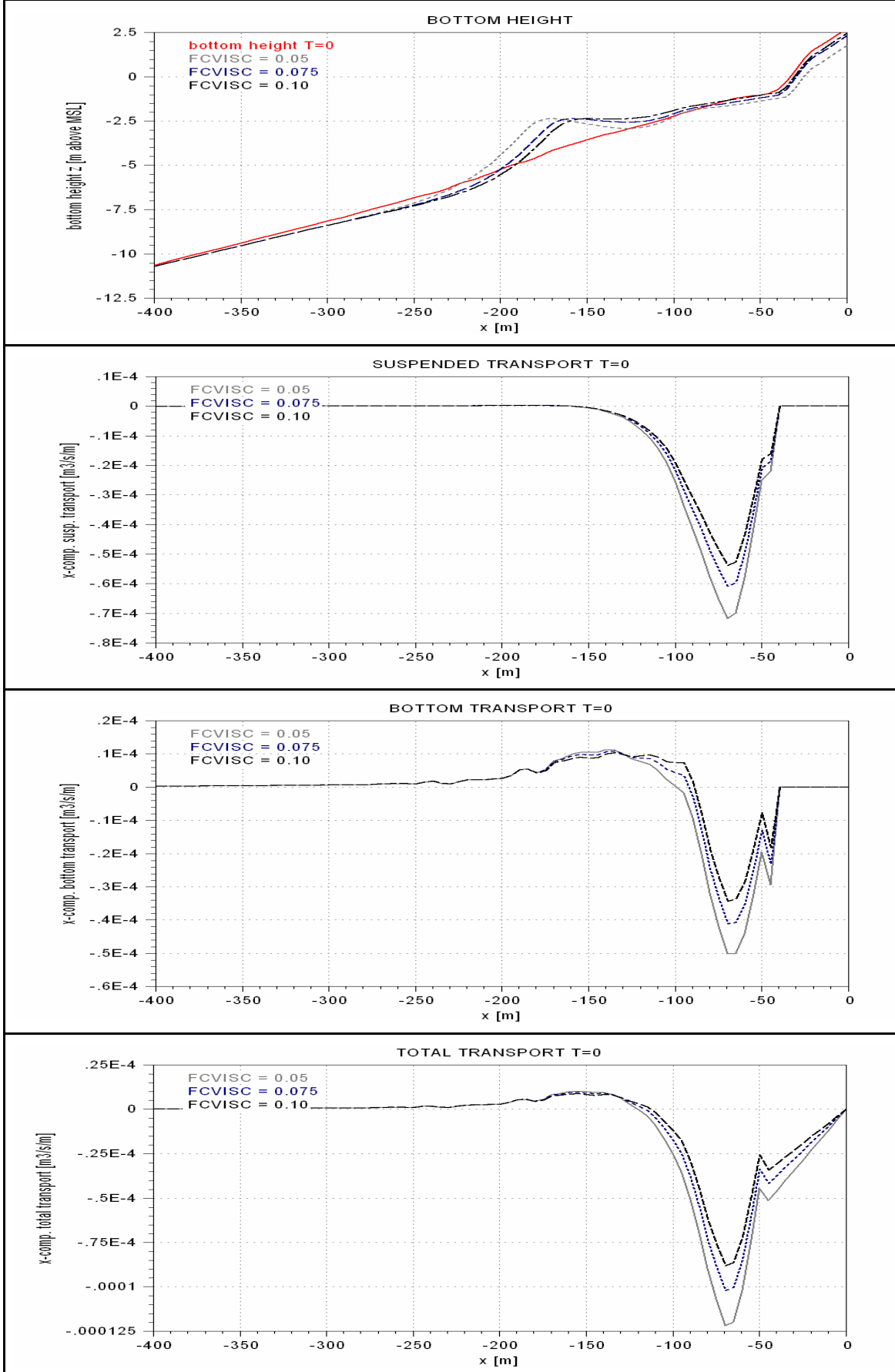
Paragraph 7.3.8



Comment: Bottom transport is influenced only indirectly.

### F.2.12 Sensitivity to model parameter FCVISC

Paragraph 7.3.9

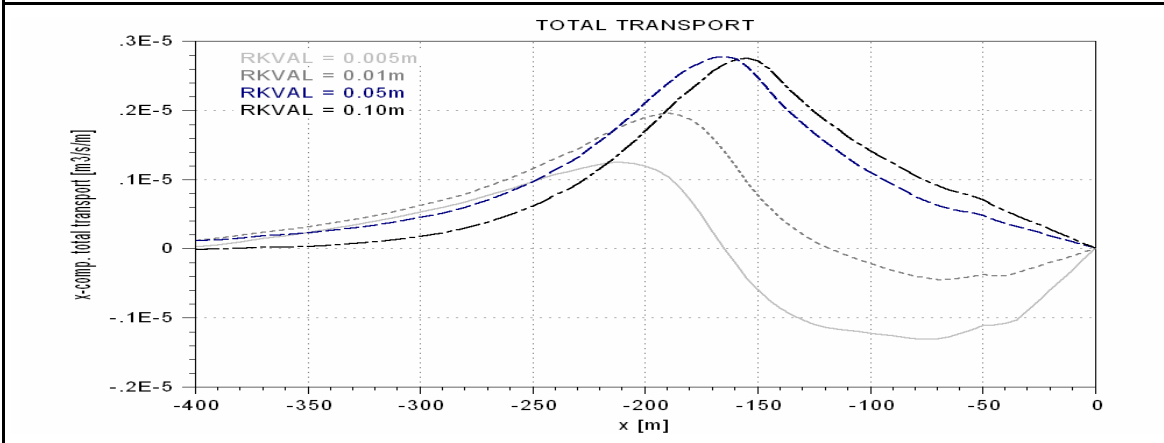
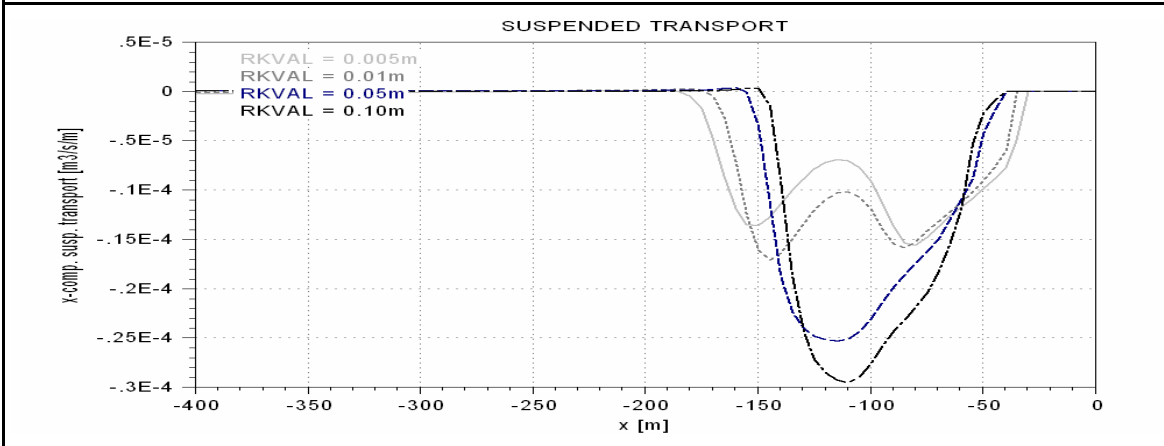
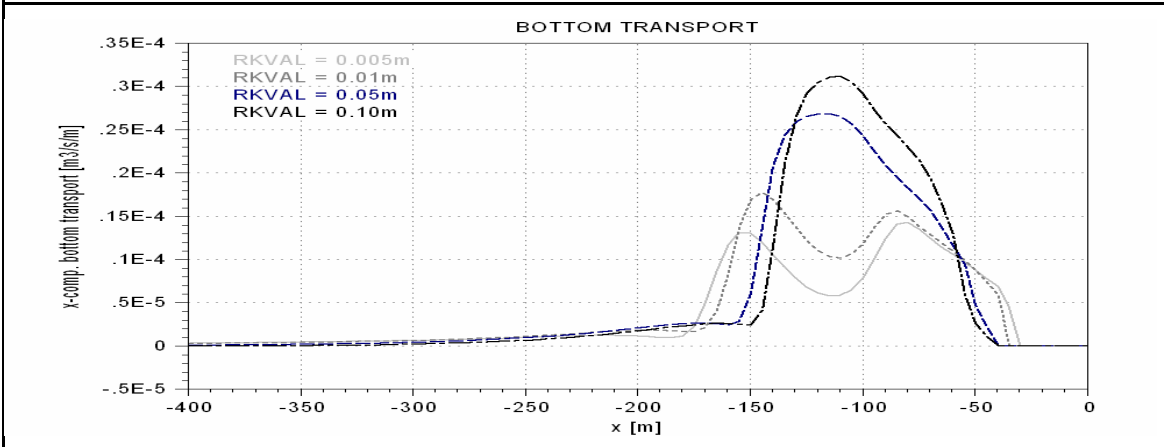
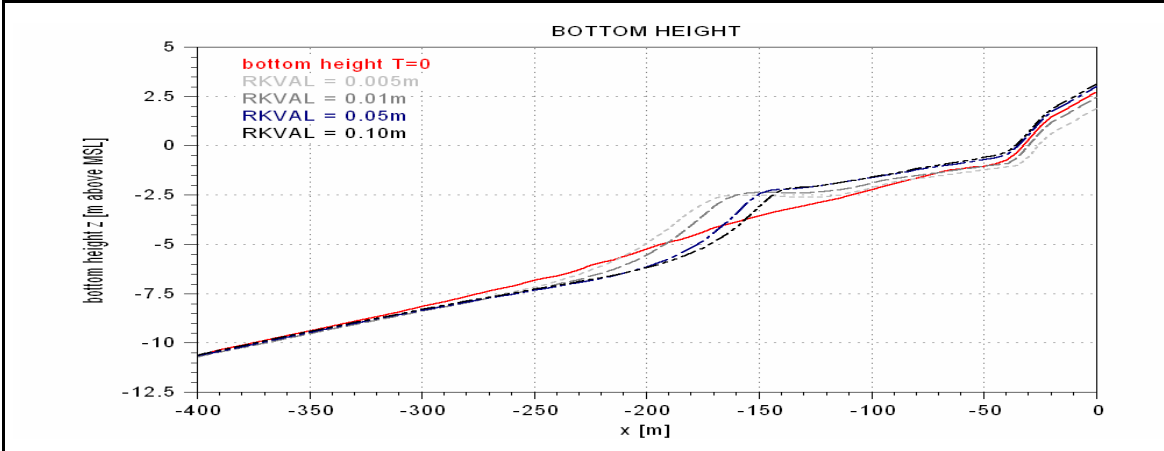


Comment: Transports are considered at T=0 to demonstrate the direct influence

### F.2.13 Sensitivity to model parameter RKVAL

Paragraph 7.3.10

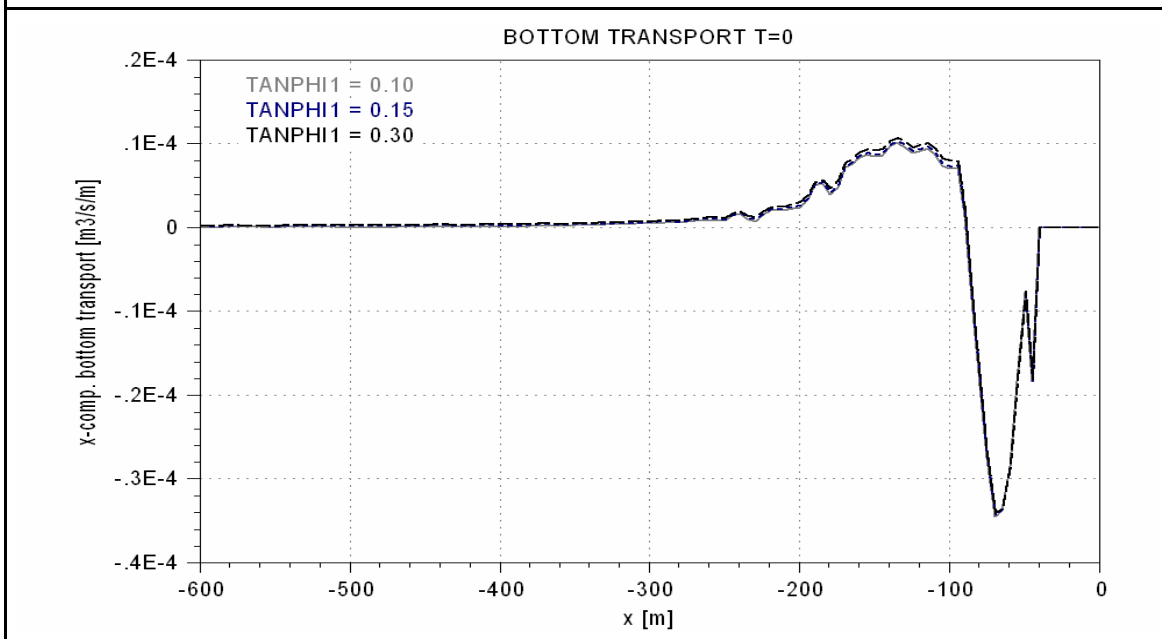
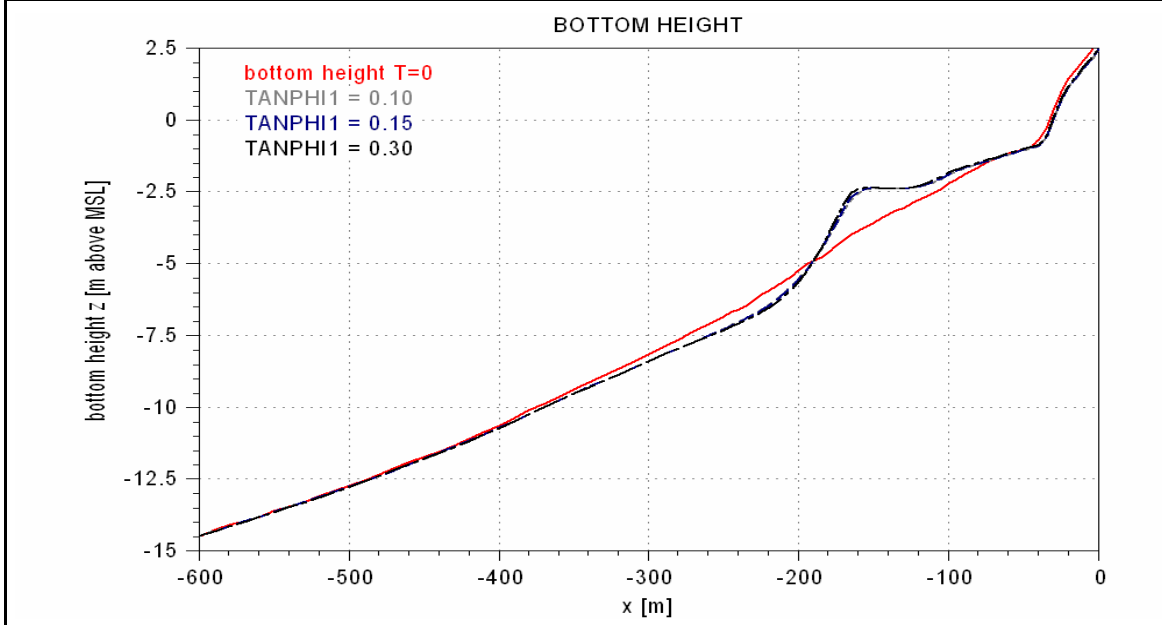
Equation (C-11), page C-5



### F.2.14 Sensitivity to model parameter TANPHI1

Paragraph 7.3.11

Equation (C-20), page C-7



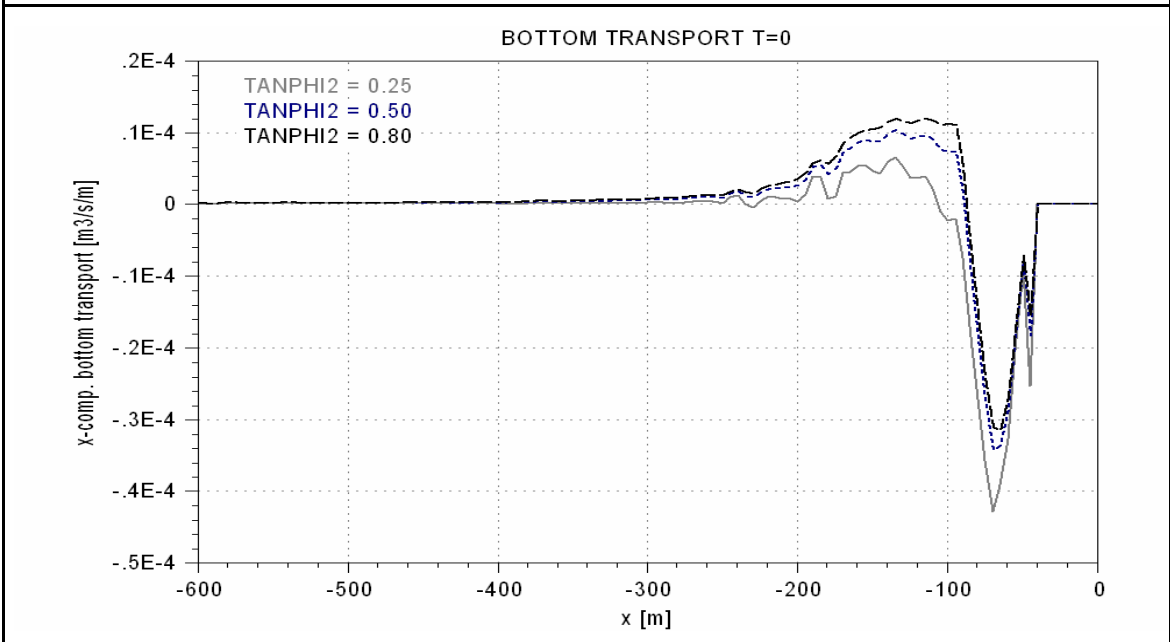
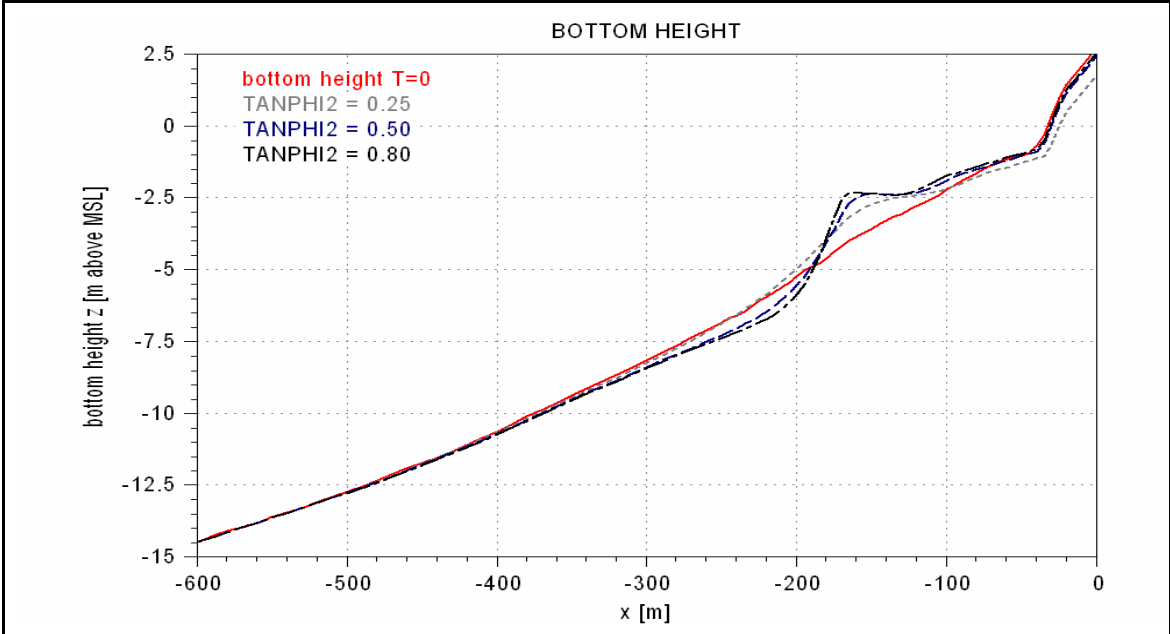
*Comment: The bottom transport is considered at T=0 to demonstrate the direct influence of the parameter TANPHI1.*



### F.2.15 Sensitivity to model parameter TANPHI2

Paragraph 7.3.11

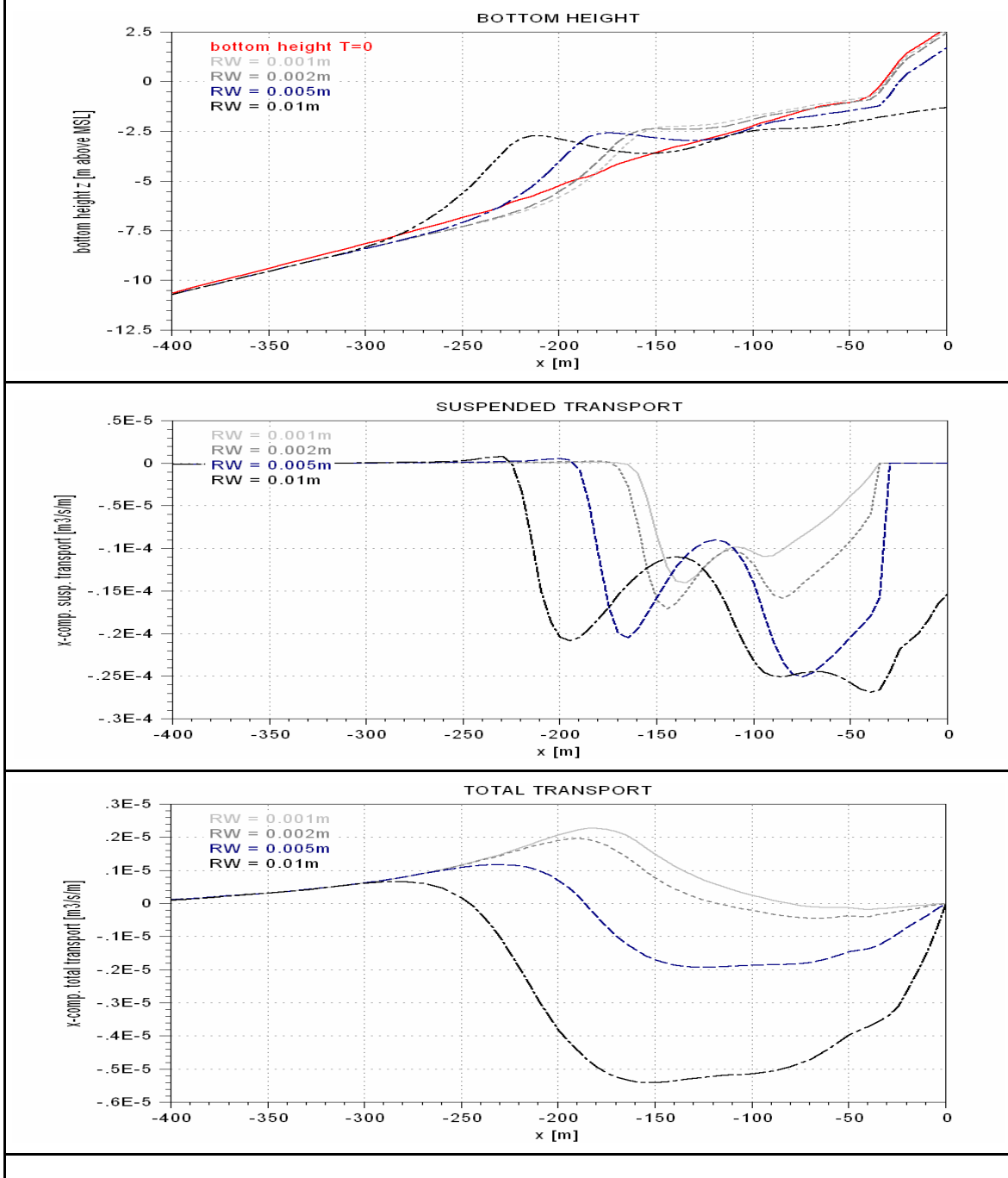
Equation (C-20), page C-7



*Comment: The bottom transport is considered at T=0 to demonstrate the direct influence of the parameter TANPHI2.*

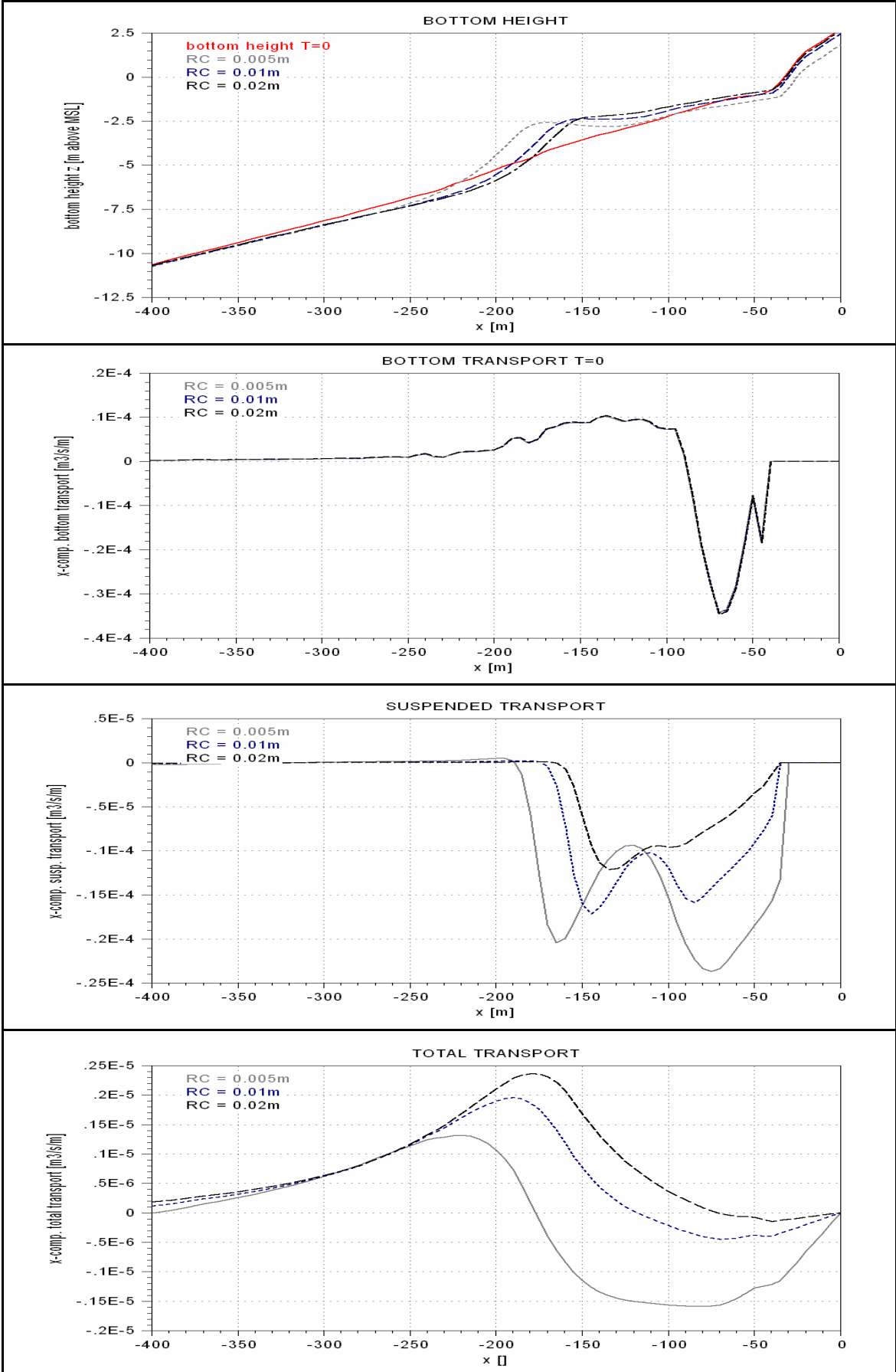
### F.2.16 Sensitivity to model parameter RW

Paragraph 7.3.12



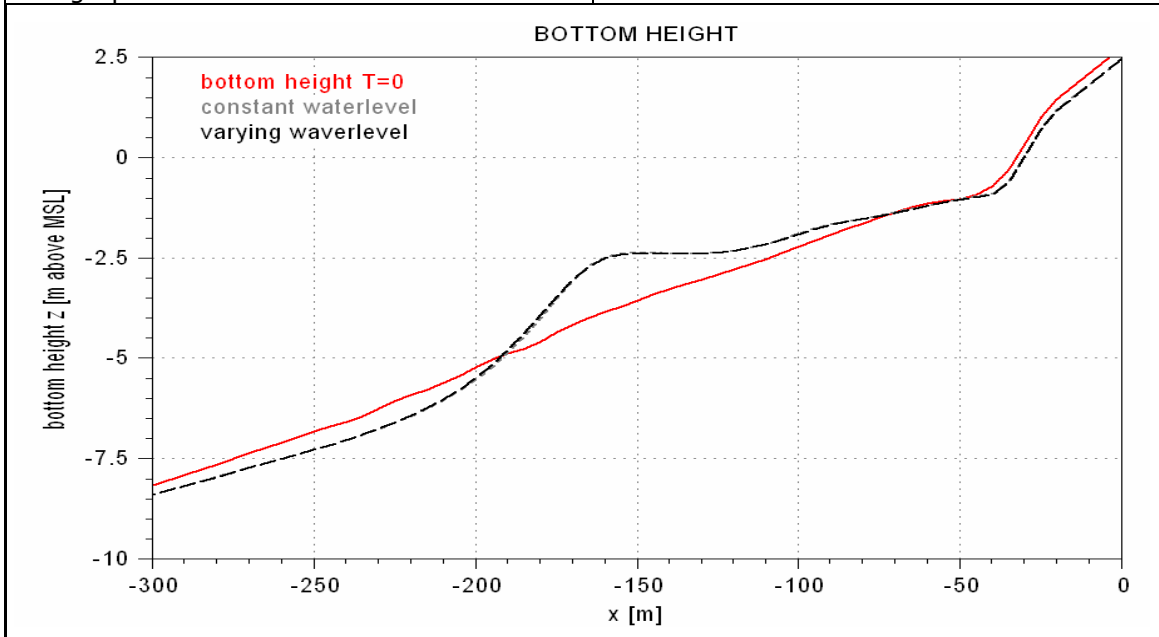
### F.2.17 Sensitivity to model parameter RC

Paragraph 7.2.17



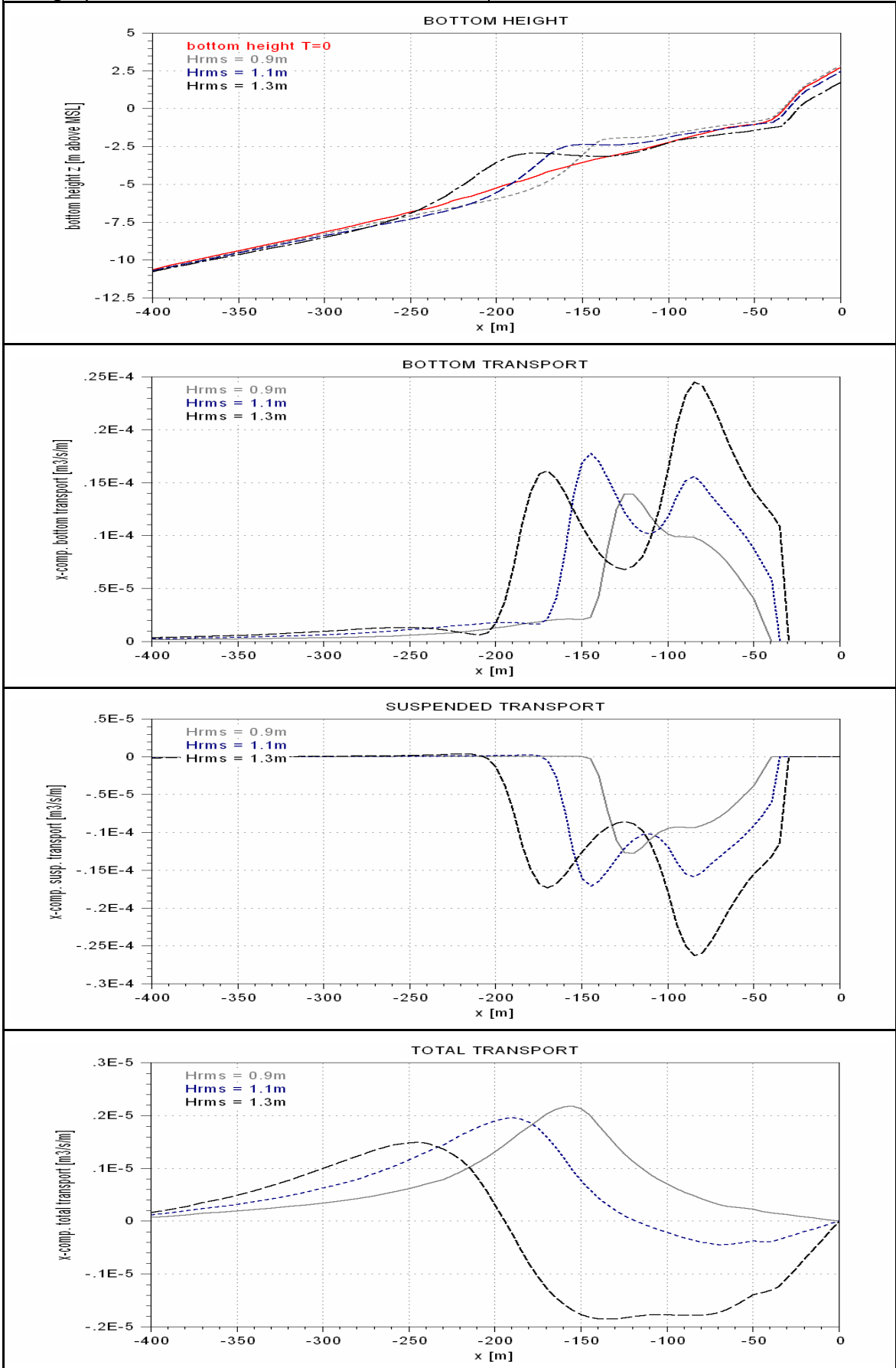
### F.2.18 Sensitivity to boundary condition $h(t)$

Paragraph 7.4.1



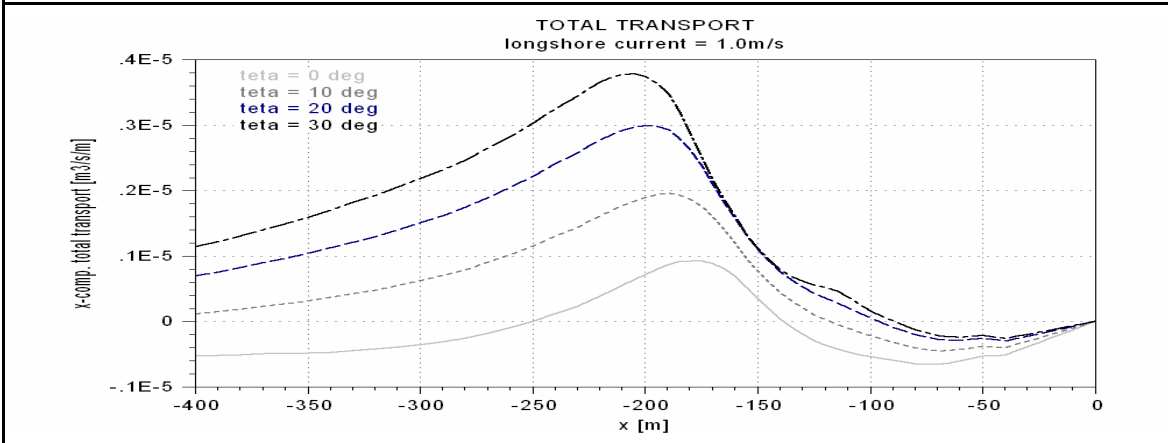
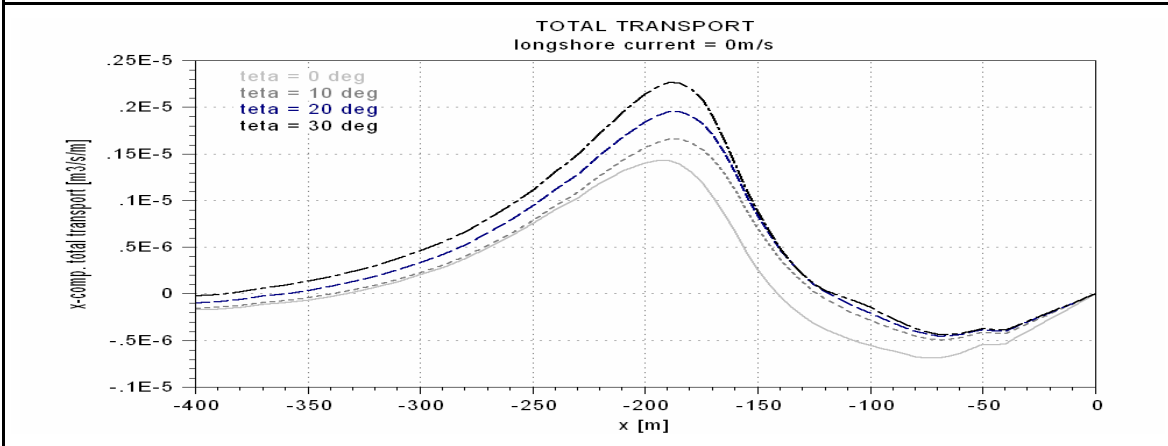
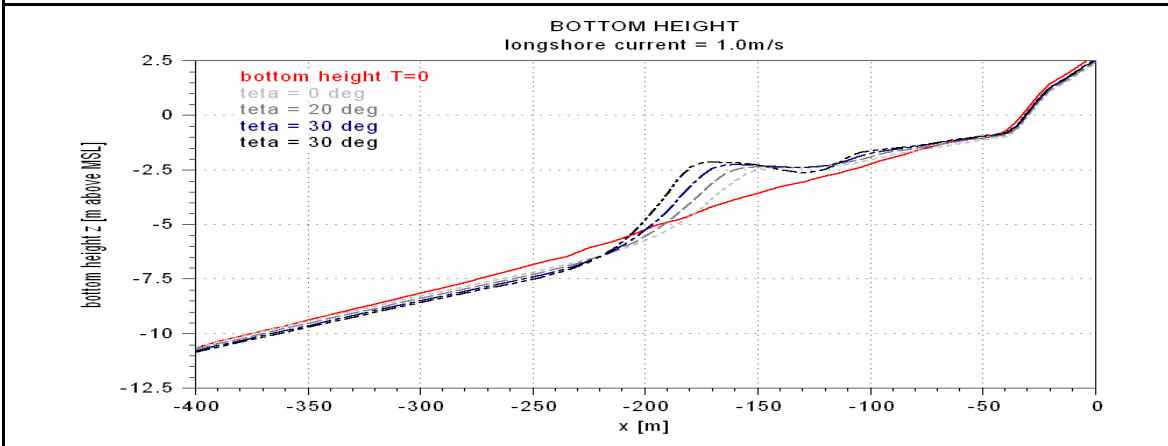
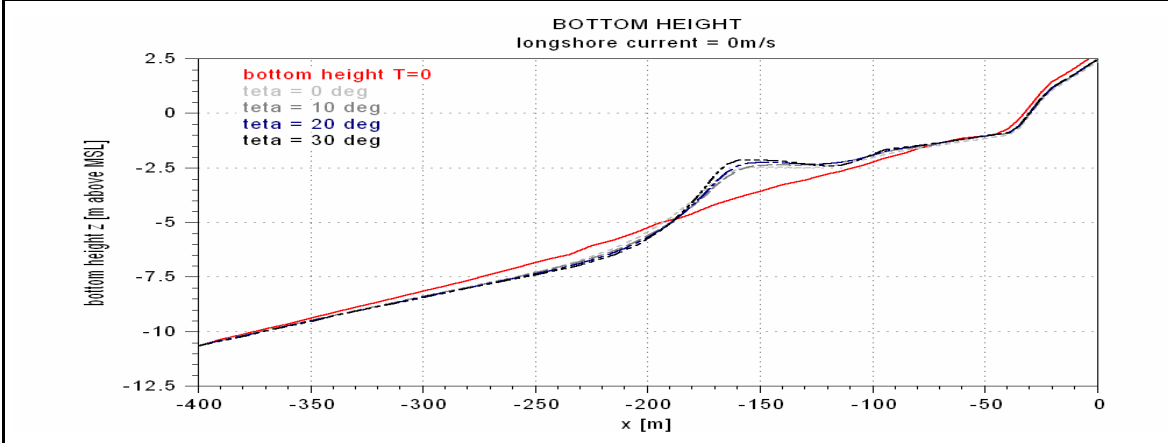
### F.2.19 Sensitivity to root-mean-square wave height $H_{rms}$

Paragraph 7.4.2



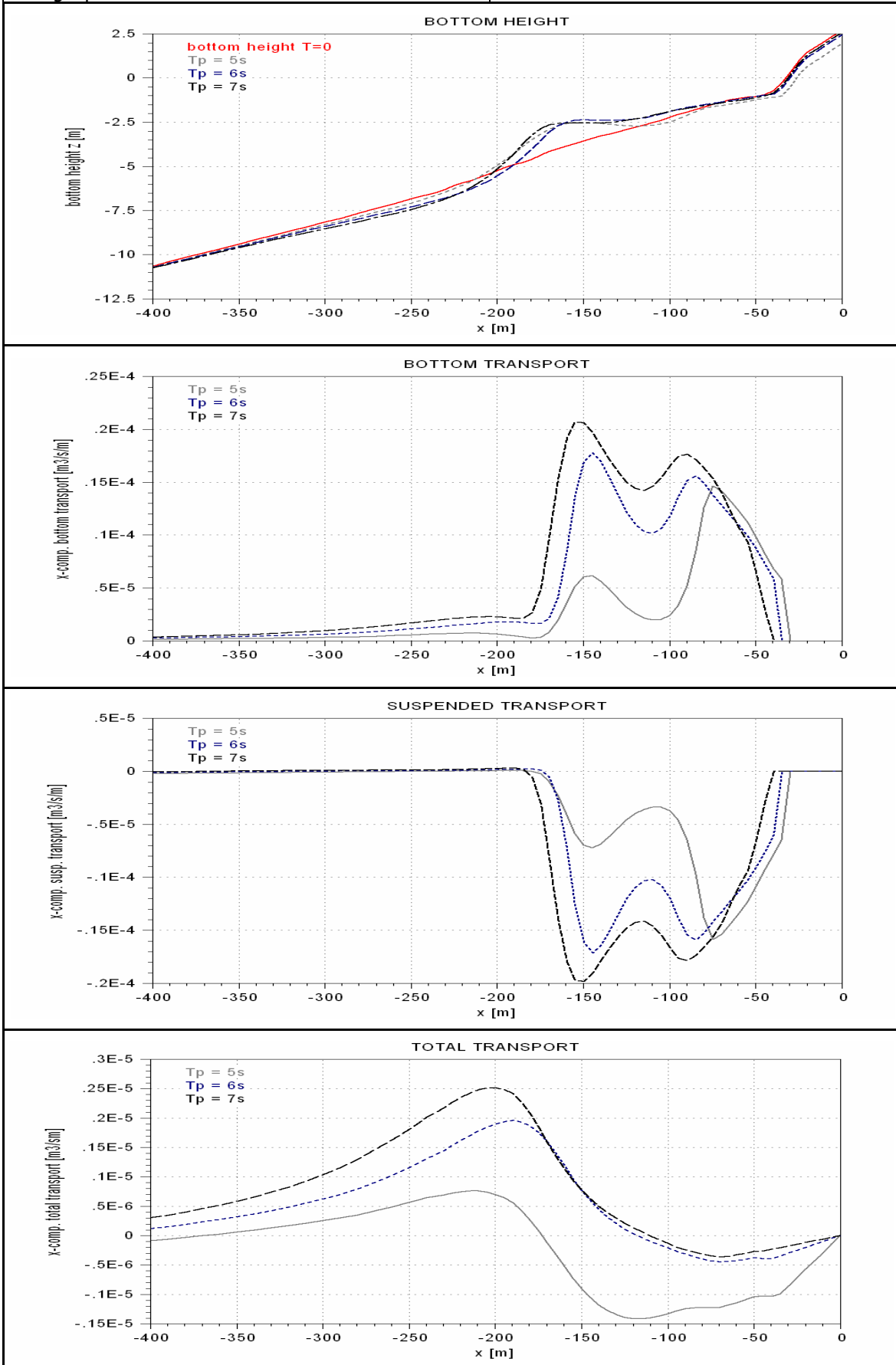
### F.2.20 Sensitivity to wave angle $\theta$

Paragraph 7.4.3



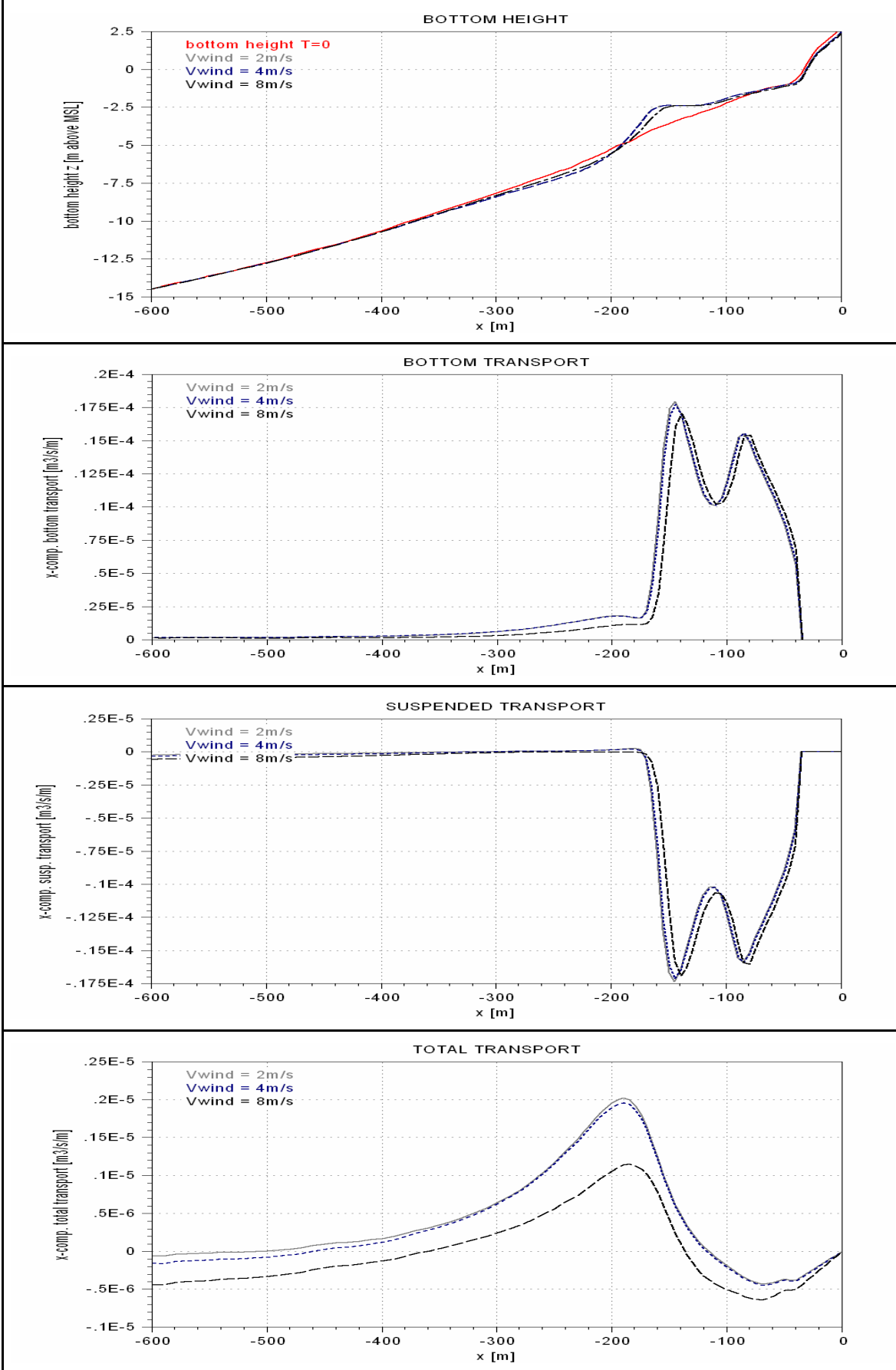
## F.2.21 Sensitivity to peak wave period $T_p$

Paragraph 7.4.4



### F.2.22 Sensitivity to wind speed $V_{wind}$

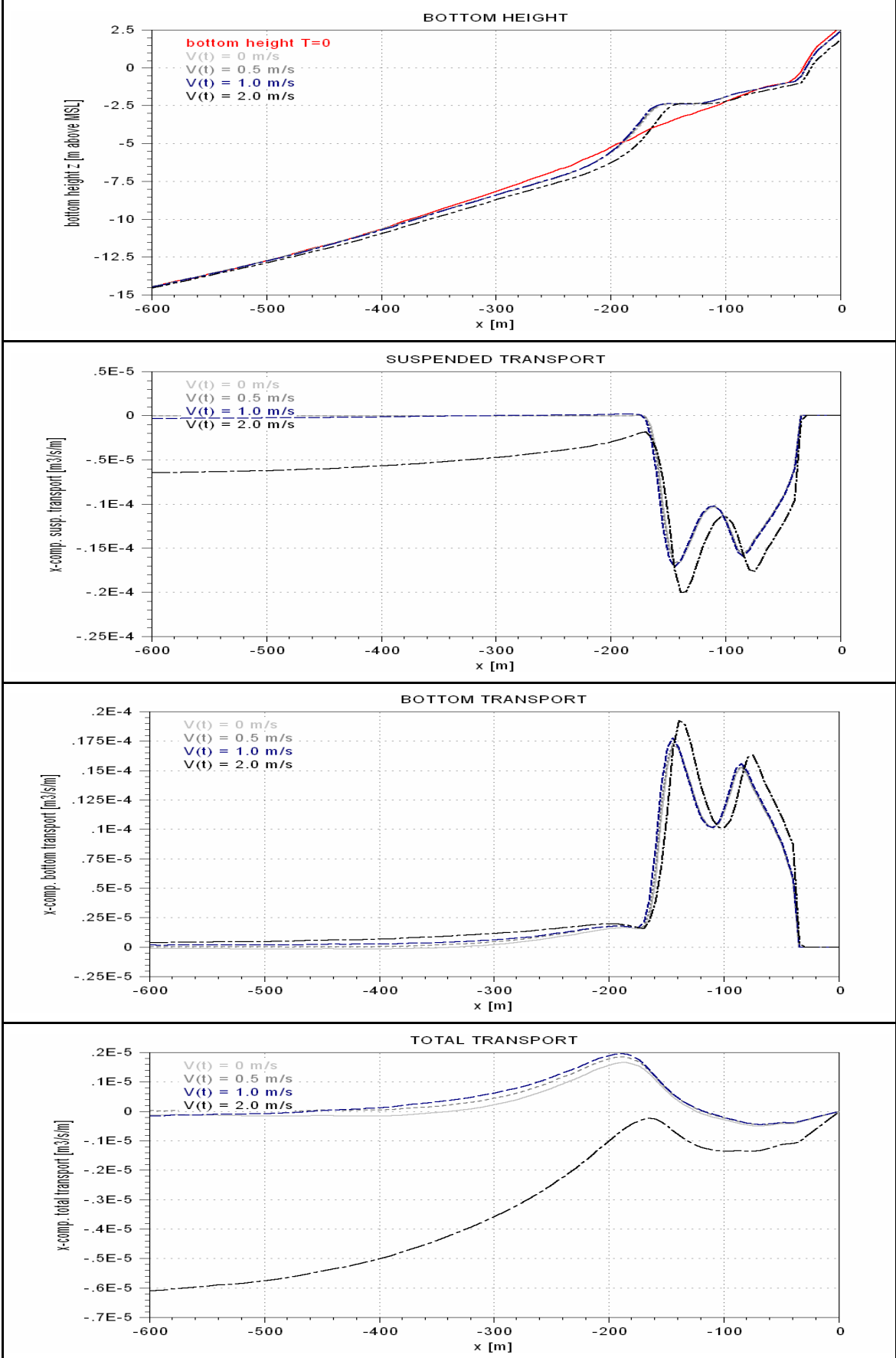
Paragraph 7.4.5





### F.2.23 Sensitivity to longshore current $V(t)$

Paragraph 7.4.6





# G RESULTS CALIBRATION PHASE

## G.1 Introduction

In this appendix the results of the calibration of the Unibest-TC model in Chapter 8 are described. Goal of the calibration is to adjust the default parameter setting of Unibest-TC in such a way that the model represents the real coastal behaviour sufficiently. The results of the sensitivity analysis of Chapter 7 serve as a reference for the calibration and verification. The final parameter setting resulting from the calibration phase can be found in Appendix D and will be used for the calculations in Chapter 9.

The sequence of the calibration procedure is as follows:

Calibration stage	Appendix	Paragraph
General shape of the profile	G.2	8.4.1
Development of individual profiles	G.3	8.4.2
Verification of the equilibration	G.4	8.4.3
Verification of the storm behaviour	G.5	8.4.4
Verification for changed boundary conditions	G.6	8.4.5

## G.2 General shape of the profile

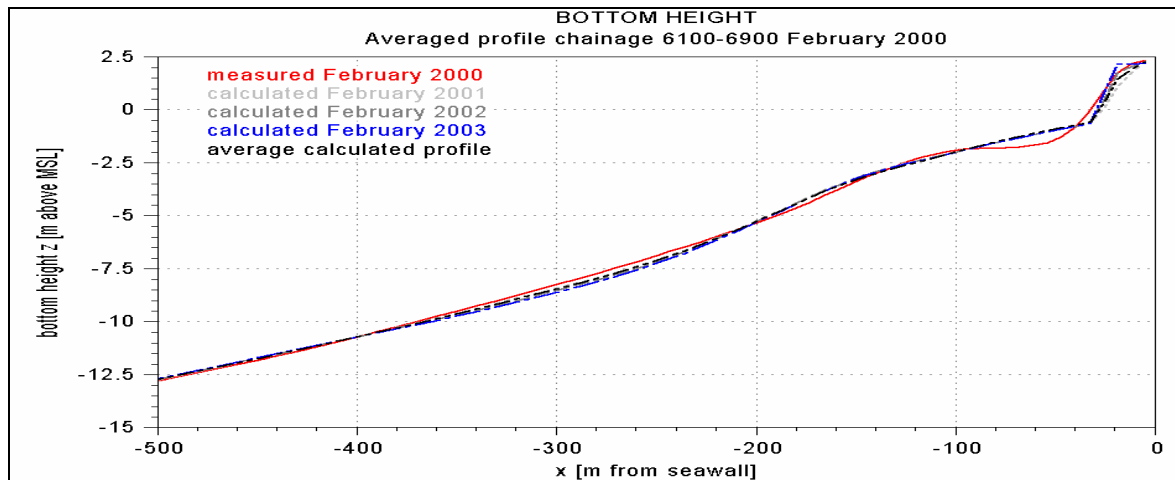


Figure G-1: Longshore averaged measured bottom heights (February 2000) and calculated bottom heights for the next three years.

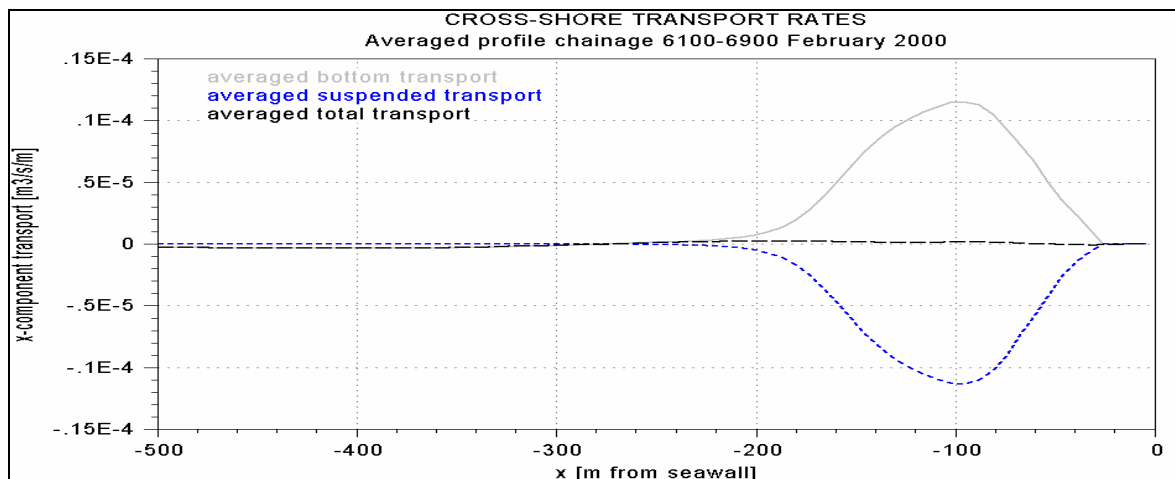


Figure G-2: Yearly-averaged cross-shore transport rates for the profile of Figure G-1.

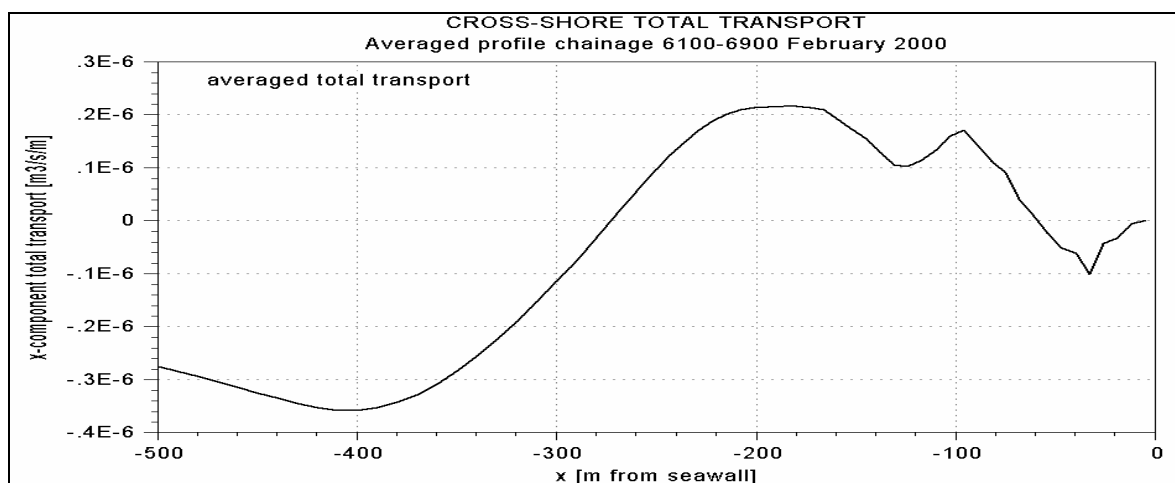


Figure G-3: Yearly averaged total cross-shore transport (enlarged from Figure G-2).

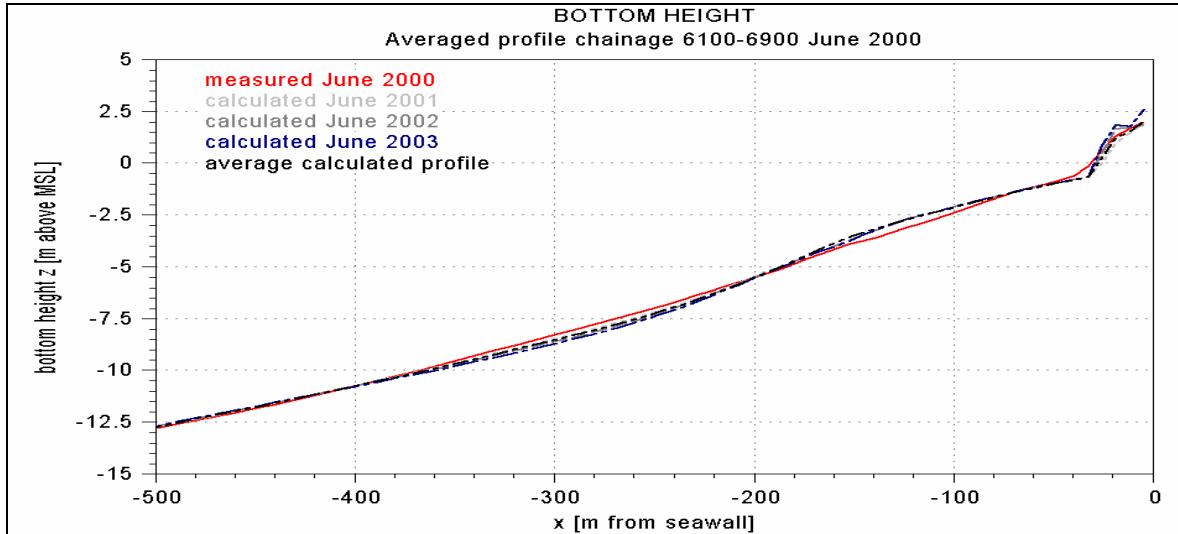


Figure G-4: Longshore averaged measured bottom heights (June 2000) and calculated bottom heights for the next three years.

### G.3 Development of individual profiles

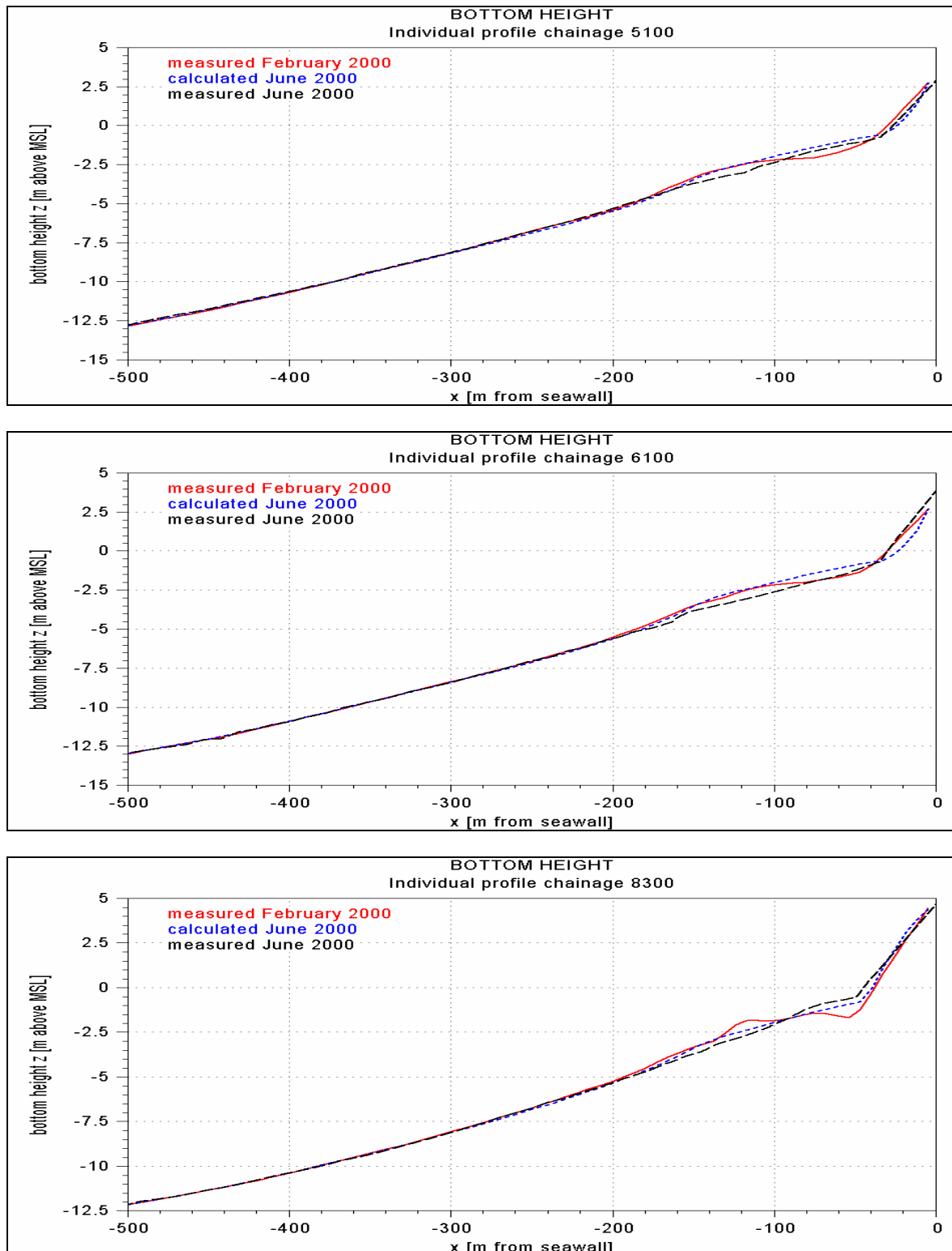


Figure G-5: Measured profiles in February 2000 (chainage 5100, 6100 and 8300), calculated profiles in June 2000 (using scaled wave conditions, see E.3.4) and measured profiles in June 2000.

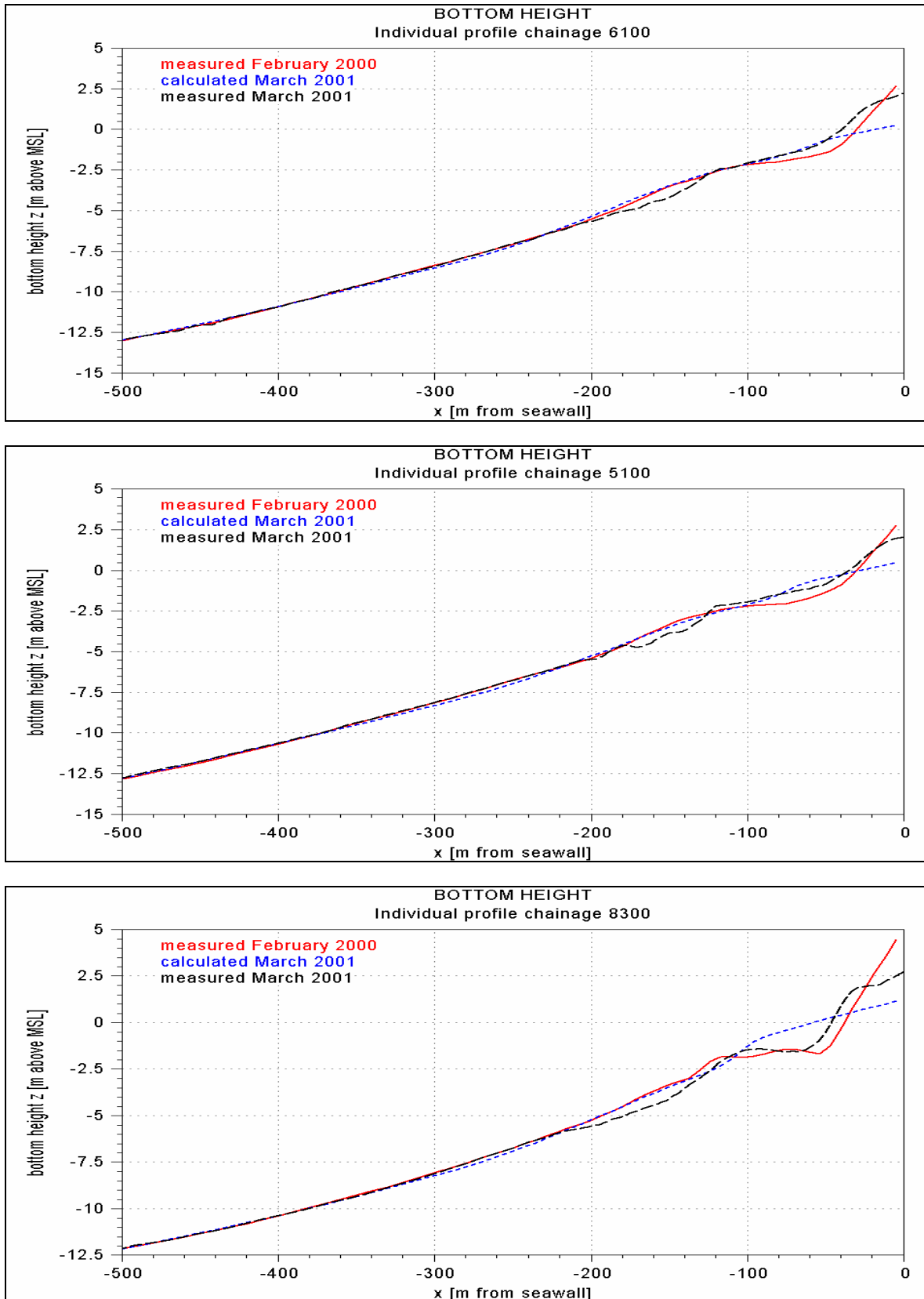


Figure G-6: Measured profiles in February 2000 (chainage 5100, 6100 and 8300), calculated profiles in March 2001 (using scaled wave conditions, see Paragraph E.3.4) and measured profiles in March 2001.

## G.4 Verification of the equilibration

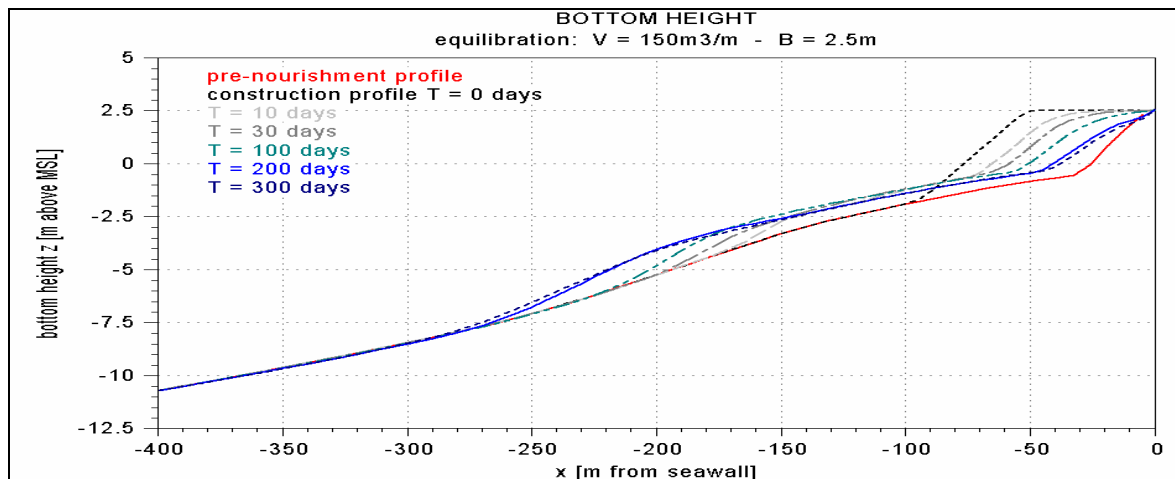


Figure G-7: A pre-nourishment profile with the imposed construction profile and the calculated bottom profiles at  $T=10, 30, 100, 200$  and  $300$  days, with the use of average boundary conditions.

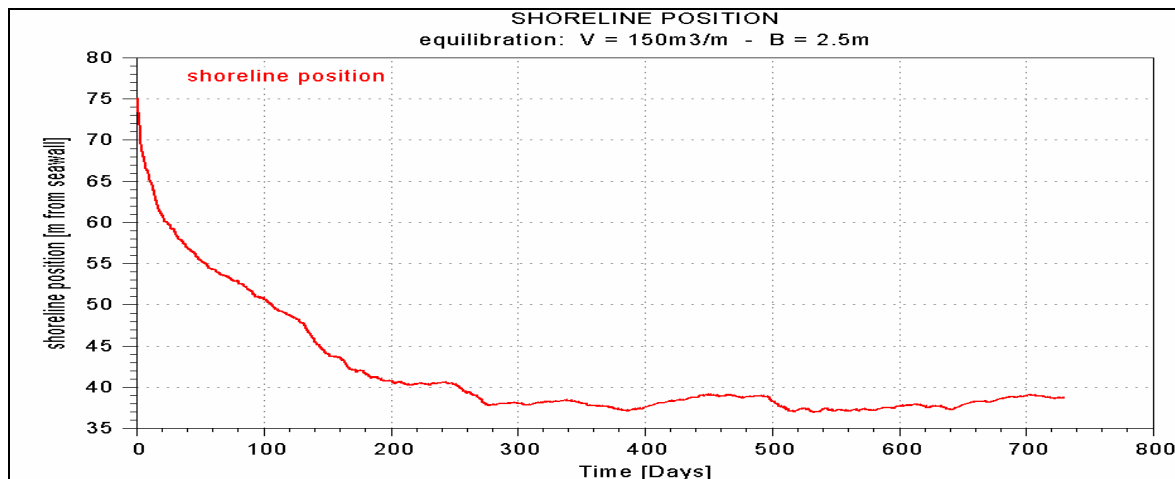


Figure G-8: The shoreline position during the equilibration of the construction profile indicated in Figure G-7.  $T=0$  is at 15 July, directly after construction.

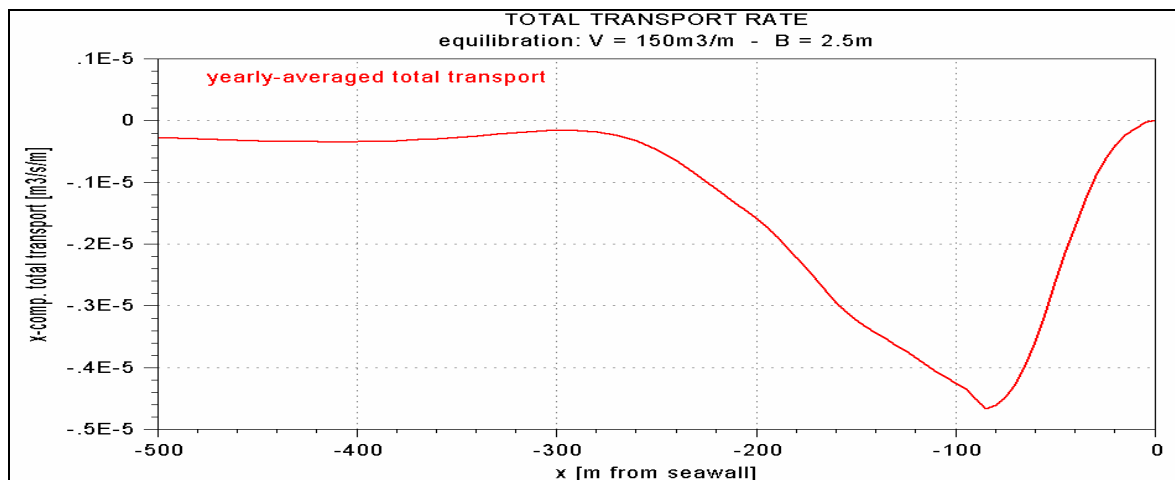


Figure G-9: Average cross-shore total transport in the first year after construction.



## G.5 Verification of the storm behaviour

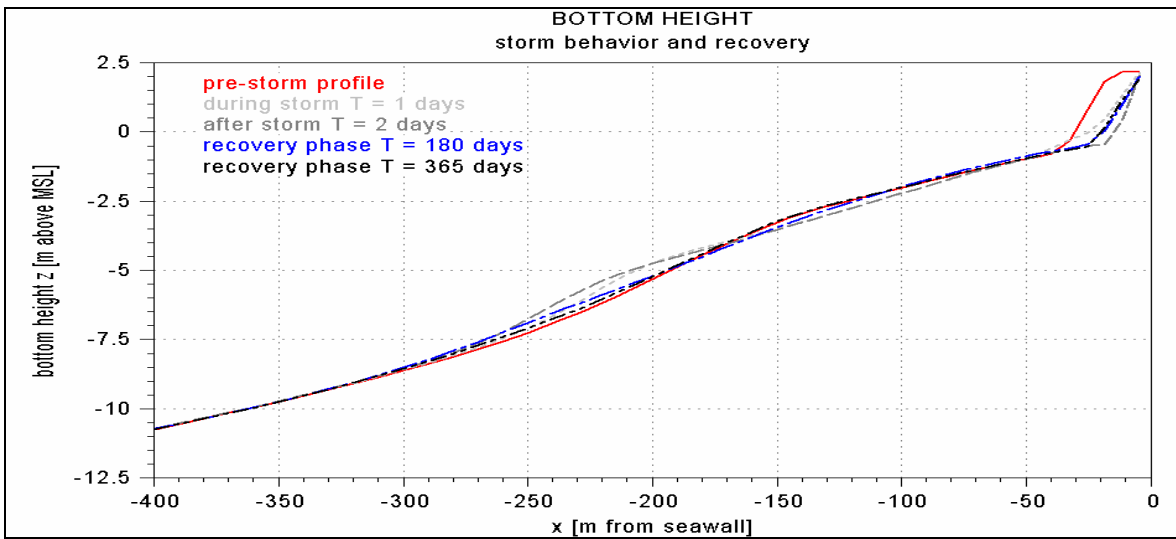


Figure G-10: A pre-storm profile and the calculated profiles after 1 day of storm conditions and at the end of the storm (after 2 days). The calculated profiles after 180 and 365 days of recovery are also plotted.

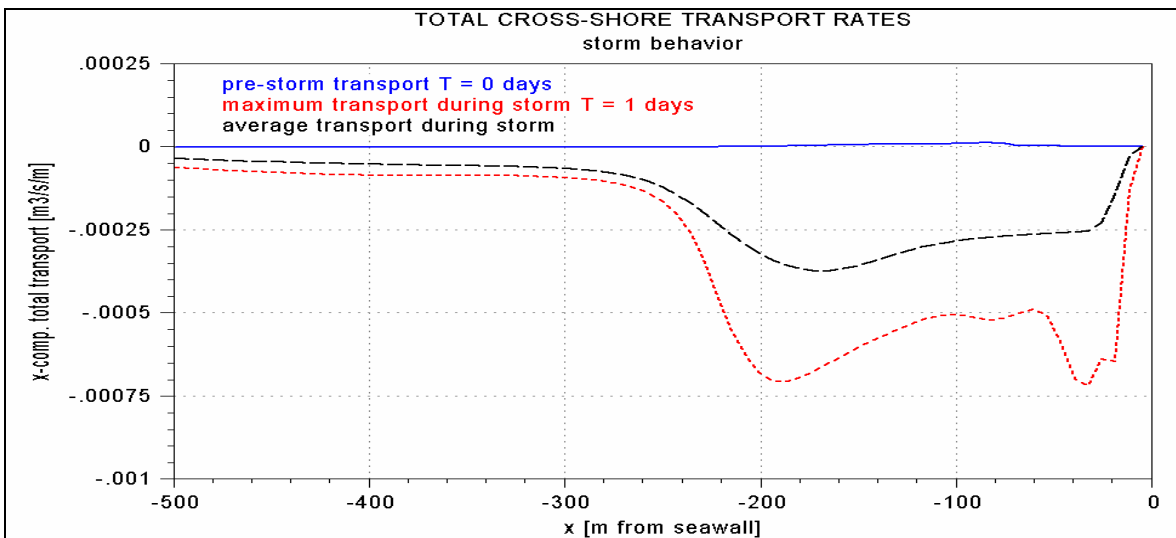


Figure G-11: The transport rates during storm conditions (black + dashed and red + dotted line) compared with the normal transport rates (blue + solid line).

## G.6 Verification for changed boundary conditions

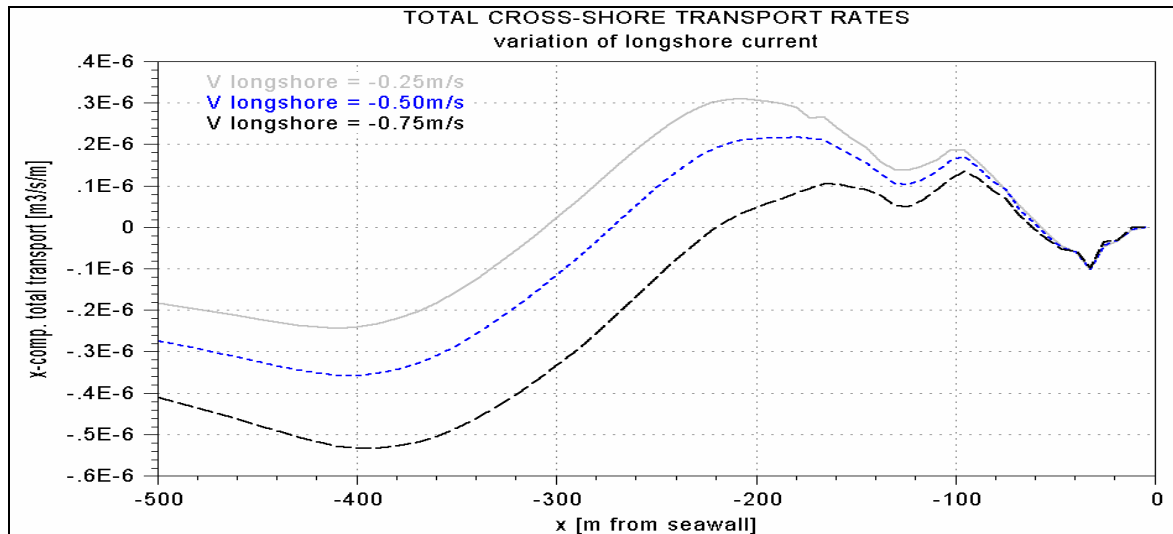


Figure G-12: The yearly-averaged cross-shore total transports for three different values of the longshore current velocity:  $-0.25$  m/s (grey solid line),  $-0.50$  m/s (blue dotted line) and  $-0.75$  m/s (black dashed line).

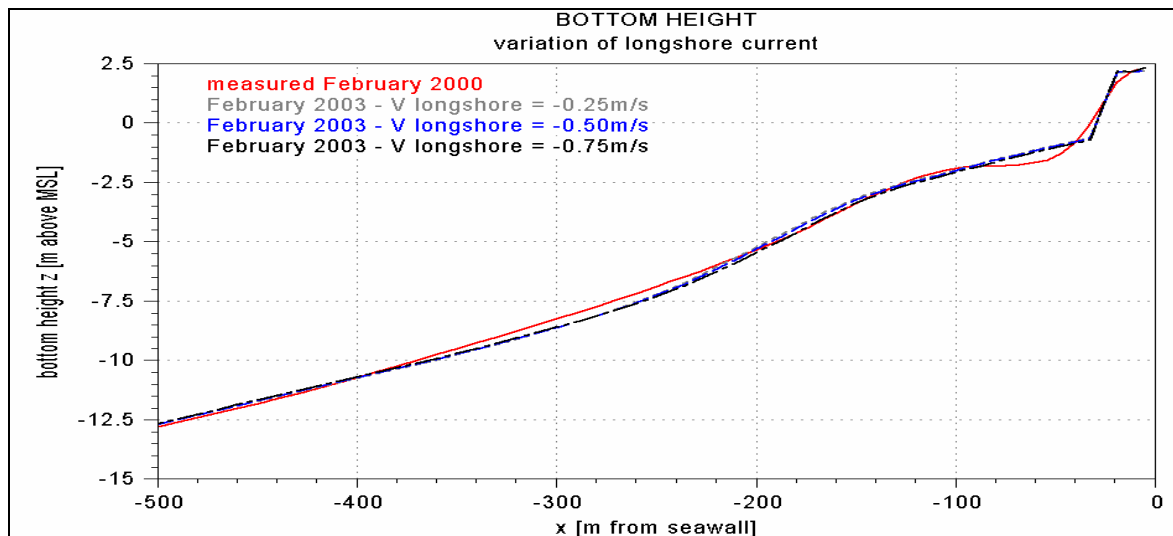


Figure G-13: The calculated bottom heights after 3 years for three different values of the longshore current velocity:  $0.25$  m/s (grey solid line),  $-0.50$  m/s (blue dotted line) and  $-0.75$  m/s (black dashed line).

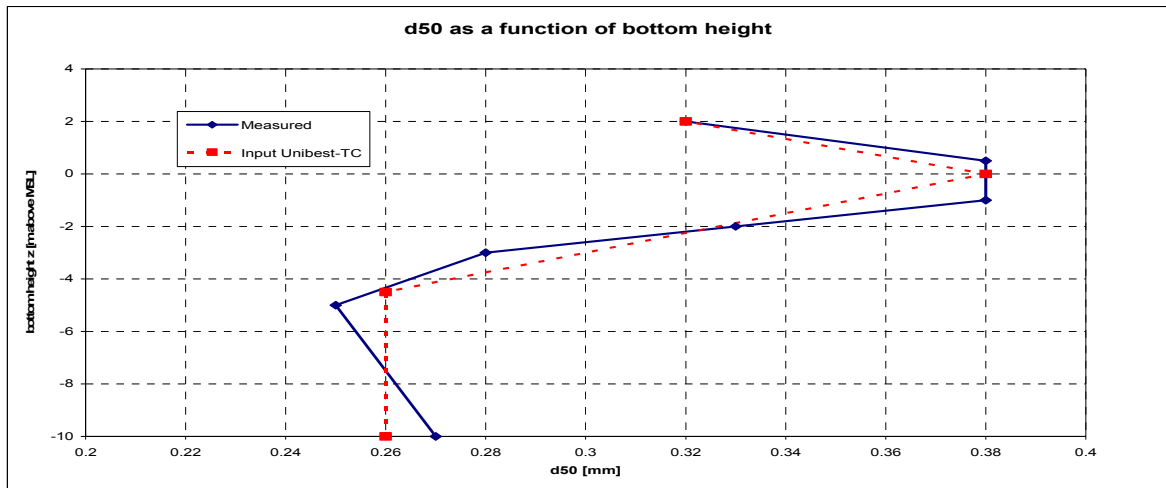


Figure G-14: The variation of the  $d_{50}$  over the depth as has been measured (blue solid line) and as has been used in Unibest-TC (red dotted line).

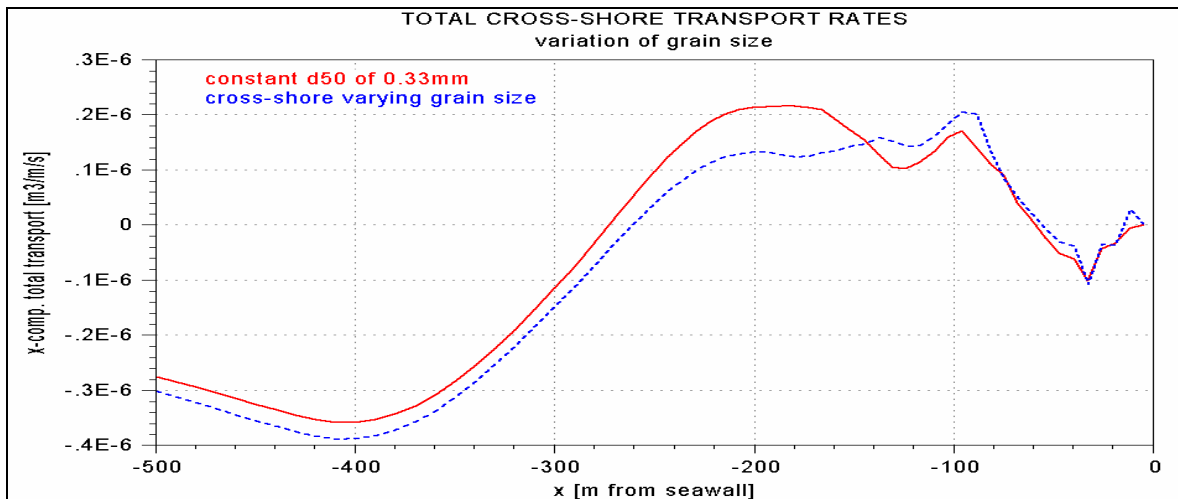


Figure G-15: The yearly averaged total cross-shore transport rates for a constant grain size and for a depth-varying grain size according to Figure G-14.

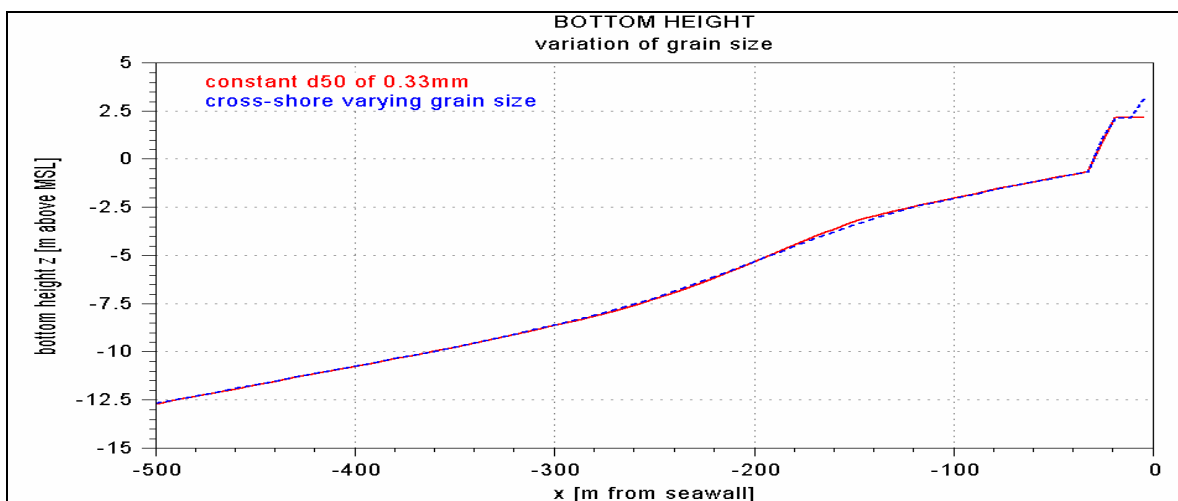


Figure G-16: The resulting bottom elevations after three years of calculations for the depth-constant and depth-varying grain size.



## H RESULTS EQUILIBRATION DESIGN METHODS

In this appendix the results of the equilibration design methods are given. In Table H-1 the calculated shoreline advancement after equilibration is presented for a closure depth of 7.5 m and a berm height of 2.5 m.

Table H-1: Additional dry beach widths  $\Delta y_{0,EQ}$  for three borrow areas according to the methods of Dean [1974], James [1975], the USACE [1994], Dean [2002] and the Unibest-TC model, using  $h_s = 7.5$  m and  $B = 2.5$  m. (\* means intersecting profile).

Dean [1974] method								
Description fill sediments			Volume [m <sup>3</sup> /m]					
Fill source	$d_{50}$ [mm]	fill factor	150	200	250	300	350	400
Native	0.33	1.00	15.00	20.00	25.00	30.00	35.00	40.00
Area I - Puerto Juárez	0.27	1.16	12.93	17.24	21.55	25.86	30.17	34.48
Area II – Punta Sam	0.42	1.00	15.00	20.00	25.00	30.00	35.00	40.00
James [1975] method								
Description fill sediments			Volume [m <sup>3</sup> /m]					
Fill source	$d_{50}$ [mm]	fill factor	150	200	250	300	350	400
Native	0.33	1.05	14.29	19.05	23.81	28.57	33.33	38.10
Area I - Puerto Juárez	0.27	1.50	10.00	13.33	16.67	20.00	23.33	26.67
Area II – Punta Sam	0.42	1.08	13.76	18.35	22.94	27.52	32.11	36.70
USACE [1994] method								
Description fill sediments			Volume [m <sup>3</sup> /m]					
Fill source	$d_{50}$ [mm]	A [m <sup>1/3</sup> ]	150	200	250	300	350	400
Native	0.33	0.175	14.81	19.66	24.47	29.25	33.98	38.69
Area I - Puerto Juárez	0.27	0.159	0.31	4.94	9.53	14.10	18.63	23.13
Area II – Punta Sam	0.42	0.198	*26.88	*33.11	*38.83	*44.17	49.22	54.19
Dean [2002] method								
Description fill sediments			Volume [m <sup>3</sup> /m]					
Fill source	$d_{50}$ [mm]	A [m <sup>1/3</sup> ]	150	200	250	300	350	400
Native	0.33	0.175	14.81	19.66	24.47	29.25	33.98	38.69
Area I - Puerto Juárez	0.27	0.159	13.10	17.40	21.70	26.00	30.20	34.40
Area II – Punta Sam	0.42	0.198	14.81	19.66	24.47	29.25	33.98	38.69
Unibest-TC model								
Description fill sediments			Volume [m <sup>3</sup> /m]					
Fill source	$d_{50}$ [mm]		150	200	250	300	350	400
Native	0.33		7.83	14.21	19.23	22.94	27.97	34.09
Area I - Puerto Juárez	0.27		1.06	7.38	12.42	17.33	22.24	27.31
Area II – Punta Sam	0.42		13.13	19.03	23.96	28.96	33.74	37.90

On the next pages the bottom profiles after equilibration are plotted for the three considered borrow areas and design methods as indicated below:

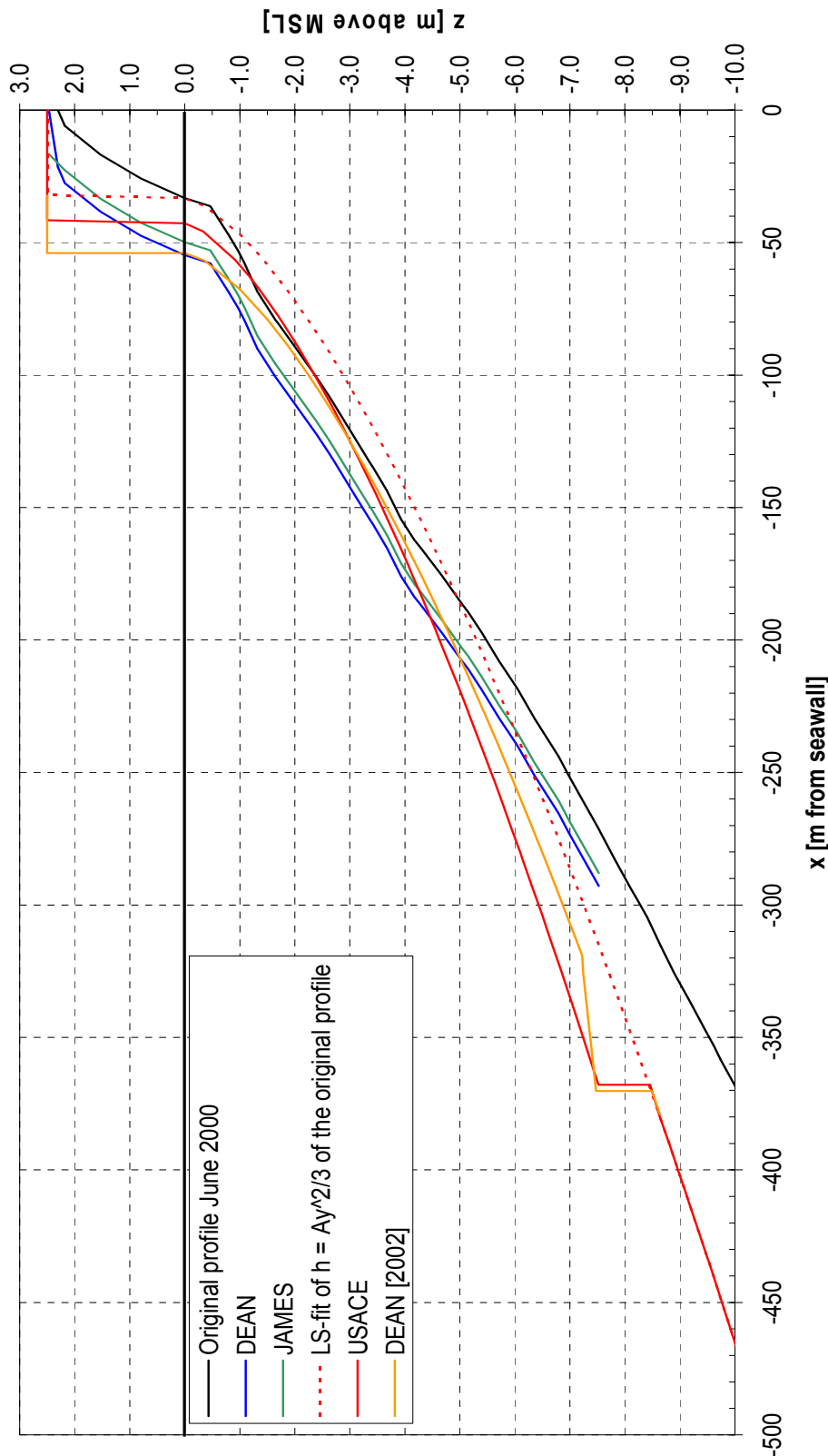
Page	Borrow area	Design methods
H-2	I – Puerto Juárez $d_F = 0.27$ mm	James [1974], Dean [1975], USACE [1994] and Dean [2002].
H-3	Fictitious $d_F = d_N = 0.33$ mm	Idem
H-4	II – Punta Sam $d_F = 0.42$ mm	Idem
H-5	I – Puerto Juárez $d_F = 0.27$ mm	USACE [1994], Dean [2002] and Unibest-TC
H-6	Fictitious $d_F = d_N = 0.33$ mm	Idem
H-7	II – Punta Sam $d_F = 0.42$ mm	Idem

Explanation: Bottom profiles after equilibration using fill sediments from borrow area I – Puerto Juárez ( $d_F = 0.27 \text{ mm}$ ) according to the methods of James [1974], Dean [1975], USACE [1994] and Dean [2002]. The least-square fit of  $h = Ay^{2/3}$  to the original profile has been made to MSL-7.5 m.

Reference: Paragraph 5.3

**BOTTOM PROFILES AFTER EQUILIBRATION FOR  $d_{F50} = 0.27 \text{ mm}$**

$h^* = 7.5 \text{ m}$  -  $B = 2.5 \text{ m}$  -  $V = 250 \text{ m}^3/\text{m}$   
chainage 6100 - 6900



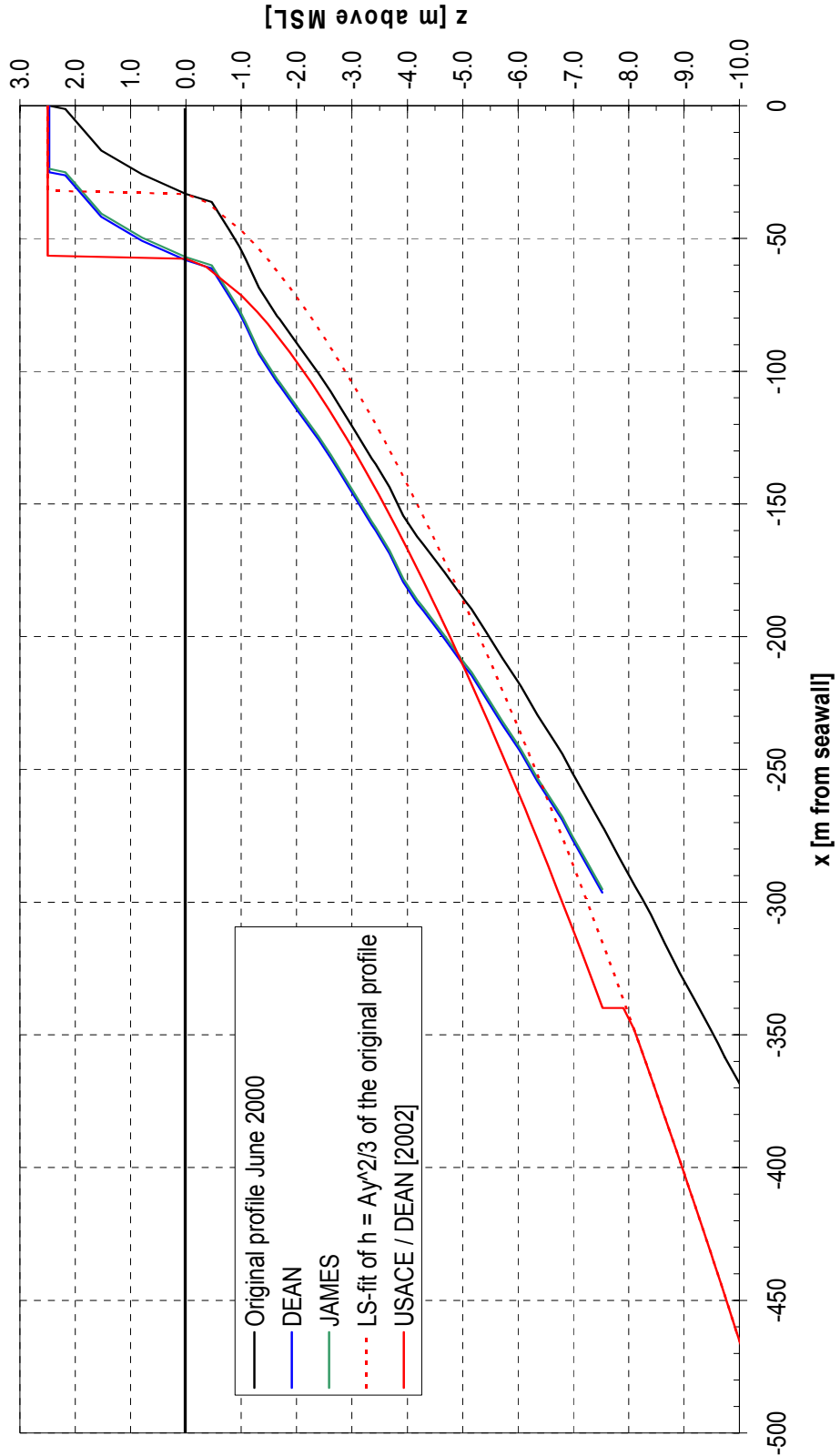
- Original profile June 2000
- DEAN
- JAMES
- ... LS-fit of  $h = Ay^{2/3}$  of the original profile
- USACE
- DEAN [2002]

Explanation: Bottom profiles after equilibration using fictitious fill sediments equalling native ( $d_F = 0.33 \text{ mm}$ ) according to the methods of James [1974], Dean [1975], USACE [1994] and Dean [2002]. The least-square fit of  $h = Ay^{2/3}$  to the original profile has been made to MSL -7.5 m.

Reference: Paragraph 5.3

**BOTTOM PROFILES AFTER EQUILIBRATION FOR  $d_{F50} = 0.33 \text{ mm}$**

$h^* = 7.5 \text{ m} - B = 2.5 \text{ m} - V = 250 \text{ m}^3/\text{m}$   
chainage 6100 - 6900



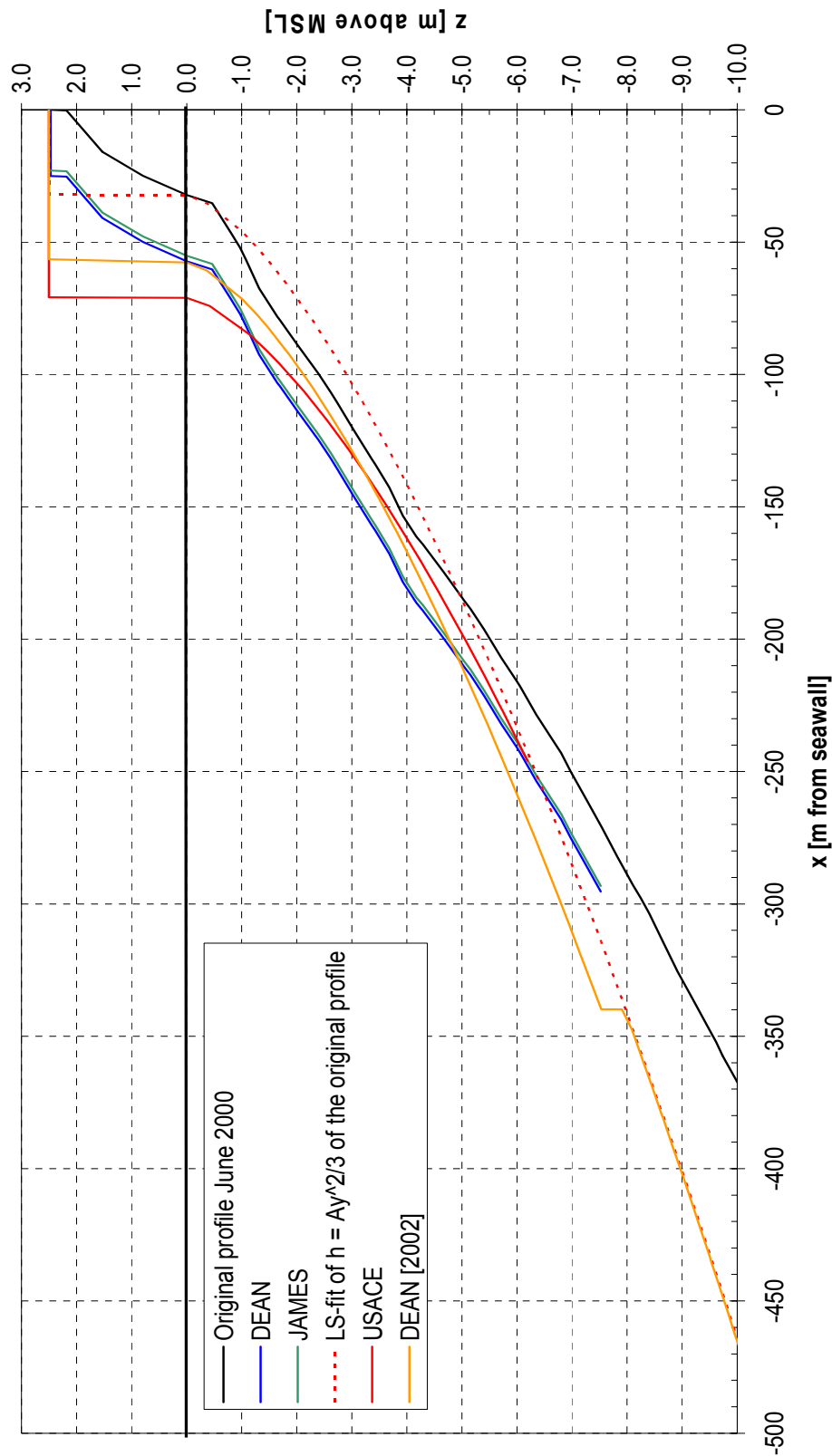
- Original profile June 2000
- DEAN
- JAMES
- ... LS-fit of  $h = Ay^{2/3}$  of the original profile
- USACE / DEAN [2002]

Explanation: Bottom profiles after equilibration using fill sediments from borrow area I – Punta Sam ( $d_F = 0.42 \text{ mm}$ ) according to the methods of James [1974], Dean [1975], USACE [1994] and Dean [2002]. The least-square fit of  $h = Ay^{2/3}$  to the original profile has been made to MSL -7.5 m.

Reference: Paragraph 5.3

**BOTTOM PROFILES AFTER EQUILIBRATION FOR  $d_{F50} = 0.42 \text{ mm}$**

$h^* = 7.5 \text{ m} - B = 2.5 \text{ m} - V = 250 \text{ m}^3/\text{m}$   
chainage 6100 - 6900



- Original profile June 2000
- DEAN
- JAMES
- ... LS-fit of  $h = Ay^{2/3}$  of the original profile
- USACE
- DEAN [2002]



Explanation:

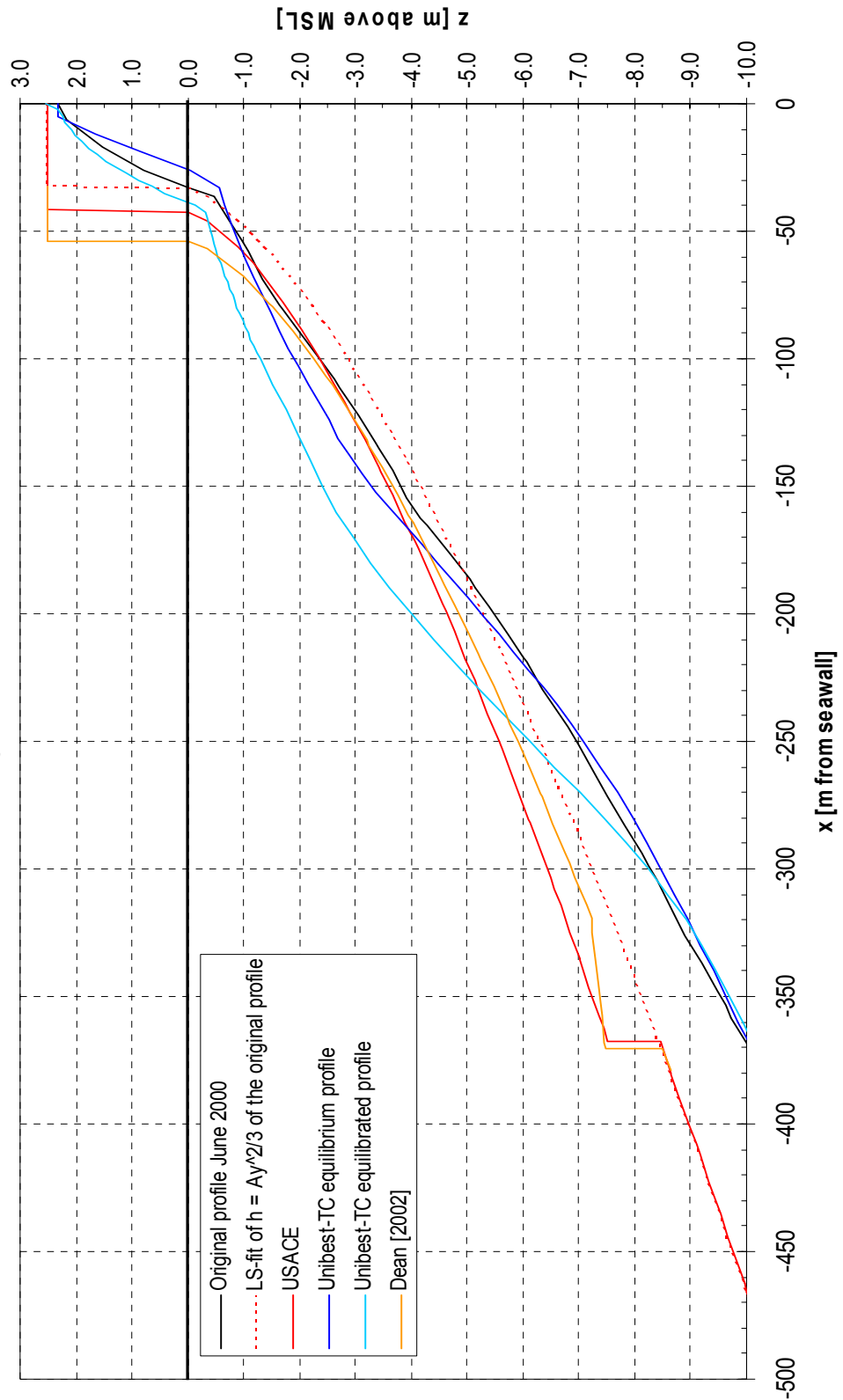
Bottom profiles after equilibration using fill sediments from borrow area I – Puerto Juárez ( $d_F = 0.27 \text{ mm}$ ) according to the methods of USACE [1994], Dean [2002] and Unibest-TC. The least-square fit of  $h = Ay^{2/3}$  to the original profile has been made to MSL -7.5 m.

Reference:

Paragraph 10.2

**BOTTOM PROFILES AFTER EQUILIBRATION FOR  $d_{F50} = 0.27 \text{ mm}$**

$h^* = 7.5 \text{ m} - B = 2.5 \text{ m} - V = 250 \text{ m}^3/\text{m}$   
chainage 6100 - 6900

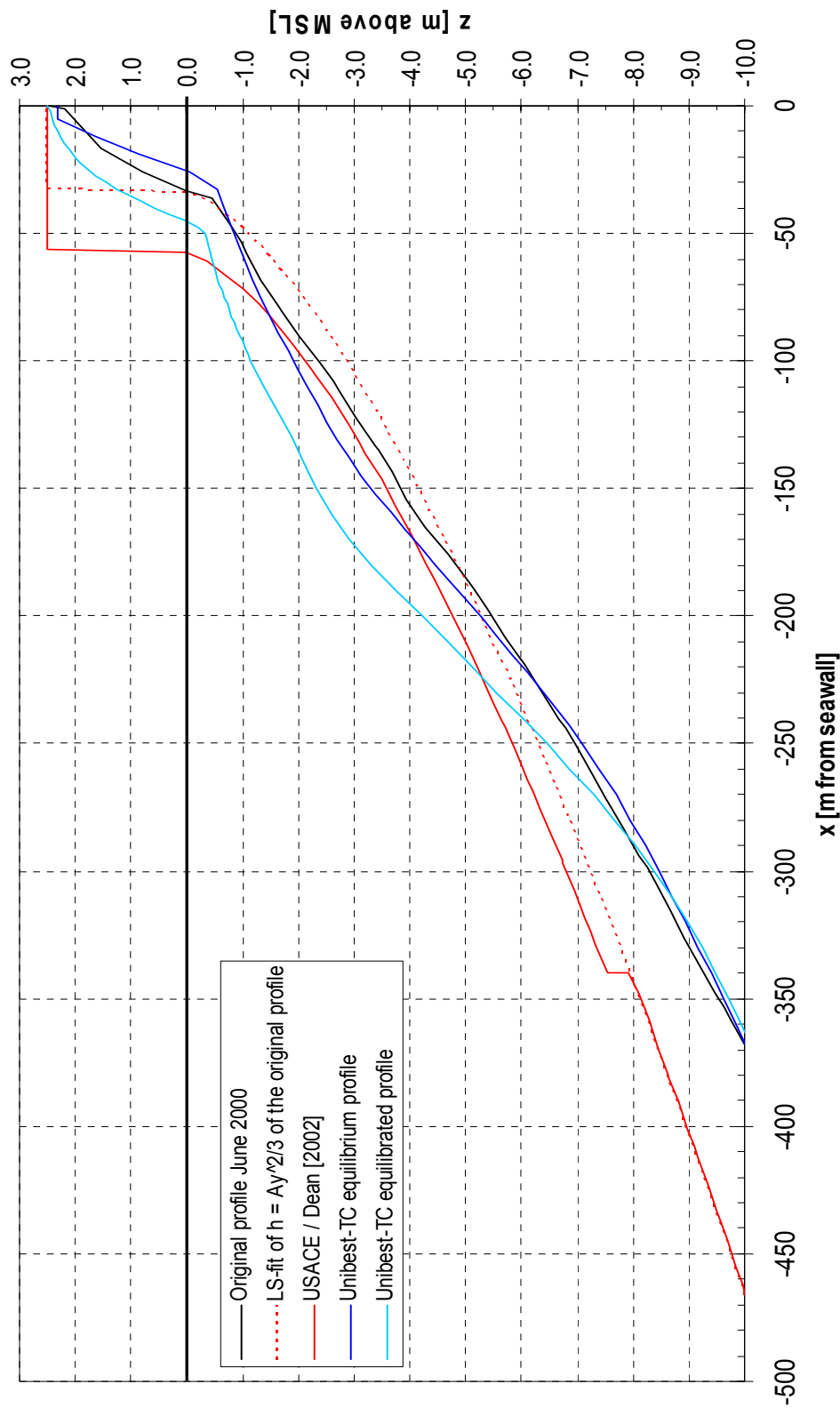


Explanation: Bottom profiles after equilibration using fictitious fill sediments equalling native ( $d_F = 0.33 \text{ mm}$ ) according to the methods of USACE [1994], Dean [2002] and Unibest-TC. The least-square fit of  $h = Ay^{2/3}$  to the original profile has been made to MSL -7.5 m.

Reference: Paragraph 10.2

**BOTTOM PROFILES AFTER EQUILIBRATION FOR  $d_{F50} = 0.33 \text{ mm}$**

$h^* = 7.5 \text{ m} - B = 2.5 \text{ m} - V = 250 \text{ m}^3/\text{m}$   
chainage 6100 - 6900

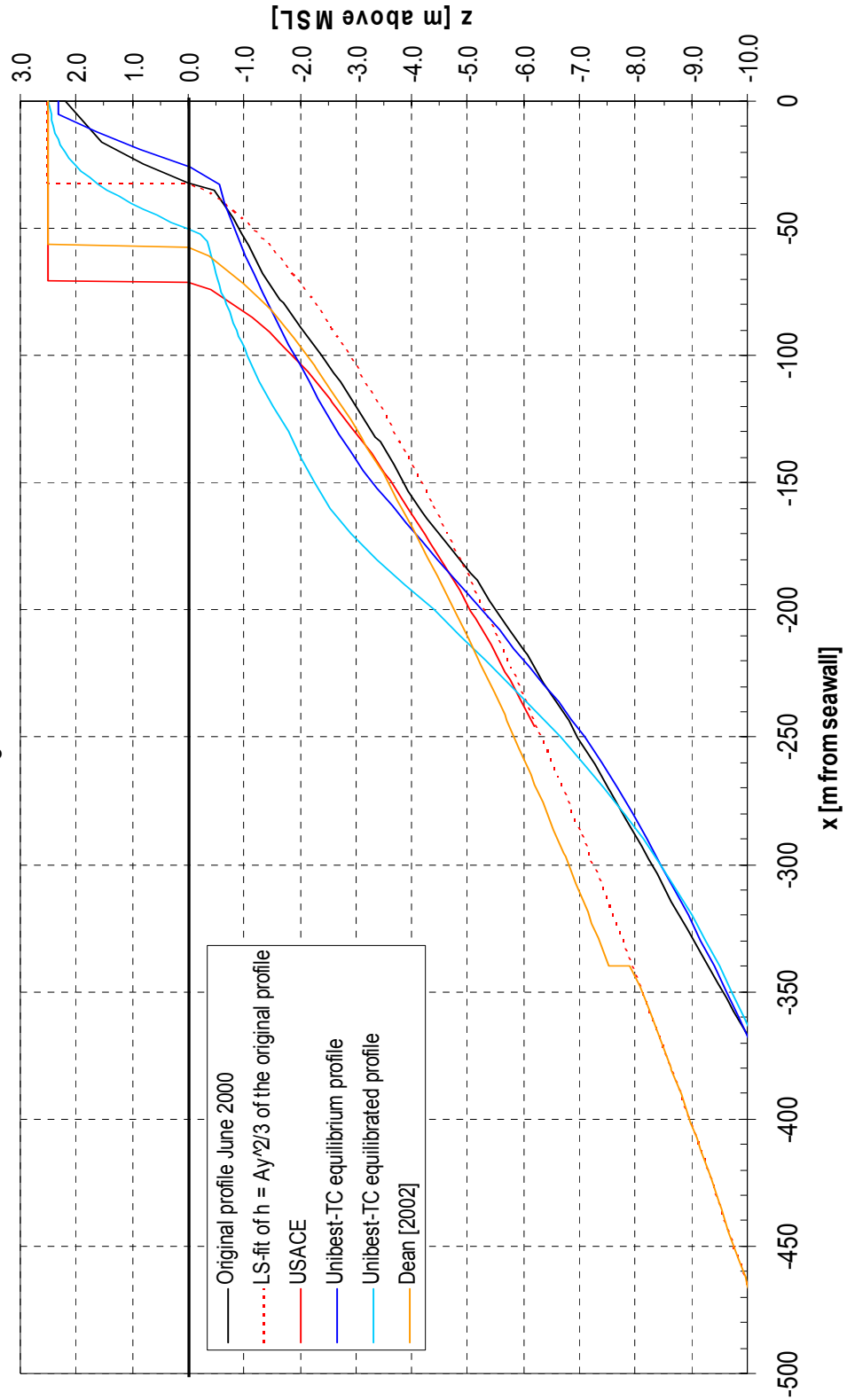


Explanation: Bottom profiles after equilibration using fill sediments from borrow area I - Punta Sam ( $d_F = 0.42 \text{ mm}$ ) according to the methods of USACE [1994], Dean [2002] and Unibest-TC. The least-square fit of  $h = Ay^{2/3}$  to the original profile has been made to MSL -7.5 m.

Reference: Paragraph 10.2

**BOTTOM PROFILES AFTER EQUILIBRATION FOR  $d_{F50} = 0.42 \text{ mm}$**

$h^* = 7.5 \text{ m} - B = 2.5 \text{ m} - V = 250 \text{ m}^3/\text{m}$   
chainage 6100 - 6900





# I SEDIMENT FALL VELOCITY

## I.1 Introduction

The fall velocity of the sediments is an important parameter in coastal engineering. In this report the fall velocity is necessary to apply the dune erosion prediction model of Vellinga [1986] in Chapter 11. In this appendix an equation will be derived for the fall velocity depending on the water density and temperature.

## I.2 Sediment fall velocity

The fall velocity of a grain in water depends on:

- The shape of the grain.
- The density of the grain (in this case equal to quartz sand = 2650 kg/m<sup>3</sup>).
- The density of the water, which depends on the temperature and salinity.
- The kinematic viscosity of the water, which depends on the temperature and salinity.

### Fall velocity according to Van Rijn [1993]

Van Rijn [1993] suggested the following expression for the fall velocity, taking into account all above parameters:

$$w_s = \frac{10\nu}{D} \left[ \left( 1 + \frac{0.01(s-1)gD^3}{\nu^2} \right)^{0.5} - 1 \right] \quad \text{for } 0.1 \text{ mm} < D < 1.0 \text{ mm} \quad (\text{I-1})$$

Where:	$w_s$	sediment fall velocity	[m/s]
	$\nu$	kinematic viscosity of the water	[m <sup>2</sup> /s]
	$D$	grain diameter	[m]
	$s$	specific density ( $\rho_s/\rho$ )	[m]
	$g$	gravity acceleration	[m/s <sup>2</sup> ]

In which  $\nu$  depends on the temperature of the water:

$$\nu = (1.14 - 0.031(T - 15) + 0.00068(T - 15)^2) \cdot 10^{-6} \quad (\text{I-2})$$

Where:  $T$  water temperature [°C]

### Fresh water fall velocity according to Sisternans [2002]

According to Sisternans [2002], the fall velocity of Van Rijn [1993] is too high compared with the fall velocity according to WL | Delft Hydraulics [1983], based on experiments. He defined the following equation for the sediment fall velocity for quartz sand in fresh water:

$$w_f(T) = w_f(18) \left[ \frac{1 + (T - 22)\gamma}{1 - 4\gamma} \right] \quad [\text{Sisternans, 2002}] \quad (\text{I-3})$$

Where:	$w_f(T)$	fall velocity at temperature T in fresh water	[m/s]
	$w_s(18)$	fall velocity according to WL   Delft Hydraulics [1983] for fresh water at 18 °C, see Equation (I-4)	[m/s]
	$\gamma$	temperature correction factor according to Equation (I-5)	[1/°C]

$$\log(1/w_f(18)) = A \log^2 D + B \log D + C \quad [\text{WL} \mid \text{Delft Hydraulics, 1983}] \quad (\text{I-4})$$

Where: A empirical parameter for fresh water and 18 °C = 0.476 [-]  
 B empirical parameter for fresh water and 18 °C = 2.18 [-]  
 C empirical parameter for fresh water and 18 °C = 3.19 [-]

$$\gamma = 75370D^2 - 84.70D + 0.02815 \quad [\text{Sisternans, 2002}] \quad (\text{I-5})$$

### Salt water fall velocity

The fall velocity of Sisternans [2002] (see Equation (I-3)) is for fresh water ( $\rho_w = 1000 \text{ kg/m}^3$ ) and is changed to salt water ( $\rho_w = 1025 \text{ kg/m}^3$ ) according to Equation (I-1), which leads to a correction factor  $\alpha$  which is almost independent of the grain size, for the grain sizes considered in this thesis. Applying Equation (I-1) leads to  $\alpha = 0.973$ . The fall velocity of the grains in salt water is calculated according to:

$$w_s(T) = \alpha \cdot w_s(18) \left[ \frac{1 + (T - 22)\gamma}{1 - 4\gamma} \right] \quad (\text{I-6})$$

Where:  $w_s(T)$  fall velocity at temperature T in salt water [m/s]  
 ( $\rho_w = 1025 \text{ kg/m}^3$ )  
 $w_s(18)$  fall velocity according to Delft Hydraulics [1983] for fresh water at 18 °C, see Equation (I-4) [m/s]  
 $\gamma$  temperature correction factor according to Equation (I-5) [1/°C]  
 $\alpha$  water density correction factor. [-]  
 For  $0.27 \text{ mm} < D < 0.42 \text{ mm}$ :  $\alpha = 0.973$

Equation (I-6) will be used to determine the sediment fall velocity for the dune erosion prediction model of Vellinga [1986] in Chapter 11.

## J POST-STORM PROFILES

In this appendix the post-storm profiles according to the dune erosion prediction model of Vellinga [1986] and the Unibest-TC model are plotted. Three beach sediments have been considered as indicated below:

Page	Borrow area
J-2	I – Puerto Juárez $d_F = 0.27$ mm
J-3	Fictitious $d_F = d_N = 0.33$ mm
J-4	II – Punta Sam $d_F = 0.42$ mm

The pre-storm profiles are equilibrated nourished (fill volume  $V = 300$  m<sup>3</sup>/m, berm height  $B = 2.5$  m) profiles calculated by Unibest-TC.

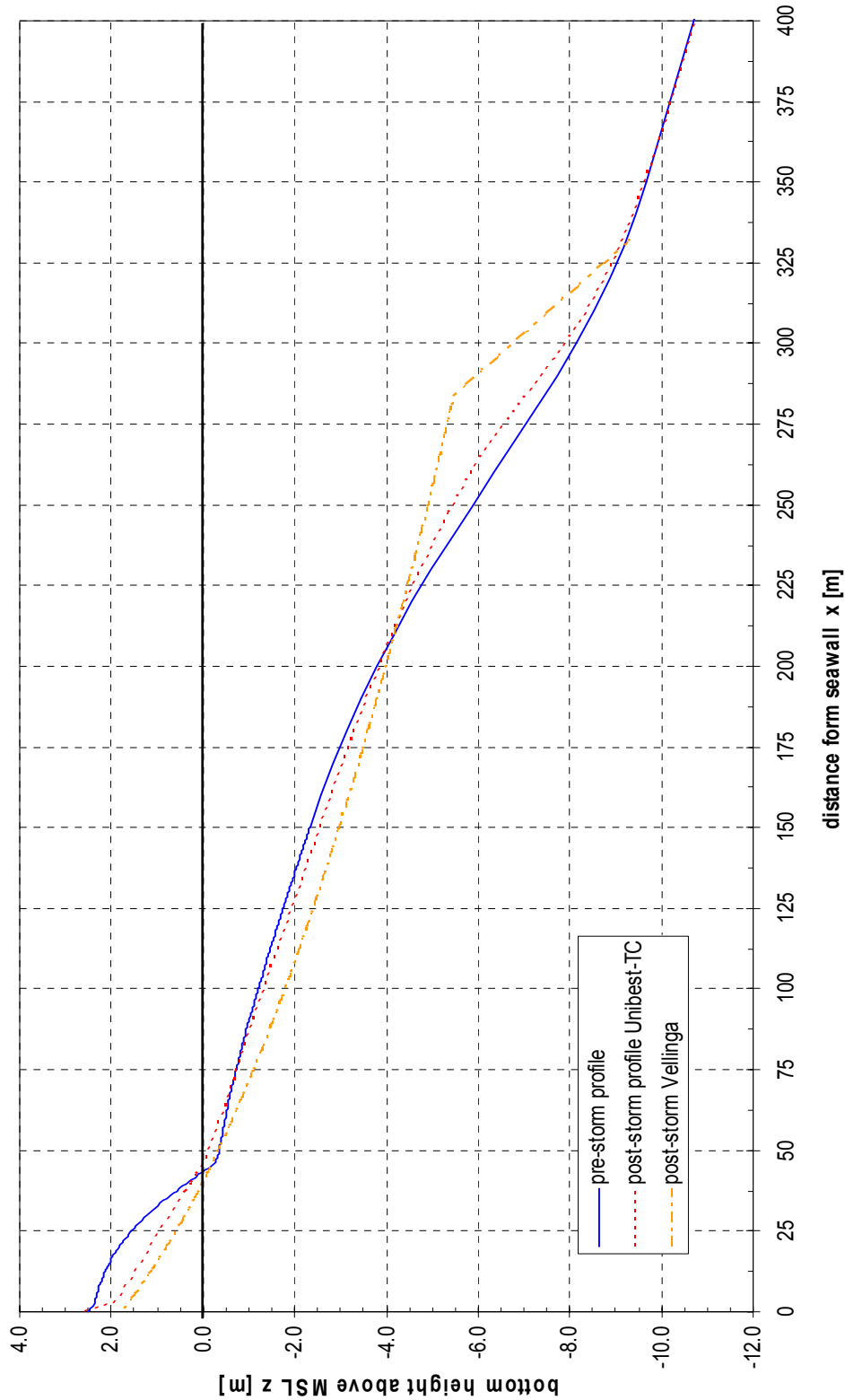
These plots are of importance for Chapter 11.

Explanation: *Bottom profiles before and after the occurrence of a design storm on the equilibrated profile for sediments from borrow area I - Puerto Juárez ( $d_F = 0.27 \text{ mm}$ ). The pre-storm profile is an equilibrated profile calculated by Unibest-TC for a fill volume of  $V = 300 \text{ m}^3/\text{m}$  and berm height  $B = 2.5 \text{ m}$  at the end of September, 15 months after construction.*

Reference: *Paragraph 11.4 & 11.5*

**STORMEROSION**

storm surge = MSL + 2.0 m -  $H_{s,0} = 10 \text{ m}$  -  $d_F = 0.27 \text{ mm}$



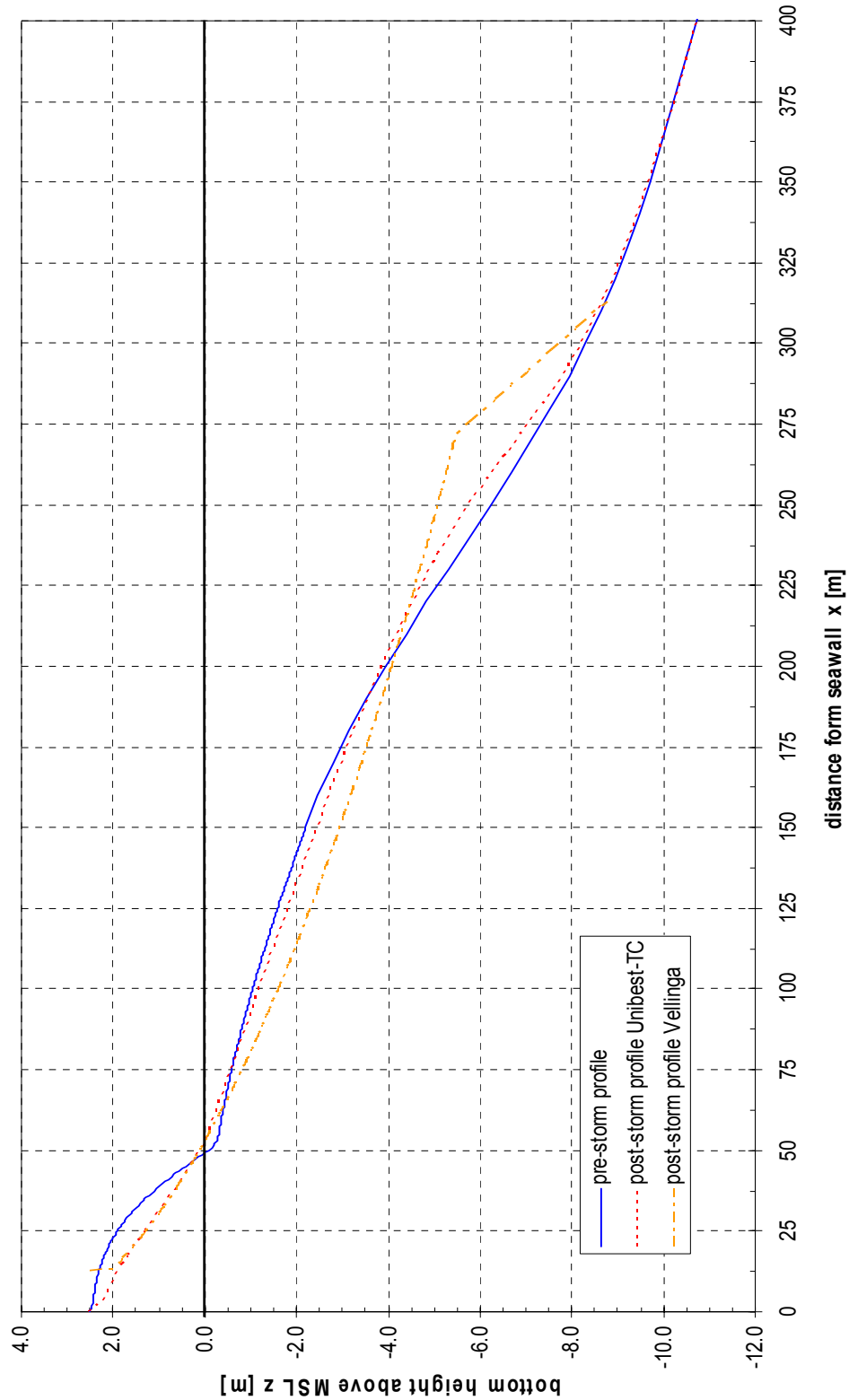


Explanation: Bottom profiles before and after the occurrence of a design storm on the equilibrated profile for fictitious fill sediments equalling native ( $d_F = 0.33 \text{ mm}$ ). The pre-storm profile is an equilibrated profile calculated by Unibest-TC for a fill volume of  $V = 300 \text{ m}^3/\text{m}$  and berm height  $B = 2.5 \text{ m}$  at the end of September, 15 months after construction.

Reference: Paragraph 11.4 & 11.5

**STORMEROSION**

storm surge = MSL + 2.0 m -  $H_{s,0} = 10 \text{ m}$  -  $d_F = 0.33 \text{ mm}$



Explanation: *Bottom profiles before and after the occurrence of a design storm on the equilibrated profile for sediments from borrow area I - Puerto Juárez ( $d_F = 0.27 \text{ mm}$ ). The pre-storm profile is an equilibrated profile calculated by Unibest-TC for a fill volume of  $V = 300 \text{ m}^3/\text{m}$  and berm height  $B = 2.5 \text{ m}$  at the end of September, 15 months after construction.*

Reference: *Paragraph 11.4 & 11.5*

**STORMEROSION**

storm surge = MSL + 2.0 m -  $H_{s,0} = 10 \text{ m}$  -  $d_F = 0.42 \text{ mm}$

